2

LRC-5258
September 1981

RECEIVED BY TIC NOV 9 1981

Babcock & Wilcox
a McDermott company

IMPROVEMENT OF THE MECHANICAL RELIABILITY OF MONOLITHIC REFRACTORY LININGS FOR COAL GASIFICATION PROCESS VESSELS

Submitted by
Babcock & Wilcox
Contract Research Division
P.O. Box 835
Alliance, Ohio 44601

MASTER

Prepared for
United States Department of Energy

DOE Contract No. EX-76-C-01-2218 (old no.)
DOE Contract No. DE-AC05-76ET10434 (new no.)
B & W Contract No. CRD-1000

DISTRIBUTION OF THIS DOCUMENT IS UNLIMITED

DISCLAIMER

This report was prepared as an account of work sponsored by an agency of the United States Government. Neither the United States Government nor any agency Thereof, nor any of their employees, makes any warranty, express or implied, or assumes any legal liability or responsibility for the accuracy, completeness, or usefulness of any information, apparatus, product, or process disclosed, or represents that its use would not infringe privately owned rights. Reference herein to any specific commercial product, process, or service by trade name, trademark, manufacturer, or otherwise does not necessarily constitute or imply its endorsement, recommendation, or favoring by the United States Government or any agency thereof. The views and opinions of authors expressed herein do not necessarily state or reflect those of the United States Government or any agency thereof.

DISCLAIMER

Portions of this document may be illegible in electronic image products. Images are produced from the best available original document.

B&W makes no warranty or representation, expressed or implied:

- with respect to the accuracy, completeness, or usefulness of the information contained in this report
- that the use of any information, apparatus, method, or process disclosed in this report may not infringe privately owned rights.

B&W assumes no liability with respect to the use of, or for damages resulting from the use of:

- any information, apparatus, method, or process disclosed in this report
- experimental apparatus furnished with this report.

LRC-5258
Dist. Category - UC-90H
September 1981

LRC--5258

DE82 007251

IMPROVEMENT OF THE MECHANICAL RELIABILITY OF MONOLITHIC REFRACTORY LININGS FOR COAL GASIFICATION PROCESS VESSELS

Final Report

Compiled by
R. A. Potter
Materials & Chemistry Laboratory
Lynchburg Research Center

DISCLAIMER

This book was prepared as an account of work sponsored by an agency of the United States Government. Neither the United States Government nor any agency thereof, nor any of their employees, makes any warranty, express or implied, or assumes any legal liability or responsibility for the accuracy, completeness, or usefulness of any information, apparatus, product, or process disclosed, or represents that its use would not infringe privately owned rights. Reference herein to any specific commercial product, process, or service by trade name, trademark, manufacturer, or otherwise, does not necessarily constitute or imply its endorsement, recommendation, or favoring by the United States Government or any agency thereof. The views and opinions of authors expressed herein do not necessarily state or reflect those of the United States Government or any agency thereof.

DOE Contract EX-76-C-01-2218 (Old No.)
DE-AC05-76OR10434 (New No.)
B&W Contract No. CRD-1000

Prepared for

United States Department of Energy

by

BABCOCK & WILCOX
Research and Development Division
Lynchburg Research Center
P.O. Box 1260
Lynchburg, Virginia 24505

DISTRIBUTION OF THIS DOCUMENT IS UNLIMITED

"This report was prepared as an account of work sponsored by the United States Government. Neither the United States nor the United States DOE, nor any of their contractors, subcontractors, or their employees, makes any warranty, express or implied, or assumes any legal liability or responsibility for the accuracy, completeness, or usefulness of any information, apparatus, product or process disclosed, or represents that its use would not infringe privately owned rights."

ACKNOWLEDGEMENTS

The following people are acknowledged for their role in the program:

E. M. Anderson - Program Manager
R. P. Glasser - Strain Gage Development
M. A. Schroedl - Mathematical Modeling
R. W. Sheriff - Acoustic Emission Analysis
R. S. Williams - Acoustic Emission Analysis
C. E. Zimmer - Test Facilities Design

Recognization is also extended to the following technicians: B. E. Burnette, J. Coleman, W. A. Crawford, P. D. Keith and R. G. Komoroski.

SUMMARY

Monolithic refractory designs based on practices in the petrochemical industry have been used in many of the non-slagging coal gasifier processes being developed or partially sponsored by the Department of Energy. These linings are easy to install, relatively inexpensive, and generally insulate vessel shells more effectively than brick linings. They are prone to crack and degrade thermomechanically, however, and it is this characteristic that concerns those involved with the operation and overall performance of coal conversion processes.

It is generally believed that the cracking and associated thermomechanical degradation of monolithic refractory linings is most significantly affected by their performance during the initial dry-out and heat-up. It was the objective of this work to improve the thermomechanical reliability, i.e., reduce or eliminate the cracking, of monolithic refractory linings of coal gasification process vessels (operating to 2000°F) during the initial dry-out and heat-up.

The scope of work developed to achieve this objective involved performing a systematic engineering study of standard and experimental monolithic refractory linings to learn why they crack and degrade and how to reduce or eliminate the causes. The expected output of the program was to be recommendations and guidelines on materials, design configurations, and installation and operational procedures for monolithic refractory linings that would improve their performance and reliability.

To perform this work, a test facility was designed and built; nine linings, of both conventional and new or improved designs and materials, were tested; a mathematical model, high temperature strain gage technique and nondestructive examination technique, such as acoustic emission monitoring, were developed; and mechanical property data were determined on the materials of interest. A seminar was given at the end of the program to present the results and findings of the study to the coal gasification and petrochemical industries and other interested groups.

This report summarizes the test procedures used, the findings of the work and the recommendations developed. The significant results of the work are outlined below and discussed in detail in the report:

1. Eighteen heat-up tests were run on nine standard and experimental dual component monolithic refractory concrete linings. These tests were run with a five foot diameter by fourteen foot high Pressure Vessel/Test Furnace designed to accomodate a twelve (12) inch thick by five foot high refractory lining, heat the hot face to 2000°F and expose the lining to air or steam pressures up to 150 psig.

   The results obtained from standard type linings in the test facility indicated that lining degradation duplicated that observed in field installations.

2. The lining performance was significantly improved due to information gained from a systematic study of the cracking that occurred in the

linings; the analysis of the lining strains, shell stresses and acoustic emission results; and the stress analyses performed on the standard and experimental lining designs with the finite element analysis computer programs, REFSAM and RESGAP, developed on this contract.

3. The material, design and operating procedure guidelines which led to this improved performance included the use of:

   - A 50% Al_2O_3 dense refractory concrete with a low cement content, very low shrinkage, good fracture toughness and superior creep resistance compared to conventional 50% Al_2O_3 dense refractory concretes. This material also has a lower coefficient of thermal expansion and a lower thermal conductivity than 90+% Al_2O_3 dense refractory concretes which reduced the thermal stresses generated in the lining and shell and insulated the shell better.

   - The use of 4 w/o 310 stainless steel fibers in the 50% Al_2O_3 dense component.

   - A weaker, lower thermal conductivity insulating component than the original material tested.

   - Wider anchor spacings--two to three feet rather than six inches to one foot.

   - Coated anchors using an asphalt based tape which burns out and leaves a ≥50 mil expansion gap around the anchor.

   - Bonding barriers between the lining components and between the lining and the shell.

   - A corrosion resistant material attached to the shell which also acts as a compliant layer between the shell and the lining.

   - A slow (25 to 50°F/hr) continuous initial heat-up rate to top operating temperature with no holds.

4. These improved material, design and operating procedure guidelines were successfully field tested on the HYGAS gasifier during a reline of the high temperature reactor portion of the unit in early 1980. They were also reviewed during a seminar given at the Lynchburg Research Center of Babcock & Wilcox.

5. A user's manual, "Mathematical Model For the Thermo-Mechanical Analysis of Refractory-Lined Process Vessels," has been written on the finite element analysis computer programs, REFSAM and RESGAP, developed on this contract. This manual is available from NTIS.

CONTENTS

CONTENTS (Cont'd)

List of Figures

List of Figures (Cont'd)

List of Figures (Cont'd)

List of Figures (Cont'd)

List of Figures (Cont'd)

List of Figures (Cont'd)

List of Figures (Cont'd)

List of Figures (Cont'd)

List of Figures (Cont'd)

List of Tables

List of Tables (Cont'd)

1. INTRODUCTION

1.1 Background - The Problem

The use of coal to help solve our energy problems has generated numerous research and commercial ventures in the USA during the 1970's. Many of these ventures involve the gasification of coal, lignite or peat to produce low, intermediate or high BTU gas (130, 350 and 1000, respectively). Both non-slagging and slagging processes at ambient pressure to thirty atmospheres or more are being, or have been, evaluated. Non-slagging processes generally operate at temperatures below 2000°F, and slagging processes operate at temperatures above 2000°F (usually in the 2500-2800°F range). Monolithic refractory concretes have been used predominantly in the non-slagging gasifiers; and brick linings, often backed up with monolithics, have been used in the slagging gasifiers.

The monolithic lining designs used in the non-slagging gasifiers were based on standard practices in the petrochemical industry and to some extent, the practices in the steel industry. These designs are usually dual or multi-component and utilize a low silica, low iron, calcium aluminate bonded high alumina (50-95% Al_2O_3) dense refractory concrete backed up with an intermediate alumina (40-60%) insulating refractory concrete. Examples of such monolithic refractory linings in some non-slagging coal gasification pilot plants are listed below.

Pilot Plant	Refractory Linings
HYGAS	12-16" dual component lining w/90+% Al_2O_3 dense hot face material and 50% Al_2O_3 insulating material
SYNTHANE	9" dual component lining w/90+% Al_2O_3 dense and 50% Al_2O_3 insulating castable
CO_2 ACCEPTOR	17" multi-component lining w/50% Al_2O_3 dense hot face material, 45% Al_2O_3 insulating component and insulating block at cold face

Monolithic refractory concrete linings are generally easy to install, relatively inexpensive compared to brick linings and thermally insulate the process vessel shell. However, they have a tendency to crack and degrade thermo-mechanically and, as a result, are considered to be unreliable. Examples of this degradation are shown in Figure 1 and 2 respectively, for the CO_2 Acceptor gasifier and the upper portion of the HYGAS Gasifier.

This degradation usually causes thinning of the lining and paths through which hot corrosive gases can flow. The combined effect is overheating and corrosion

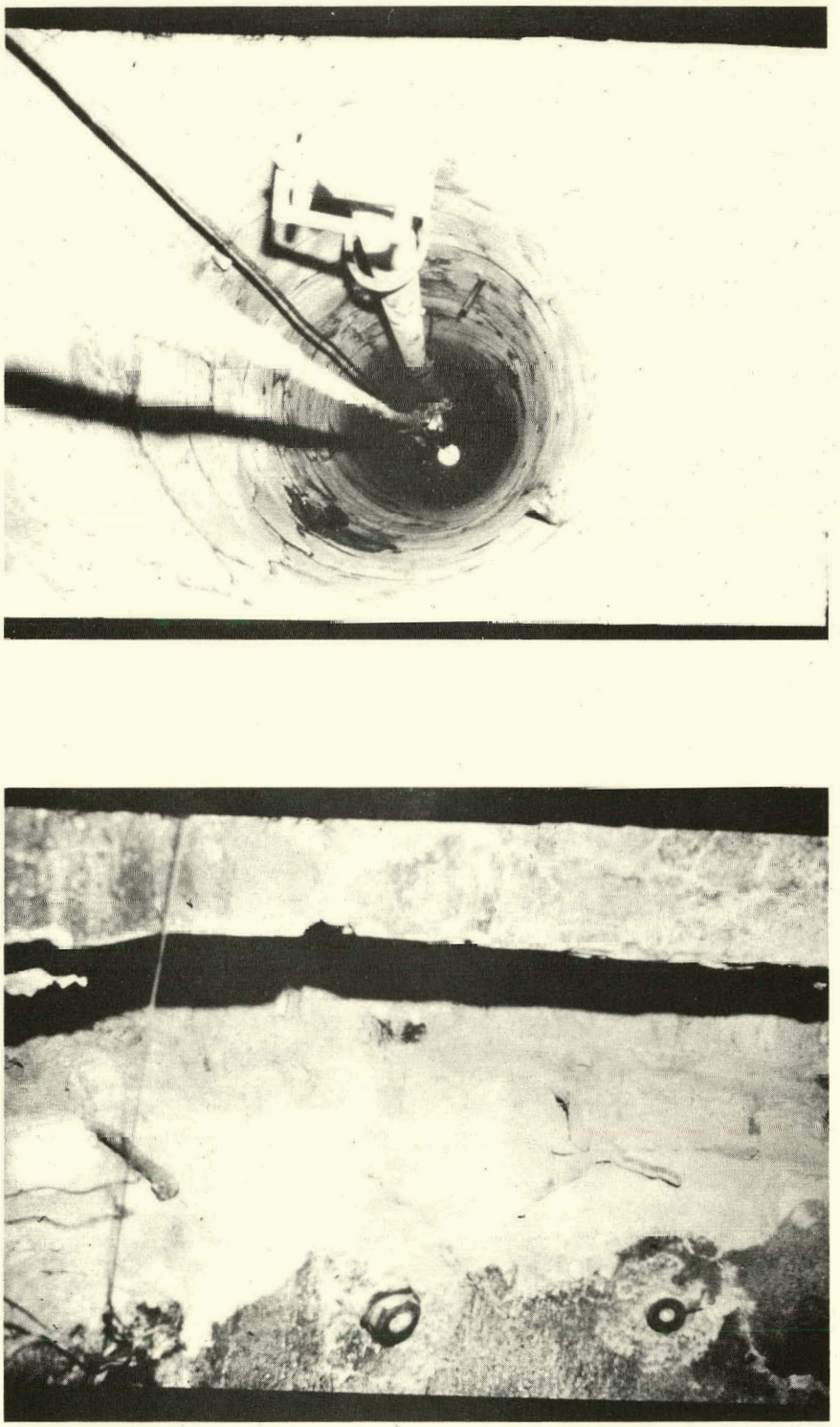

FIGURE 1. Appearance of Monolithic Refractory Lining in CO_2 Acceptor Gasifier after Approximately Five Years of Intermittent Service.

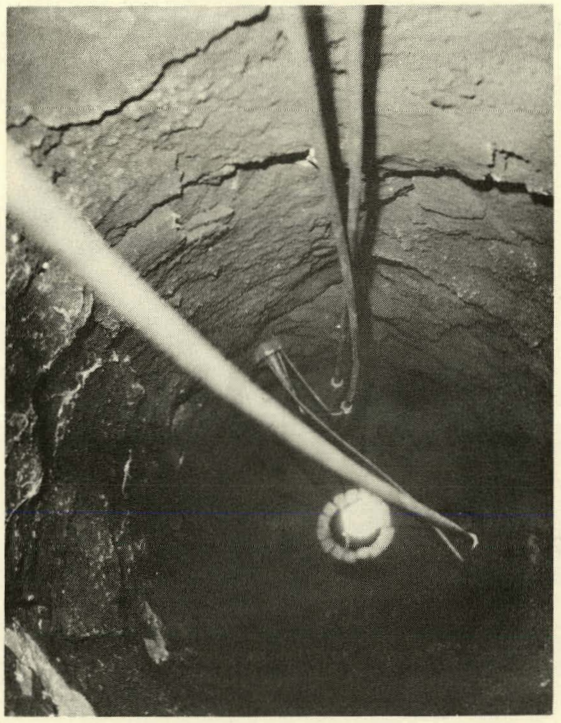

FIGURE 2. Appearance of Monolithic Refractory Lining in High Temperature Reactor Region of HYGAS Gasifier.

of the metal pressure vessel shell and short refractory life (six months to two years). In a severe condition the refractory linings can separate from the shell and cause a blow-by condition to occur which can lead to major damage to the vessel. Similar problems can also occur with brick linings.

Much of the monolithic refractory lining degradation is believed to be related to the cracking, spalling, etc. which occur on the initial dry-out, heat-up and cool-down of the monolithic refractory concrete lining. It is during this time that the uncombined and hydraulically bonded water is removed from the concrete and shrinkage and other changes in the material occur.

Since the majority of the coal gasification processes under development in the early to mid 1970's were of the non-slagging type, DOE chose to sponsor an engineering study on monolithic refractory concrete linings. The experiments were to be performed on standard and improved lining designs in a test facility that simulated the conditions which existed in pilot plant and commerical sized gasifiers. The linings were to be instrumented with strain gages, acoustic emission transducers and other devices to generate the test data wanted. The tests were to be run at temperatures to 2000°F and at pressures to at least 100 psi.

A user oriented model was also to be developed which would permit scale-up stress analysis predictions relevant to refractory lined pressure vessels up to 30 feet in diameter.

The ultimate goal of the program was to develop a better understanding of how monolithic refractory linings degrade and how to improve their reliability. The key deliverables wanted were: guidelines on material specifications, lining designs, installation procedures and operating procedures that would minimize cracking and improve overall lining performance.

The specific deliverable items requested by DOE were to include:

1. Computer programs (Fortran Language) for math modeling and analysis.
2. Furnace designed and constructed for the program.
3. Test procedures to measure stress, strain, and pressure and acoustic emissions (AE) in monolithic refractory linings.
4. Experimental data for heating tests and supporting data.
5. Specifications for refractories to prevent cracking during heat-up.
6. Guidelines for the design of monolithic refractory linings to prevent cracking during heat-up.
7. Guidelines on operating procedures to minimize crack formation during heat-up.
8. Improved monolithic refractory lining designs to resist cracking and other forms of thermo-mechanical degradation.

The report which follows summarizes the results of the work done during the four (4) year life of the program.

1.2. Objective

The objective of this program was to improve the thermo-mechanical reliability of monolithic calcium aluminate bonded refractory concrete linings

of coal gasification process vessels by reducing or eliminating the cracking and thermo-mechanical degradation which occurs in them on the initial dry-out, heat-up and cool-down.

1.3. Scope of Program

The scope of work planned to develop the guidelines for the improved performance wanted and to achieve the overall objective of the program was subdivided into nine tasks and is outlined below.

Tasks

I. Critical Literature Search. The literature was to be searched for information on the volume stability, mechanical properties and chemical changes of monolithic refractory linings of large process vessels as they are related to crack formation. The cracking which occurs during curing, dry-out, heat-up and cool-down was of prime consideration.

II. Derivation of Mathematical Model. A mathematical model was to be developed using thermal and finite element analysis computer programs to determine the stresses and strains occurring in twelve inch thick monolithic refractory linings of gasifier vessels of various sizes (2-30 foot I.D.). The model was to be developed for single and multicomponent linings but would not consider the effect of anchors. This effect was to be studied independently by the Civil Engineering Dept. at MIT under a separate DOE contract. Materials properties available in the literature or those being generated in Task III of this or other programs on 50-95 percent alumina insulating or dense refractories were to be utilized. The model would cover the temperature range from room temperature to 2000°F, but could be expanded to higher temperature if wanted.

III. Determination of Relevant Mechanical Properties. The relevant physical and mechanical properties of nine monolithic calcium aluminate and phosphate bonded refractories (five generic formulations and four commercial refractories) was to be determined. These properties were to include density, porosity, pore size and structure, hot and cold tensile and compressive strength, thermal expansion, permanent linear and volume change, creep and other related mechanical properties. These properties were to be used in the development of the math model and to support work in other tasks of this program.

IV. Development of New or Improved Refractories. New or improved monolithic refractories that have been developed to resist cracking during heat-up and cool-down will be evaluated. The work done in Tasks I, II and VI was expected to generate ideas for this task.

V. Design and Construction of Test Furnace. A pressure vessel/test furnace was to be designed and constructed. This test facility would be cylindrically designed and have a three foot I.D. when lined with twelve inches of refractory. It would be seven feet high to give a four foot working height for the lining. The facility would have a temperature capability of 2000°F, heat-up rate capability to 300°F/hr., a temperature gradient of no more than $\pm$20°F over the four foot height and pressure capability of 250 psi. It would also be instrumented to measure temperature, strains, acoustical emissions, pressure and other pertinent experimental parameters.

VI. Heat-up Tests With Stress-Strain and NDT Measurements. The pressure vessel/test furnace was to be used to test nine linings. The twelve inch refractory linings were to be instrumented to measure the strain developing in them as a function of heat-up rate, temperature, cool-down rate, gaseous atmosphere and pressure, materials used, lining design (single and multicomponent and different anchor spacings) and other practical considerations. The linings were to be monitored with visual and acoustic emission techniques for evidence of cracking during these tests. High temperature strain gage qualification activities were to be done under this task prior to the start of the heat-up tests. This work would be done to determine if and how the strain gages presently available or under development could be used at high temperatures (1000°F and above) in monolithic refractories. Babcock & Wilcox expertise on strain gages was to be used in this activity.

VII. Testing of Refractory Linings After Heat-up Tests. The linings were to be inspected for physical damage after the heat-up tests were completed. The shrinkage and crack widths were also to be determined. NDT and destructive test techniques were to be used during these inspections. Some physical and mechanical property testing was to be done on samples removed from the lining.

VIII. Correlation and Analysis of Data. The data collected during this program were to be analyzed and correlated with the mathematical model thermal and stress predictions generated on each lining. Relationships would be sought between the physical and mechanical properties of the refractories, the lining design, operating procedures (heat-up rate, atmospheric conditions, etc.) and vessel size and the probability of crack formation. These analyses and correlations were to serve as a basis for specifications on monolithic refractory lining materials for various size vessels.

IX. Seminar. A seminar was to be organized to present the data generated and the conclusions drawn from the work. It would also serve to transfer the technology developed on this program to the refractories industry, architectural engineering firms and to other interested parties.

2. TECHNICAL APPROACH

This section of the report describes the technical approaches and procedures used to perform the work.

2.1. Critical Literature Search

The search was accomplished by using a number of different data bases. These included a retrospective computer search on a number of data bases available through the Company's Corporate Information Center, a review of the Chemical and Ceramic abstracts, and a review of the literature that had been collected previously at Babcock & Wilcox on monolithic refractories. References were also sought on refractory studies that had been published since November or December 1975.

Table 1 lists the specific data bases searched and the proportioning of the 850 references that were considered of interest after the titles of the initial two thousand "hits" were reviewed. When the abstracts of these 850 references were reviewed, about 100-125 were considered relevant.

Since crack growth as well as crack initiation are important to the proper understanding and modeling of the performance of monolithic refractories, references which covered the thermal shock, crack growth, stress analysis and acoustic emission characteristics of ceramics and refractories were sought and reviewed. References that had been identified by the DOE Technical Representative as pertinent to this program, including work underway by other DOE contractors, were covered during this activity.

Six sets of key word combinations were used for the retrospective computer search. These sets are listed in Table 2.

TABLE 1. Data Bases Searched and Number of References Identified for Each

Data Bases	Period Covered	Initially Identified References
Engineering Index Computer	1970 - to present	446
NTIS Computer	1964 - to present	85
Smithsonian Science Info. Exchange	no specific search	
Claims(Chemical Patents File)	1970 - to present	150
Miscellaneous (Chemical Abstracts, etc)	1969 - to present	150
NASA/RECON	1962 - to present	19
TOTAL		850

TABLE 2. Sets of Key Words Used in Retrospective Computer Literature Search

Set 1	Set 2	Set 3	Set 4	Set 5	Set 6
Refractory with	Concrete with	Coal	Castable and	Castable and	Castable and
Thermal Analysis	Crack	Gasification with	Monolithic	Monolithic	Monolithic
Cylinder	Finite Elements	Castable	Refractory with	Refractory with	Refractory with
Thermal Shock	High Temp.	Monolithic	Phosphate	Creep	Carbon Monoxide
Heat Transfer	Elevated Temp.	Refractory	Calcium Aluminate	Dryout	Hydrogen
Transient		Reaction	Calcium Monoaluminate	Hydration	Steam
Lining			Calcium Hexaaluminate	Curing	Atmosphere
Anchor				Thermal Expansion	Heating Rate
Spalling				Hot Strength	
Monolithic				Tensile Strength	
Shrinkage				Cracking	
Analysis					
Stress					
Cracking					

2.2. Analytical Procedure/Model Development

2.2.1. Overview of the Model Capabilities

One of the objectives of this contract was the development of a mathematical model capable of calculating the strains and stresses in monolithic refractory linings resulting from thermal and mechanical loads. The mathematical model was to be user oriented and sufficiently documented to facilitate its use for structural analysis of monolithic linings used in a circular pressure vessel. With this objective in mind, two finite element computer programs were developed. The first computer program developed to achieve this objective consisted of a sophisticated non-linear finite element computer program capable of analyzing linings for the effects of creep, cracking, crushing, shrinkage, and thermal and mechanical loads. This program contains a one-dimensional thermal analysis capability which can be used to calculate the transient temperature distribution in the radial direction of the vessel. Inherent in the one-dimensional heat transfer capability is the assumption that there is no circumferential or axial variation of temperature in the lining or shell. This temperature distribution can then be used in conjunction with the finite element program to calculate the mechanical, thermal, creep and shrinkage strains in monolithic linings as well as in the shell. The computer program contains an axisymmetric generalized plane strain finite element. This element is based on the assumptions of uniform strain in the axial direction of the vessel and no variation in the radial or hoop strain in the circumferential direction of the vessel. That is, only one axial strain is computed for the vessel; whereas, radial and hoop strains are calculated at different radial locations through the vessel wall and these strains are not allowed to vary in the circumferential direction of the vessel due to axisymmetry. In addition to strains, the total stress state and radial displacements are calculated at various locations through the vessel wall. This computer program is called the Refractory Failure and Stress Analysis Model (REFSAM).

The second finite element computer program (RESGAP) is a simplified version of REFSAM which allows the user to define the vessel configuration, materials and loading with a minimum of input. It also allows the user to analyze the effects of gaps between various linings or between the linings and shell. The primary restriction of this simplified model is that it does not account for the temperature dependence of the material properties or the variation in response of the vessel in the hoop or axial direction of the linings or shell. However, these simplifications result in a program which requires little input from the user to define the analysis and can be executed with limited computer facilities. It is envisioned that this computer program can be used to investigate different lining configurations, the gross interaction between the linings and shell, and the effect of various heat-up rates for the vessel.

These models are thoroughly discussed in the user manual which is being delivered to DOE under separate cover.[1]

2.2.2. REFSAM and RESGAP Model Developments

The writeup which follows summarizes briefly the computer systems and approach used to develop these models. Much of this information is detailed in the user manual.

Computers Used

The computer systems initially used included a Digital Equipment Corporation PDP-11/70, stationed at the Alliance Research Center, which served as a terminal to an IBM 370/155 computer, located at Barberton, Ohio, and a CDC 7600 computer system, located at Lynchburg, Virginia. The CDC 7600 computer system has a CDC 7614 central computer which has 65,000 word, high speed, small core memory and 256,000 word, slow speed, large core memory capacities. The CDC 7614 is tied to a CDC 7638 disc that has a storage capability of 800 million characters. The CDC 7614 is driven by a CYBER 73-16 computer which has a 98,000 word core memory capacity. The system has multiple line printers, graphical plotters and magnetic tape drives. This system was later changed to include a VAX 11/780 computer instead of the PDP 11/70 computer. This computer is comparable in speed to the IBM 370 series computers at about 1/10th the cost.

The VAX 11/780 computer was used for the development of the simpler user oriented model and was tied to a CALCOMP plotter or line printer to generate plots from the analyses. This computer has a 32 bit word core memory, a two million bytes storage capability, CRT display, and a line printer.

Model Development

The failure analysis of refractory linings is a formidable task involving a thermal analysis with variable properties through the refractory wall; a stress analysis taking account of such effects as strains due to thermal expansion, irreversible shrinkage, nonlinearity of stress-strain relations and creep; and, most importantly, a failure criteria that defines the combinations of stress and strain which will result in cracking or crushing of the material.

The basic tool initially planned in the development of a mathematical model was the nonlinear program ADINA. The program, ADINA, is a 3D finite element stress analysis program which has extensive capabilities to analyze thermal stresses due to prescribed temperature distributions when the material properties vary with temperature.

Difficulty was expected with the program ADINA, since none of the individual options currently available in it could model all of the important aspects of the refractory analysis. For example, the creep model did not take into account the variation of thermal expansion with temperature, or simultaneous shrinkage, creep and cracking. Thus, the overall goal of the initial model development was to first identify appropriate models for the individual aspects of creep, expansion, shrinkage, and cracking; and incorporate a new material model into ADINA which could include all of these effects.

The program ADINA was acquired from MIT with Company funds and implemented on the Company computer system. Ten test cases supplied with the program were successfully executed. The project engineer attended a one-week course at MIT on the use and theoretical basis of the program ADINA. Inquiries were made to Dr. Bathe[2,3], the program originator, concerning the feasibility of modifying mathematical models in ADINA so that they would be applicable to refractory materials. The specific modifications discussed were the combination of Models 5 (concrete material model) and 11 (thermo-elastic-plastic-creep model) for the two-dimensional

and axisymmetric continuum elements (see Reference 1). Dr. Bathe saw no major difficulties in the proposed changes; he suggested that the coding would be simplified by adding the concrete cracking option to Model 11 rather than vice-versa. In response to questions about the physical validity of Model 5, Dr. Bathe stated that the failure criteria in the cracking model was purposely kept relatively simple, but was thought to be general enough for practical application. He mentioned that both Professor Connors at MIT and Professor Argyrus at the University of Stuttgart in West Germany have done a significant amount of work in this area using more sophisticated models. According to his philosophy, the material models in ADINA should be used in conjunction with tests in the laboratory to insure that physically meaningful results are being obtained with the model.

The program ADINA did not have a heat transfer analysis capability; and since the existing B&W heat transfer codes are proprietary, an auxiliary program was developed for use in the refractory analysis. The code is for one-dimensional transient analysis of cylindrical geometries. It is a finite element program based on quadratic temperature interpolations over each element. The basic equation in matrix form is

$$\{C\}\ \dot{T} + \{K\}\ T = Q \qquad (1)$$

where C is the specific heat matrix
K is the thermal conductivity matrix
T is a vector of nodal temperatures
Q is a vector of nodal heat flows
and a dot indicates differentiation with respect to time.

The element specific heat and conductivity matrices are formed by numerical integration over individual elements. The necessary material properties at each integration point are found by interpolating from user input tables of specific heat and conductivity versus temperature. As many as five different materials can be used through the wall, each having its own variation of properties with temperature. Since relatively small systems of equations are envisioned, an in-core equation solver based on Gaussian elimination is used. The program currently uses a constant time step and a simple implicit integration operator which, as proven in reference 2, is unconditionally stable. The heat transfer program also includes plotting capabilities which allow the temperature profile through the wall to be plotted at user-selected time steps. In addition, the temperatures are written on tape and cataloged in a format which is compatible with the required input data for the ADINA stress analysis program.

An attempt was made to use the ADINA cracking model with a refractory configuration as shown in Figure 3 but the results were not satisfactory. It appeared that the finite element grid was not refined enough to perform a successful cracking analysis.

It became apparent at this point that the program ADINA was too general and incomplete to be a viable user oriented model. A simpler, design

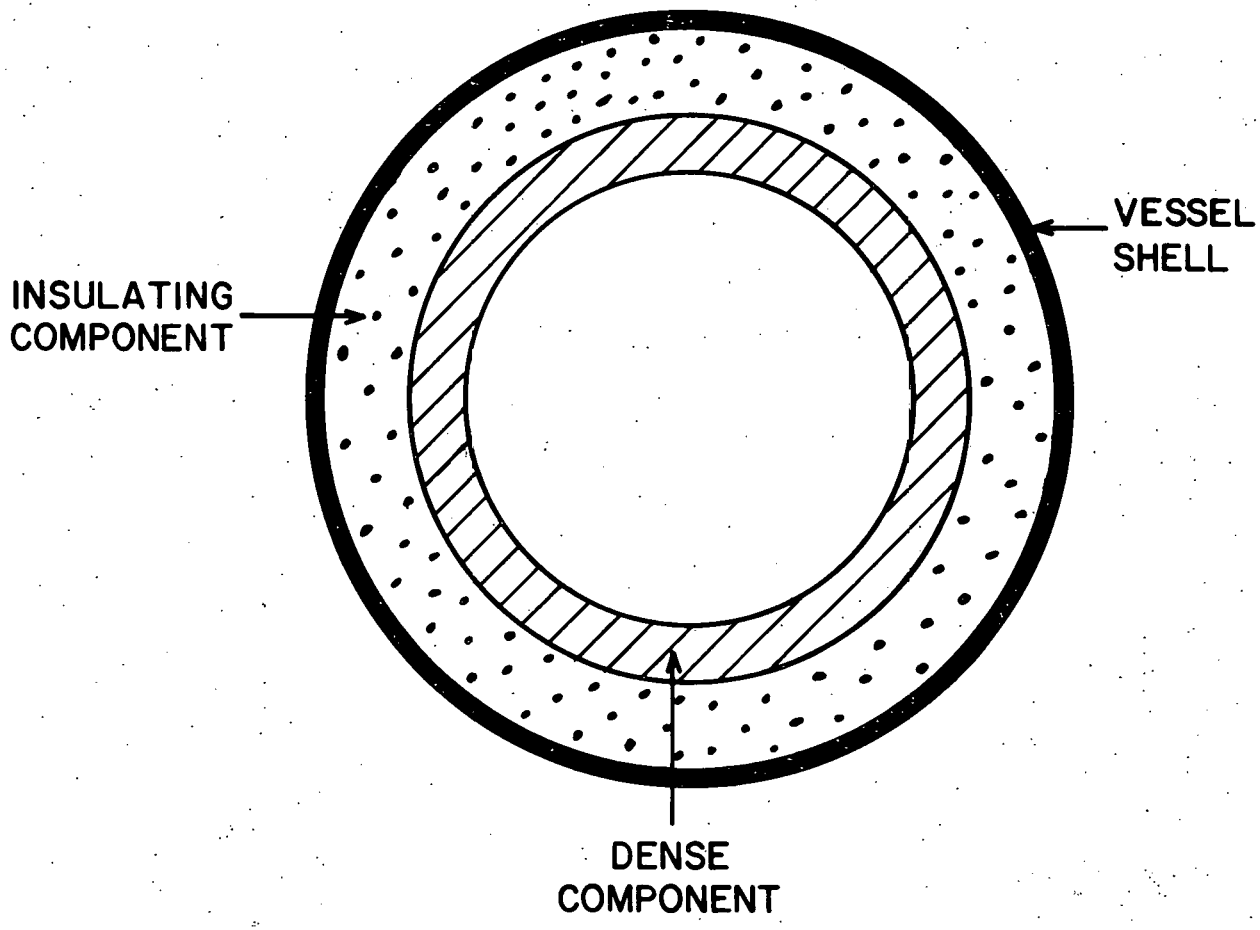

FIGURE 3. Refractory Lined Vessel Configuration Being Modeled

oriented, special purpose program was then developed which had generalized plane strain stress analysis capability for multicomponent cylindrical refractory lined vessels and had uncoupled thermal and stress analysis models in it. This meant that the transient temperature distribution was obtained independently of the stress analyses.

This model which became REFSAM included the effects of shrinkage, creep and temperature-dependent material properties. The shrinkage and creep models were developed from experimental data collected on the refractory concretes of interest. The details of the experimental techniques and data generated on shrinkage and creep to develop these models are summarized in other sections of this report and in the user's manual.

The overall program flow of REFSAM is shown in Figure 4 and indicates the material type properties required over the range 0 to 2000°F. These property data are:

Thermal Properties	Mechanical Properties	Time-Dependent Properties
Thermal conductivity	Tensile strength	Creep data
Specific heat	Compressive strength	Shrinkage data
Convective film coefficients	Biaxial compressive strength	
	Proportional limit in tension and compression	
	Modulus of elasticity	
	Poisson's ratio	
	Thermal expansion coefficient	

The thermal properties are used in the heat transfer analysis which at each stage of the analysis, predicts the temperature distribution through the refractory. The mechanical properties are used in the constitutive law which generalizes the results of uniaxial tests to multiaxial stress states and accounts for changes in the stress-strain response due to local cracking or crushing. The creep law consists of an analytical expression for creep strain, and also includes the transition from uniaxial to multiaxial creep predictions. Finally, the results of the thermal analysis are used along with the creep and constitutive laws to perform a finite element stress analysis.

The geometric idealization is shown in Figure 5. The refractory is divided into a number of finite elements. Each element consists of three nodes and has its own temperature-dependent material properties. The unknowns at each node are the radial and axial displacements and the nodal temperature. The main assumptions in the analysis are axial symmetry and generalized plane strain, which indicate that only radial variations of stress and strain are considered. The axial force or corresponding axial strain which are constant over the length are prescribed as a function of time as input data.

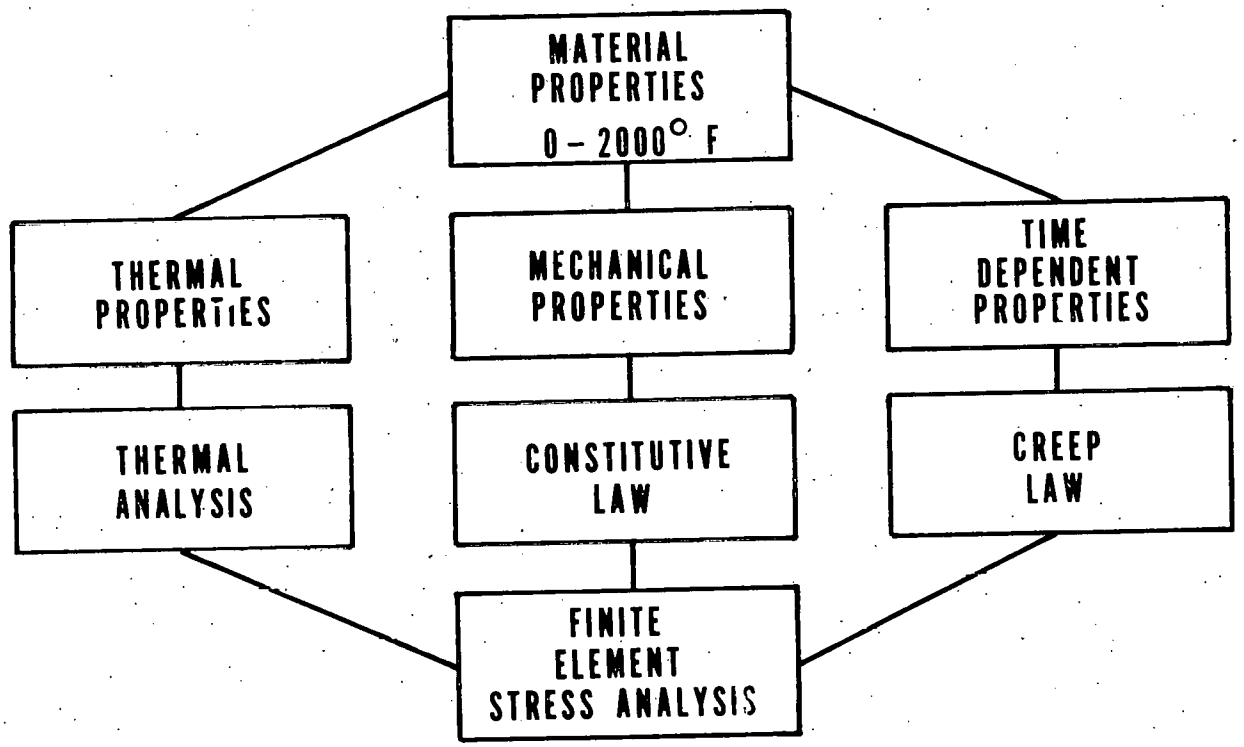

FIGURE 4. REFSAM Organization Diagram

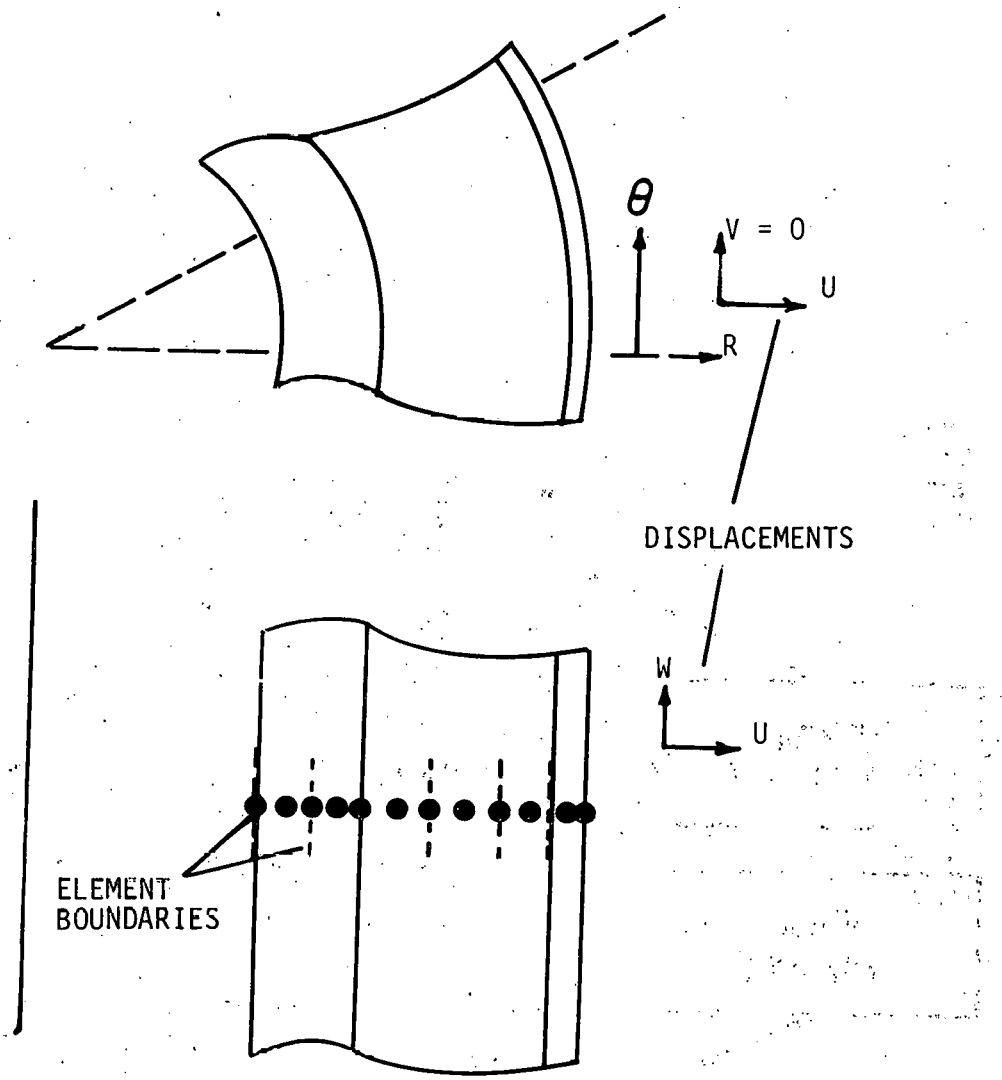

ASSUMPTIONS:

- AXIAL SYMMETRY
- GENERALIZED PLANE STRAIN

NODAL UNKNOWNS: U, W, TEMPERATURE

FIGURE 5. Geometric Idealization of Refractory

When this model was used to predict lining and shell strains and compared to the experimental results of the first two lining tests, it was found that the experimental strains were higher than those predicted. The main explanation proposed for this difference was the possibility that the model assumption of generalized plane strain (G.P.S.) was not very rigorous for the present vessel configuration. To investigate this aspect of the analysis, an elastic steady state analysis was carried out using an in-house axisymmetric finite element program FESAP. The refractory consisted of a two component liner and was subjected to a radial temperature profile similar to that after the hold at 1000°F in the Lining #2 experiment. The effect of interest was primarily a geometric effect and was not expected to be dependent on the particular loading or on material nonlinearities. Hence, the use of an elastic analysis was considered to be sufficient. The properties chosen for the modulus of elasticity and thermal expansion coefficient were average values over the temperature range and the expansion coefficient was reduced to simulate the effect of shrinkage.

It was learned from this investigation that end effects did exist at the top and bottom of the test vessel used in this contract. Furthermore, it was realized that the end effects were not adequately modeled by generalized plane strain predictions in the REFSAM. This model did appear to be adequate for predicting strains and stresses in the refractory lining and possibly the shell for larger vessels (>10 ft. high) away from the ends of the vessel.

The conclusions drawn from this investigation were:

1) An axisymmetric analysis of refractory lined vessels considering end effects is desirable to predict peak shell stresses.

2) Membrane shell stresses due to the thermal expansion of the refractory lining can be substantial.

3) When stress analyses of pressure vessels are performed, these membrane shell stresses and end effect shell stresses should be factored into the analysis, and

4) Strain measurements should be taken at the center of the refractory lined test vessel to reduce erroneous results due to end effects.

Pore Pressure/Mass Transfer Effects

During the initial lining tests experiments, it was found that the temperatures of the insulating component near the shell differed significantly from the temperatures predicted with the REFSAM. The lining was found to be hotter than predicted, rose to a temperature of 212°F very quickly during the initial temperature ramp, and maintained that temperature for an extended period (until the water had been driven away). The lining temperature then rose quickly. This effect of moisture migration in portland cement based concrete was shown by England [4] to be due to the gradient in temperature and vapor pressure. Bazant and Thougulhu [5] expanded on this concept and developed both 1 and 2D models to predict its effect on shrinkage, permeability, pore pressure and explosive spalling in heated concretes.

Both these models were acquired from Dr. Bazant under a subcontract and the ID pore pressure program was modified and incorporated into the B&W CDC computer system. Some of the modifications included a new equation solver, a change of units for data input and a grid generator to minimize data input. This program was to be used to select an appropriate permeability value for the refractory concrete to best match the weight loss data generated from special tests. Since multiple computer runs were required, the one dimensional program was the most efficient program for that purpose.

An initial test case was run to verify the operation of the program. The program executed; however, the computed temperatures and pressures were erratic, particularly near the heated surface. Subsequent runs with a more refined grid indicated that the program was very sensitive to grid refinement near the surface and would require numerous elements through the thickness for accurate prediction of pore pressures. The difficulty was thought to be due to the low order interpolation used for pressure and temperature in the program. It appeared that it would be desirable to replace the simple triangular elements used in the program with a higher order element such as the Isoparametric Quadrilateral. This would be compatible with the stress analysis program which used the higher order interpolation scheme, since no interpolation would be required to obtain nodal point temperatures and pressures used in the stress analysis.

As an indication of the type of results that are predicted by the one dimensional pore pressure model, some typical output is included in Table 3. The analysis is for a 3 inch O.D. cylindrical specimen which is sealed at the ends and heated from the outer surface at 100°F/hr. The coordinate X(I) is the proportion of the distance from the center to the outside surface. A time step of 15 minutes was used in this analysis and the results shown are at a particular time (T = 3 hours). Note that the program provides the spatial variation of pore pressure, temperature, and humidity, H. The humidity value indicates the rate of drying and will be used to estimate shrinkage. Although the accuracy of the absolute values shown in Table 3 were questionable, it is interesting to note the sharp gradient in moisture content near the heated surface. If these results are qualitatively correct, shrinkage stresses very near the surface are likely to be important considerations.

However, since problems still existed in the pore pressure program, and the completion of the basic model was the primary objective, no further effort was expended on it.

Parameter Study

The parameter study was to be done with REFSAM and was to involve a systematic study of the following variables:

1. Geometrical variables - lining thicknesses
   - shell thicknesses
   - vessel diameter
   - expansion allowances
   - anchor configurations.

TABLE 3. Typical Output of One Dimensional Pore Pressure Program*

	X(I)	Pore Pressure(psi)	Temperature(F°)	Relative Humidity
1	0.000	62.9178	299.99	0.93901
2	0.010	62.9172	299.99	0.93900
3	0.020	62.9161	299.99	0.93898
4	0.080	62.9159	299.99	0.93898
5	0.140	62.9147	299.99	0.93896
6	0.200	62.9128	299.99	0.93893
7	0.260	62.9101	299.99	0.93888
8	0.320	62.9067	299.99	0.93883
9	0.380	62.9012	299.99	0.93874
10	0.440	62.8938	299.99	0.93863
11	0.500	62.8864	299.99	0.93851
12	0.560	62.8779	300.00	0.93838
13	0.620	62.8605	300.00	0.93811
14	0.680	62.7299	300.00	0.93615
15	0.740	61.8254	300.00	0.92265
16	0.800	61.3564	300.00	0.91564
17	0.860	51.3603	300.00	0.76646
18	0.920	31.3075	300.00	0.46720
19	0.980	7.0078	300.00	0.10458
20	0.990	5.0603	300.00	0.07551
21	1.000	0.0043	300.00	0.00006

*

Time	3.00 Hours
Time Increment	15.00 Minutes
No. of Iterations	2
No. of Steps	21

2. Material variables
   - creep characteristics
   - elastic moduli
   - shrinkage and expansion properties
   - porosity and permeability.

3. Applied loads
   - heating and cooling rates
   - effects of holds at temperature
   - internal pressure
   - long term or steady state response.

In order to limit the number of computer runs, attention was to be focused on four particular material configurations as listed below:

Configuration	Dense	Insulator
1	90 percent alumina	Litecast 75-28
2	Phosphate bonded	Litecast 75-28
3	50 percent alumina	Litecast 75-28
4	50 percent alumina w/4% SS Fibers	Litecast 75-28

The material properties, creep, and expansion characteristics determined previously in this program were to be used.

The remaining variables were to be subjected to a wide range of values. Some typical ranges to be investigated are listed below:

Thickness of dense component (2 to 6 inches)
Total lining thickness (9 to 15 inches)
Shell thickness (1/2 to 4 inches)
Heating rates (50 to 500°F per hour)
Maximum temperature (1000 to 2000°F)
Internal pressures (0 to 1000 psi)

For each particular analysis, some of the key criteria to be investigated were:

Maximum tensile stress (in each component)
Maximum compressive stress (in each component)
Maximum shell stress
Time, location, and extent of predicted cracking if strength properties are exceeded

In addition, several key comparisons to be made were:

Transient versus steady state results (assuming that long term creep data were available)
Constrained (anchored) versus unconstrained linings
Single versus dual component linings

Analyses involving hypothetical material property variations were also of interest to determine which improvements in material properties are most desirable.

Finally, some special configurations were to be analyzed, such as multiple linings (three or more) or possibly special purpose cement compounds which harden at higher temperatures after some of the shrinkage has occurred.

In order to perform this study quickly and efficiently, REFSAM was simplified and placed on a VAX 11/780 computer. The rationale behind this activity was that analyses of gross effects could be done quickly and optimization of the lining design could be developed rapidly. This new program used average properties over the temperature range of interest instead of temperature dependent properties, and eliminated the complicated cracking and crushing models. It also operated with the minimum of temperature input or experimental data. This simplified model was designated RESGAP.

Capabilities of Models

Table 4 summarizes the capabilities of REFSAM and the RESGAP stress analysis model. Analyses can be performed with all or parts of these models. Flat wall configurations can be run as special cases with either of these models.

The operation of the RESGAP model can be learned in about one half day whereas the operation of REFSAM will take about two days. A relatively simple computer such as the IBM 5100 series or the PDP 11 series can be used for the RESGAP model whereas more sophisticated computers are needed for REFSAM. These would include the PDP 11/70, VAX 11/780, IBM 370 or CDC 7600 systems.

TABLE 4. Mathematical Model Capabilities

Capability	RESGAP*	REFSAM
Heat Transfer	X	X
Mechanical Loads	X	X
Pressure	X	X
Temperature Dependent Properties	*	X
Shrinkage	X	X
Creep	X	X
Cracking	-	X
Crushing	-	X
Gaps	X	-
Non-Linear Stress-Strain	-	X

*Uses average material properties over temperature range of interest

2.3. Material Property Determinations

2.3.1. Materials Tested

A total of eleven generic or commercial monolithic refractory materials were tested. They included dense and insulating refractory concretes and phosphate bonded ramming mixes. Table 5 lists these eleven materials and Tables 6 and 7 show mix formulations of the generic materials. KAOLITE*2300 LI was substituted for the KAOLITE 2500 HS commercial product after field results on pilot plant gasifiers indicated lower service temperature insulating components would be adequate for non-slagging coal gasifiers. KAOCRETE*XD50 (Mix 36C) material was added to the list of materials to test after two years into the program. This material is a high density, high strength, low cement content refractory concrete that exhibits low shrinkage and good strength. A four percent 310 stainless steel fiber addition to Mix 36C was also tested during this work.

The metal fibers (RIBTEC**) were purchased from Ribbon Technology Incorporated and were one inch long. These fibers were relatively easy to incorporate into Mix 36C at the same water levels used without the fibers.

2.3.2. Sample Preparation

Thirty to fifty 1"x1"x6" bars and two to five 2-1/2"x4-1/2"x9" brick of each refractory concrete material were made from forty to one hundred pound batches. These batches were made in either a T-200 model Hobert mixer or a two hundred pound capacity Muller mortar mixer. The optimum water level used was based on the level which gave the best ball-in-hand consistency. Once this was established, batches of each material were made with water amounts above, below, and at this level so the effect of water content on physical and mechanical properties could be determined.

After the bars and brick were removed from the molds, the majority of them were dried for eighteen to twenty four hours at 250°F. The remaining samples were stored in a water filled desiccator for testing in the as-cured state.

A similar number of 1"x2"x6" bars and 2-1/2"x4-1/2"x9" brick of the phosphate bonded ramming mixes were made from fifty to sixty pound batches. The generic batches were made in a Lancaster Muller mixer and had workabilities in the 25-30 range. The 90 RAM HS*** had a similar workability.

The bars and brick were made by ramming the generic and commercial phosphate bonded ramming mixes into the bar and brick molds with a pneumatic ramming hammer. In cases where laminations were found in the samples, the ramming mixes were air dried overnight to make them less plastic. This usually prevented laminations from occurring during subsequent ramming.

Once the bars were stripped from the mold, they were heated at a 50°F rate to 450-500°F and held for twenty four hours and then cooled slowly.

---

* KAOLITE and KAOCRETE are registered trade names of the Babcock & Wilcox Co.
** Registered trade name.
*** Registered trade name of Combustion Engineering Refractories

TABLE 5. Refractory Materials Tested

Generic Materials

Type	Bond
90+% Al_2O_3 (Castable)	CA-25
90+% Al_2O_3 (Castable)	SECAR 250
50% Al_2O_3 (Castable)	CA-25
90+% Al_2O_3 (Ramming Mix)	Phosphate
45% Al_2O_3 (Ramming Mix)	Phosphate

Commercial Materials

Type	Brand	Supplier
Lightweight 55% Al_2O_3 (Castable)	LITECAST*	General Refractories
Lightweight 42% Al_2O_3 (Castable)	KAOLITE 2300 LI	Babcock & Wilcox
Lightweight 42% Al_2O_3 (Castable)	KAOLITE 2500 HS	Babcock & Wilcox
90% Al_2O_3 Phosphate Bond (Ramming)	90 RAM HS	C. E. Refractories
Dense 50% Al_2O_3 (Castable)	KAOCRETE XD50 (36C)	Babcock & Wilcox

* Registered trade name

TABLE 6. Ramming Mix Formulations, w/o

Materials	Ramming Mixes 90+% Al_2O_3	45% Al_2O_3
Tabular Alumina		
6+10 Mesh	30	--
10+20 Mesh	20	--
-20 Mesh	15	--
-48 Mesh	17	--
Calcined Alumina A-2, -325 Mesh	15	15
Calcined Kaolin		
-6+10 Mesh	--	30
10+20 Mesh	--	20
-20 Mesh	--	15
Ball Mill Fines (-100 Mesh)	--	17
Bentonite (Wyoming)	3	3
Hydrated Alumina	1	1
Phosphoric Acid (85% Strength)	6	6

TABLE 7. Mix Formulations and Characteristics of Dense Generic Castables

Materials	Mix Formulations, w/o			
	50% Al_2O_3		90+% Al_2O_3	
	Standard	Modified	Standard	Modified
Tabular Al_2O_3				
6+10 Mesh	--	--	25	--
-10+20 Mesh	--	--	20	--
-20 Mesh	--	--	20	--
-6 Mesh + Fines	--	--	--	70
Calcined Kaolin				
-6+10 Mesh	25	27.5	--	--
-10+20 Mesh	20	22.5	--	--
-20 Mesh	15	20	--	--
Ball Milled Fines (50% < 325 Mesh)	15	5	--	--
A-2 Calcined Al_2O_3 -325 Mesh	--	--	10	5
CA-25 Cement Casting Grade	25	25	25	25
Water Added	11	10	9.3	8.5
Mixing Character (12 Cu. Ft. Muller Mixer)	Fair	Good	Fair	Good
Ball-In-Hand	Good	Good	Good	Good
Casting Characteristics	Stiff, Poor Flow	Good Flow	Stiff, Poor Flow	Good Flow
Set Time, Minutes	10	30+	10	25

2.3.3. Mix Modifications

After performing preliminary experiments with the generic 50 and 90+% Al_2O_3 dense castable formulations proposed by DOE, it became apparent that they were difficult to mix and place without adding extra water. This was expected to cause problems with the twelve cubic foot mortar/concrete mixer planned for use in the lining test work. As a result, some experiments were performed to coarsen both mixes by reducing the minus 325 mesh fractions by from five to ten percent and increasing the intermediate and coarse fractions by an equal amount. The modifications made are summarized in Table 7. Since there was a definite improvement in the mixing, casting and working time characteristics of the original generic mixes, the modified mixes were used to prepare the materials needed for the lining tests.

2.3.4. Properties Determined

The following physical properties were determined for evaluation of the quality and uniformity of the refractory materials tested:

Bulk Density
Apparent Porosity
Mean Pore Size
Microstructure
Loss on Ignition (LOI)

Standard ASTM and Babcock & Wilcox test procedures were used to determine these properties. All the properties were determined at room temperature on as-cured, dried and fired samples.

To perform thermal and stress analyses on the refractories and refractory lined vessels, the following thermal and mechanical properties were required:

Tensile Strength
Compressive Strength
Fracture Strain: (Strain at Failure)
Modulus of Elasticity
Poisson's Ratio
Thermal Expansion Coefficient
Linear and Volume Shrinkage
Creep
Thermal Conductivity

Since the analyses were to be run on linings heated in the room temperature to 2000°F range, the properties required were determined in this same range. In addition, since the objective of the work was to reduce or eliminate degradation on the initial dry-out and heat-up of the monolithic refractory linings, the majority of the testing was done on as-cured and/or 250°F dried samples. Some testing was done on prefired refractory samples. High temperature, intermediate pressure (150 psi) steam exposed samples were tested at room temperature so comparisons could be made with samples removed from the tested linings.

2.3.5. Physical, Thermal and Mechanical Properties Test Procedures

Physical Properties

This was determined on one third of the as-cured samples and all of the dried and fired samples. A minimum of five samples was normally used.

Apparent Porosity

This was determined on a least three samples of each material using either the ASTM boiled porosity procedure (C-20-20) or the mercury porosimetry technique which employed an Aminco-Winslow porosimeter (5-7107). Samples were usually prepared from modulus of rupture tested specimens.

Mean Pore Size

This was determined with the Aminco-Winslow Porosimeter (5-7107) using the work sheets supplied by Aminco. These sheets are identified Cat. No. 5-7133, 5-7134 and 5-7135. At least three samples were tested to determine an average "effective" mean pore size for pores in the 40 to 120 μm range. The "effective" mean pore size was determined from the pore size distribution curve for each sample at fifty (50) percent of total mercury volume penetration.

Loss On Ignition

This was done on samples that were either dried for twenty four hours or fired for five hours. The samples were usually either full size bars or half bars and were tested at temperatures of 250°F to 1832°F.

Mechanical Properties

Tensile Strength (Modulus of Rupture)

The ASTM Hot Modulus of Rupture test procedure [C-583-67 (1972)] with 1"x1"x6" or 1"x2"x6" bars and a three point bending arrangement was used for this testing. A ten thousand pound capacity Instron tester with a 3000°F furnace and ceramic rams and pedestal were the equipment used for this work. A photograph of this unit is shown in Figure 6. The samples were loaded at a rate of .02 in/minute to failure. All the samples of one or more materials were loaded in the furnace and then heated to various test temperatures at 250°F/hr, held for at least one half hour and then tested. At least five samples of each refractory were tested at each temperature. The dense monolithic refractories were tested at room temperature, 500, 1000, 1500, 1750 and 2000°F while the insulating refractories were tested at room temperature, 500, 1000, 1250 and 1500°F.

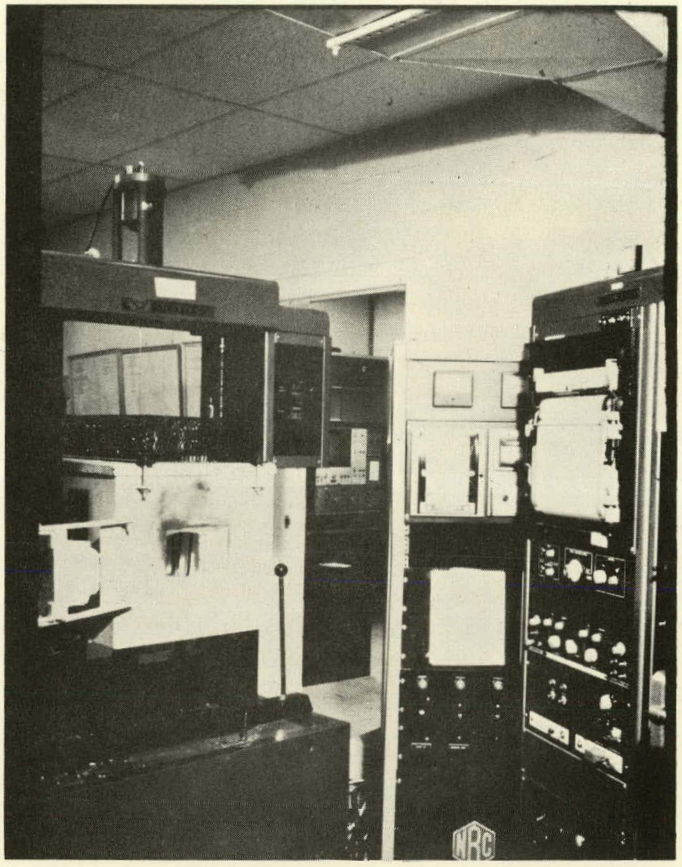

FIGURE 6. Instron Test Equipment With Furnace

During the tensile test work, a number of dense refractory concretes were tested with the modified modulus of rupture technique described by Ainsworth and Herron[6]. This was done to determine if the technique could be used to distinguish the differences in toughness between the refractory concretes of interest. The procedure used involved machining the test bars with a 0.25 inch deep by 0.030 inch wide slot at the midpoint of the bars and testing the bars in the modulus of rupture test arrangement. The bars were tested with the slot pointed down.

Since the compliance of the Instron tester and ceramic tooling was too large to accurately measure the strain of the samples during this modified modulus of rupture test, a linear variable differential transducer strain measuring system was incorporated onto the test equipment. It involved attaching an alumina sensing rod directly to the upper ceramic loading ram so it would make contact with the top surface of the pedestal on which the test specimens were placed. The movement of this sensing rod was monitored by an LVDT attached to a fixed point on the test equipment. This strain was used in the following equation to calculate fracture energy:

Fracture Energy Equation

$$\gamma = \frac{3l}{2bd^2} \times A$$

Where γ = Fracture Energy in in.-lb/in^2

l = Span of lower bearing edges in inches

b = Width of specimen in inches

d = Height of specimen in inches

A = Area under load/displacement curve

Compressive Strength

A uniaxial compressive test technique was developed for use with the Instron tester and furnace equipment. The technique involved five steps. They included:

1. Preparing 1/2"x1"x1" specimens of the dense monolithic refractories and one inch cubes of the insulating refractory concretes from 220°F dried bar samples. Enough samples of each refractory were prepared to test at least five at the same test temperatures used for the modulus of rupture testing. The cross section of the dense refractories had to be reduced below one inch square after it was found that they could not be tested to failure with the ten thousand pound capacity Instron tester. The top and bottom surfaces of each sample were trued up to assure parallelism,

2. Loading the samples in the Instron test furnace and heating them at a rate of 250°F/hr to the various test temperatures indicated,

3. Applying the load uniaxially at a .020 in/min strain rate,

4. Monitoring the strain with the same LVDT strain measuring system used for the fracture energy determinations, and

5. Using a computer program developed for an Hewlett-Packard 9830 computer to calculate, tabulate and plot the compressive strength and stress/strain results.

Modulus of Elasticity

Young's modulus was determined from the uniaxial compressive strength test data by calculating the slope of the stress/strain curves for each sample in the most linear part of the curve. The same computer program used to generate the stress/strain curve was used for this work.

Fracture Strain

This property was determined from the same above mentioned stress/strain curves. Corrections were made to the curves for compliance of the test equipment by extending the linear portion of the curve back to the X axis. The fracture strain of the specimen was determined by subtracting the X intercept value from the maximum strain value measured. This was the same method used by P. J. Pike, et al.[7].

Poisson's Ratio

This property was not determined. Instead the value of 0.20 was acquired from the literature on conventional concretes and used for both the dense and insulating monolithic refractories over the entire temperature range tested.

Thermal Expansion Coefficient

A fused silica dilatometer (A. F. Molkin & Co., Ltd.) was used to determine the thermal expansion curve and coefficient of each material. The tests were run from room temperature to 1875°F or higher at rates ranging from 100°F/hr to 400°F/hr on two inch long by half inch square specimens. The change in length of the specimen was monitored continually and was recorded manually in three to ten minute intervals, depending upon the amount of change occurring in the specimen. A correction was made for the expansion of the fused silica sensing rod used with the equipment.

To most accurately simulate the thermal expansion characteristics of the lining material, the samples of material to be tested were stored in a high humidity environment for two to twenty days prior to testing. Other samples of some of the materials were dried at 250°F overnight or stored for two to twenty days in air and tested for comparison with the samples stored in the high humidity environment.

The coefficient of thermal expansion was determined in two different temperature ranges. One was the room temperature to top test temperature which was 1500°F for the insulating materials and 1875°F for the dense materials. The second range was from 700-1875°F, i.e., the linear portion of the curve. In some cases, the materials were run on a second cycle to determine how the thermal expansion character changed and to relate it to the subsequent cycles of a lining. In this case the coefficient of thermal expansion was determined from room temperature to the top test temperature.

Linear and Volume Shrinkage

The linear and volume shrinkage was determined by two methods. One involved determining the change in length and volume of the thermal expansion specimens after the test. The second involved using ASTM procedure C269-70 on either bars, brick, or both of the materials of interest. The change in length or volume was divided by the original length or volume and multiplied by 100 to calculate the shrinkage.

Creep

A uniaxial creep test procedure was developed using a combination of techniques reported in the refractories and concrete literature [8,9,10] that were modified for this program.

Creep Test Furnace

The test facility used was a Pereney Model MRLT-3000-102 combination hot modulus of rupture/hot bond test furnace capable of temperatures to 2900°F. The unit had a 5000 lb. capacity pneumatic/hydraulic loading system on the hot modulus of rupture side of the furnace which was modified so that a flat ram could be used and a constant load applied on a sample for periods up to 48 hours or longer. This unit is shown in Figure 7.

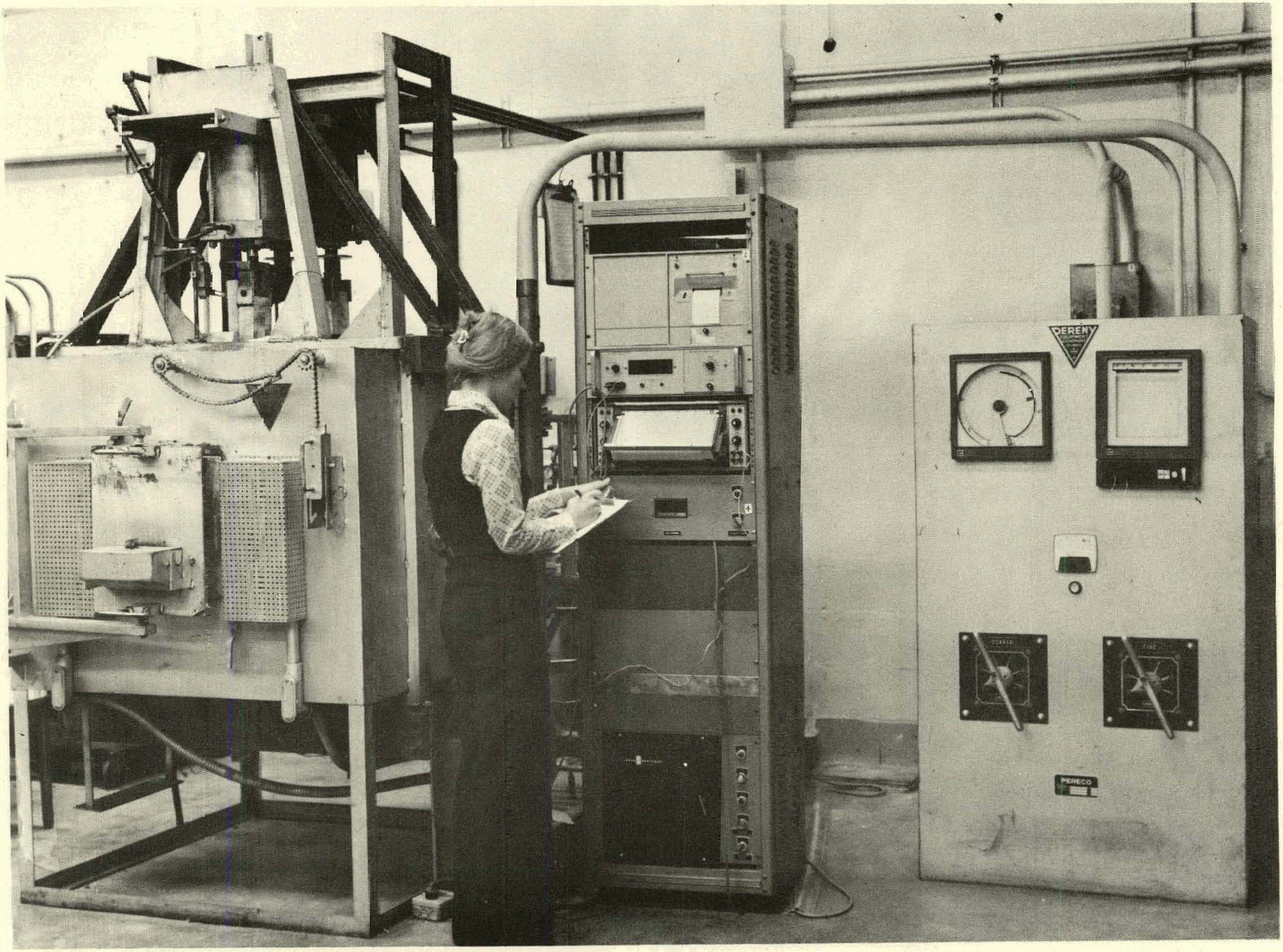

FIGURE 7. Pereny Furnace Used for Creep Testing

Sample Configuration

Six inch long samples were used for the creep work. Since preliminary stress analyses on the refractory linings indicated that very high (500 psi) stresses could be induced in the refractory components, each material was tested at three or more stress levels within the range 500 to 3300 psi to develop adequate creep data for the model. The samples were cut from 250°F dried brick. The cross section was maintained at 2"x1" for stress levels of 2000 psi and lower, but was reduced to 1"x1" for stress levels above 2000 psi.

Measuring Technique

The samples were instrumented with an LVDT arrangement as shown in Figure 8 to continuously monitor the strain occurring in the test specimen when it was loaded during a test. The two 99.9% Al_2O_3 purity sensing rods were instrumented so that strain was not sensed by the LVDT as a sample was heated to a specific test temperature prior to loading. This arrangement produced flat regions in the strain versus the curve generated during a creep test.

Test Procedure

Since the total time involved in the initial dry-out, heat-up, and cool-down of a monolithic refractory normally does not take more than one hundred hours, a test procedure was wanted that would measure the creep at periods of from ten to fifty hours and have the flexibility to be run for shorter or longer periods. A method[10] was found in the literature for determining long and short term creep with a short term test which appeared to be applicable to refractory concretes. It involved loading a sample uniaxially to 75%, or less, of its ultimate strength, monitoring the strain which occurred instantaneously and over a specific period of time, unloading the sample, and continuing to monitor the strain. Three to ten hour tests were found to be adequate to generate the data wanted. These data were then transformed into unit creep (strain/psi stress) versus log time plots and equations were written for the straight line curves which developed. The stress level was kept below 75% of the ultimate compressive strength to assure completion of the test. Stresses greater than this level generally caused stress rupture to occur which completely destroyed the sample and often damaged the strain monitoring system.

Figures 9 and 10 respectively, are representations of the loading scheme used and of the unit creep plots developed with this test procedure.

During the initial creep tests run, one sample was tested at one stress level and temperature. Figure 11 is an example of the typical type of results obtained. These tests were found to take a considerable amount of time and were expected to be expensive. As an alternate scheme, the procedure was modified so that one sample was tested at one stress level from room temperature to temperatures up to 2000°F in a stepwise manner as shown in Figure 12. The sample was loaded at room temperature for one hour and then unloaded before the furnace was heated. This was done to check the quality of the sample and to assure that it could take the stress level of interest. The sample was then heated to the first test temperature at 250°F/hr, held at temperature for one hour, loaded as quickly as possible to the stress wanted and held for three hours, unloaded as quickly as possible, heated to the next test temperature, and the cycle repeated. A ten hour

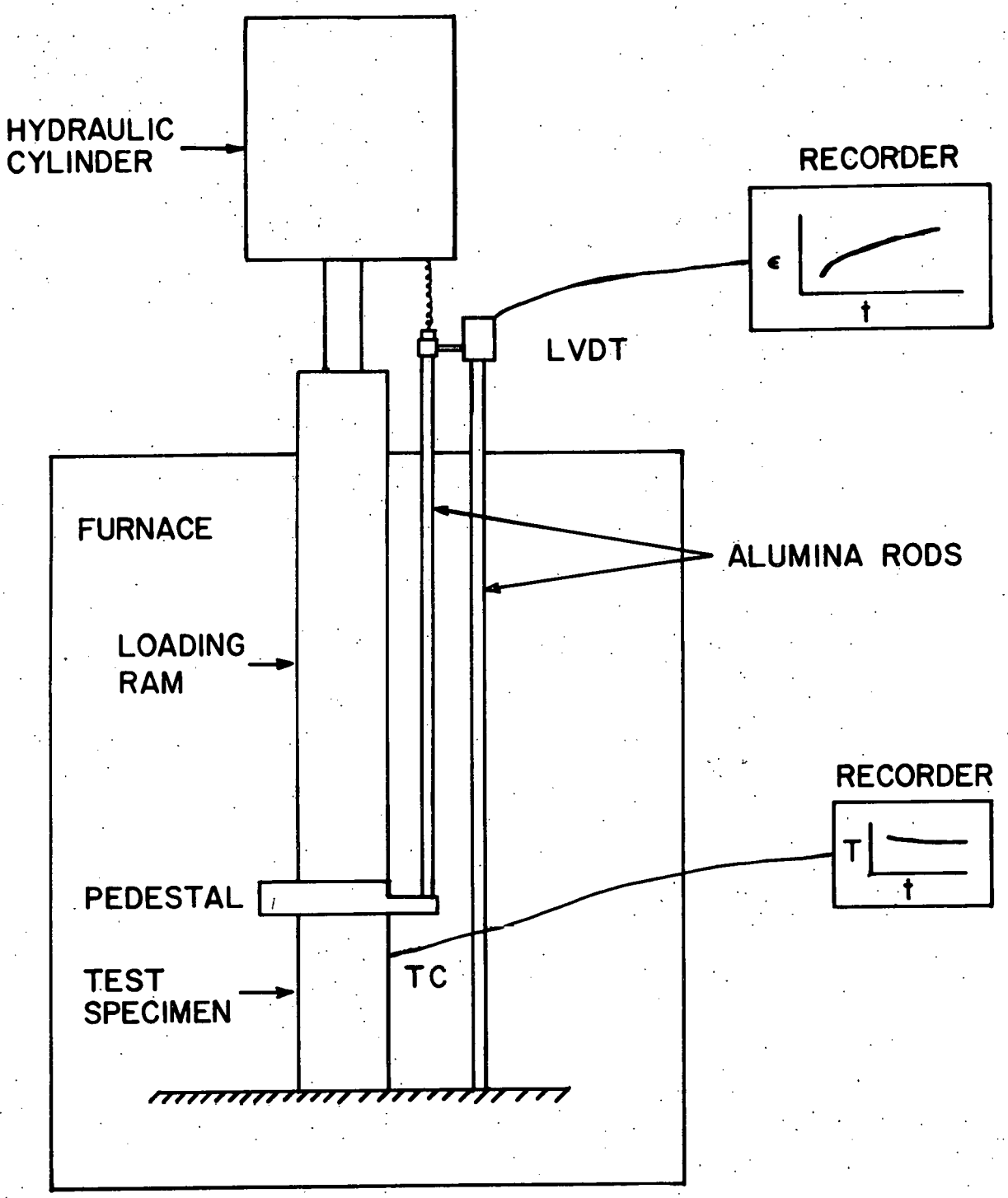

FIGURE 8. Schematic of Creep Test Set-Up

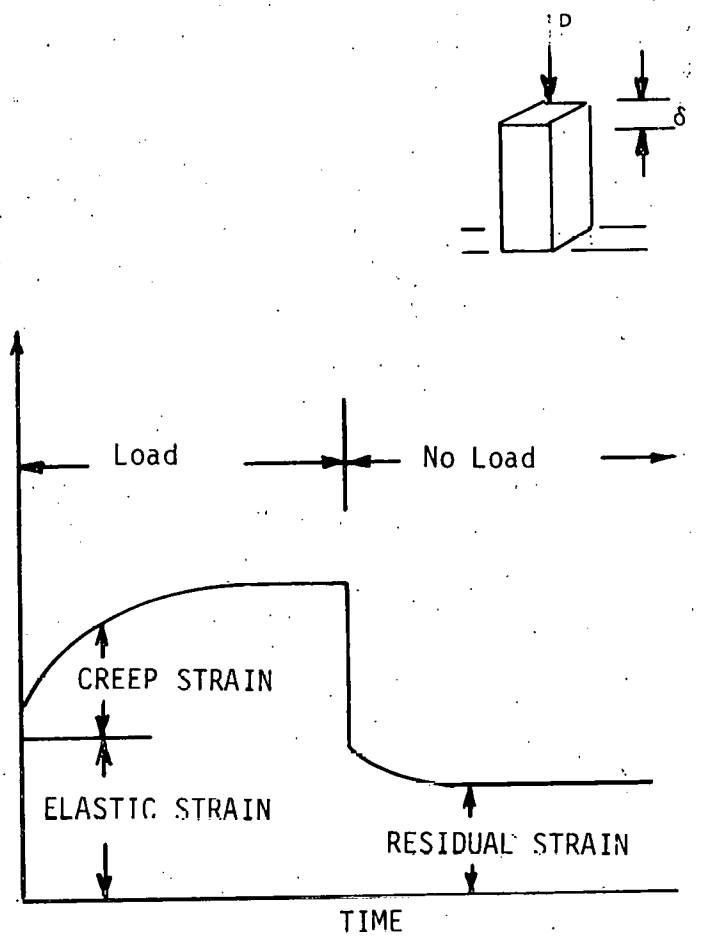

FIGURE 9. Loading Scheme for Determination of Unit Creep Plots

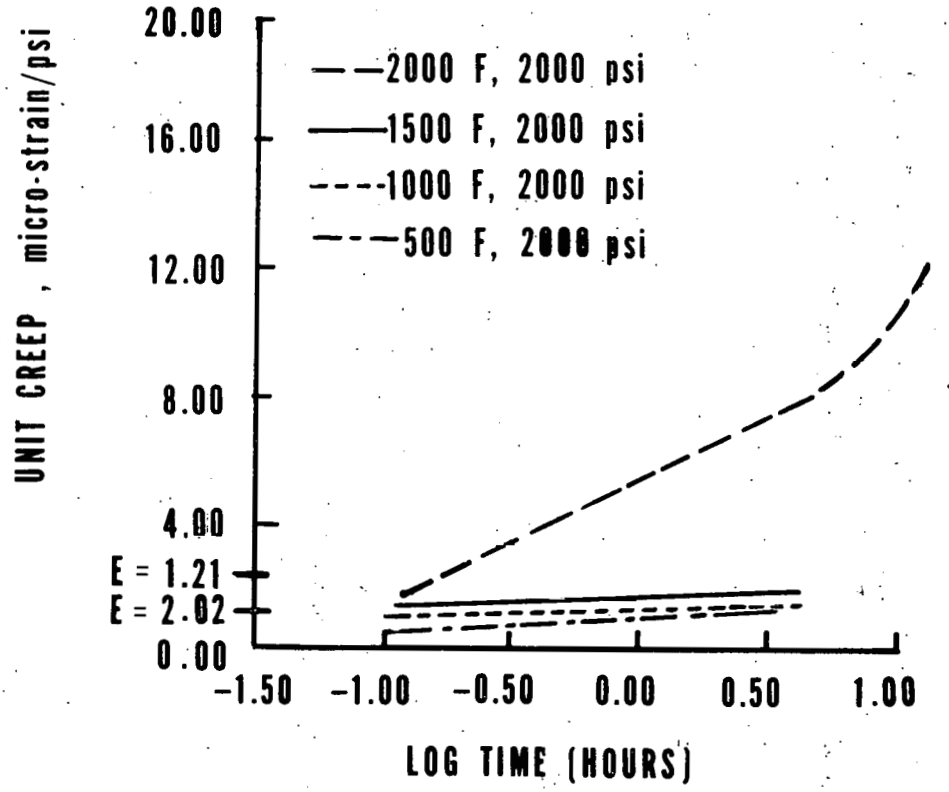

FIGURE 10. Unit Creep Plot

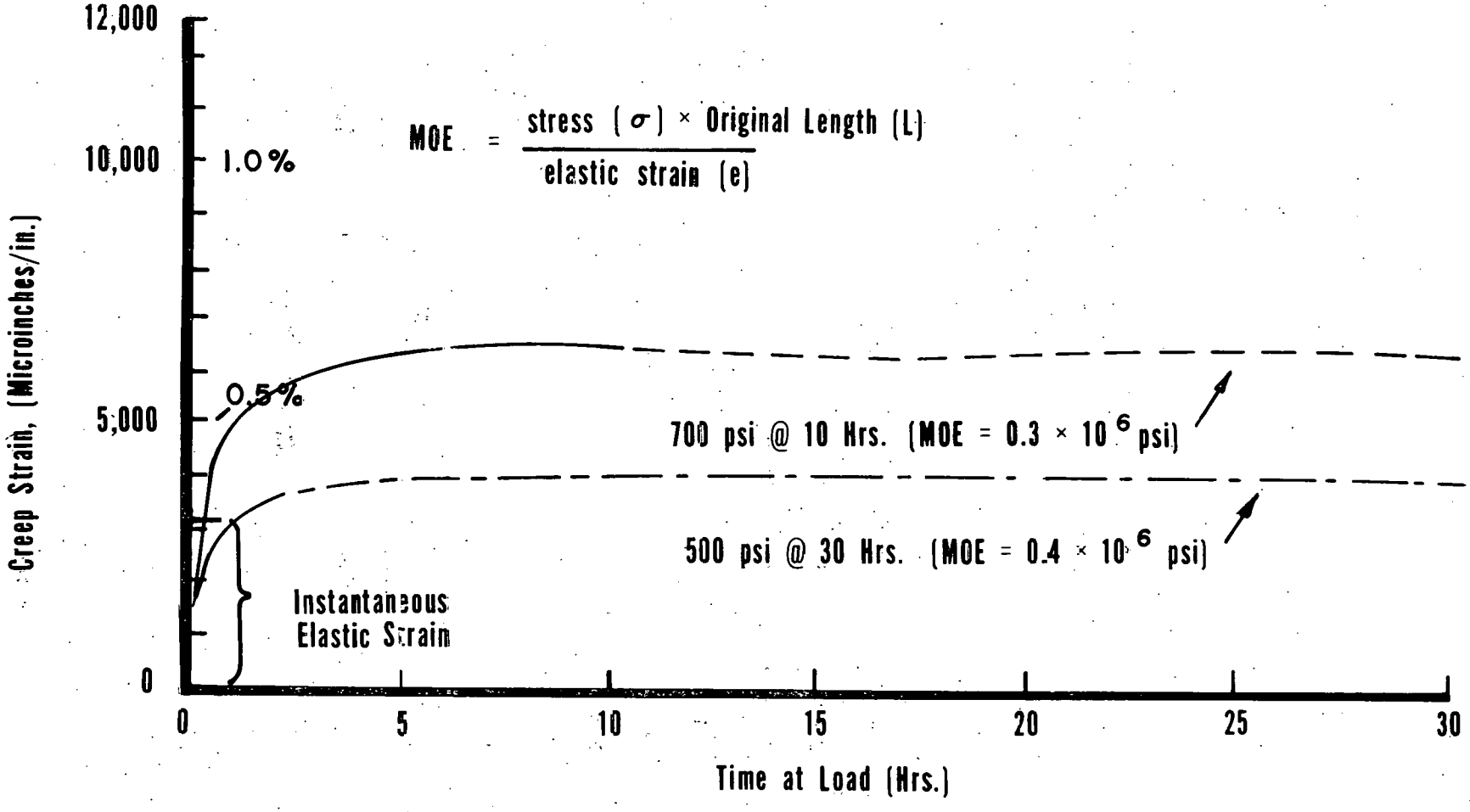

FIGURE 11. Results from Single Stress Level/Temperature Creep Test

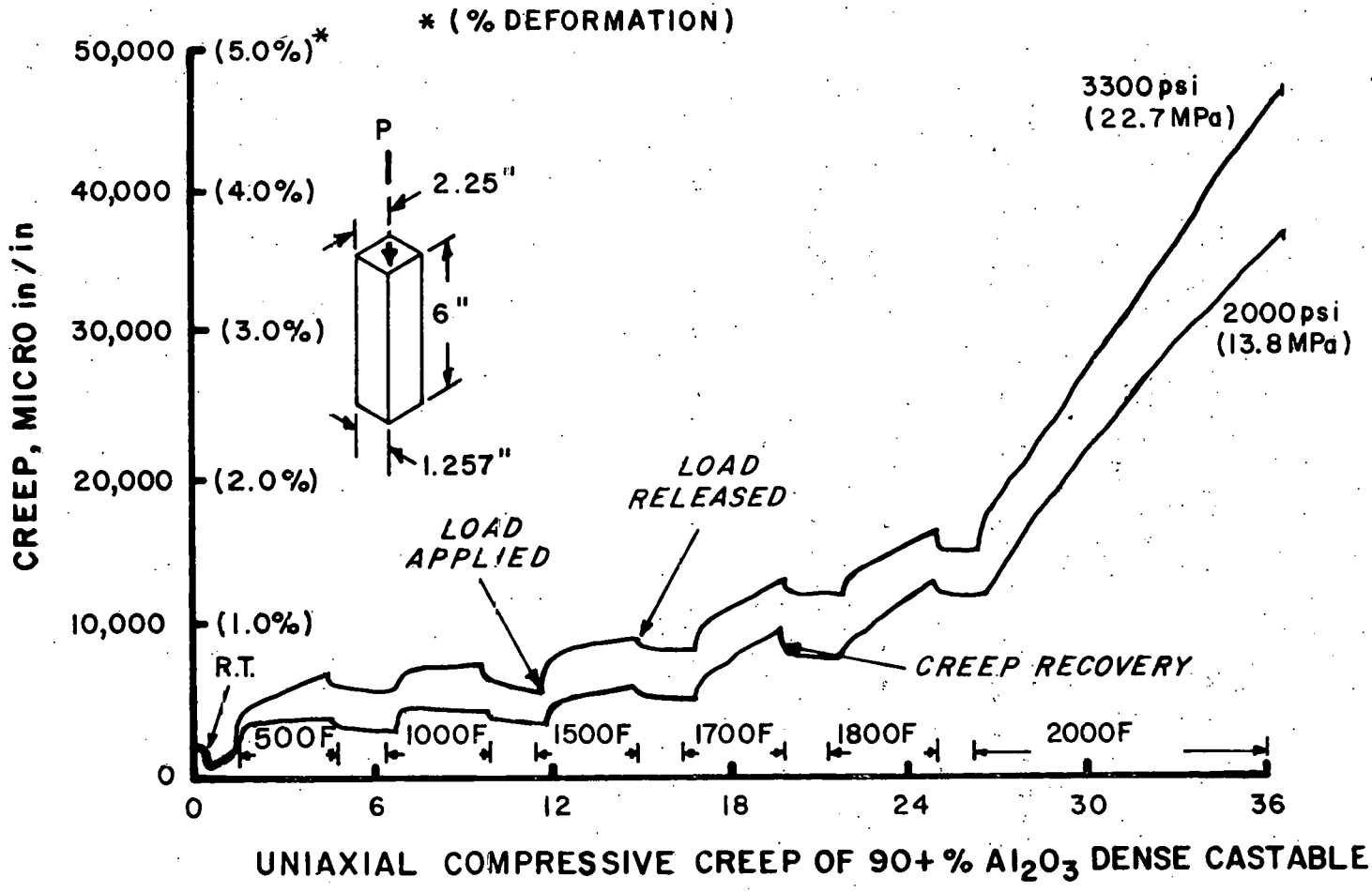

FIGURE 12. Prccedure for Single Stress Level/Increasing Temperature Creep Test

hold was used at the top test temperature. The following test temperatures were generally used for the dense and insulating refractories:

Temperature (°F)	Dense	Insulating
Room Temperature	X	X
500	X	X
1000	X	X
1250	-	X
1500	X	X
1800	X	-
2000	X	-

The strains were recorded after .05, 0.1, 0.2, 0.25, 0.5, 0.85, 1.0, 2.0, and 3.0 hours for the short hold; and then every hour from 3 to 10 hours for the longer holds. These data were then fed to a computer program, reduced to the unit creep curves wanted and equations written for the curves obtained.

If a sample creeped more than 5.0%, the test was stopped to prevent failure of the sample and damage to the strain monitoring system. All samples tested were measured after the test to determine the total percent deformation.

Hot Load Testing

The two hot load stations of the Pereny Furnace were used during the creep test to measure the hot load deformation of selected materials at either 100 and/or 200 psi. The specimens were loaded at room temperature, heated to the top test temperature, and cooled to room temperature. The change in length of the specimen was calculated as percent deformation.

This testing was done to develop some data on the relatively low stress creep resistance of the materials of interest.

2.4. Evaluation and Verification Tests

To aid in the evaluation of the refractory materials to be used in the lining tests, a series of heat-up tests was run on panels, hollow cylinders and other types of cast samples. In addition, these tests were used to develop empirical data to verify thermal analyses being done with REFSAM, and to collect data on the cracking tendency of monolithic refractories due to either shrinkage or transient thermal stresses.

Other small scale special tests were run to develop pore pressure related data or measuring techniques.

The procedures used during these tests are described below:

2.4.1. Panel Tests

Single and dual component panels of the designs and materials of interest were made and run on the numerous heating schedules. These panels were 12" thick x 15" x 18", weighed approximately 300 lbs. and were designed to fit into the door of a gas fired catenary kiln. Figure 13 is a schematic of the test panel configuration and Figure 14 is a photograph of a test panel installed in the catenary door.

As can be seen from these figures, the metal plate of the panel is the base of the panel mold used during casting and simulates the vessel shell during the test. Handles were installed on the plate to aid in the movement and handling of the panel. Metal anchors were welded to the base plate prior to casting of the panel as shown in Figure 15. Dual component panels were cast on two separate days and the single component panels were cast in one day. Both 4 and 12 cu. ft. mortar mixers and concrete pencil vibrators were used to mix and place the materials tested. After the panels were cast, they were sealed in plastic bags and stored in a temperature controlled laboratory for three days to one month or more. The panels were instrumented with Type K thermocouples (TC's) at various positions through the twelve inch panel thickness. This was done by drilling 1/8" holes through the metal plate to permit placement of the TC's to the desired position, or gluing the TC's to the metal plate and hot face with a high alumina sodium silicate bonded mortar. The temperature profile through the panel was continuously recorded with an Leeds & Northrup multipoint recorder.

Table 8 lists the materials, mixing and casting procedures, and designs of the ten panels made. It also lists the heat-up schedules used during the tests. Four panels were monitored with acoustic emission (AE) equipment to evaluate an AE technique being developed for the lining tests.

Most of the panels were run prior to the start of the lining tests.

2.4.2. Hollow Cylinder Tests

As a means of evaluating the relative thermal shock resistance and thermal stress damage of the initial materials to be tested, any new materials identified or developed during the program and new systems of interest, a special test was developed. This test involved heating (internally) multi-layered hollow cylinders of each material, or a combination of materials, at various heating rates

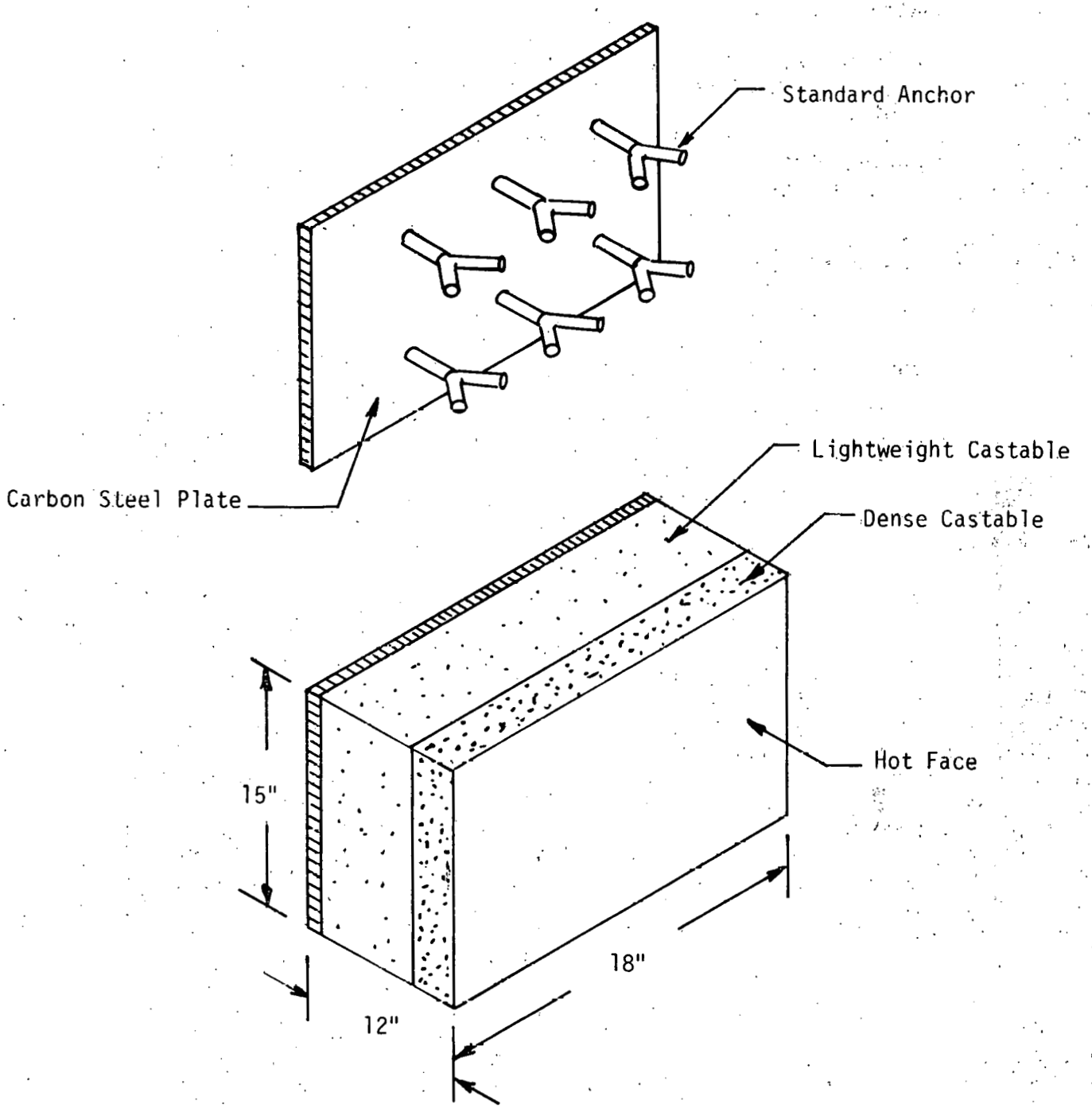

FIGURE 13. Schematic of Test Panel

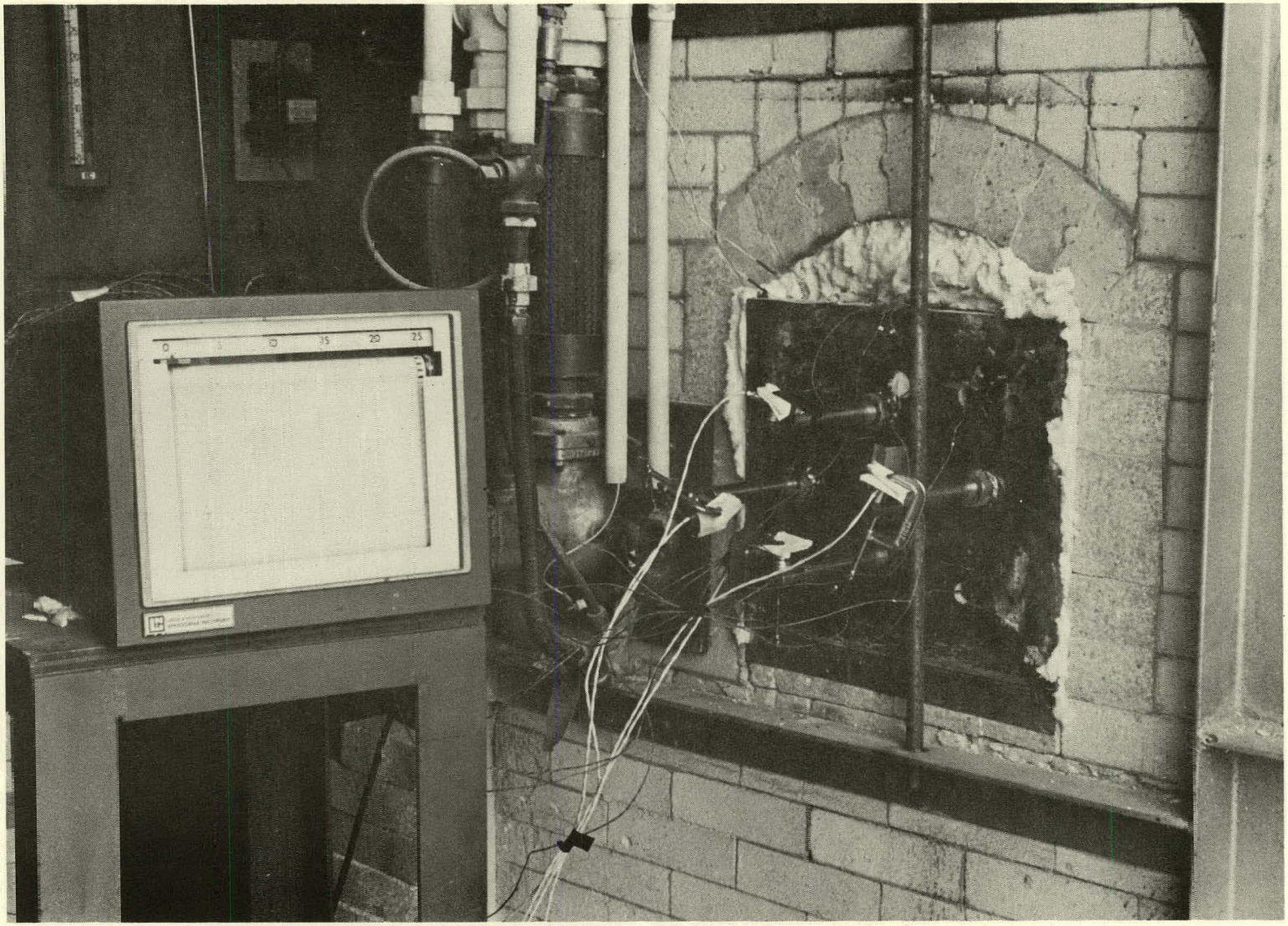

FIGURE 14. Test Panel Equipped With Temperature and Acoustic Emission Monitoring System

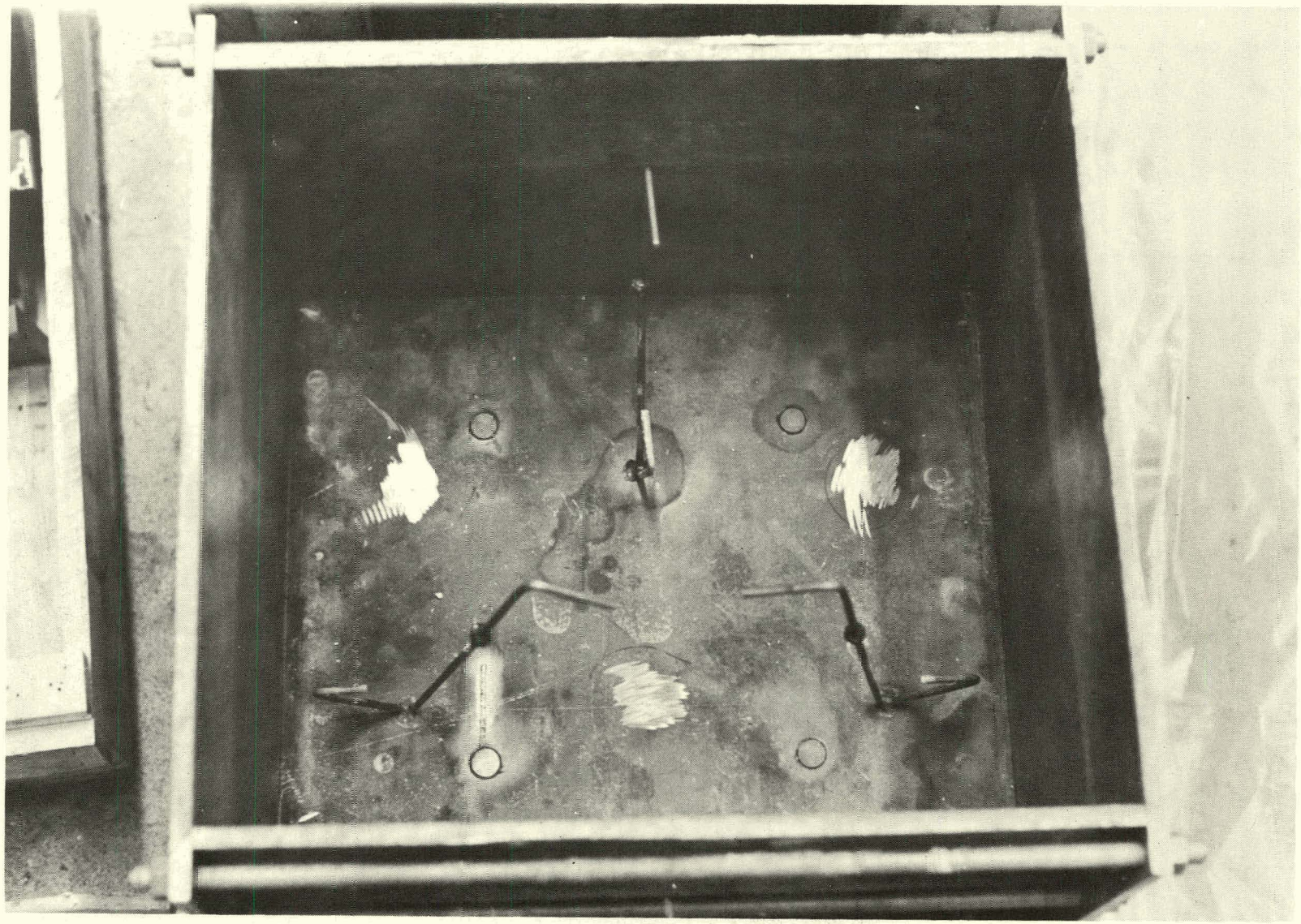

FIGURE 15. Panel Mold With Anchors Welded In-Place

TABLE 8. Panel Casting and Testing Summary

Panel #	Composition	Anchors	Comments on Mixing and Casting Procedure	Firing Schedule	Crack Pattern
(Date) #1 (11-23-76)	Litecast 75-28 7" 26% H_2O 90+% Al_2O_3 generic 5" 10.3% H_2O w/C.G. CA-25	None	Lightweight / Dense Mixer - 4 cu. ft. / 4 cu. ft. Batch size - 75 lb. / 175 H_2O/pour temp.- - / - / - / - Ball-in-hand - -- / sticky Vibration - table / concrete vib. Other - LC 75-28 covered w/plastic and cured 60 hrs. Dense troweled lightly and covered w/plastic overnight. Six day (@ 70°F) cure outside of mold. 4 cu. ft. mortar mixer stalled on both components. Some settling in LC 75-28 from table vibration.	(Date) 16 hrs. @ 400°, 100°/hr to 1000°, 3 hrs. @ 1000°, 100°/hr to 1800° T_{max}. Cool @ 100°/hr. Irregular (12-1-76)	Many small interconnected cracks on hot face. Propagated from 1 to 5 inches into dense component.
#2 (12-10-76)	Litecast 75-28 7" 26% H_2O 90+% Al_2O_3 generic 5" 10.3% H_2O	Standard Y uncoated 6" spacing	Mixer - 4 cu. ft. / 4 cu. ft. Batch size - 100 lbs. / 175 lbs. H_2O/pour temp.- - / - / - / - Ball-in-hand - good / wet, sticky Vibration - concrete vib. in & outside mold. Other - Motor hp. increased on mixer. OK for LC 75-28 but mixer stalled with dense. Concrete vibrator worked well against mold. 3 day cure in mold with plastic cover at ~ 70°F.	16 hrs. @ 400°, 100°/hr to 1000°, 3 hrs. @ 1000°, 100°/hr to 2000° T_{max}. Cool @ 100°/hr. Irregular (12-13-76)	Many small interconnected cracks on hot face. Propagated from 1 to 5 inches into dense component. Other cracks at interface and in insulator.
#3 (12-22-76)	Litecast 75-28 7" 26% H_2O 90+% Al_2O_3 generic 5" 9.3% H_2O	Standard Y wax coated 6" spacing	Mixer - 4 cu. ft. / 4 cu. ft. Batch size - 75 lbs. / 2-75 lbs. H_2O/pour temp.- - / - / - / - Bail-in-hand - good / wet to good Vibration - concrete vib. in and outside mold. Other - Dense cast in 2 parts. Mixer OK. Concrete vib. only good when placed against mold. Six day cure in mold with plastic cover @ 70°F.	18 hrs. @ 300°, 100°/hr to 1800°, 12 hrs. @ 1800° T_{max}. Cool @ 100°/hr.	Separation between panel and base plate. Almost no visible cracks in hot face. Few cracks in insulator perpendicular to base plate.

TABLE 8. Panel Casting and Testing Summary (Cont'd)

Panel #	Composition	Anchors	Comments on Mixing and Casting Procedure	Firing Schedule	Crack Pattern
(Date)			Lightweight / Dense	(Date)	
#4 (12-31-76)	Litecast 75-28 7" 20% H_2O 90+% Al_2O_3 generic 5" 9.3% H_2O	6-V type with straight legs 6" spacing uncoated 	Mixer - 4 cu. ft. / 4 cu. ft. Batch size - 100 lb. / 2-100 lb. H_2O/pour temp. - - / - / - Ball-in-hand - good / good Vibration - concrete vib. in & outside mold. Other - Dense surface troweled smooth to identify cracks. Cast surface covered w/wet blotter paper & plastic. Cured 4 days at 65°F.	16 hrs. @ 200°, 100°/hr to 700°, 260°/hr to 770° when explosively spalled. Case #1, T_{max} - 770°. Panel blown out of furnace door. Many small pieces from front 2 in. of dense. Firebrick baffle used to distribute heat. (1-5-77)	Explosively spalled at 770°F.
#5 (1-25-77)	Litecast 75-28 7½" 21% H_2O 90+% Al_2O_3 generic 4½" 9.3% H_2O	6-V type with leg ends bent inward 6" spacing uncoated 	Mixer - 4 cu. ft. / 4 cu. ft. Batch size - 100 lb. / 2-100 lb. H_2O/pour temp. - 84°/78° / 86°/79° Ball-in-hand - good / good Vibration - concrete vib. in & outside mold. Other - Warm H_2O caused fast set in both components. Surface wire brushed when cast. Wrapped in Kaowool to maintain hydration temp. Panel wt. - 284 lbs.	13 hrs @ 200°F, 480°/hr to 1000°F when explosively spalled. Controller malfunction. Hot face spalled into 4 large pieces w/ anchors imbedded and threads stripped. AE antenna welded to base plate over an anchor. AE monitored. (1-27-77)	Explosively spalled at 1000°F
#6 (1-31-77)	Litecast 75-28 7½" 21% H_2O 90+% Al_2O_3 generic 4½" 9.3% H_2O	3-Y type 1-V type set in insulator 8½"x8½"x12" spacing 	Mixer - 4 cu. ft. / 4 cu. ft. Batch size - 100 lb. / 2-100 lb. H_2O/pour temp. - /70° / /70° Ball-in-hand - good / good Vibration - concrete vib. in & outside mold. Other - Surface wire brushed when cast. Cool H_2O temp. gave better mixing & working time. Wrapped in plastic & Kaowool. Panel wt. = 284 lbs.	22 hrs. @ 170°, 26 hrs @ 450°, 100°/hr to 1000°, 14 hrs @ 1000°, 125°/hr to 2000°, 3 hrs @ 2000°F, cool @ 100°/hr. AE monitored w/1 antenna. 10% H_2O loss after firing. (2-1-77)	Random and interconnected network of shallow cracks on hot face with some extending from anchor/refractory interface.

TABLE 8. Panel Casting and Testing Summary (Cont'd)

Panel #	Composition	Anchors	Comments on Mixing and Casting Procedure	Firing Schedule	Crack Pattern
(Date) #7 (2-18-77)	Litecast 75-28 7½" 21% H_2O Modified 90+% Al_2O_3 generic 4½" 8.5% H_2O	3-Y type 1-V type set in insulator 8½"x8½"x12" spacing 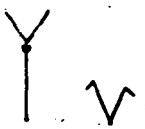	Lightweight / Dense Mixer - 4 cu. ft. / 12 cu. ft. Batch size - 100 lbs. / 600 lbs. H_2O/pour temp. - 110°/78° / /73° Ball-in-hand - poor, crumbly / excellent Vibration - concrete vib. in & outside mold. Other - Litecast mat'l. temp. = 58°. Hot H_2O resulted in 15 min. set time. Lightweight & dense wrapped in plastic & Kaowool. Excellent mixing action with large mixer.	(Date) 14 hrs. @ 110°, AE breakdown 22 hrs @ 170°, 26 hrs @ 450°, 100°/hr to 1000°, 3 hrs @ 1000°, 100°/hr to 2000; 4 hrs @ 2000°F, cool 100°/hr to 900, 50°/hr to 500°. AE monitored using 4 wave guides. (3-22-77)	Very few cracks on hot face. Those found are shallow and not interconnected.
#8 (2-24-77)	50% Al_2O_3 generic single component 12" 11% H_2O	3-V anchors with legs bent outwards 8½"x8½"x12" spacing 	Mixer - 12 cu. ft. Batch size - 600 lbs. H_2O/pour temp. - 83°/78° Ball-in-hand - excellent Vibration - concrete vib. in & outside mold. Other - Initially balled up w/10% H_2O. Final 11% H_2O after extra 7 min. mixing. Poor flow & set up in mixer. Sealed in plastic. Panel wt. - 324 lbs.	Stored for future testing	
#9 (3-2-77)	Modified 50% Al_2O_3 generic single component 12" 10% H_2O	3 anchors straight legs 7" long 8½"x8½"x12" spacing 	Mixer - 12 cu. ft. Batch size - 550 lbs. H_2O/pour temp. - 70°/70° Ball-in-hand - fair Vibration - concrete vib. in & outside mold. Other - Used 5% ball mill fines plus 0.1% boric acid as hydration retarder. Wrapped in plastic & Kaowool. Stored w/wet sponge. Panel wt. = 285 lbs.	16 hrs. @ 180°, 16 hrs @ 450° 100°/hr to 1000°, 3 hrs @ 1000°, 100°/hr to 2000°, 5 hr @ 2000°F, cool 300°/hr to 1600°, 100°/hr to 1000, 50°/hr to R.T. AE monitored using 4 wave guides. (3-29-77)	Single crack across hot face. Several cracks parallel to and approximately 5" from hot face.

TABLE 8. Panel Casting and Testing Summary (Cont'd)

Panel #	Composition	Anchors	Comments on Mixing and Casting Procedure	Firing Schedule	Crack Pattern
(Date) #10 (4-13-77)	Litecast 75-28 single component 7½", 12" 21% H_2O	Modified panel 2-V anchors from side 2-St. legs down 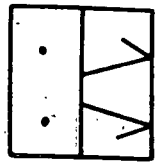	Lightweight Dense Mixer - 12 cu. ft. Batch size - 350 lbs. H_2O/pour temp. - 72°/88° Ball-in-hand - very good Vibration - concrete vib. in & outside mold. Other - Mat'l. temp. = 86°. Excellent mixing and working time. New material ordered for use in lining tests.	(Date) Stored for future testing.	

until they cracked. Small (7-1/5" dia. x 24" long) silicon carbide heating elements were arranged, as shown schematically in Figure 16, to heat the cylinders. The initial work was done with well insulated 6 inch high x 5 inch OD x 3 inch ID cylinders and instrumented with Type K TC's cemented to the ID and OD surface to monitor thermal history. This set-up is shown in Figure 17. This cylinder configuration was found to be very difficult to crack regardless of the material tested unless unrealistically high heating rates of 600 to 1000°F/hr were used. In addition, the tests were time consuming. As a result, the cylinder configuration was changed to 3 inch high x 6 inch OD and 2 inch ID. This change permitted the testing of two cylinders at one time and increased their tendency to crack at heating rates that more reasonably approximated safe heating rates for refractory lined vessels.

Further changes that were made in the original test scheme involved 1) preparing hollow cylinders with metal restraining rings around them to simulate the vessel shell/refractory interactions expected or observed in the lining tests, 2) water cooling the metal restraining rings and 3) experimenting with the use of compliant layers between the refractory and the restraining ring or with a thermal barrier coatings on the ID of the cylinder.

The cylinders were tested in the as-cast and cured state to simulate the condition of an as cast monolithic refractory lining. The cylinders were cast at the optimum water levels and stored in plastic bags at ambient conditions until tested. A James Electronic V-meter was used to non-destructively test the cylinders before and after each test.

The experimental materials evaluated with this test are summarized below:

ERDA 90 (Generic 90+% Al_2O_3) w/10 w/o Raw Kyanite added

ERDA 90 (Generic 90+% Al_2O_3) w/1/4" thick, HES* mortar layer on ID of restraining rings

LITECAST 75-28 w/ 4 w/o 1-3/8" 304 stainless steel fibers

LITECAST 75-28 w/ RX-14 High Emissivity Coating on ID

KAOLITE 2300 LI w/ 1 2/o 1" 310 stainless steel fibers

KAOLITE 2300 LI (Same as above with 3/8" thick HES* mortar layer on ID of restraining ring and 4 mil plastic sheet between HES and refractory)

Mix 36C w/ 10 w/o Raw Kyanite added

Mix 36C w/ 10 w/o Pyrophyllite

Mix 36C w/ RX-14 High Emissivity Coating on ID

Mix 36C w/ 1/4" thick HES mortar layer on ID of restraining ring

* HES is a registered trademark of Pennwalt Corp.

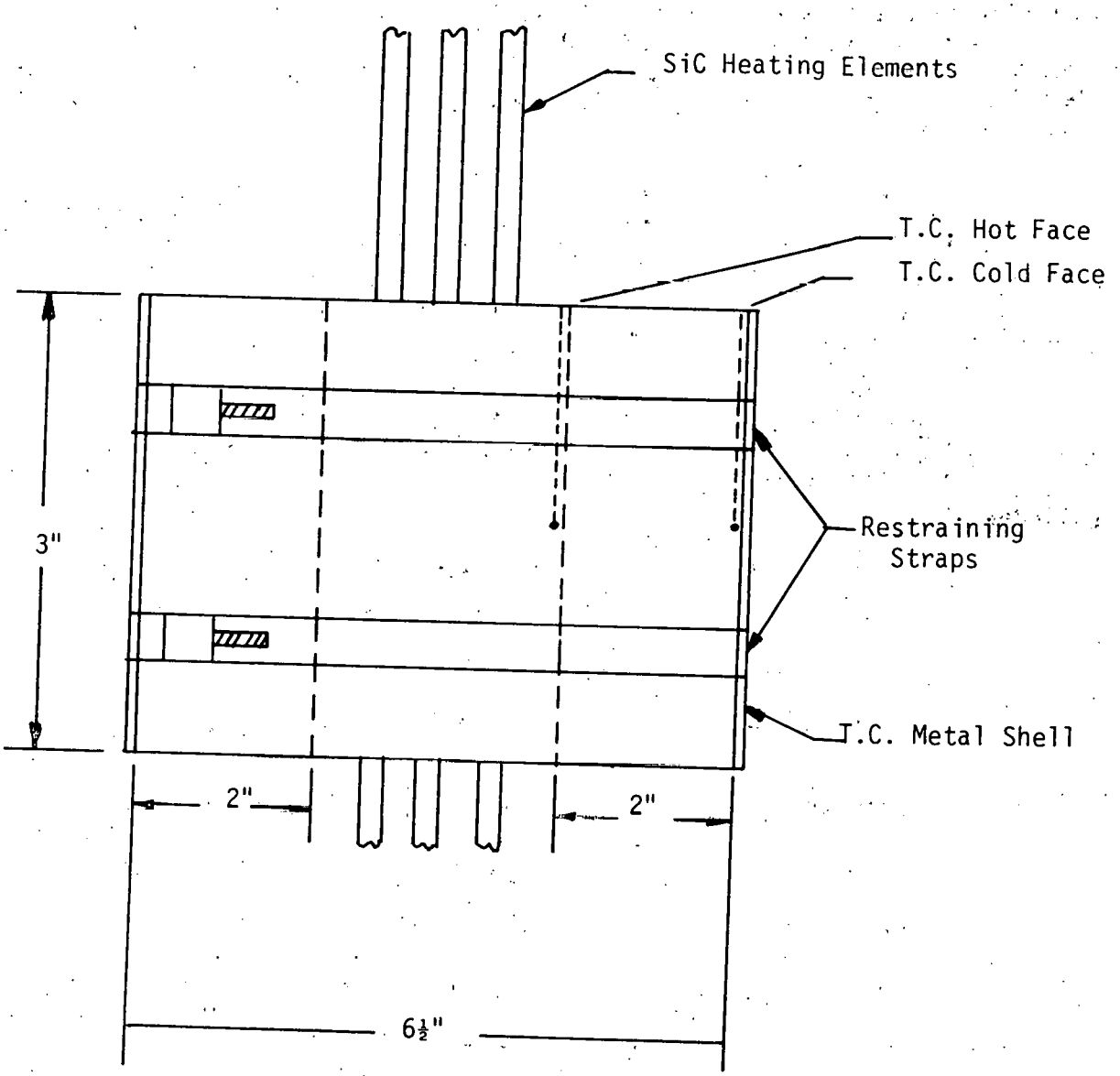

FIGURE 16. Schematic of Cylinder Cross Section With Thermocouple Placements for Thermal Analysis Verification Tests

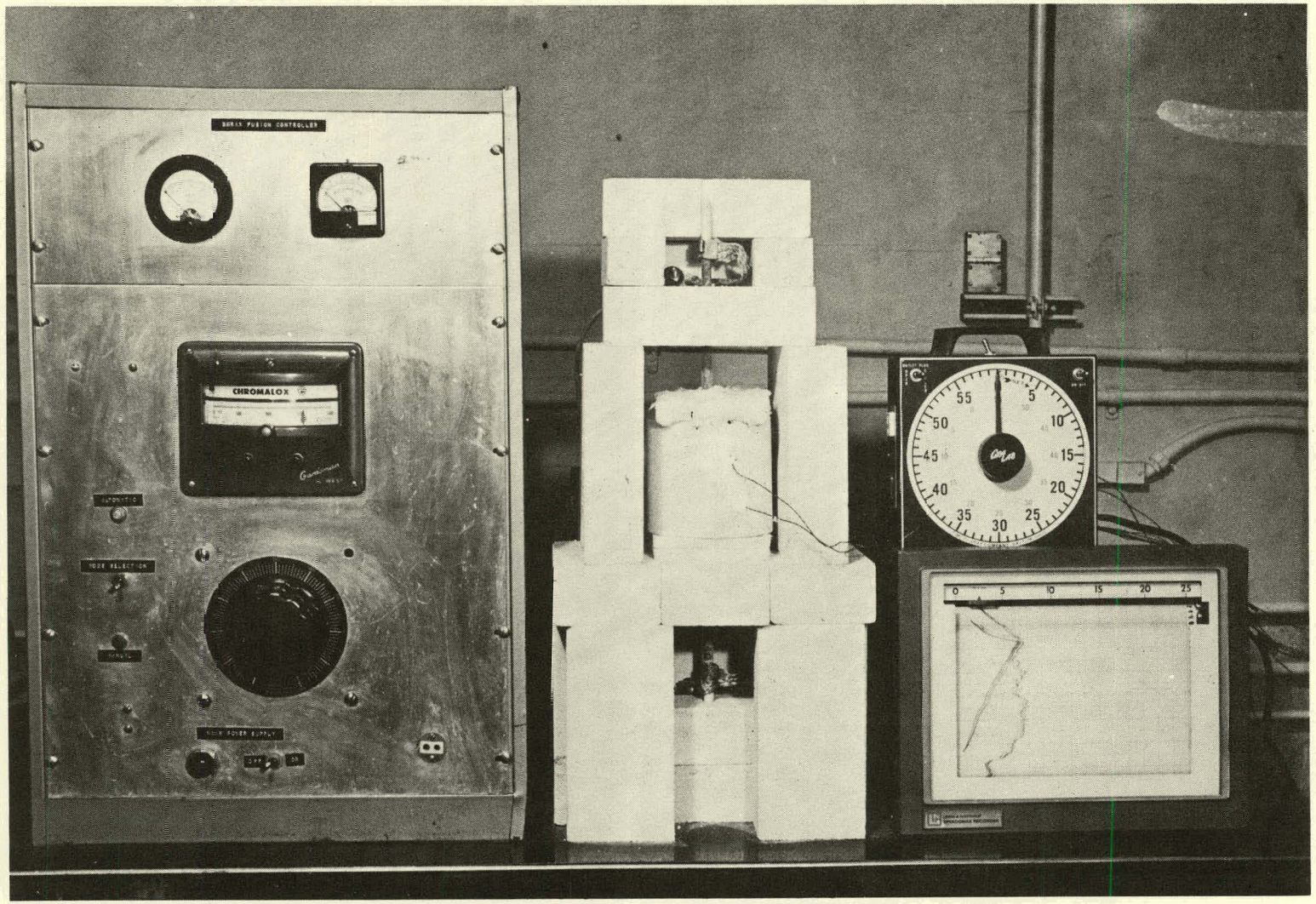

FIGURE 17. Test Set-Up For Hollow Cylinder Heat-Up Tests

2.4.3. Pore Pressure

To support the incorporation of Z. Bazant's[5] pore pressure model into the 1 and 2 OD finite element analysis models and to expand on an internal pore pressure technique developed by Kistler[11] for use in the lining tests, a series of experiments was performed.

Pore Pressure Model Input

The support data for the model involved determining moisture loss relative to temperature. These data could be fed directly into the pore pressure/moisture migration model acquired from Z. Bazant[5] to determine the permeability of the material. Permeability was then related to pore pressure and explosive spalling.

Test specimens were prepared by casting the materials of interest into solid cylinders (3" OD x 6" high). Different amounts of mix water were used in the castable so that permeability could be expected to vary from specimen to specimen. To direct the migration of water in a radial path, the ends of the cylinders were sealed with aluminum foil. The as-cured specimens were heated to different temperatures in the Instron test facility; and weight loss was monitored by way of a 10 pound load cell. A schematic of the test set-up is shown in Figure 18.

Pore Pressure Measuring Technique

C. Kistler[11] reported that internal pressure due to steam in a refractory concrete being heated can be measured by a pressure gage which is connected to one end of a metal tube, the other end being open and embedded in the concrete. Since the technique appeared to be a practical method of determining pore pressure in a monolithic lining during dry out and heat up, it was further investigated.

The initial technique development work was done with bricks and solid cylinders. This work involved embedding 1/4" and 1/8" dia. stainless steel tubes at various distances from the hot face and measuring pressure changes with temperature and time. To prevent the escape of moisture from the surface of the specimen, it was wrapped in aluminum foil. One face of the specimen was heated at a rate fast enough to cause the moisture to migrate at a rate sufficient to generate internal pore pressure. Pressures up to 20 psig were measured two inches from a brick surface heated to 1000°F. Figure 19 illustrates the configuration of some of the brick shapes tested. Macrostructural examination of sectioned specimens indicated that an excellent bond was attained between oxidized stainless steel tubing and the refractory. No evidence was found of any pressure leakage along the tubing due to poor bonding. Figure 20 indicates some of the pressures measured at various distances from the hot face and the associated temperatures during one of the brick tests. Hot face heating rates were generally ≥2000°F/hr although internal heating rates at the pressure tube locations were about 400°F/hr. These rates are considered high for the initial firing of refractory concretes; however, the pressures recorded were somewhat lower than had been anticipated.

Further investigations of the technique were investigated to determine the effect of system error on the experimental results. Both open and closed end tubes were embedded in cylindrical specimens; some filled with water,

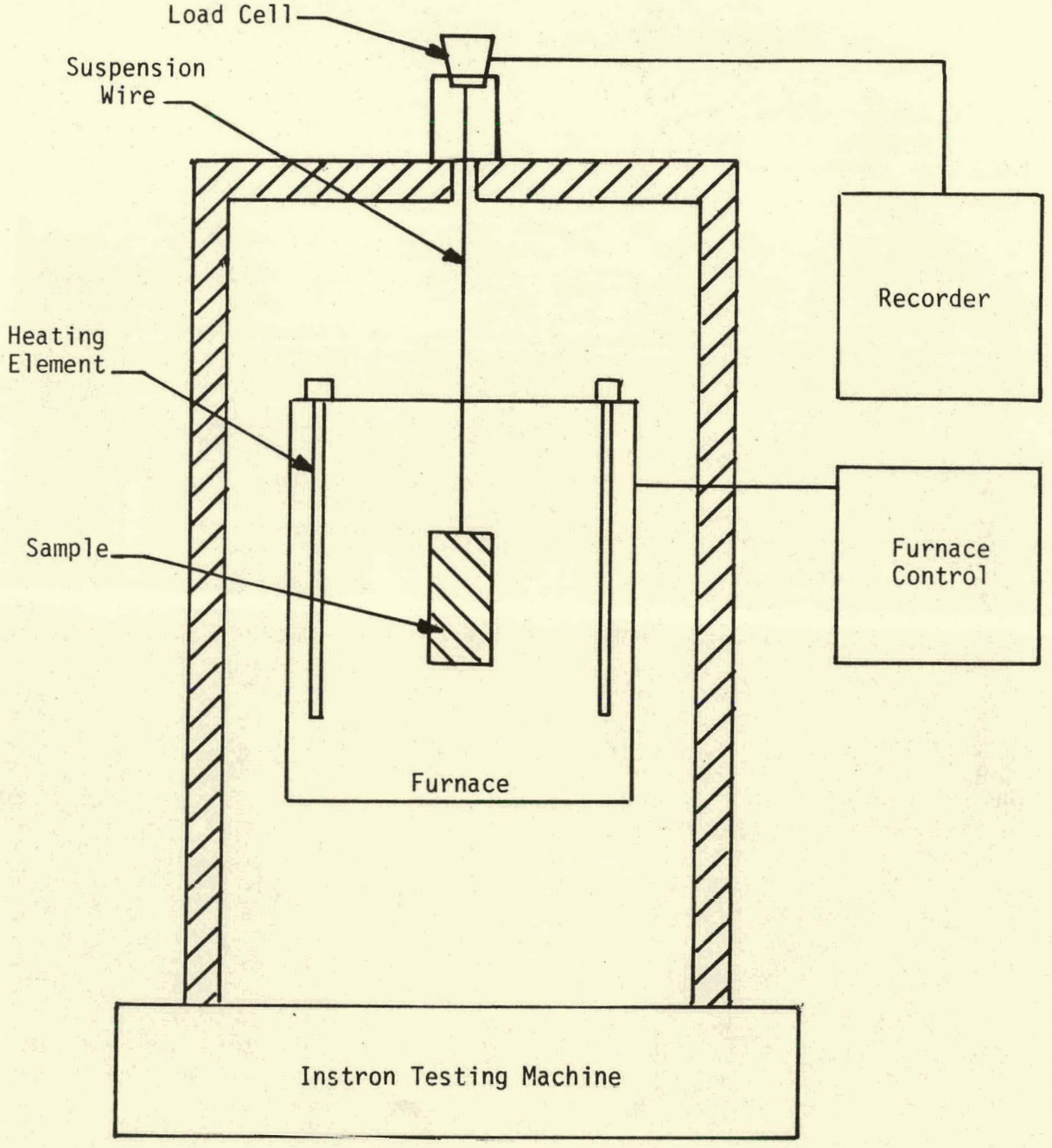

FIGURE 18. Schematic of Test Unit Used to Determine Water Loss Vs. Time and Temperature of Refractory Concrete Lining Materials.

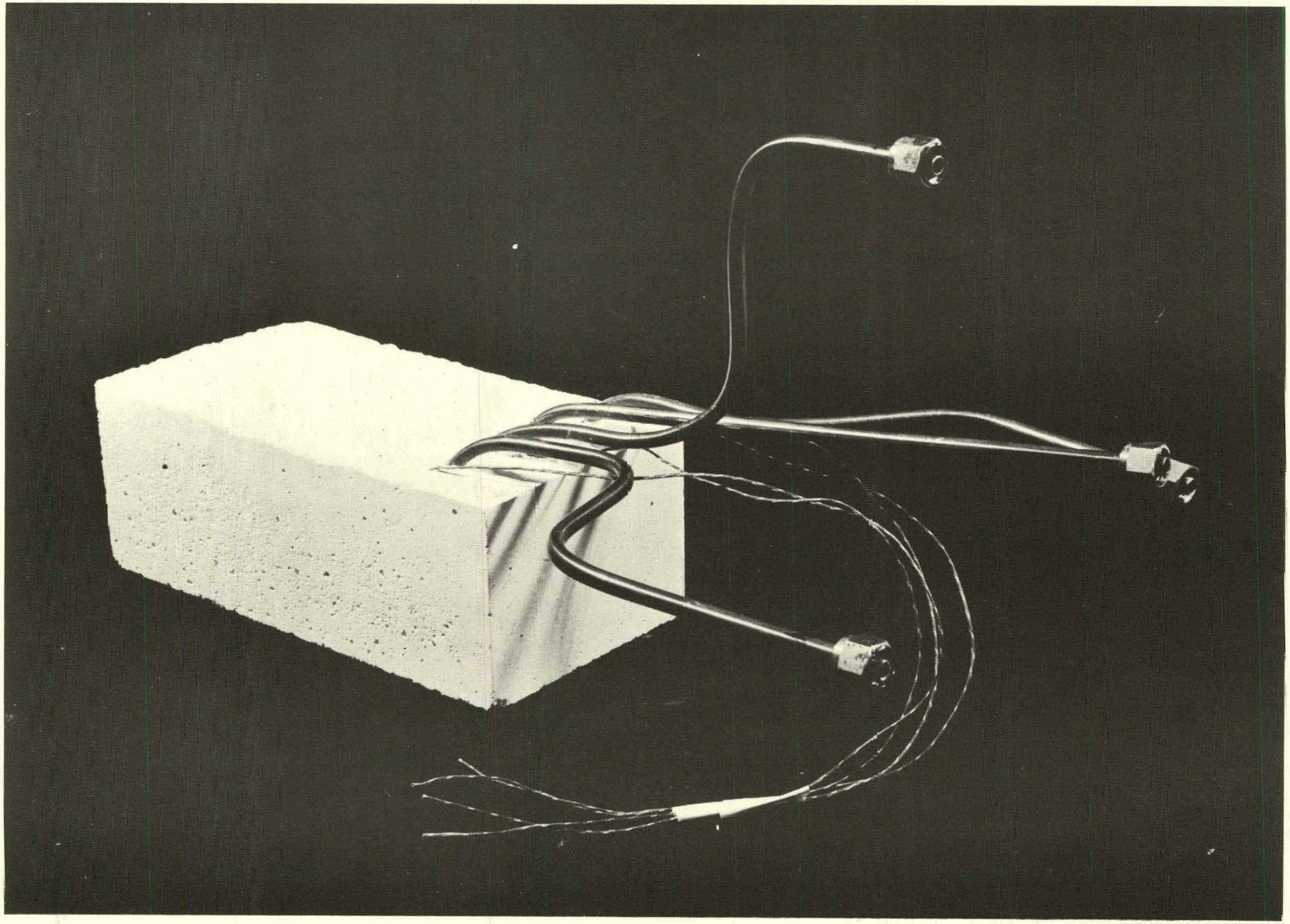

FIGURE 19. Refractory Specimen Equipped With Embedded Tubes and Thermocouples for Determination of Pore Pressure Vs. Temperature.

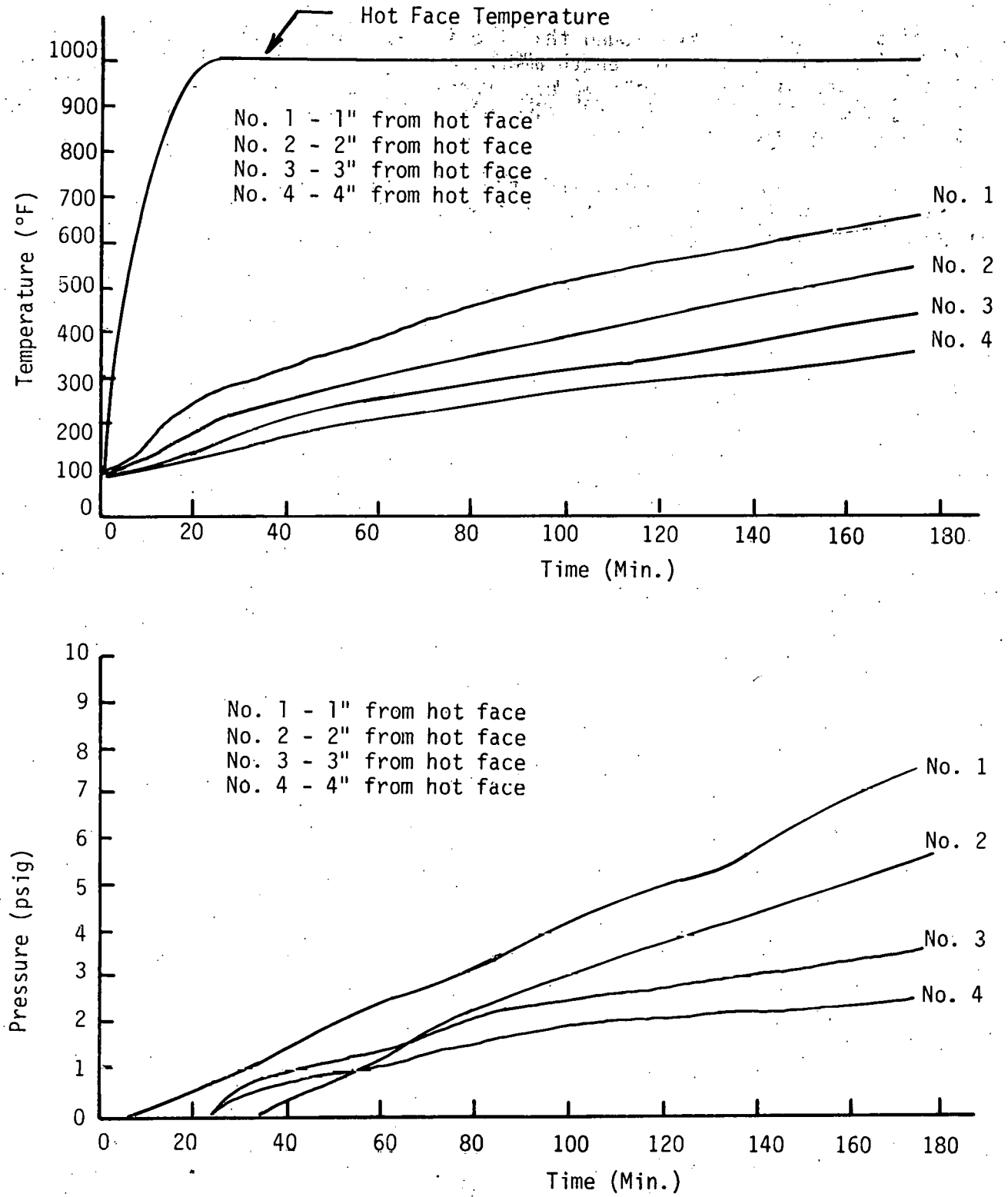

FIGURE 20. Pore Pressure Vs. Temperature and Distance from Hot-Face of Refractory (90+% Al_2O_3).

and others with air. It was found that the increase in pressure due to the increase in temperature along the tube length amounted to 1-2 psi, regardless of whether the tube was filled with air or with water. Pressures were also measured using two different sizes of tubes (1/4" and 1/16" dia.); however, no significant differences between the two were noted.

It was concluded from the investigation that an embedded, open ended, air filled tube connected to a pressure gage can be used to measure internal pressure in a refractory concrete.

2.5. Acoustic Emission (AE) Development Procedures and Results

2.5.1. Procedures

The intent of applying acoustic emission (AE) monitoring in this study was to detect the occurrence of refractory degradation due to cracking. By determining the time and relative severity of cracking, AE techniques can provide realtime feedback of a given lining's response to stresses developed during thermal cycling. This information may be used to control the firing schedule during the initial heat-up and cure of refractory lined vessels to improve lining performance and reliability.

The initial stages of the AE development program were designed to demonstrate the feasibility of refractory crack detection using AE methods. The specific objectives of the initial stages were:

- Define AE monitoring parameters, system gain, and sensor configurations to be used on the first series of lining tests.
- Determine preliminary technique feasibility and the effect of scale-up to full size lining tests on detection sensitivity.
- Analyze features from AE data which allow differentiating signals related to cracking from less significant sources such as moisture release and noise interference.

These objectives were accomplished by performing tests on a series of brick and panel refractory specimens. All specimens were cast using a vibrating table assist and common casting practices. Figure 21 shows the configuration of the brick and panel specimens used in these preliminary experiments. As shown in the Figure, each brick had a fused silica rod (waveguide) embedded approximately 3/8" into the refractory material. The fused silica provided a smooth surface to which AE sensors could be attached. The excellent insulating and acoustic properties of the silica rods also provided a means to protect the AE sensors from heat damage with no loss in detection sensitivity.

Table 9 contains a summary of the brick tests performed. Two basic refractory compositions (ERDA 90 and LITECAST) were used with small variations in water content to produce the nine specimens. Each brick specimen was heated in a programmable Harrop electric furnace. The bricks were placed vertically in the furnace door and packed around the edges with fibrous insulating material (KAOWOOL*) to form a secure fit. One face of each brick was exposed to the furnace heat; the opposite face remained exposed to the surrounding laboratory environment. When heated according to the firing schedules shown in Table 9, this configuration produced a thermal stress gradient from the hot face (inside furnace) to the cold face (room temperature). This thermal stress gradient, also present in refractory lined vessels, had a tendency to induce cracking.

---

*KAOWOOL is a registered trade name of the Babcock and Wilcox Co.

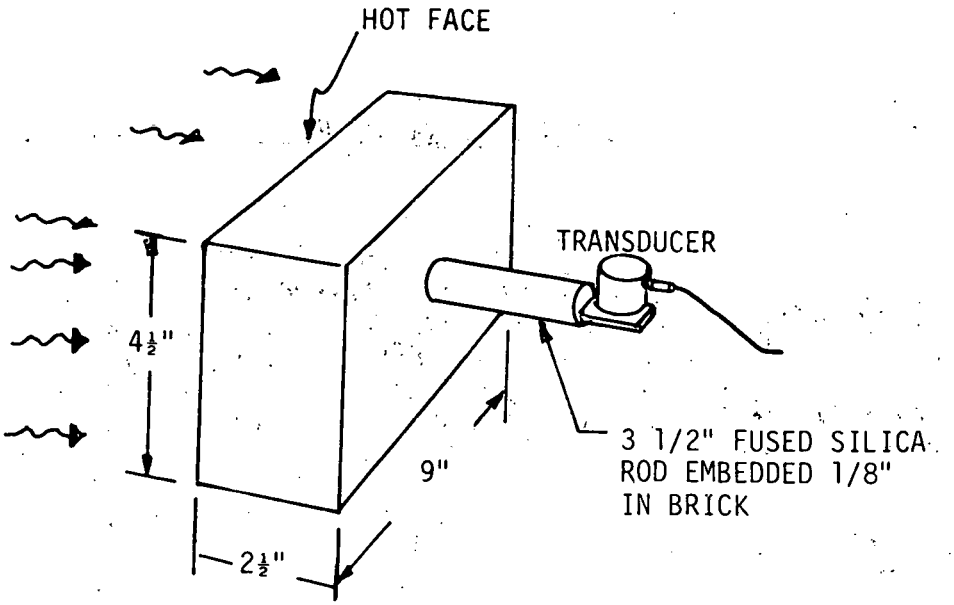

a) Brick Specimen

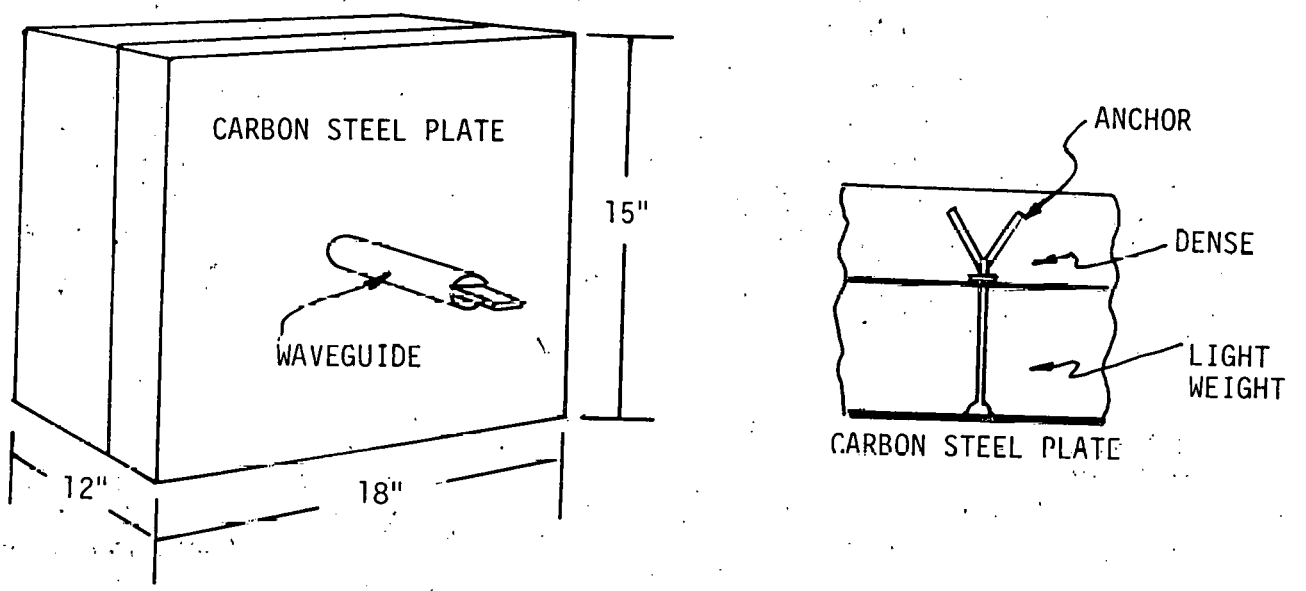

b) Panel Specimen

FIGURE 21. Specimen Configurations for Brick and Panel Tests in AE Feasibility Study

TABLE 9. Summary of Brick Tests Performed During Initial AE Feasibility Study

Brick#	Composition	Heating Schedule	*Relative Visual Cracking
1	LITECAST 75-28 26% H_2O	400-600°F/Hr to 1400°F; Furnace Cool (Specimen run twice)	5
2	90+% Al_2O_3 Generic 9.3% H_2O	700-600°F/Hr to 1500°F; Furnace cool	3
3	LITECAST 75-28 26% H_2O	200°F/Hr to 1800°F; Furnace cool	4
4	90+% Al_2O_3 Generic 9.3% H_2O	200°F/Hr to 2850°F; Furnace cool	1
5	LITECAST 75-28 21% H_2O	100°F/Hr Case #1 heatup and cooldown	3
6	90+% Al_2O_3 Generic 9.3% H_2O	100°F/Hr Case #1 heatup and cooldown	1
7	50% Al_2O_3 Generic 10% H_2O	100°F/Hr Case #1 heatup and cooldown	4
8	LITECAST 75-28 24% H_2O	50°F/Hr with same holds as Case #1	2
9	LITECAST 75-28 24% H_2O	100°F/Hr Case #1 8-hour hold during cooldown at 1500°F	1

* Rating of 1 is least severe; 5 is most severe

Panel tests were performed in a similar fashion as the brick tests; however, a larger gas-fired programmable furnace was used to accommodate the larger specimens. AE monitoring of panel tests was concurrent with the materials evaluation. Their investigations started earlier than AE investigations, so not all panel tests were acoustically monitored. Table 10 contains a summary of the panel tests which were monitored for AE. These tests served as an intermediate step in the scale-up to full sized liner monitoring using AE techniques. Whereas brick specimens consisted of single components, the panels were cast as dual component samples (LITECAST backing ERDA 90) to more closely simulate a portion of a lined vessel. Y-anchors were used to fix the two components to the steel support backing, also simulating standard monolithic lining installation practices.

Figure 22(a) is a photograph of some of the AE equipment used during the brick and panel tests. Figure 22(b) is a photograph of a brick sample positioned in the furnace with KAOWOOL as a packing material. A single AE sensor was attached to the left silica waveguide using a C-clamp. All of the brick and preliminary panel tests were monitored with a single channel Dunegan/Endevco 3000 AE system. Figure 23 contains a block diagram of that system. A broad-band differential AE sensor (D9202) was attached to the 3-1/2" silica waveguides using high temperature silicone grease as a couplant. The output of the sensor was preamplified 40 dB, then further amplified for a total gain of 85 dB. Electrical and mechanical noise interference was reduced by passing the signals through a high pass filter with a lower cut-off frequency of 100 KHz. Total ringdown and envelope (event) counts were accumulated using two 301 totalizers and a 905 digital envelope processor. Outputs were displayed on strip chart and x-y recorders.

Later panel tests were acoustically monitored using a multi-channel AE source location system. The system was manufactured by Acoustic Emission Technology Corporation (AETC), Model RTM024. The AETC system processed AE signals in the same basic manner as the Dunegan system (ringdown and event counts); however, it provided additional information about the AE signals such as two-dimensional source location and pulse height analysis. It also provided increased noise discrimination using software implemented accept/reject criteria.

The AETC sensors used for these tests had a center frequency of 357 KHz (Model AC-375). The preamplifiers incorporated 250-500 KHz band-pass filters to reduce noise interference while amplifying the sensor outputs 40 dB. Additional amplification was introduced with the main system signal processors whose gain was continuously variable over the range of 0-60 dB. The gain for the panel tests was fixed at 88 dB total. Figure 24 contains a block diagram of the AETC system as used for the later panel tests.

The AE signals from the first few brick and panel tests were recorded on a modified Sony video tape recorder. The video recorder enabled "freezing" the transient AE waveforms during playback so that selective frequency analysis could be performed. Frequency analysis, however, did not produce signal features which could discriminate between the various source mechanisms (including noise), so it was abandoned in further investigations.

TABLE 10. Summary of Panel Tests Performed During Initial AE Feasibility Study

Panel	Composition	Firing Schedule (^{o}F)	Crack Pattern	*Relative Visual Cracking
#5	LITECAST 75-28 7½" 21% H_2O 90+% Al_2O_3 Generic 4½" 9.3% H_2O	13 hrs @ 200^{o}, 480^{o}/hr to 1000^{o}. when explosively spalled. Controller malfunction. Hot face spalled into 4 large pieces w/ anchors imbedded and threads stripped. AE waveguides welded to base plate over an anchor. AE monitored.	Explosively spalled at 1000^{o}	(Failed)
#6	LITECAST 75-28 7½" 21% H_2O 90+% Al_2O_3 Generic 4½" 9.3% H_2O	22 hrs @ 170^{o}, 26 hrs @ 450^{o}, 100^{o}/hr to 1000^{o}, 14 hrs @ 1000^{o}, 125^{o}/hr to 2000^{o}, 3 hrs @ 2000^{o}, cool @ 100^{o}/hr AE monitored w/1 waveguide 10% H_2O loss after firing.	Random and interconnected network of shallow cracks on hot face with some extending from anchor/refractory interface.	3
#7	LITECAST 75-28 7½" 21% H_2O 90+% Al_2O_3 Generic 4½" 8.5% H_2O	14 hrs @ 110^{o}, AE breakdown 22 hrs @ 170^{o}, 26 hrs @ 450^{o}, 100^{o}/hr to 1000^{o}, 3 hrs @ 1000^{o}, 100^{o}/hr to 2000; 4 hrs @ 2000^{o} cool 100^{o}/hr to 900, 50^{o}/hr to 500^{o}. AE monitored using 4 wave guides.	Very few cracks on hot face. Those found are shallow and not interconnected.	3
#9	Modified 50% Al_2O_3 Generic Single component 12' 10% H_2O	16 hrs @ 180^{o}, 16 hrs @ 450^{o} 100^{o}/hr to 1000^{o}, 3 hrs @ 1000^{o}, 100^{o}/hr to 2000^{o}, 5 hr @ 2000^{o} cool 300^{o}/hr to 1600^{o}, 100^{o}/hr to 1000, 50^{o}/hr to R.T. AE monitored using 4 wave guides.	Single crack across hot face. Several cracks parallel to and approximately 5" from hot face.	5

* Rating of 1 is least severe; 5 is most severe

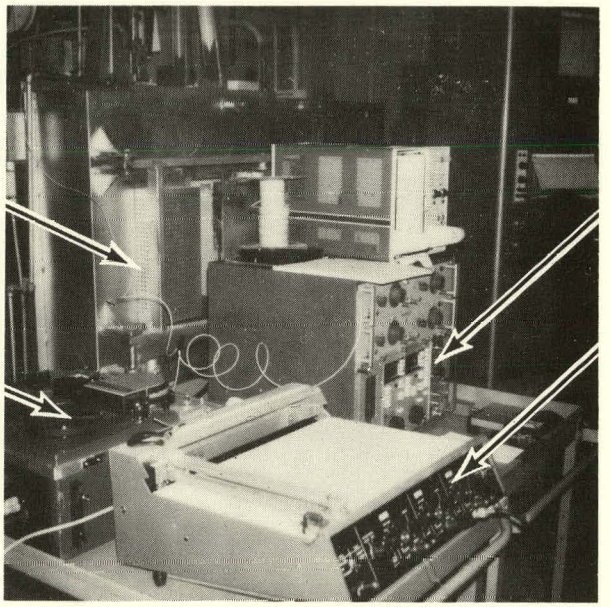

(a) Instrumentation for Brick and Panel Tests.

(b) Brick Sample Positioned in Furnace for Evaluation.

FIGURE 22. Photographs of Set-Up for AE Evaluation.

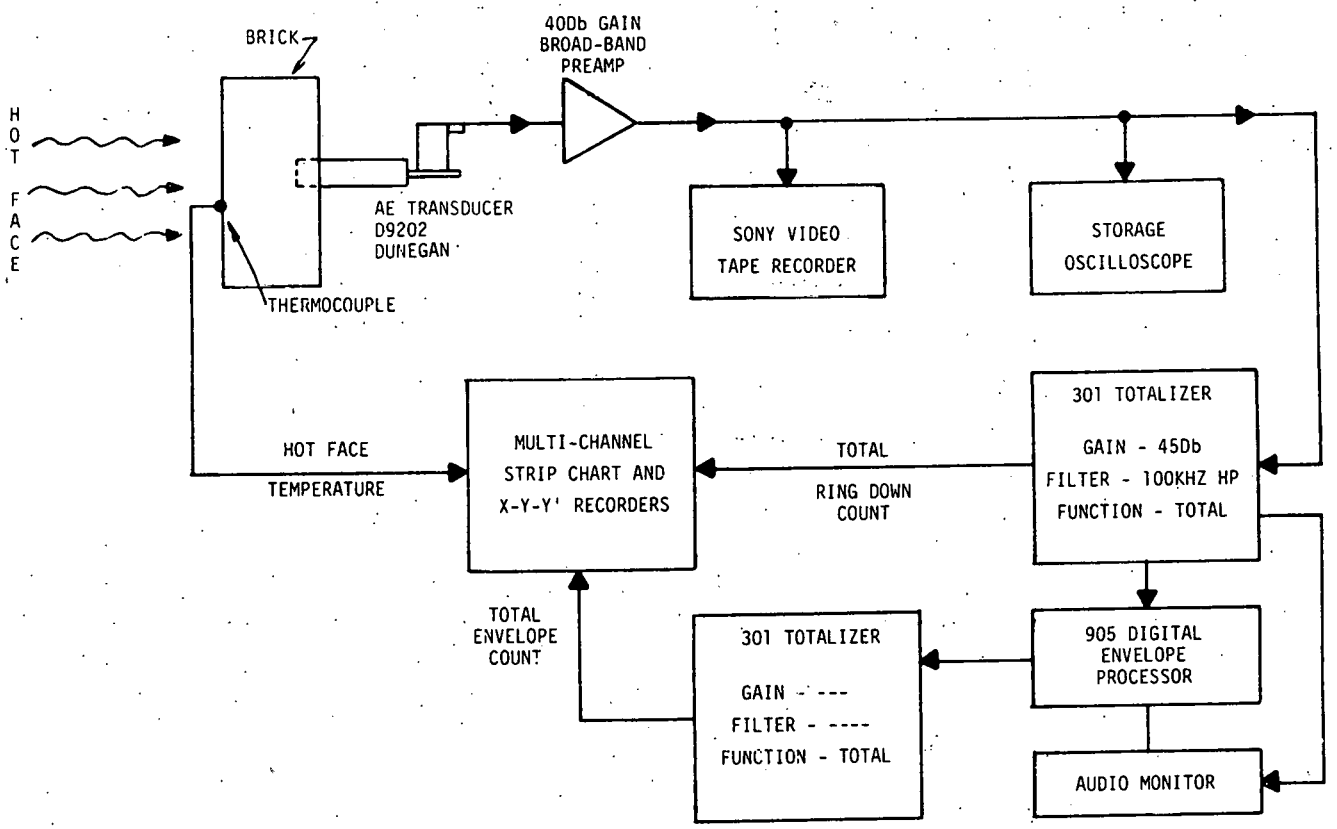

FIGURE 23. Block Diagram of Dunegan/Endevco AE System Used to Monitor Brick and Preliminary Panel Tests

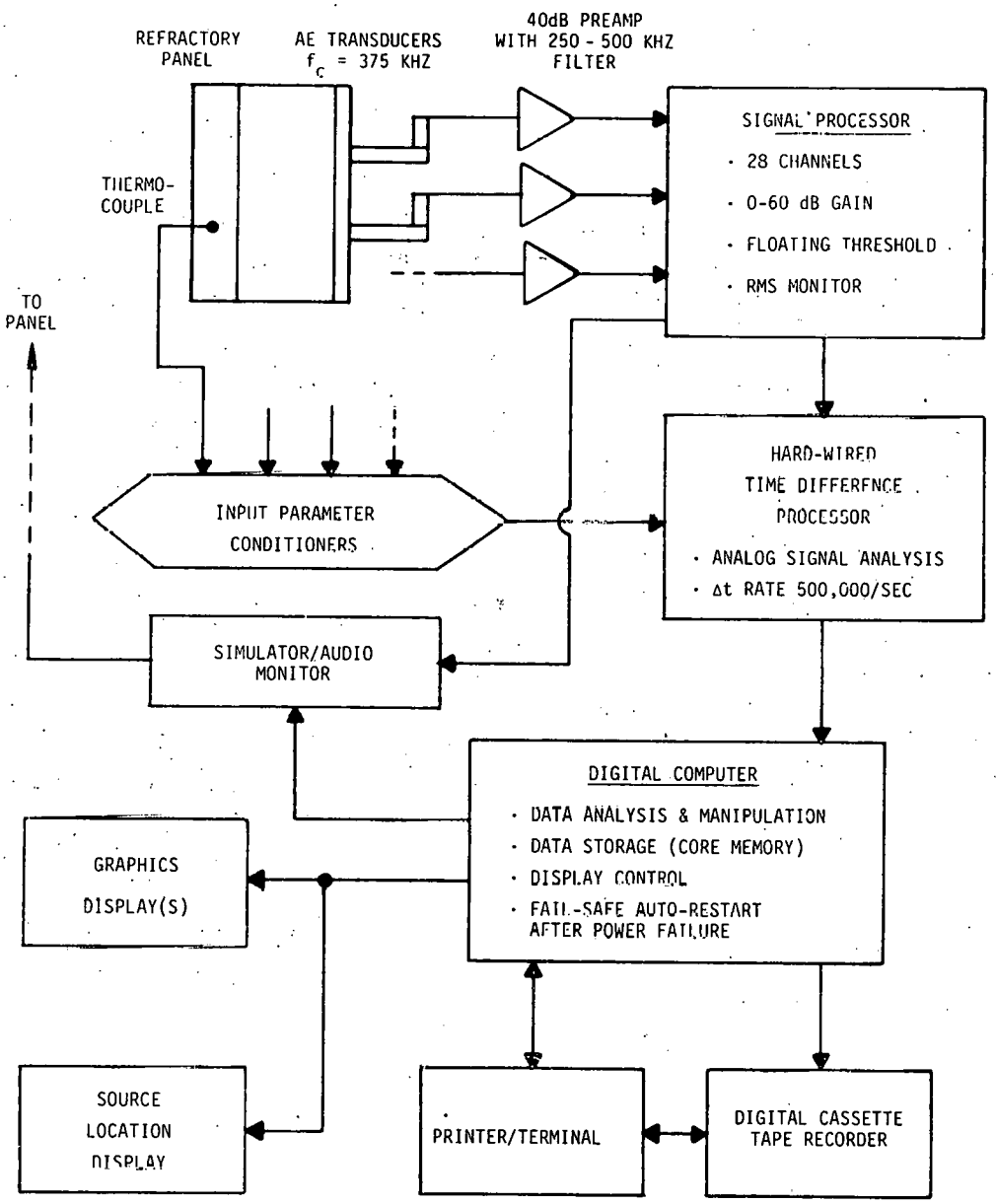

FIGURE 24. Block Diagram of AETC RTM-24 AE System Used for Panel Tests

2.5.2. Brick and Panel Test Results

Figure 25 is a plot of AE data generated during the initial tests of two LITECAST brick samples. This data is typical of all early LITECAST brick tests performed. One sample was heated to 1400°F (hot face temperature) at a rate of 400-600°F/hour. The other was heated to 1800°F (hot face temperature) at a rate of 200°F/hour. These two samples correspond to brick numbers 1 and 3 referred to in Table 9.

Figure 26 is a plot of AE data generated during analogous tests of two ERDA 90 brick samples. The same heating rates were used as for the LITECAST samples to allow a qualitative comparison of the two types of materials' responses. The ERDA 90 samples in Figure 26 correspond to brick numbers 2 and 4 in Table 9.

These initial brick tests were used to determine if AE could be detected from refractory materials during thermal cycling, and whether it could be correlated with other test parameters. At this point it was an assumption that the primary source of the AE was cracking. The results did lead to some interesting observations, however. First there was a definite temperature dependance of AE activity for both Materials and both heating rates. For the LITECAST material, the majority of the acoustic activity occurred at temperatures exceeding approximately 1000°F on the hot face. For the denser ERDA 90 material, the transition temperature was lower, occurring at approximately 600°F. Since the data in Figures 25 and 26 were not recorded with time as a variable, it is difficult to assess the influence of the heating rate upon the results. It can be stated, however, that faster heating rates produced greater cumulative counts regardless of the material. Another significant observation is that the LITECAST materials were more active (greater accumulated AE counts) than the ERDA 90 materials at the same corresponding heating rates. These observations support the assumption that the major source of AE from the refractories was cracking. LITECAST was a weaker material and more susceptible to cracking than the denser ERDA 90. (See Section 2.3. Material Property Determinations). It therefore should have produced more AE activity because of its additional cracking tendency. Visual observations of the brick's crack patterns after heating confirmed a larger number of cracks for the LITECAST samples.

Figure 27 depicts typical results obtained from a dual component (LITECAST backing ERDA 90) panel test. In particular, these results were obtained from panel #6 as listed in Tabel 10. Little AE activity was detected until the hot face temperature reached approximately 1300°F. It then increased in activity and continued for the remainder of the test, even through the cooldown. There were a few large bursts which occurred between 1850°F and 2000°F, but for the most part the increases in counts were uniform with time. (The bursts appear as the sharp vertical steps in the ringdown count curve in Figure 27).

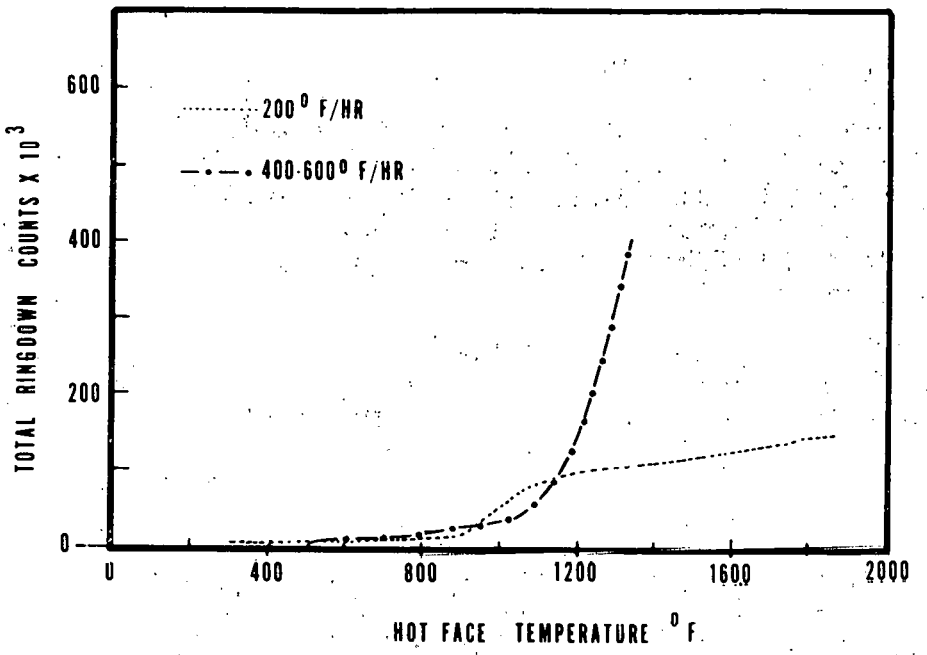

FIGURE 25. Plots of Accumulated AE Ringdown Counts vs. Hot Face Temperature for Two LITECAST Samples at Different Heating Rates

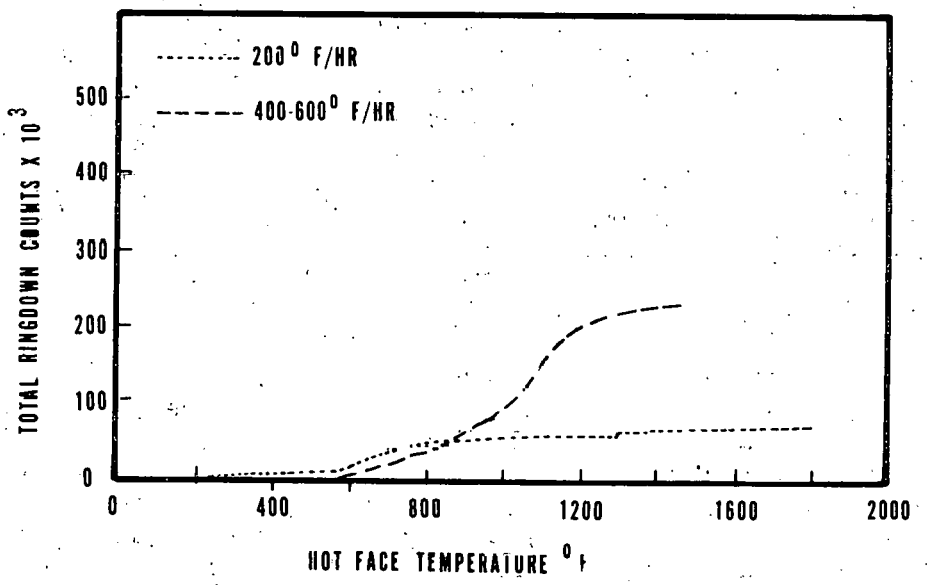

FIGURE 26. Plots of Accumulated AE Ringdown Counts vs. Hot Face Temperature for Two ERDA-90 Samples at Different Heating Rates

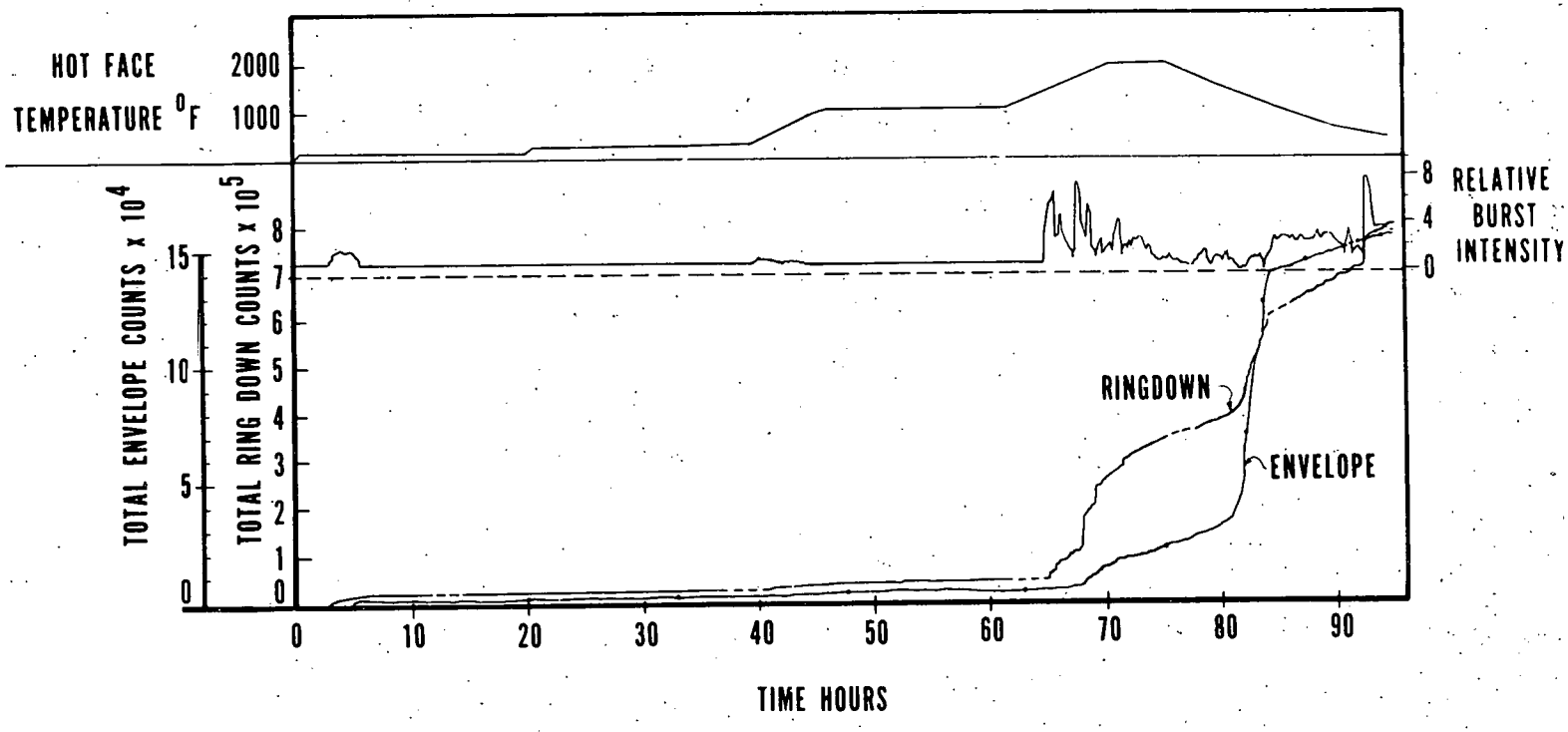

FIGURE 27. AE Results Recorded During Panel Test #6

In addition to the temperature, ringdown counts, and event count curves, Figure 27 also contains a plot termed Relative Energy per Event. This is an AE parameter developed from the analysis of the brick and panel AE data, intended to allow easier interpretation of AE data and to highlight significant (high energy) AE activity. Relative Energy per Event incorporates both envelope (event) counts and ringdown counts according to the following relationship:

$$\text{Relative Energy per Event} = \frac{\Delta r_i}{\Delta e_i}$$

where Δr_i = change in accumulated ringdown counts over time interval i

Δe_i = change in accumulated envelope (event) counts over time interval i

i = 5 minutes for panel tests; 15-30 minutes for lining tests.

As can be seen in Figure 27, the Relative Energy per Event graph did give a clearer representation of the AE activity. Consequently further analyses of AE data concentrated on this parameter.

Less typical but highly significant AE results were obtained during the testing of panel #5. This panel had a dual component configuration that failed by explosive spalling. The spall occurred at 1000°F after the furnace control malfunctioned and caused a severe heating rate of 480°F/hour. Figure 28 is a photograph of the spalled panel and furnace as they appeared immediately after the explosion. Prior to the controller malfunction, the panel had been heated at 100°F/hour to 200°F where it was held for thirteen hours. Little AE was recorded during that period. Figure 29 details the acoustic events for the two hours following the 200°F hold and preceding the spall. Up to about 1.3 hours following the end of the hold the Relative Energy per Event graph displayed amplitudes and patterns that were similar to those recorded from panel #6 (Figure 27). At about 1.4 hours, the relative activity showed a sharp increase, as indicated in Figure 29. Three minutes later this "precursor" activity resumed a momentary low level, followed by rapidly increasing activity which continued until failure. Note that the amplitude of the Relative Energy per Event graph continued to increase up to the spall's occurrence.

FIGURE 28. Photograph of Panel #5 and Test Furnace After Specimen Failed by Explosive Spalling

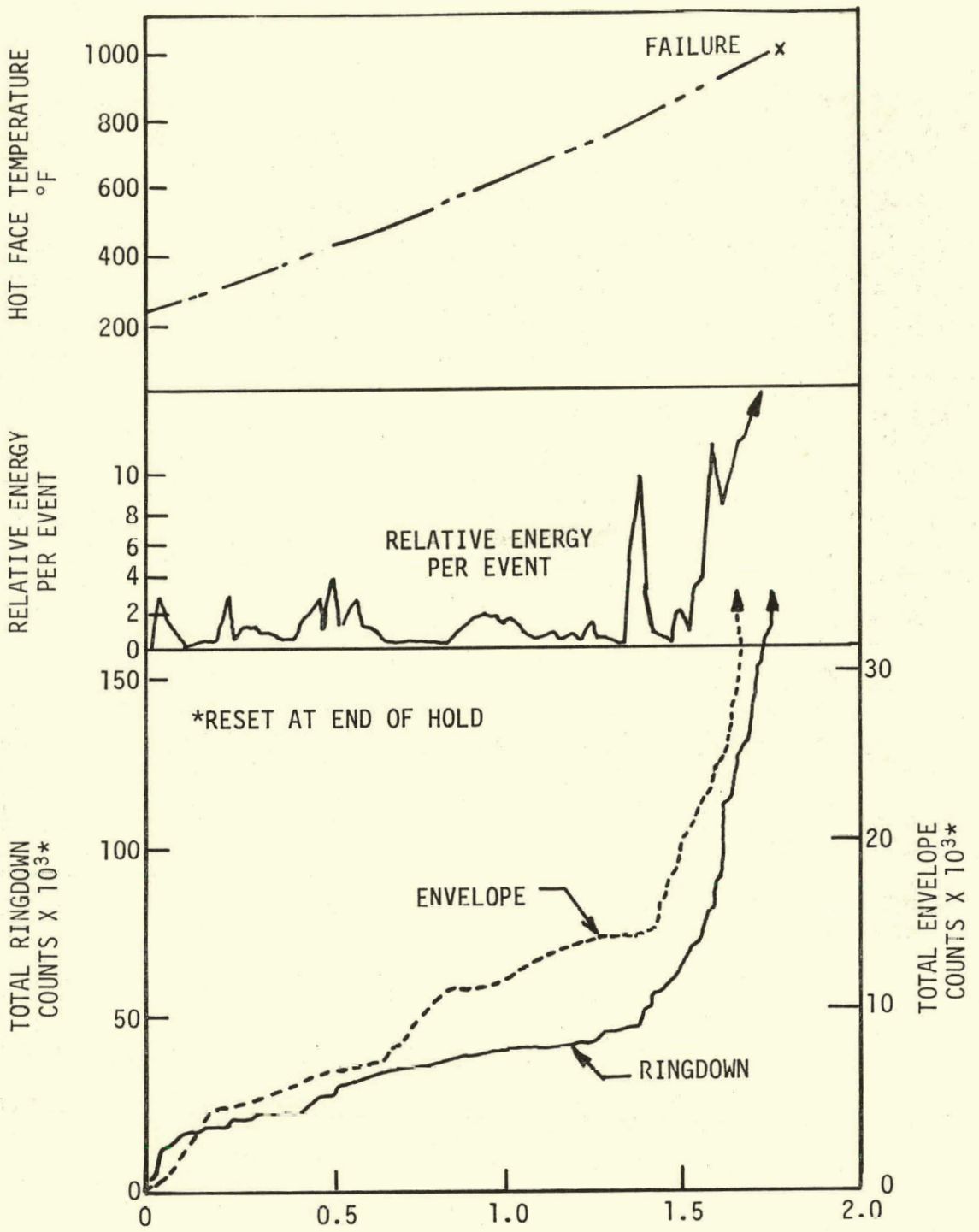

FIGURE 29. AE Results From Panel Test #5 Which Failed By Explosive Spalling

2.5.3. Additional Small-Scale Brick Testing

During the course of the lining tests monitored for AE, it became increasingly evident that an understanding of the basic materials' response to the variables imposed during a lining test had not been obtained. It was not economically feasible to change only one or two test parameters from lining to lining in order to isolate individual effects. Therefore, many parameters (material composition, anchor type and location, heating rates and schedules, etc.) were changed to empirically achieve a bulk improvement in the refractory performance. This approach prompted additional small-scale experiments to study the isolated effects of material composition, heating rate, and combined thermal/mechanical loading upon the AE response. The objective of this phase of the AE development program was to enable better interpretation of the AE data from the lining tests.

The last phase of the AE development effort involved designing another series of tests using brick samples. Figure 30 shows the various test cases examined in these additional small scale experiments. The following list explains the separate conditions they represented.

Case I - Material response to a moderate heating rate

Case II - Material response to a moderate mechanical load

Case III - Material response to a rapid heating rate

Case IV - Material response to a combined mechanical load and moderate heating rate

Case V - Material response to a combined mechanical load and rapid heating rate

Case VI - Prototype material response to a combined mechanical load and rapid heating rate

The preliminary brick and panel tests were largely qualitative in nature; that is, they were intended to demonstrate that AE related to cracking could be detected from refractory materials and that the technique could be scaled-up to the large test vessel. These secondary brick tests differed from the initial experiments in that they were designed to enable direct comparison of data according to material type and loading conditions. The anticipated degradation occurring in these additional test cases just outlined was least for Case I with progressively more damage in each consecutive test. LITECAST samples were expected to degrade more quickly than ERDA 90 samples under similar loads because of their weaker physical properties. The greatest amount of cracking was expected in Cases IV and V, which best simulated lined vessel conditions.

CASE I

LITECAST	ERDA 90
100°F/hr to 1600°F (No Load)	200°F/hr to 1600°F (No Load)

CASE IV

LITECAST	ERDA 90
100°F/hr to 1600°F	200°F/hr to 1600°F

Initial Load of 400 lbs/leg From Loading Fixture

CASE II

LITECAST	ERDA 90
Room Temperature Load (Fired Samples From) Case I	

CASE V

LITECAST	ERDA 90
400°F/hr to 1600°F	400°F/hr to 1600°F

Initial Load of 400 lbs/leg From Loading Fixture

CASE III

LITECAST	ERDA 90
400°F/hr to 1600°F (No Load)	400°F/hr to 1600°F (No Load)

CASE VI

B&W Prototype 50

400°F/hr to 1600°F

Initial Load of 400 lbs/leg From Loading Fixture

FIGURE 30. Test Cases Designed to Study Isolated Effects of Material Composition, Heating Rate, and Thermal/Mechanical Loading Upon AE Response

In these tests, the bricks were placed in the door of a programmable Harrop electric furnace as described earlier. To allow application of a mechanical load during the heating of the brick samples, a loading fixture was designed and constructed. Figure 31 shows the appearance and dimensions of the fixture and the locations of strain gages for applied load determination. The two protruding legs of the fixture contacted the outside edges of the brick samples as shown in Figure 32. On the interior of the test furnace, a pointed edge ceramic ram was used to brace the brick at its center line. When an applied load was desired, the turn-down screws at each end of the fixture were tightened against the fixture. This action resulted in a three point bending load, placing the cold face of the bricks in tension and the hot face in compression. AE was monitored by attaching sensors to fused silica waveguides embedded 3/8" into the samples. Hot face temperatures were measured by contact mounted thermocouples on the hot face surface of each sample.

Calibration of the AE loading fixture was obtained through experiments on a Materials Test Systems (MTS) machine. The fixture was mounted on the machine with each leg individually contacting the hydraulic ram. Incremental loads were applied to each leg and the fixture's strain gage readings were plotted against the load cell readout from the MTS machine. The calibration curve so generated allowed application of known loads to each brick by converting the strain readings measured from the legs of the loading fixture.

In order to allow direct comparison of the AE data generated from one brick sample to the next, it was necessary to obtain equivalent sensitivity settings on the AE instrumentation. To accomplish this calibration, each brick was positioned in the furnace with sensors (AET AC 375) mounted to each of the two silica waveguides. A pulser unit contained in the AETC system was used to excite an external AE simulator transducer (Dunegan-S140B) at 30 pulses per second. During calibration, the AE simulator was coupled to the end of one of the silica waveguides. The output of the AE sensor on the opposite waveguide was displayed on an oscilloscope. That sensor's output level was then adjusted to obtain 0.64 V peak to peak on the leading edge of the received signals. The AE simulator was then coupled to the other waveguide and similarly the output of the opposite sensor was adjusted to the same level. This technique was selected to compensate for differences in the acoustic attenuation of LITECAST and ERDA 90 samples, and for differences in sensor coupling efficiency. Injecting a calibration signal into one waveguide implied that the signal had to propagate through the various coupling interfaces and the specimen. Adjustments to the sensor output levels therefore were direct compensation for the variations in coupling and material properties.

Figures 33-43 contain the AE responses recorded from each brick sample in test Cases I-VI, respectively. With the exception of the Case I and IV LITECAST samples, all the scales denoting the Relative Energy per Event of the AE activity are identical. This allows direct comparisons of the magnitudes between the various material/loading conditions. The hot face temperature measurements (where applicable) are all plotted on identical scales. Load applications are also noted in the figures where applicable.

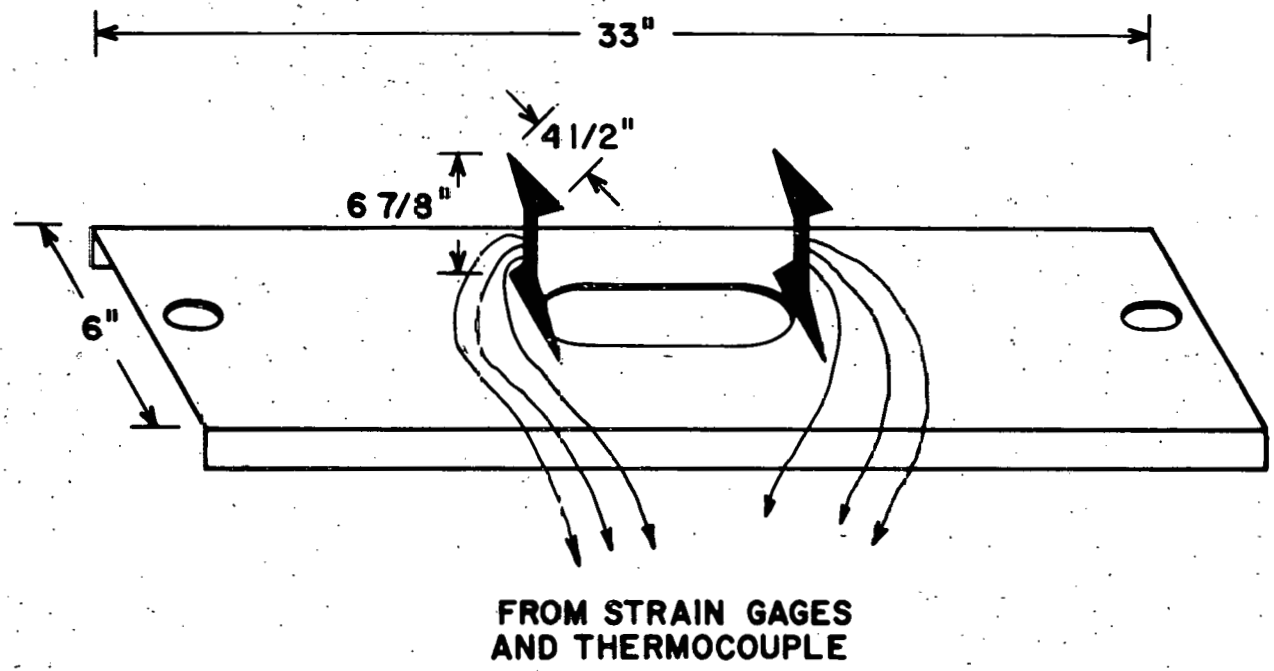

FIGURE 31. Fixture Used to Apply Mechanical Loads To Brick Specimens While Heated During AE Development Effort

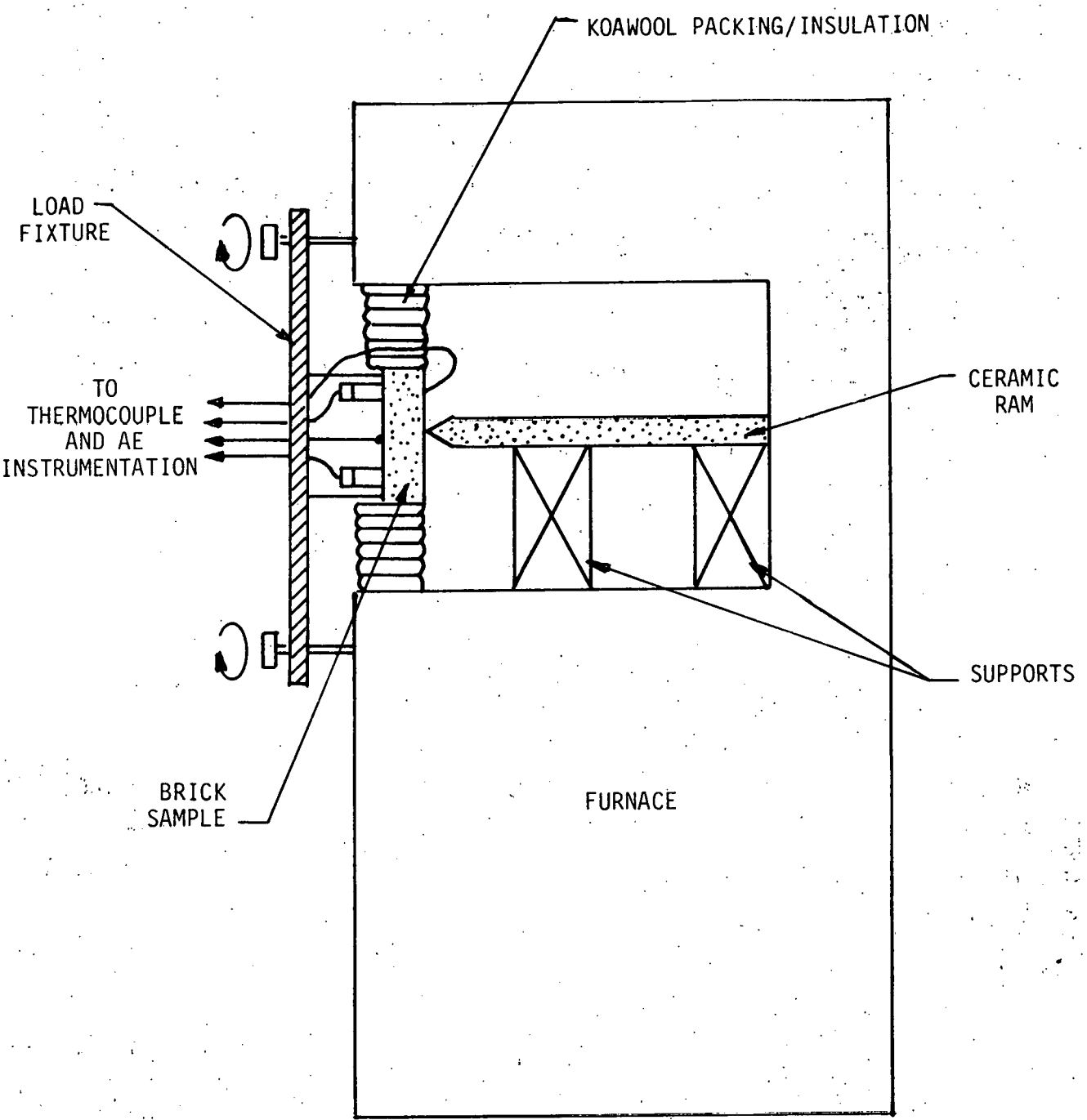

FIGURE 32. Cut-away View of Furnace Depicting Method to Apply Three-point Load to Bricks While Heating and AE Monitoring

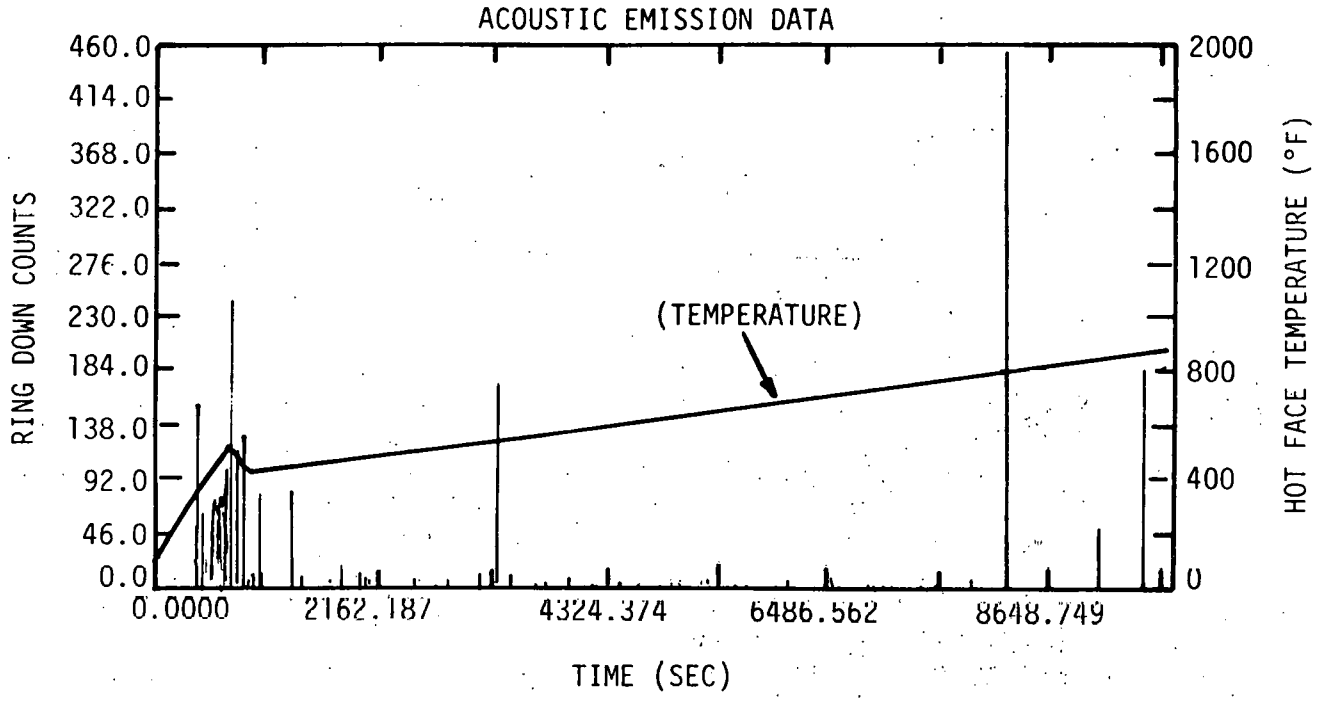

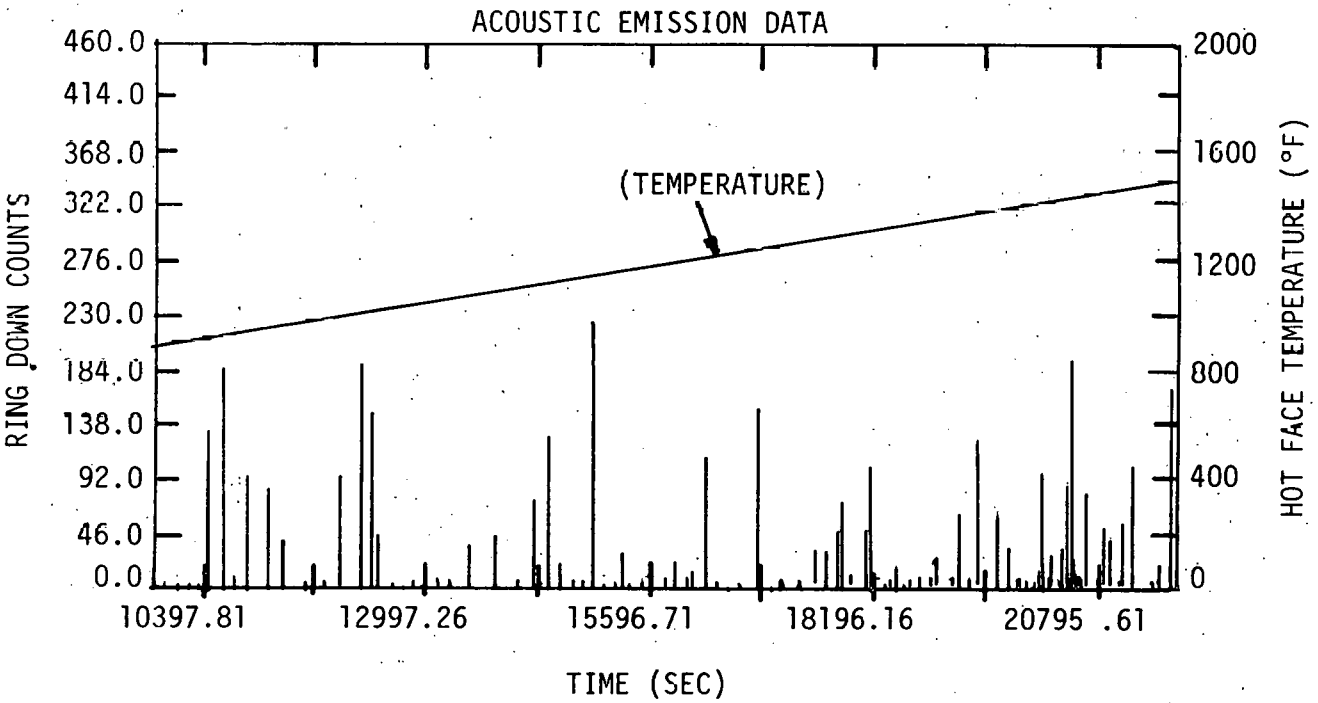

FIGURE 33. AE Results for CASE I Brick Test - LITECAST.

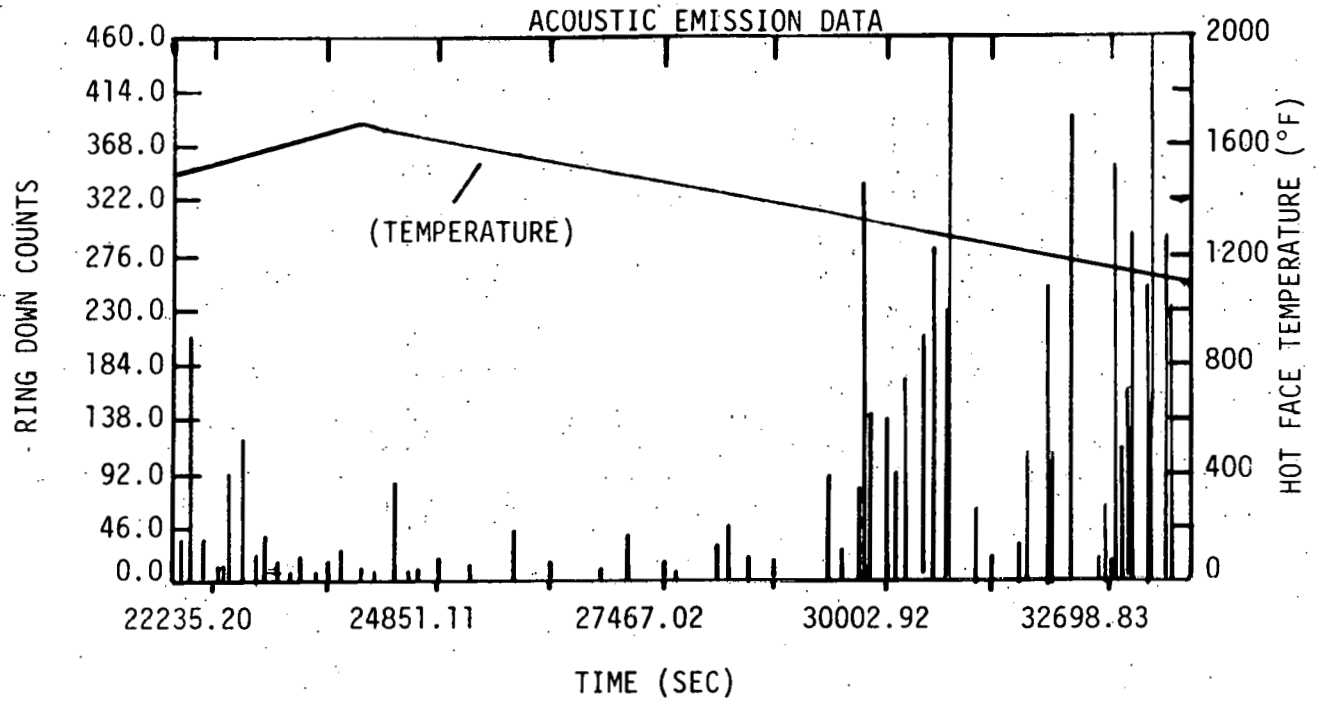

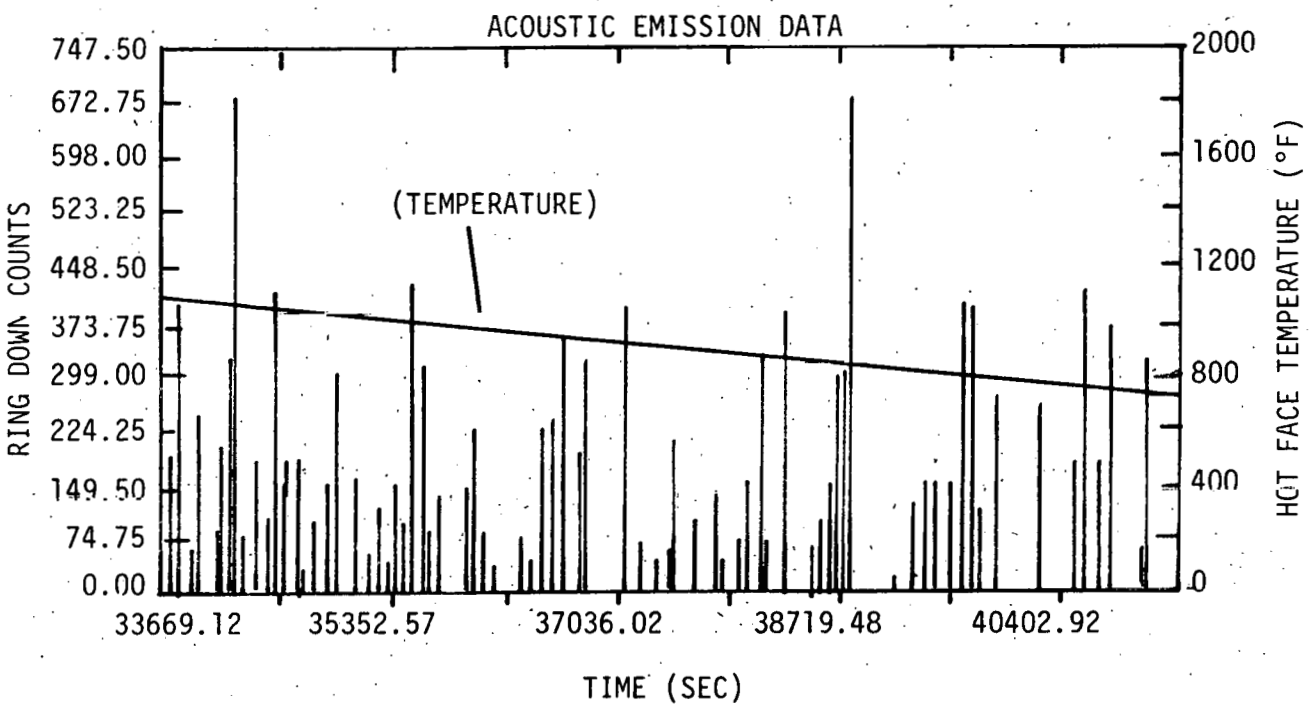

FIGURE 33. AE Results for CASE I Brick Test - LITECAST (Cont'd).

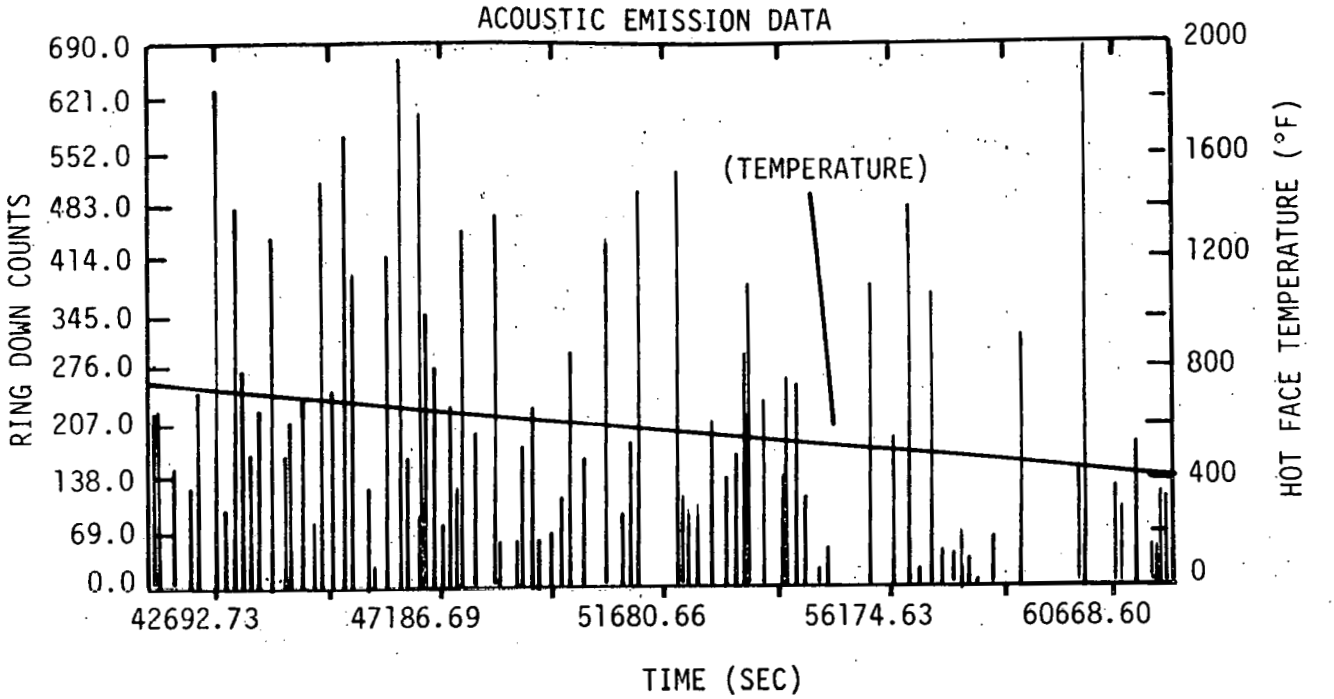

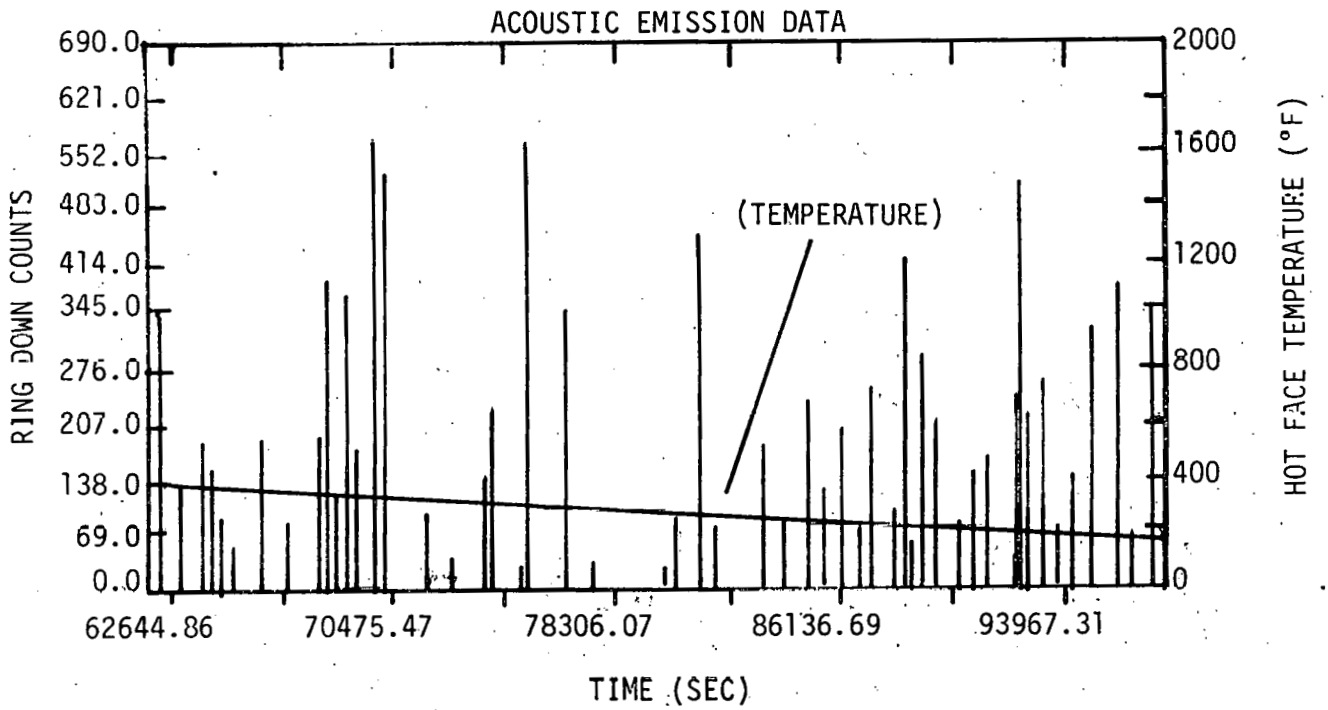

FIGURE 33. AE Results for CASE I Brick Test - LITECAST (Cont'd).

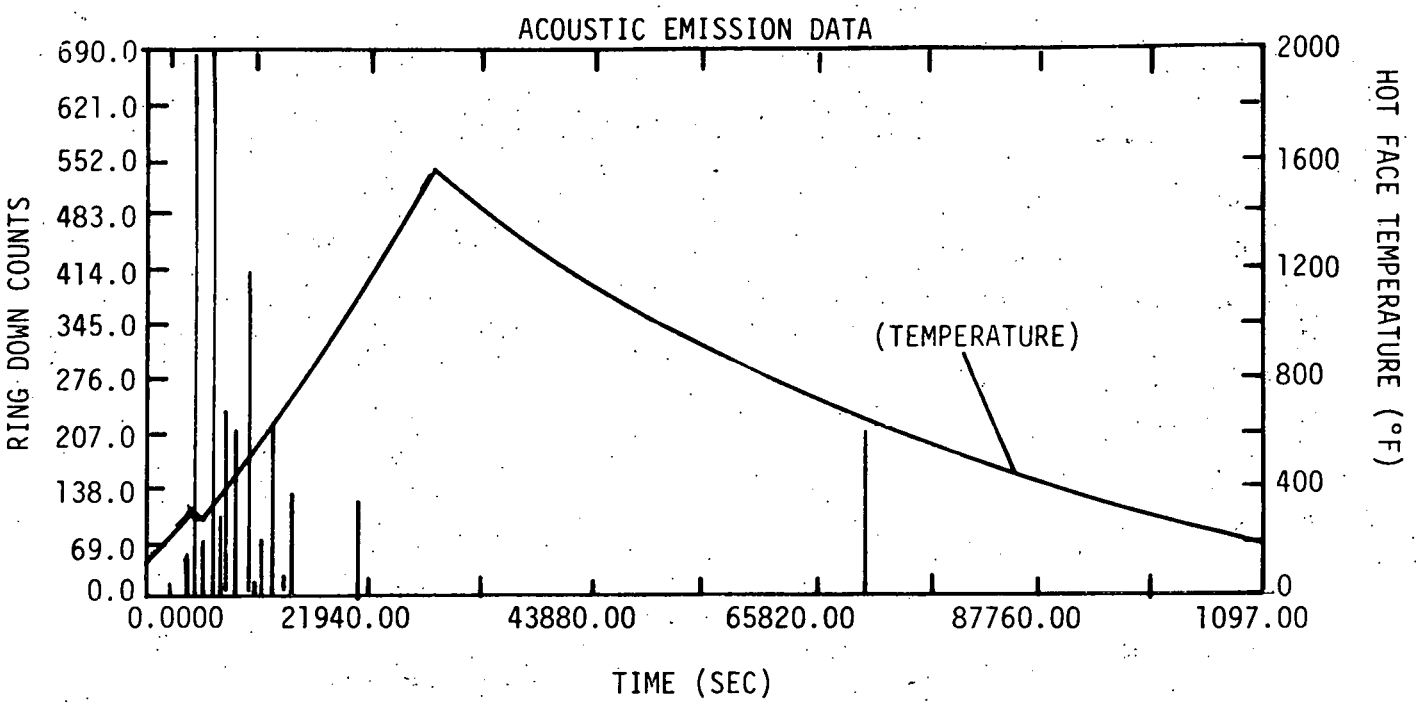

FIGURE 34. AE Results for CASE I Brick Test - ERDA 90.

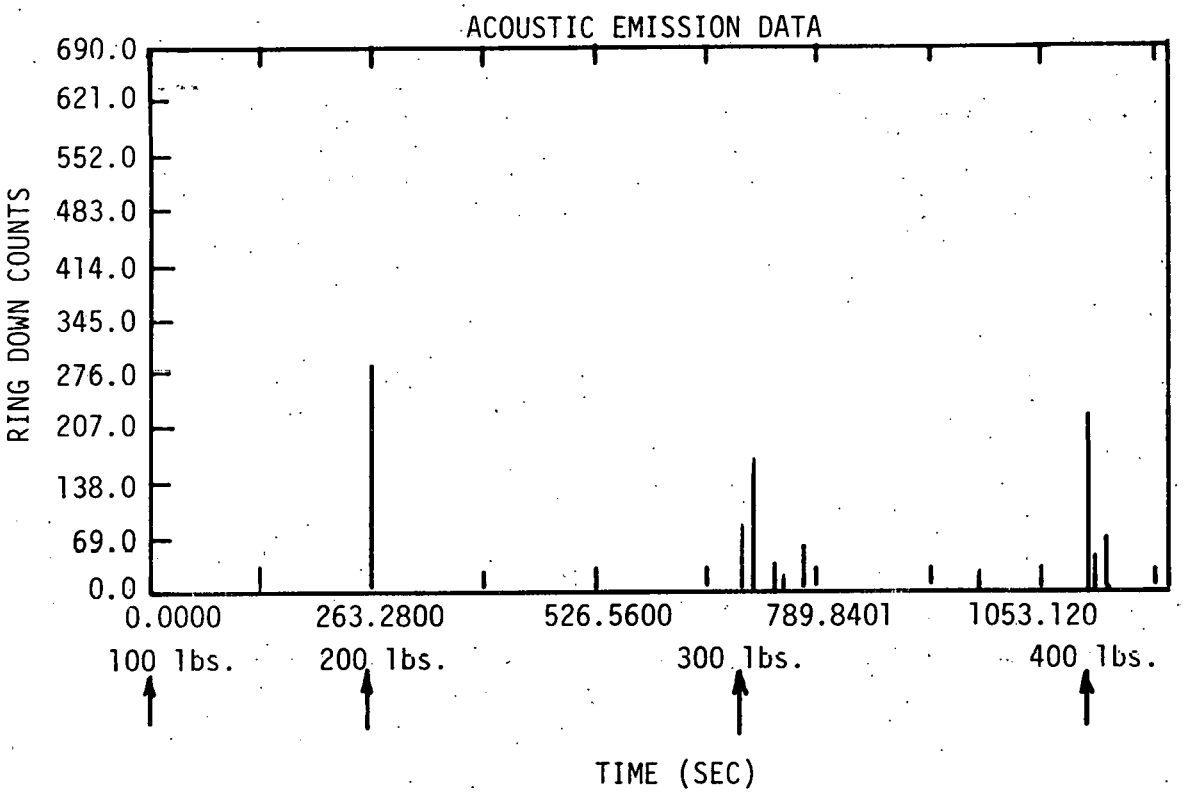

FIGURE 35. AE Results for CASE II Brick Test - LITECAST.

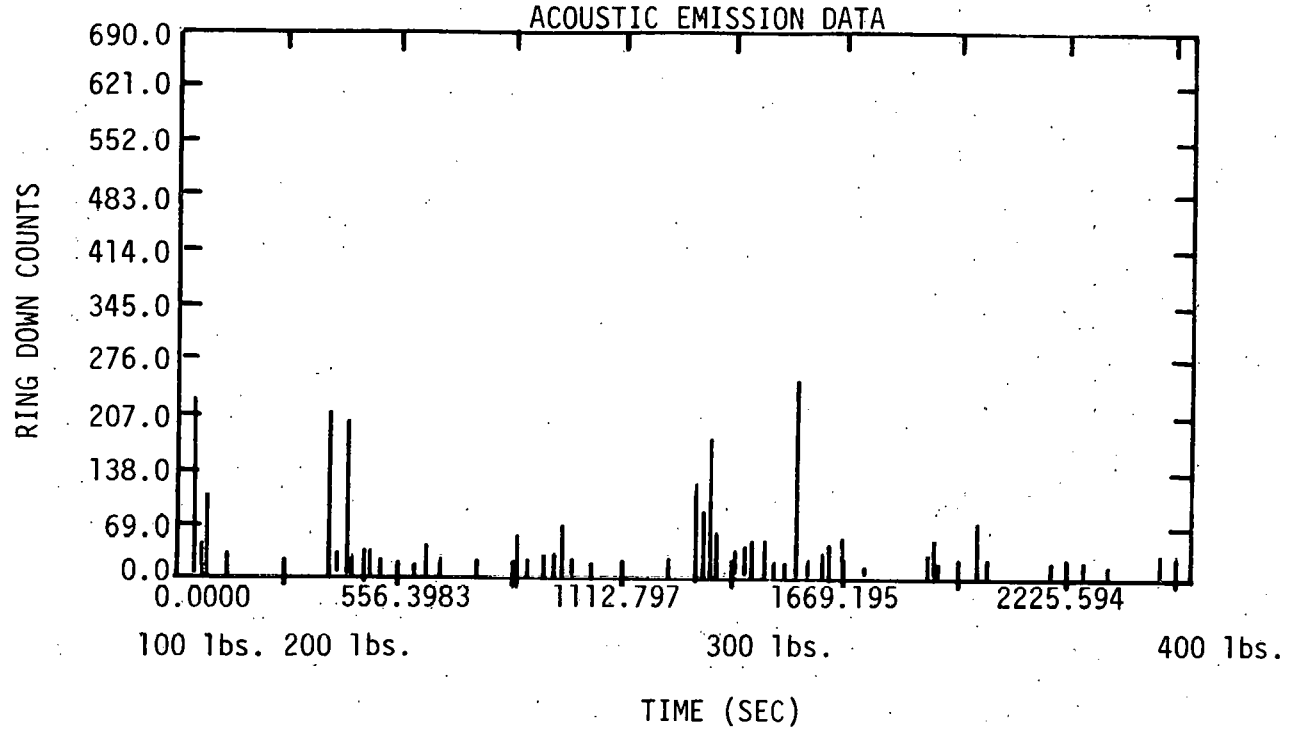

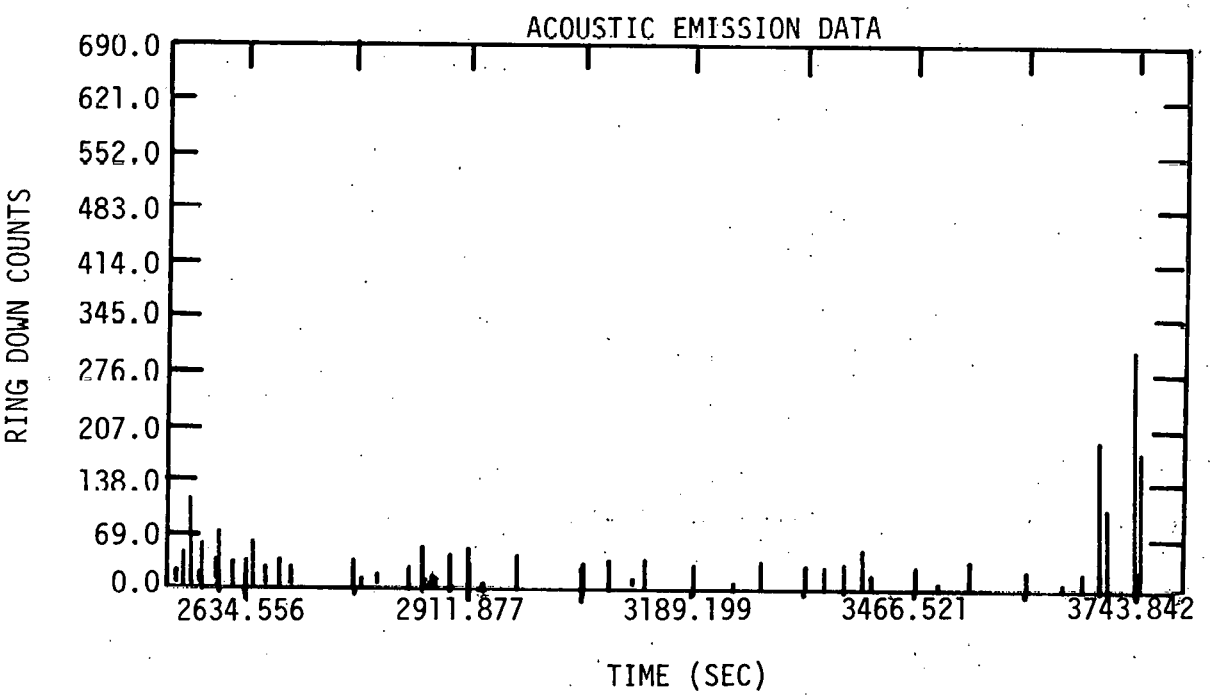

FIGURE 36. AE Results for CASE II Brick Test - ERDA 90.

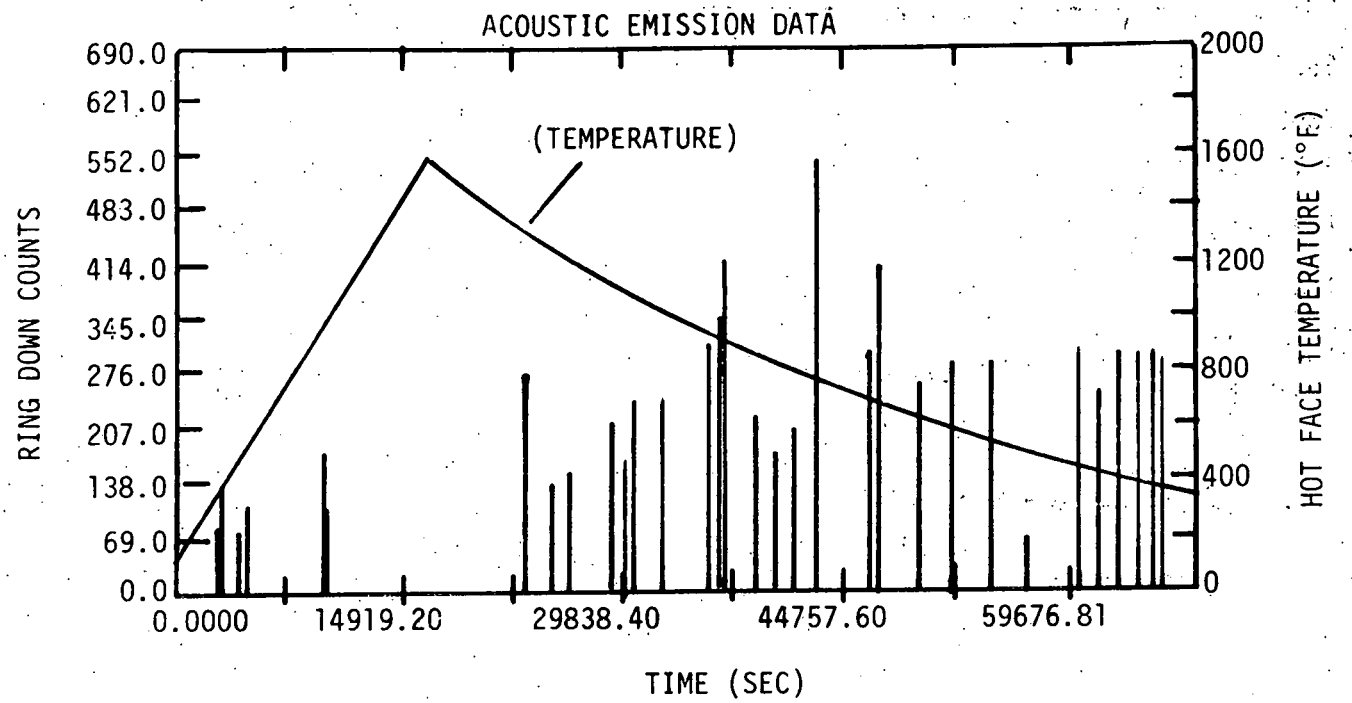

FIGURE 37. AE Results for CASE III Brick Test - LITECAST.

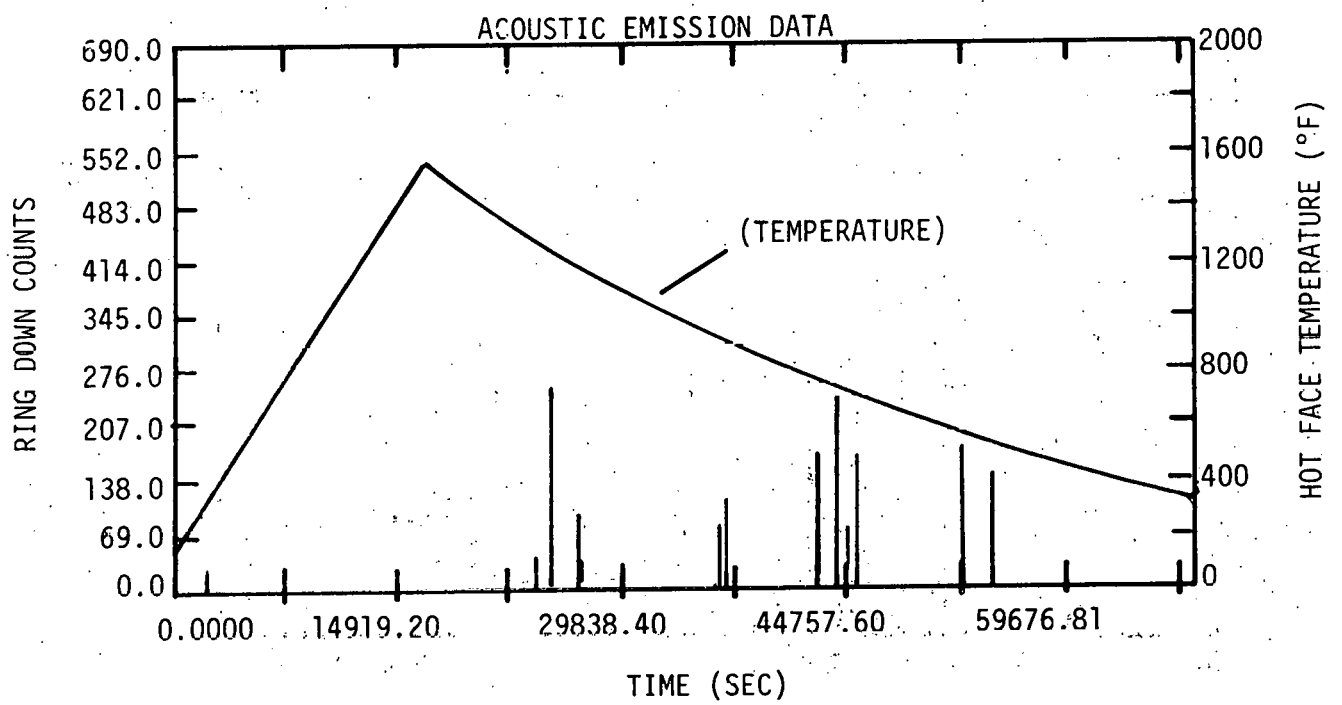

FIGURE 38. AE Results for CASE III Brick Test - ERDA-90.

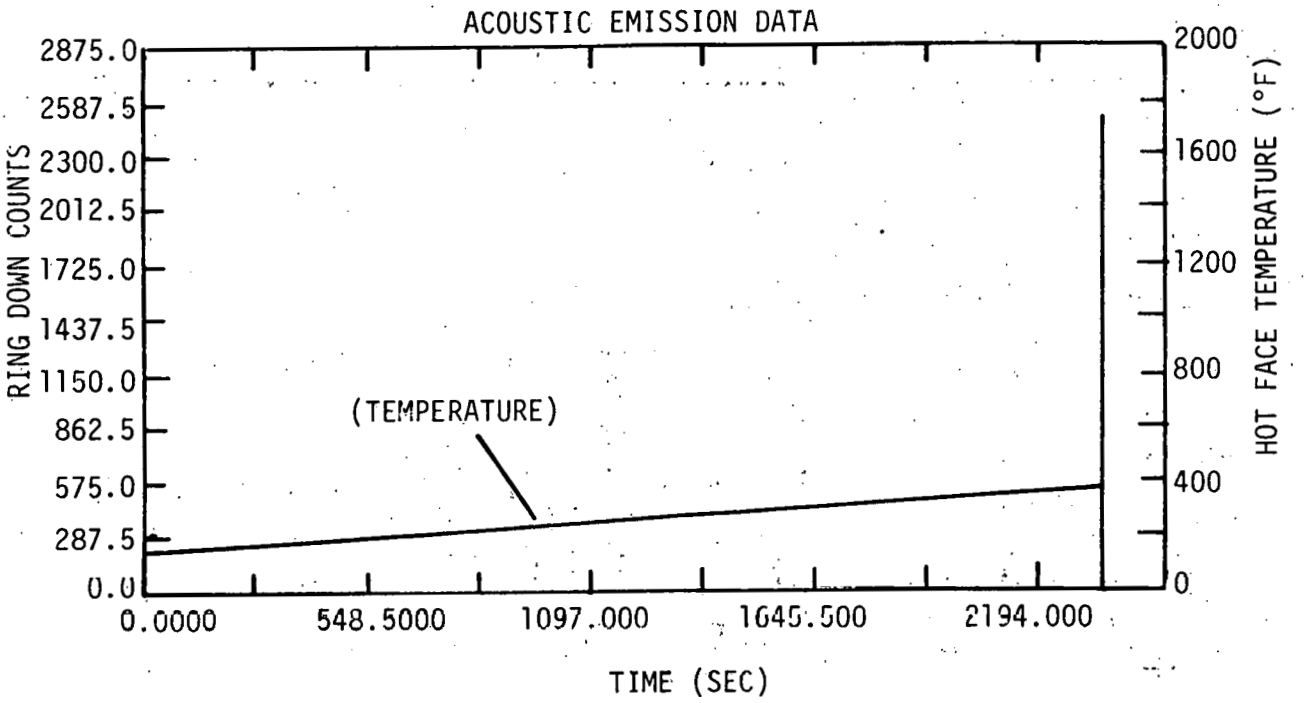

FIGURE 39. AE Results for CASE IV Brick Test - LITECAST.

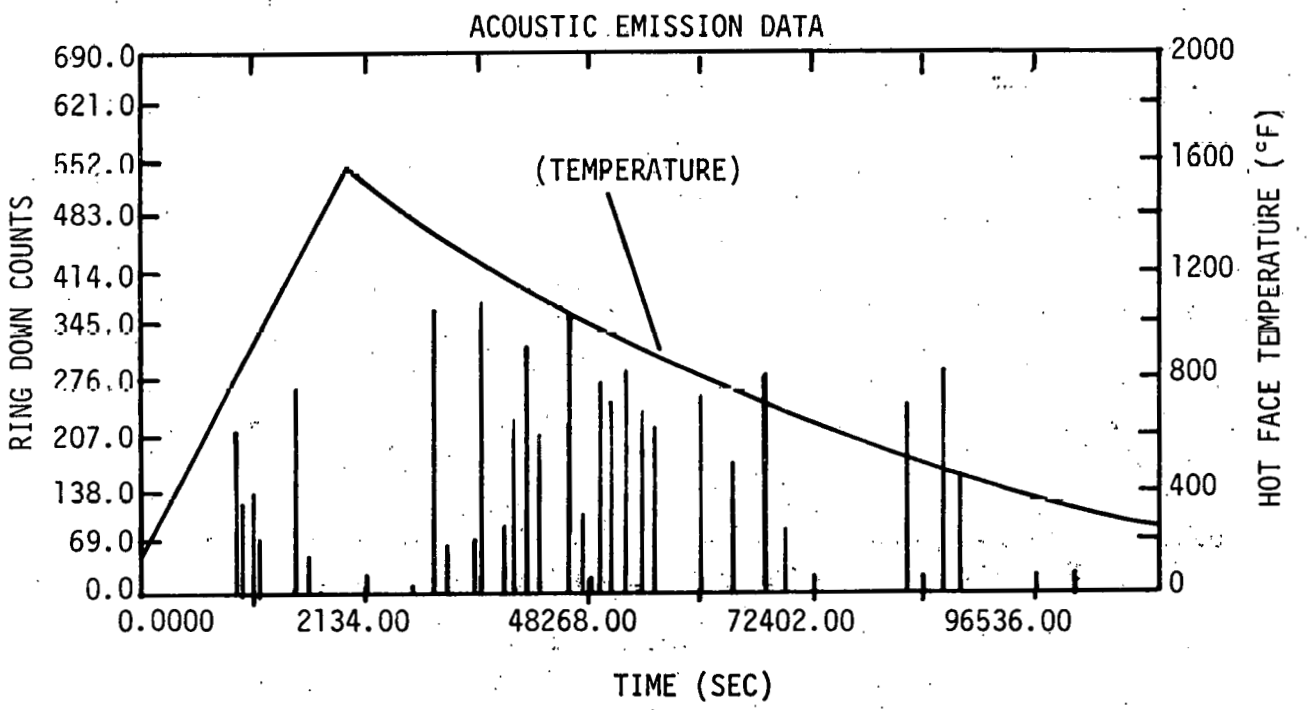

FIGURE 40. AE Results for CASE IV Brick Test - ERDA-90.

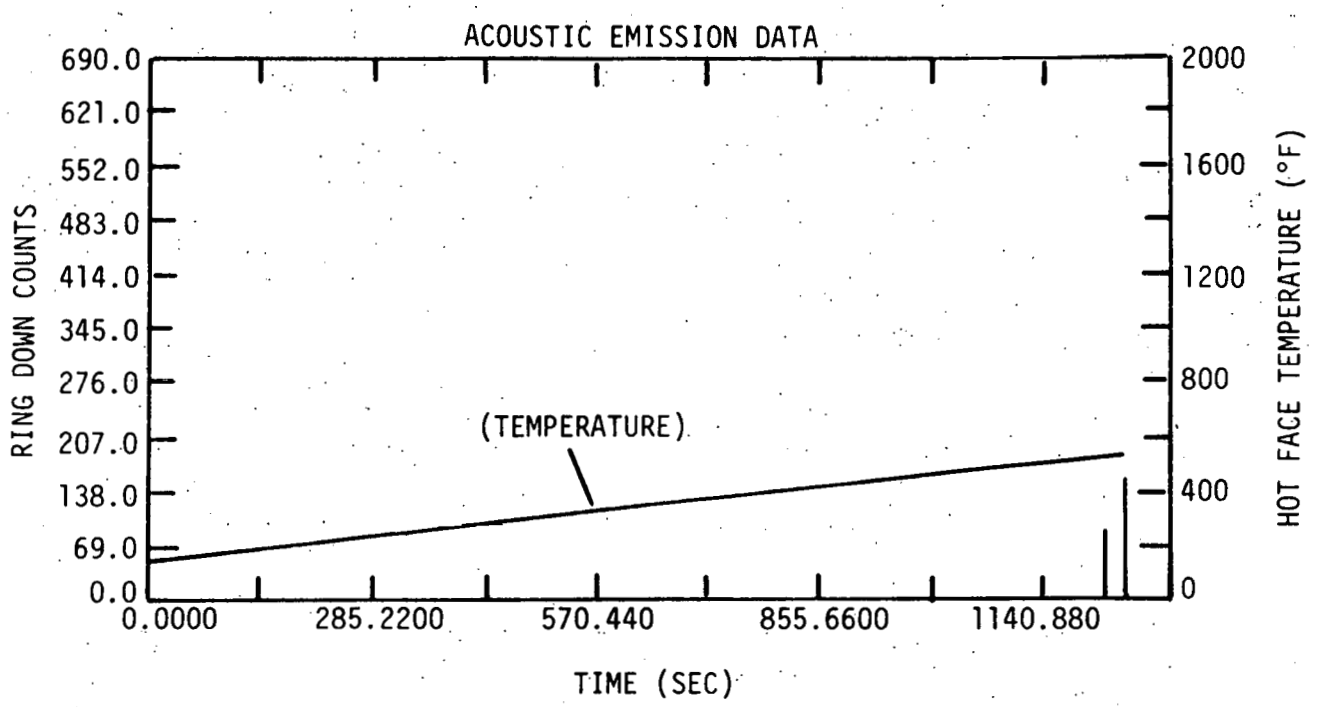

FIGURE 41. AE Results for CASE V Brick Test - LITECAST.

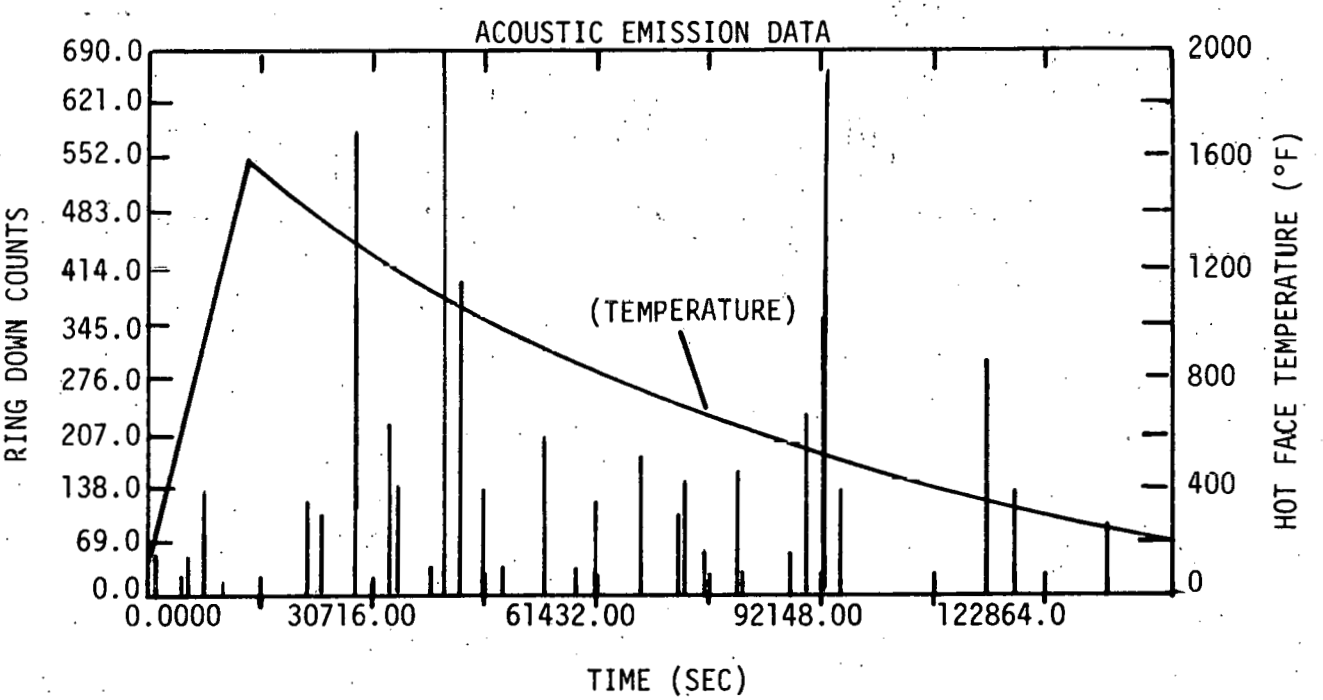

FIGURE 42. AE Results for CASE V Brick Test - ERDA-90.

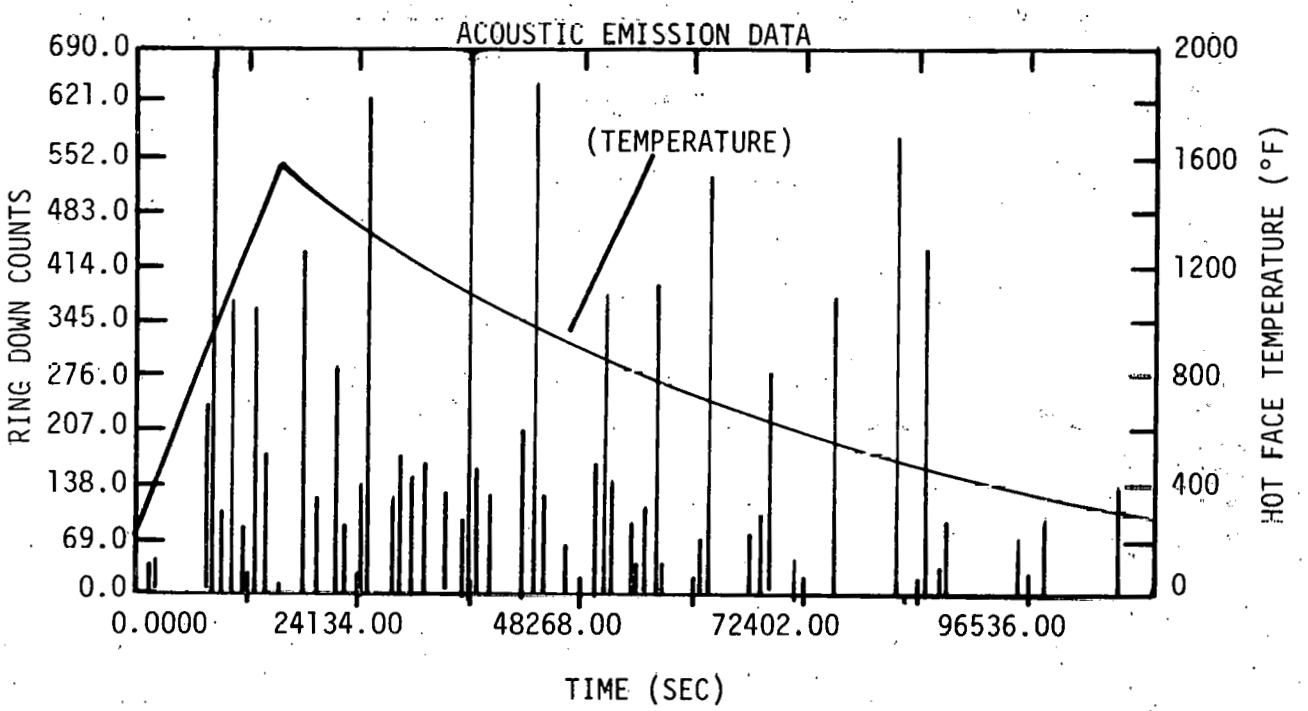

FIGURE 43. AE Results for CASE VI Brick Test - FRDA-50.

During the course of these small scale brick tests, three LITECAST samples failed (broke in half) prematurely. This limited the amount of correlation that could be drawn from the scheme outlined by the various test cases. A number of observations were made, however, which do lend supporting evidence that the AE detected from these samples was directly related to their tendency to crack. These observations are listed as follows:

- The surfaces of the mechanically loaded and heated specimens showed more evidence of cracking when compared to those that were not. The corresponding AE responses monitored from those specimens also tended to have greater numbers of occurrences and greater Relative Energy per Event than non-loaded samples. (Case IV vs. Case I, Case V vs. Case III).

- LITECAST samples' surfaces cracked more than ERDA 90 samples under the same test conditions. The AE from LITECAST bricks in general was more frequent and of higher energy than corresponding ERDA 90 tests.

- LITECAST samples subjected to combined mechanical and thermal load had a greater tendency to fail catastrophically than corresponding ERDA 90 samples. Three LITECAST bricks broke in half while none of the ERDA 90 bricks had surface cracks greater than 1/2". Moments prior to the catastrophic failures, the AE Relative Energy per Event increased rapidly until failure occurred. These responses were similar to panel tests that failed by explosive spalling. (Cases II, IV, and V - LITECAST).

- The ERDA 50 specimen (Case VI) produced similar numbers of high energy events at corresponding times in the thermal cycle as the ERDA 90 specimen in Case V. The ERDA 50 sample, however, had a significant amount of lower level activity not detected in the ERDA 90 test. This low level activity was similar in nature to LITECAST responses, especially during cooldown. There was not a significant difference in the surface crack patterns on the ERDA 50 and ERDA 90 samples.

- Samples that were AE monitored through a complete temperature cycle (heat-up and cooldown) attained a quiescent state (little detected AE activity) at elevated temperatures. This suggests that the materials became less brittle and therefore had less tendency to crack from induced stresses. The specific temperatures at which quiescence occurred varied several hundred degrees depending upon each sample's particular load and thermal stress state. On the average the quiescent state began at 1000 - 1100^{o}F hot face temperature upon heat-up, and ended at 1200^{o} - 1300^{o}F on cooldown.

2.6. Experimental Procedures - Lining Tests

The sections which follow describe the equipment, the refractory installation procedures, the instrumentation techniques, the post testing procedures and other miscellaneous techniques employed to perform the lining tests.

2.6.1. Test Facility

Pressure Vessel

A pressure vessel was designed by Babcock & Wilcox and built by Chattanooga Boiler and Tank (CB&T), Chattanooga, Tennessee under a subcontract. The vessel was delivered to and installed at the Babcock & Wilcox Lynchburg Research Center in March 1977. Figures 44 and 45 show, respectively, a schematic of the vessel as planned and a photograph of the vessel as delivered.

The vessel is oriented in a vertical position. The overall height of the three sections is approximately 14 feet. The vessel is 5 feet in inside diameter. The complete assembly is supported by columns affixed to the bottom head. The vessel is made of carbon steel since no extremely corrosive atmospheres were scheduled to be tested. The top and bottom dished heads and the cylindrical center section are flanged. This permits the furnace vessel to be easily taken apart. The top head weighed 3580 lbs., the center section weighed 10,660 lbs. and the bottom head with support legs weighed 4475 lbs. When the three flanged sections are attached, the test furnace facility can be operated at up to 250 psig and shell temperatures of 650°F. Both compressed asbestos and FLEXITALLIC* gaskets of 1/8 inch thickness were used to seal the vessel flanges. The vessel was built according to Section VIII, Division I of the ASME Code and has a U code stamp. To meet this code, the vessel was instrumented with a consolidated (Dresser Industries) 250 psig pressure relief valve rated at 1284 lb/hr of saturated steam and with a one inch diameter nickel rupture disc rated for 287 psig burst pressure at 72°F and 253 psig burst pressure at 450°F. The vessel was also designed with a steam trap, special sight glass and a pressure/steam venting system. The steam trap was made by Wright-Austin and had a 0-350 psig operating range and a one quart storage capacity. Pre Sure Products Co., high pressure high temperature sight glasses, model "A," were used on the sight ports in the bottom head of the vessel and were rated for 250 psig. The pressure steam venting system was designed to vent pressurized gases out of the test bay in the event the vessel operating pressure was exceeded. This system was combined with the pressure relief and rupture disc systems.

The bottom head contained flanged viewports set at skewed angles to the radius (Figure 46) to permit visual observations of the interior surface of the lining during testing. Additional penetrations were located in the top and bottom heads to accommodate strain gage leads, thermocouple leads, atmospheric control connections, and pressure gages. The cylindrical test section which contains the refractory lining had nozzles for strain gage and thermocouple leads, penetrations for electrical connectors, external mounts for acoustic emission antennas, and brackets for pneumatic vibrators. A second identical

*FLEXITALLIC is a registered trade name of Flexitallic Gasket Co., Inc.

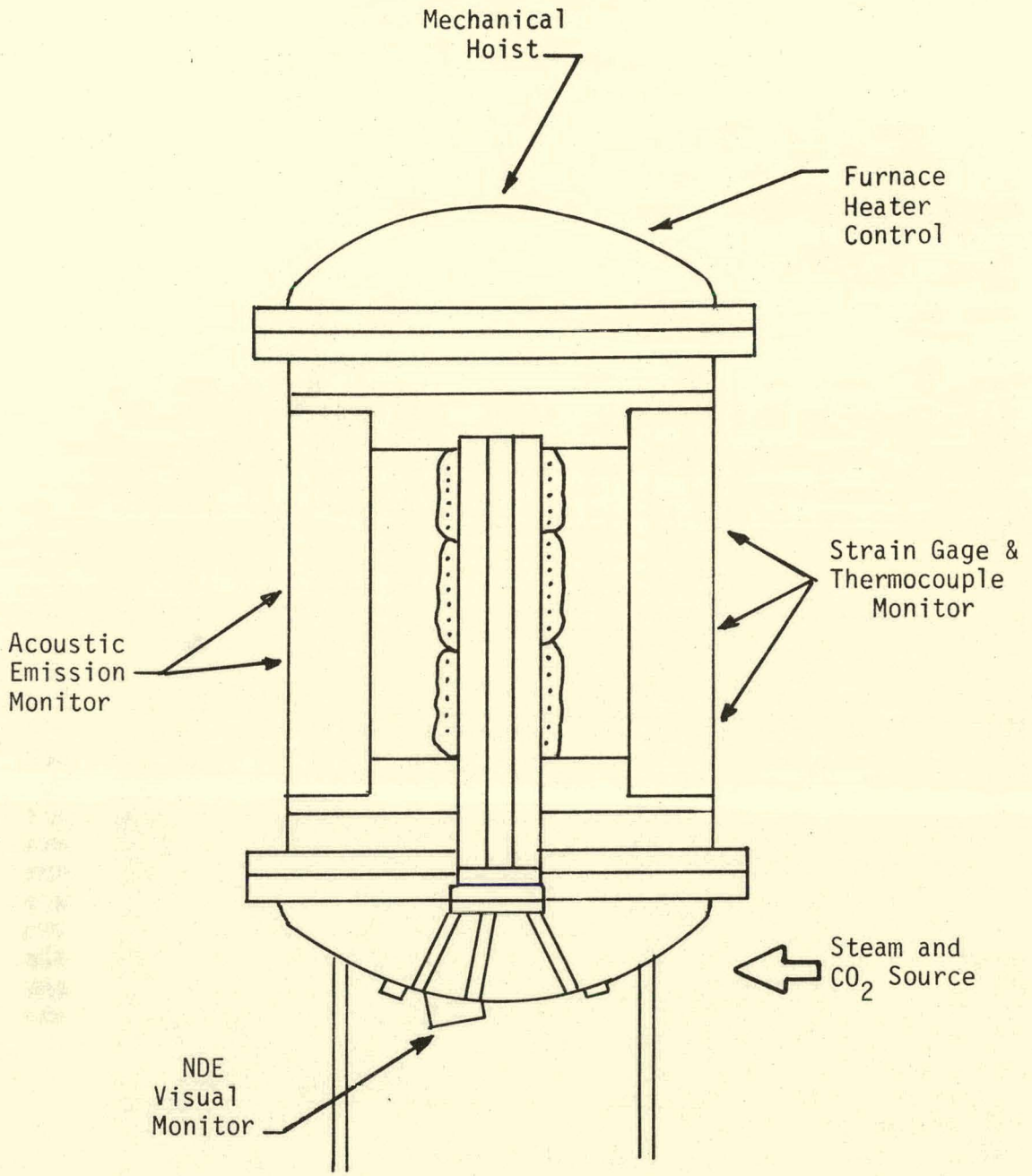

FIGURE 44. Schematic of Overall Test Facility Lay-out For Heating and Cooling Refractory Linings.

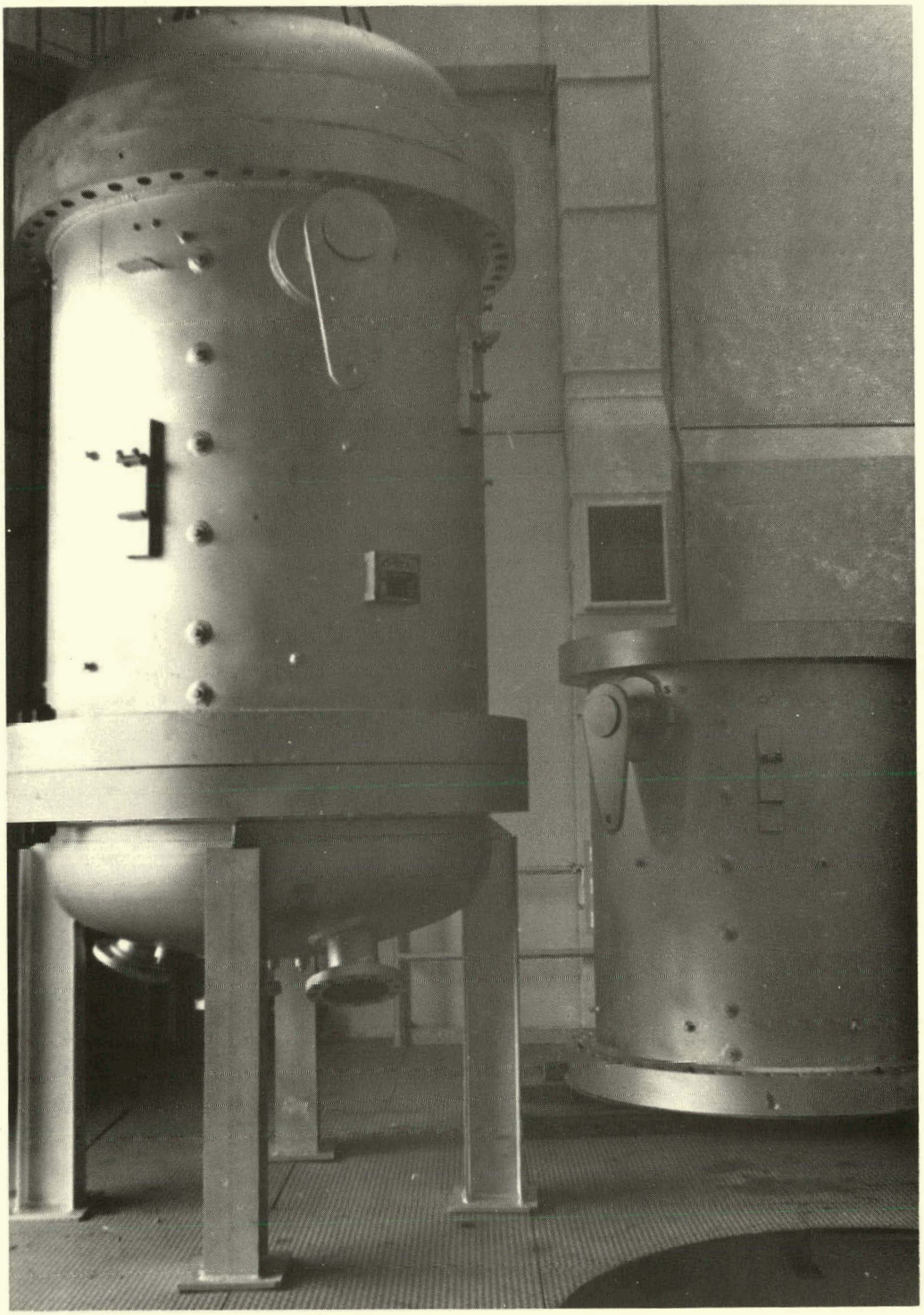

FIGURE 45. Assembled Three-Part Pressure Vessel/Test Furnace (14 ft. x 5 ft.) and Extra Center Section.

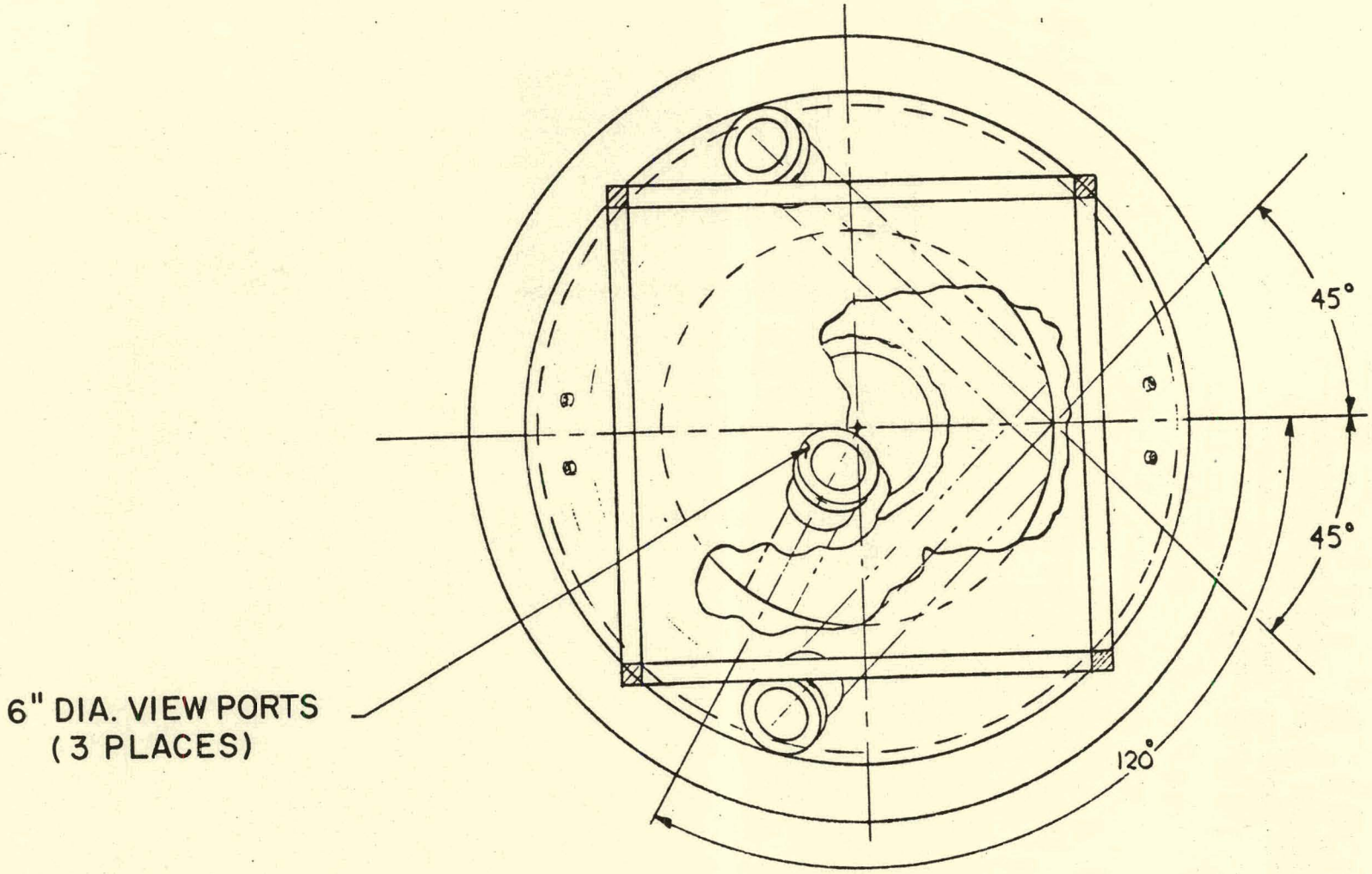

FIGURE 46. Location of Viewports and Support Columns on Bottom Head of Pressure Vessel.

cylindrical test section was made to facilitate the schedule for testing and data collection.

As shown in Figure 47, the test section had heavy duty hex nuts welded to the inside surface at 6 inch spacings for attachment of metal anchors at various spacings. The vessel design required that any and all openings or attachments anticipated during the entire testing program which required welding, be made before hydrotesting. This was done because any welding done after receipt of the vessel would invalidate the code stamp.

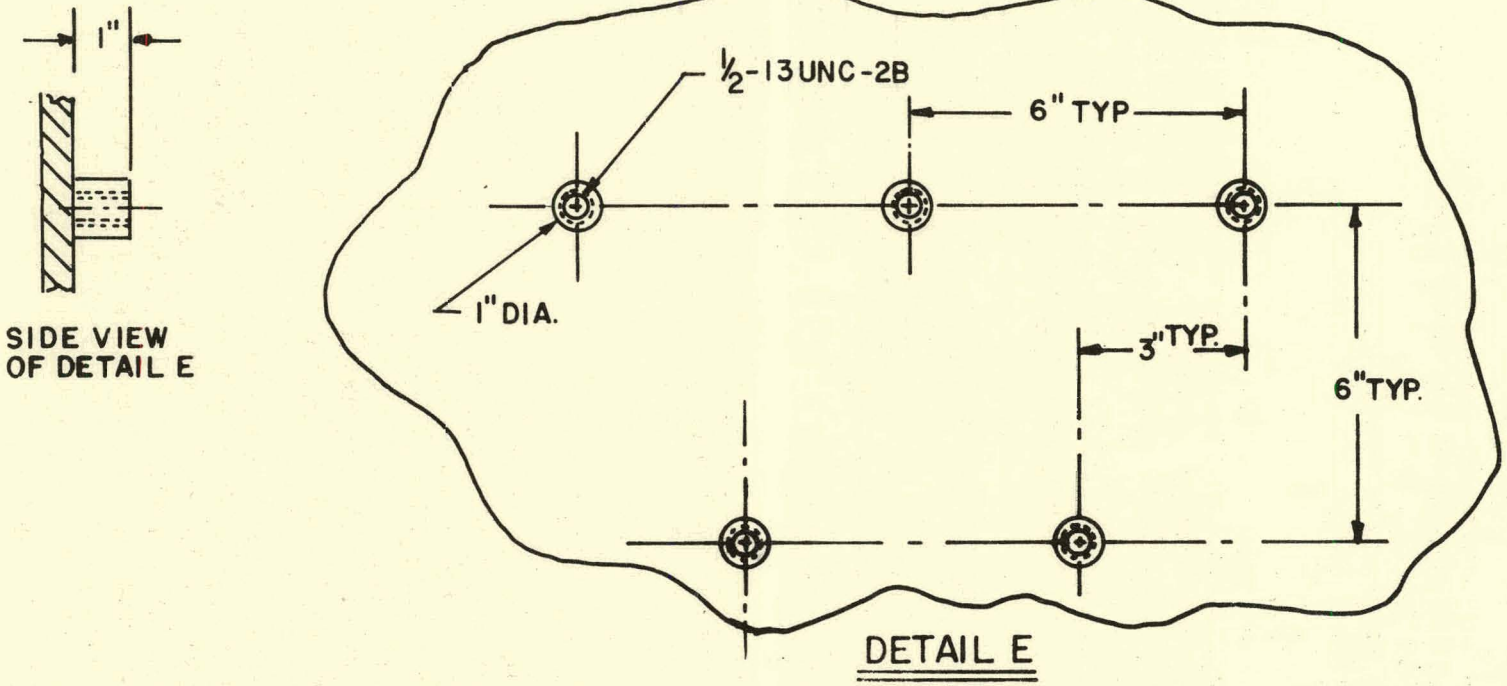

FIGURE 47. Spacing of Anchor Receptacles on Inside of Pressure Vessel Wall.

The only significant change made from the initial design was related to the shell wall thickness of the center section. The shell thickness was originally designed to be 5/8" but when initial analyses were started on the refractory liner-shell interactions with the ID finite element stress analysis model developed, much higher hoop stresses (35,000 psi) than those originally anticipated were indicated. These stresses are generated primarily from the greater thermal expansion of the refractory liner than the shell at 2000°F hot face temperature. When they are analyzed as radial stresses, they are equivalent to an internal shell pressure of > 500 psig. Since the vessel was originally designed for 250 psig gas pressure and 400°F shell temperature capability and with no significant refractory-metal shell interactions using the Section 8, Division I of the ASME Code, this additional pressure (radial stress from the refractory liner expansion) was expected to make the shell thickness marginal. A shell thickness of about one inch was considered necessary to reduce these stresses. When this information was combined with the fact that many pressure vessels associated with high BTU gasifier pilot plants had shell thicknesses of 1 to 2-1/2 inches, a decision was made to increase the center shell thickness to 1-1/8 inch. This thickness was the upper limit that CB&T could roll and gave a pressure vessel shell that was safely hydrotested to approximately 375 psig.

Test Zone and Sensor Placement

The middle five feet of the seven foot high center shell was to be covered with refractory material. The remaining one foot adjacent to each flanged end of the center section was not to be lined. The refractory was installed as a continuous lining. A 4 foot test zone was centrally located in the vessel with an additional 6 inches on the top and bottom to allow for thermal gradient effects from the heating element. Only the central 4 foot region was to contain monitoring devices and be evaluated for the test parameters.

Insulation of Test Zone

The 6 inches of extra lining on each end of the test section and the 1 foot of unlined shell adjacent to each end was for the purpose of reducing temperatures at the end of the test furnace chamber. A thermal barrier system consisting of nine inches of ceramic fiber blanket in a circular configuration that fit tightly inside the top of each lining was used to reduce the temperature sensed by the flanges and the dished heads. The blanket was held in place on Inconel 601 studs by Inconel 601 washers over ceramic washers.

Under ambient pressure conditions the head temperatures did not exceed 250-260°F with the hot face at 2000°F. This helped maintain temperature uniformity of ±20°F wanted in the 4 foot test zone. This insulation could be removed and reused for other tests. A picture of this insulation scheme is shown in Figure 48. Additional reflectance type insulation was considered for the top insulation if a chimney effect became a problem. Line-of-sight holes were made in the lower insulation to permit the illumination and viewing of the hot face of the lining through the sight ports.

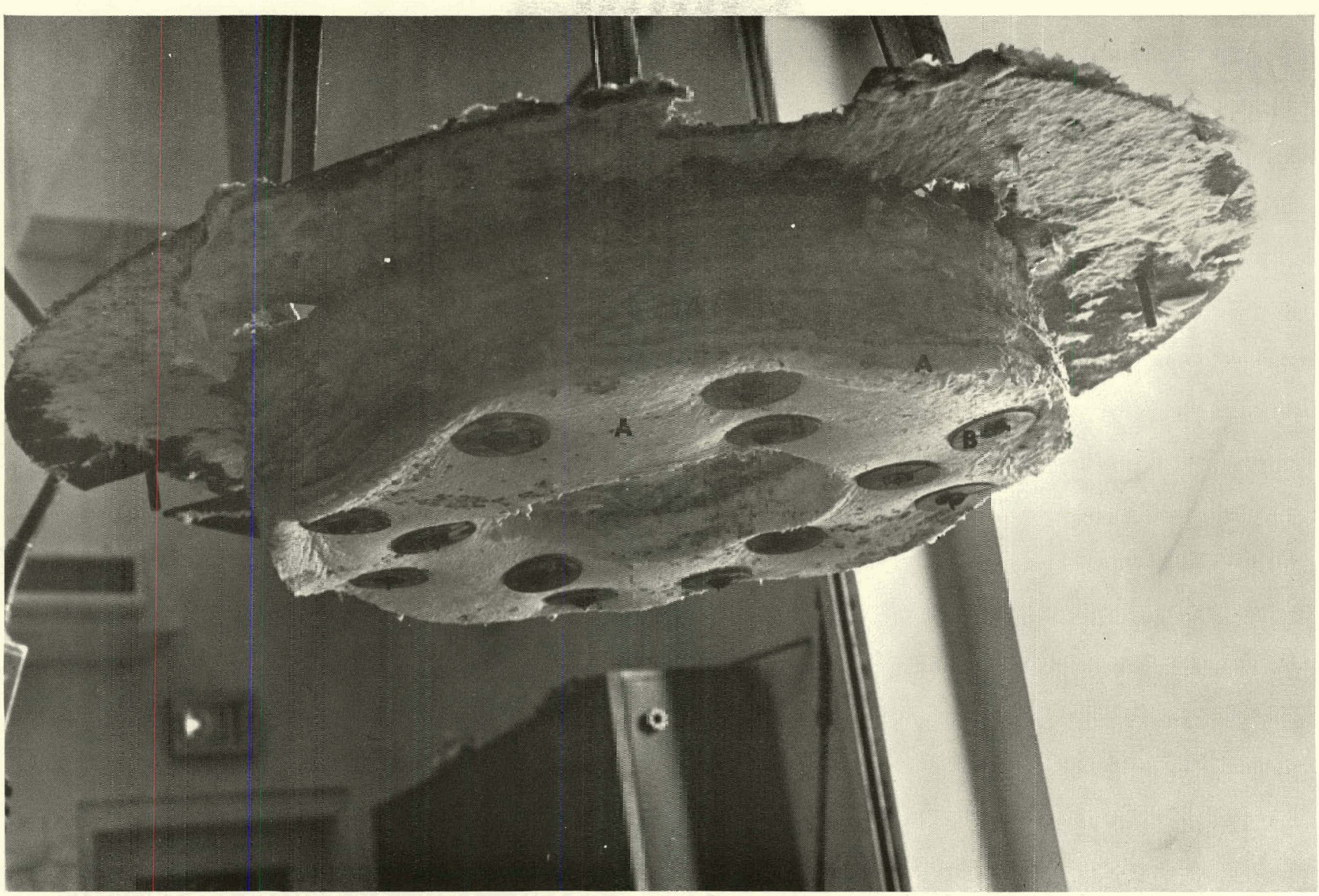

FIGURE 48. View of Upper Insulation after Removal From Lining #4 Test to 1850F with Steam. Ceramic Fiber Blanket (A) is Held in Place with Ceramic and Inconel 601 Washers (B) Over Inconel 601 Studs

Vertical Restraint of Test Linings

The refractory lining is restrained in the vertical as well as other directions by the presence of anchors and to a lesser degree by its own weight. Additional restraining in the vertical directions was accomplished by the use of reinforced metal "L-shaped" angles which would restrain the top stabilizer ring plate as shown in Figures 49 and 50. Its basic design is as follows: short, open ended U-shaped metal plates were welded onto the side of the shell. The top stabilizer ring had notches at specifically spaced locations on the perimeter which permitted the ring to slide down past the properly spaced welded restrainer support plates. Once in place the stabilizer ring was rotated a few degrees. The metal angles were then slid in between the shell and the welded retainer support plates. Threaded bolts tightened these metal angles against the shell wall so they could not move. This configuration allowed the refractory lining to be cast without any extra anchors or metal rings at the top end. It also permitted flexibility for ease of installation and removal of the lining. Figure 51 shows the restraining ring in position in Lining #1. The first test to 1200°F indicated this ring plate worked, but a test to 2000°F resulted in the upward warpage of the inner 5 inches of the ring. The ring was therefore remade with twice the thickness (1 inch) of the first plate and did not warp in future tests.

Control and Monitor of Test Facility

The test facility includes the pressure vessel, heating unit control, strain gage-thermocouple monitor, acoustic emission monitor, NDT camera monitor, steam generator, CO_2 tanks, pressure monitor, crane assembly and other supporting equipment for lining installation and data collection. Bottled CO_2 was used when a CO_2 atmosphere was required. When a steam atmosphere was required, a steam generator with 150 psig capability was used. The steam was injected into the vessel through a distribution ring arranged as shown in Figure 44 to evenly expose the lining to steam. Two separate computer data acquisition systems which were housed in an isolated room built for monitoring instrumentation on the vessel and control of the pressure vessel/test furnace during heat-up and cool-down cycles were used. Photographs of this control and data acquisition equipment are shown in Figures 52-54.

Transporting of Test Section

In cases where the lined test section had to be moved, the introduction of cracks in the lining due to distortion of the shell were prevented by the use of external lifting supports at the flanges and by the use of internal ring plates. In addition the shell was designed to have sufficient thickness to minimize distortion of the steel wall during lifting and movement by the overhead crane. Internal ring plates fabricated to the necessary tolerances but not welded to the shell, as shown in Figure 49, were used to insure dimensional stability of the refractory lining during installation (both with and without anchors).

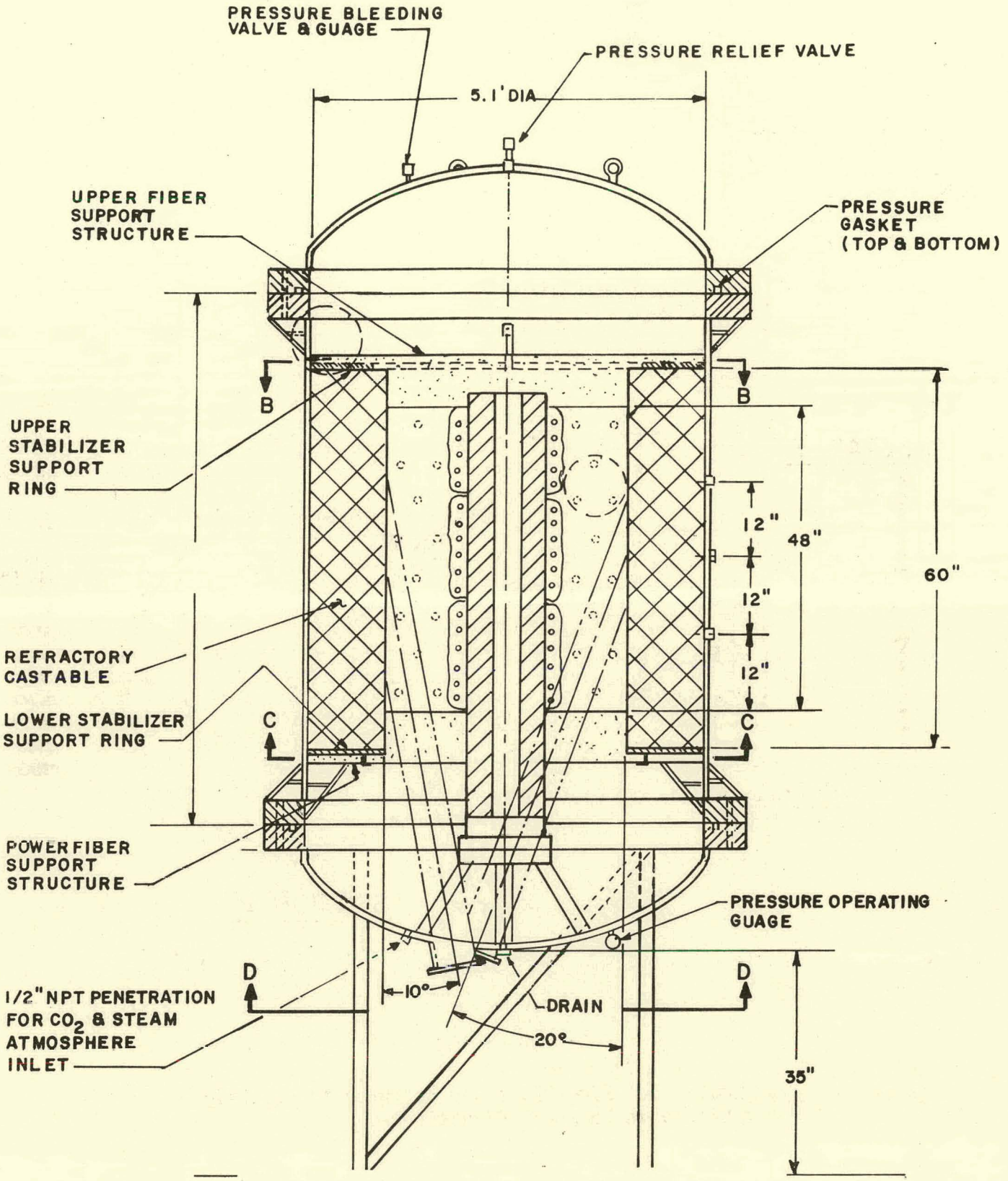

FIGURE 49. Engineering Drawing of Pressure Vessel/Test Furnace.

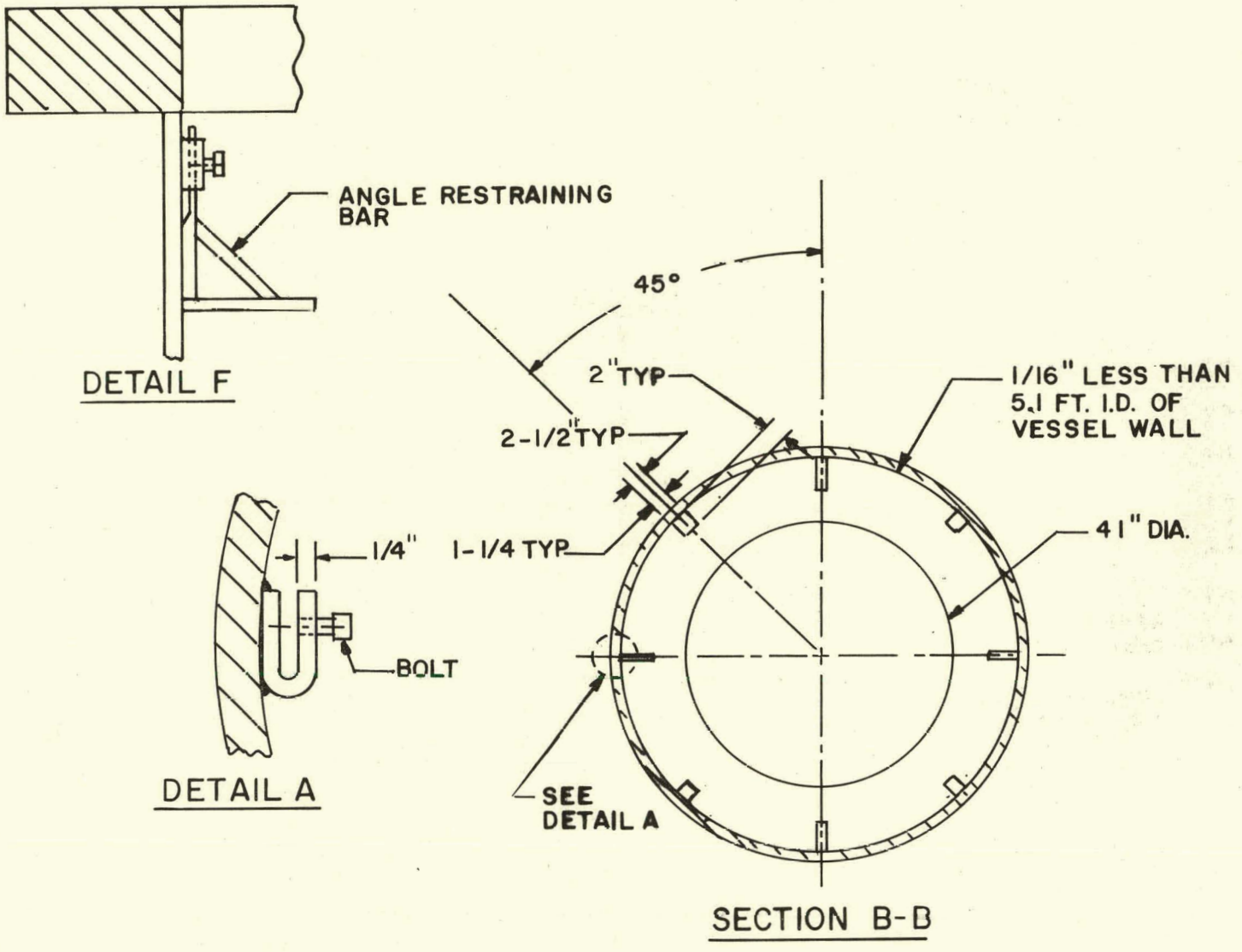

FIGURE 50. Top Stabilizer Ring Plate and Hardware to Restrain Cast Lining in Vertical Direction.

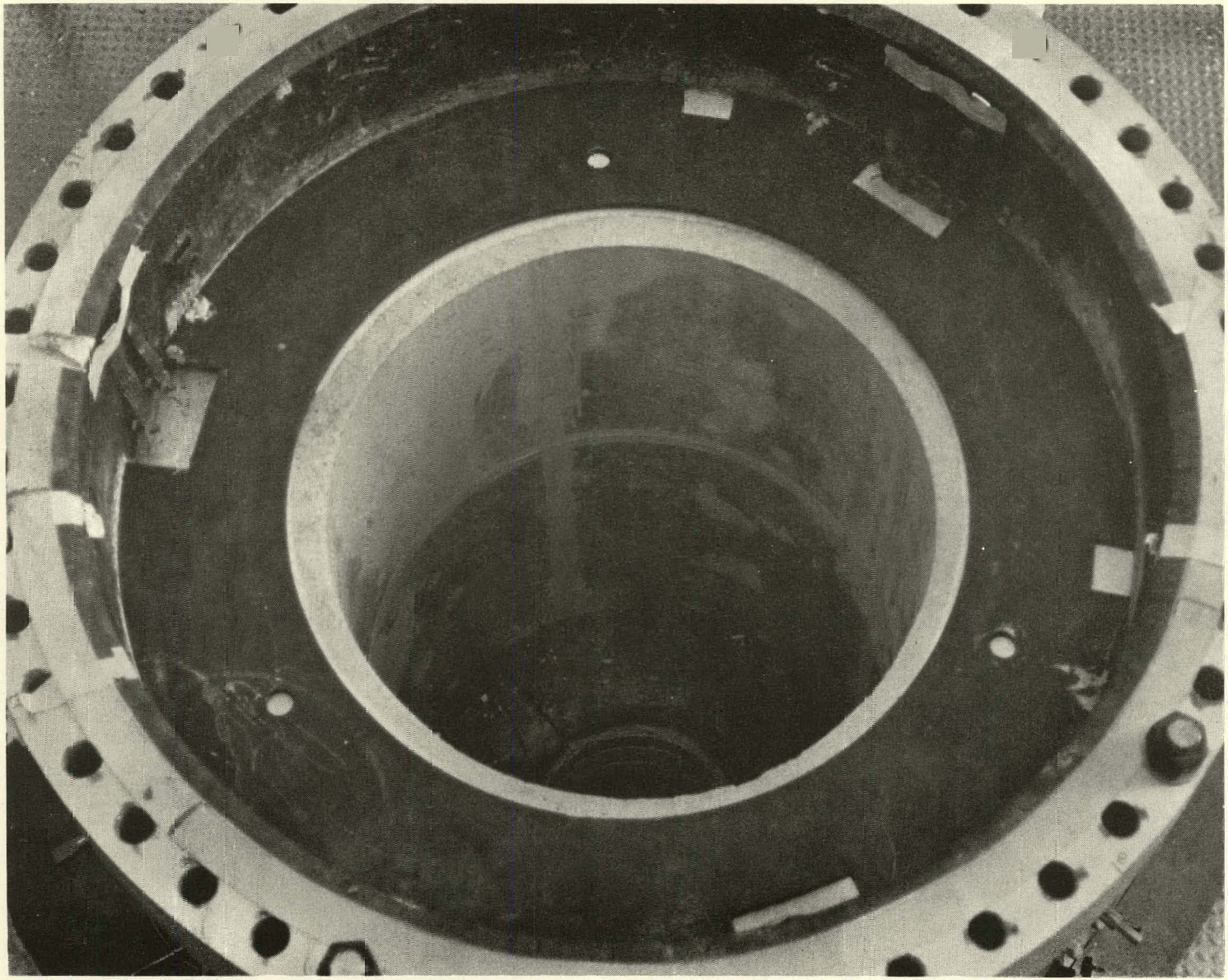

FIGURE 51. Top View of Lined Vessel With Upper Stabilizer Ring Plate Installed to Restrain the Lining in the Vertical Direction.

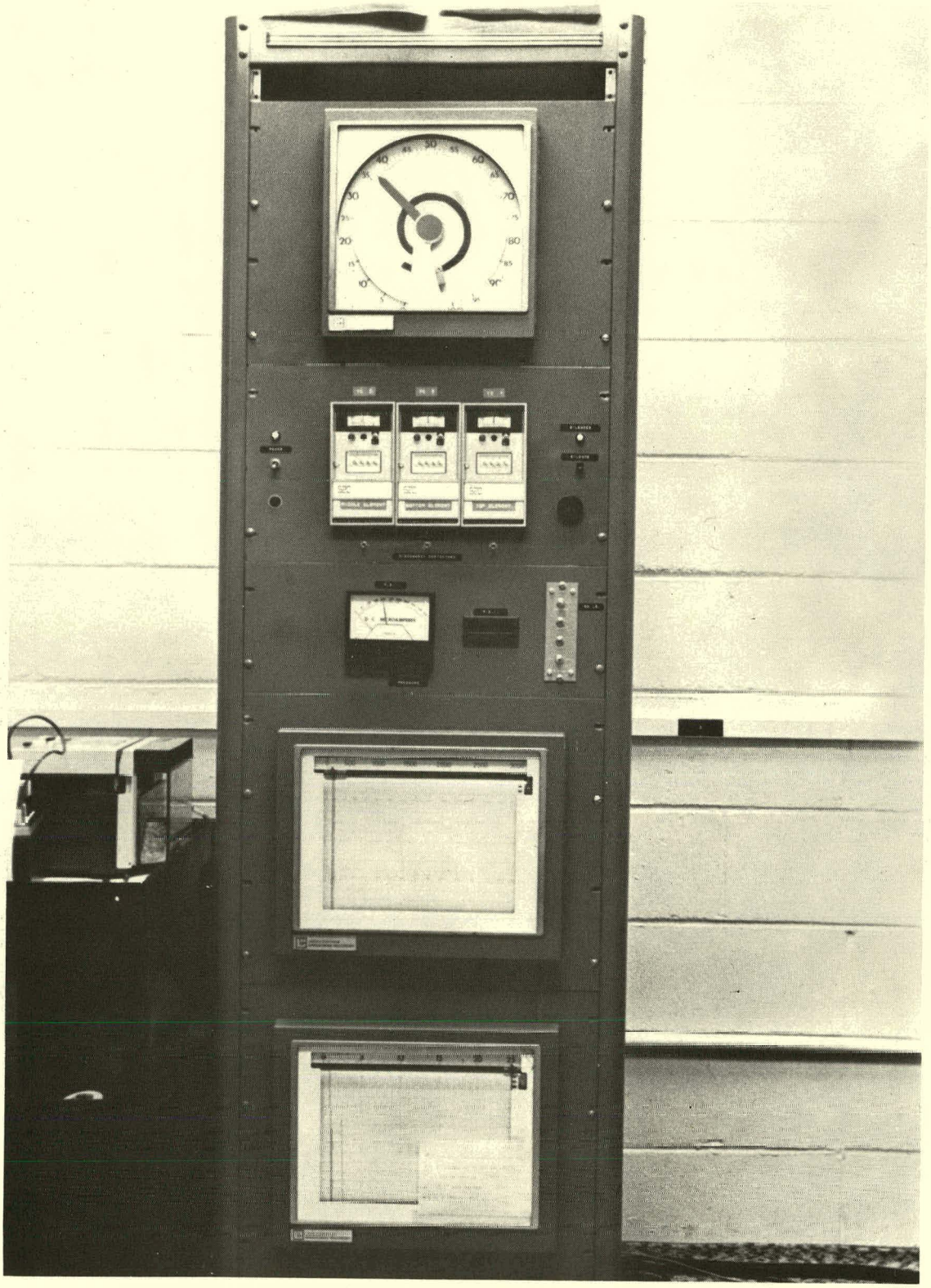

FIGURE 52. Furnace Control.

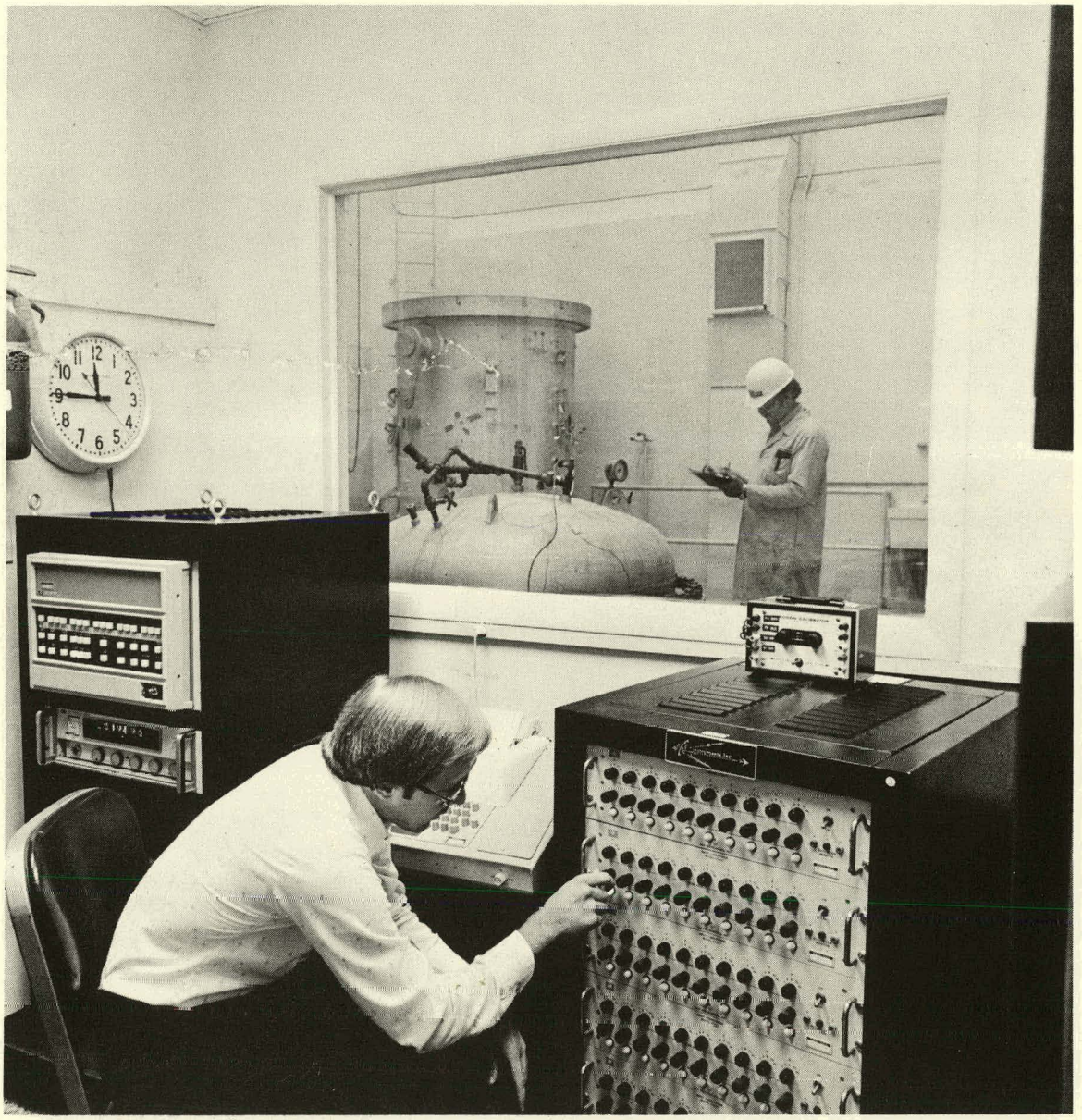

FIGURE 53. Thermocouple, Strain Gage, and AE Data Acquisition System.

FIGURE 54. AE Data Acquisition System.

Furnace Heating Element

Heating the "hot face of the refractory lining was accomplished by radiant heating using a multizone externally wound electric resistance wire element fabricated by Electro-Applications, Inc., Washington, PA. Figure 55 schematically illustrates the configuration and location of the heating element assembly. The element was capable of supplying 80 KW of heat, a hot face temperature at 2000°F and a 300°F/hr. heating rate. It could maintain a ±20°F from nominal hot face temperature over a 4 foot zone. Kanthal A-1 resistance heating wire made up the coil of the heater. This was not a stock heater system and was difficult to acquire. A spare element was therefore also acquired.

Figure 56 shows what a heating element looked like when assembled and positioned in the unlined shell after a checkout test. It was designed as a removable plug assembly and was inserted and removed after each separate test. Each zone was 18 inches in diameter, had a 2 inch wall thickness and was 16-18 inches tall. This design permitted the zones to be stacked one on top of the other in a stable manner. The element was covered with a high alumina type cement to protect the metal windings from steam and carbon dioxide environments. The three zone heating element was positioned in the 4 foot test section on a ceramic spacer cylinder and was supported by a metal pedestal that set inside the bottom head. The face of the refractory lining was approximately 9 inches from the heating element surface. The lightweight insulation systems described above helped stabilize and position the heating assembly in the center of the lined vessel.

The leads for each zone are located in the core of the element and are brought out the top of the assembly. After placement into the lined vessel, the six leads were connected to flexible leads which crossed the upper insulation support plates as shown in Figure 57 and exited the vessel through conax fittings near the top of the center section. These leads were then connected to a 230 volt 3 phase transformer and drew up to 100 amperes in their on-off mode of operation. Each zone had its own thermocouple, contactor and Barber-Coleman controller with all three interconnected to the same programmer. When the top head was separated and the leads disconnected, a long rod threaded at one end could be extended down the central opening of the element and threaded into the metal lifting plate underneath the ceramic spacer cylinder. This rod permitted the element to be removed from the vessel with a crane.

Because they were of inferior quality, each as-received assembly required a significant amount of repair to upgrade its integrity. Furthermore, after the initial checkout test of an unlined vessel, the construction of the elements became suspect. This was verified in the first lining test to 2000°F. The Kanthal A-1 wire which was helically wound around each ceramic core, went through an irreversible thermal expansion which caused the cement bond holding the grooved Al_2O_3 spacers to fail. This permitted the wire windings to separate from the ceramic cores and to shift en masse downward. When this happened the bottom winding of the middle heater shorted out with the wire on the bottom heater and caused a termination of the test. This problem is shown in Figures 58 and 59. This problem was corrected by improving the bonding of the windings to the ceramic cores, adding ceramic supports to the Kanthal A-1 strips which were the leads from the winding to the flexible connections and putting ceramic plates between each zone of the heating element. This improved arrangement is shown in Figure 60.

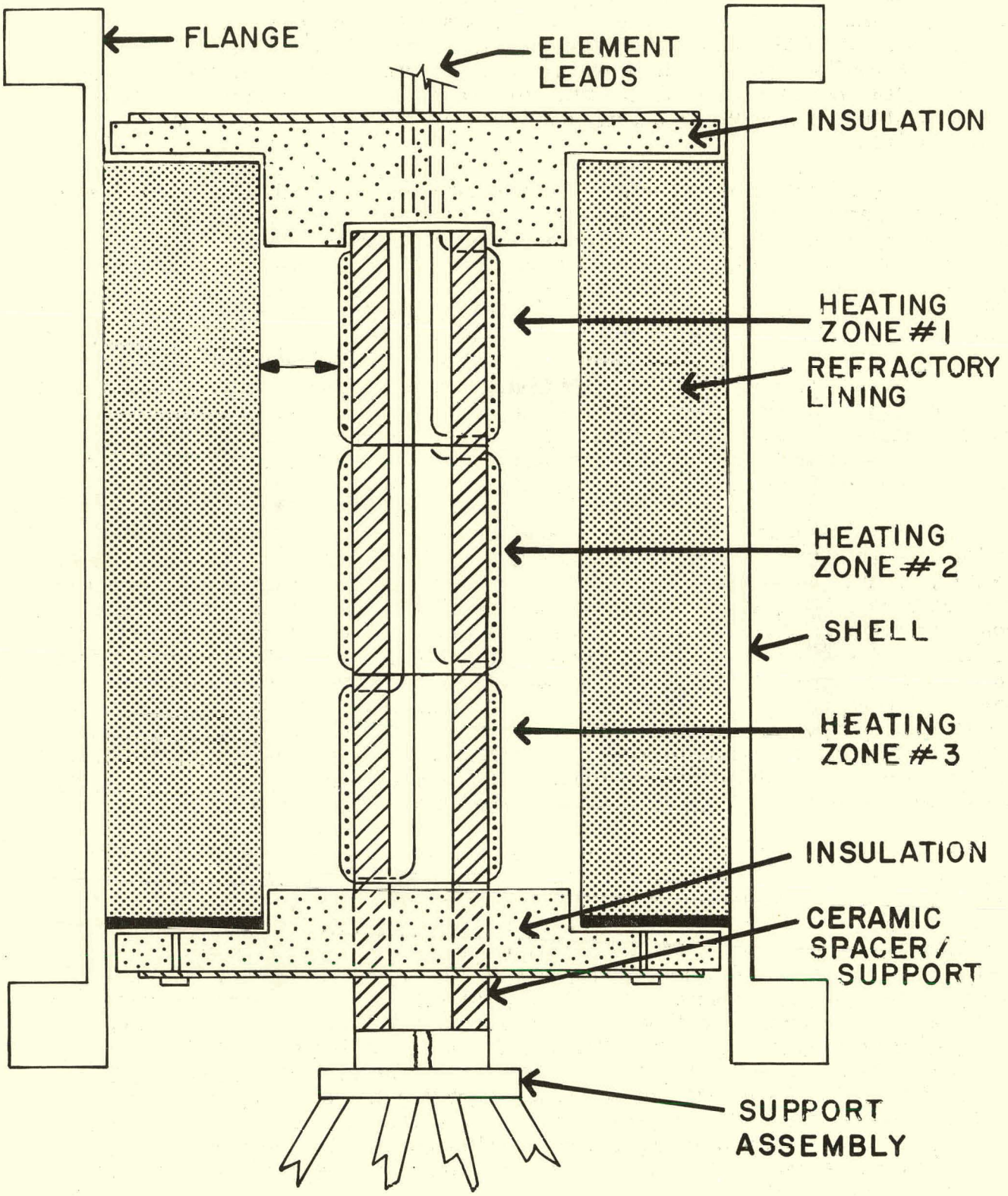

FIGURE 55. Schematic of Heating Elements.

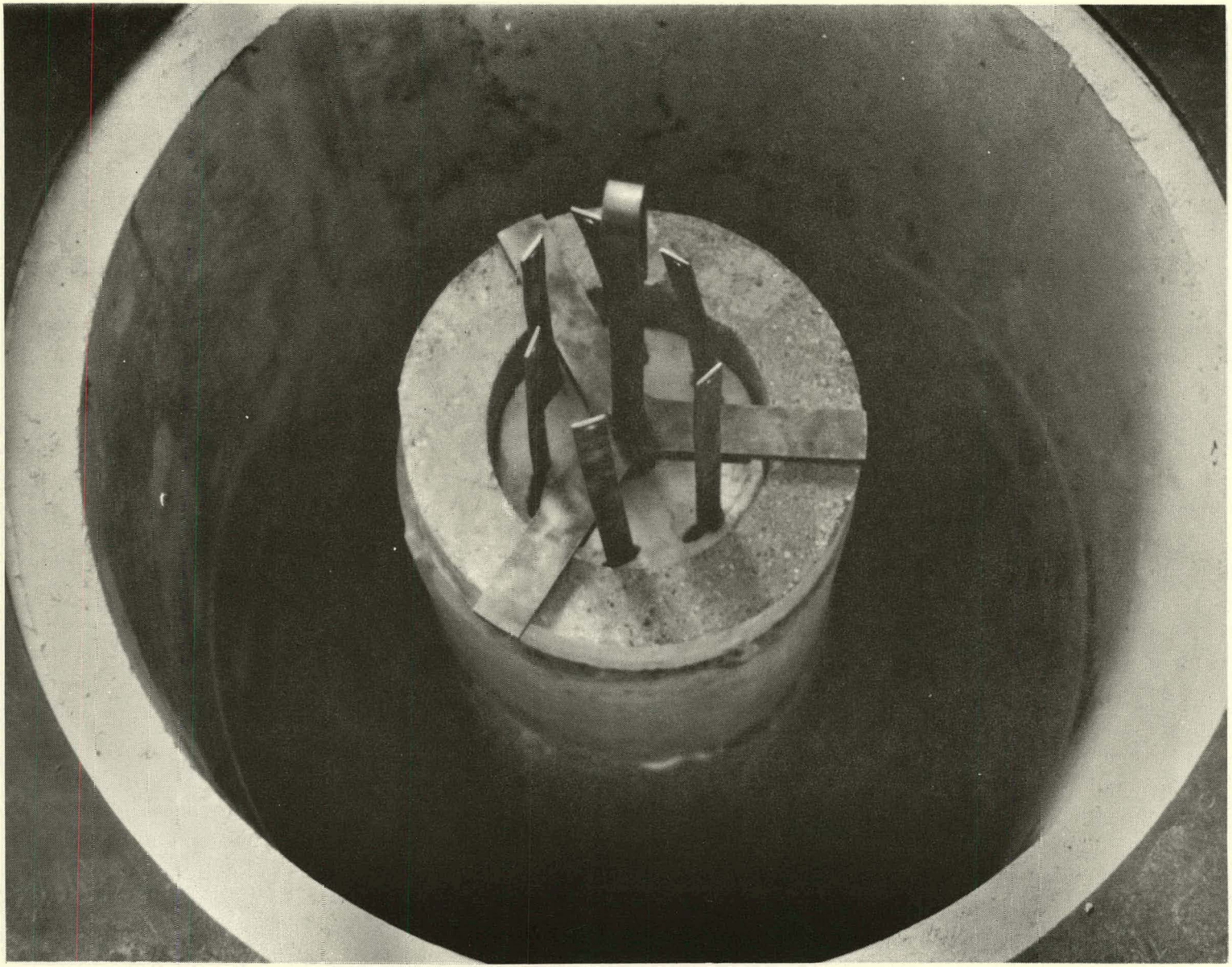

FIGURE 56. Multizone Heating Element Assembly Installed in Unlined Vessel.

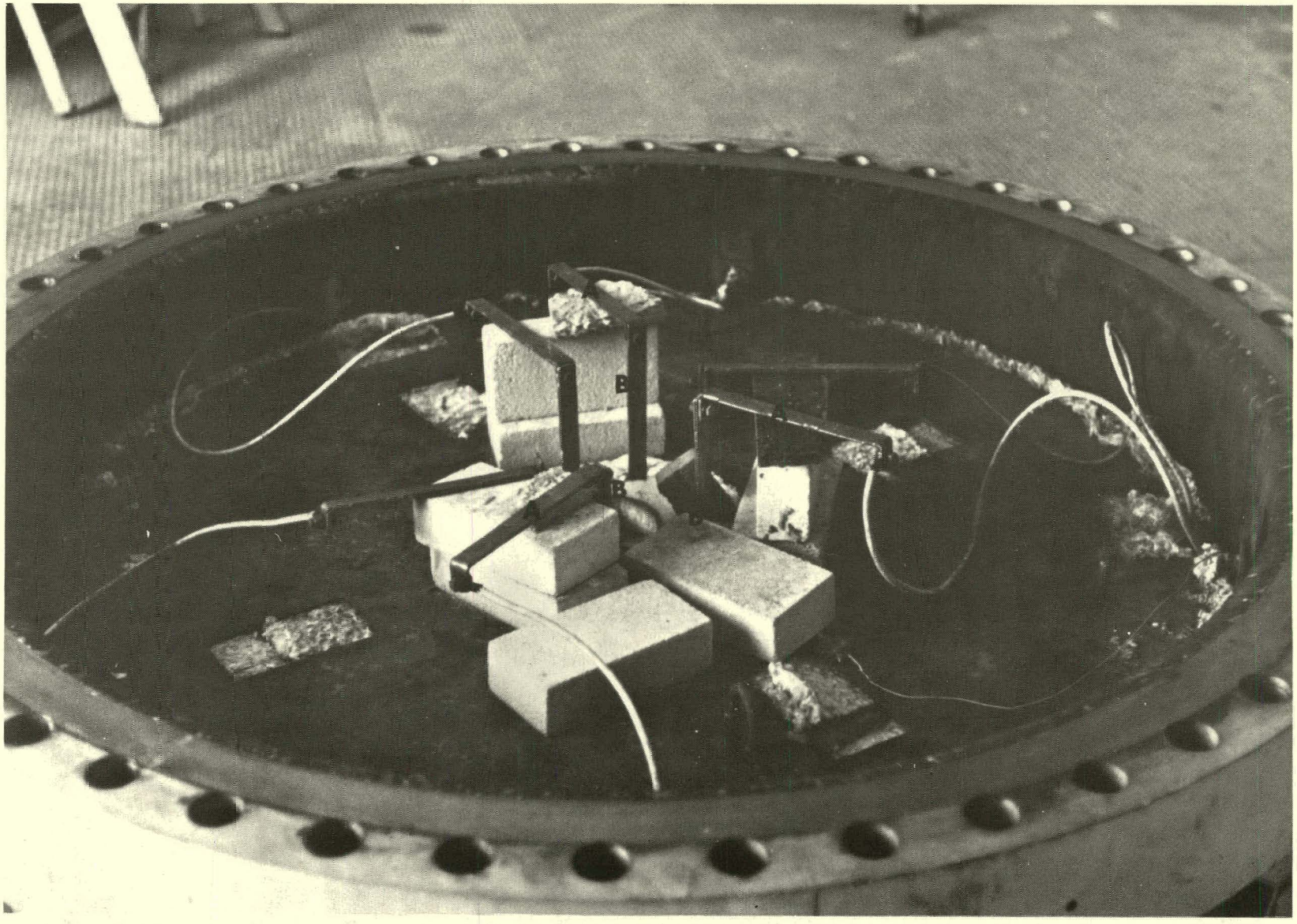

FIGURE 57. Electrical Lead Connections and Top of Upper Fiber Insulation Support Plate Prior to Placement of Top Head on the Vessel.

FIGURE 58. Top View of Externally Wound Ceramic Core after Test to 2000°F.

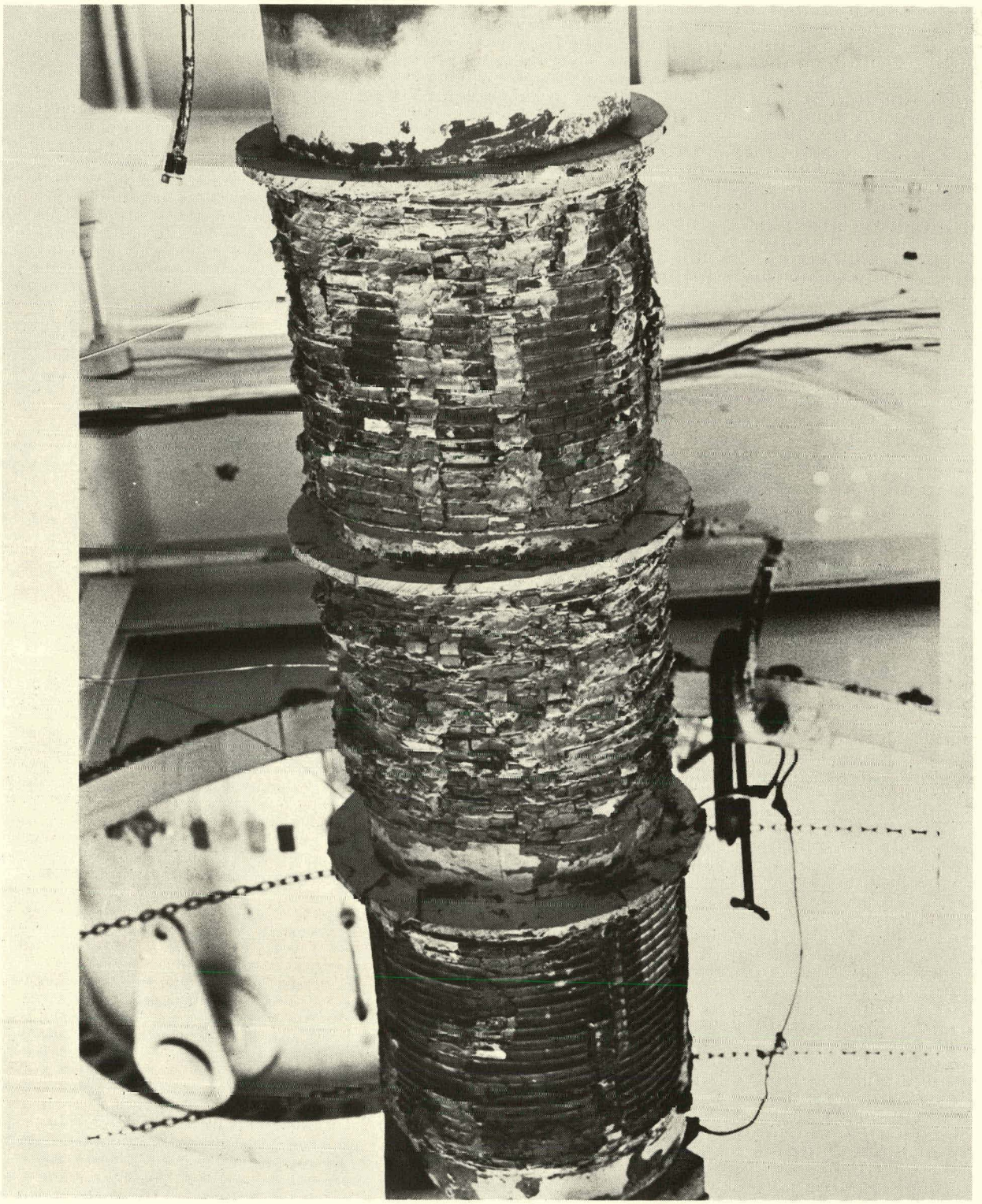

FIGURE 59. Multizone Heating Element Assembly after Termination of Test to 2000°F.

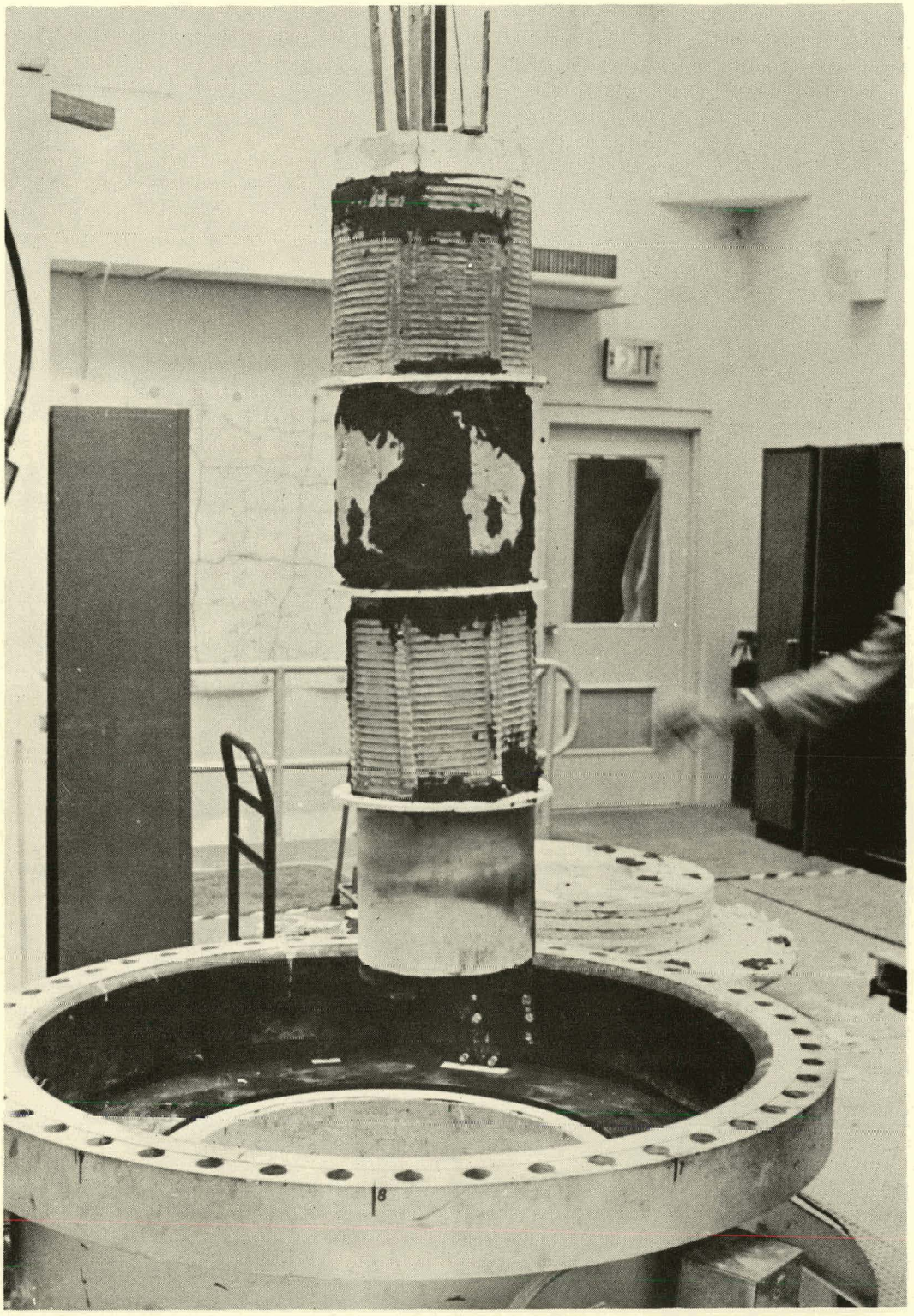

FIGURE 60. Improved Arrangement of Externally Wound Resistance Wire Heating Elements.

Test Vessel Capability

Summarized below is the capability of the test vessel:

High Temp. Test Zone - 4 ft.
Pressure - 250 psi Top & Bottom Heads, 375 psi Center Sections
Shell Temp. - 650°F
Hot Face Temp. -2000°F
Control - Temperature, Pressure
Versatility - 2 Center Sections
Inspection of Lining in Vertical Direction
Restraint of Lining in Vertical Direction
Atmospheres - Air, Steam, CO_2, Others
Lining Thickness - 12 Inches or Less
Heat-up Rates - 300°F/hr and Less

Mixing and Distribution System

A mixing and distribution system was built for installing linings in the 5 foot diameter vessel. It was designed for use with the short working times (30 minutes) of the refractory concretes and consideration of personnel safety. The mixing and casting sequence was accomplished by utilizing two 12 cu. ft. Muller mortar mixers positioned on a 4 segment, circular, elevated track surrounding the vessel. The mixers were modified with swivelling railroad wheels which permitted them to ride on the tracks and be easily moved. The mixers had dual screw blades which quickly and efficiently mixed up to 800 lb. batches of the dense and 400 lb. batches of the lightweight materials. The mixers discharged (via chutes) into the vessel fitted with circular metal forms. Figure 61 shows a schematic of this mixing and distribution system, and Figure 62 is a photograph of the actual system.

Casting Forms

Two sets of metal forms were used; one for the outer, insulating component and the other for the inner, dense component. These forms were readily collapsible so they could be removed from the cast furnace without difficulty and without generating cracks and other defects in the cast lining. To achieve this, the forms were divided into quadrants and further divided into a top and bottom section.

The metal forms were equipped with pneumatic vibrators which were attached to brackets welded to the inside of the forms. The pressure vessel was also equipped with vibrators to assist in the placement of the refractory concrete lining.

The vibrators for the forms were Dynapac EB-25 ball vibrators. Two of them were used and were operated at 80 psi with plant compressed air. They each generated 540 lb. of impact force. The vibrators used for the shell were Dynapac EP-56 heavy duty railroad hopper type vibrators and were operated at 90 psi with diesel powered air compressors. Two of them were also used and each generated up to 5000 lb. of impact force. A picture of the insulating component metal forms after placement in the vessel is shown in Figure 63.

Test Site

The test furnace/pressure vessel was located at the Lynchburg Research Center of Babcock & Wilcox in a 34 foot high by 30x34 foot bay. This bay was air conditioned and was equipped with a 10 ton overhead crane, a large access door to the outside and a 480 KW power transformer. There were two levels to the high bay. A circular hole was cut through the main floor of the bay so the pressure vessel could be counter sunk down onto the concrete basement floor below.

An 8x10 foot air conditioned control and data acquisition room was added to the bay to house the furnace controls and the data acquisition equipment. Figure 64 is a photograph of the main floor of the test site and shows the arrangement of the pressure vessel and control room.

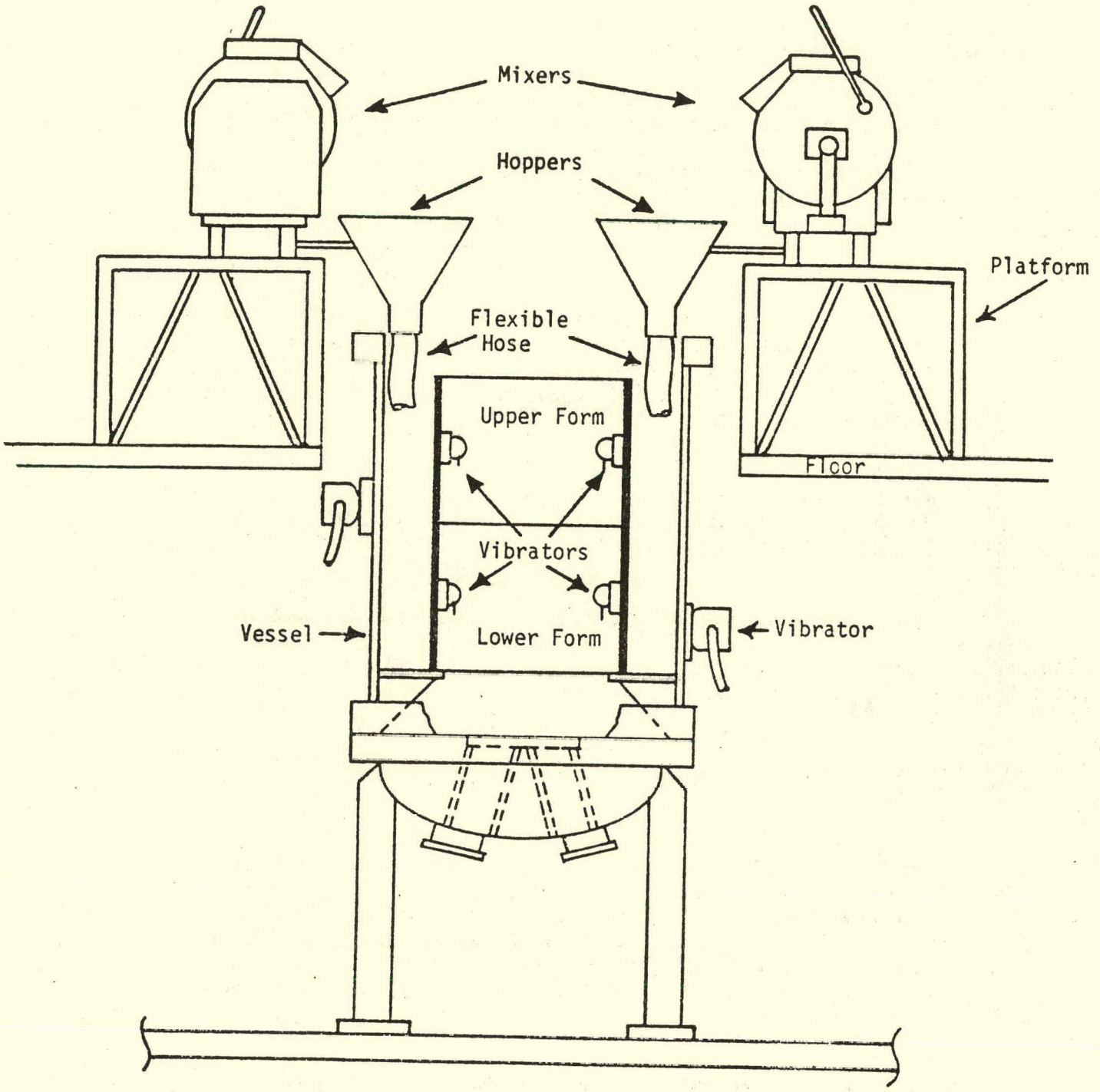

FIGURE 61. Mixing and Distribution System for Casting Monolithic Linings.

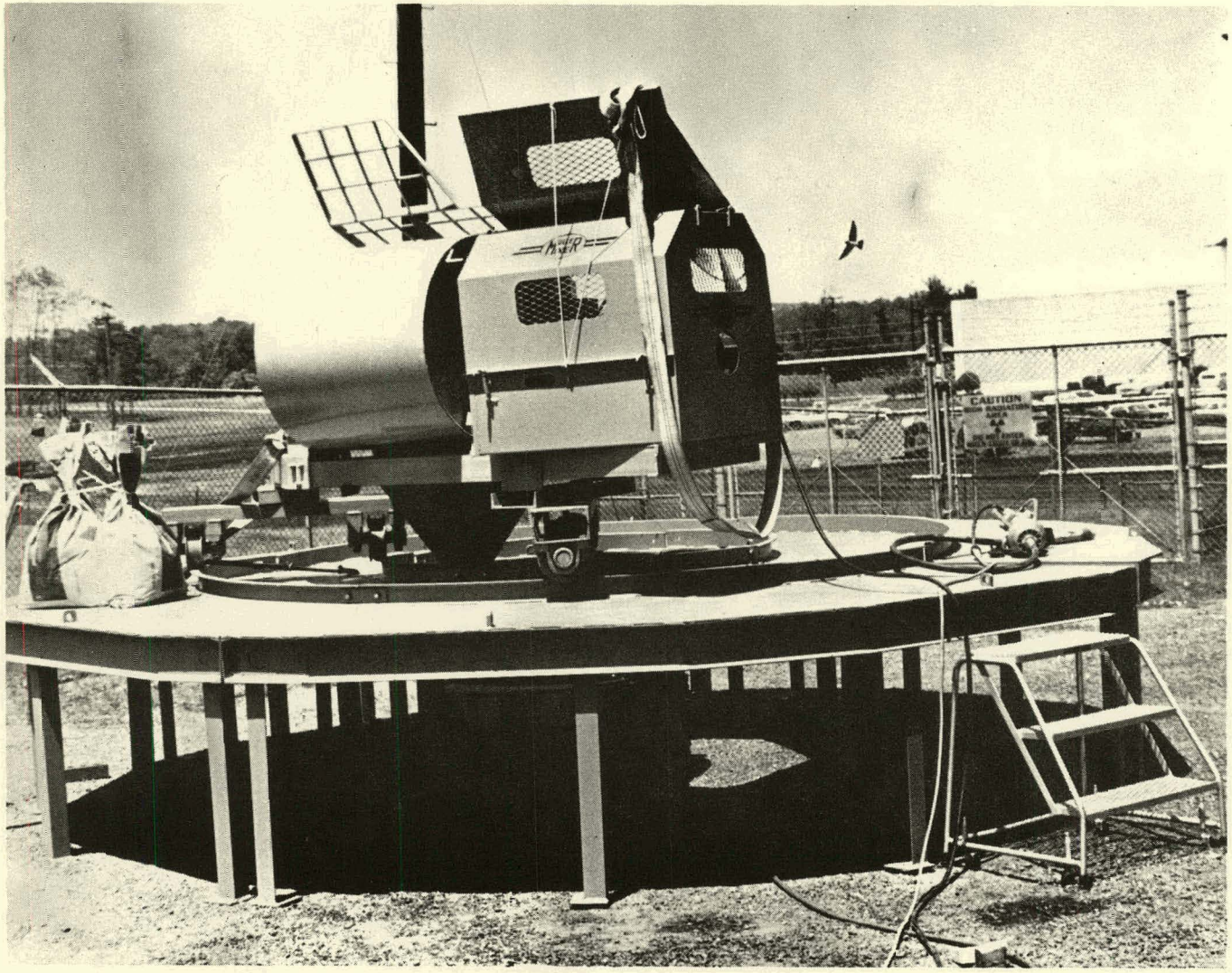

FIGURE 62. Photograph of Mixing and Distribution System.

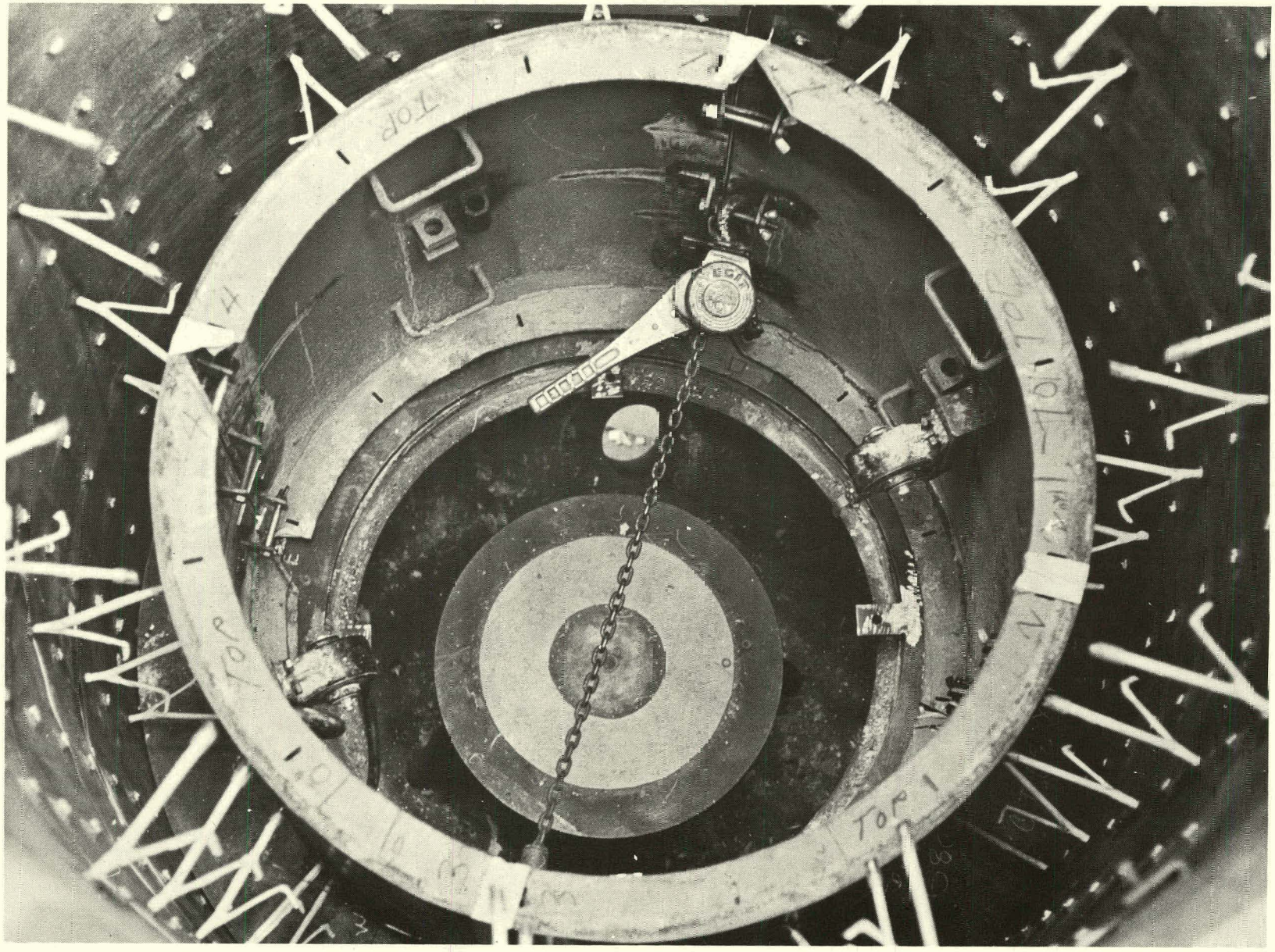

FIGURE 63. Metal Forms with Vibrators and Anchors.

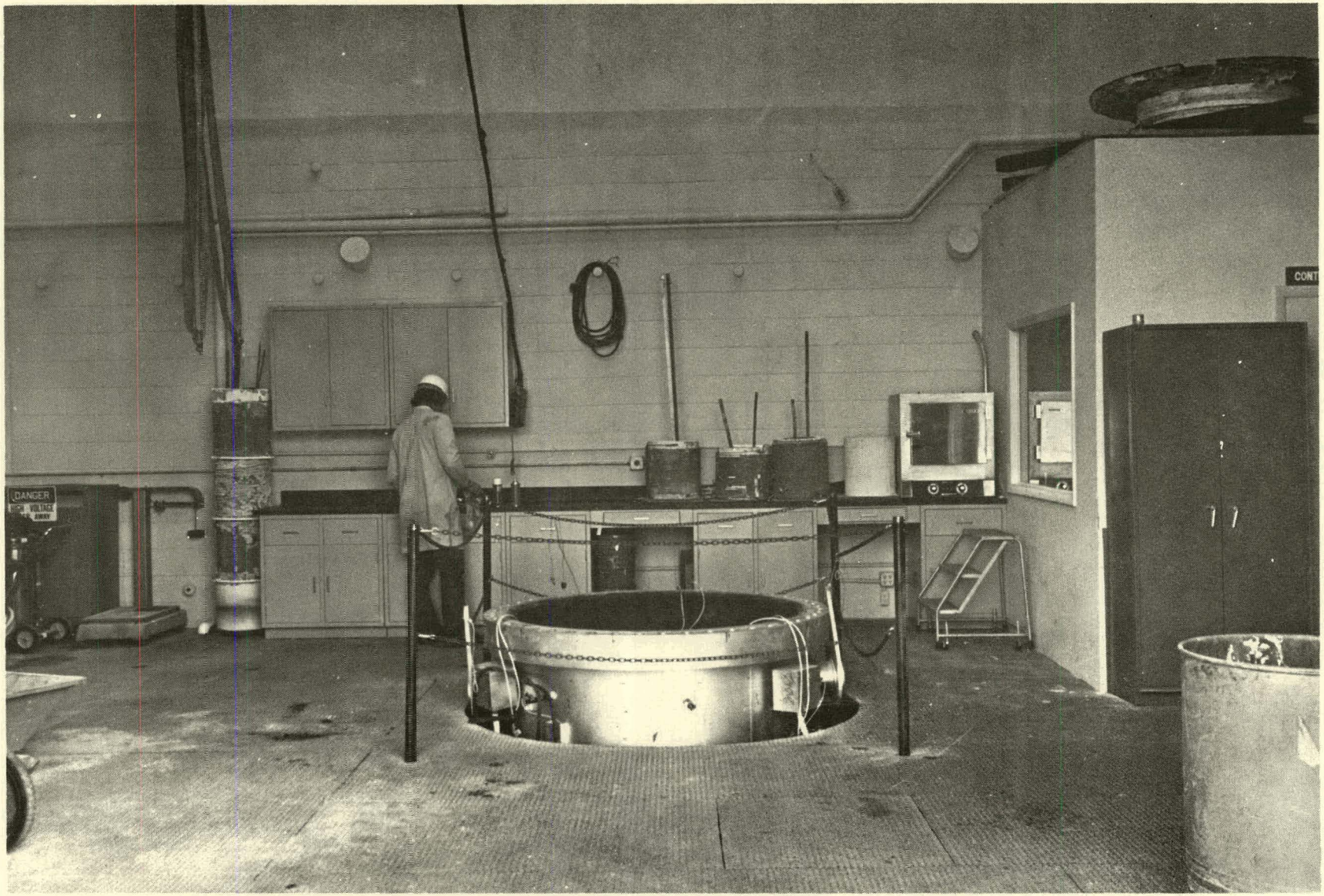

FIGURE 64. View of Test Site in High Bay Area at the Lynchburg Research Center.

2.6.2. Lining Test Matrix Planned

A series of nine single or dual component monolithic refractory concrete linings were to be run at two specific heating rates, with different anchor spacings and in air at one atmosphere and under pressurized steam or CO_2 to 100 psig or more. Other heating rates, refractory materials and operating conditions were to be considered as the test program progressed. The original design to be studied was a dual component monolithic refractory lining like those used in ammonia reformers in the petrochemical industry and like those being used in a number of the non-slagging coal gasifier pilot plants listed in Section 1.1 of this report. This design has been designated as the "Standard" lining design and is schematically represented in Figure 65. The actual lining configuration chosen was a twelve inch thick lining with 7.5 inches of insulating backup material and 4.5 inches of dense hot face material. This lining configuration and design was to be modified as information was acquired on the causes of cracking and degradation of the standard lining.

Table 11 lists the lining test matrix originally developed. Summarized below are the original two heating schedules to be studied:

Case #1

Heat-up and hold at 200-400°F for 16 hrs.

Heat-up at 100°F/hr. to 1000°F

Hold at 1000°F for 3 hrs.

Heat-up to 2000°F at 100°F/hr.

Hold at 2000°F for 5 hrs.

Case #2

Heat-up at 50°F/hr. to 1000°F and at 100°F/hr. from 1000-2000°F with no holds until 2000°F.

In the event cracking had not occurred after heating under Cases 1 and 2, faster heating rates were to be tried until cracking did occur.

STANDARD LINING DESIGN

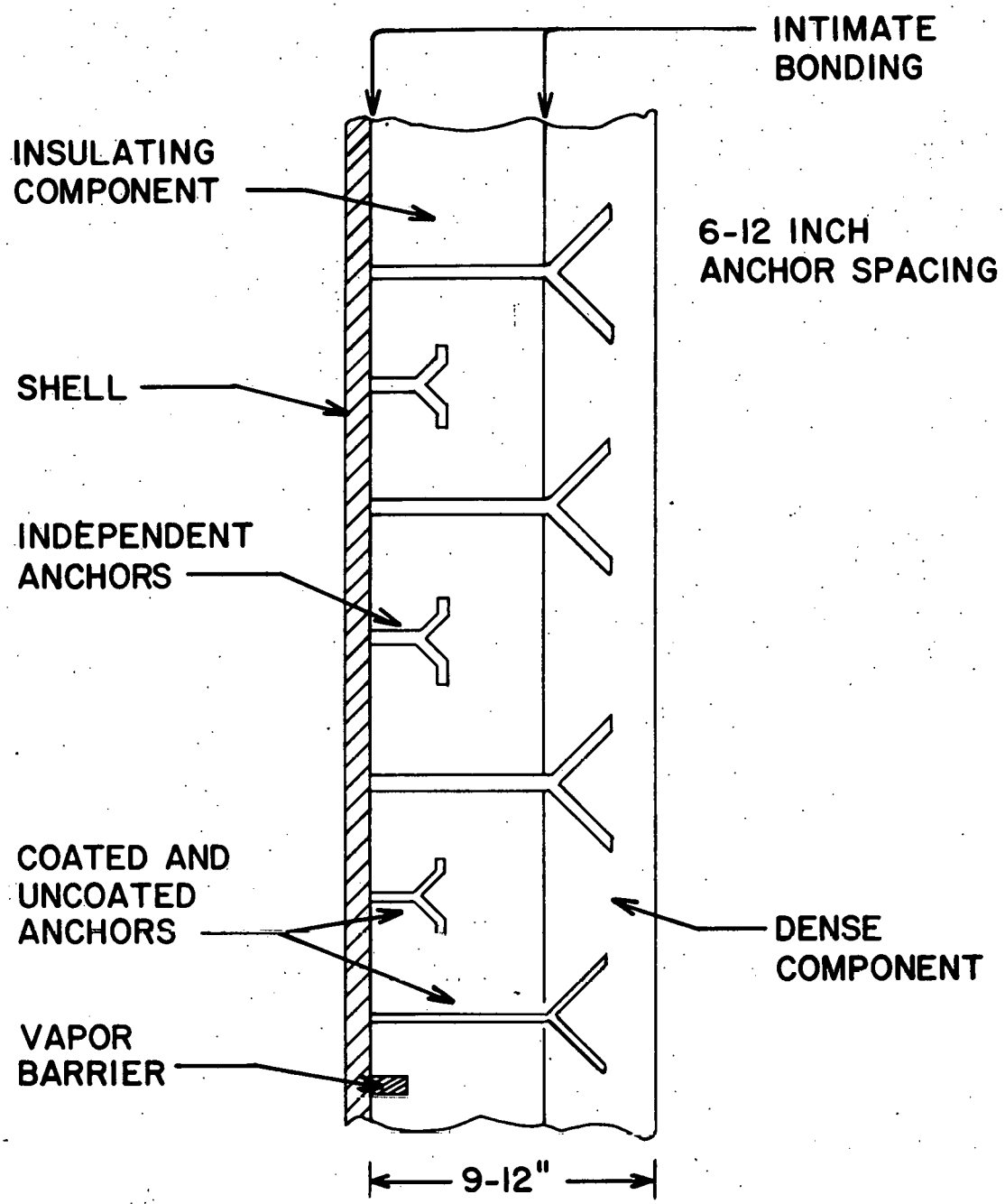

FIGURE 65. Standard Lining Design.

TABLE 11. Plan for Proposed Lining Tests on 12" Thick Monolithic Refractory Linings (Vertically Restrained)

Test No.	Lining Configurations		Anchor Configurations					Atmospheres			Pressures		Heating Schedules to 2000°F		
	Single	Dual	Spacing, in. 6	12	24	Coated	Uncoated	Air	Steam	CO_2	1 Atm.	100 psig	1	2	3
Lining Material #1															
Test 1		X		X			X	X			X		X		
Test 2		X		X		X		X			X		X		
Test 3		X		X		Open		X			X			X	
Test 4		X		X		Open			X			X	X		
Test 5		X		X		Open				X		X	X		
Lining Material #2															
Test 6	X			X		Open			Open		Open			Open	
Lining Material #3															
Test 7	X 6" Only OPTION-PATCH CASTABLE			None		Open			Open		Open			Open	
Lining Material #4															
Test 8		X		Open		Open			Open		Open			Open	
Lining Material #5															
Test 9		X		Open		Open			Open		Open			Open	

NOTE: Materials 1-3 generic or commercial monolithic refractories.
4-5 new or improved monolithic refractories.

2.6.3. Installation of Linings

All of the linings tested were cast using the mixing and distribution system described earlier. The installation of a complete lining usually took two full weeks and was done in two steps. The insulating component was installed and cured. The dense component was then installed and cured. The steps normally followed during the installation of the lining are outlined below:

Installation Steps

1. Silicone caulking was applied around the outer edge of the base plate of the center section of the pressure vessel. This was done to seal the space between the shell and the plate and to prevent leaking of refractory concrete down into the lower head during the pour.

2. Ceramic paper, silicone grease or fine alumina grain covered with plastic were used to cover the base plate prior to the pouring of the lining. This was done to create a parting agent between the plate and the lining which was expected to simplify the removal of the lining during the tear out activities.

3. The anchors were installed in the vessel at the spacings wanted by screwing one of the threaded ends of the anchor into the heavy duty hex nuts welded to the inside of the shell. Three types of anchors were used. One was a "V", the second was a "Y" type anchor and the third was a "Steer horn" type anchor. The "V" and "Y" were designed as shown in Figure 66 with a threaded end which terminated at the interface. An extension was attached to this piece after the insulating component was installed. The "V" anchors were positioned in a random array as shown in Figure 63 and the "Y" anchors were oriented so the extension was in a vertical array. The Steer horn" was designed as shown in Figure 66 and was only installed in the insulating component of the lining. It was essentially a shortened version of the "Y" anchor. The hex nuts which were not used were filled with silicone caulking and covered. This was done to assure that no refractory material filled or surrounded the nuts and caused an unusual stress concentration in the refractory.

4. The threaded ends of the anchors were covered with rubber caps to protect the threads during the casting of the insulating component and to create a space around them which permitted the extensions to be easily installed. Anchor coatings and bonding barriers were installed at this point. Masking tape and an asphalt based insulating type tape (PRESSTITE) which was about 80 mils thick were used to coat the anchors. Both silicone grease and 4 mil thick plastic sheet were used as bonding barrier materials. The plastic sheet was attached to the shell or lining by adhesive tape or silicone caulking.

5. The metal forms were assembled and installed in the vessel as one unit. The space between the bottom of the form and the base plate was filled with the asphalt base tape to seal the form. The joints of the form were sealed with silicone caulking and the outer surface of the forms was then sprayed with a silicone mold release compound. These two treatments prevented the refractory from bonding to the mold and from having joints form in it during casting.

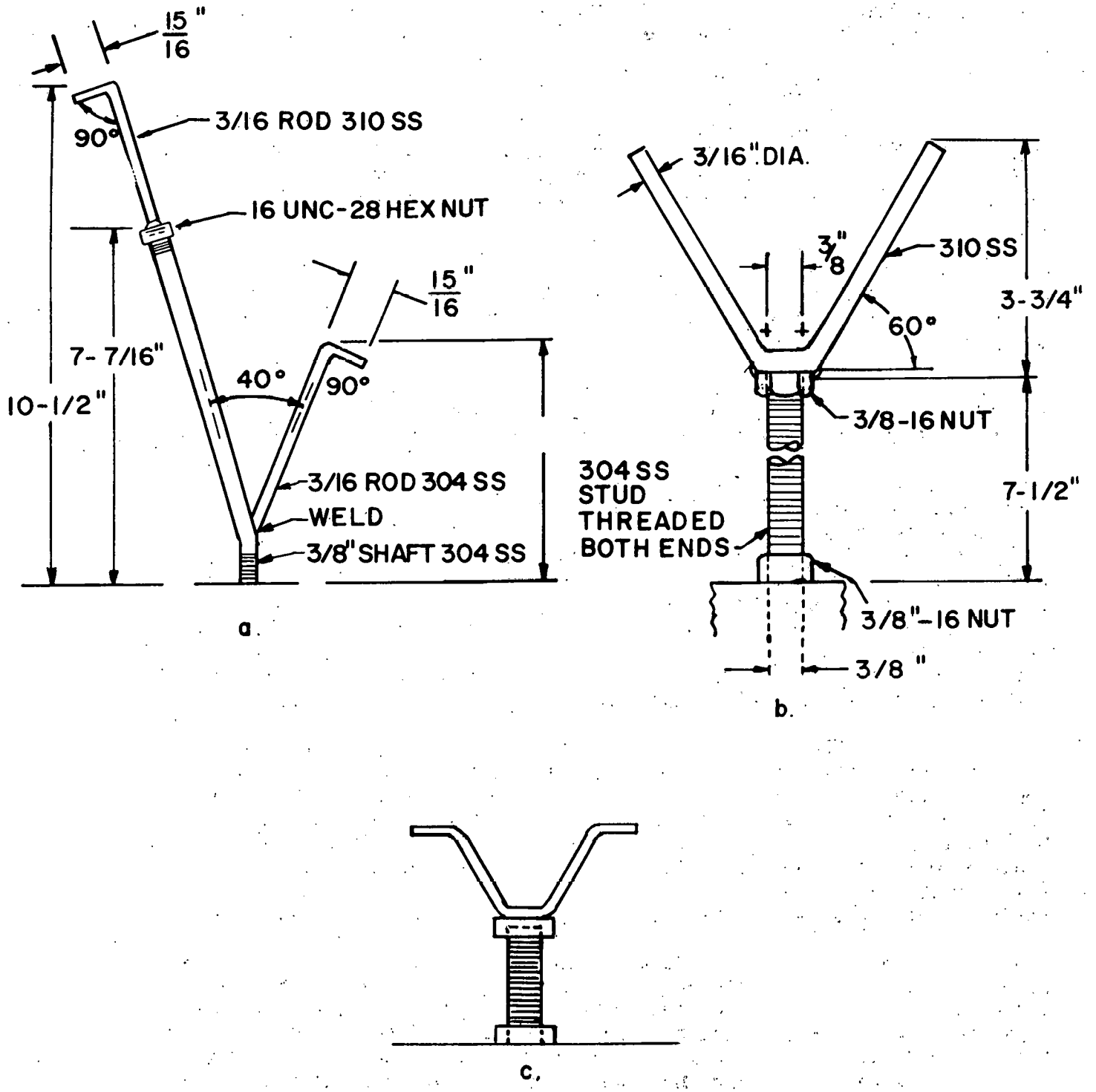

FIGURE 66. Design of Anchors Used in Lining Tests.

Great care was taken to align and true the molds. Both the insulating and dense component forms were brought into round, and maintained in that configuration, with a wench arrangement and were then bolted to the base plate. The forms had to be bolted to the plate to prevent them from floating during placement of the lining.

6. The insulating component was cast using the vibrators attached to the shell and forms; and the concrete pencil vibrators were submerged in the material during placement. The shell and form vibrators were initially placed on the bottom half of the equipment and raised to the top half after about half of the lining was installed. A similar procedure was used when the dense component was installed; however, the shell vibrators were not used.

7. Prior to mixing and casting the linings, the materials to be used and mixers were brought in to the test area from the unheated or uncooled storage area. This was done to allow the material and equipment to warm up or cool down to about 70 to 75°F. This generally took about 2 days. Since the material temperature was found to have the biggest effect on the mix temperature, additional time was used to warm up or cool down the material if necessary.

8. Since the insulating components were commercial products, (LITECAST 75-28 and KAOLITE 2300 LI) fresh casting grade material was ordered two weeks to one month before a lining was installed. The water levels used in these castings were determined in test pours prior to the actual casting. Every attempt was made to use the same water level as was used in the property determination activities. This was 21% for the LITECAST 75-28 and 59% for the KAOLITE 2300 LI.

Fresh casting grade dense component material was also ordered two weeks to one month before the lining was installed. The 90+% Al_2O_3 material was made at the Insulating Products Division (IPD) of Babcock & Wilcox using the modified mix formulation listed in Table 7. It was designated ERDA 90 and was usually made in 5000 lb. batches. Mix 36C was also made at IPD but was a stock item and was acquired as needed. Water levels of 7.75% and 7.5%, respectively, were used for these materials.

9. Two mixers were alternately used to mix and place the refractory materials. It normally took 6 to 7 batches to completely install one of the components. A 350 lb. quantity of the insulating component material was used for each batch and a 600 lb. quantity of the dense material was used.

10. After the materials were dry mixed for 30 seconds, the prescribed amount of water and other additives such as metal fibers were added all at once. The material was wet mixed for periods of 90 seconds to 5 minutes, depending upon the material, and the pour temperature and ball-in-hand consistency (BIHC) were checked.

If the material had a poor BIHC, the batch was either wet mixed another 30 seconds to one minute or more water added (usually in 0.5% increments), or a combination of the two tried. This usually improved the BIHC.

11. A target pour temperature of 75°F with a minimum of 70°F was sought. This was done to make the refractory concretes as permeable as possible and to minimize their tendency to explosively spall. In cases where the refractory concrete was not warm or cool enough, the water temperature was varied to acquire the target temperature.

12. Once the material was mixed, checked and approved, it was emptied in the hopper attached to the mixer and placed in the vessel with aid of flexible chutes. The insulating materials generally had a wet sand consistency and did not flow well through the hoppers and chutes. However, they flowed well when vibrated and filled the vessel cavity. The dense component materials generally flowed better through the hoppers and chutes and vibrated well. Both components could be cast in about one hour.

13. Once the lining components were cast, they were covered with plastic sheet to keep the moisture within the refractory and to aid curing. Usually after about 2 hours, metal spacers were removed from the vertical joints in the metal forms. This was done to assure that no cracking of the lining components occurred because of the differential expansion between the lining and the metal forms.

14. The temperature of the lining components was monitored with the embedded TC's to determine whether cement hydration had occurred.

15. The metal forms were usually removed after 48 hours of curing and the lining inspected for defects, voids and general quality. In one or two cases the forms were removed after 18-24 hours. In the case of the insulating component, the material around and over the anchors was removed so the anchor extensions could be installed. A picture of this activity is shown in Figure 67. Once the extensions were installed and coated if necessary, the insulation component was repaired around the anchor. The dense component forms were then installed and the process repeated.

16. It normally took two to three weeks to prepare and install the insulating component and one week to prepare and install the dense component. The circular platform was removed from the test site after the lining was completely installed and prior to the final instrumentation and preparation for the heat-up tests.

17. In one or two tests, the effect of roughening the ID of the dense component on the tendency of that component to crack was investigated. Alternate schemes were tried to roughen the surface. One involved using a chipping hammer to remove the dense, fine textured skin on the ID. The other involved using corrugated cardboard covered with an alumina grit (minus 14 mesh or finer) as a liner around the outside of the dense component metal form. Both roughened the surface; however, the chipping hammer method removed the skin and the other method produced a corrugated surface texture but did not prevent the skin from forming.

FIGURE 67. Installation of Anchor Extensions Prior to Casting the Dense Component.

2.6.4. Instrumentation

Throughout the experiments, the test units were instrumented with thermocouples, strain gages and pressure transducers to allow the measurements of hot face and lining temperatures, temperature gradients through the lining, strain of both lining components, shell temperatures and stresses, anchor stresses, and pressures generated from within the lining materials. As an aid in studying the degradation of monolithic refractory linings under thermal and mechanical loading during heat-up and cool-down tests, the following information was obtained via the various measurement and observation techniques:

1. Lining strain
2. Temperature profile and distribution in the lining
3. Refractory pore pressure
4. Acoustic emissions from the lining
5. Video taped observations of the hot face
6. Anchor stresses
7. Vessel temperature profiles
8. Vessel stresses
9. Vessel pressure

Of primary significance were the techniques enabling measurement of strain, acoustic emission, and temperature within the refractory lining. In conjunction with conventional instrumentation, new techniques were developed, tested, and evaluated prior to the testing of the various lining designs. Where appropriate, these techniques are described and the results of development tests are presented in the following sections.

Lining Instrumentation

Strain

A technique was developed whereby strain within refractory materials can be measured using commercially available high-temperature strain gages. These instruments are referred to as Ailtech electric resistance weldable type strain gages (Eaton Corporation, Electronic Instrumentation Division). The gages are hermetically sealed and are rated for use to 1200°F; thus, they are suitable for use in a refractory embedment mode. The selection of this type gage as a candidate for the lining tests was based on the lining test conditions, a review of internal and external references on the performance and problems associated with high temperature strain gages, and on B&W's extensive experience in high temperature strain measurement.

The evaluation of the Ailtech gage for this application was based on its thermal output performance and its strain transfer characteristics in an embedment mode. In considering the embedment application of this gage it was speculated that normal data reduction procedures may require revision since the gages cannot be spot welded, which is the mounting mechanism for which the gages are calibrated. Such modifications would thus be related to the fact that the transfer of strain from the refractory to the gage is dependent upon the bond that exists between the two after embedment. This point was thought to be particularly important with regard to the more porous castables, such as the insulating type refractories.

To study this area of concern, cleats were attached to the mounting (strain transfer) shims of several of the evaluation test gages. These cleats were to serve as a means of enhancing the bond and strain transfer. Results from the evaluation tests of the cleated and as-manufactured gages were to identify the necessary data reduction modifications, if any, or lead to optimal techniques of modifying and embedding the strain gages. A visual comparison between a cleated and an as-manufactured Ailtech resistive strain gage is provided in Figure 68. The cleats are attached to the bottom side of the gage's mounting shim by spot welding. The proposed lining strain measurement technique was thus developed and evaluated through in-air testing of these gages and through tests of refractory brick specimens in which these gages were embedded.

The in-air test phase of this development effort was performed to characterize the output of the Ailtech gage in an unbonded state as a function of temperature and time. Data obtained from one of the eight gages so tested are plotted in Figures 69 and 70, respectively, and are typical of the results obtained from all the gages tested. In acquiring thermal output as a function of temperature, the eight gages were suspended in air and subjected to four thermal cycles between room temperature and 1200°F. Gage temperatures were obtained from thermocouples which were spot welded to each gage. The data of Figure 69 corresponds to the fourth thermal cycle for one of the gages. From this plot and the data from the previous three cycles, it was found that the strain gage output is linear and repeatable with temperature, thus indicating that the thermal response characteristics of the Ailtech gages are predictable. These results also show that the shift of the strain temperature curves, which is a normal result of thermal cycling, is tolerable. This phenomenon is depicted in Figure 69 where a zero shift of only 24 micro-inches per inch was observed at 72°F at the end of the fourth thermal cycle. Data obtained from these gages as a function of time show that the strain output remains essentially constant for a reasonable period of time while operating at a temperature comparable to that expected to exist during the lining tests. This result is exemplified in Figure 70, where the values plotted were derived from the same gage as that corresponding to Figure 69. Thus, the drift in strain output associated with the Ailtech gage was found to be insignificant over a short term, indicating that strain drift would not be of concern throughout the duration of a refractory lining heat-up test. In summary, the in-air test data was favorable and suggested that, based on its thermal performance, the proposed gage would be adequate for the lining tests up to 1200°F.

The second phase of the strain measurement development effort consisted of testing the strain gage in an embedment (bonded) mode. The same cleated and as-manufactured gages that were tested in-air were cast within eight refractory brick specimens which, in turn, were subjected to separate thermal and mechanical loading. The resulting strain gage outputs were compared with reference strain values derived simultaneously from displacement transducers. Performance of the Ailtech gage was investigated in two types of refractory materials. The first was a dense 90+% Al_2O_3 generic refractory, the second was an insulating type; namely, LITECAST 75-28. The eight refractory brick test specimens were two inches square by six inches long. While casting them, an Ailtech gage was positioned at the center of each brick and was oriented to sense strain in the length direction.

The thermal load portion of the bonded strain gage testing was performed first, followed by room temperature mechanical load tests. Thermal

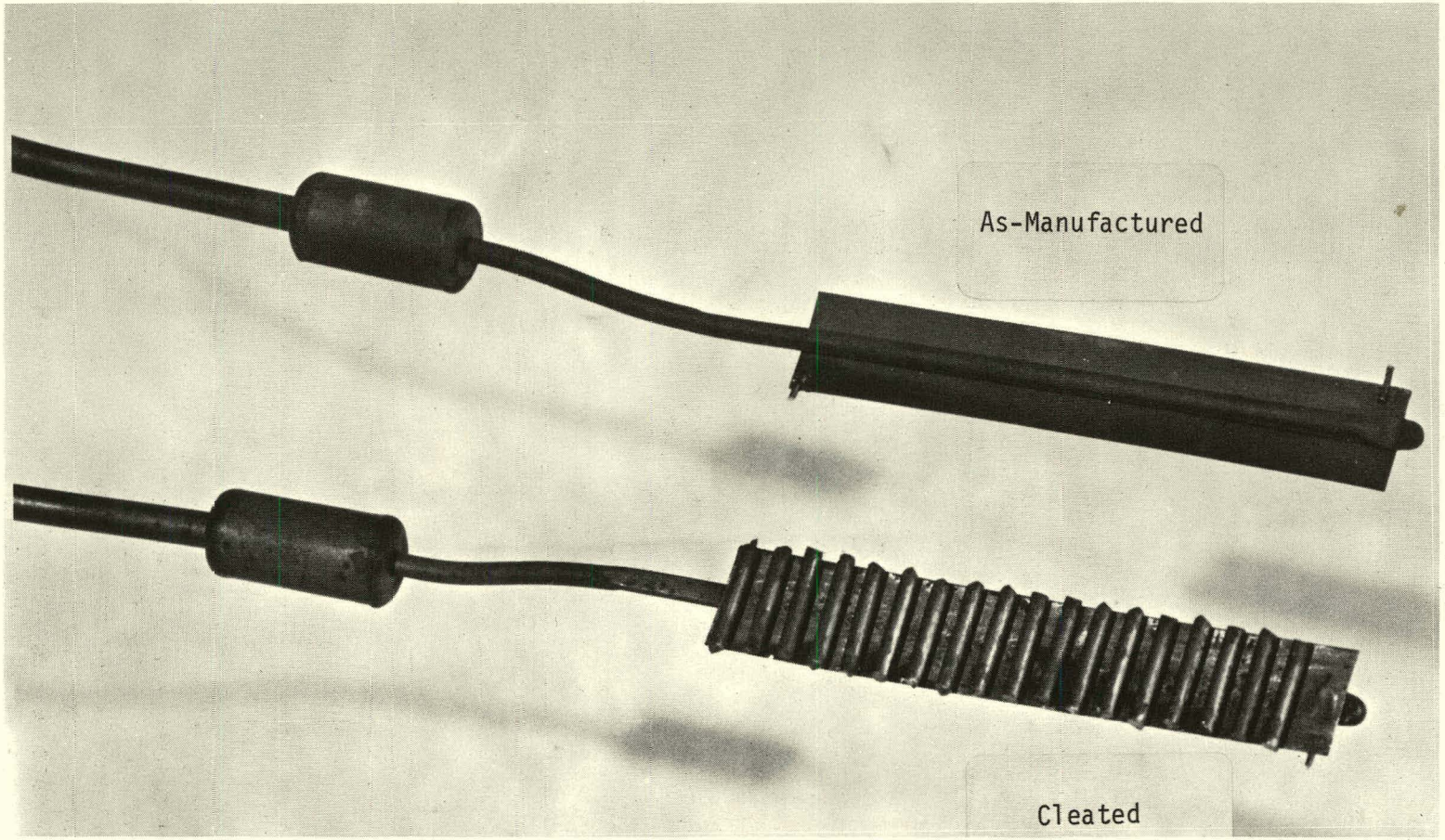

FIGURE 68. As-Manufactured and Cleated Embedment Strain Gage.

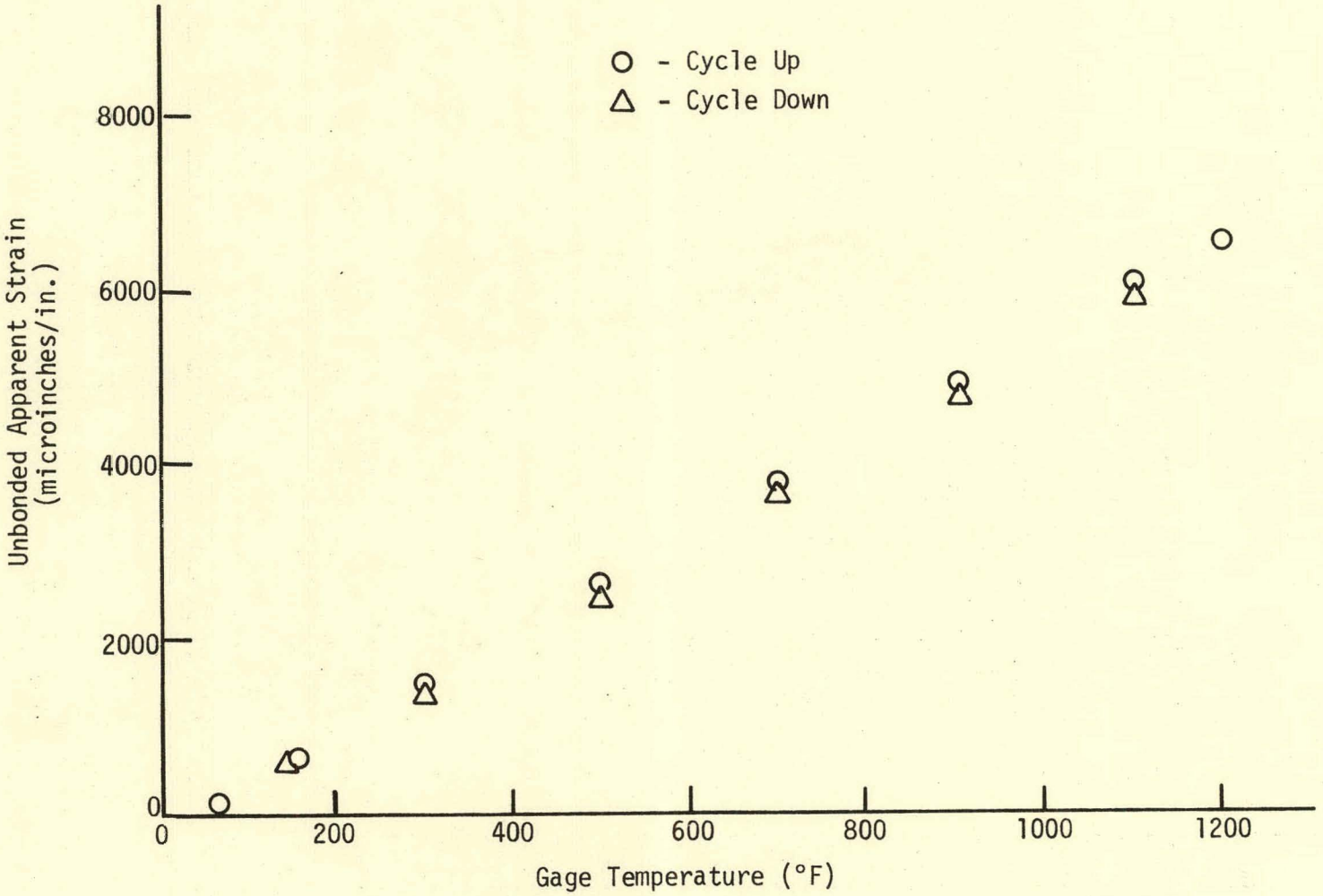

FIGURE 69. In-Air Test Data for Strain Gage No.4038 - Experiment 1, Temperature Cycle No. 4.

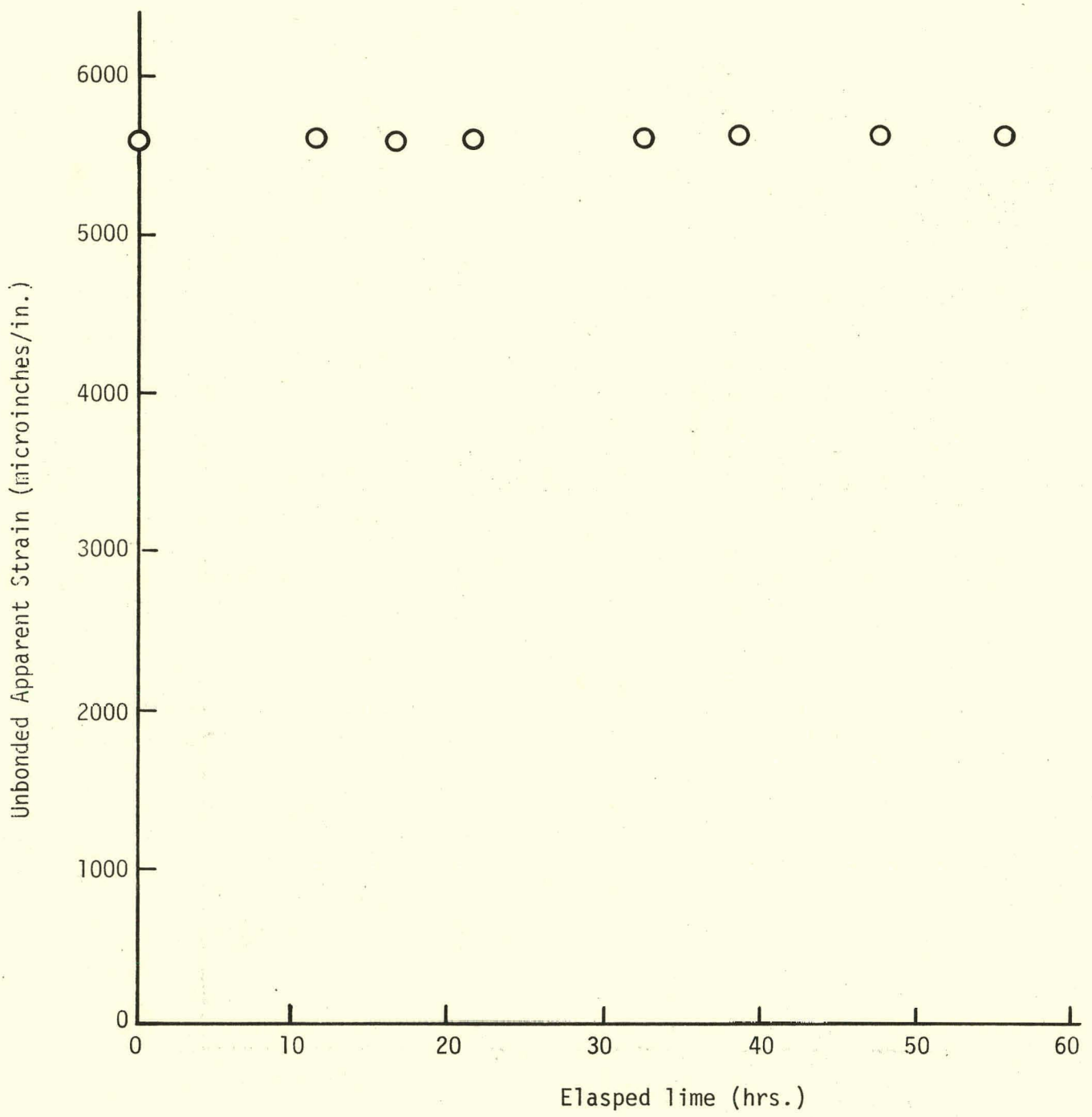

FIGURE 70. In-Air Drift Data at 1000°F.

loading consisted of heating the strain-gaged brick specimens to 1200°F at about 200°F/hr, then cooling to room temperature, while allowing the bricks to expand and contract in an unconstrained manner. During this thermal cycle, the expansion, shrinkage, and contraction of each brick was measured using a displacement transducer positioned over each as illustrated in Figure 71. Figure 72 shows the physical arrangement of the dense brick specimens in the oven prior to testing. Strain gages were embedded within only four bricks. The other two bricks were included in the test to detect any differences in the thermal expansion characteristics of the refractory due to the presence of the strain gages. Figure 72 also shows external thermocouples cemented to the faces of selected bricks to assure minimal temperature gradients during testing. Also shown are alumina rods used to transfer the growth and contraction of the bricks to the displacement transducers located above the test oven. A computer-based data acquisition system, shown in Figure 73, was used to record all the temperature, displacement, and strain gage data generated during the thermal load tests. Reference strain values were computed from the brick displacements, and then compared with the strain gage measurements. A discussion of the thermal load test results obtained for both the dense and insulating refractory bricks follows.

Figure 74 through 77 are representative test results for the cleated and as-manufactured Ailtech strain gages embedded in both the dense and insulating refractory bricks. The strain gage results shown were reduced from the strain gage data using the standard procedures specified by the vendor for a welded application. This approach was chosen to identify what revisions, if any, would be required to obtain accurate strain measurements in an embedment application. Based on the comparative plots, it is evident that the cleats hinder the transfer of strain from the refractory to the gage in the dense materials (Figures 74 and 75), but they enhance strain transfer in the insulating refractory (Figures 76 and 77). Even though the strain gage predictions in Figures 75 and 76 do not completely match the reference strain curves derived from the direct current displacement transducers (DCDT's), it was felt that the thermal load test results were favorable, considering this as an initial approach in refractory strain measurements.

After completing the thermal loading tests, the dense and insulating strain-gaged brick specimens were subjected to room temperature mechanical tests. These tests were performed by placing each specimen into an Instron testing machine, applying a series of compressive loads, and monitoring the resulting strain gage outputs and overall brick displacements using a displacement transducer. This testing arrangement is shown in Figure 78. As with the thermal load tests, the strain gage results were compared with the reference strain data derived from the brick displacements. These test results are plotted in Figures 79 through 82 and correspond to the same bricks previously subjected to the thermal load test. Conclusions based on these plots were generally the same as those derived from the thermal load testing. Comparing Figure 79 with 80 and Figure 81 with 82 again reveals that it is not advantageous to attach cleats to Ailtech gages embedded within the dense refractory, but that cleats are favorable to use in the insulating materials. As with the thermal load tests, the strain gage data from the mechanical load tests were reduced using the standard procedures for these gages in a weldable application.

After the bonded strain gage tests were completed, each brick specimen with an embedded Ailtech strain gage was cut into several sections to visually examine the refractory-to-strain gage bond. In addition, the exposed

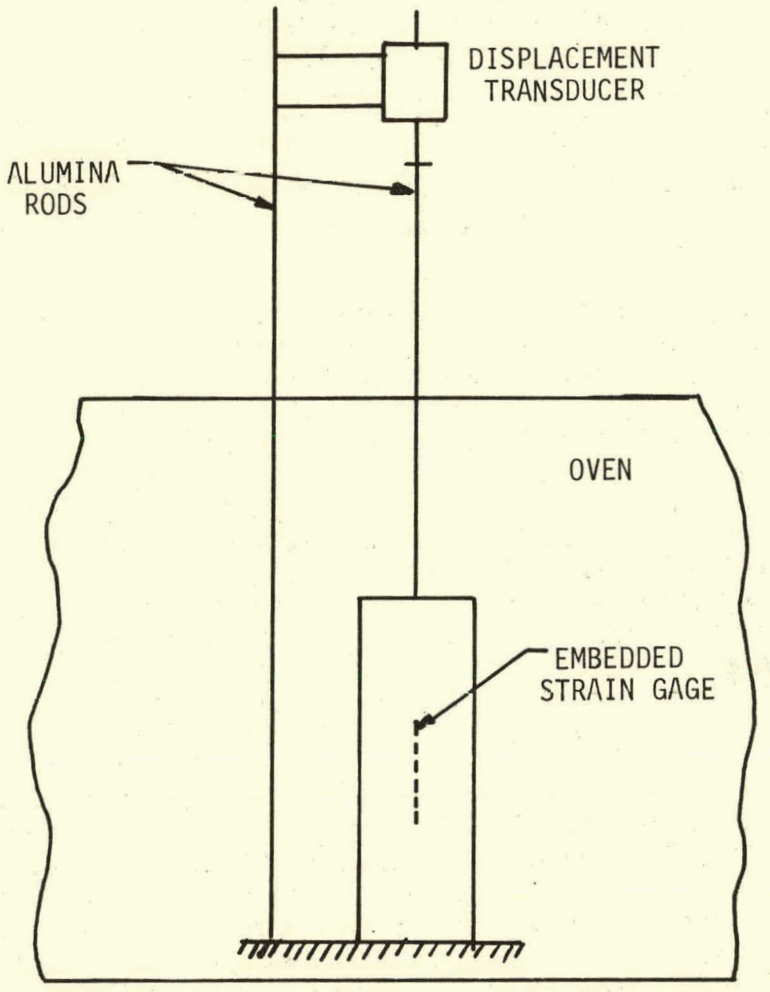

FIGURE 71. Schematic of Thermal Load Test.

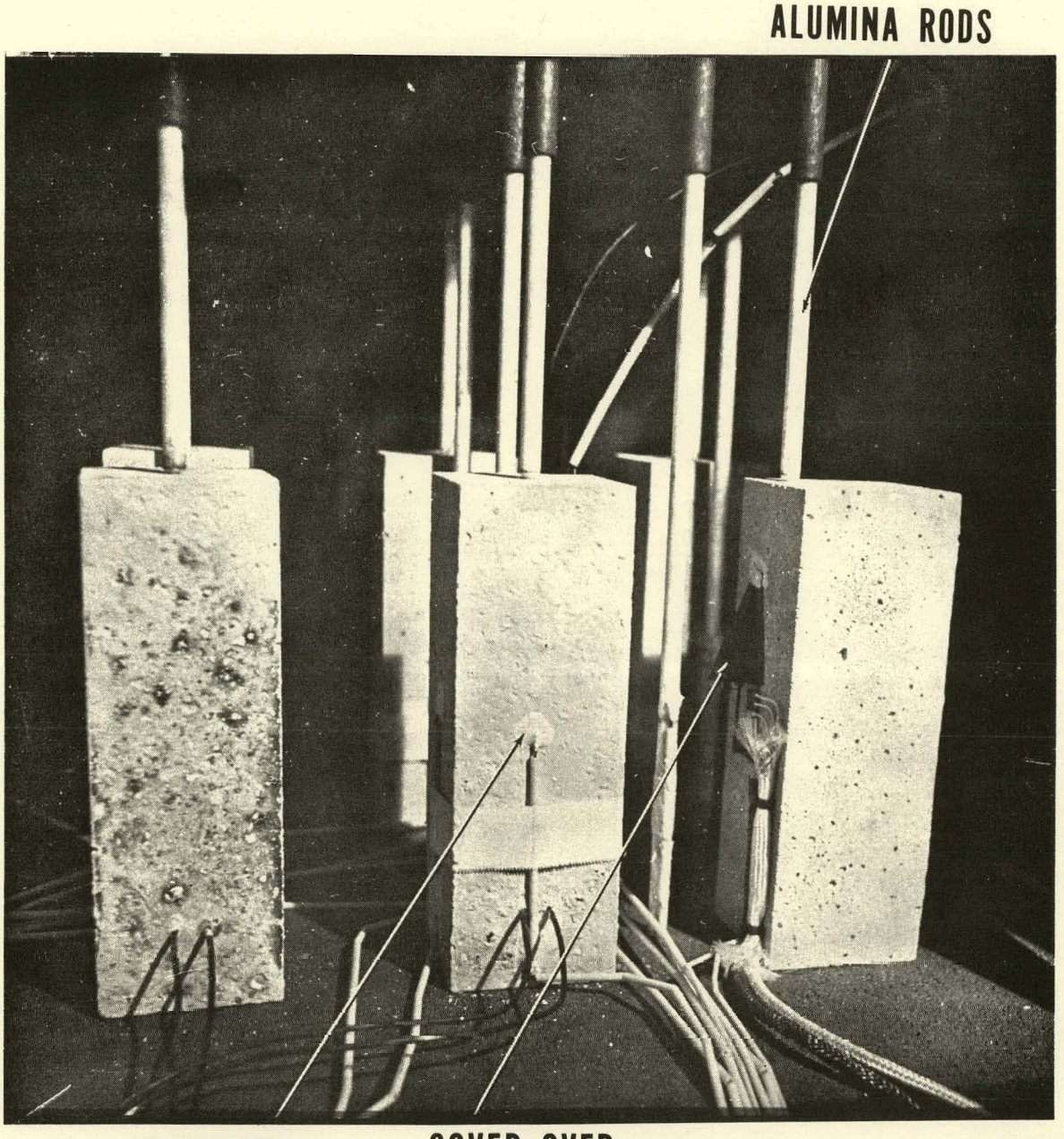

FIGURE 72. Thermal Load Test Set-Up (Embedded Strain Gaged).

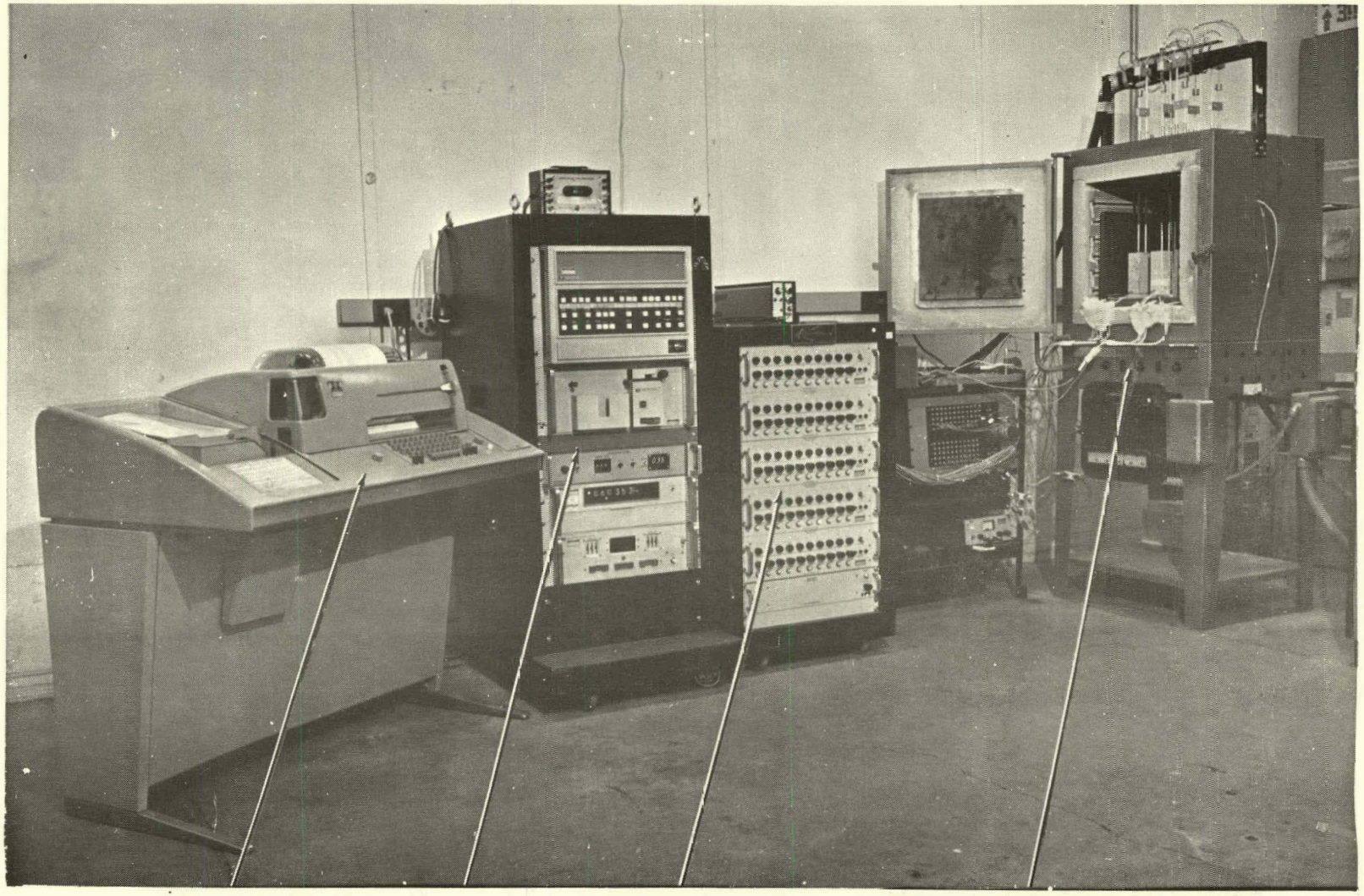

FIGURE 73. Thermal Load Test Data Acquisition System.

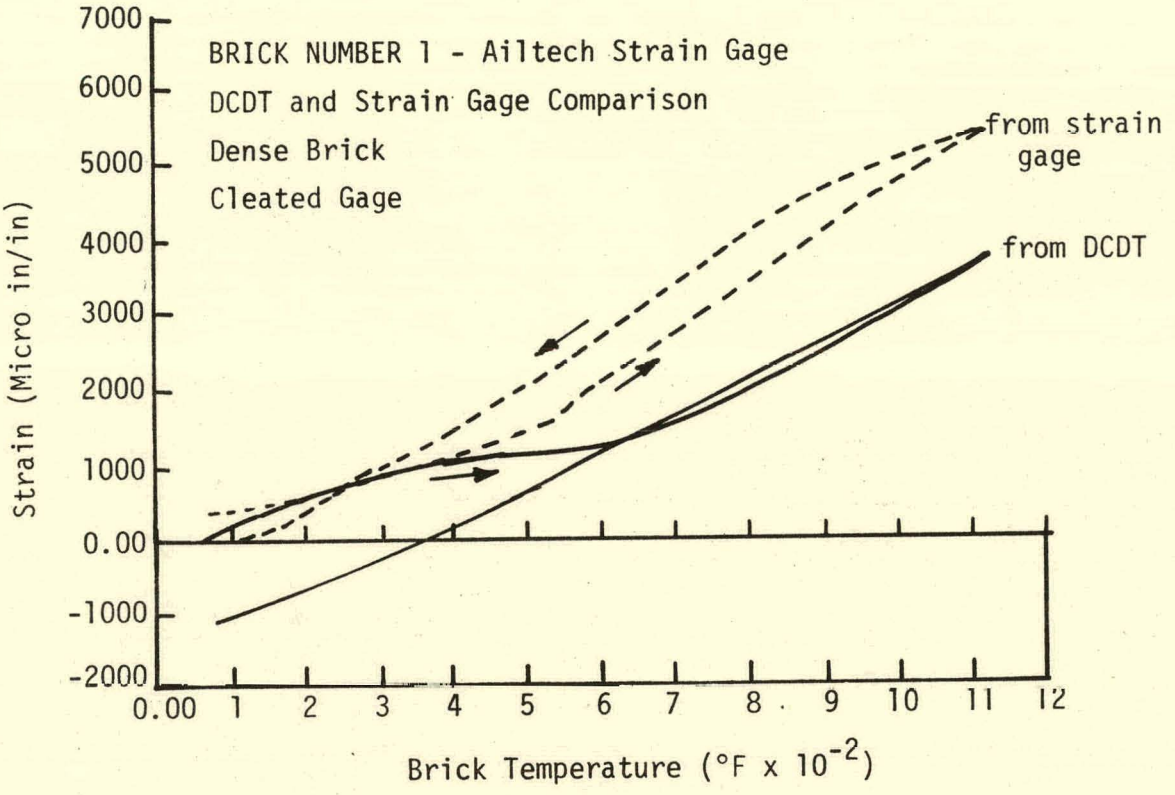

FIGURE 74. DCDT and Cleated Gage Comparison During Thermal Load Test on Dense Brick.

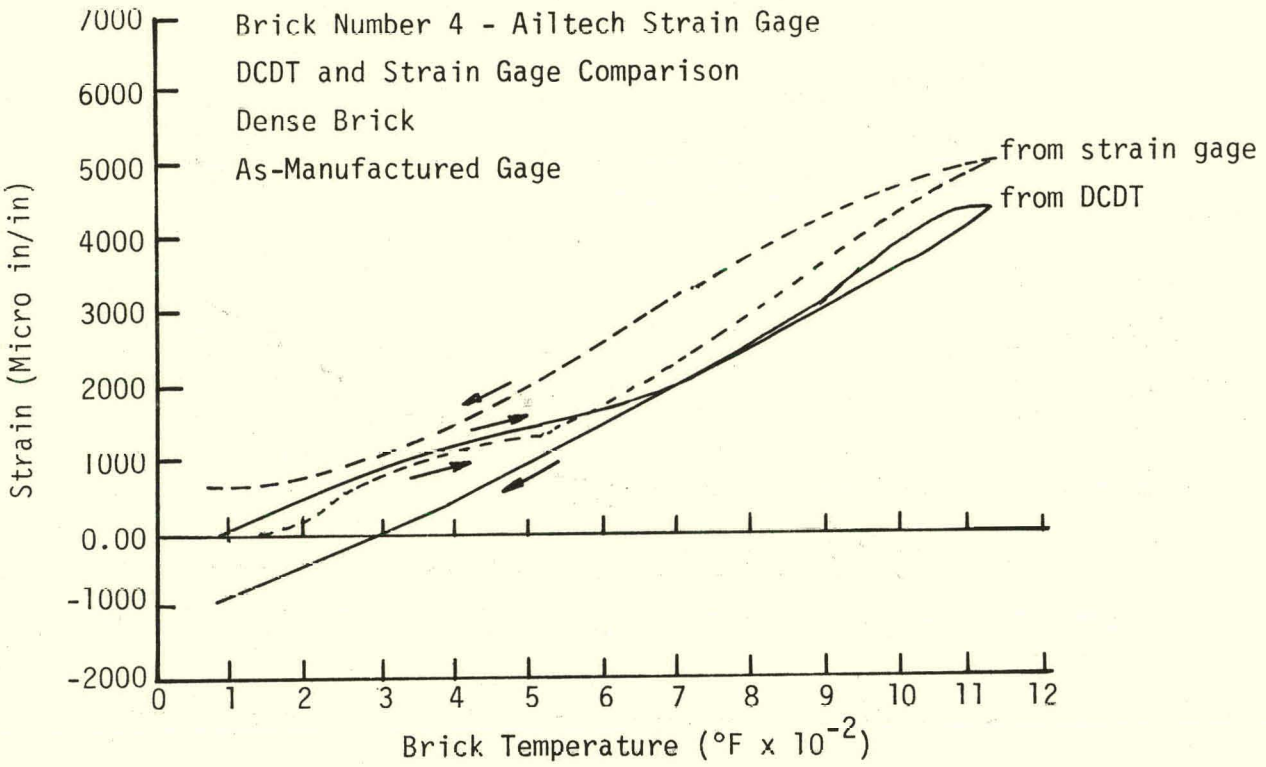

FIGURE 75. DCDT and As-Manufactured Gage Comparison During Thermal Load Test on Dense Brick.

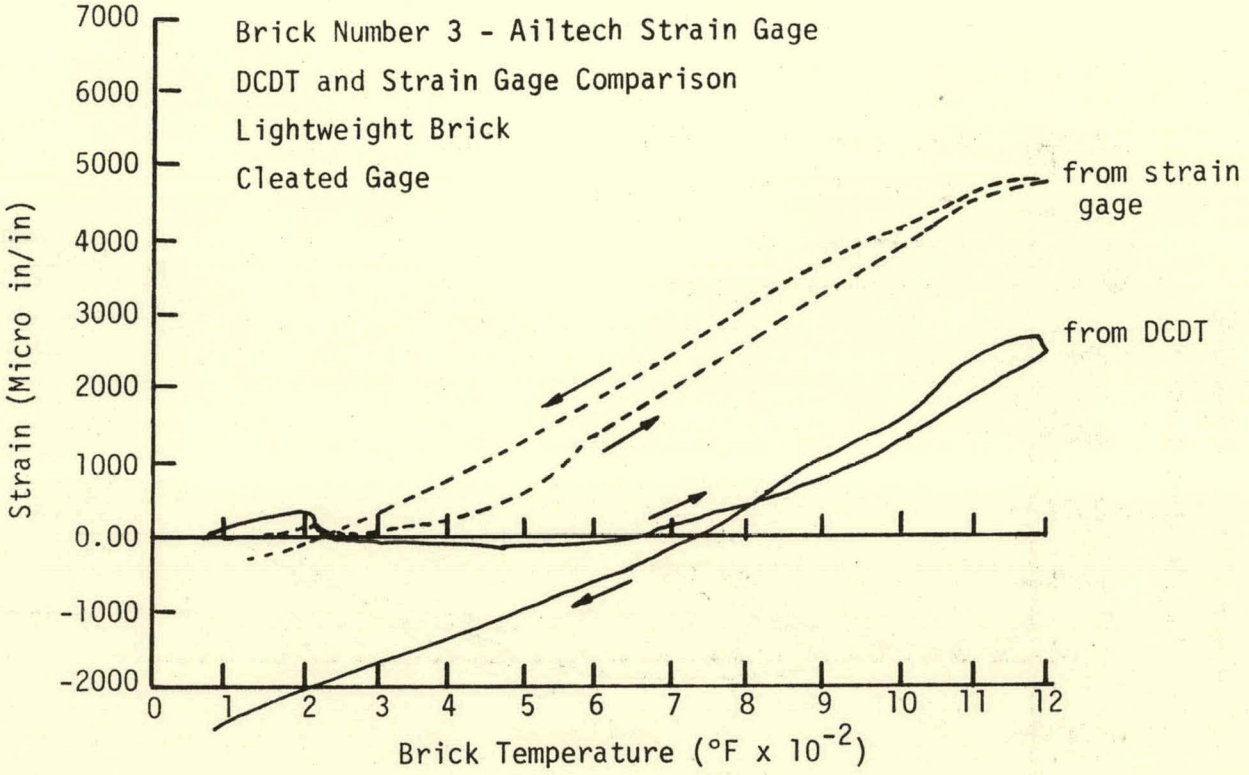

FIGURE 76. DCDT and Cleated Gage Comparison During Thermal Load Test on Lightweight Brick.

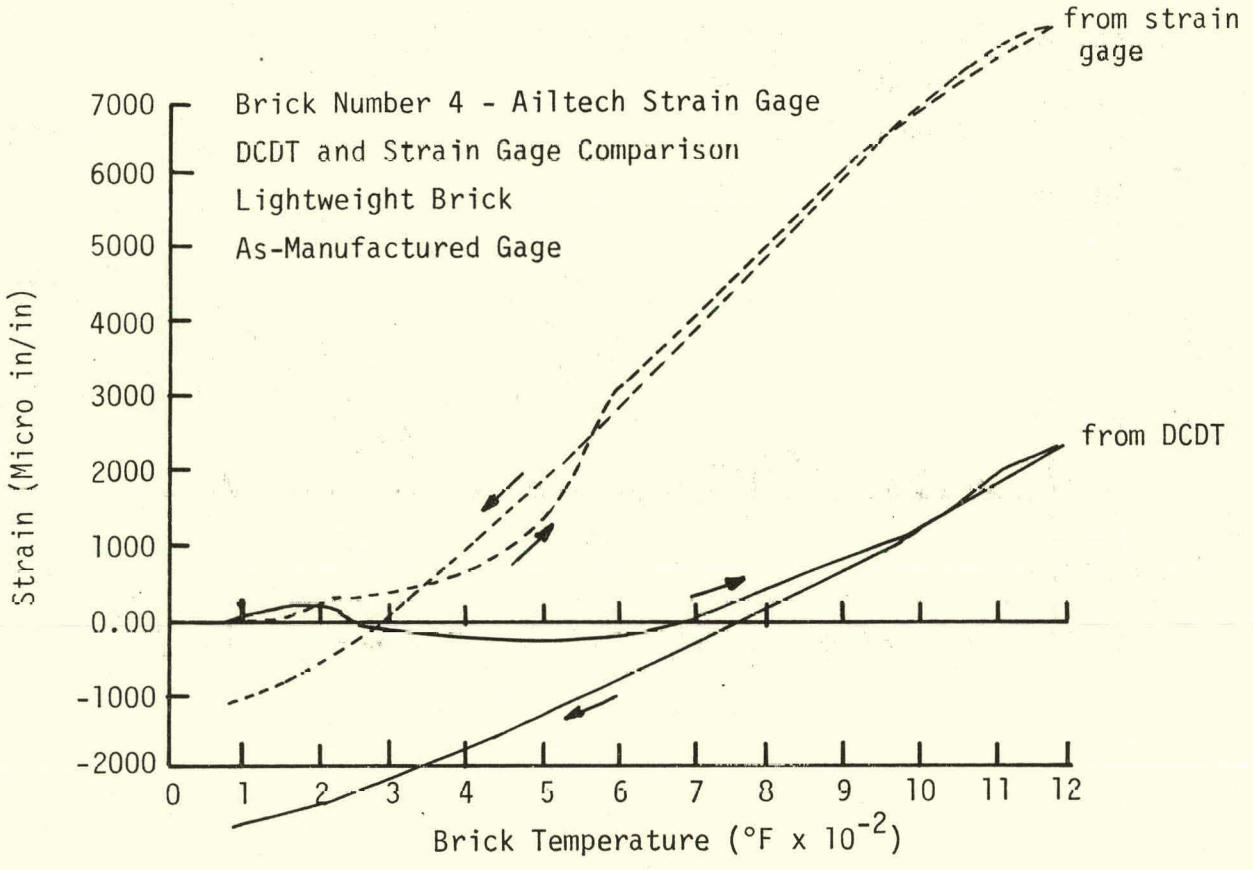

FIGURE 77. DCDT and As-Manufactured Gage Comparison During Thermal Load Test on Lightweight Brick.

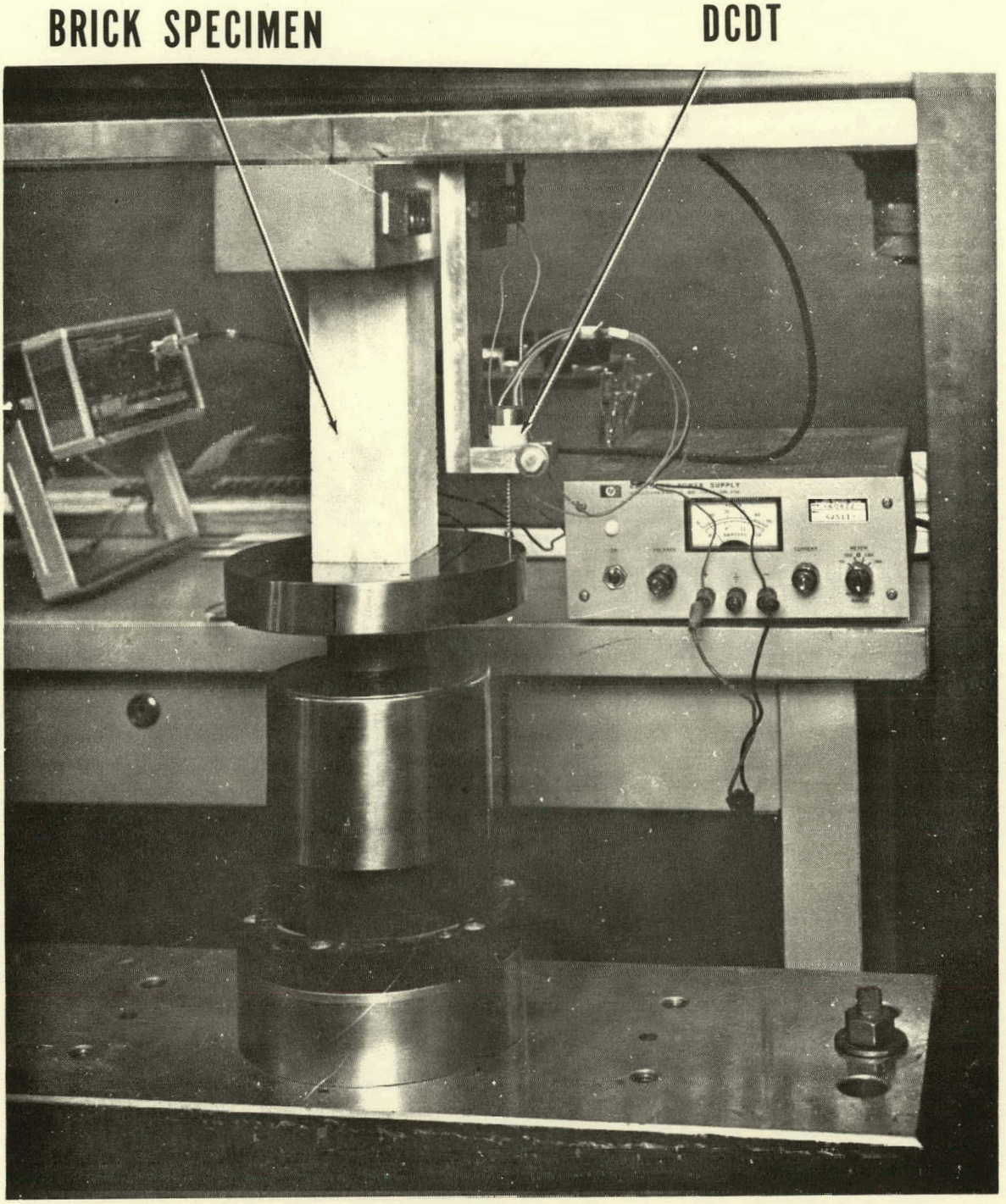

FIGURE 78. Mechanical Load Test Set-Up

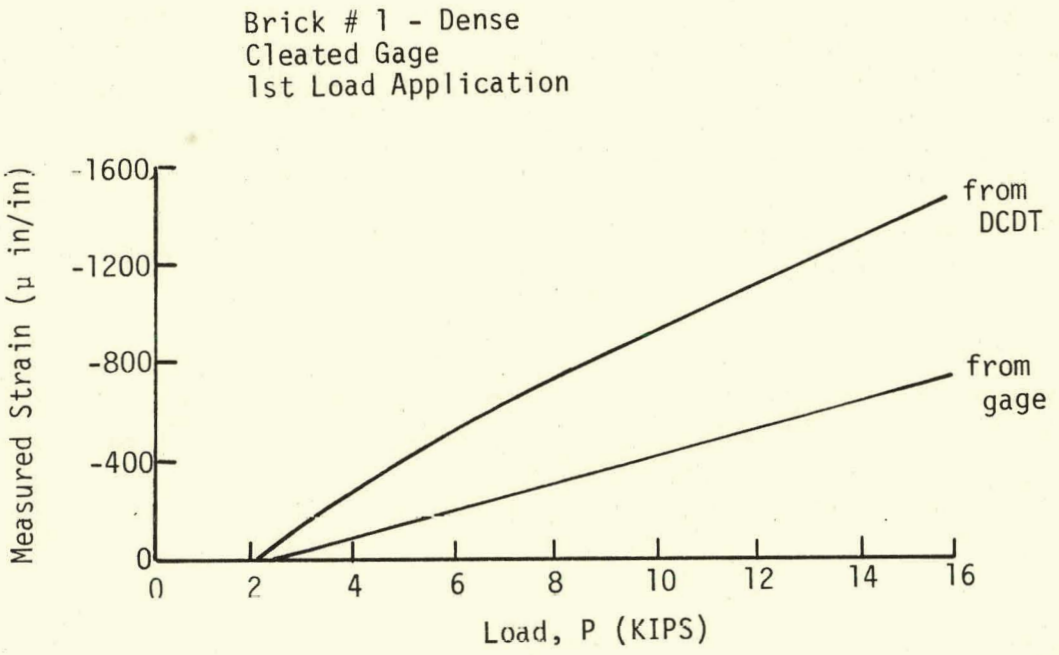

FIGURE 79. DCDT and Cleated Gage During Mechanical Load Test on Dense Brick.

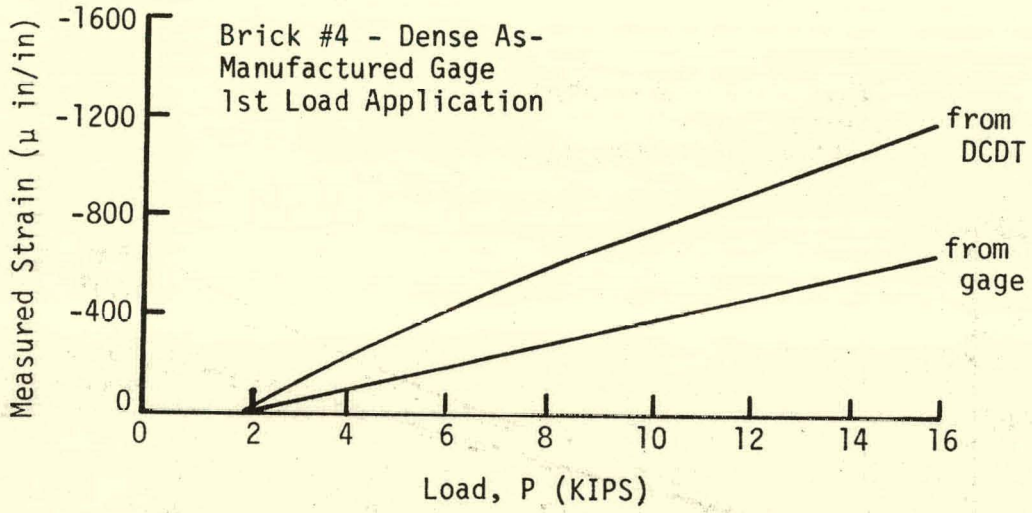

FIGURE 80. DCDT and As-Measured Gage Comparison During Mechanical Load Test on Dense Brick.

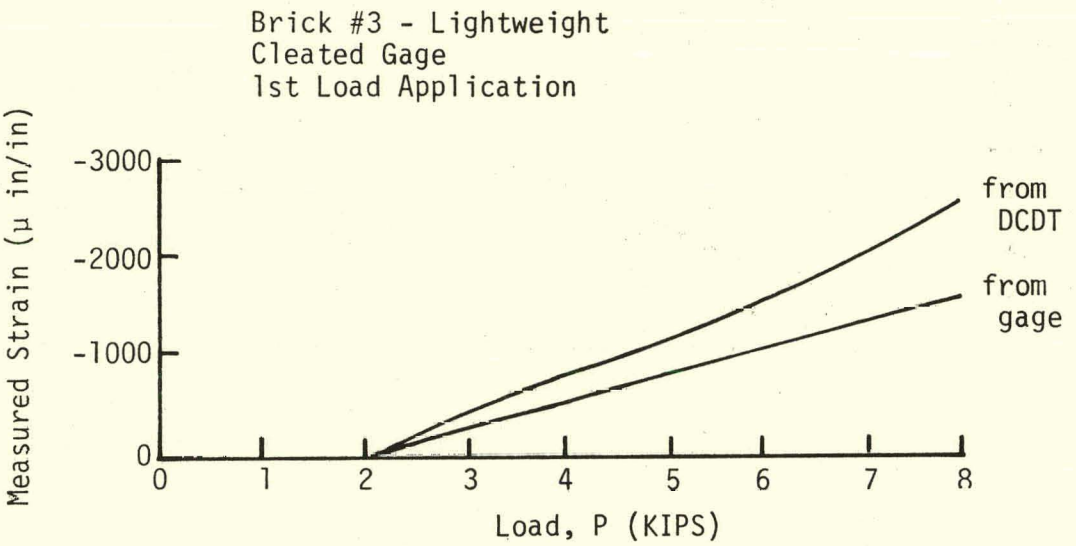

FIGURE 81. DCDT and Cleated Gage Comparison During Mechanical Load Test on Lightweight Brick.

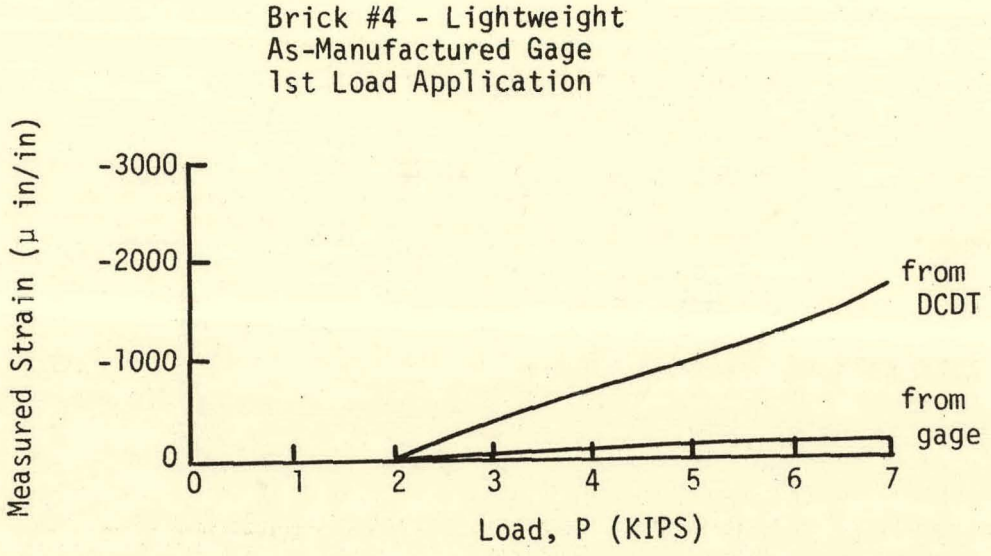

FIGURE 82. DCDT and As-Manufactured Gage Comparison During Mechanical Load Test on Lightweight Brick.

cross-sections were to reveal whether the presence of the strain gages causes cracking within the refractory material. Typical examples of the sliced brick cross-sections are provided in Figures 83 and 84 for the dense and insulating materials, respectively. In all cases, the bond between the refractory and gage was good. It was apparent that the gages did not cause cracking within the bricks and that the gages would not be likely to be sources of cracking within the refractory linings.

Results from the strain gage development work demonstrated that acceptable tensile and compressive strain measurements can be obtained at the interior points of refractory linings up to 1200°F using the Ailtech resistive gage. However, inaccuracies exist with this measurement technique as exhibited by these initial development test results. The differences noted between the strain gage results and the reference strain values were thought to be related to a strain gage data reduction parameter referred to as the gage factor. This factor relates measured strain (strain gage output) with the true or actual strain, and is an important factor in strain gage data reduction. The gage factors used to reduce the thermal and mechanical load test data were specified for each gage by the gage manufacturer. These values, however, apply to normal installations where the gages are spot-welded to a surface where strain measurements are desired. Thus in order to improve the accuracy of the proposed refractory strain measurement technique, it was necessary to determine the gage factor for the Ailtech gage in this unique embedment application.

Determining the appropriate gage factor for the embedment application of these gages required that additional refractory brick specimens be tested. Six dense (90% Al_2O_3) and six insulating (LITECAST 75-28) type refractory brick specimens, each having an embedded strain gage, were tested. Testing consisted of applying axially compressive loads to the brick specimens at various temperatures through two thermal cycles to 1200°F. By combining thermal and mechanical loads, the gage factor could be determined as a function of temperature for the gages embedded in both types of refractory. These specimens were tested in the Pereny furnace (Figure 7) rather than the facilities shown in Figures 72 or 78 since the Pereny was capable of providing combined thermal and mechanical loading. As with the initial development tests, the reference strains to which the strain gage results were compared were computed from the overall brick displacements which were measured using a displacement transducer. Results from one of the dense bricks is plotted in Figure 85 as measured strain (from embedded strain gage) versus true (from brick displacement). These results are typical of the six dense bricks tested. Shown are the curves derived from compression loading at room temperature, 300°F, and 580°F, during the first thermal cycle. For clarity, the remaining family of curves from the continued heat-up to 1200°F and cool-down to room temperature (in 300°F increments) are not shown. The family of curves associated with the second thermal cycle testing are likewise not presented in Figure 85. However, gage factor values were computed from each of the measured strain versus true strain curves generated during both thermal cycles of this brick, and these are shown graphically in Figure 86. The gage factors (GF) were derived from each of the curves that would appear in Figure 85 using the standard relation:

$$\varepsilon_t = \varepsilon_m \left(\frac{GFS}{GF}\right)$$

or

$$GF = \left(\frac{\varepsilon_m}{\varepsilon_t}\right) GFS$$

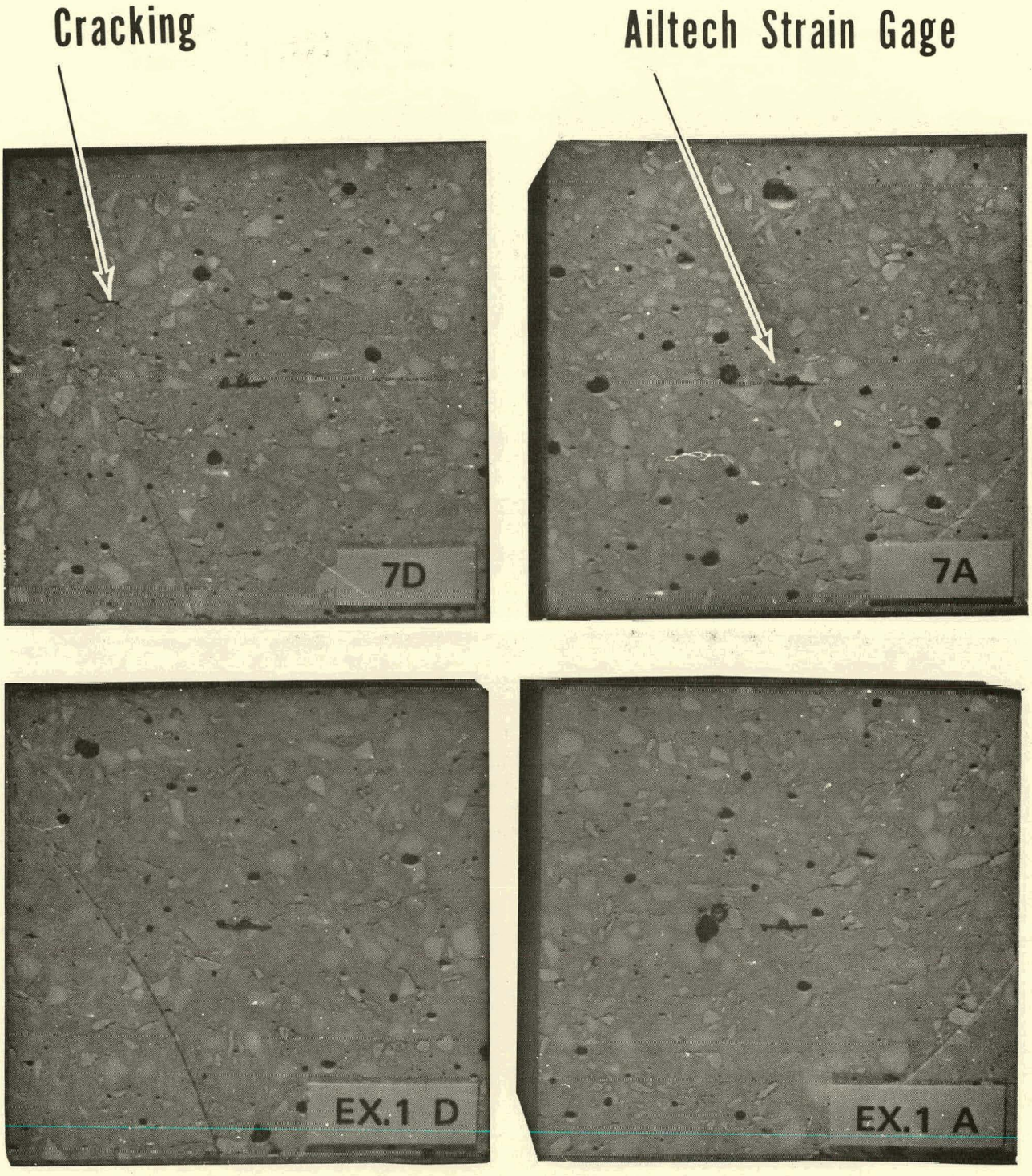

FIGURE 83. Cross-Sections of Dense Brick Showing Bonding to Embedded Strain Gage and Cracking Throughout Specimens.

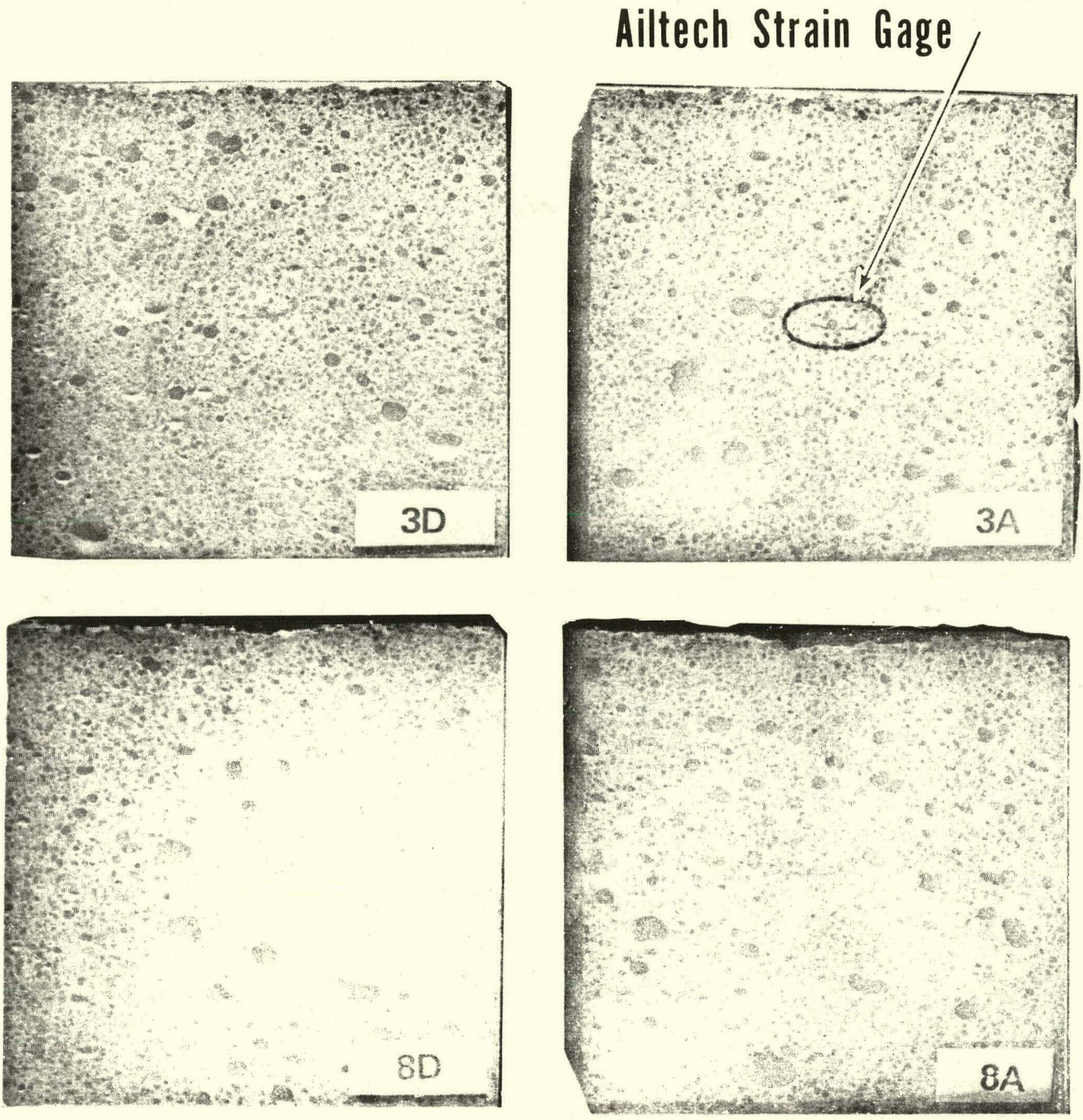

FIGURE 84. Cross-sections of Lightweight Brick Showing Bonding to Embedded Strain Gage and Absence of Cracking.

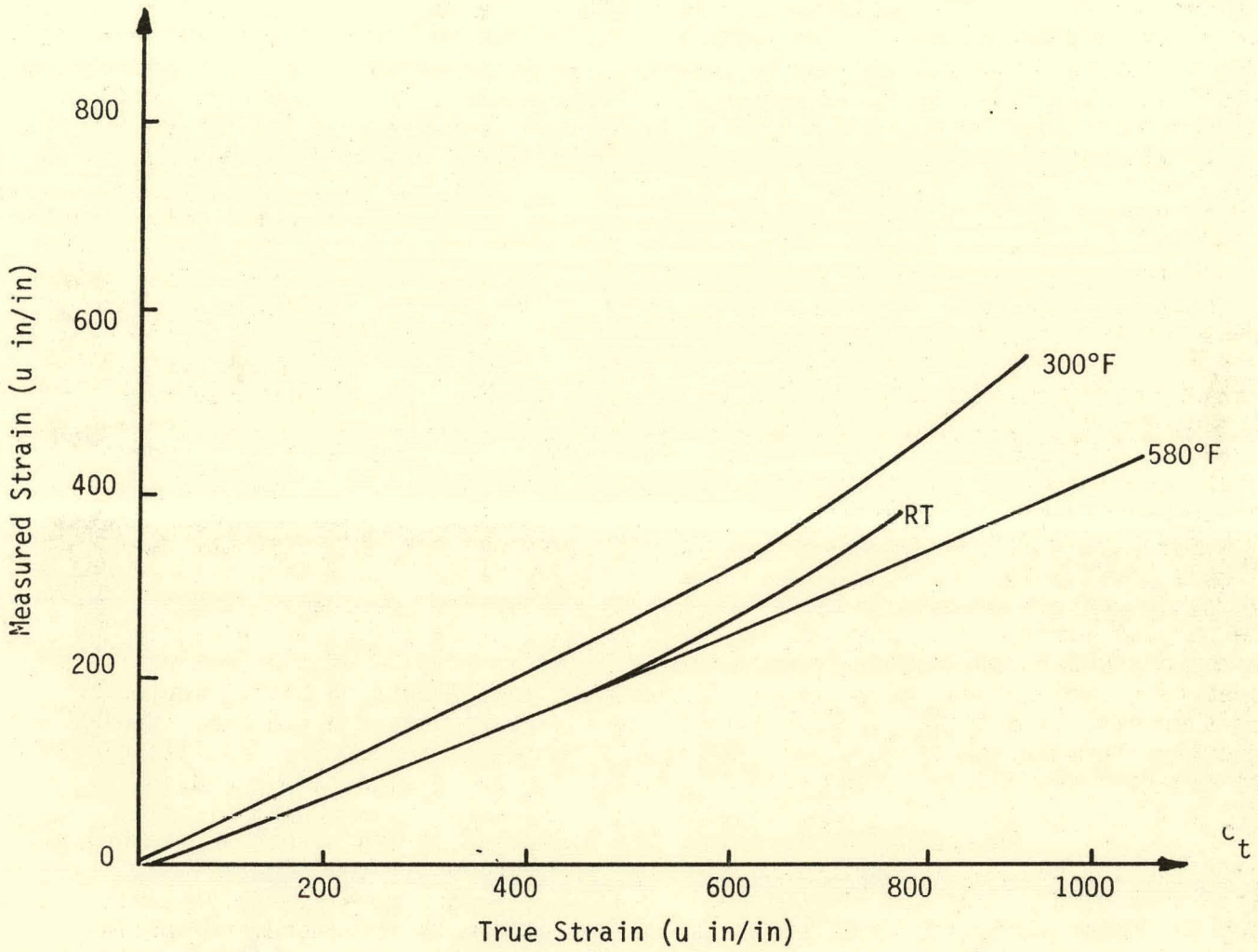

FIGURE 85. Measured Vs. True Strain of Dense Specimen (2"x2"x6") Under Axial Compressive Loading.

where GFS = gage factor setting of the strain measurement instrument,
ε_m = measured strain
ε_t = true strain
and $(\frac{\varepsilon_m}{\varepsilon_t})$ = slope of curve in Figure 85 at any temperature.

Figure 86 thus shows the variation of gage factor with temperature during the initial heat-up and cool-down and also illustrates the difference in gage factor between the initial and second thermal cycles. A significant result of Figure 86 is that the cool-down portion of the gage factor curve during the first thermal cycle does not follow the heat-up portion. In contrast to this first cycle curve is the gage factor data supplied by the manufacturer for a weldable application of this gage, regardless of the number of thermal cycles. For a weldable application the gage factor decreases gradually with increasing temperature and retraces the same curve on cool-down to room temperature, much like the second thermal cycle curve shown in Figure 86. As previously noted, the manufacturer's gage factor curve was used to reduce the strain gage data for the thermal load tests of the brick specimens performed initially. Thus, the inaccuracies noted in the previous thermal load tests (Figures 74 through 77), particularly the divergence between the strain gage and reference strain curves during cool-down from 1200°F, were believed to exist because of the significant difference between the vendor-supplied gage factor curve and the derived first cycle curve shown in Figure 86. The curves plotted in Figure 86 also suggest the need for two separate data reduction procedures. One reduction procedure would treat heat-up and cool-down data separately on an initial thermal cycle, and the second would be applied to heat-up and cool-down of subsequent thermal cycles. Formulating these strain gage data reduction procedures for both the dense and insulating refractory materials was hindered due to time constraints associated with the parallel effort of instrumenting, casting, and testing the refractory linings. In addition, the reliability of the gage factor curves derived from the insulating refractory specimens was questionable because limited data were acquired. Three of the six bricks tested failed prematurely under compressive loads during the initial stages of the testing procedure. The low quality of the test specimens was thought to be attributed to either old mix material or an error in the mixing and casting process. Consequently, formulation of modified data reduction procedures on the insulating type material was not completed because of time constraints and limited data.

An acceptable technique for measuring strain within refractory linings during heat-up to 1200°F was developed and applied to the eight linings tested during this contract. From the initial strain gage development testing, the gage factor variation with temperature associated with the embedment application of the proposed strain gage was identified as a possible source of error in the data reduction procedure. Formulation of more accurate procedures through additional testing of strain-gaged refractory bricks was used but not completed. Unique gage factor versus temperature curves were derived from these tests and it is recommended that the above development work be continued to establish and verify a more accurate strain gage data reduction procedure utilizing these unique gage factor curves.

A method of measuring strain on the inside diameter surface (hot face) of the test linings was also investigated during this development effort. One type of strain gage considered suitable for this application was a capacitance gage developed by the Boeing Company. Like the Ailtech resistance gage, the Boeing gage was also designed to be attached to a specimen by spot welding.

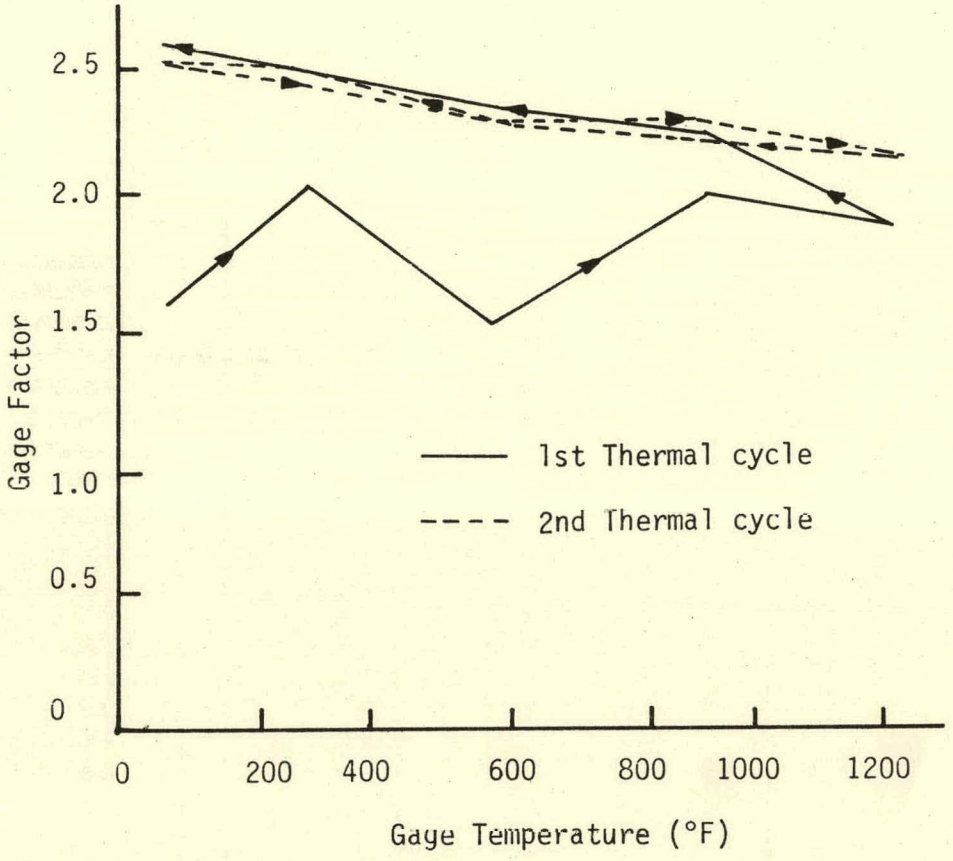

FIGURE 86. Gage Factor Vs. Temperature

This gage is not sealed but is rated for operation to 1500°F. Evaluation tests performed on this gage were similar to those for the Ailtech embedment gage in that thermal and mechanical loads were applied to a refractory brick specimen to which a Boeing gage was attached. Based on the cost of this capacitance gage, its evaluation was limited to testing of only one gage. The gage was attached to one side of a dense brick specimen by spot welding to Inconel mounting pads which were embedded into the surface of the brick during casting. The dense brick was of the same type refractory as that planned for the dense components (hot face) of the test linings. A close-up view of the installed gage with the leadwires attached is shown in Figure 87.

Results of the separate thermal and mechanical load testing of the Boeing gage are presented in Figure 88. These results are plotted in the same format as the initial Ailtech embedment strain gage results presented earlier since both gage types were tested simultaneously. Results from the Boeing capacitance gage were not as favorable as those derived from the Ailtech resistance gages. Under compressive mechanical loading at room temperature, the strain gage output is in good agreement with the reference strains derived from the displacement transducer (Figure 86). However, this gage did not adequately measure strain of the brick specimen under thermal loading beyond 350°F(Figure 88). The deviation between the strain gage prediction and the reference strain was thought to be caused by several factors. One possibility was that the brick "curled" during heat-up thereby inducing a bending strain at the strain-gaged surface of the brick which would not be completely sensed in the axial direction by the displacement transducer. Another possible explanation of the strain gage response is that a transverse strain gradient may have existed within the brick causing the strain gage attachment pads to rotate with respect to the strain-gaged surface. This occurrence would also induce an erroneous bending strain sensed by the gage. The data reduction equation associated with this gage was also examined, particularly with regard to a term which is related to the thermal expansion of the strain gage compensating rod. An independent dilatometer test was performed on a sample of this rod material to verify the thermal expansion data supplied by the gage manufacturer. However, substitution of these new data into the gage data reduction equation did not significantly improve the variation between the strain gage predictions and the reference strains.

Because of the cost, the proposed use of the Boeing capacitance strain gage was to install several gages on the hot face of the initial test lining, then reuse these gages on the hot face of the subsequent linings. This plan assumed that reconditioning of these gages would be necessary after each test. In discussing the feasibility of this plan with the strain gage manufacturer, it was their opinion that because of the fragile nature of the gage, and the 2000°F temperature to which it would be exposed, the gages could possibly be reused two or three times at most. Our observation of the gage after completing the thermal load phase of the bonded strain gage testing confirmed this opinion. Attempts to remove the gage were difficult because of the oxidation, and hence, were not successful. It was concluded that significant reworking of the gages would be required by the manufacturer if they were completely removed and considered for reuse. Alternate methods of gage attachment were not studied under the originally planned evaluation work primarily because the spot welding approach is the sole recommended procedure set forth by the manufacturer. Because of these problems and the unfavorable evaluation test results, use of the Boeing gage to measure hot face strain during the lining tests was not considered further.

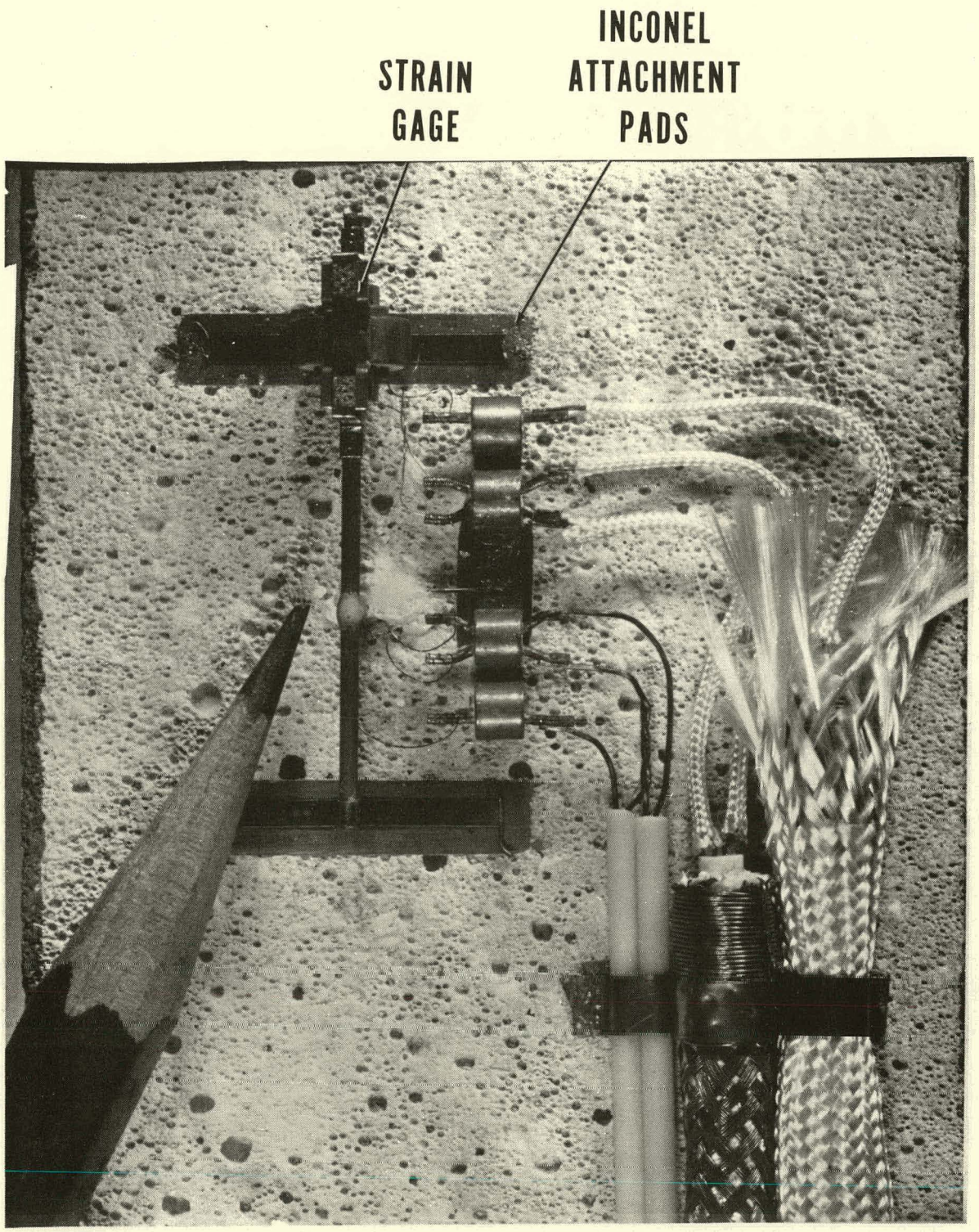

FIGURE 87. Capacitance Strain Gage Attached to Surface of Dense Brick Specimens

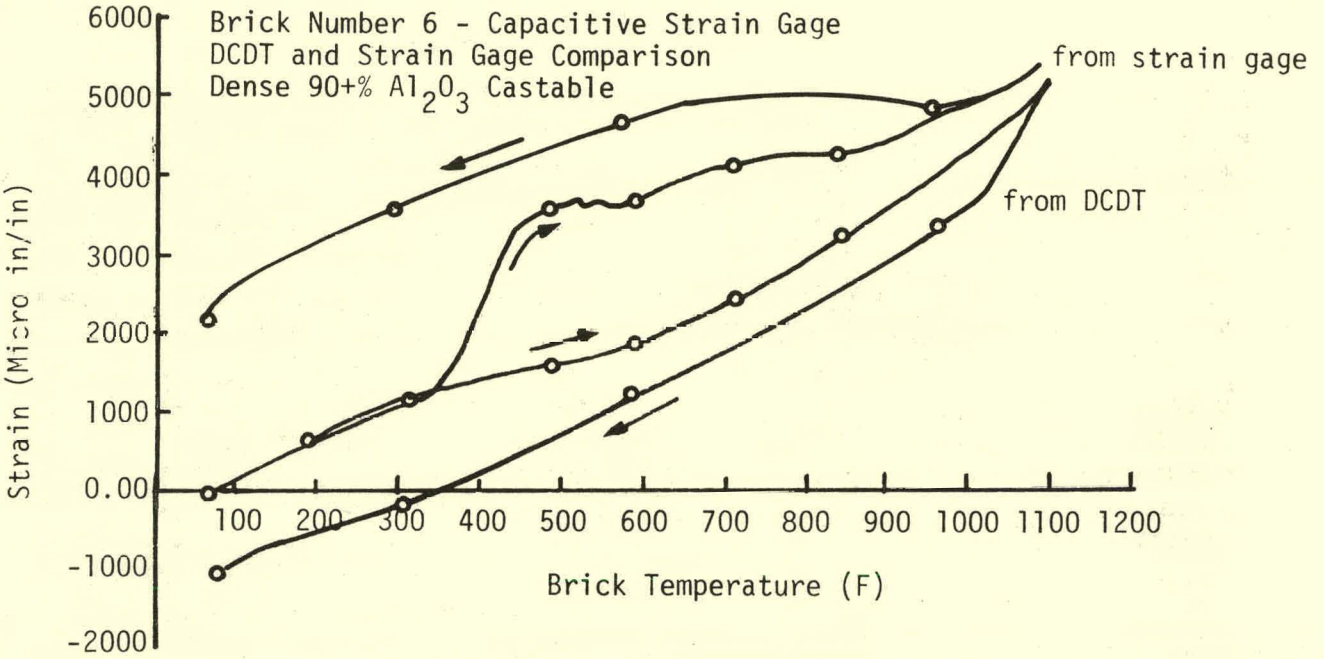

a) Thermal Load Test Results

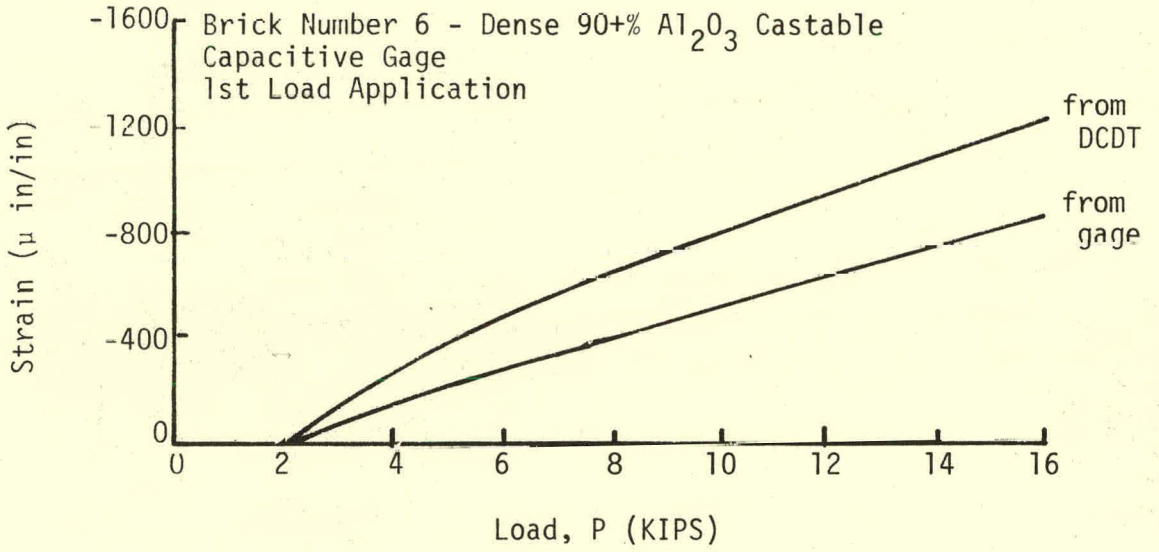

b) Mechanical Load Test Results

FIGURE 88. Bonded Strain Gage Test Results for Boeing Capactive Gage.

Battelle Columbus Laboratories Subcontract

One of the findings that arose while reviewing external references on high temperature strain gages for the lining tests was the work that Battelle-Columbus Laboratories (BCL) had performed for the National Aeronautics and Space Adminstration (NASA) in developing a free-filament gage for use to 2000°F. Personnel at Battelle involved with the development and characterization of this gage system were contacted to discuss the feasibility of modifying this gage to make it suitable for use in the refractory linings. The fact that the BCL gage is a free-filament type prohibited its direct use in the refractory application. It was learned from these discussions that the BCL gage was not commercially available but that Battelle would attempt to develop a 2000°F gage for a refractory embedment application on a subcontract basis. A subcontract with Battelle was pursued with the intent that these gages would be embedded in the hot face region of the test linings where temperature would exceed 1200°F, the operating limit of the commercial Ailtech gages.

The approach suggested by Battelle involved modifying commercial 1200°F Ailtech strain gages to incorporate the special Fe-Cr-Al alloy wire that was developed for the BCL 2000°F gage. Specifically, this entailed substituting the special BCL alloy wire as the strain sensing filament in place of the platinum-tungsten alloy which Ailtech uses to fabricate their standard gages. Thus, the modified gage would be similar in appearance to the Ailtech gage (Figure 68), and the alloy substitution would extend the operating temperature of the standard Ailtech gage to 2000°F.

Fourteen modified strain gages were to be fabricated by Ailtech under Battelle's supervision. Four of these were to undergo characterization and evaluation tests at Battelle and the remaining ten would be delivered to B&W for use in the lining tests. It was realized that this development activity represented a first-of-a-kind effort and, as such, difficulties were encountered during the gage fabrication process. Out of about 40 fabrication trials, only four were totally successful. The failed gages were described as having poor insulation resistance, shorted or open filaments, or abnormal gage resistance. It was suspected that these failure modes were related to a special heat-treatment required of the BCL alloy during the gage fabrication process. Since only four rather than fourteen operative gages were available, B&W and Battelle mutually agreed that characterization tests of the modified gages planned to be performed at Battelle should be eliminated from the subcontract workscope. Thus, B&W received these four gages along with several of the failed gages. Battelle issued a report summarizing their subcontract activities, elaborating on the gage fabrication difficulties. The four modified gages were not included in any of the lining tests since time was not available to characterize these gages prior to installation within the test linings as was done with the 1200°F Ailtech gages.

Lining Strain Embedment Technique

A technique was developed for embedding the Ailtech strain gage within the insulating and dense components of the test linings. Before pouring the insulating component of each lining, the cleated strain gages were placed at their prescribed locations in the annular region formed by the vessel shell and the insulator casting form. They were oriented to sense strain in either the hoop, axial, or radial direction of the lining. The gages were rigidly fixed into proper orientation by attaching their leadwires to guy wires which were stretched diagonally between adjacent anchors fastened to the shell in the vicinity of the gaged areas. Figure 89 shows the arrangement used to install the strain gages and the guy

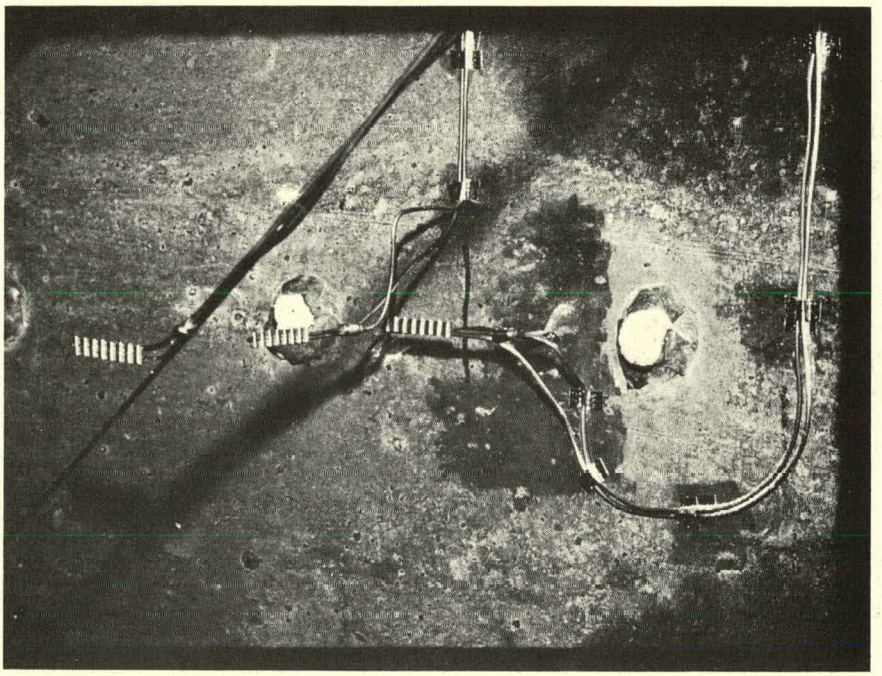

FIGURE 89. Strain Gage Installation Technique for Insulating Component.

wires. The lead wires were routed through penetrations in the vessel shell to the outside of the vessel where they were connected to the data acquisition equipment cables. Split-gland Conax fittings threaded into these penetrations (Figure 90) served to seal the lining and test environment within the vessel. After completing the leadwire routing and attachment activity, the insulating castable was poured, thereby embedding the strain gages. While casting, the gages were protected from direct impact of the refractory, and were also hand-held to provide further support and assure orientation as the castables assumed their level. A similar procedure was followed to embed the uncleated strain gages in the dense component of each of the linings after the insulating component had cured. Guy wires were again used to secure the strain gages. In this case, the guy wires were attached to anchor extensions which were threaded onto the anchor bases previously installed in the insulating component. This arrangement is shown in Figure 91 .

Temperature

Because strain gage temperature relates to a necessary strain data reduction parameter, a thermocouple was attached to each of the embedded gages. In addition, the thermocouples provided useful data with regard to temperature profiles and histories through the lining and at hot face positions. Type K thermocouples were used in both the lining and at the hot face position; however, those in the lining were sheathed in 304 stainless steel and those at the hot face were sheathed in Inconel. Hot face position thermocouples were placed by welding them to embedded metal tabs (positioned during liner pouring) at the hot face surface. The signals from the thermocouples were fed directly to the data acquisiton system and converted to temperature values.

With the exception of one test run without strain gages, the thermocouples were used in conjunction with the strain gages. Their location during a specific test(Lining #3) is indicated in Table 12. Table 13 indicates the location of thermocouples in the test run without strain gages.

Refractory Pore Pressure

Measurements of pore pressure within the refractory lining were obtained so that comparisons could be made with analyses obtained with REFSAM and related to explosive spalling. Both the test and its experimental developments are described in Section 2.4.3.

The orientation and location of pressure tubes, gages, and transducers are shown in Figure 92. Subsequent modifications were made to the pressure tubes so that they were straight, rather than curved as shown in the illustration. The modifications were based on experimental trials whereby it was shown that there was no advantage in bending the tubes.

Application of Acoustic Emission (AE)

As was discussed in Section 2.5., AE technique feasibility was successfully demonstrated through the brick and panel tests. It was therefore decided to instrument the full sized test vessels for AE monitoring during selected lining tests. Prior to the first lining test, the unlined shell of the test vessel was instrumented with both the Dunegan and AETC AE systems. The unlined vessel was heated to a shell temperature of 400°F and monitored for AE. The purpose of this test was to detect, locate, and minimize potential noise interferences associated with the vessel itself, the heater assemblies, and the structural attachments. Minimal amounts of AE signals were generated during this test and it was therefore concluded that the precautions taken to acoustically isolate the vessel were successful. These precautions included power supply isolation and filtering, sensor channel filtering, and electrical isolation of the sensors from the vessel shell.

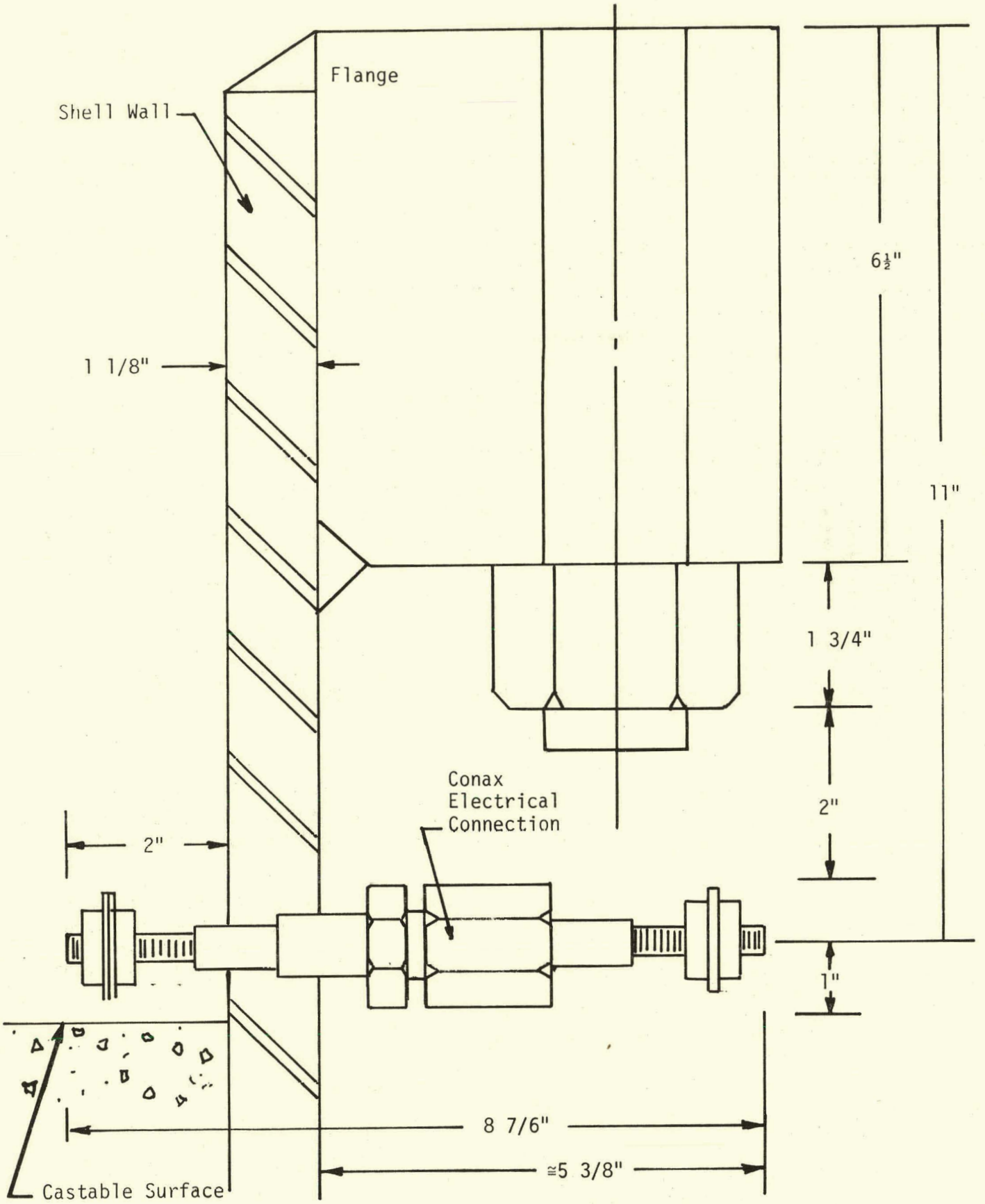

FIGURE 90. Schematic of Split-gland Conax Fitting Attached to Vessel Shell Through Penetrations.

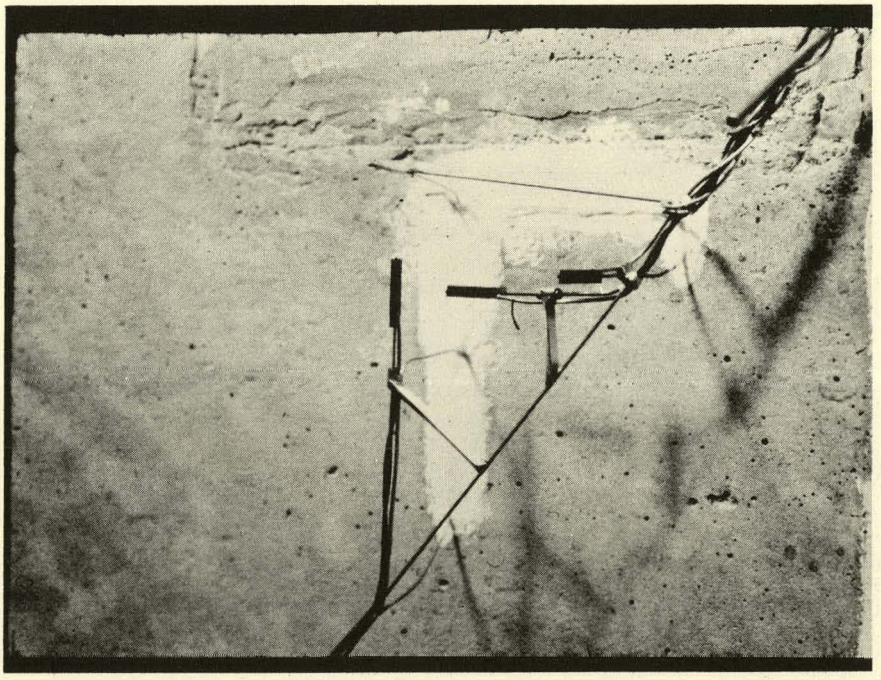

FIGURE 91. Strain Gage Installation Technique for Dense Component.

TABLE 12. Geometric Location & Orientation of Embedment, Anchor, and Shell Strain Gages in Lining #3

Embedment Strain Gage Number	Circumferential Location θ-Degrees	Axial Location Z-Inches	Radial Distance From Hot Face D-Inches	Strain Sensing Direction	Liner Component
1	17	-6	1	Hoop	Dense
2	17	-6	1	Axial	Dense
3	208	-6	1	Radial	Dense
4	17	-6	3 1/2	Hoop	Dense
5	17	-6	3 1/2	Axial	Dense
6	208	-6	3 1/2	Radial	Dense
7	17	-6	5 1/2	Hoop	Insulator
8	17	-6	5 1/2	Axial	Insulator
9	208	-6	5 1/2	Radial	Insulator
10	17	-6	11	Hoop	Insulator
11	17	-6	11	Axial	Insulator
12	208	-6	11	Radial	Insulator
Anchor (Radial Stud)	112	0			
Shell	17	0	13 1/8		
Shell	208	0	13 1/8		

TABLE 13. Location of Embedded Thermocouples in Lining

Embedded Thermocouple Number	Circumferential Location θ-Degrees	Axial Location Z-Inches	Radial Distance From Hot Face D-Inches	Lining Component
1	17	0	0	Hot Face
2	17	0	1	Dense
3	17	0	3 1/2	Dense
4	17	0	4 1/2	Interface
5	17	0	5 1/2	Insulator
6	17	0	11	Insulator
7	17	+15	0	Hot Face
8	17	+15	3 1/2	Dense
9	17	+15	11	Insulator
10	17	-15	0	Hot Face
11	17	-15	3 1/2	Dense
12	17	-15	11	Insulator

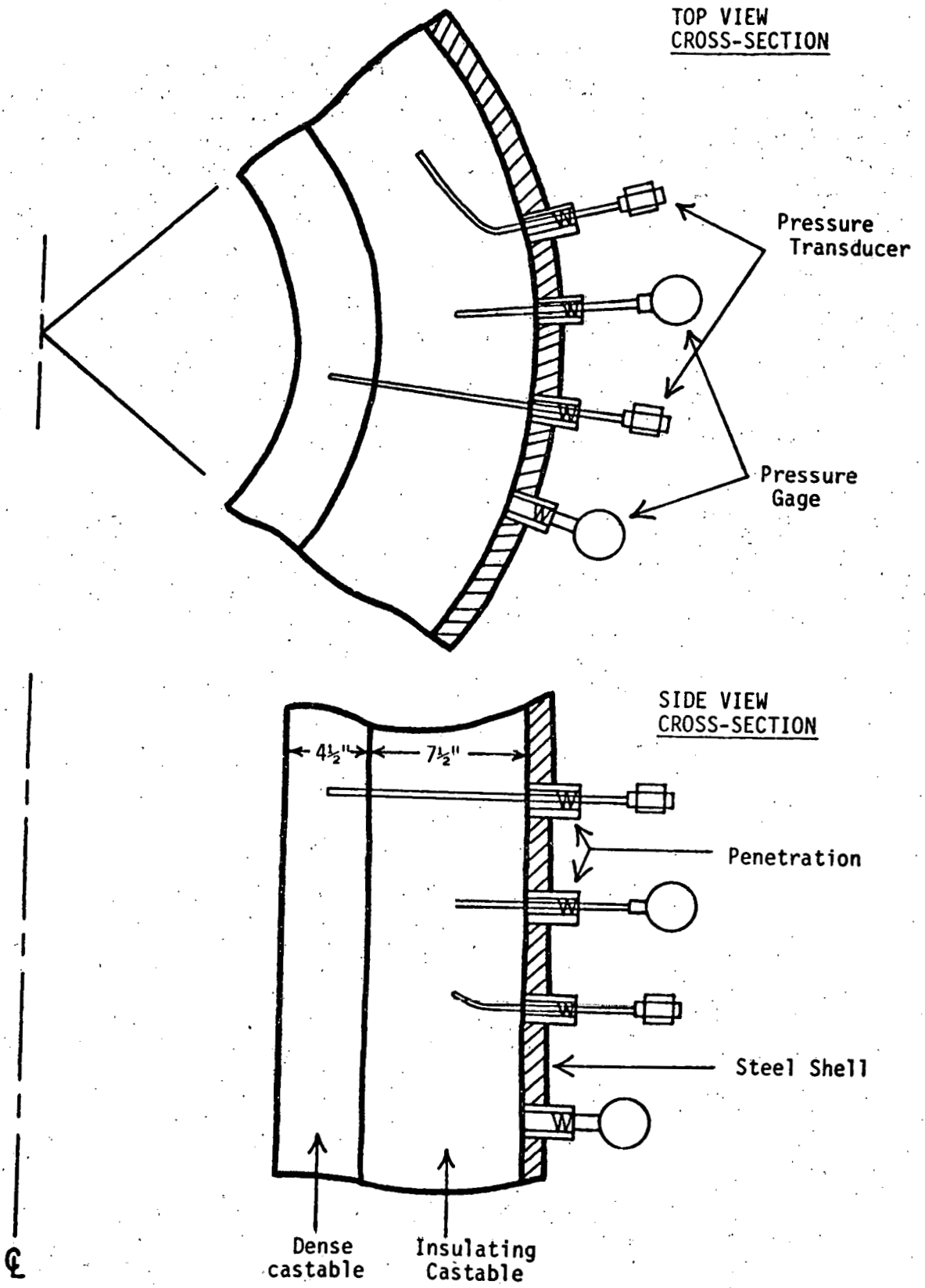

FIGURE 92. Cross-section of Refractory Geometry of Two Component Lining.

Figures 93 and 94 depict the mode for attaching the various AE sensors to the shell of the large test vessels. Each sensor was attached to the shell by means of threaded steel waveguides. The waveguides screwed into nuts welded at the locations shown in Figure 93. The three centrally located waveguide positions were used to attach the Dunegan sensors. Although the Dunegan system was a single channel unit, the highly attenuative nature of the refractory linings necessitated mixing the outputs from three evenly spaced sensors in order to achieve full coverage of the vessel.

The inherent nature of the AETC system necessitated using fourteen waveguides and sensor channels to perform source location. The fourteen AETC waveguides were spaced as shown in Figure 94 to provide two bands of sensor positions, each band containing seven sensors. The waveguides in the lower band were circumferentially offset approximately 26 degrees from the upper band waveguides to form triangular sensor arrays. The triangular sensor arrays were a necessary condition to allow the AETC system's software to accept the incoming AE data and compute its source location.

The waveguide attachment points were selected not only within the geometrical constraints imposed by the vessel and AE system designs, but also in consideration of the refractory anchor positions. It was predicted that AE signals generated within the innermost portion of the linings (dense component, hot face) would be severely attenuated and possibly undetectable by attaching sensors to the shell. The reasons for these concerns were as follows:

- The refractory materials used in these tests were highly attenuative to acoustic signals in the frequency range of interest (roughly 100-500 KHz). The one foot total thickness of the dual component linings could completely damp even large amplitude crack-related signals.

- The dual component (two separately cast materials) nature of the linings formed a mechanical interface between the two materials which could impede acoustic propagation across the interface. Therefore, AE signals generated within the innermost casting (dense component) may not have been detected, even if the attenuation was not a significant problem.

- An additional acoustic interface existed between the shell and the LITECAST component due to the difference in acoustic impedances of the shell material and the refractory.

To avoid the potential complications presented by the conditions above, the acoustic waveguides on the shell were positioned directly over the anchor positions where possible. The anchors attached directly to the inner wall of the shell and penetrated through both lining components in most cases. AE signals therefore had direct propagation paths through the anchors to the shell and AE sensors, and could be detected from either component. Since anchor-refractory interactions were known contributors to cracking tendencies, this technique also provided good sensitivity to those interactions.

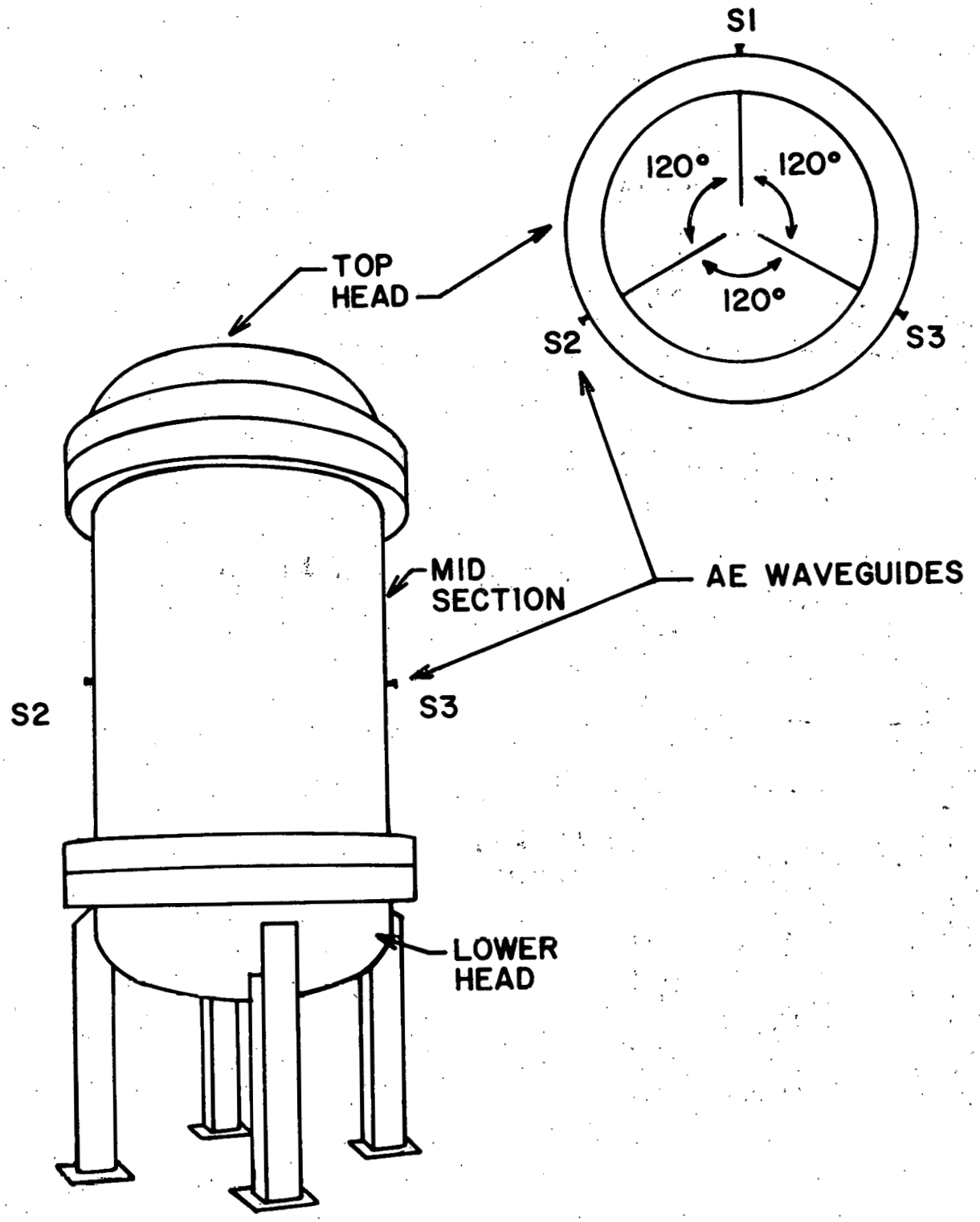

FIGURE 93. AE Sensor Positions on Large-Scale Test Vessel (Dunegan System)

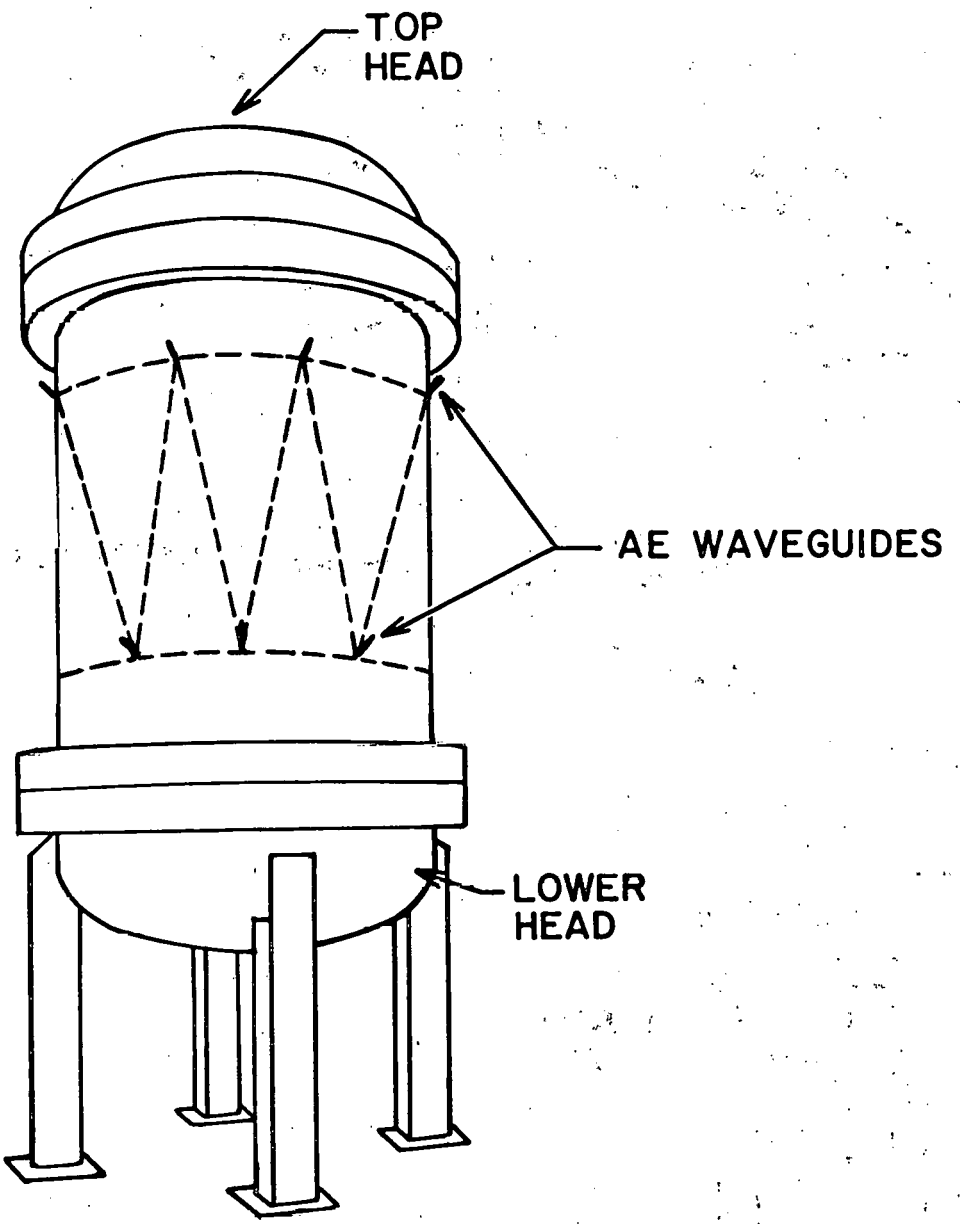

FIGURE 94. AE Waveguide Positions on Large-Scale Test Vessel(AETC System)

Anchors

Although predictions of anchor strains and stresses were not planned with the math models developed on this contract, their measurement was considered to be of great value to the understanding of refractory lining/anchor interactions which occur in monolithic lined process vessels. In addition, the data collected were expected to give MIT some important experimental data for their DOE sponsored refractory lining/anchor modeling study.

To make these measurements, state-of-the-art strain measurement techniques for metal components were used. These techniques involved spot-welding 4 uniaxial Ailtech weldable strain gages to the 3/8" shaft of the "V" and "Y" type anchors about two inches from the end that was attached to the shell. These gages were the same type used in the embedment work. The gages were originally spaced 90 degrees apart around the circumference of the anchor and were oriented such that their axes coincided with the anchor axes. This arrangement enabled the determination of both axial and bending stresses which were induced in the anchors during the heat-up of the linings. A thermocouple was also spot-welded to the anchor near the strain-gages to properly reduce the strain data at elevated temperature.

In all cases, the strain gaged anchors were located at the center (Z = 0 in.) of each lining. Leadwires from the strain gages and thermocouples were routed through sealed penetrations in the vessel shell in the same manner as was used for the embedded lining strain gages and thermocouples.

This technique was modified slightly in the later linings. The modification involved using only two strain gages instead of four and positioning them 180° apart around the circumference of the anchor. This was done to reduce the cost of strain gaging the anchors and to make more channels available on the data acquisition system for other test data.

Figures 95 & 96 are, respectively, photographs of the strain-gaged "V" and "Y" anchors.

Vessel

The two test vessel shells were instrumented to measure temperature, stress and pressure while the top and bottom heads were instrumented to measure temperature and pressure. The methods used to make these measurements are outlined below.

Temperature

Type K thermocouples were either spot-welded to the shell and heads or bonded with a high temperature mortar. These thermocouples were placed at various strategic locations on the shell, such as at the center and at circumferential locations, that coincided with the embedded thermocouple locations. Most of the vessel shell thermocouples were associated with strain gages. The output of these thermocouples was fed to the data acquisition system.

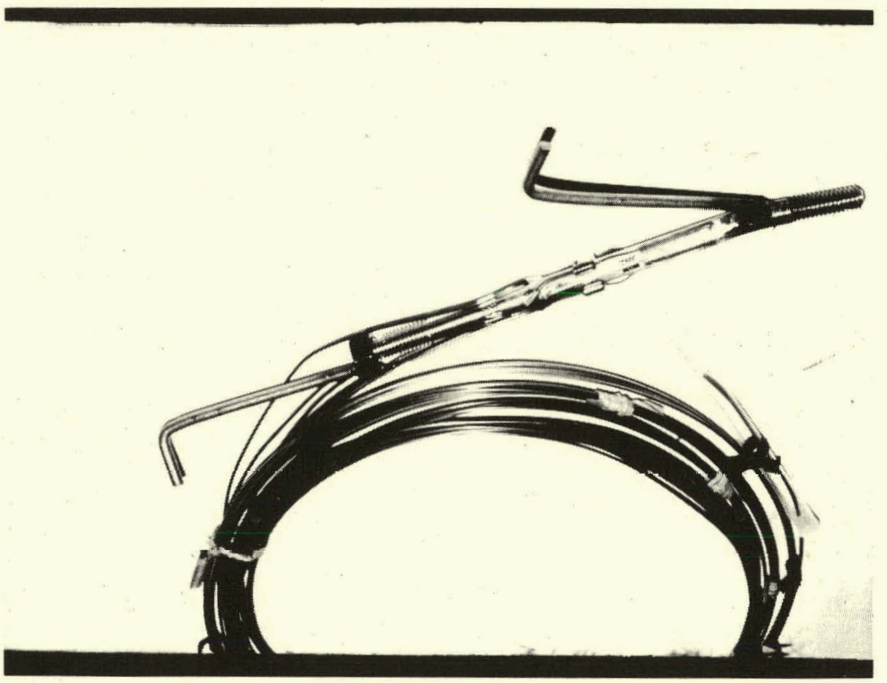

FIGURE 95. Strain Gaged "V" Anchor.

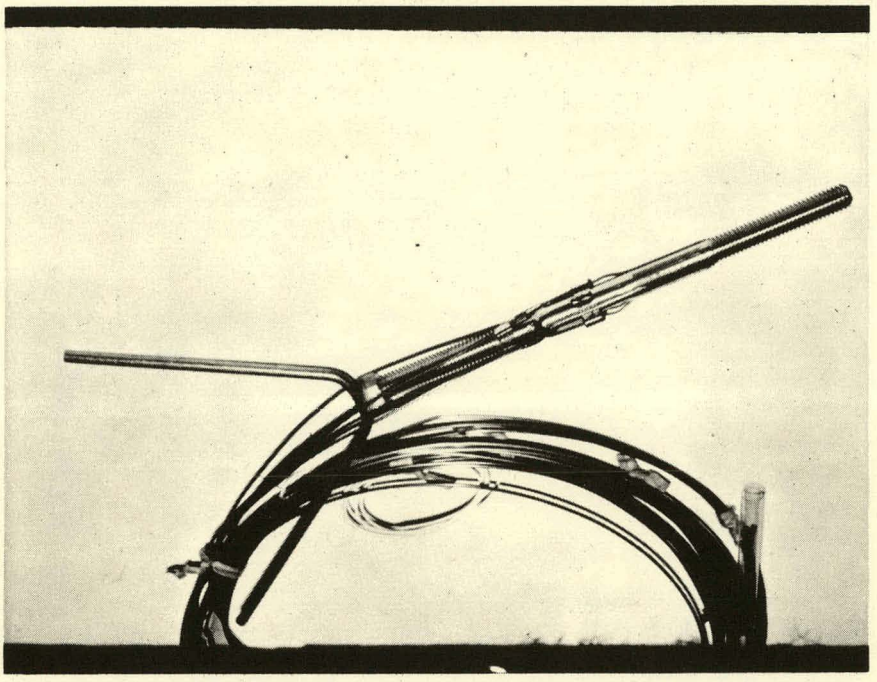

FIGURE 96. Strain Gaged "Y" Anchor.

Strain/Stress

To acquire an appreciation for the lining/shell interactions occurring during the heat-up tests and to generate data that could be correlated with the math model predictions, the vessel shells were instrumented with biaxial foil type strain gages. State-of-the-art techniques were used to install and use these strain gages. Initially two types of biaxial gages were evaluated and were placed 180° apart at the center (Z = 0 in.) of the vessel shell. Later a third type of gage was used and the gages were placed 90° apart at the center (Z = 0 in). of the vessel shell and along the length of the vessel at one circumferential location. These gages were designated LWK, CEA and WK, respectively.

The CEA and WK were bonded to the shell with a high temperature adhesive and the LWK was spot welded. The gages were oriented such that their biaxial grid axes coincided with the hoop and axial axes (principal stress directions) of the shell as shown in Figure 97. The LWK and CEA gages were used in the early tests (first five linings) and the WK was used in the last four lining tests. The shell stress results which lead to this change in the type of biaxial strain gage used are discussed in the lining test results section of the report(3.5.)

Pressure

Pressure gages and pressure transducers with >250 psig capacity were used to measure the pressure in the test vessel during the pressurized steam and air runs. These gages and transducers were attached to the shell and top or bottom heads through the 1/2 to 3/4 inch penetrations available in these sections. The gages were read routinely during the tests while the transducers were connected to a pressure alarm system and a digital display. This latter system would ring an alarm if the pressure exceeded a preset value. The alarm was routinely set at 225 to 250 psig maximum.

Video Taped/TV Monitoring of the Hot Face

A remote video camera (Sony) was set up to monitor the hot face through one of the bottom viewports. Two of the three viewports in the bottom head were designed to project at an angle of 20° to the same region in the middle of the test zone on the hot face. Figure 98 is a top view of Lining #3 and shows two holes in the lower insulation for illumination and camera angle as well as the illuminated viewing area on the hot face. Good resolution was obtained with a telescoping lens used on the camera shown in Figure 99. Numerous filters were available to obtain optimum contrast. A television was located in the control and data acquisition room so the hot face could be monitored continuously during the test. A video recorder was used to record the image at periodic intervals.

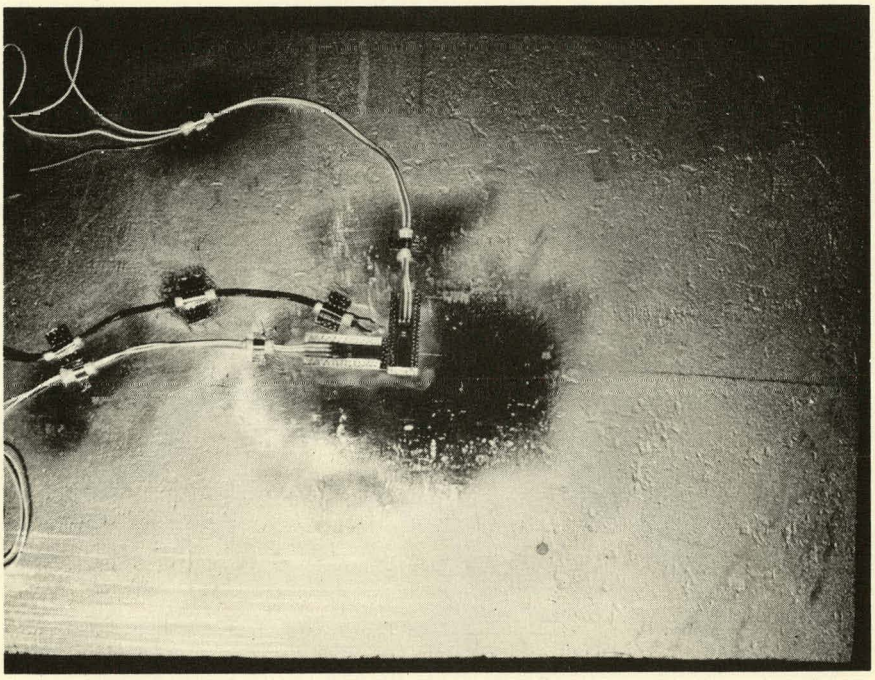

FIGURE 97. Orientation of Biaxial Strain Gage Attached to Outside of Pressure Vessel Shell in Hoop and Axial Directions.

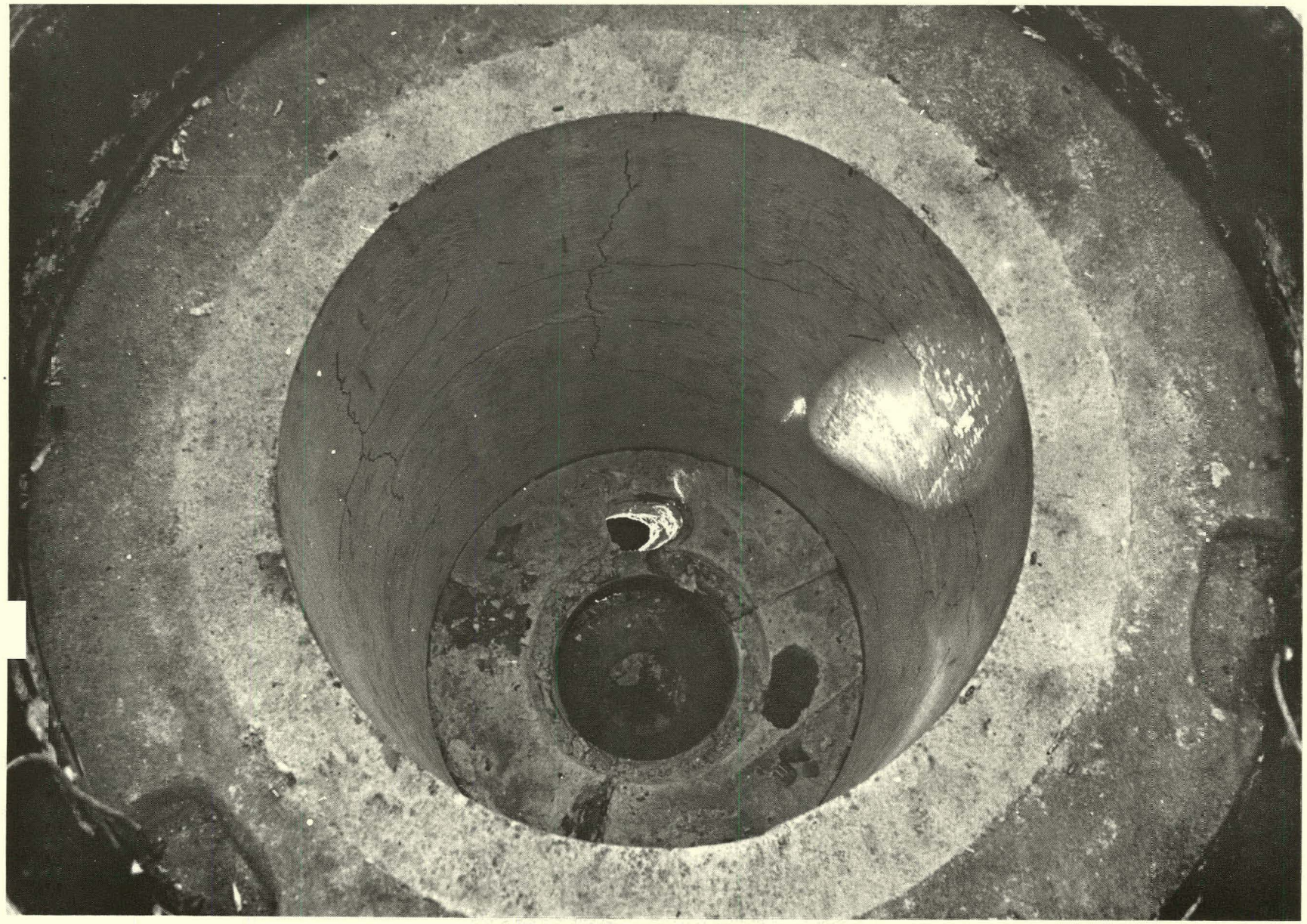

FIGURE 98. Top View of Pressure Vessel/Test Furnace Showing Crack Pattern After Heat-up Test of Lining #3 to 400°F.

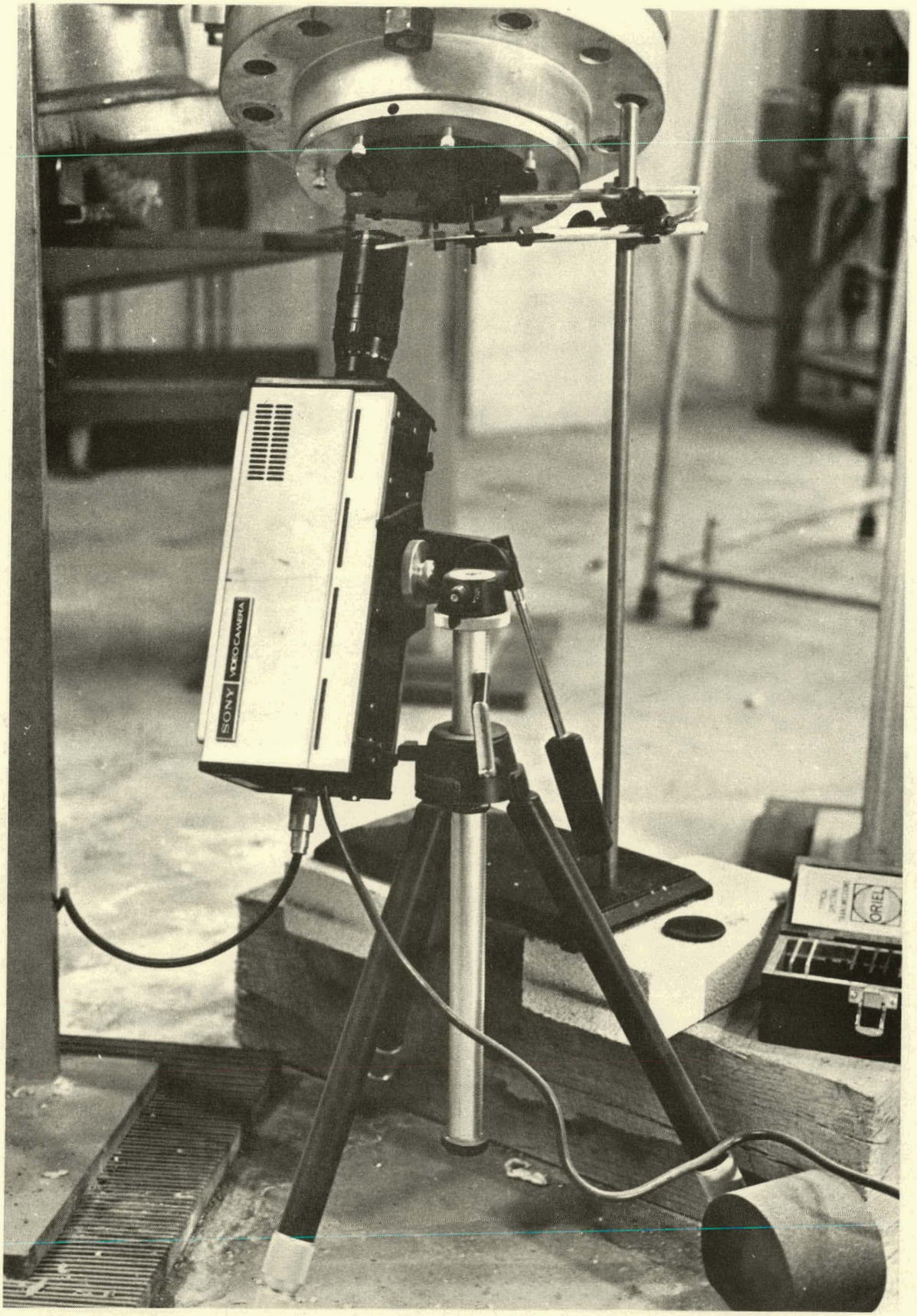

FIGURE 99. Television Camera With Telescoping Lens Positioned Under Viewport for Remote Monitoring of Hot Face.

2.6.5. Post Testing

Post testing included the nondestructive examination, visual inspection measurement, sample collection, sample testing, and tear out of a lining. Of particular interest was the crack pattern and crack widths which occurred throughout the lining after a heat-up test. To perform this work, test equipment and a number of techniques were acquired or developed. The sections which follow describe this equipment and the techniques used.

Test Equipment

To make crack width measurements, shrinkage determinations and a full inspection of the cracking pattern in a lining, special equipment was acquired or made. This equipment included:

- A gage for measuring the diameter of the lining. This gage was made by attaching a 34.5 inch long aluminum rod to a 1 inch vernier depth caliper to give a device capable of measuring accurately from 35 to 37 inches.

- A PEAK LUPE 7X Optical Comparator (a magnifying eyepiece with a graduated objective lens). This device was used to measure the crack widths to hundredths of an inch.

- A lighted magnifying glass which was used to locate fine (.005 inch wide or smaller) cracks.

- A 36 inch long caliper with a dial micrometer. This was used to measure the thickness of the lining components at various locations along the length of the lining.

- Feeler gages which were used to measure or estimate the gap formed between the dense and insulating components.

- Pneumatic chipping hammers (Black & Decker) which were used to roughen the inner surface of the dense component and to chip out samples of lining material for testing.

- An electric concrete drill coring rig designed for vertical drilling which was purchased and then modified so horizontal drilling could be done with it. The drill was manufactured by Christensen Diamond Products and was designated model E-2-15. It had a 15 amp, 1000 rpm motor and accessories which allowed drill bits from 1 to 6 inch diameter, or larger, and 6 to 18 inch long to be used. The overall length of the unit was approximately 32". The drill could be lengthened with extensions and blocks to 36" or more. Photographs of this equipment are shown in Figure 100.

- A pneumatic diamond wall saw and attachment assembly which were purchased to make vertical slices through the lining. This equipment was to be used to aid in the tear out of the lining and also to produce a good

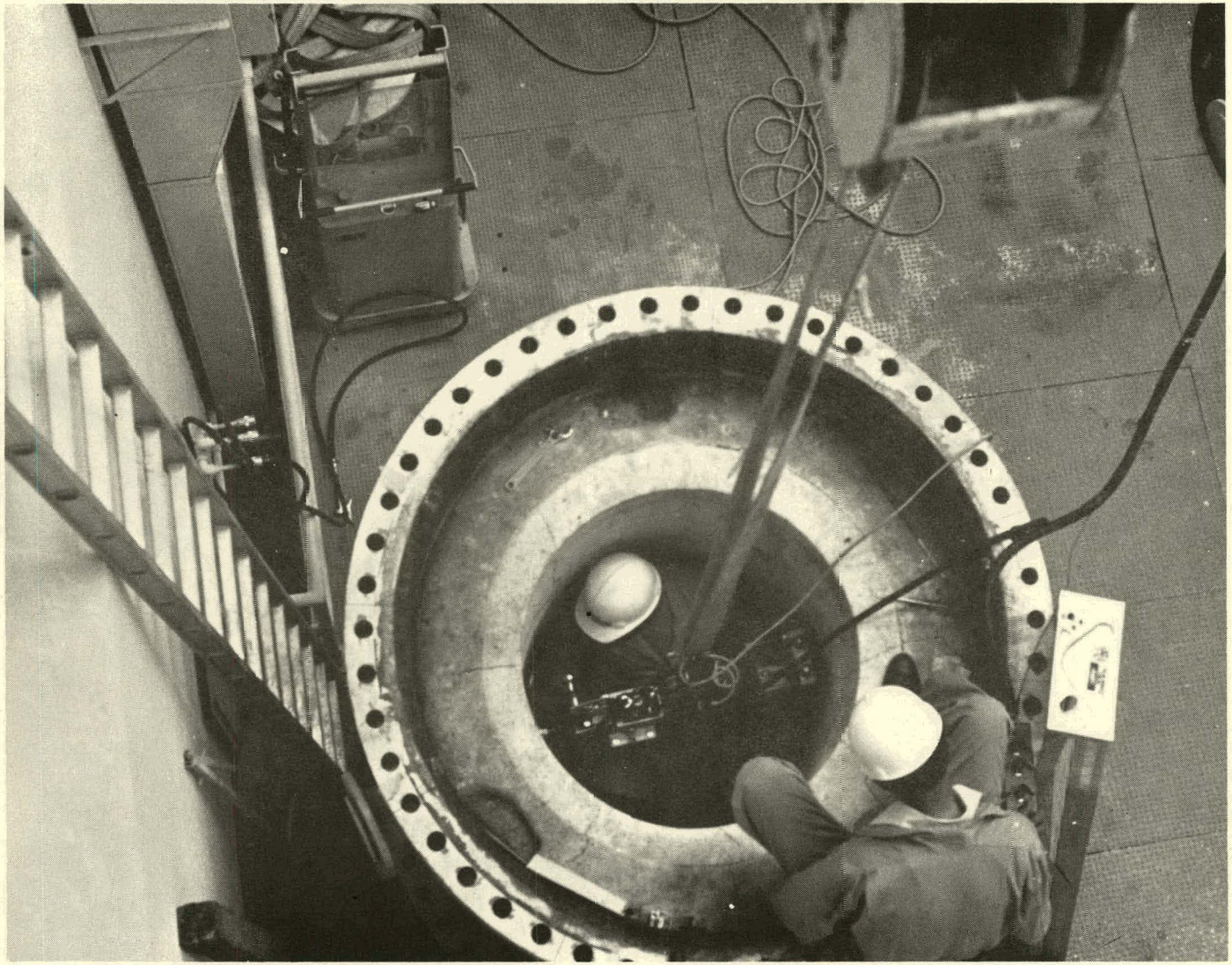

FIGURE 100. Drill Core Rig.

cross-sectional view of a lining. The saw was made by GDM, Inc. and was identified as Model 14. It was mainly sold to the concrete industry and was capable of making 5 inch deep cuts.

- A tear out station which was built to handle the center section of the pressure vessel/test furnace during all or part of the post test inspection, sample retrieval, and tear-out. A photograph of this facility is shown in Figure 101.

- Heavy duty pneumatic jack hammers and diesel power air compressors which were rented to tear-out the lining.

- A Cobalt 60 gamma source which was used to nondestructively examine (radiograph) two linings. The equipment was supplied by the Argonne National Laboratory.

Post Testing Techniques

The normal sequence and description of test techniques used during post testing work were as follows:

- Prior to the testing of a lining the thickness of the components and inner diameter and height of the lining were determined at prescribed points. These points were marked with a high temperature Tempil pencil so they would be visible after the heat-up tests. Any cracks or other defects in the lining were noted for future reference. Once this was done, four 2 inch diameter drill cores were taken from the as cast lining. Two were taken about 8 inches up from the bottom while the other two were taken about 8 inches down from the top. These holes were patched with identical material.

- After a heat-up test was made and the top head, upper insulation and heating element were removed from the vessel, a general visual inspection of the lining was made. The diameter and other dimensions of the lining were then measured at the predetermined locations using the various calipers and gages mentioned above and the crack widths were measured in the vertical and horizontal directions with the optical comparator. Figure 102 is a schematic drawing of the locations where the cracks were measured.

- The appearance of the lining was then photographed after which the cracks were marked (highlighted) with ink and the lining again photographed.

- Some maps of the hot face crack pattern were made at this point by attaching paper to the ID of the lining. Tracks were made over the inked cracks. In cases where second and third heat-up cycles were run on linings, the mapping was continued to indicate crack growth and new cracking.

- The lining was then drill cored at specific locations to collect samples for testing, to get a better look at the crack pattern, to retrieve the strain gages and check their orientation, and to retrieve anchors.

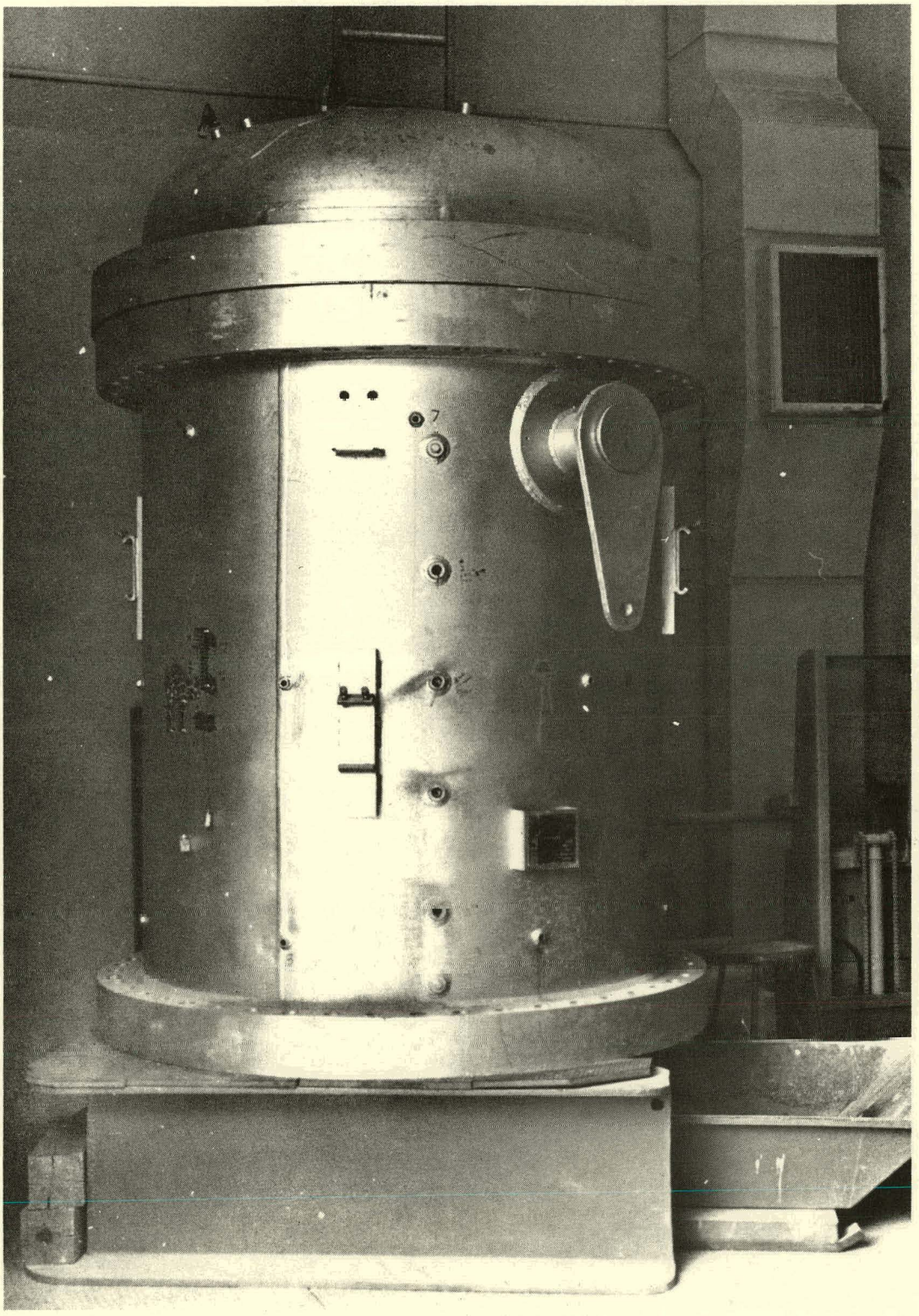

FIGURE 101. Tear Out Station.

FIGURE 102. Schematic Showing Location of Cracks Measured for Shrinkage Determinations.

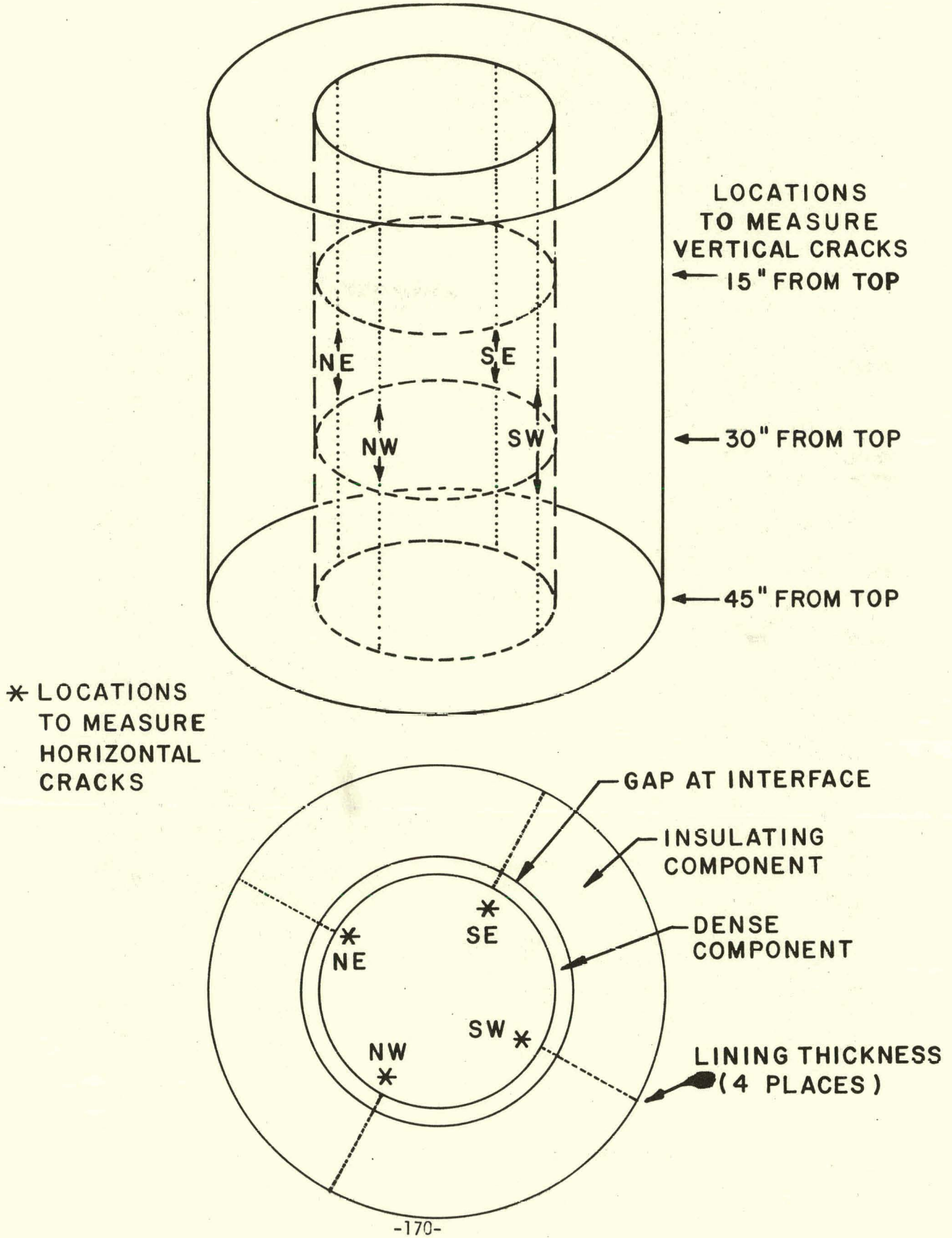

The number of drill cores taken varied from one lining to another depending upon the condition of the lining and the number of times it was heated. Generally at least 4 drill cores were taken from a lining. One each was taken from the top and bottom of the lining in a crack free area near the locations of the drill cores taken from the as cast lining. The remaining drill cores were taken over the largest and smallest cracks and from crack free regions of the lining.

- In cases where gaps formed between the refractory lining components and the shell, the feeler gages were used to measure the gap. This was difficult to do with the 2 inch drill core holes but by using a 6 inch drill core this problem was eliminated. This large drill core was also used to extract whole anchors and to get a better idea of the cracking present in the insulating component.

- To nondestructively examine a lined vessel, the ^{60}Co source was placed in the vessel as shown in Figure 103. Prior to this step, the outside of the vessel was covered with film as shown in the figure. This film became exposed when the ^{60}Co source was placed in position for about 40 minutes and was found to be successful for detecting cracks, voids, discontinuities, and anchors in the lining. It took approximately one day to completely radiograph a lining.

- The center section of the vessel was usually moved to the post testing/tear out section for the final core drilling, sawing and tear-out activities.

- To produce a cross sectional view of a lining the dense component of the lining was sliced vertically at 1 inch depth of cut passes with the diamond saw. Since the saw had only a 5 inch depth of cut, no cutting of the insulating component was possible. Instead, this component was chipped away with a chipping hammer and then dressed up so that its surface paralleled that of the dense. Once this was done, the cracks were highlighted with ink and the cross section was photographed.

- In cases where the dense component could be removed separately from the insulating component, the same type measurements, inspections, highlighting of cracks, and photographing were done with the insulating component.

- The lengths of the "Y" anchor studs were measured after the lining was torn out with a caliper and compared to the original length for evidence of yielding. Each stud was stamped with a number to aid in its identification.

- Once the lining was removed, the vessel was wire brushed and cleaned to prepare it for the next test. It normally took one week to complete this activity.

- The shrinkages which occurred in a lining were determined by dividing the original thickness or length into the changes in thickness or length measured. In addition, the shrinkage at the hot face and hot face side of the insulating component were determined by adding up all of the crack widths in the vertical and horizontal directions and dividing these numbers by the original circumference and height of the lining, respectively. These shrinkages were reported as percentages.

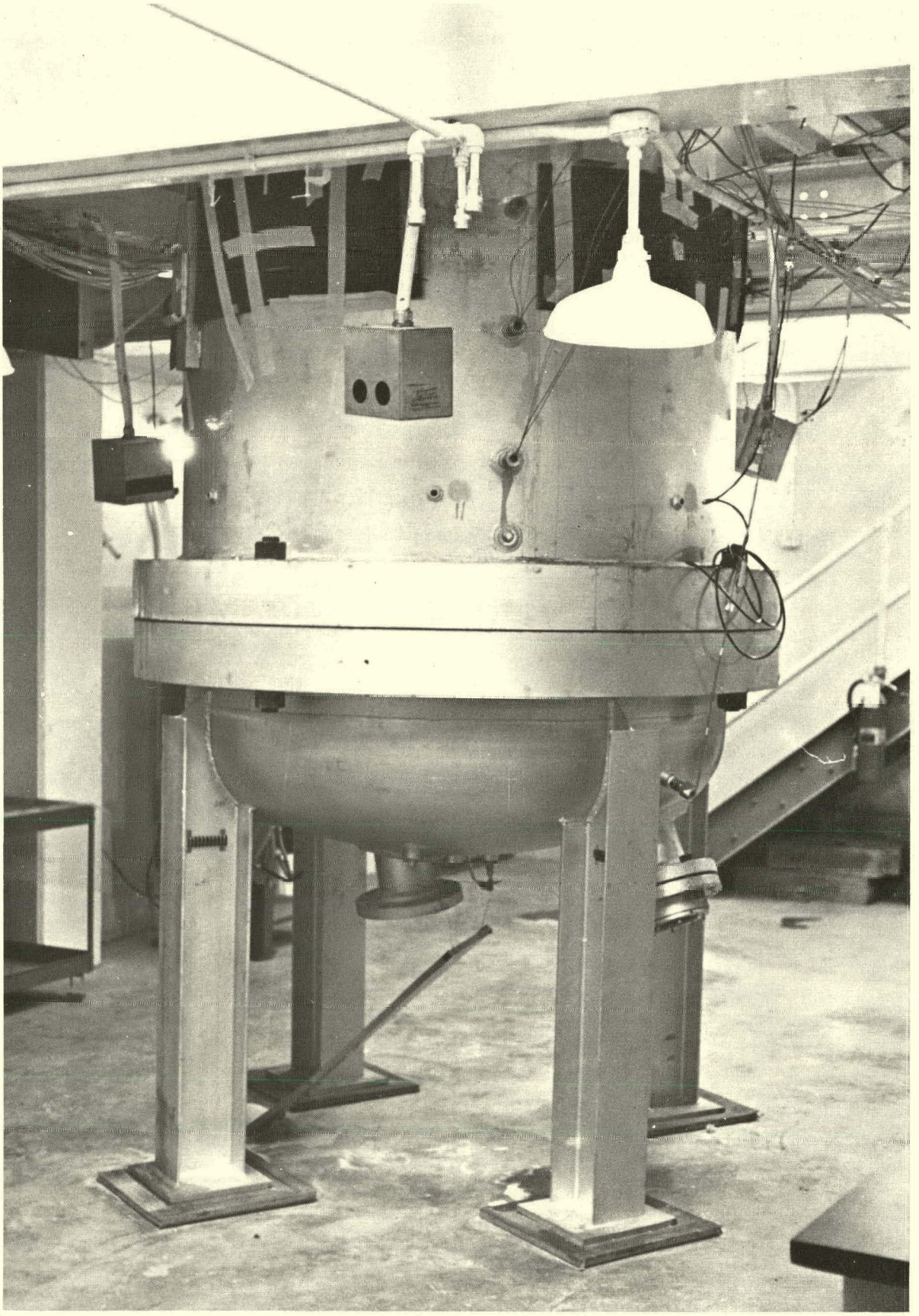

FIGURE 103. Gamma Radiography of Lined Vessel.

• The drill cores were usually photographed before and after slicing and sectioning and were often x-rayed and/or petrographically examined for evidence of mineralogical changes. Density, weight loss and porosity were determined routinely on the drill core samples using the same procedures used to determine the properties of the refractories which were discussed in Section 2.3. of the report. To determine the strength of the core samples, rectangular test pieces were cut from the hot face and cold face side of each component of each drill core. However, the preparation of samples with parallel surfaces was very difficult. As a result, an alternate method of determining the strength was used.

This method was the diametral compression (splitting tensile) test used in the concrete industry to determine the tensile strength of cements and concretes. The procedure was designed around the ASTM test (C496-71) and the findings of Marion and Johnstone[12]. One inch thick discs were sliced from the hot and cold face sides of each component of each 2 inch core and compression tested to failure at room temperature. The test scheme shown in Figure 104 was used to make these determinations.

The specimen was tested to failure and the equations indicated were used to calculate the splitting tensile strength. The Instron testing machine was used for this testing.

2.6.6. Special Tests

A series of special tests were run on the Pressure Vessel/Test Furnace prior to and after it was used to test linings. Both of the center sections of the vessel were used for all, or portions of, these tests. The tests were run to determine how the facility responded to pressurization and to thermal and mechanical loading.

The pressurization tests involved monitoring the axial and circumferential strains occurring in the shell as the vessel was pressurized with the strain gages attached to the shell; and monitoring the radial strain (diametral growth) of the shell with dial gages independent of the vessel. A similar procedure was used to monitor the thermal loading effect on the shell strains. The heating element was installed in the empty vessel and the shell heated up to approximately 450°F in this test.

To simulate a point loading (mechanical loading) condition which could be produced by an anchor transmitting the force of the expanding lining to the shell, a test procedure as shown in Figure 105 was used. It involved applying a point load at two points 180° apart which were on either side of strain gages attached to the OD of the shell at the center line of the vessel with the hydraulic device shown. The purpose of the activity was to determine if the strain gages detected localized loading effects.

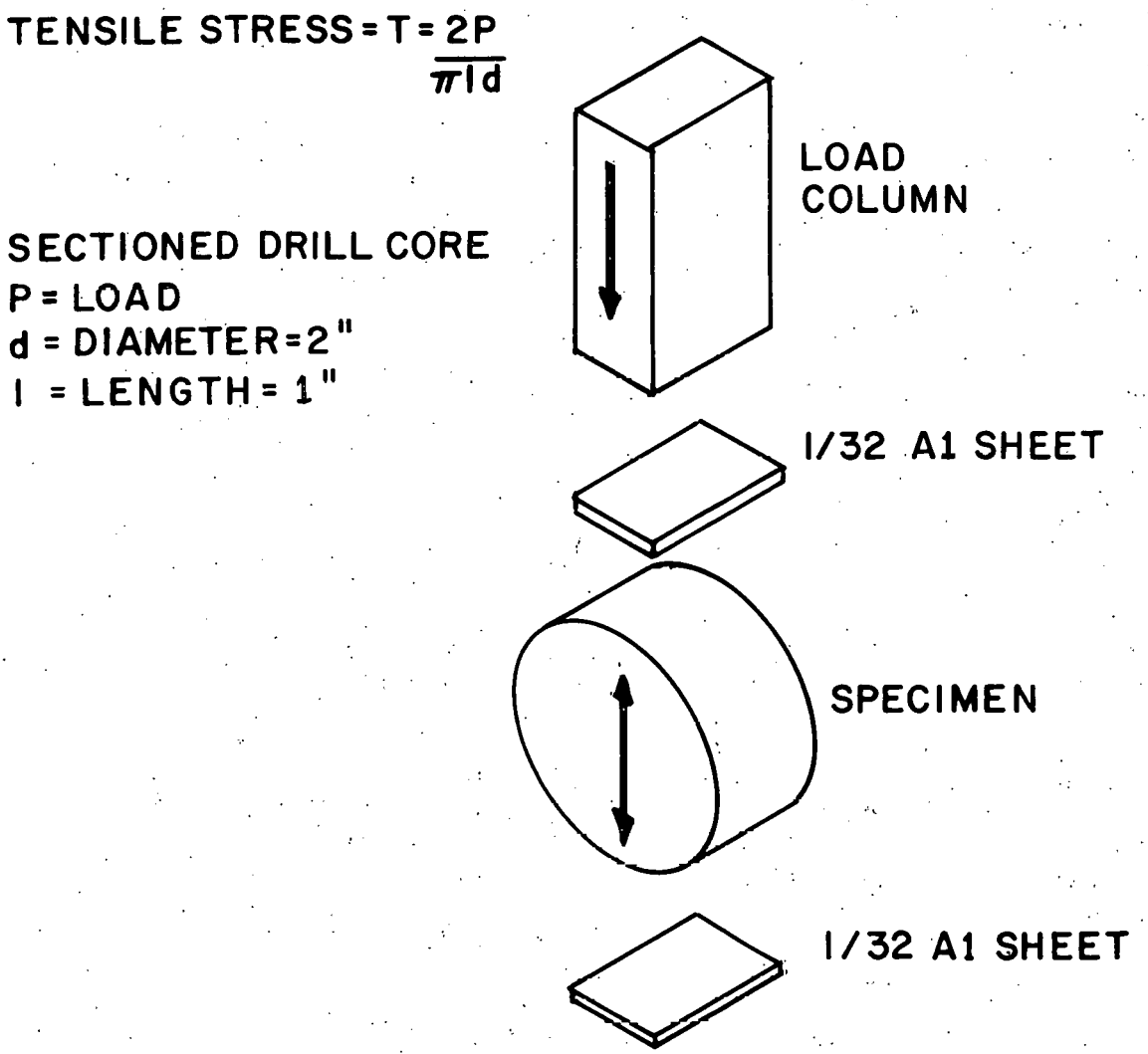

FIGURE 104. Mechanical Loading Test to Simulate Transmission of Lining Force to the Shell.

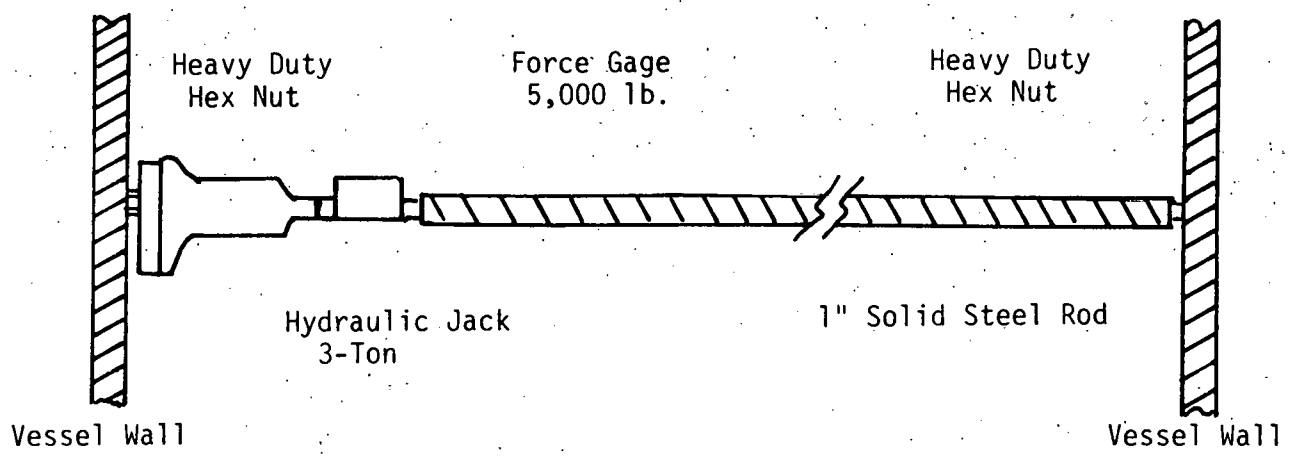

POINT LOADING LOCATIONS

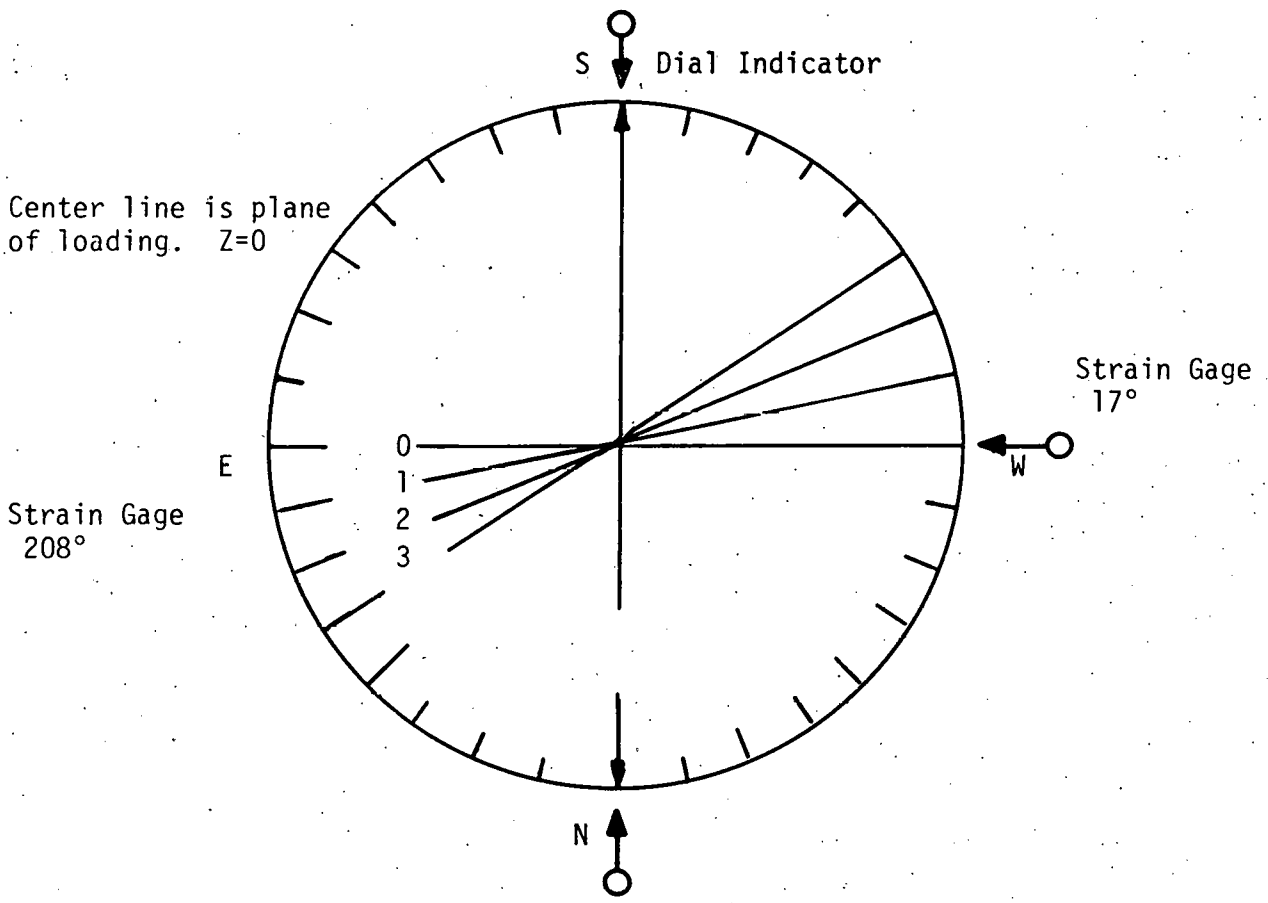

FIGURE 105. Schematic of Internal Point Loading Assembly and Location of Force Application.

3. RESULTS

3.1. Literature Search

During the first year of the program, an extensive literature search was conducted to provide information relating the cracking of monolithic refractory linings to the physical and mechanical properties and chemical stability of the refractories during curing and heat up. The findings of this search are discussed in detail in a report, Critical Literature Search, FE-2218-14, December 1977, under the old contract number (EX-76C-01-2218). Outlined below is a brief summary of the findings of the search and of additional information acquired after the search was published.

Summary

A considerable number of references were found which documented the failures of refractory concrete and phosphate bonded ramming mix monolithic linings used in process vessels. The causes for these failures were mostly associated with chemical degradation of the materials which lead to a reduction in strength and abrasion resistance. These property changes caused the material to crack, erode and spall during service. A few papers discussed failures due to explosive spalling of monolithics during the initial dry out and due to cracking and spalling caused by metal anchor/refractory interactions.

Only two references (9 & 13) were found that considered the thermo-mechanical aspects of refractory lined vessels. Wygant and Crowley's[9] paper reviewed the state-of-the-art on monolithic refractory designs from the late 1950's and early 1960's and reported engineering calculations on the effect of creep to 1000°F. The stress analyses performed were very simplistic elastic analyses and developed gross approximations at best. They did not consider a circular cross section or multicomponent lining designs.

Huggett's[13] paper was more practical in nature. He indicated the need to keep shrinkage of monolithic linings below 0.1% and to use wide (2 foot) anchor spacings to reducing cracking of single component linings. He recommended keeping the shell cool to keep the lining in compression as a means to keep cracks closed during service.

Other solutions or guidelines recommended to minimize the effect of cracking or prevent spalling included the use of replaceable metal shrouds inserted on the inside of the lined vessel, vapor barriers every three to five feet along the length of the shell, more anchors and curing temperatures above 75°F. Independent anchoring of the insulating component of a dual component lining to keep it tightly in contact with the shell was another approach taken.

The use of 90+% Al_2O_3 monolithic refractories with less than 0.1% by weight Fe_2O_3 and SiO_2 was recommended for petrochemical[14] and steel industry applications to reduce the effect of chemical corrosion caused by hydrogen, steam or carbon monoxide.

Some evidence[15,16,17] was beginning to develop in the mid-70's which indicated that contrary to Crowley's[14] findings, 50% Al_2O_3 refractory concretes were improved by exposure to high pressure (500 psi and greater) steam or steam containing atmospheres while 90+% Al_2O_3 refractory concretes were degraded. These results were quite surprising to the refractories industry and further testing was planned to confirm it.

No references were identified in which a monolithic refractory lining was instrumented to measure the stress and strains which develop during the initial heat-up or to listen to cracking with acoustic emission techniques. Some guidelines[18] were published on installation procedures and safe and economical heat-up schedules to prevent failure of a lining.

A number of references were found in the Portland cement based concrete literature which discussed the relationships between properties, curing and thermomechanical performance and were found to be helpful in the development of the REFSAM and the creep test procedures used. Some of these references were identified earlier(4 &10)while the others are listed in the literature search.

After the literature search was reported, two additional references[19,20] were identified which discussed the thermo-mechanical aspects of the refractory lined vessels. Both discussed elastic analyses and only one[14] considered temperatures above 1000°F. Neither of them, however, considered the effects of creep or the stress state of the lining during the initial dry-out and heat-up.

Pierce's [20] work appeared to be the most closely allied to the objective of this program. He was designing acid resistant refractory linings and was most concerned about cracks forming in the lining that could lead to vessel corrosion and mechanical degradation. Mr. Pierce became an important contact during this program.

The conclusions drawn from the search were as follows:

(1) Cracking of monolithic refractory linings and the subsequent corrosion and/or over heating and failure of the metal shell is a well recognized problem and has been fairly well documented in the literature. There are very few references, however, that discuss the interrelationship between the physical, mechanical and chemical properties of monolithic refractories and the cracking of these refractories in large process vessels.

(2) Guidelines do exist on material specifications and installation procedures to prevent cracking or explosive spalling due to shrinkage and steam entrapment. However, few mechanical property guidelines, cool-down guidelines or lining design configurations on refractory concretes or phosphate bonded ramming mixes used in cylindrical process vessels exist to prevent cracking. Most of the guidelines that do exist are based mainly on field experience in commercial facilities and consider the effects of the cement type and level, curing temperature and dry-out and heat-up schedules on the tendency of the monolithic refractory linings to crack and/or explosively spall during the initial heat-up cycle.

(3) Very little stress analysis work has been performed on monolithic refractory linings in cylindrical process vessels and as a result there is only a limited understanding of what causes monolithic refractory linings to crack and how to prevent it. For these reasons it is thought that a systematic study of the thermo-mechanical aspects of monolithic refractory lined cylindrical process vessels such as was done on this contract was needed. The determination of engineered properties of monolithic refractories such as creep rates and modulus of elasticity versus temperature was also needed.

(4) Some very useful references on the modeling and engineered properties of Portland cement based concretes have been identified and have been used to develop the math model required for this program.

(5) This contract work should result in the necessary data for determining whether monolithic refractory linings for coal gasification process vessels should be considered more seriously in the future or if brick linings should be used to protect the vessel shell.

3.2. Material Properties

This section includes a summary of the physical, thermal and thermo-mechanical properties of the key monolithic refractories used in the lining tests. These properties were the ones used in the stress analyses. It also includes general comments about these refractories and a discussion of the similarities and differences between them. The remaining data collected on the other materials listed in Table 5 and on these key materials at varying water levels, heat treatments, etc., are summarized in Appendix B. The key refractory materials include the modified 90+% Al_2O_3 dense generic (ERDA 90), the 50% Al_2O_3 dense generic, the KAOCRETE XD 50 (Mix 36C) with and without stainless steel fibers, LITECAST 75-28 and KAOLITE 2300 LI. The ERDA 90 and LITECAST 75-28 were used in Linings #1-4, KAOCRETE XD 50 (Mix 36C) and LITECAST 75-28 were used in Linings #5 and 6, KAOCRETE XD 50 (Mix 36C) with 4 w/o 310 stainless steel fibers and LITECAST 75-28 were used in Lining #7 and KAOCRETE XD 50 (Mix 36C) with 4 w/o 310 stainless steel fibers and KAOLITE 2300 LI were used in Lining #9.

Tables 14 through 23 list the properties of these key refractories and Figures 106 through 120 show some of the thermal expansion, thermal conductivity and thermo-mechanical properties obtained. Some data are also included on commercial products in the same class as the generic materials and on samples of the key materials which were made during the installation of the linings for comparative purposes.

Generally, the water levels required to achieve good ball-in-hand consistencies for these materials were found to agree with the levels recommended by the refractory vendors on the commercial products tested or commercial products similar to the generics. Every attempt was made to use as low a water level as possible to give these good consistencies. The as cast and dried bulk densities and modulus of ruptures of these key materials were also found to agree well with bulk densities and modulus of ruptures reported by the refractory vendors and give further evidence of this good agreement. These results were interpreted to mean that acceptable refractory materials were being tested.

As expected the ERDA 90 had the highest bulk density, coefficient of thermal expansion, thermal conductivity, strength and creep resistance of the key refractories tested while the KAOLITE 2300 LI had the lowest properties by comparison. The general order of decreasing properties was ERDA 90, KAOCRETE XD 50 (Mix 36C), KAOCRETE XD 50 (Mix 36C) with 4 w/o 310 stainless steel fibers, 50% Al_2O_3 dense generic, LITECAST 75-28 and KAOLITE 2300 LI. Within each type of material as the water level was increased above the optimum, the physical and mechanical properties generally degraded. Figure 106 shows an example of this effect on the thermal expansion and shrinkage of LITECAST 75-28 as the water level was increased from 21 to 24%. Other examples which indicate the effect on density, strength and creep resistance are included in Appendix B.

Figure 107 shows a thermal expansion curve for the as-cast 90+% Al_2O_3 dense generic refractory which was stored in a one hundred percent humidity environment and a curve of the same material which was allowed to dry prior to the test. The difference in shrinkage and overall thermal expansion of these two materials indicate why the curve for the one hundred percent humidity stored sample was used in the stress analyses. It showed more shrinkage but a similar expansion character to the dried sample. This difference in shrinkage character was thought to be very important to the overall performance of the refractory lining. If it were not

Table 14. Chemical Analyses of Monolithic Refractories (Published Data)

Chemical Analysis, %	90 RAMHS Phosphate Bonded Ramming Mix	90 + % Al_2O_3 Dense Generic (ERDA 90)	50% Al_2O_3 Dense Generic	KAOCRETE XD 50 (Mix 36C)	LITECAST 75-28	KAOLITE 2300 LI
SiO_2	2.7	0.1	40.0	43.2	36.3	37.0
Al_2O_3	93.6	95.0	51.0	52.3	54.5	41.0
Fe_2O_3	0.5	0.1	1.0	0.7	1.1	0.9
TiO_2	0.2	Trace	2.0	1.5	1.1	1.7
CaO	Trace	4.6	5.0	2.1	4.8	18.6
MgO	Trace	Trace	0.1	0.1	0.1	0.4
P_2O_5	2.9	-	-	-	-	-
Alkalies (Na_2O & K_2O)	0.3	0.1	0.3	0.3	0.8	0.3

TABLE 15. Properties of Modified 90+% Al_2O_3 Dense Generic (ERDA 90) and KAOTAB 95

Properties	90+% Al_2O_3 Dense Generic Lab	ERDA 90 (Lining #3)	KAOTAB 95
Water Level, %	8.5	7.75	8.0
Bulk Density, pcf (220°F Cured)	175	176	172
Coefficient of Thermal Expansion, α			
X 10^{-6} in/in/°F 1st Cycle RT-1875°F	3.94	3.86	3.84
700-1875°F	5.90	5.42	-
2nd Cycle RT-1875°F	4.88	4.80	-
Linear Shrinkage, %			
after 220°F	0.05	0.05	0.1
after 1000°F	0.1	0.1	-
after 1500°F	0.2	0.2	0.2
after 2000°F	0.2	0.2	0.2
Thermal Conductivity, k BTU, in/Hr/Ft^2/°F (at temp)	13.1	-	13.1
Specific Heat, c	2.5	2.5	2.5
Poisson's Ratio, ν	0.2	0.2	0.2
Hot Modulus of Rupture, psi			
RT	1790 ± 330	2550	1620
500°F	980 ± 150	-	-
1000°F	890 ± 170	-	1320
1500°F	865 ± 55	-	-
1750°F	610 ± 210	-	-
2000°F	760 ± 320	-	1320
Hot Compressive Strength, psi			
RT	9100 ± 1750	12140	5940
500°F	9220 ± 580	-	-
1000°F	9690 ± 1040	-	-
1500°F	9130 ± 1480	-	-
1750°F	7300 ± 1160	-	-
2000°F	8455 ± 420	-	-
Hot Modulus of Elasticity, psi x 10^6			
RT	1.5 ± 0.5	-	-
500°F	0.8 ± 0.3	-	-
1000°F	0.8 ± 0.3	-	-
1500°F	0.7 ± 0.3	-	-
1750°F	0.4 ± 0.1	-	-
2000°F	0.4 ± 0.2	-	-
Hot Compressive Fracture Strain, mil/in			
RT	3	-	-
500°F	13	-	-
1000°F	13	-	-
1500°F	12	-	-
1750°F	27	-	-
2000°F	24	-	-

TABLE 16. Properties of 50% Al_2O_3 Dense Generic, KAOCRETE XD 50 (Mix 36C) With and Without 4 W/O 310 SS Fibers and LABORDE

Properties	50% Al_2O_3 Generic	KAOCRETE XD 50 (Mix 36C) Without	KAOCRETE XD 50 (Mix 36C) With 4 w/o 310SS (Lining #7)	LABORDE
Water Level, %	10	7.5	7.5	11
Bulk Density, pcf (220°F Cured)	140	140	143	136
Coefficient of Thermal Expansion, α				
$X10^{-6}$ in/in/°F 1st Cycle RT-1875°F	2.06	2.71	5.00	2.2
700-1875°F	2.90	3.15	5.73	3.1
2nd Cycle RT-1875°F	-	-	4.51	-
Linear Shrinkage, %				
after 220°F	0.0	0.1	0.1	0.1
after 1000°F	0.1	0.1	0.1	0.1
after 1500°F	0.2	0.1	0.1	0.1
after 2000°F	0.2	0.1	0.0	0.2
Thermal Conductivity, k BTU, in/Hr/ft^2/°F (at temp)	7.0	10.0	11.0 (Calculated)*	7.5
Specific Heat, c	2.5	2.5	2.5	2.5
Poisson's Ratio, ν	0.2	0.2	0.2	0.2
Hot Modulus of Rupture, psi				
RT	1125 ± 140	980	1990 ± 430	1150
500°F	860 ± 85	-	1080 ± 430	-
1000°F	890 ± 50	950	1070 ± 190	-
1500°F	1030 ± 150	1080	990 ± 175	-
1750°F	660 ± 85	-	730 ± 90	-
2000°F	435 ± 90	850	757 ± 160	-
Hot Compressive Strength, psi				
RT	8020 ± 880	4000	3220 ± 410	-
500°F	6705 ± 850	4195	3480 ± 850	-
1000°F	8570 ± 910	3370	3520 ± 650	-
1500°F	10130 ± 490	5680	4725 ± 370	-
1750°F	8690 ± 390	4550	4380 ± 435	-
2000°F	6300 ± 1020	3865	3680 ± 270	-
Hot Modulus of Elasticity, psi x 10^6				
RT	0.9 ± 0.5	0.2	0.1	-
500°F	0.6 ± 0.3	0.2	0.1	-
1000°F	1.0 ± 0.4	0.2	0.2	-
1500°F	0.6 ± 0.2	0.2	0.1	-
1750°F	0.6 ± 0.3	0.2	0.1	-
2000°F	0.2 ± 0.1	0.1	0.1	-
Hot Compressive Fracture Strain, mil/in				
RT	10	30	36	-
500°F	12	30	45	-
1000°F	-	30	50	-
1500°F	21	45	60	-
1750°F	16	50	60	-
2000°F	-	60	60	-

*Added 10% to k due to presence of 310SS Fibers

TABLE 17. Properties of LITECAST 75-28 and KAOLITE 2380 LI

Properties	LITECAST 75-28	KAOLITE 2380 LI
Water Level, %	21	59
Bulk Density, pcf (220°F Cured)	85	62
Coefficient of Thermal Expansion, α		
$X10^{-6}$ in/in/°F 1st Cycle RT 1875°F	2.61	-0.12
700-1875°F	4.04	1.19
2nd Cycle RT 1875°F	4.1	3.30
Linear Shrinkage, %		
after 200°F	0.3	0.1
after 1000°F	0.4	0.4
after 1500°F	0.4	0.6
Thermal Conductivity, k BTU, in/Hr/Ft^2/°F (at temp)	2.8	1.6
Specific Heat, c	0.83	0.83
Poisson's Ratio, ν	0.2	0.2
Hot Modulus of Rupture, psi		
RT	570 ± 65	230 ± 30
500°F	320 ± 30	170 ± 20
1000°F	225 ± 55	150 ± 15
1250°F	220 ± 25	140 ± 10
1500°F	185 ± 115	150 ± 25
Hot Compressive Strength, psi		
RT	3945 ± 350	430 ± 55
500°F	3490 ± 180	505 ± 25
1000°F	3940 ± 340	540 ± 25
1250°F	4245 ± 740	560 ± 30
1500°F	5330 ± 430	820 ± 20
Hot Modulus of Elasticity, psi $x10^6$		
RT	0.6 ± 0.3	0.02
500°F	0.3 ± 0.1	-
1000°F	0.4 ± 0.2	0.02
1250°F	0.4 ± 0.2	-
1500°F	0.2 ± 0.1	0.03
Hot Compressive Fracture Strain, mil/in		
RT	11	25.5
500°F	11	-
1000°F	11	24.0
1250°F	15	-
1500°F	33	31.5

Table 18. Creep Results on the Modified 90+% Al_2O_3 Dense Generic Refractory Concrete at Different Stress Levels and Temperatures

	Percent (%) Deformation		
	1500 psi	2000 psi	3300 psi
Time, hr. / Temperature, °F			
1 hr. / RT	0.02	0.08	0.16
3 hrs. / 500°F	-	0.23	0.52
3 hrs. / 1000°F	0.26	0.08	0.16
3 hrs. / 1500°F	0.34	0.20	0.36
3 hrs. / 1800°F	0.90	0.32	0.58
10 hrs. / 2000°F	1.70	1.80	3.60
Total	3.22	2.71	5.38
Post Test Results	3.54	2.36	5.00

Table 19. Creep Results on the Modified 90+% Al_2O_3 Dense Generic Refractory Concrete at Different Stress Levels and Temperatures (ERDA 90 - Lining #4)*

	Percent (%) Deformation		
	1500 psi	2500 psi	3300 psi
Time, hr. / Temperature, °F			
1 hr. / RT	0.03	0.10	0.08
3 hrs. / 1000°F	0.08	0.25	0.22
3 hrs. / 1500°F	0.14	0.32	0.40
3 hrs. / 1800°F	0.49	0.85	0.87
10 hrs. / 2000°F	1.08	1.54	2.77
Total	1.82	3.06	4.34
Post Test Results**	1.45	2.33	3.75

* Samples were prepared while Lining #1 was being installed.
** Measured at RT on Stepwise Tested Specimens.

Table 20. Creep Results on the 50% Al_2O_3 Dense Generic Refractory Concrete at Different Stress Levels and Temperatures

Time, hr. / Temperature °F	Percent (%) Deformation	
	1500 psi	2000 psi
1 hr. / RT	0.0	-
3 hrs. / 250°F	-	0.08
3 hrs. / 500°F	-	0.30
3 hrs. / 1000°F	0.07	0.11
3 hrs. / 1500°F	0.31	0.41
10 hrs. / 1800°F	0.65	0.87
Total	1.03	1.76
Post Test Results	1.0	1.70

Table 21. Creep Results on the KAOCRETE XD 50 (Mix 36C) Refractory Concrete at Different Stress Levels and Temperatures

Time, hr. / Temperature °F	Percent (%) Deformation		
	1000 psi	2000 psi	2500 psi
1 hr. / RT	0.06	0.08	0.04
3 hrs. / 500°F	0.17	0.22	0.08
3 hrs. / 1000°F	0.09	0.14	0.10
3 hrs. / 1500°F	0.21	0.34	0.37
3 hrs. / 1800°F	0.18	0.49	0.46
10 hrs. / 2000°F	0.76	1.95	2.69
Total	1.47	3.22	3.74
Post Test Results	1.06	2.73	3.45

TABLE 22. Creep Results on the KAOCRETE XD 50 (Mix 36C) Refractory Concrete With 4 W/O 310 Stainless Steel Fibers at Different Stress Levels and Temperatures.

	Percent (%) Deformation		
	1000 psi	1500 psi	2000 psi
Time, hr. / Temperature °F			
1 hr. / RT	0.08	0.14	0.29
3 hrs. / 500°F	0.23	0.27	0.52
3 hrs. / 1000°F	0.18	0.20	0.28
3 hrs. / 1500°F	0.35	0.37	0.50
3 hrs. / 1800°F	0.27	0.38	0.49
10 hrs. / 2000°F	1.68	2.08	Failed @ 3.64
Total	2.79	3.44	5.72
Post Test Results	1.78	2.29	-

Table 23. Creep Results on LITECAST 75-28 Insulating Refractory Concrete at Different Stress Levels and Temperatures

	Percent (%) Deformation		
	700 psi	1000 psi	1500 psi
Time, hr. / Temperature °F			
1 hr. / RT	-	0.21	0.19
3 hrs. / 250°F	0.08	0.27	0.28
3 hrs. / 500°F	0.30	0.39	0.44
3 hrs. / 1000°F	0.20	0.29	0.33
3 hrs. / 1250°F	-	0.36	0.50
10 hrs. / 1500°F	1.50	2.93	5.66
Total	2.08	4.45	7.40
Post Test Results	1.73	3.79	6.40

THERMAL EXPANSION OF DENSE AND INSULATING CASTABLES

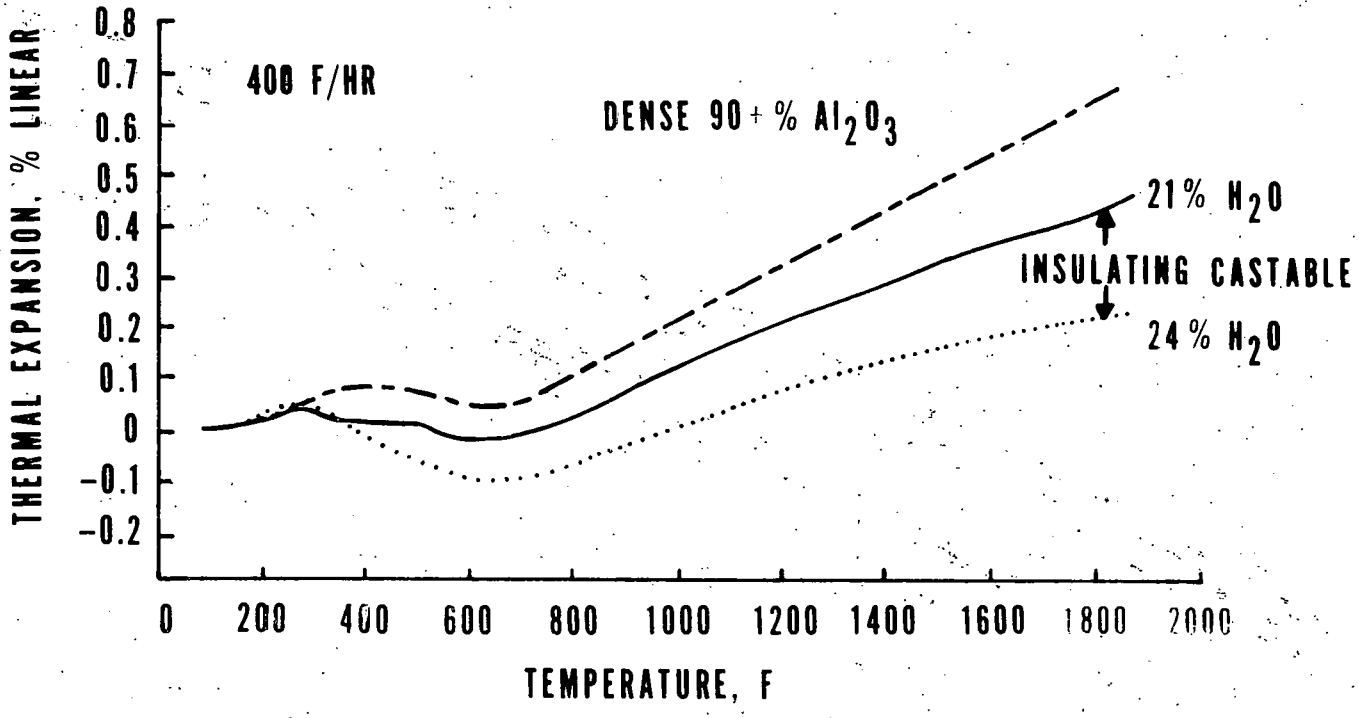

FIGURE 106. Thermal Expansion Curves of Castables during Initial Heat-up.

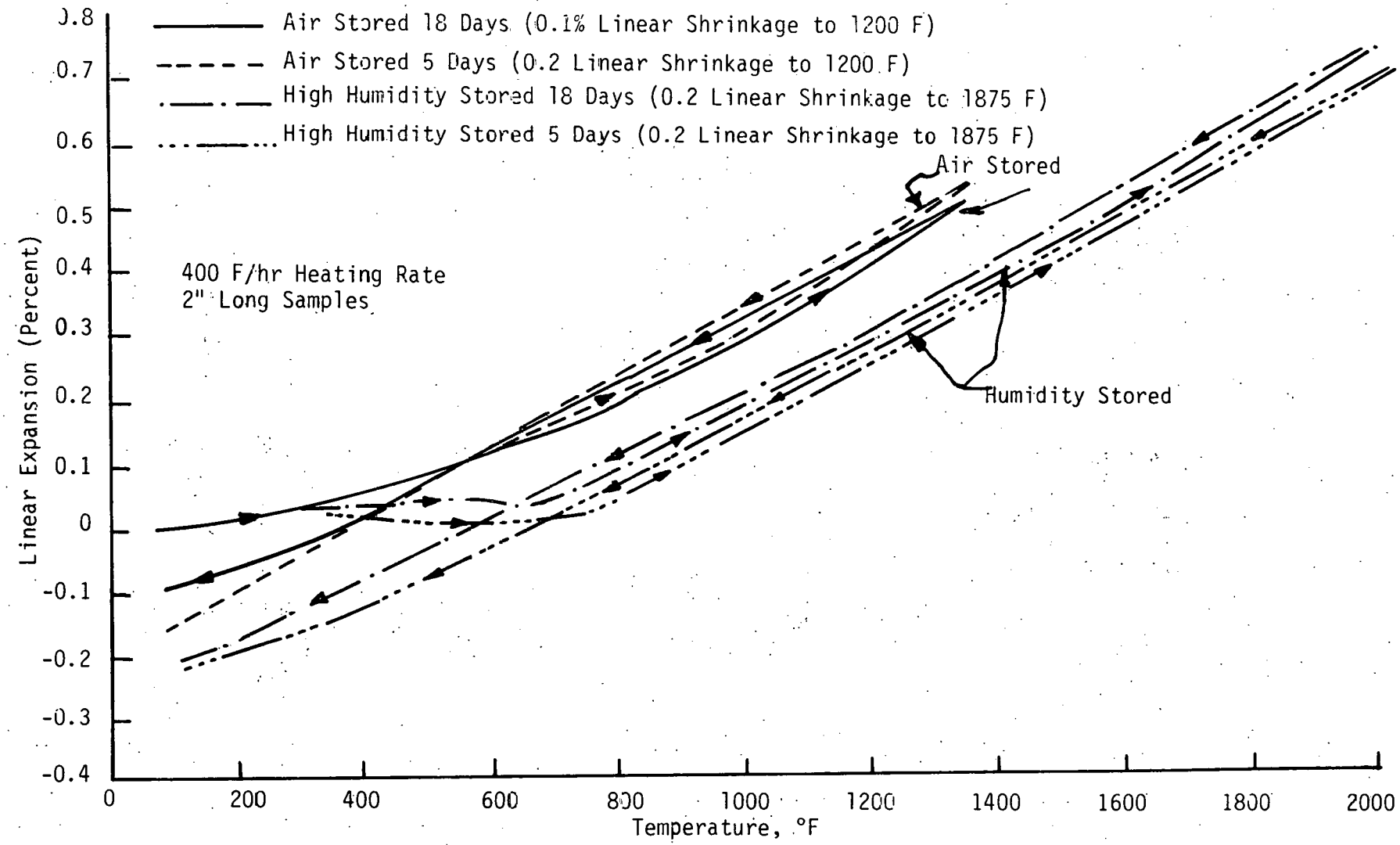

FIGURE 107. Thermal Expansion Curves of ERDA 90 After Storage in Different Environments.

THERMAL CONDUCTIVITY OF A DENSE AND INSULATING MATERIAL

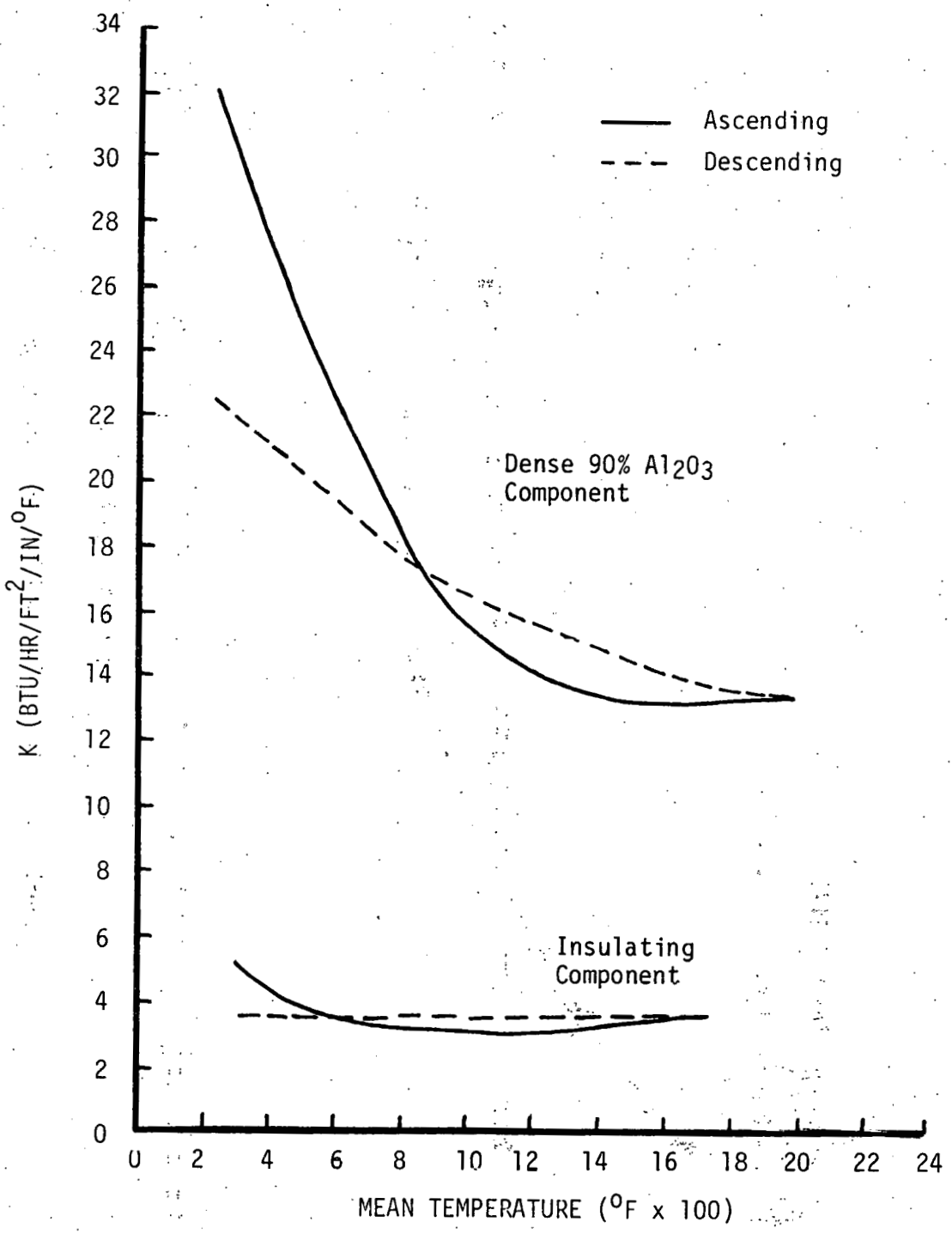

FIGURE 108. Thermal Conductivity Vs. Temperature of 90+% Al_2O_3 Dense Generic and LITECAST 75-28 Refractory Concretes.

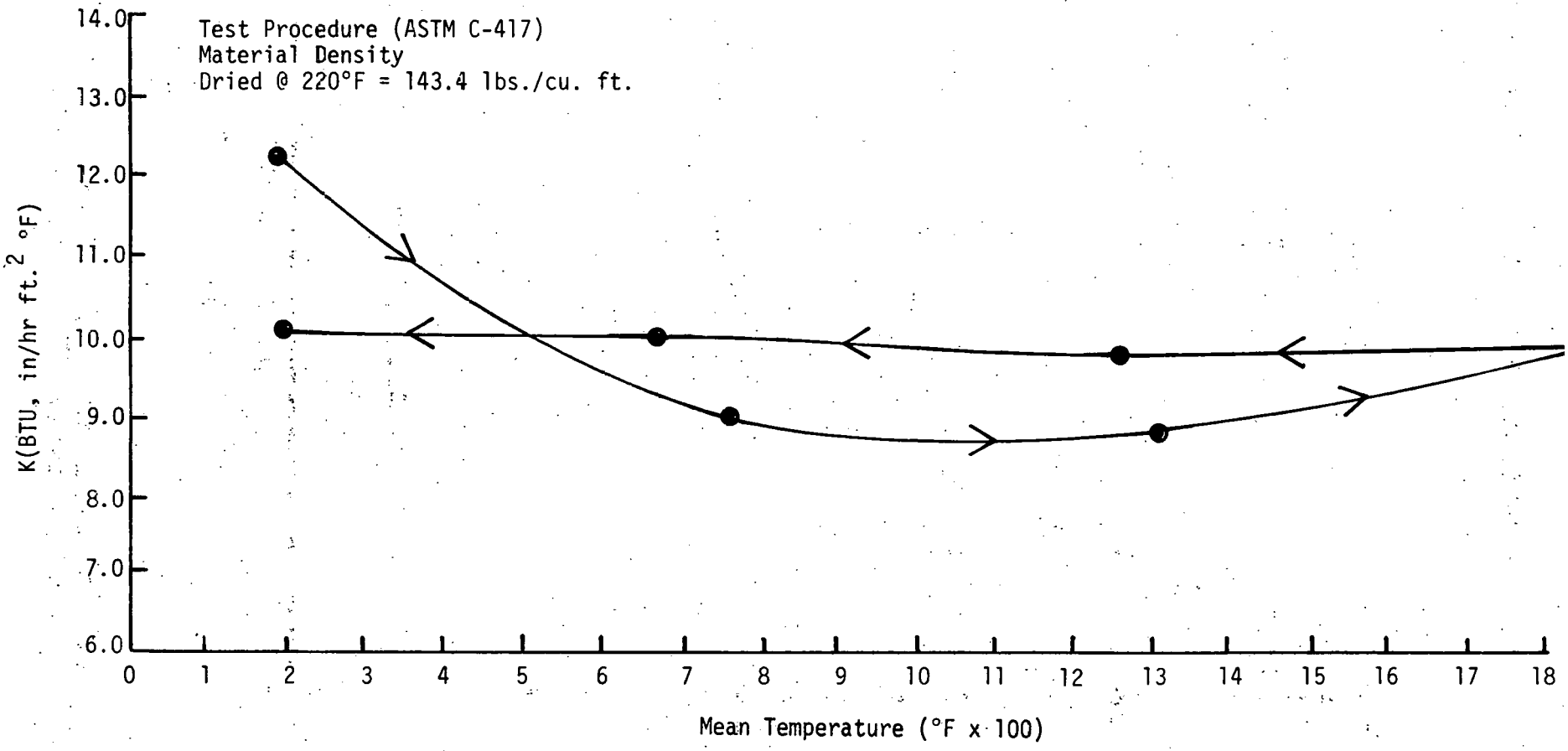

FIGURE 109. Thermal Conductivity Vs. Temperature of KOACRETE XD-50.

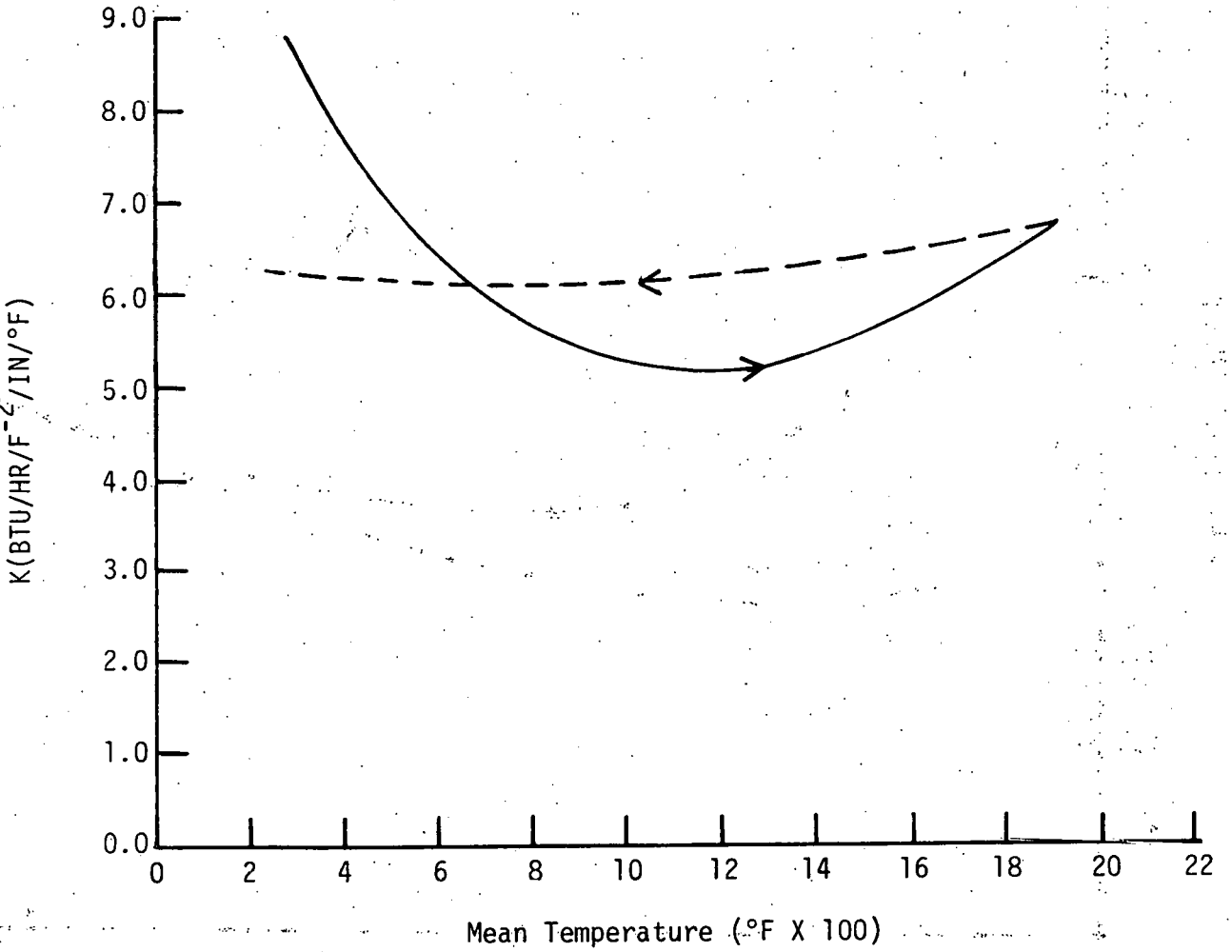

FIGURE 110. Thermal Conductivity Vs. Temperature of 50% Al_2O_3 Dense Generic Refractory.

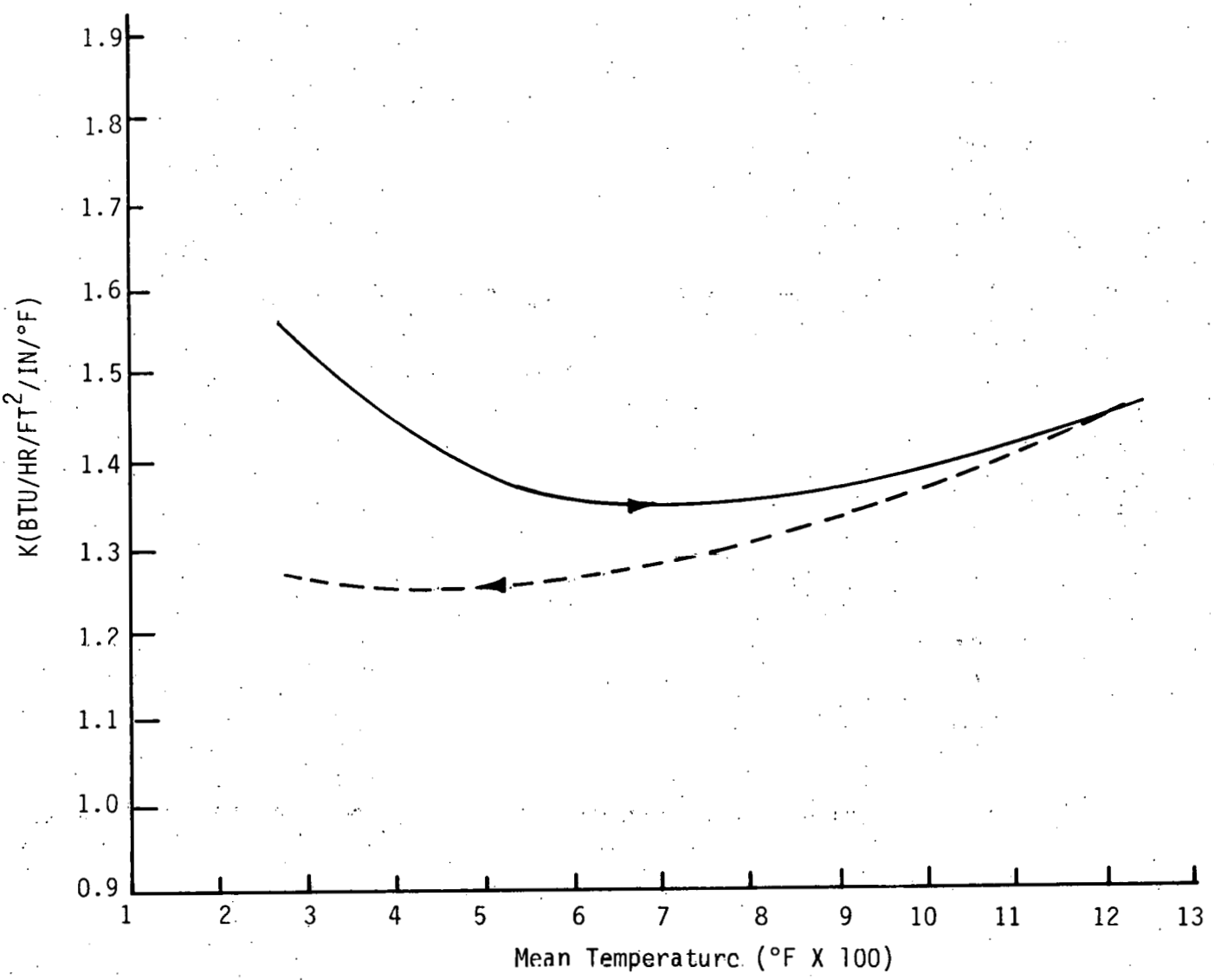

FIGURE 111. Thermal Conductivity Vs. Temperature of KAOLITE 2300-LI.

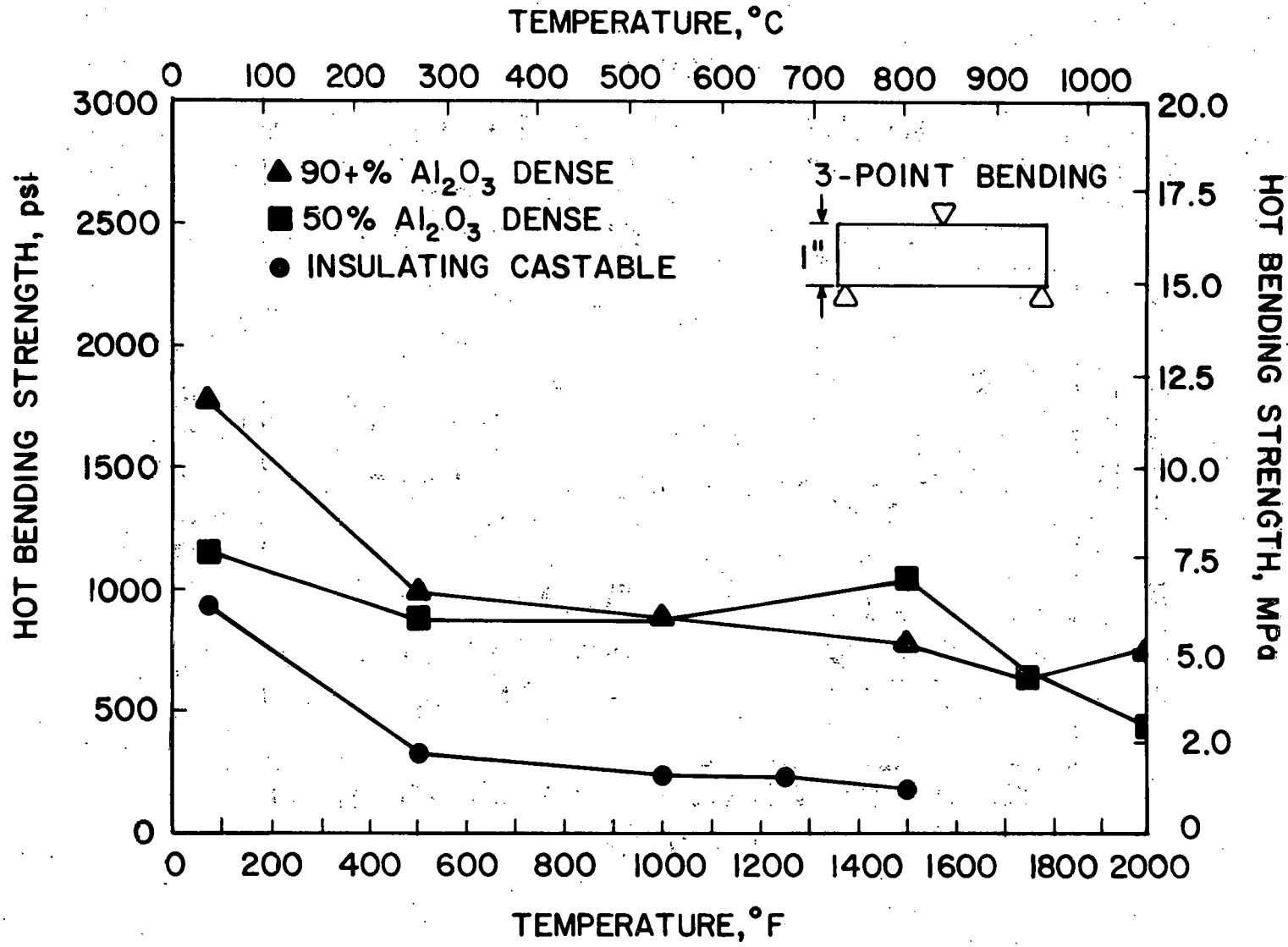

FIGURE 112. Hot Bending Strength Vs. Temperature of Dense Generic and Insulating Castables.

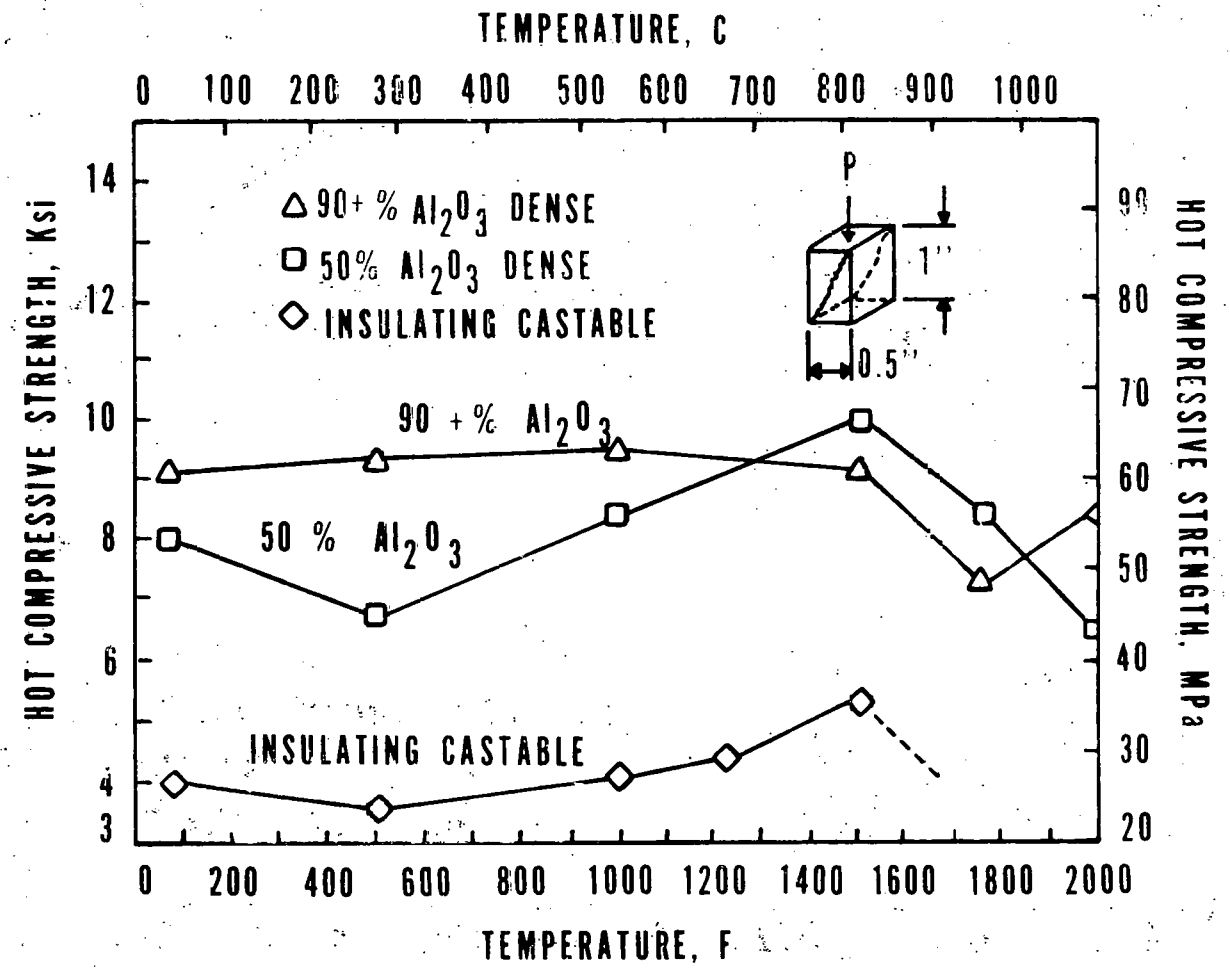

FIGURE 113. Hot Compressive Strength Vs. Temperature of Dense Generic and Insulating Castables.

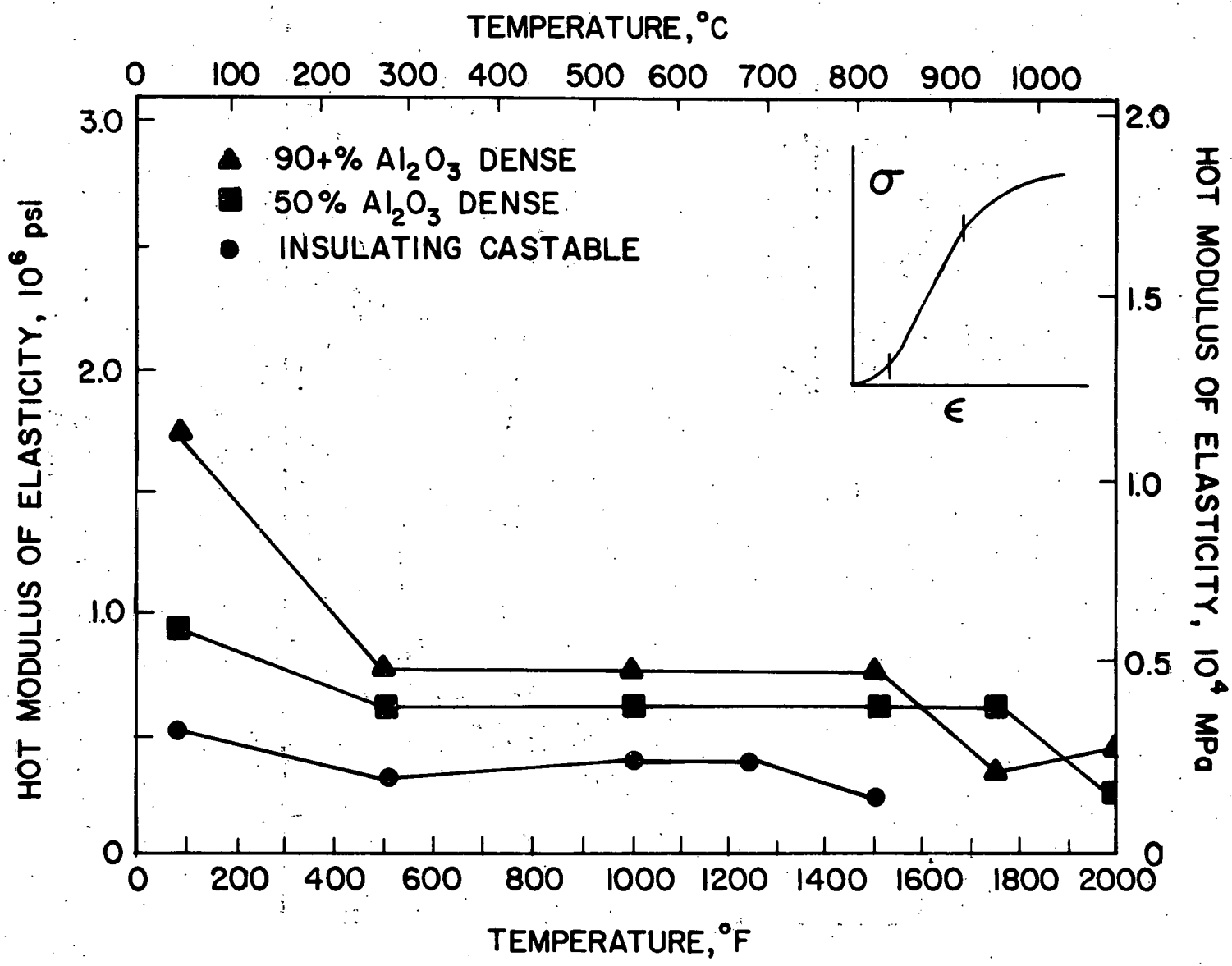

FIGURE 114. Hot Modulus of Elasticity Vs. Temperature of Dense Generic and Insulating Castables.

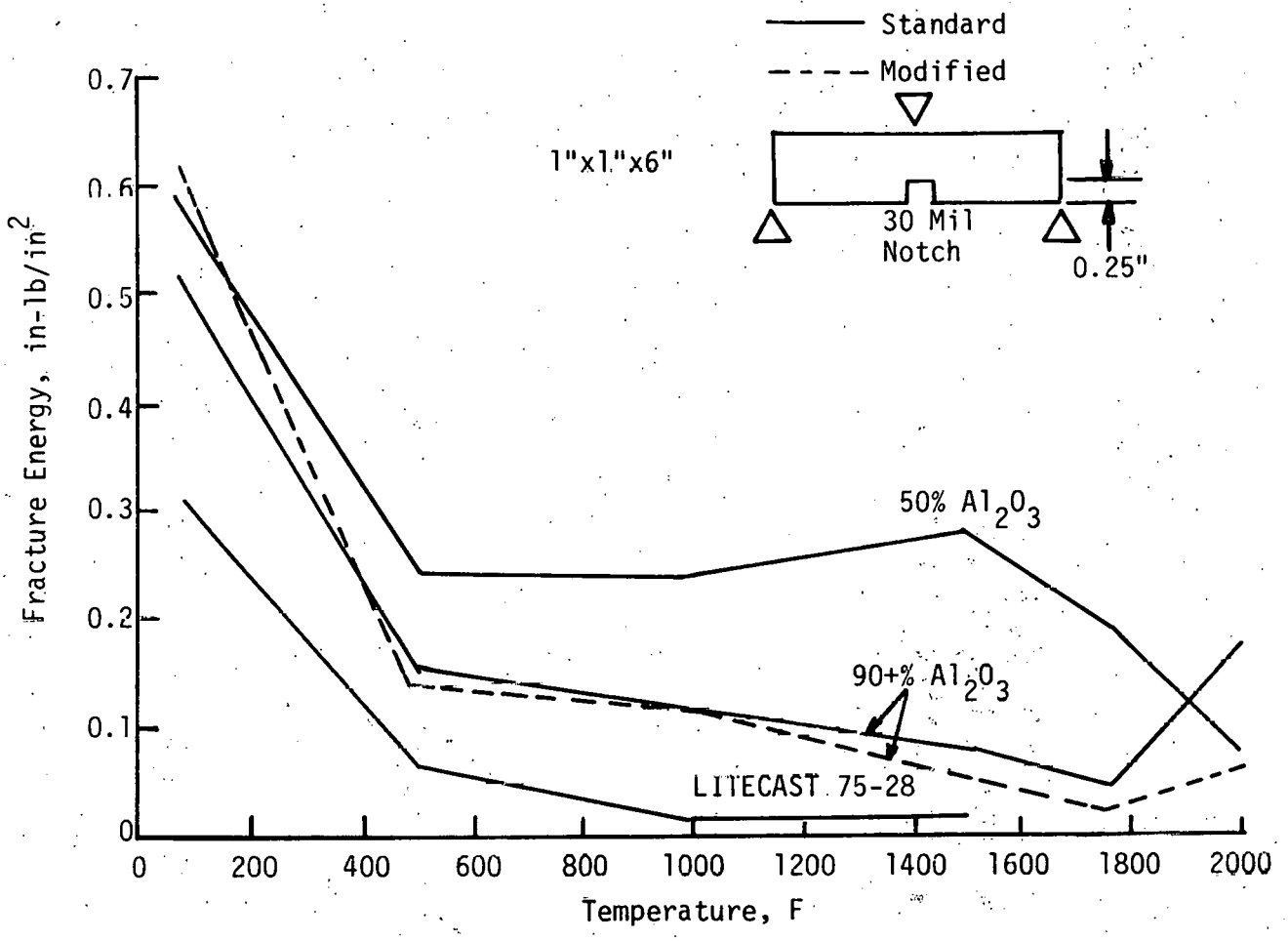

FIGURE 115. Fracture Energy Results Vs. Temperature For Dense and Insulating Castables.

accounted for accurately in a stress analysis, that analysis could be grossly in error.

As shown in Figures 112-115, the strengths of the key monolithic refractories were fairly uniform over the temperature ranges used and the materials all generally broke in a brittle manner. The modulus of rupture, modulus of elasticity and fracture energy values generally showed an initial loss at 500°F of up to 50% but then remained fairly constant above that temperature. The compressive strength values on the other hand showed little initial loss and only minor variations over the temperature ranges studied. The use of 4 w/o 310 stainless steel fibers in KAOCRETE XD 50 (Mix 36) did not appreciably change the strength of this material but did improve its toughness as noted during the modulus of rupture testing by the greater area under its load/deflection curves compared to the fiber free material.

Although the compressive strength tests were run on small samples, the room temperature measured results were found to agree well with strengths determined on brick size samples of the same or similar types of materials. In addition, as diagrammed in Figure 113 the samples generally broke in a near perfect shear failure mode which would be expected for uniform uniaxial compressive loading of brittle materials. Based on these findings, the hot compressive strengths determined on these small samples were used with confidence in the stress analysis work.

The modulus of elasticity values determined on these key monolithic refractories were generally smaller (less than 2×10^6 psi and usually less than 1×10^6 psi) than those of fired refractories but they were similar to the values reported for Portland cement based concretes [5,10]. The values were also considerably lower (by an order of magnitude) than the values reported [21] for dense refractory concretes when measured with a sonic method. It appears that a mechanical method of determining modulus of elasticity is a more realistic method for stress analysis work than a sonic method.

Tables 18 through 23 list the creep results on most of the key refractories at three stress levels and the temperatures of interest. The actual creep data collected on these key refractories at these different stress levels and temperatures and a typical tabulation of the same creep data on the 50% Al_2O_3 dense generic refractory concrete which have been reduced to Unit Strain are included in Tables B-18 through B-24 in Appendix B. Figures 116 through 123 show typical Unit Creep plots obtained on these materials, the difference in macroscopic appearance of the 50% Al_2O_3 dense generic refractory concrete and the KAOCRETE XD 50 (Mix 36C) after creep testing and the microscopic appearance of some of the refractories before and after creep testing.

As can be seen from these creep data and the stepwise creep plot shown in Figure 12 for the modified 90+% Al_2O_3 dense generic refractory concrete, steady state creep appeared to be attained in three to five hours. These creep data also showed that the creep of the materials was more temperature dependent than stress dependent in the temperature and stress ranges used. Generally, very little creep occurred for any of the materials below 1000°F. This was further confirmed with the stress relaxation results which are included in Appendix B and by the creep work of McGee, Smyth and Bray [22]. The LITECAST 75-28 began to creep dramatically somewhat above this temperature and generally deformed the most while the other materials did not creep significantly until higher temperatures. The critical temperatures at which creep became significant for the various key monolithic refractories were found

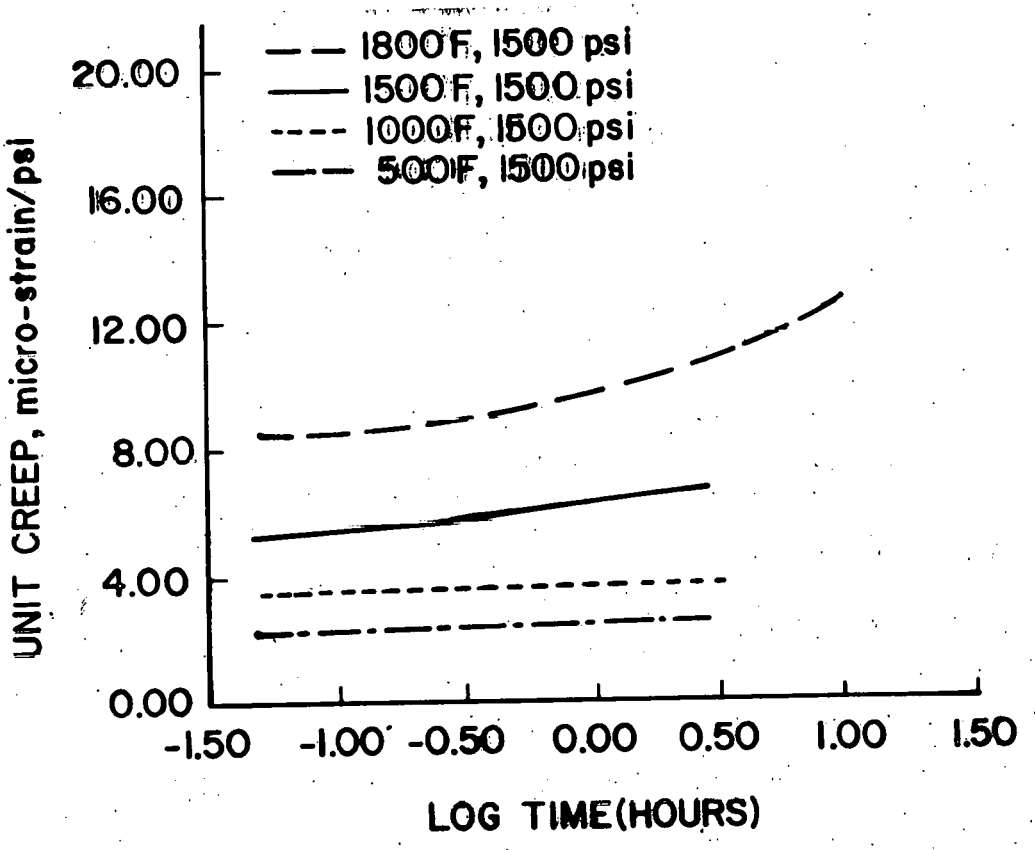

FIGURE 116. Unit Creep of 50% Al_2O_3 Dense Generic at One Stress Level.

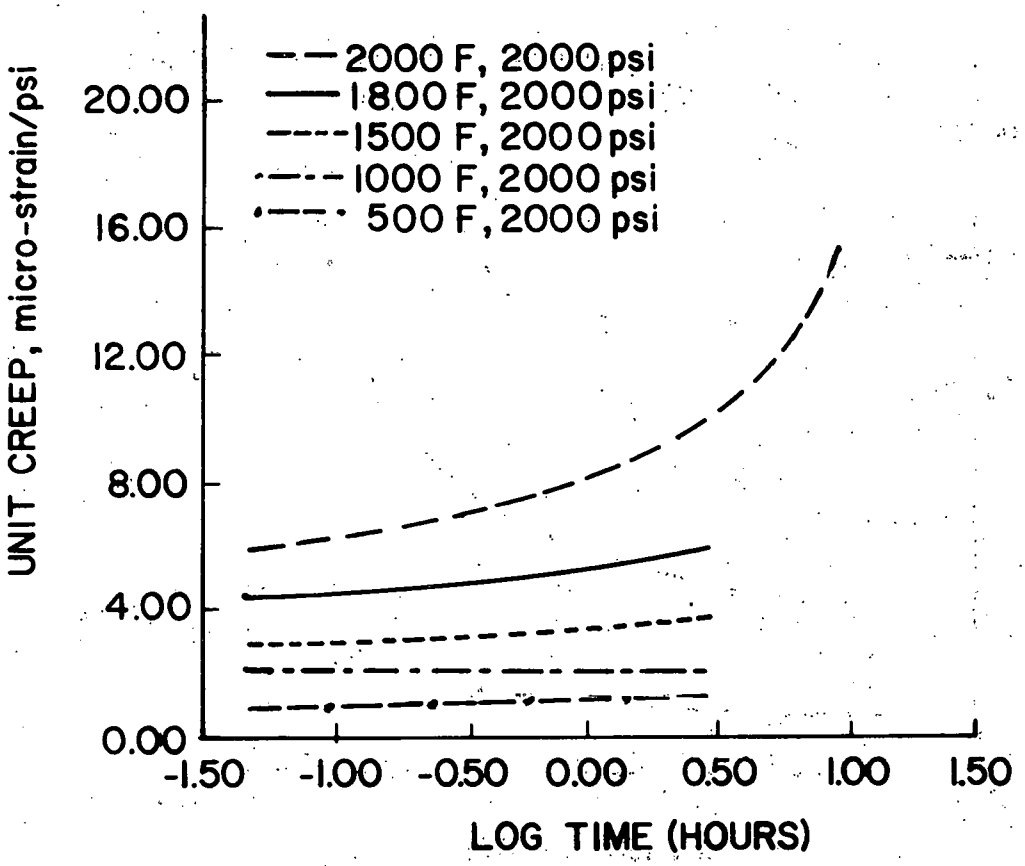

FIGURE 117. Unit Creep of KAOCRETE SD-50 (Mix 36C) at One Stress Level.

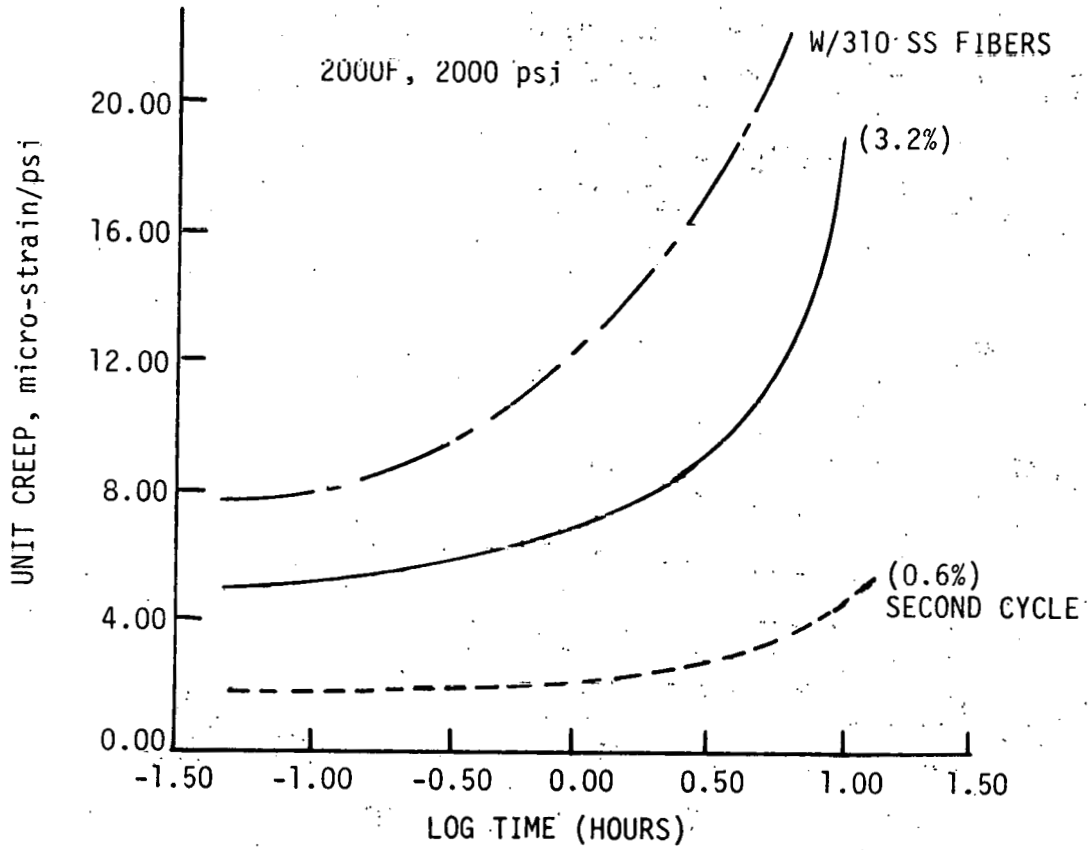

FIGURE 118. Unit Creep of Various Samples of KAOCRETE XD-50 (Mix 36C) at One Stress Level.

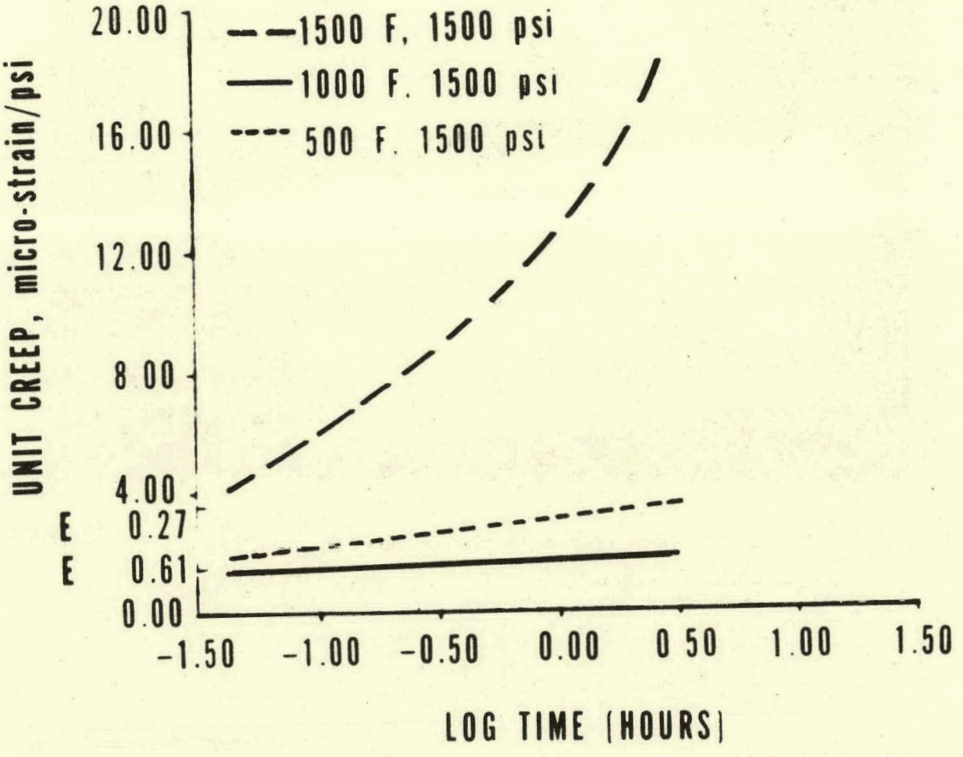

FIGURE 119. Unit Creep of LITECAST 75-28 at One Stress Level.

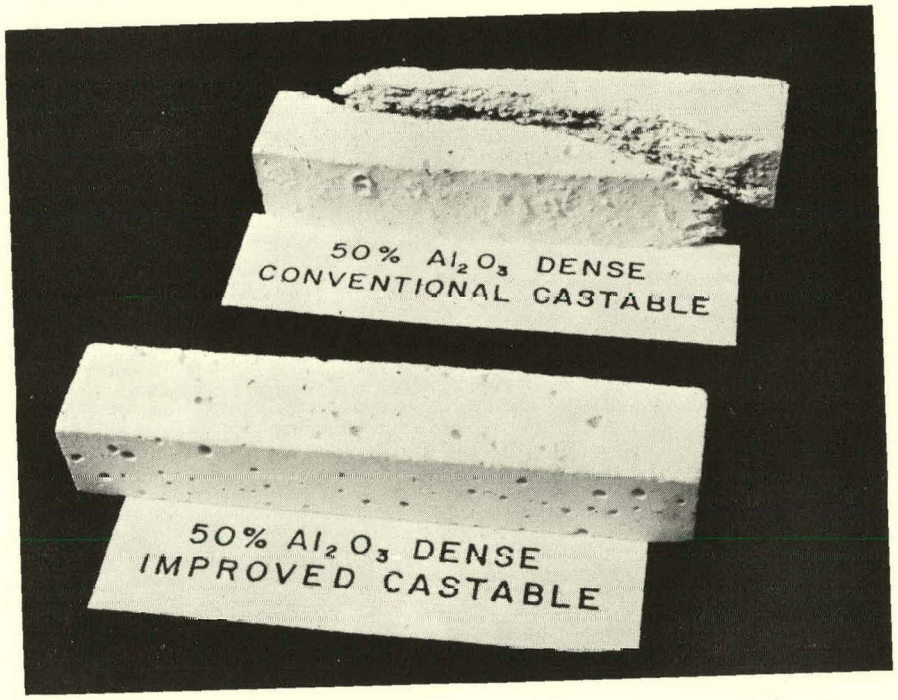

FIGURE 120. Appearance of 50% Al_2O_3 Dense Generic and KAOCRETE XD-50 (Mix 36C) After Creep Testing.

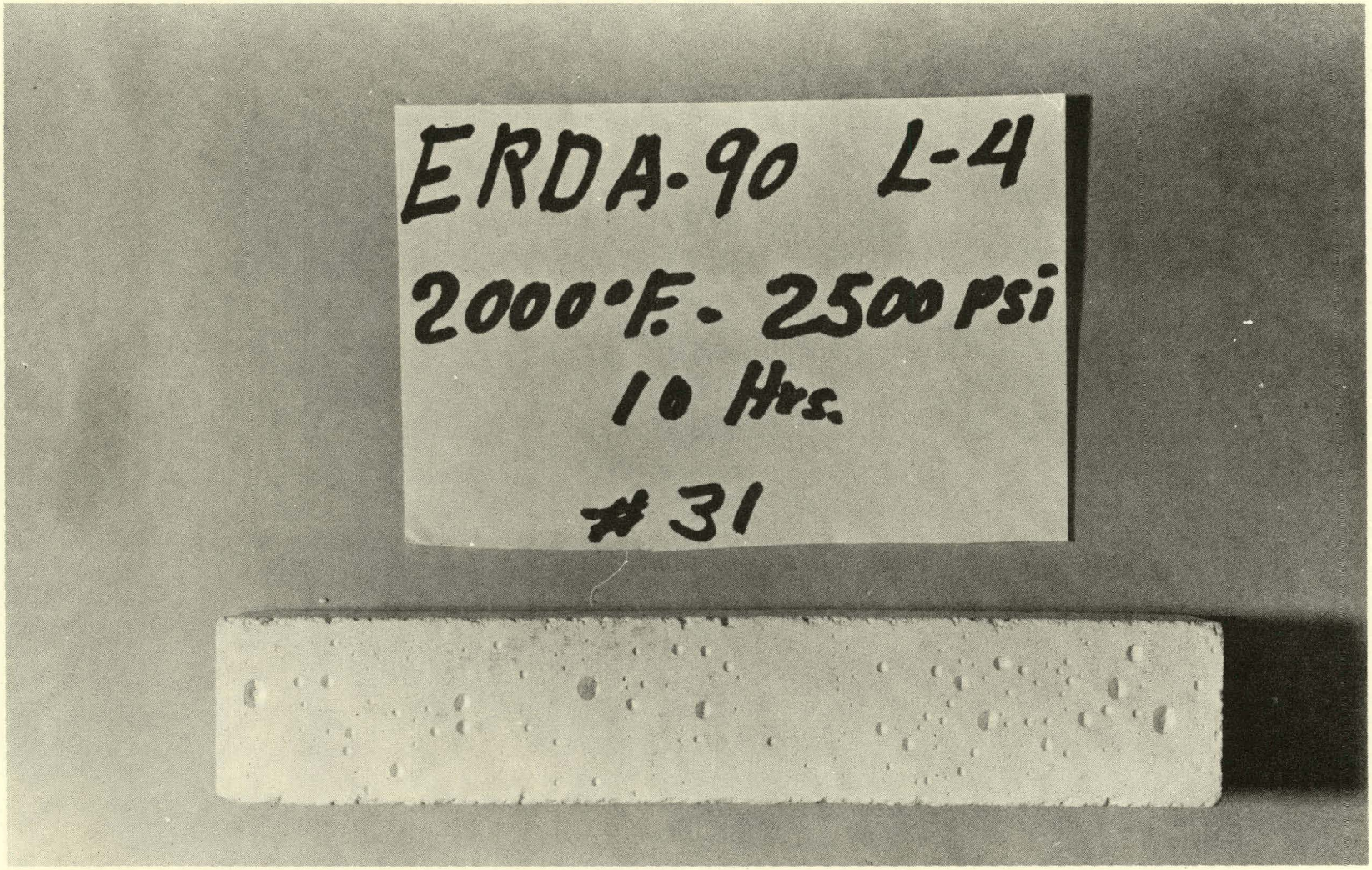

FIGURE 121. Appearance of 90+% Al_2O_3 Dense Generic (ERDA 90 - Lining #4) After Creep Test.

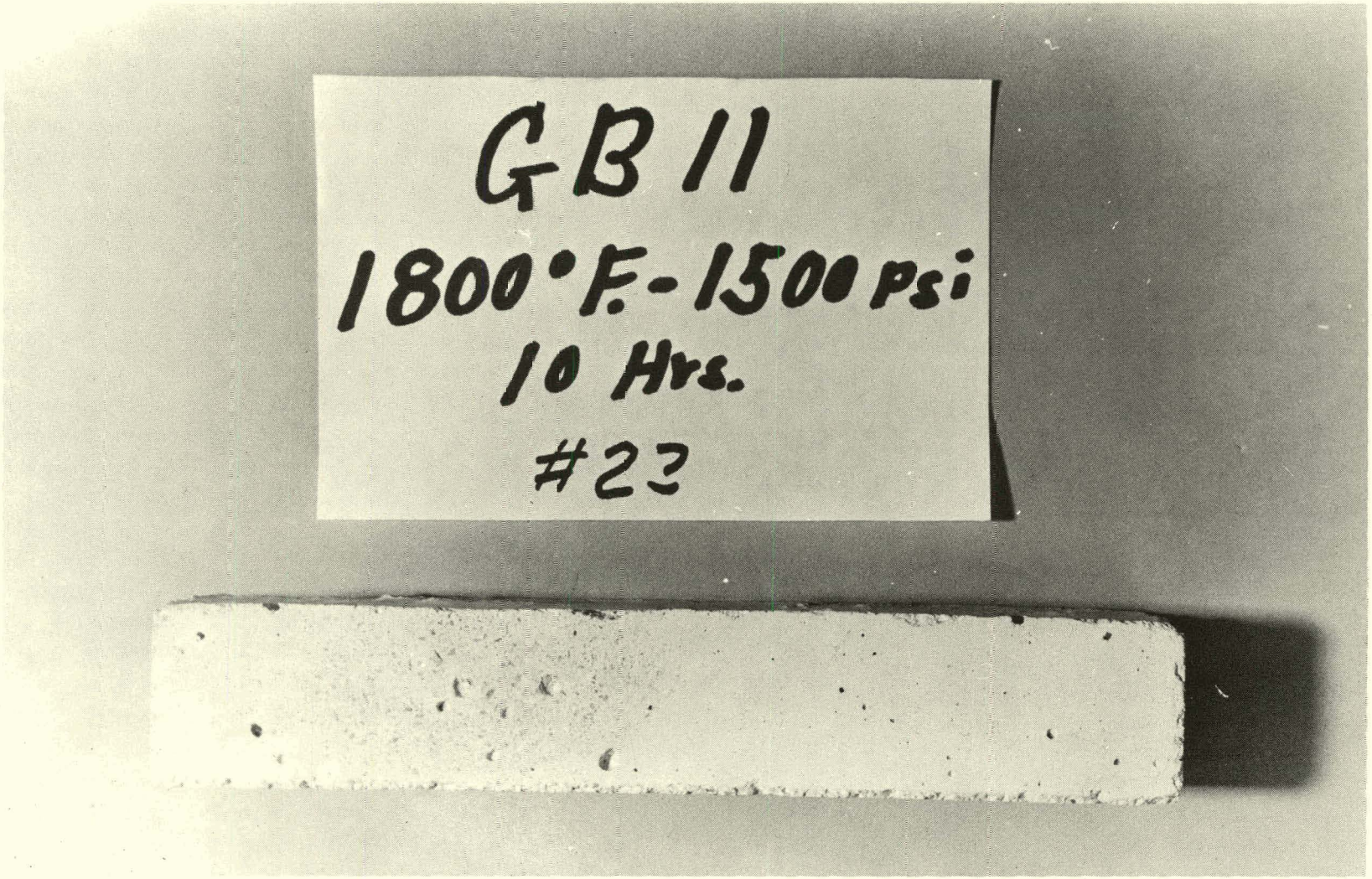

FIGURE 122. Appearance of 50% Al_2O_3 Dense Generic After Creep Test.

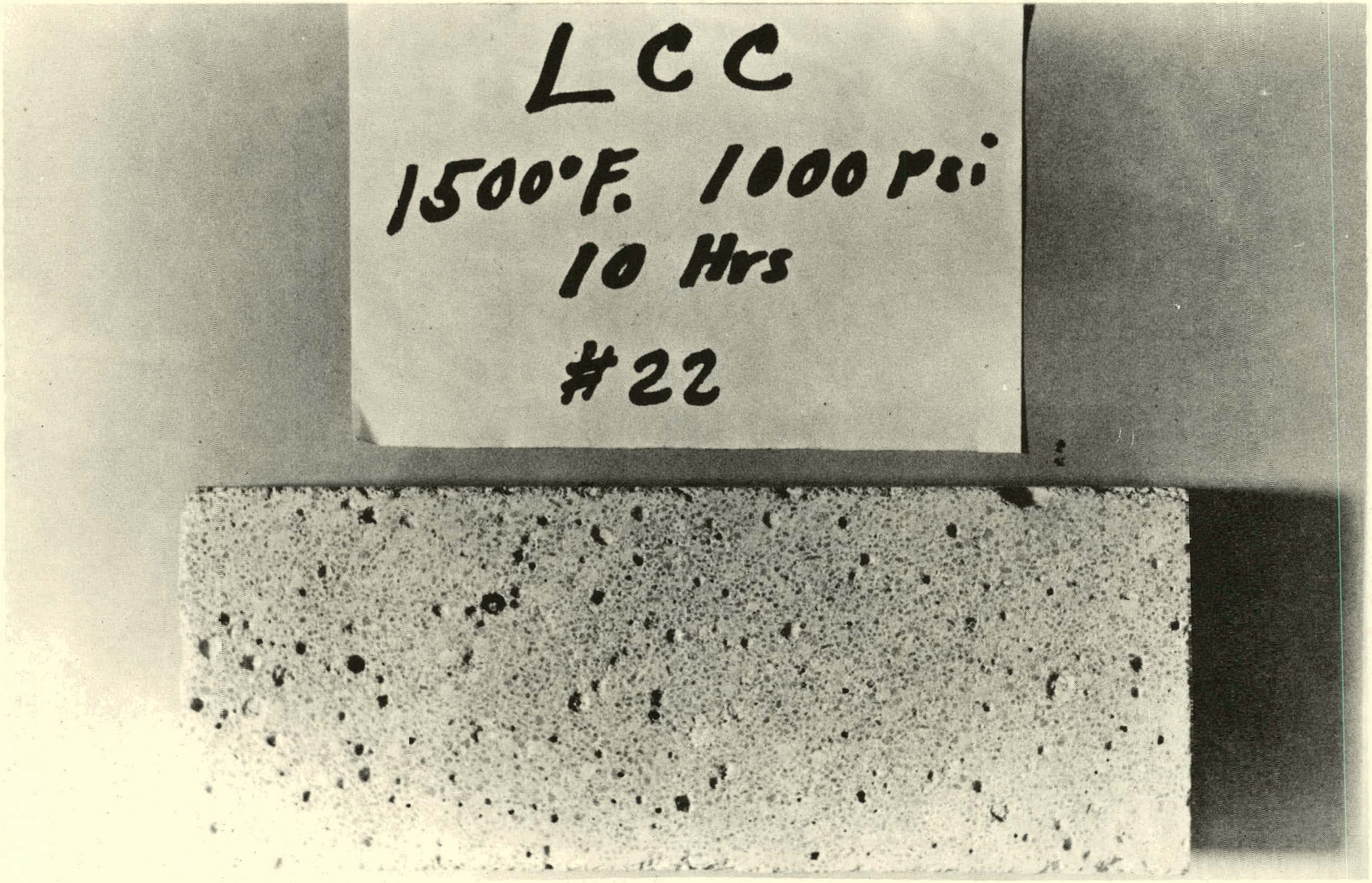

FIGURE 123. Appearance of LITECAST 75-28 After Creep Test.

to be:

90+% Al_2O_3 dense generic	1800°F
KAOCRETE XD 50 (Mix 36C)	1800°F
KAOCRETE XD 50 (Mix 36C) with 4 w/o 310 stainless steel fibers	~1700°F
50% Al_2O_3 dense generic	~1700°F
LITECAST 75-28	1250°F
KAOLITE 2300 LI	Not Determined

The amount of creep generally followed this same order.

The LITECAST 75-28 could be tested at 1500°F but could not withstand stresses above 1500 psi. The 50% Al_2O_3 dense generic could be tested at 1800°F and stresses to 2500 psi but would fail if tested at 2000°F and 1000 psi or more as shown in Figure 120. The 90+% Al_2O_3 dense generic and KAOCRETE XD 50 (Mix 36C) could be tested at 2000°F and 2500-3300 psi without failing. This was not true for the 90+% Al_2O_3 dense generic, however, if the water level used was 0.5 to 1.0% higher than the optimum. The material lost considerable creep resistance and would fail at 2000°F and 2000 psi. This was also not true for the KAOCRETE XD 50 (Mix 36C) when stainless steel fibers were added to it. The material could no longer survive a creep test at 2000°F if it contained 4 w/o 310 stainless steel fibers and it was tested at 2000 psi or higher stress. As shown in Appendix B, the material had even poorer creep resistance when it contained 2 or 4 w/o 446 stainless steel fiber and was tested at 2000°F and stresses greater than 1000 psi.

The creep results listed in Tables 18-23 generally show a difference in creep between the cummulative total and the post test total. This difference was thought to be due predominantly to the creep recovery which occurs in the samples during the unloading portion of the test. This creep recovery was not accounted for in the cummulative total but is essentially accounted for on the specimen measured after the test. The creep recovery generally appears to be greater, the greater the creep.

These creep results indicate that the chemical composition, refractoriness of the bond and density (porosity) of these key refractory concretes are major factors in controlling creep. The difference in creep between the 90+% Al_2O_3 and 50% Al_2O_3 dense generics is mainly due to the former two property effects while the difference in creep between the 50% Al_2O_3 dense generic and the KAOCRETE XD 50 (Mix 36C) is due to the latter two property effects. Specifically, these are the lower cement level (<15% vs 25%) and the optimized grain sizing of the KAOCRETE XD 50 (Mix 36C) compared to the 50% Al_2O_3 dense generic refractory. The loss of creep resistance of the KAOCRETE XD 50 with 4 w/o 310 stainless steel fibers is apparently due to the effective increase in porosity created by the presence of the soft fibers and to the enhancement of shearing caused by the soft fibers during the high temperature tests.

Very few materials were tested on a second cycle or monitored for creep during the cooldown but those that were tested on a second cycle generally showed a reduced level of creep. This latter effect is shown in Appendix B for the 90+% Al_2O_3 and KAOCRETE XD 50 (Mix 36C) materials. More data on these effects on creep are available in the work of McGee, et al [22].

The microscopic examination of the creep tested refractories showed that they had densified and developed microcracks during the tests. The degree of densification and microcracking was dependent on the stress level used in the test. Figures 121-123 show the typical appearances of the 90+% Al_2O_3 dense generic, the 50% Al_2O_3 dense generic and the LITECAST 75-28 before and after testing.

Although only limited testing was done to specifically evaluate the crack resistance of the key refractories, the fracture energy results showed an interesting trend that would be followed in the lining tests. This trend which is shown in Figure 115 indicated that the 50% Al_2O_3 dense generic was more resistant to crack growth than the 90+% Al_2O_3 dense generic and LITECAST 75-28 in that order. The KAOCRETE XD 50 (Mix 36C) was expected to act like the 50% Al_2O_3 dense generic and the use of metal fibers in it was expected to make it even more resistant to crack propagation.

3.3. Evaluation and Verification Tests

The following two sections describe results of panel and hollow cylinder tests:

3.3.1. Panel Tests

Ten panels were made for heat-up testing as described earlier in Table 8. The purpose of this work was multi-faceted and included evaluating or investigating:

(1) The temperature profiles on twelve (12) inch thick linings.

(2) The design and performance of the experimental V-type anchor, and different anchor configurations including no anchors.

(3) The performance of dual component panels using lower water levels, different mixing and curing times and curing conditions.

(4) The performance of the 50% Al_2O_3 single component lining.

(5) The effect of independent anchoring of the insulating component on the cracking tendency of the dual component lining.

(6) The effect which the 12 cu. ft. Muller mixer and larger batch sizes (600-700 lbs.) would have on the quality of the panel produced and the heat-up performance obtained.

(7) Various Acoustic Emission (AE) monitoring techniques.

(8) The sample collection and tear out procedures planned for the linings.

The work was found to be very beneficial to the rest of the program. Through it a better appreciation was gained of the explosive spalling tendency of the dual component linings with the dense 90+% Al_2O_3 castable and the factors, especially the rapid heat-up rates (>250°F/hr in 400-1000°F range), which caused it. In addition, this work indicated that the V-type anchor design should be modified to improve its performance, a six (6) inch spacing was too close and could have contributed to the explosive spalling problem, less cracking could occur when Y-type anchors are used, the modified 90+% Al_2O_3 generic formulation looked acceptable for the lining tests, the 50% Al_2O_3 single component lining appeared to be susceptible to cracking, independent anchoring of the insulator did not have any noticeable effect on the lining performance, and a viable acoustic emission monitoring technique had been developed for use in the lining tests.

Figure 124 is an example of the type of thermal profile obtained during a typical panel test. It is for the panel containing the uncoated Y anchors. Figure 125 shows the crack pattern observed in the 90+% Al_2O_3 and insulating castable portions of this panel on the hot face and through its cross section. The cracks have been highlighted with black ink.

The results showed that the metal shell could get up to 250°F when a 6" anchor spacing was used and a 2000°F hot face temperature was achieved. They also indicated that the insulating castable could get as hot as 1600°F at the interface between the two components and that the dense castable cooled very quickly and at

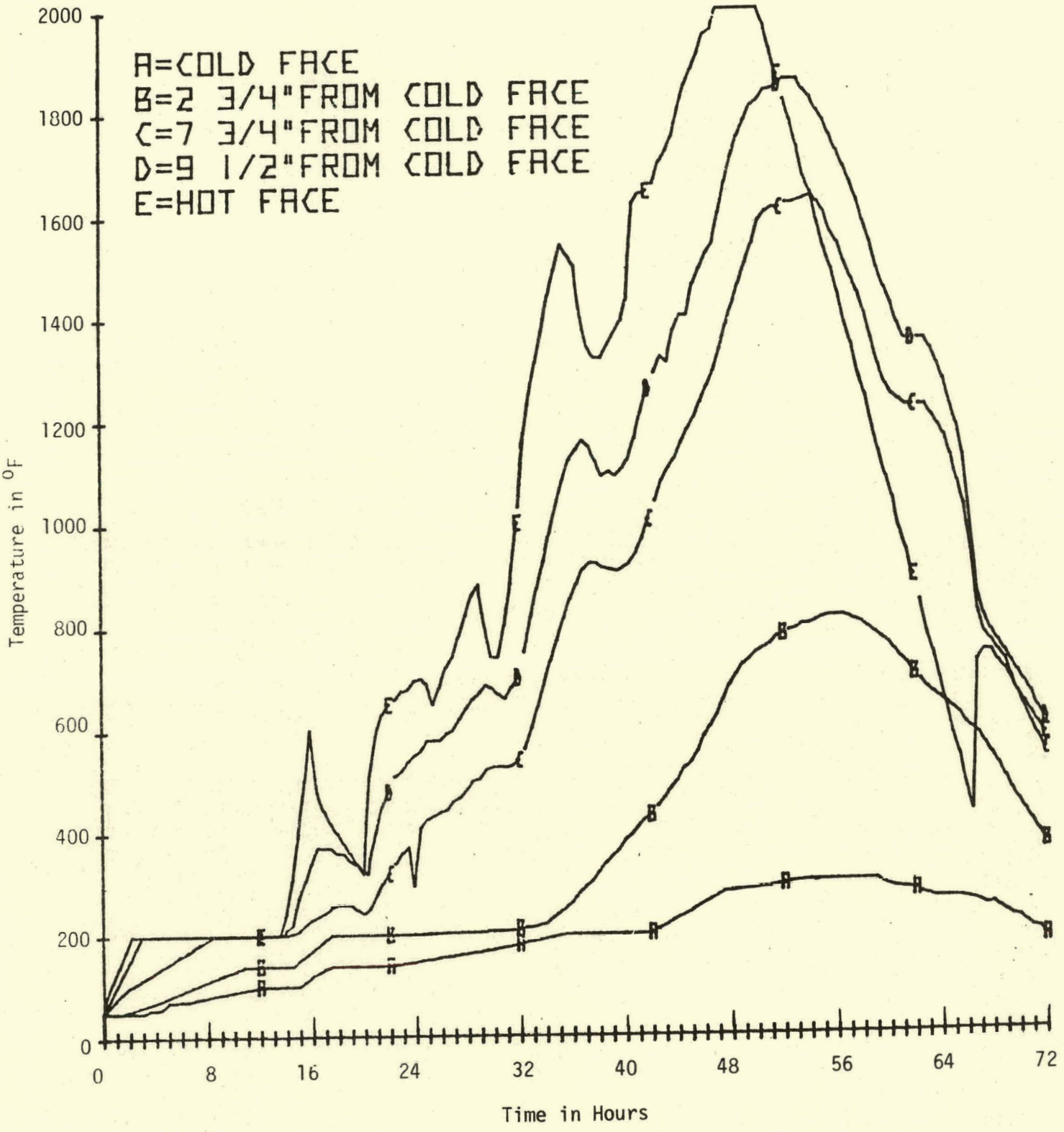

FIGURE 124. Temperature Profile of Panel Test.

one point was cooler than the hottest region of the insulating castable.

By comparison to the Y anchor containing panel, the anchorless panel had a 50 to 100°F lower shell temperature. This difference indicated that the anchors which extended out into the dense castable acted as heat sinks and conducted considerable heat to the shell. In either case, however, even with cracking, the pressure vessel shell wall should remain below 650°F, the shell wall design temperature.

The cracking pattern seen in Figure 125 for the uncoated Y anchor containing panel was fairly typical of the appearance of all the panels except that the degree of cracking in the dense castable varied. It was hardly cracked at all in the coated anchor containing panel whereas it was severely cracked in the uncoated anchor containing panel and contained shallow surface cracks only in the anchorless panel. The cause for the big differences between the cracking tendency of the anchorless and wax coated anchor containing panels and the uncoated anchor containing panel is apparently due to the absence or reduction of anchor-refractory interactions. However, the use of 1.0% less water in the dense castable component of the coated anchor containing panel could also have helped reduce the cracking tendency of this component.

The consistent cracking of the LITECAST 75-28 indicated that the 26% water level was too high and that lower water levels would be necessary. Through experiments with 100 lb. quantities of this castable in a 4 cu. ft. mortar mixer, it was found that 21% water was a minimum level to produce good castings; and some amount between 23 and 24% appeared to be the optimum level.

The 9.3% water level used with the dense 90+% Al_2O_3 castable in the uncoated anchor containing panel was generally considered to be the minimum level to produce good castings. A 9.8% level was considered to be closer to the optimum level for this castable when the 4 cu. ft. mixer was used.

Thermal profiles for two panels which underwent explosive spalling are shown in Figures 126 & 127. Photographs of the spalled panel appear in Figures 28 & 128. When panel 4 explosively spalled, the front 2-1/2 inches of the 90+% Al_2O_3 generic hot face material separated from the rest of the panel with such force, it blew the 285 lb. panel out of the furnace door. The panel continued to explode for a number of minutes after it landed on the floor. Even though this explosion occurred, the insulating component and some of the dense component remained intact (and anchored) to the metal plate. The straight anchor legs were also intact and did not appear to be bent or distorted by the explosive spalling of the dense castable. They obviously had provided very little holding force for the failed dense component.

This explosive spalling of the panel 4 identified the need for a retaining bar on the front of the furnace to prevent panels from blowing out of the furnace door if explosive spalling occurred again. This event also led to a review of the mixing, casting and curing history of this panel to determine if something had contributed to the spalling. It became apparent from this review that a number

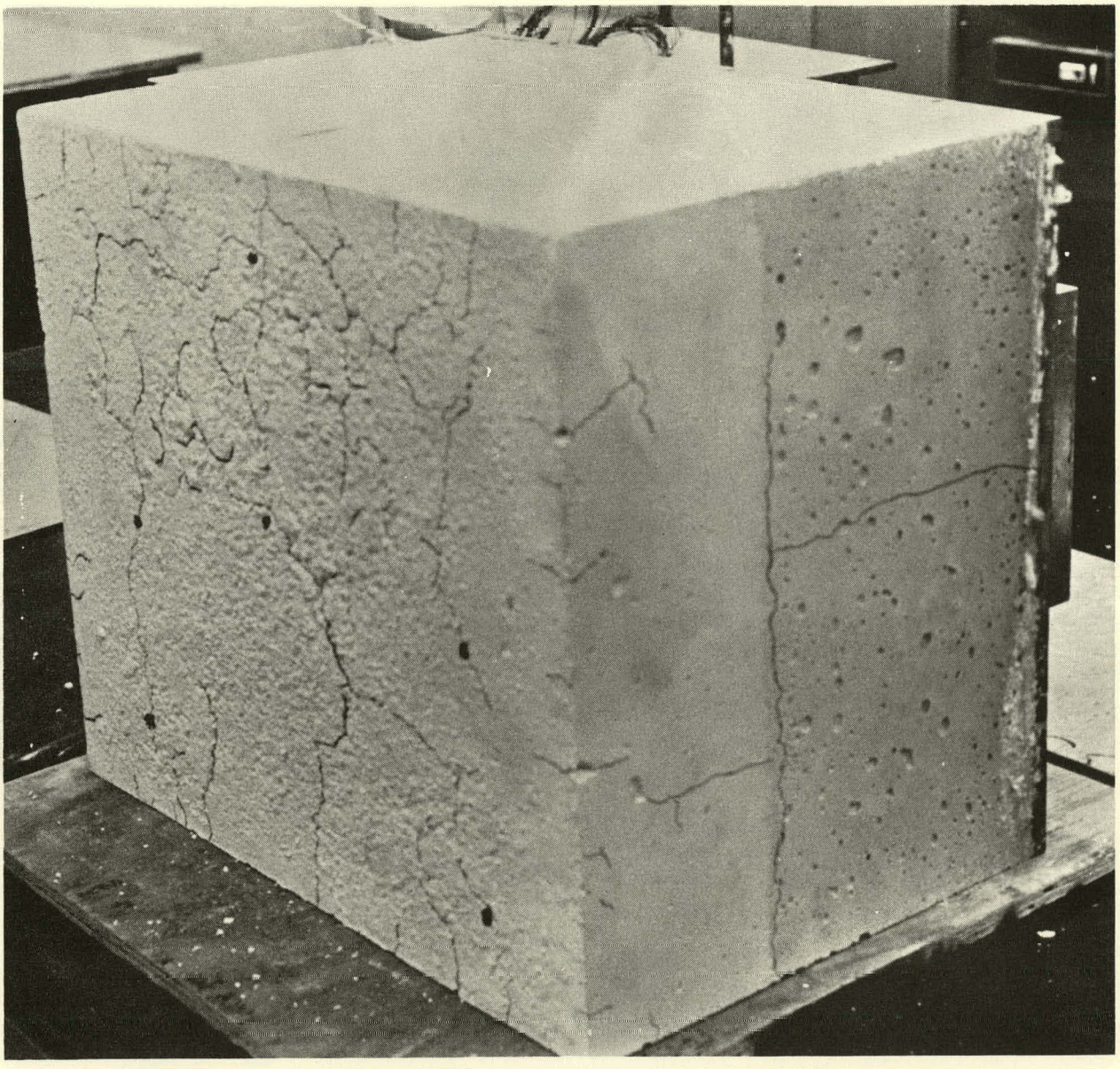

FIGURE 125. Front and Side View of Two Component Panel (#6) After Heat-Up Test to 2000°F.

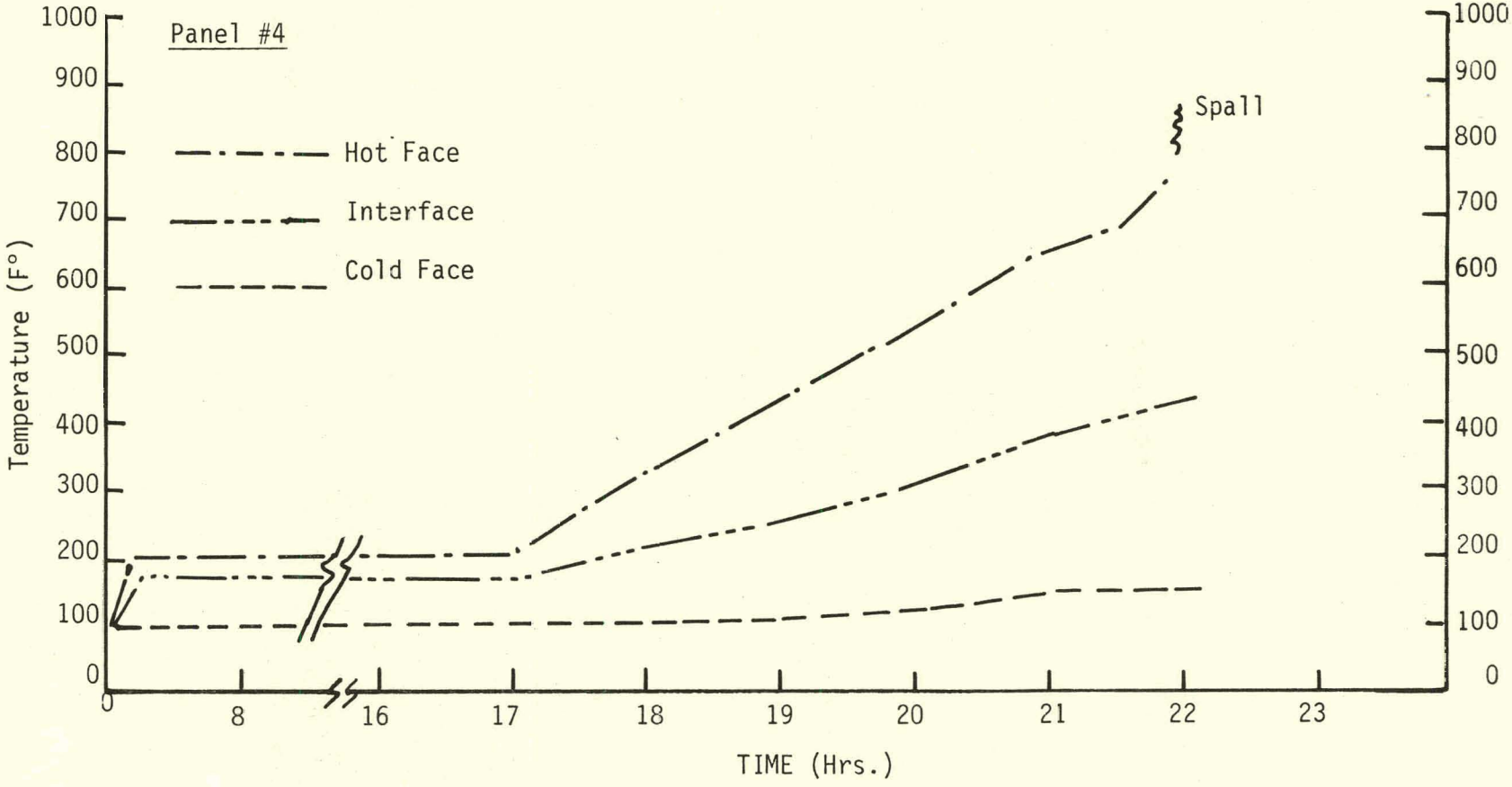

FIGURE 126. Temperature Profile of Spalled Panel #4.

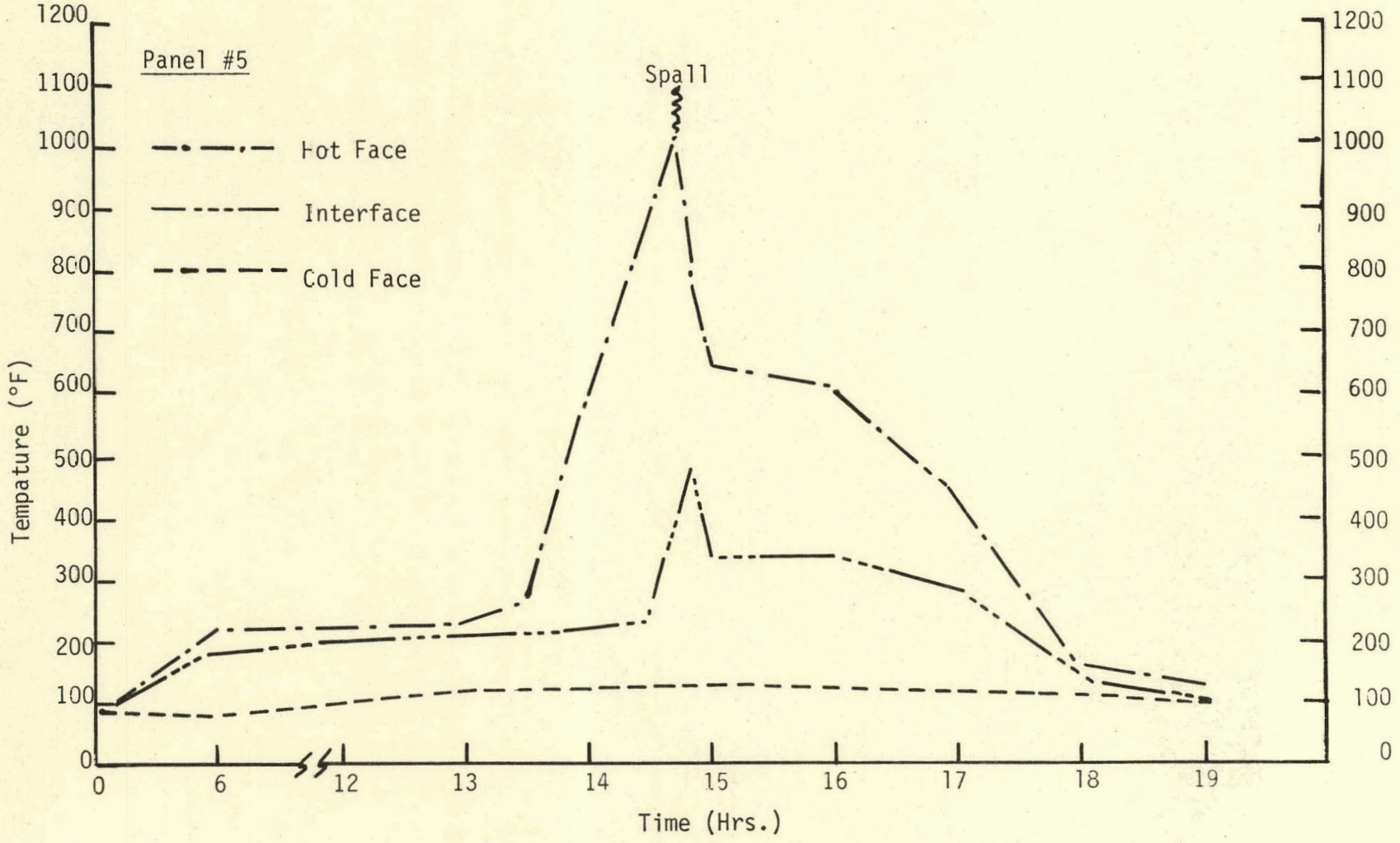

FIGURE 127. Temperature Profile of Spalled Panel #5.

FIGURE 128. Spalled Panel #4.
Straight Anchor Sticking Out of Insulator.

of factors contributed to the high sensitivity of panel 4 to explosive spalling during an inadvertent rapid heat-up rate in the 700°F temperature range. These factors included:

(1) 5" of 90+% Al_2O_3 generic castable were used rather than the 4-1/2" originally planned.

(2) The 90+% Al_2O_3 generic was cast in two (2) separate pours from a 4 cu. ft. mortar mixer. (This could have produced a discontinuity in this component in the location of the fracture surface.)

(3) The hot face surface was troweled smooth and covered with wet blotter paper before being covered with plastic to maintain a high humidity during curing.

(4) The panel cured over a long weekend when the laboratory temperature was lowered to ∿65°F.

These last two factors were thought to be the main contributors to this sensitivity and give credence to the findings of other investigators who have reported the explosive spalling sensitivity of high alumina castables that have been cured at below 75°F. This sensitivity becomes apparent at temperatures of 800°F and higher during rapid heat-up rates (250°F/hr or higher).

To test the validity of these 4 factors, panel 5 was made and heated. Great care was taken during the fabrication of this panel to eliminate the factors which made panel 4 sensitive to heat-up rate, and included:

(1) Repeating the same anchor spacing but bending the last one inch of each leg inward 90°.

(2) Using warm water during the placement of both components to maintain a pour temperature above 75°F.

(3) Roughening the hot face surface with a wire brush after casting to open the surface pores.

(4) Wrapping the panel with plastic and ceramic fiber blanket to maintain a ∿80°F or higher curing temperature environment.

(5) Deleting spray water on the cast surface.

This greater care apparently reduced the sensitivity of panel 5 to explosive spalling by permitting it to remain intact at the rapid heat-up rate (460°F/hr) due to a controller malfunction until the 800 to 1000°F temperature range had been reached. The panel exploded with the same force as panel 4 but the restraining bar installed on the front of the furnace prevented the panel from being blown out of the furnace. The panel failed in the same manner as the previous panel except that the hot face component spalled into four (4) pieces and the bent anchor extensions remained embedded in these pieces. The force of the explosion was great enough when failure occurred, that the threaded nuts of the anchor extensions were stripped off the welded leg. These items are shown in Figure 129.

Despite the furnace controller problems, the results indicated that the six (6) inch spacing which was common to panels 4 and 5 should not be used further.

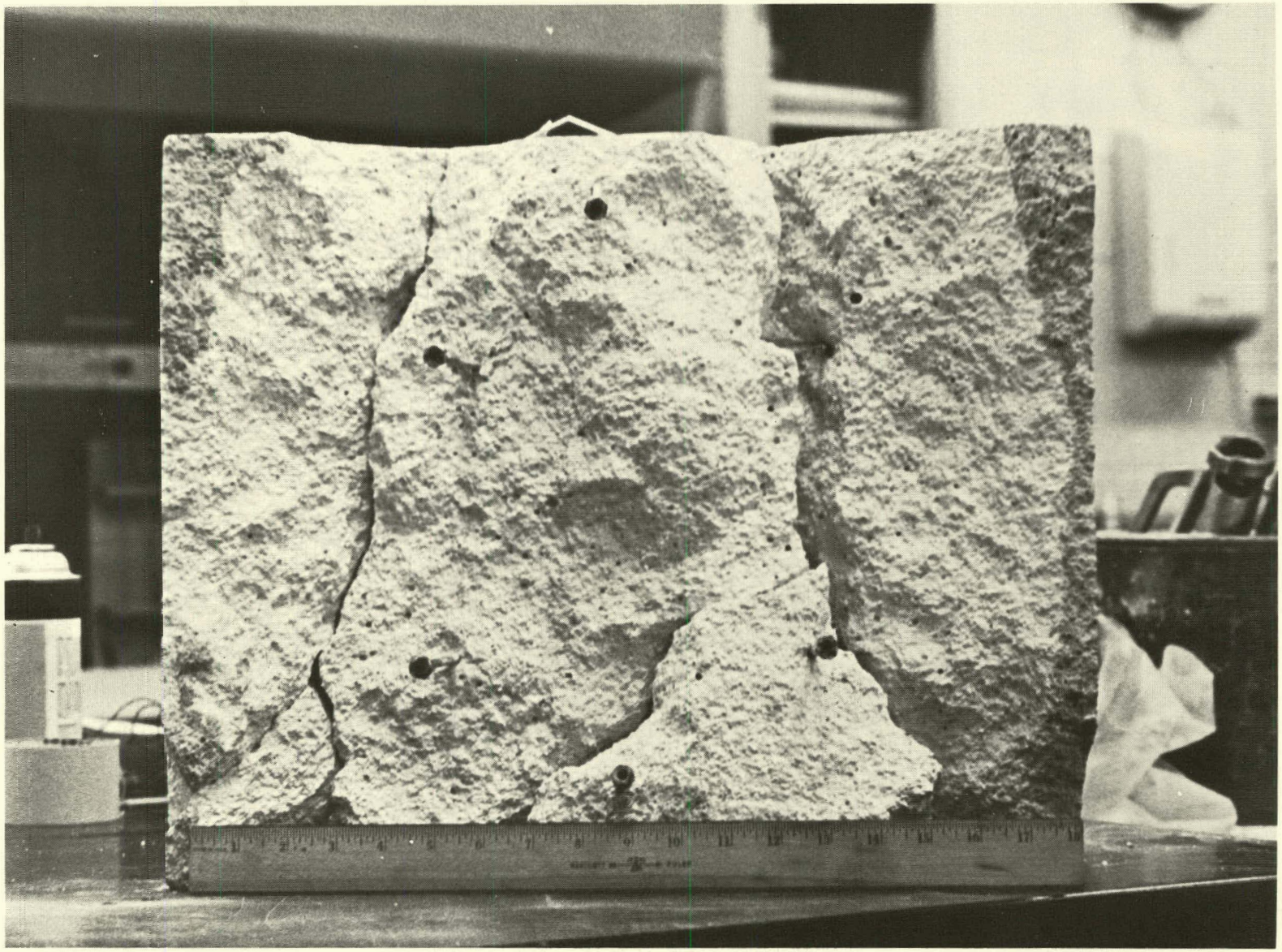

FIGURE 129. Spalled Panel #5 Showing Stripped Anchor Nuts.

They also indicated that the dry-out portion of the Case #1 heat-up schedule should be extended to remove as much mechanical water as possible from the lining before the heat-up to 1000°F is started. These results on panel 5 also indicated the need for a fail-safe system on the pressure vessel/test furnace and around the clock surveillance of the lined vessel heat-up tests.

These factors were investigated in panel 6 along with the previous factors studied in panel 5. In addition, a different anchor configuration (see Figure 15) was used. It included three (3) Y-type anchors spaced between 8-1/2" and 12" apart and an independent V-type anchor in the insulator component. Since the modified Case #1 heat-up schedule was achieved during the running of this panel as indicated by the thermal profile in Figure 130, no rapid heating rates or explosive spalling were experienced. The panel was cracked through both the dense and insulator components after the test. The crack pattern was mainly random but some cracks appeared to parallel the anchor orientations.

Since neither the modified 90+% Al_2O_3 generic castable or materials mixed with the 12 cu. ft. mortar mixer had been evaluated in any of the panel tests, panel 7 was made to investigate these points. It was practically identical to panel 6 except for the differences mentioned above and for the fact that the materials were mixed and poured at slightly higher temperatures. This caused the LITECAST 75-28 to be somewhat stiff during placement. Thirdly, a lower water level was used with the modified 90+% Al_2O_3 generic castable (8.5% vs 9.3%).

It was found that panel 7 had only minor surface cracks compared to panel 6 after the modified Case #1 heat-up schedule and for all practical purposes was uncracked. Since the main differences between panels 6 and 7 were the formulations of the dense material, the water level used in the dense component and the mixing and curing temperatures used, these differences must be primarily responsible for the better performance of panel 7. Based on these findings, the modified 90+% Al_2O_3 generic material with the mixing and curing conditions for panel 7 was used in the first lining test.

The panel tests also provided an opportunity to evaluate the lining tear-out procedures planned. The anchorless panel split apart quite readily along the dense-lightweight interface. It was then sectioned by a diamond saw to determine the extent of crack propagation. Although it was difficult to determine, the cracks did not appear to propagate completely through the thickness of the dense material. A hammer and chisel were used on the panels with anchors. Splitting followed the larger, deeper cracks in the surface of the dense castable as chunks were chipped away from the panel. Axial cracks in material adjacent to anchors were noted in both the dense and insulating refractory when chunks of lining were pulled away from the anchors. Generally, the panels could be torn apart without too much difficulty and the same anchors were used for the two anchor containing panels.

In summary, the panel work was very helpful and informative. It had indicated the severity of the explosive spalling of the 90+% Al_2O_3 dense generic type material and the sensitivity of this material to heating rates of 250°F/hr or greater in the 700 to 1000°F temperature range especially when it is cured at below 75°F. A heating rate of 200°F/hr or less appears to be a safe one to use to prevent explosive spalling.

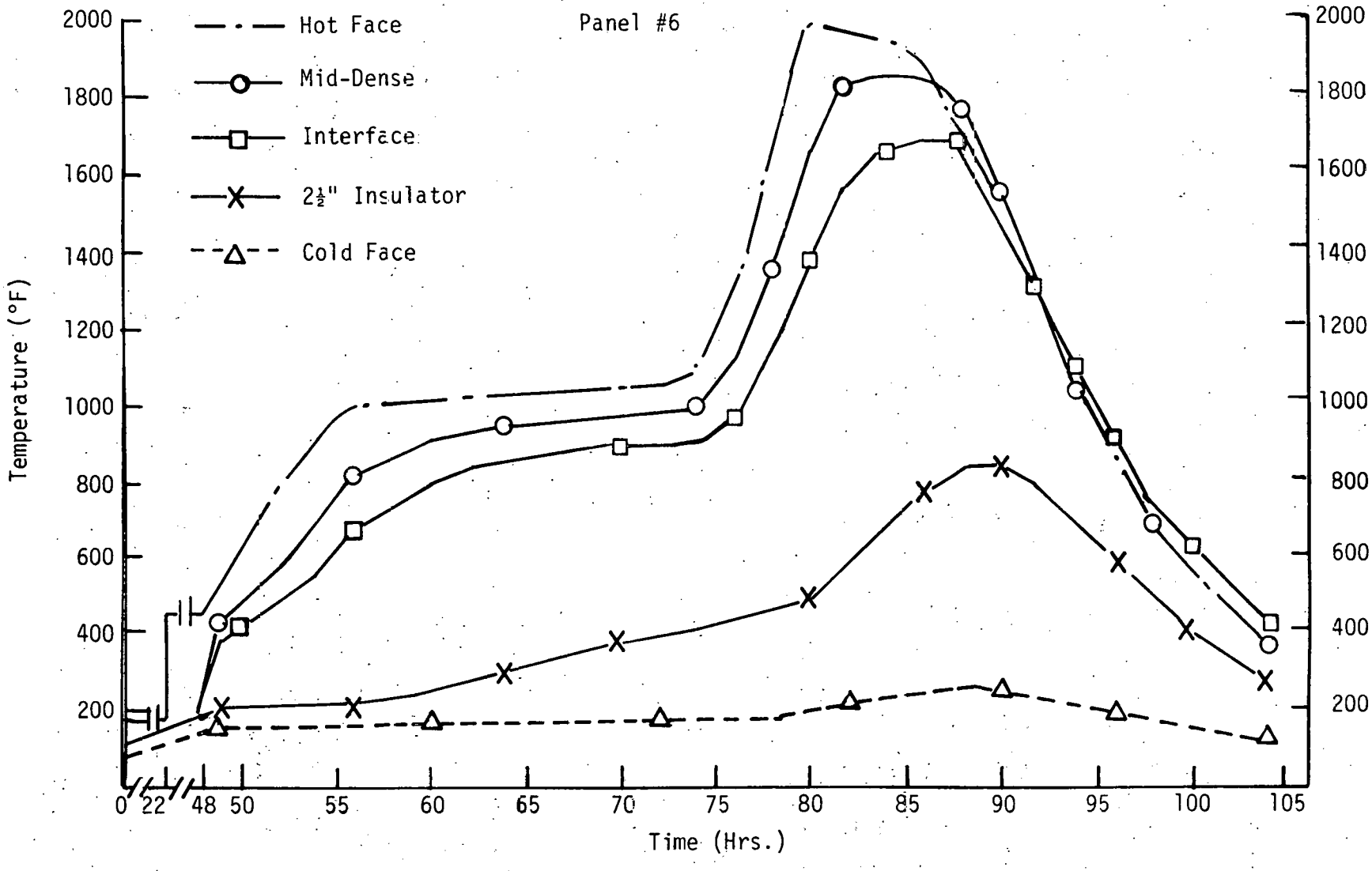

FIGURE 130. Modified Case #1 Used on Panel #6.

This work has also showed that:

(1) The modified Case #1 heat-up schedule should be used in the initial vessel lining tests.

(2) A fail-safe system should be installed on the pressure vessel/test furnace to prevent rapid heating rates from occurring.

(3) A six (6) inch anchor spacing is too close and probably contributes to stress build-up in the lining.

(4) Y-type anchors may produce less cracking than V-type anchors.

(5) The modified 90+% Al_2O_3 generic castable mixed with the 12 cu. ft. mortar mixer at a 8.5% water level or lower is an acceptable dense component material to use in the liner tests. LITECAST 75-28 cast at 21% water gives a low shrinkage material which is acceptable for use as the insulator component.

(6) Batch temperatures of at least 70°F and preferably 75°F should be used to reduce cracking and explosive spalling tendencies.

(7) Surface roughening of the dense component hot face helps reduce the sensitivity of this type material to explosive spalling.

(8) The V-type anchor design should be modified to improve the strength of the threads.

(9) Independently anchoring the insulating component did not appear to have a positive or negative effect on the tendency of the lining to crack.

The findings of this work dealing with explosive spalling were published in 1978.[23,24]

3.3.2. Hollow Cylinder Tests

Tables 24 through 27 summarize the materials, design configurations, operating conditions, heating schedules, and results obtained on four of the key monolithic refractories (modified 90+% Al_2O_3 dense generic, KAOCRETE XD 50 (Mix 36C), LITECAST 75-28 and KAOLITE 2300 LI) and modifications to them in the hollow cylinder tests. The purpose of these tests was to evaluate various materials and/or designs and operating parameters to acquire additional direction on how best to improve the performance of monolithic refractory linings and direct the plans for the last three to four lining tests. The findings of this testing are discussed in the following paragraphs.

The order of cracking tendency was in general the highest for the LITECAST 75-28 followed by KAOLITE 2300 LI, the modified 90+% Al_2O_3 dense generic and KAOCRETE XD 50 (Mix 36C). In general, it only took a heating rate of about 400°F/hr to crack the LITECAST 75-28 and KAOLITE 2300 LI materials

TABLE 24. Cylinder Test Results for Modified 90+% Al_2O_3 Generic

Cyl. No.	Composition and Design	Casting History	Firing Schedule	Temperature Profile	Crack Width Ranking	Crack Pattern	I.D. Shrinkage	V Meter
1	7.75% H_2O Liner 4* Unrestrained	Stored 13 months Sealed	600°F/hr. to 1660°F, 200°F/hr cool	HF.-1660°F CF.-1170°F ΔT -490°F	4	2 Medium large cracks 95% penetration	.13%	25.7
2	7.75% H_2O Liner 4 Attached Restraint	Stored 13 Months Sealed	600°F/hr to 1760°F, 200°F/hr	HF-1760°F CF/shell-1210°F** ΔT-550°F	5	2 Large cracks 90% penetration	N.C	32.9
3	10 w/o Kyanite Added, 8% H_2O Cast in Restraining ring(1/2"SS)- Ring coated w/silicone grease	Stored 4 days Sealed	600°F/hr to 1860°F, 200°F/hr cool	HF-1860°F CF-1060°F Shell-780°F*** ΔT-880°F	3	3 Fine cracks 65% Penetration	.30%	34.6
4	10 w/o Kyanite Added, 8-1/2% H_2O, Cast in restraining ring-ring coated w/silicone grease	Stored 4 days Sealed	600°F/hr to 1820°F, 200°F/hr cool	HF-1845°F CF-1140°F Shell-1040°F ΔT-805°F	2	1 Fine crack 1 Med. crack (portion) 54% Penetration	.32%	43.8
5	8.25% H_2O cast in re-straining ring prelined with 1/4" HES mortar	Mortar air dried 5 days castable stored 1 day Sealed	600°F/hr to max heating of mortar (750°F), 200°F/hr cool	HF-1320°F CF-790°F Shell-700°F ΔT-620°F	2	3 very fine cracks 50% penetration	.16%	31.5
6	10 w/o Kyanite Added, 10.25% H_2O Unrestrained	Stored 14 days Sealed	600°F/hr to 1850°F 200°F/h4 cool	HF-1660°F CF-1140°F ΔT-520°F	4	2 Medium large cracks Penetration	.13%	37.9

Legend: Crack Widths:
Rank 5 - Large - .010"+
Rank 4 - Med. Large - .007"-.010"
Rank 3 - Med. - .005"-.007"
Rank 2 - Fine - .002"-.005"
Rank 1 - Very Fine - .002"

This ranking applies to all four tables (23-26)

Penetration Average: An average of the penetration depths, hot face to cold face, in a given sample.

* Denotes that cylinder was made during pour of Lining #4.
** Aluminum ring melted - no effective restraint during hold or cool down.
*** Stainless steel ring slipped 1/2" during test, siezed solid during cool down.

TABLE 25. Cylinder Test Results for KAOCRETE XD 50 (Mix 36C)

Cyl. No.	Composition and Design	Casting History	Firing Schedule	Temperature Profile	Crank Rank	Crack Pattern	I.D. Shrinkage	V Meter
1	7.5% H_2O Liner 5* Unrestrained	Stored 11 Months Sealed	900°F/hr to 1600°F, Fast cool	HF - 1620°F CF - 980°F ΔT - 640°F	1	No cracks	.04%	29.7
2	7.5% H_2O Liner 6 Unrestrained	Fired Stored 6 Months Sealed	600°F/hr to 1760°F, 200°F/hr cool	HF - 1760°F CF - 1200°F ΔT - 560°F	2	2 Fine Cracks 30% Penetration	.03%	32.9
3	7.5% H_2O Liner 5 Unrestrained	Stored 11 Months Sealed	600°F/hr to 1720°F, 200°F/hr cool	HF - 1720°F CF - 1120°F ΔT - 500°F	2	2 Very fine cracks 15% Penetration	.021%	36.7
4	7.75% H_2O Cast in Restraining ring - Ring pre-lined w/ 1/4" HES mortar	Mortar air dried 5 days, castable stored sealed 1 day	600°F/hr to max rating of mortar (750°F), 200°F/hr cool	HF - 1540°F CF - 740°F Shell - 620°F ΔT - 920°F	1	No cracking	None	36.7
5	7.5% H_2O, Unrestrained-Hot Face coated w/RX-14	Cast with Lining 6 Stored 8 Mo. Sealed	600°F/hr to 1850°F, 200°F/hr cool	HF - 1850°F CF - 940°F ΔT - 910°F	2	2 Very fine cracks 36% Penetration	**	29.3
6	7.9% H_2O 10 w/o Kyanite Added, Restrained w/SS ring	Air dried 24 hrs.	600°F/hr to 1850°F, 200°F/hr cool	HF - 1830°F CF - 790°F Shell - 740°F ΔT - 1090°F	2	1 Fine Crack + Random very fine pattern 25% Penetration	None	39.7
7	7.5% H_2O Restrained w/ SS ring	Air dried 24 hrs.	600°F/hr to 1850°F, 200°F/hr cool	HF - 1850°F CF - 770°F Shell - 720°F ΔT - 1130°F	2	Extensive very fine random cracks apparent penetration 10% or less	.042%	36.3
8	7.5% H_2O+ 4 w/o 1" Ribtec SS fiber, Restrained w/ SS ring	Stored 48 hrs. Sealed	600°F to 1850°F 250°F/hr cool	HF - 1900°F CF - 610°F Shell - 500°F ΔT - 1400°F	1	Few random Surface Cracks	.28%	35.9
9	9% H_2O 10 w/o Pyrophyllite Added, Restrained w/SS ring	Stored 4 Days Sealed	600°F/hr to 1850°F 200°F/hr cool	HF - 1840°F CF - 560°F Shell - 480°F ΔT - 1360°F	2	2 Very fine cracks 40% Penetration	.46%	36.9
10	7.5% H_2O Restrained w/SS ring-water cooled***	Stored 7 days Sealed	600°F/hr to 1850°F 200°F/hr cool	HF - 1840°F CF - 300°F Shell - 170°F ΔT - 1670°F	3	3 Fine to Med. large cracks 40% Penetration	.064%	37.1
11	7.5% H_2O+ 4 w/o 1" Ribtec SS fiber	Stored 48 hrs. Sealed	600°F/hr to 1830°F 250°F/hr cool	HF - 1780°F CF - 660°F ΔT - 1120°F	3	2 Fine cracks + random fine pattern top surface and hot face 88% penetration	.32%	39.8

Legend:

* Denotes that cylinder was made during pour of Lining #5.
** Coating on H.F. made accurate measurements impossible.
*** Water cooled: sample had copper tubing wrapped around restraining ring, water was circulated thru tubing to carry off heat.

TABLE 26. Cylinder Test Results for LITECAST 75-28

Cyl. No.	Composition and Design	Casting History	Firing Schedule	Temperature Profile	Crack Rank	Crack Pattern	I.D. Shrinkage	V Meter
1	21% H_2O Liner 5* Unrestrained	Stored 11 Months Sealed	400°F/hr to 2100°F, fast cool	HF - 2100°F CF - 820°F ΔT - 1280°F	5	2 large - 1 small crack 100% pene-	.34%	43.7
2	21% H_2O Liner 6 Unrestrained	Stored 5 Months Sealed	400°F/hr to 1440°F, 200°F/hr cool	HF-1440°F CF-700°F ΔT-740°F	5	2 large cracks 95% penetration	.26%	40.0
3	21% H_2O Liner 6 attached re-straint*	Stored 5 Months Sealed	400°F/hr to 1520°F, 200°F/hr cool	HF-1520°F CF/shell-700°F ΔT-820°F	3	2 med. cracks 50% penetration	.26%	44.5
4	21% H_2O+4% w/o Ribtec 1-3/8" SS fibers-unre-strained	Stored 2 days sealed ex-posed to air 4 days	400°F/hr to 1500°F, 200°F/hr cool	HF-1500°F CF-300°F ΔT-700°F	2	3 very fine cracks 25% penetration	.25%	47.3
5	21% H_2O cast in SS restraining ring-ring coated w/silicone grease	Stored 2 days Sealed ex-posed to air 4 days	400°F/hr to 1500°F, 200°F/hr cool	HF-1490°F CF-465°F Shell-450°F ΔT-1035°F	4	2 med. large cracks 86% penetration	.096%	52.5
6	21% H_2O Liner 6 Unrestrained-I.D. coated w/RX-14	Stored 18 Weeks Sealed	400°F/hr to 1500°F, 200°F/hr cool	HF-1500°F CF-480°F ΔT-1020°F	5	2 large cracks 95% penetration	--	--
7	21% H_2O Re-strained in SS ring-water cooled	Stored 4 days Sealed 2 days air ex-posure	400°F/hr to 1500°F, 200°F/hr cool	HF-1500°F CF-200°F Shell-200°F ΔT-1300°F	5	5 fine large cracks 50% penetration	.25%	--

Legend: * - Attached restraint: split aluminum ring tightened with stainless steel clamps.

TABLE 27. Cylinder Test Results for KAOLITE 2300 LI

Cyl. No.	Composition and Design	Casting History	Firing Schedule	Temperature Profile	Crack Rank	Crack Pattern	I.D. Shrinkage	V Meter
1	1 v/o 1" SS fibers, 59% H_2O restrained in SS ring	Stored 19 days Sealed	400°F/hr to 1500°F, 200°F/hr cool	HF-1460°F CF-210°F Shell-210°F ΔT-1250°F	2	Very fine random pattern 10% penetration	.042%	--
2	59% H_2O, restrained in SS ring-water cooled	Stored 17 days Sealed	400°F/hr to 1500°F, 200°F/hr cool	HF-1500°F CF-180°F Shell-140°F ΔT-1360°F	4	3 med-med large cracks+ extensive very fine surface cracks 65% penetration	.23%	--
3	1 v/o 1" SS fiber, 59% H_2O, restrained in SS ring. Ring lined w/ 1/4" HES mortar, protected w/4ml plastic	Mortar air dried 24 hrs., Castable stored 48 hrs., sealed 24 hrs. air exposure	400°F/hr to 1500°F, 200°F/hr cool	HF-1500°F CF-220°F Shell-200°F ΔT-1300°F	4	Extensive random fine-med. cracks 30% penetration Large separation between mortar & shell	No change	--

while it took heating rates of 600 to 900°F/hr to crack the two dense materials. Within each material the cracking tendency appeared to be higher for the unrestrained cylinders than for the stainless steel ring restrained cylinders. Water cooling appeared to worsen cracking slightly. Also within each material the higher the test temperature, the greater the tendency to crack.

The casting and storage history did not have a significant effect on the cracking tendency of the materials and the addition of raw kyanite or pyrophyllite which are expanding type minerals, did not reduce cracking. However, the use of 4 w/o 310 SS fibers was found to reduce the cracking tendency of both insulating materials and the KAOCRETE XD 50.

The use of 1/4" of HES mortar between the restraining ring and these same materials had opposite effects on them. It significantly helped the modified 90+% Al_2O_3 dense generic and KAOCRETE XD 50 but detrimentally affected the KAOLITE 2300 LI. The LITECAST 75-28 was not tested with this material. The use of the RX-14 high emissivity coating had no beneficial effects when tested with either the dense or insulating materials.

This series of tests indicated that the KAOCRETE XD 50 (Mix 36C) combined with a layer of HES mortar will give good performance in a cylindrically lined vessel. The effect of adding SS fibers was minimal in these cylinder tests. In addition, some improvement in lining performance was achieved with the use of KAOLITE 2300 LI instead of the LITECAST 75-28 from both the cracking and insulating points of view. Water cooling of the vessel shell was expected to increase the tendency of a lining to crack.

3.3.3. Weight Loss Data For Pore Pressure Analyses

Table 28 lists the weight loss data generated on the solid cylinders of the 90+%Al_2O_3 dense generic (ERDA 90), LITECAST 75-28 and KAOCRETE XD 50 (Mix 36C) at different heat-up rates and/or maximum test temperatures. The weight loss versus time curves generated on these refractories are included in Appendix C.

These data do not show any unusual weight loss characteristics and were found to show the same weight loss trends Z. P. Bazant published[5] on conventional concretes. Since these data were not analyzed with the Bazant 1.D. model, there will be no further discussion of these data.

Table 28: Weight Loss Data on As-Cured 90+% Al_2O_3 Dense Generic (ERDA 90), KAOCRETE XD 50 (Mix 36C) and LITECAST 75-28 Refractory Concretes For Pore Pressure

Material	$\%H_2O$	Diametral Shrinkage %	Bulk Density pcf	Heating Rate °F/hr	Maximum Temperature °F	Weight Loss, % 300°F (200°F)	Weight Loss, % Maximum Temperature
ERDA 90	10	.15	179	125	1000	1.4	8.7
ERDA 90	10	.15	178	110	500	1.3	7.0
ERDA 90	7.5	.10	182	110	500	0.6	5.2
ERDA 90	7.5	.10	181	100	250	(0.0)	3.1
ERDA 90	10	.05	180	100	250	(1.0)	5.0
ERDA 90	10	.14	181	100	500	2.4 (0.5)	7.6
KAOCRETE XD 50	7.5	.05	145	100	250	(0.4)	4.4
KAOCRETE XD 50	7.5	.13	146	100	500	1.6 (0.6)	5.7
LITECAST 75-28	21	.15	96	100	500	5.2 (1.2)	14.9
LITECAST 75-28	21	.08	96	100	250	(1.3)	12.3

3.4. Analytical Predictions

During and after the RESAM and RESGAP model developments, thermal and elastic and inelastic stress analyses were performed on the standard and modified lining designs and on vessels of various shell thicknesses and diameters. These analyses were performed, using the property data summarized in Section 3.2 of this report, to develop information which could guide the program. This information was expected to enhance the understanding of the mechanisms of lining degradation during the initial heat-up, assist in the design of the Pressure Vessel/Test Furnace and test procedures, aid in the evaluation of scale-up effects on lining performance and give direction to improved lining designs. The sections which follow discuss the results of these analyses. They are grouped into analyses that were mainly elastic, others that were thermal and, finally, elastic or inelastic analyses which were run on the lining designs being tested.

3.4.1. Elastic Stress Analyses

Figures 131 through 134 show, respectively, the transient elastic stress analysis done on the standard dual component lining design used for Linings #1 and 2 and the steady state elastic stress analyses done on a twelve inch thick single component lining which had properties that approximated the average properties of the standard dual component lining. These approximated properties were also temperature independent. These latter analyses show the general effect of shell thickness and vessel diameter variations on the stresses induced in the shell and lining and on the effective pressure exerted by the lining on the shell. These results essentially summarize the limited parameter study done with the model in some key areas of interest.

Design of Pressure Vessel/Test Furnace Facility

The change in the shell thickness of this facility after stress analyses were done on the lined vessel configuration to be used initially in this work are discussed in Section 2.6.1. These analyses are shown in Figure 131 and 132 and indicated that at steady state conditions, tensile circumference (hoop) stresses up to 3500 psi would be induced in a half inch thick shell by a twelve inch thick monolithic refractory lining heated to a 2000°F hot face temperature. This stress was believed to be great enough to yield the vessel shell. By increasing this shell thickness to one inch, the analysis indicated that the stresses would be reduced by about half. Further reductions were also possible by increasing the thickness from one inch to three inches but they were not as significant as those obtained with the initial increase. When these stresses were converted to the effective pressure that the lining would exert on the vessel shell as shown in Figure 134, the results indicated that significant pressure would be induced in the shell. This pressure was in the fifty to sixty psi range for a five foot diameter vessel with a shell thickness in the one half to one inch range. This pressure is generally not accounted for in stress analyses on refractory lined pressure vessels to determine the code stamp. These results indicate this effect should be more seriously considered.

Although these analyses were conservative because they did not include the effects of shrinkage and creep which were expected to reduce the shell stresses, a decision was made to increase the shell thickness from the five eighths inch thickness originally planned to approximately one inch.

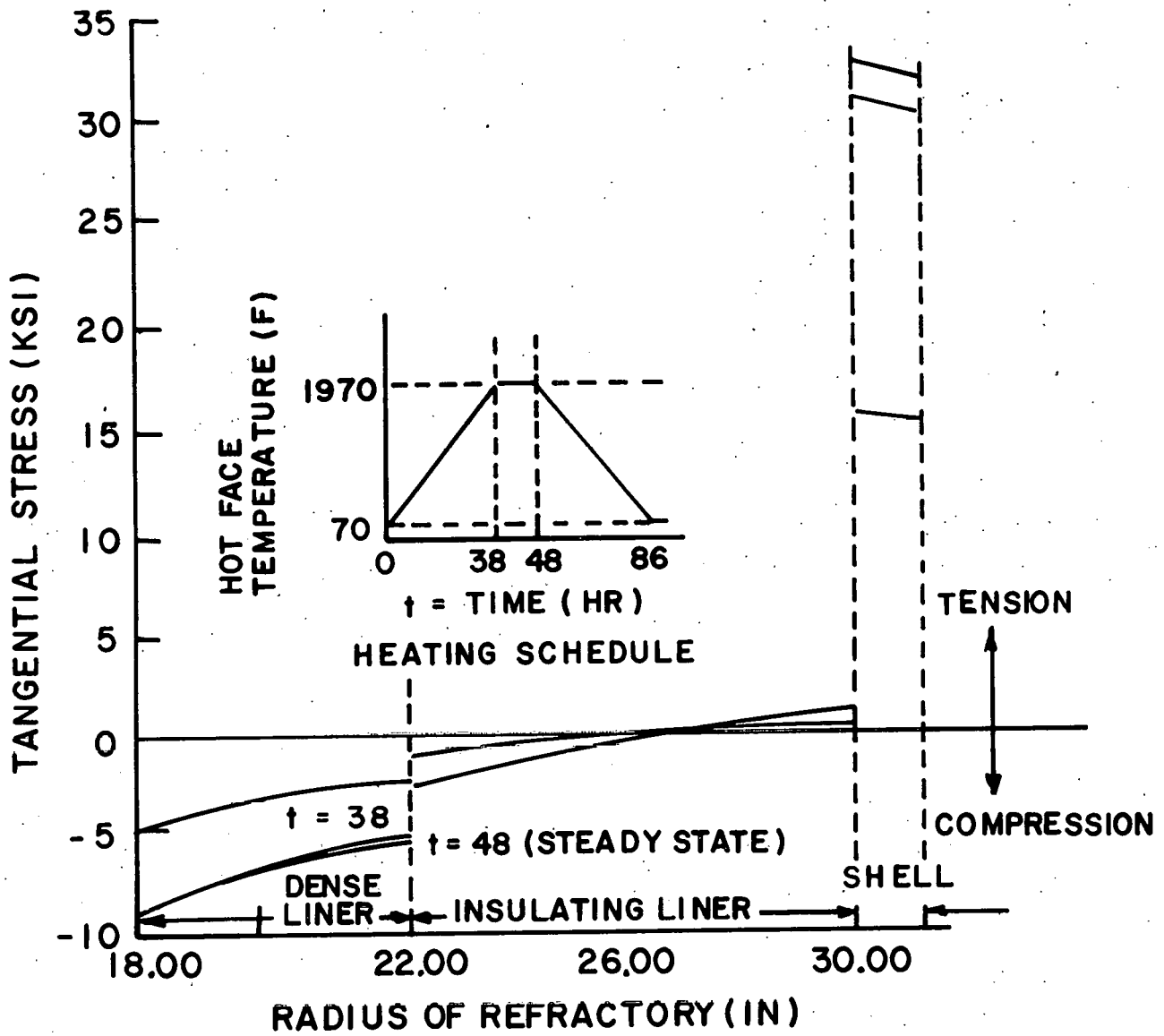

FIGURE 131. Elastic Hoop Stress Distribution Prediction Done on the Standard Lining Design (Linings #1 and 2) and Shell at Various Times During the Heat-Up Schedule.

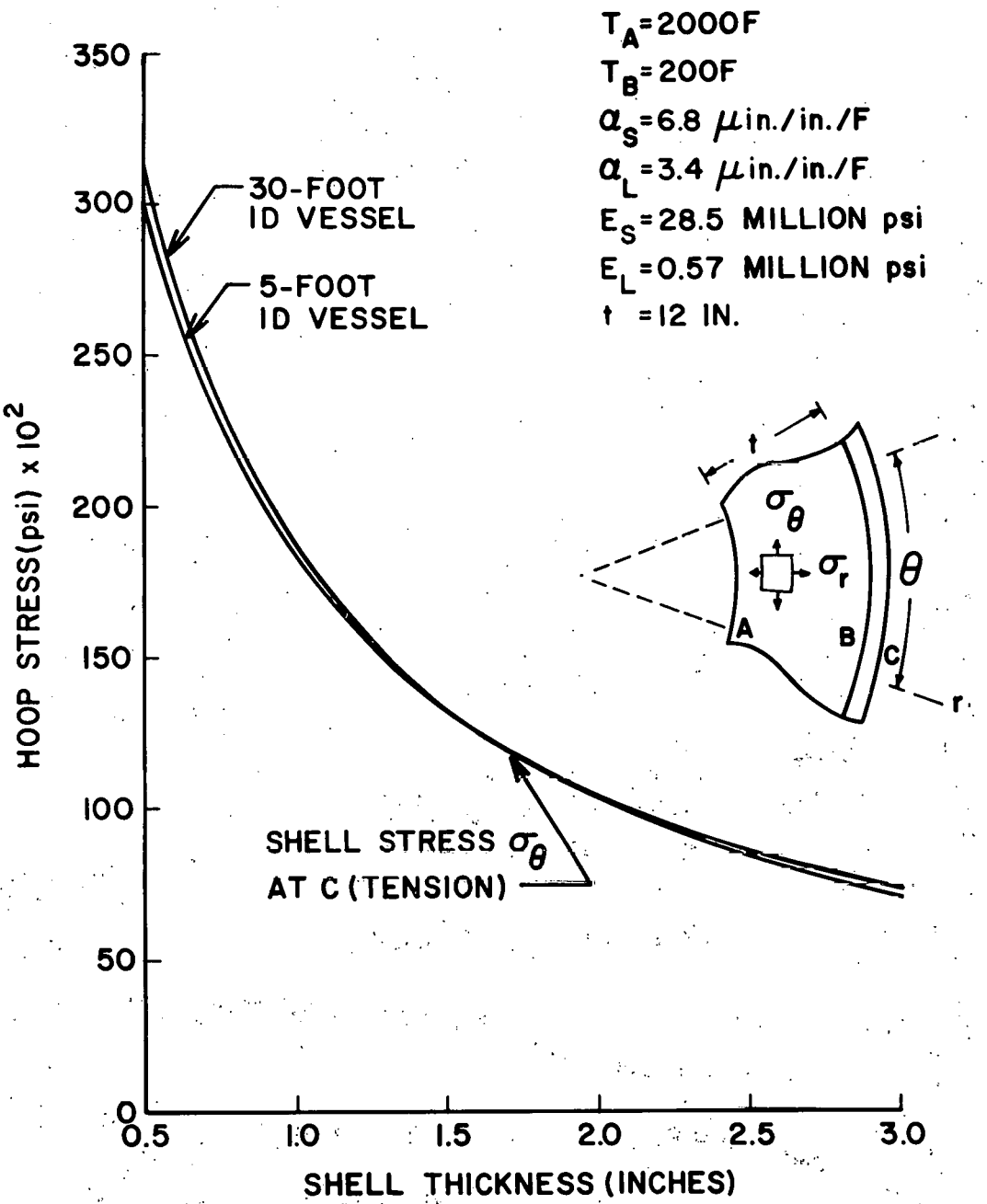

FIGURE 132. Prediction of Shell Hoop Stresses for a Monolithic Refractory Lined Vessel of Varying Shell Thickness and Diameter (Elastic Analysis).

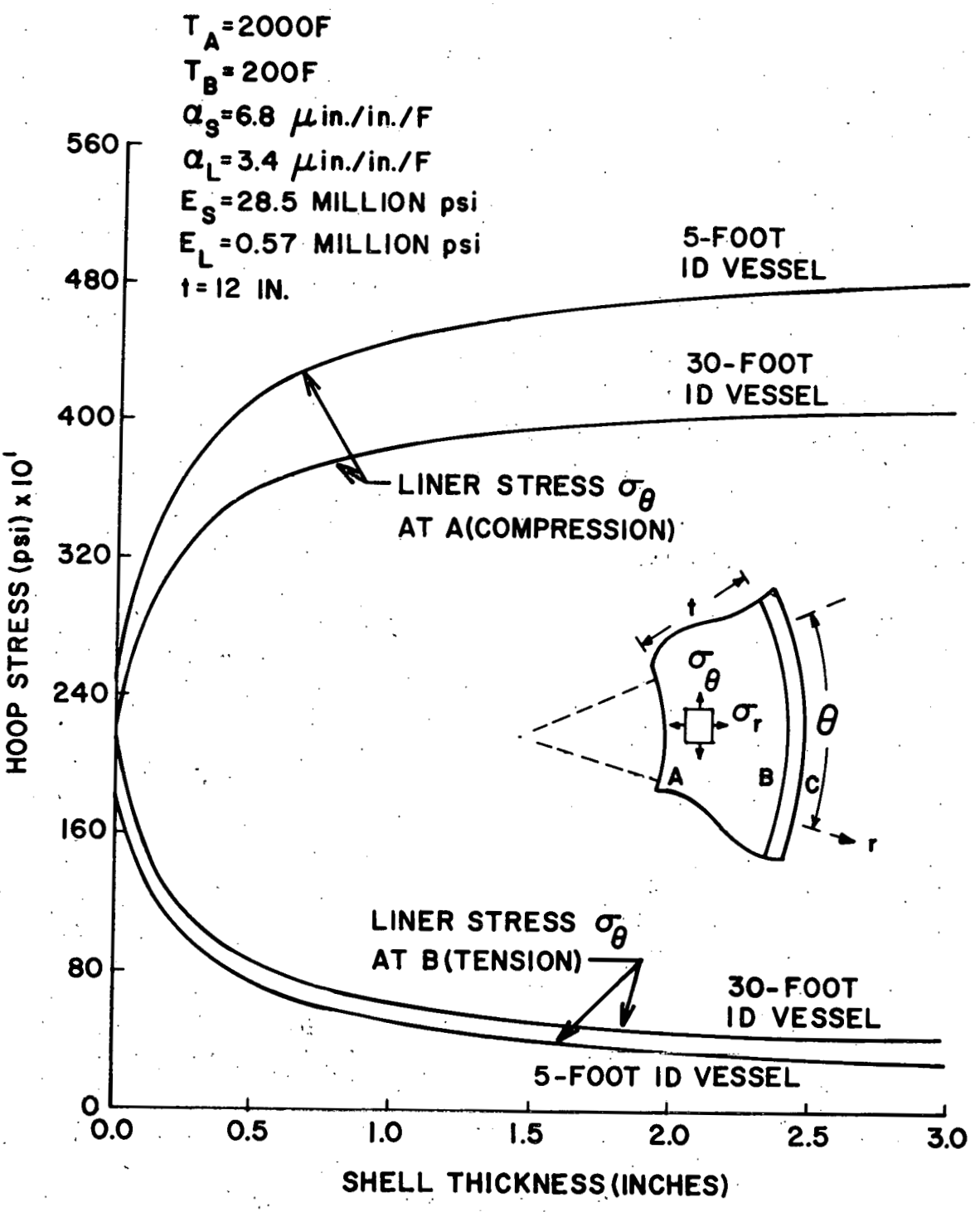

FIGURE 133. Prediction of Hoop Stresses at the Inside (Hot Face) and Outside (Cold Face) Surfaces of a Twelve Inch Thick Monolithic Refractory Lining Versus Shell Thickness and Diameter. (Elastic Analysis)

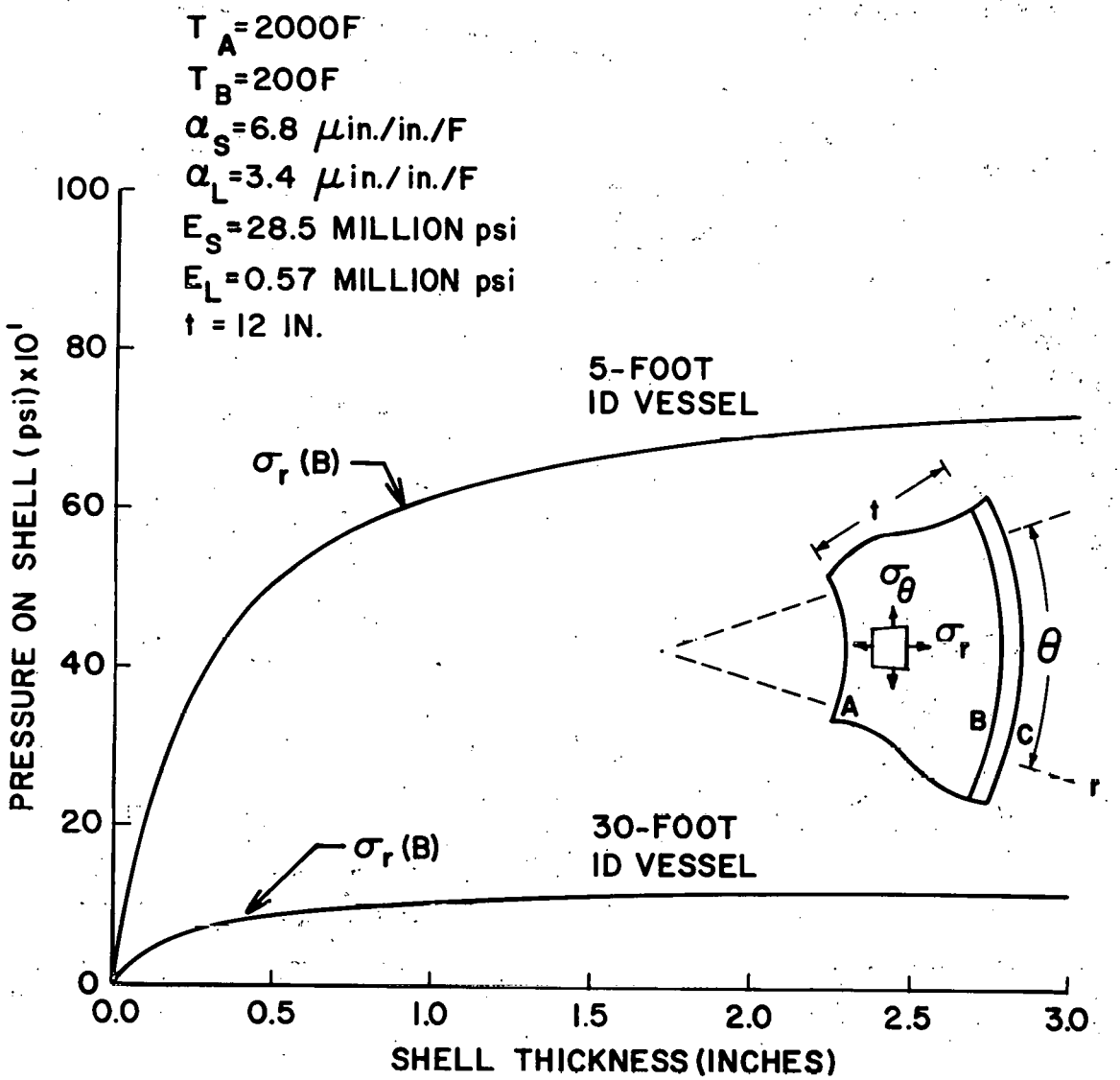

FIGURE 134. Prediction of Pressure Exerted by a Twelve Inch Monolithic Lining on a Vessel of Varying Shell Thickness and Diameters.

The test vessel was constructed by the Chattanooga Boiler and Tank Co.

Lining Stresses

As can be seen in Figure 131, when the elastic properties listed for the 90+% Al_2O_3 dense generic and the LITECAST 75-28 in Tables 15 and 23, respectively, were used in the analysis, a compressive stress is induced in the dense component of the circular lining as it expands outward during heating to approximately 2000°F at a rate of 100°F/hr and makes contact with the insulating component. This stress decreases through the four and a half inch thickness of the dense component to about half the hot face level. At 2000°F, the hot face stress is approxiamtely 10,000 psi which is equivalent to or greater than the compressive strength of the 90+% Al_2O_3 dense refractory concrete material used in this component. This result indicates that if the lining acted purely elastically, the dense component of the standard lining could crush during the heat-up of the lining.

On the other hand, the seven and a half inch insulating component is partially in compression near the interface region of the lining and partially in tension near the shell during the heat-up. The stresses induced become progressively more compressive and tensile in each region as the heat-up progresses through the ten hour hold at 2000°F. Since the compressive and tensile stresses are in the 3000 psi and 2000 psi range respectively, these results indicate that if the lining acted purely elastically, this component would tensile crack from the shell (cold face) side of the lining and might crush on the interface side during the heat-up of the lining to 2000°F.

Because the stress analysis is elastic, the stresses indicated in the lining decrease during the cool-down and finally return to the zero stress state at 70°F. Although this is not what is expected in an actual lining, the analysis is helpful in understanding the stress state that can occur in a dual component lining and the shell in a monolithic refractory lined process vessel.

Creep Test Stress Levels

From the above discussed elastic stress analysis of the dual component standard lining design, it became apparent that considerably higher stress levels than the one hundred to two hundred psi levels normally used in standard refractory creep tests would be required to perform significant stress analyses with the model. It also became apparent, however, that steady state conditions could be achieved rather quickly during the initial heat-up test. Based on these points, it appeared that the dense component type material should be creep tested at compressive stress levels up to about 5000 psi and for periods of up to ten hours. It also appeared that the insulating component should be creep tested at compressive stress levels up to about 2000 psi for a similar period; and possibly tensile creep tested to 1000 psi as well.

Scale-Up Effects

Since one objective of the program was to develop a model that could predict scale-up effects, some scale-up steady state elastic stress analyses were done. The general findings of these analyses for a twelve inch single component

lining with average properties which approximate those of a dual component lining are shown in Figures 132-134. The shell stress analysis indicates that the shell stresses are unaffected by vessel diameter in the five foot to thirty foot diameter range for a constant lining thickness but are affected significantly by shell thickness. The shell pressure analysis indicates that the effective pressure exerted on the shell significantly decreases as the vessel diameter is increased from five to thirty feet. This point indicates that present pressure vessel codes are more reliable for larger diameter vessels than small ones. The lining stress analysis indicates that little change in the tensile stress state occurs for the cold face region of the lining as the vessel is scaled-up from five to thirty feet. This was not true for the hot face region. This region showed a significant reduction in compressive stress as the vessel diameter size increased from five to thirty feet. This is considered to be beneficial to lining performance since it would reduce the potential of the lining to crush or creep.

3.4.2. Thermal Analyses of Lining Designs

Figures 135 through 137 are thermal analyses run with the uncoupled heat transfer routine of the REFSAM and RESGAP. Figure 135 is for the standard lining design which was used in Linings #1 and 2 and the other is one of the modified designs used in Lining #9. From these analyses it was learned that the dense 90+% Al_2O_3 (ERDA 90) material will have a smaller thermal gradient across it and will generally operate at higher temperature than the 50% Al_2O_3 dense material (KAOCRETE XD 50 with 4 w/o 310 Stainless Steel fibers) used at the same hot face temperature. This will make the 90+% Al_2O_3 dense materials expand more and insulate less than the 50% Al_2O_3 material and result in higher lining stresses and interface temperatures.

Since the insulating component materials have lower thermal conductivities than the dense component (k = 1.5 to 3.0 vs 7.5 to 13 BTU in/hr $Ft^2°F$), the large gradient predicted across this component compared to that of the dense component is not surprising. The results clearly show the importance of this component in insulating the shell, and indicate that the insulating component could probably be one to two inches thinner and still give adequate thermal protection to the shell.

Figure 137 compares the predicted versus the actual experimental thermal profile results on Lining #2 during the heat-up to 1200°F. The results show the overall excellent agreement of these profiles with one another except for a region in the insulating component (from the center to the shell). The delayed removal of the moisture which occurs in this component during the heat-up test at 100°F/hr is not accounted for by the thermal model included in REFSAM and RESGAP. This model does give a good overall analysis of the thermal condition of the lining, however, and is expected to be adequate for most monolithic linings. It should work very well for linings which no longer have water associated with them. The Z.P. Bazant [5] 1D thermal and mass transfer model is the type model needed to include this delayed moisture removal effect and to permit the most accurate stress analysis to be made on monolithic refractory linings.

Two additional points were learned from these analyses; the linings being studied reached steady state conditions in forty hours or less and at heating rates below 200°F/hr, transient effects were relatively small (15%) compared to steady state conditions.

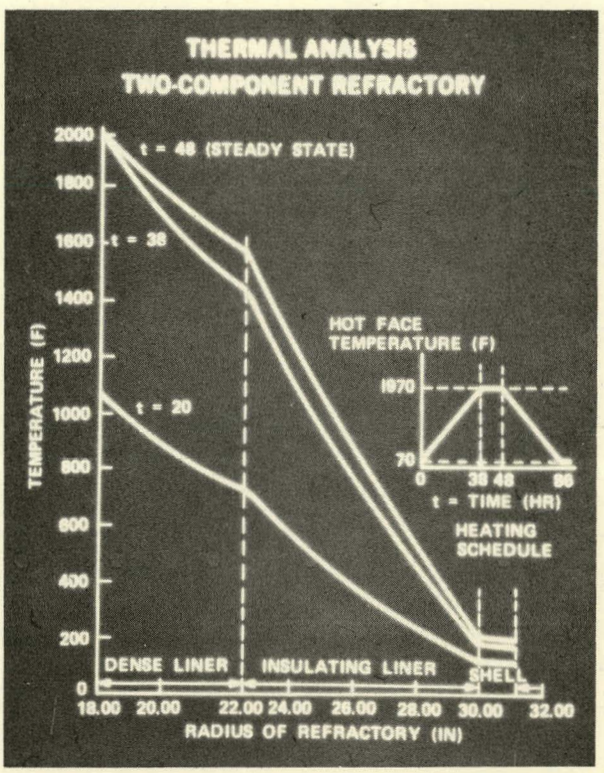

FIGURE 135. Thermal Distribution Predicted for the Standard Lining Design (Linings #1 and 2) During a 100°F/hr Heat-Up to 2000°F.

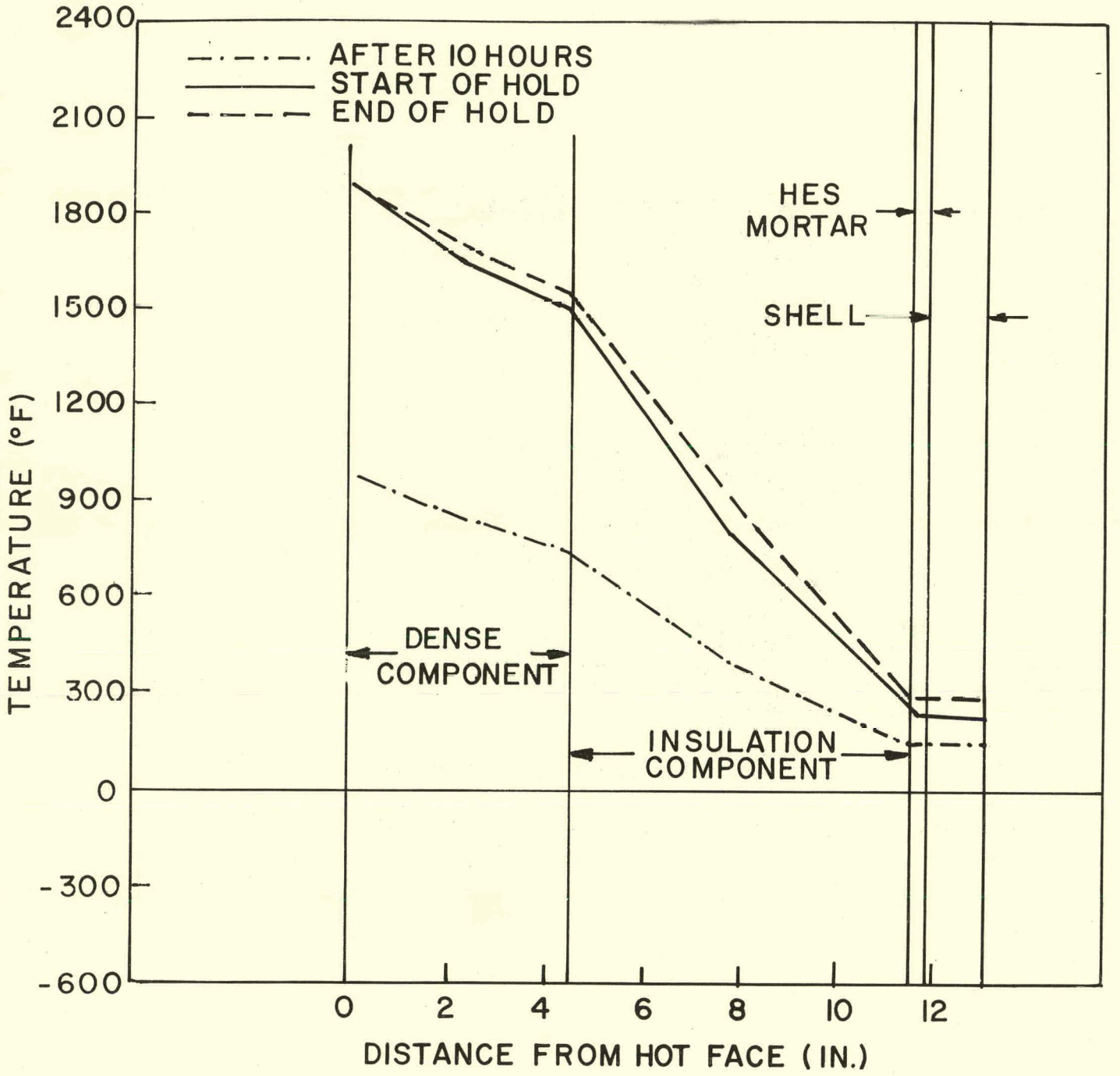

FIGURE 136. Thermal Distribution Predicted for Lining #9 During the 200°F/hr Heat-Up to 2000°F.

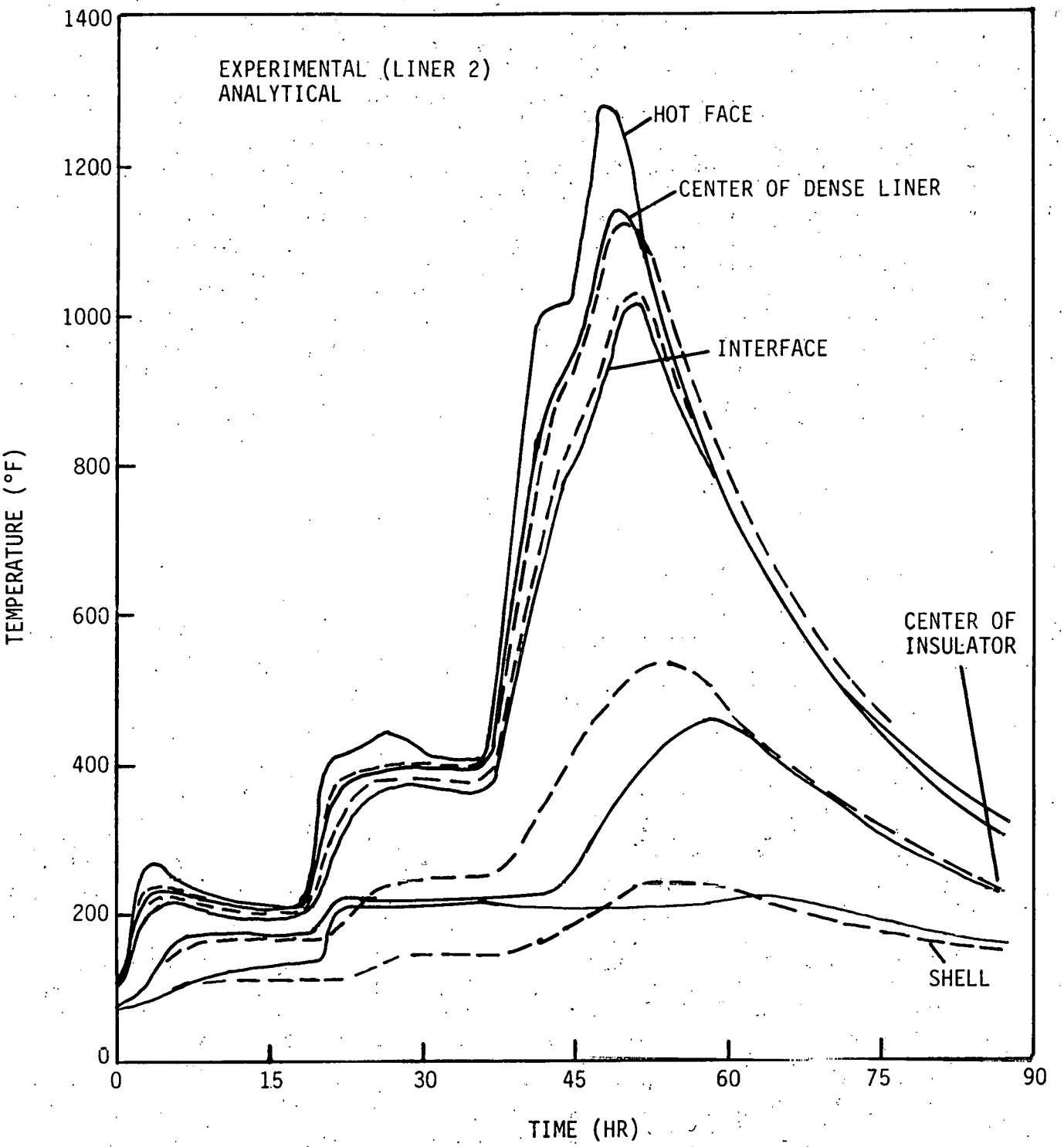

FIGURE 137. Temperature History Within the Standard Lining Design and at the Shell (Predicted vs Actual).

3.4.3. Lining Analyses

When the effect of shrinkage and creep were incorporated in the elastic analyses run on the standard lining design used for Linings #1 and 2, it was indicated that these two linings would crack. It was also indicated that these two properties were the principal factors affecting cracking. In a typical monolithic refractory lining geometry this cracking would be expected to occur at the inside surface during cooldown. Transient thermal stresses (or thermal shock) should not be significant at normal heating and cooling rates (on the order of 100°F per hour). Stresses develop due to constraints caused by bonding to the shell and to the anchors which prevent free contraction of the liner upon cooldown. The anchors are not modeled in the present program, but their effect is simulated by the continuity of displacements which prevents gaps from occurring between the liner and shell and between the insulator and dense liner upon cooldown. The hoop and axial stresses in the liner are nearly equal. There is a slight preference for radial cracks along the axis of the refractory due to a slightly greater hoop stress, but circumferential cracks due to axial stress would also be expected. The effect of creep is to cause negative inelastic strains to occur throughout the dense liner and partially into the insulator, which are indistinguishable from shrinkage strains. Both creep and shrinakge strains cause a tensile stress state upon cooldown.

Some of these effects are shown in Figure 138, which is a plot of the hot face hoop stress for the geometry described previously with a heatup rate of approximately 100°F per hour to 2000°F, followed by a 40-hour hold at temperature, and subsequent cooldown. Two analyses are shown in Figure 138. The first neglects creep effects and indicates high compressive stresses during heatup like those seen in the elastic analysis which level off during the hold period, and eventually go tensile near the end of the cooldown due to the shrinkage which has occurred during the heating cycle. The step in the curves, early in the temperature ramp, is due to the reversal which occurs in the thermal expansion curves during heatup.

This particular run did not include cracking effects, but the time of cracking can be predicted by noting that the tensile strength of the dense liner ERDA 90 is about 1200 psi (indicated by dashed line) at 1000°F, as estimated from modulus of rupture tests. Although the depth of cracking was not predicted in this analysis, it is expected that the cracking would have proceeded through the entire liner in this case, since the tensile stresses exceed the tensile strength by a large margin. The second analysis shown in Figure 138 includes creep effects. The effect of creep is seen to be very strong as soon as the hot face temperature reaches about 1700°F. The effect is a relaxation of the compressive stresses to a value which levels off at about 1000 psi toward the end of the hold period. Upon cooling the stresses become tensile and reach a higher level due to creep. The difference between the final stress values at t = 100 hours is much smaller than the compressive stress difference earlier in the test. This result is misleading, however; actually, there should be a much larger difference. The reason for this is that when this analysis was made, the creep phenomenon was modeled by a series of Kelvin elements which predicted complete creep recovery upon removal of the stress. Hence, upon cooldown the previously accumulated creep strains are disappearing. A more realistic procedure is to allow only a partial recovery of the creep strains (a value of one-third is more typical of experimental results in uniaxial compression tests).

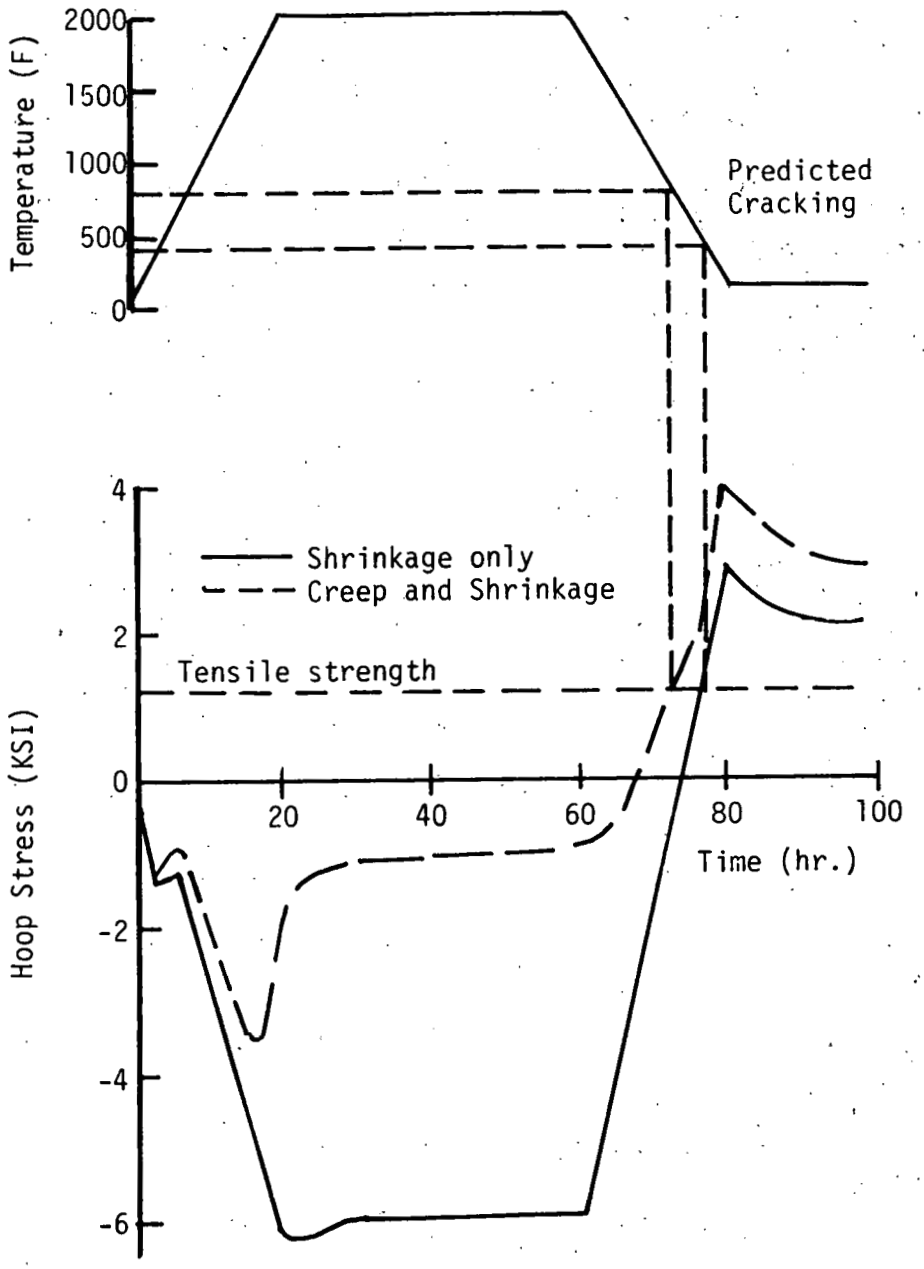

FIGURE 138. Hoop Stress Predictions at the Inside Surface of the Standard Lining Design (Linings #1 and 2) Versus Time When Heated at 100°F/hr.

This change had the effect of increasing the tensile stress at the hot face upon cooldown in the creep run. Thus, the mechanisms of creep and shrinkage both appear to be significant, and either is capable of generating hot face stresses in excess of the available tensile strength properties.

The stress distribution through the refractory and shell is shown in Figure 139 for the corresponding analyses at two particular time values: T = 20 hours, corresponding to the end of the heating ramp; and at the end of the test, T = 100 hours. The effect of creep is to reduce the hot face compressive stresses substantially and to move the location of the maximum compressive stress toward the center of the dense liner. In addition, creep is beneficial in that it significantly reduces the tensile stresses in the shell. On the other hand, at T = 100 hours the residual tensile stresses in the dense liner exceed the tensile strength by a substantial amount due to shrinkage alone; and this effect is aggravated by creep. Since this analysis did not compensate for creep recovery effects, the final tensile stress in the dense liner should be greater for the creep run. This analysis also predicts a large residual compressive stress in the shell after the heat-up test. However, since cracking is predicted to occur but the effect was not included in this analysis, these residual stresses are expected to be significantly lower. Since the modeling of shrinkage in REFSAM is a simple linear extrapolation rather than a time dependent effect, the exact time at which cracking occurs is uncertain, although the eventual occurrence of cracking is not. For example, cracking due to shrinkage might occur very early in a test run if the heat-up schedule were too slow or included holds at a relatively low temperature. This is because during the heat-up, the reversible thermal expansion counteracts the shrinkage so that only a small dimensional change actually occurs. The ultimate controlling factor in determining whether cracking will occur, however, is the extent and distribution of inelastic strain which occurs and the degree of mechanical constraint on the liner preventing the accommodation of these strains upon cooldown. Thermal stresses are important in that they determine the amount of creep which will occur, but should not themselves cause cracking in a constrained (anchored) liner. In a less constrained liner, thermal stresses might be expected to cause cracking in the insulator during heatup.

The creep predictions discussed above are based on relatively short time creep tests and were intended to be reliable for initial heatup and cooldown. The above results suggest that long term creep effects would be significant at even lower stress levels.

From these initial analyses done with REFSAM, it became apparent that cracking in monolithic refractory linings could be reduced or eliminated in two different ways as follows:

1. Material Modifications:
   a. By reducing shrinkage through modified materials or curing procedures.
   b. By improving creep properties or by alternately operating at lower temperatures where the creep rate is much less severe (1750°F or less in dense liner, 1250°F or less in insulator).
   c. Improving tensile strength characteristics by composition changes, or mechanical or fibrous reinforcement.

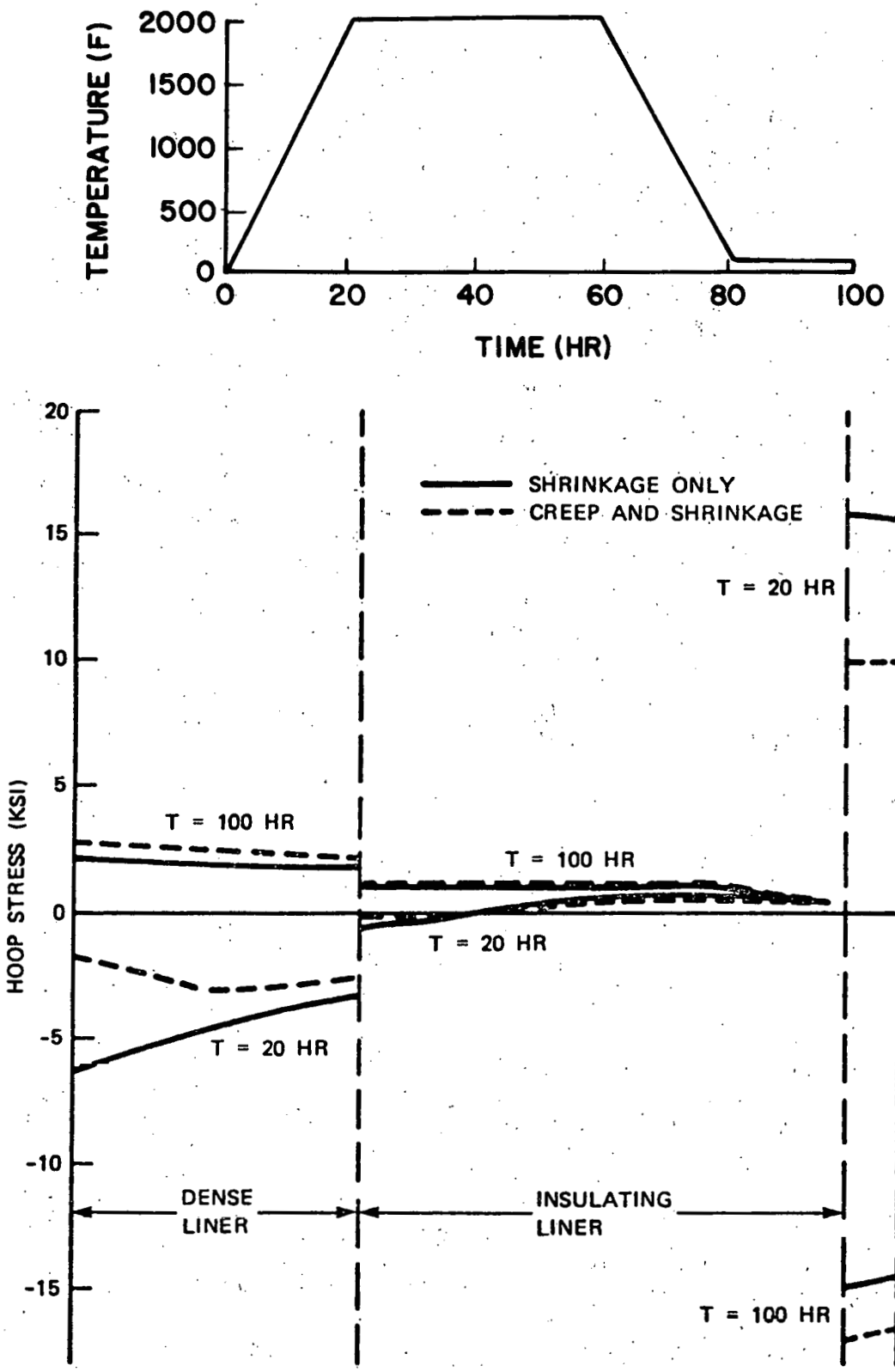

FIGURE 139. Hoop Stress Distribution Prediction Through the Standard Lining Design and Shell at the End of the Heating Ramp (T = 20 hrs) and the Residual Stresses After Cooldown (T = 100 hrs).

d. By improving the fracture toughness of the materials.

2. Design Modifications:

   a. Eliminate constraints on liner so that shrinkage can occur as freely as possible (alternate anchoring schemes).

   b. Reduce compressive stresses on the liner by an expansion allowance to reduce the interference with the shell. (There is a tradeoff here, because reduced compression at the hot face will result in increased tension and possible cracking in the insulator).

These approaches became the basis for much of the experimental material property work and lining test work done on the rest of the program. They emphasized the need to keep shrinkage and creep to a minimum by the use of as little water as possible in the refractory concretes; and the use of materials with low cement levels and optimized grain sizing. They also emphasized the need to look at materials with fiber additions to increase strength and/or fracture toughness. Finally, they stressed the need to study lining designs which reduced the constraining effects of anchors and the bonding of the components to one another and to the shell and which reduced the interaction of the shell with the lining during the test. Any or all of these changes were expected to reduce the cracking of the monolithic refractory linings for use to 2000°F.

During the latter part of the program, a number of these effects were analyzed with the RESGAP program for comparison with the lining test results. This analysis was done on the Lining #9 type configuration which included four mil gaps between the two refractory components and a third layer (HES mortar) attached to the shell. The results are illustrated in Figures 140 through 144 for elastic stress analyses. Figures 140 through 143 show the temperature histories for each component of the lining and the shell obtained with a 200°F/hr heat-up to 2000°F and the accompanying hoop stresses. Figure 144 shows the hoop stress distribution through the Lining #9 cross section at various times during the heat-up test when LITECAST 75-28 was used as the insulating component material. Appendix D lists the computer printout of Lining #9 with KAOLITE 2300 LI as the insulating component material.

The results indicate that the dense component material (KAOCRETE XD 50 with 4 w/o 310 Stainless Steel fibers) will not crack during the heat-up test to 2000°F at 200°F/hr; however, the insulating component materials (LITECAST 75-28 or KAOLITE 2300 LI) and the HES mortar will. The compressive stresses generated in the dense component and the stresses induced in the shell are predicted to be less than those for the standard lining design (Linings #1 and 2) and are believed to be low enough to keep the effect of creep to a minimum. Actually the shell stresses are predicted to be compressive during this heat-up test but are suspect because of the high tensile stresses predicted for the HES mortar. The use of KAOLITE 2300 LI instead of LITECAST 75-28 further lowers the stresses generated in the dense component and the shell and, therefore, its use should improve the performance of both the KAOCRETE XD 50 with or without 4 w/o 310 Stainless Steel fibers and the 90+% Al_2O_3 dense generic refractory concrete in a dual or multicomponent lining. The tensile strengths of the insulating component materials are too low, however, to resist the tensile stresses induced in this component during the heat-up tests.

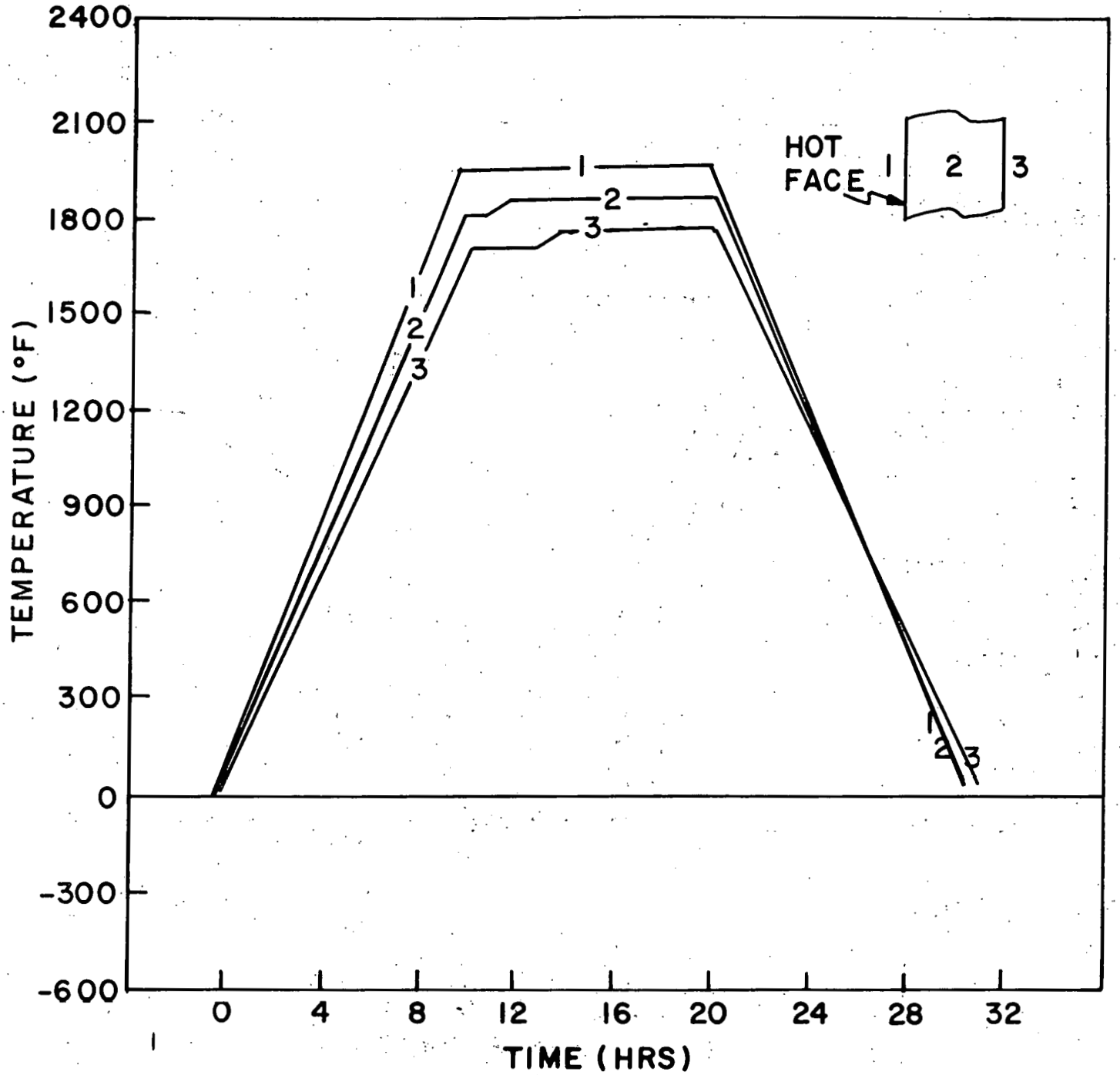

FIGURE 140. Temperature and Hoop Stress Predictions of the Dense Component of Lining #9 During 200°F/hr. Heat-up to 2000°F.

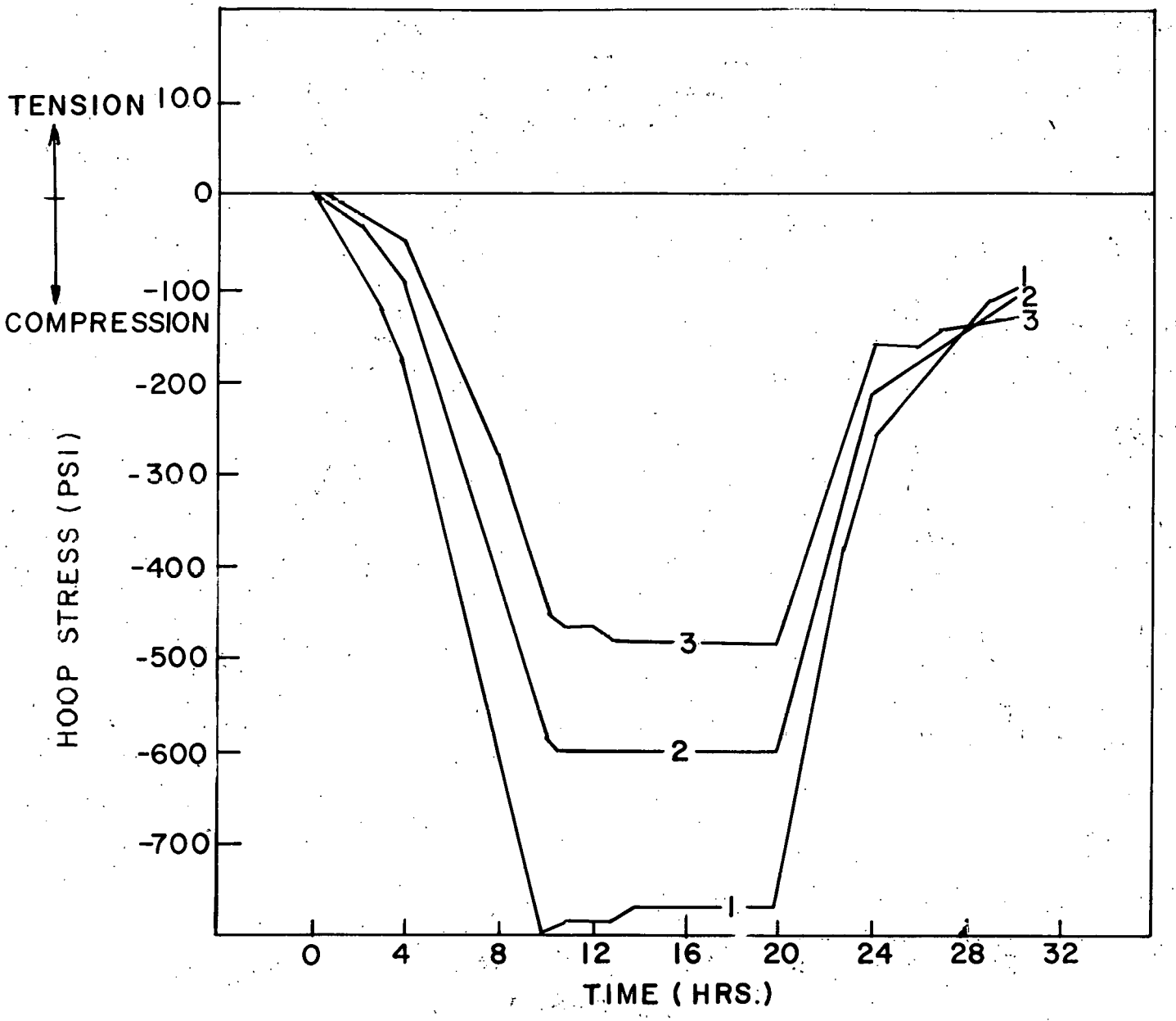

FIGURE 140 (CONT'D).

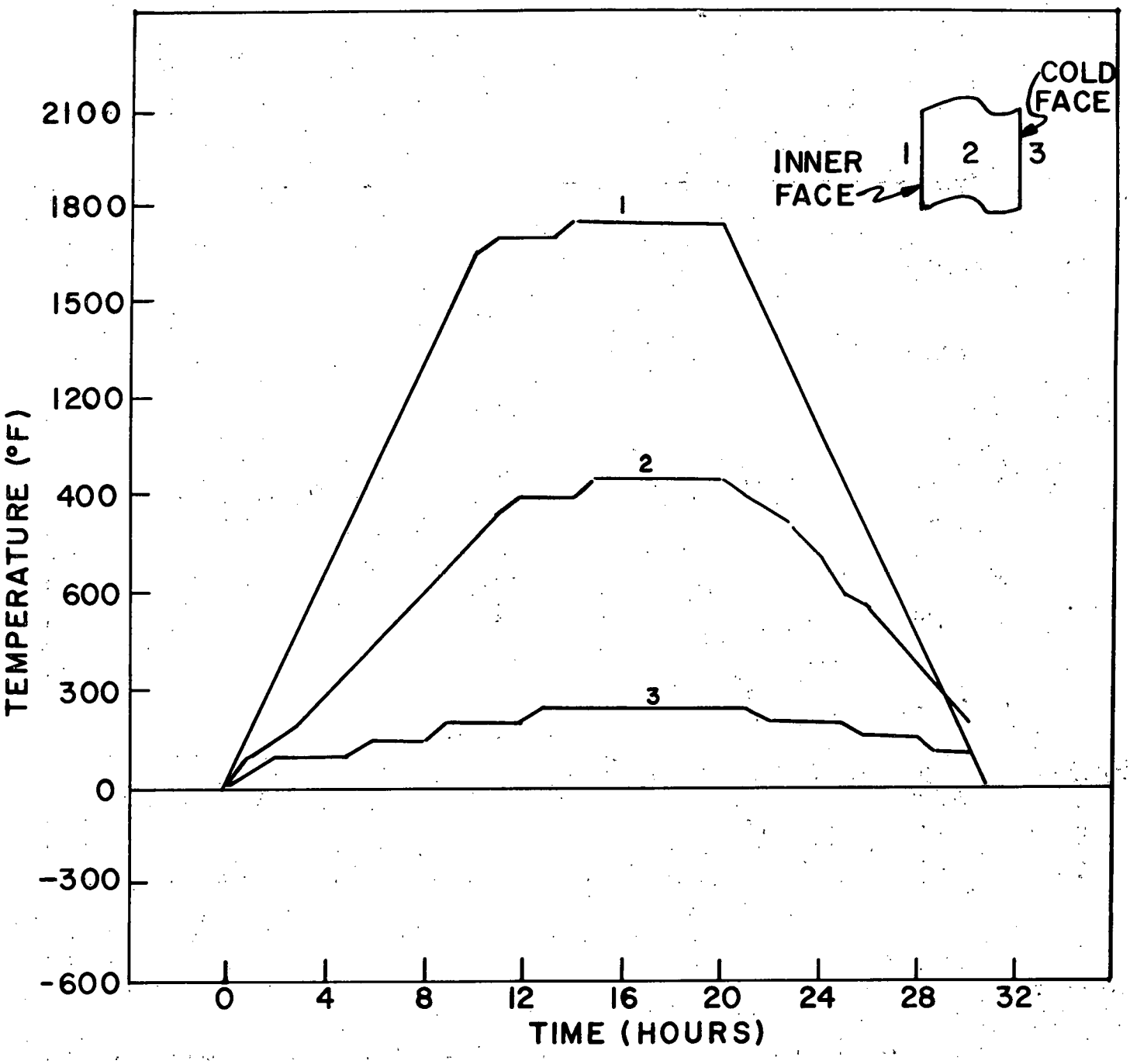

FIGURE 141. Temperature and Hoop Stress Predictions of the Insulating Component of Lining #9 During 200°F/hr. Heat-up to 2000°F.

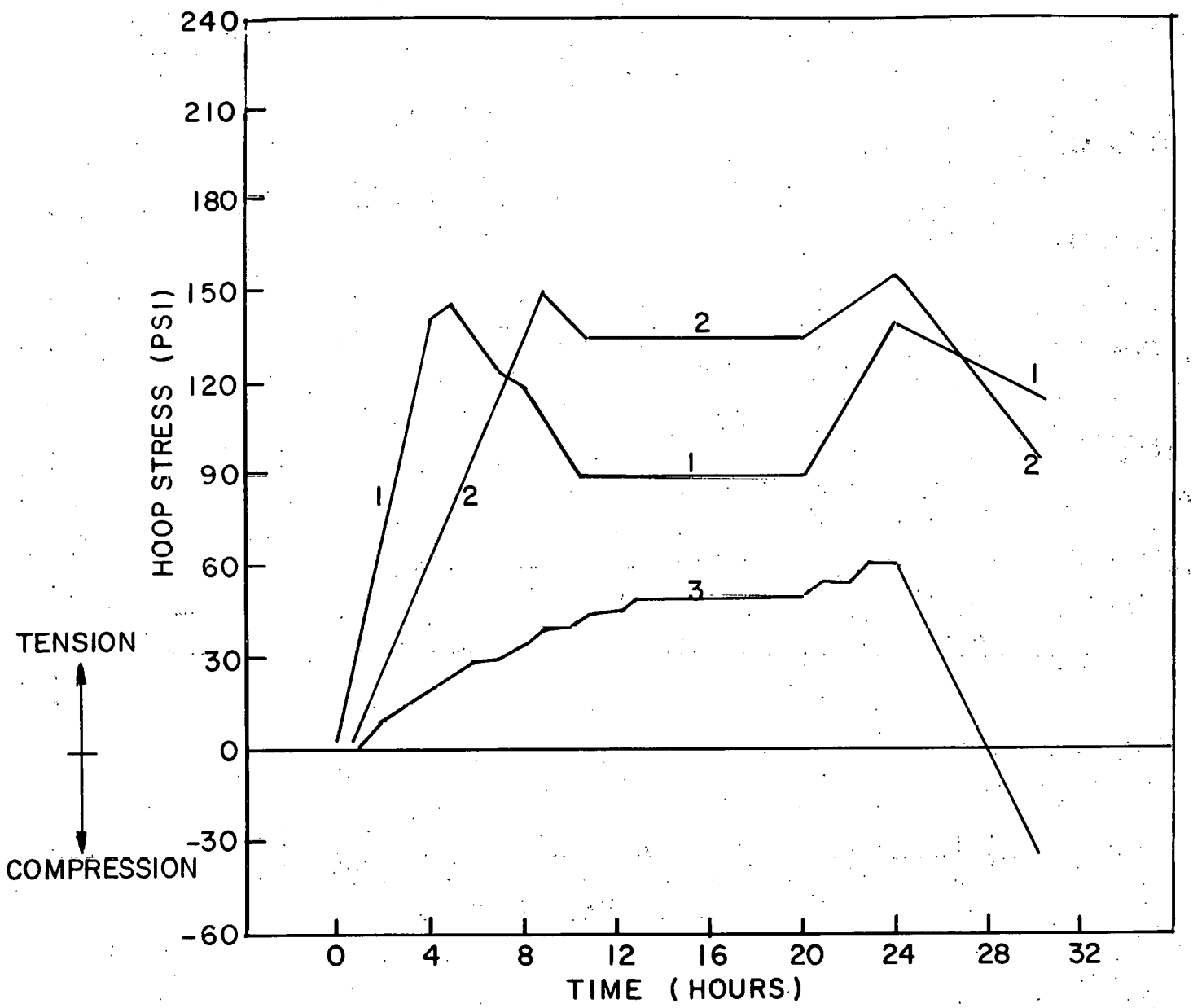

FIGURE 141 (CONT'D).

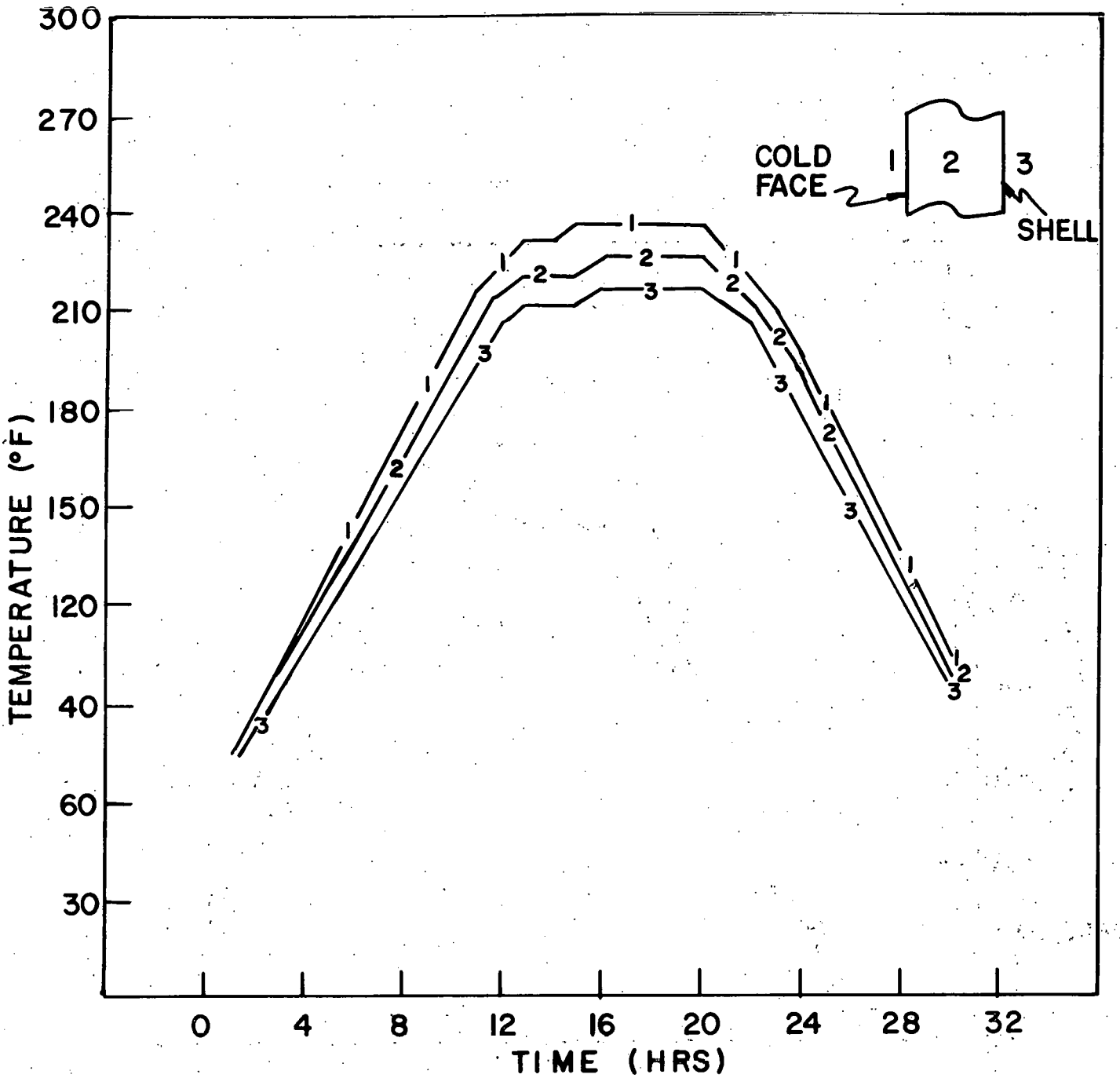

FIGURE 142. Temperature and Hoop Stress Predictions of the HES Mortar of Lining #9 During 200°F/hr. Heat-up to 2000°F.

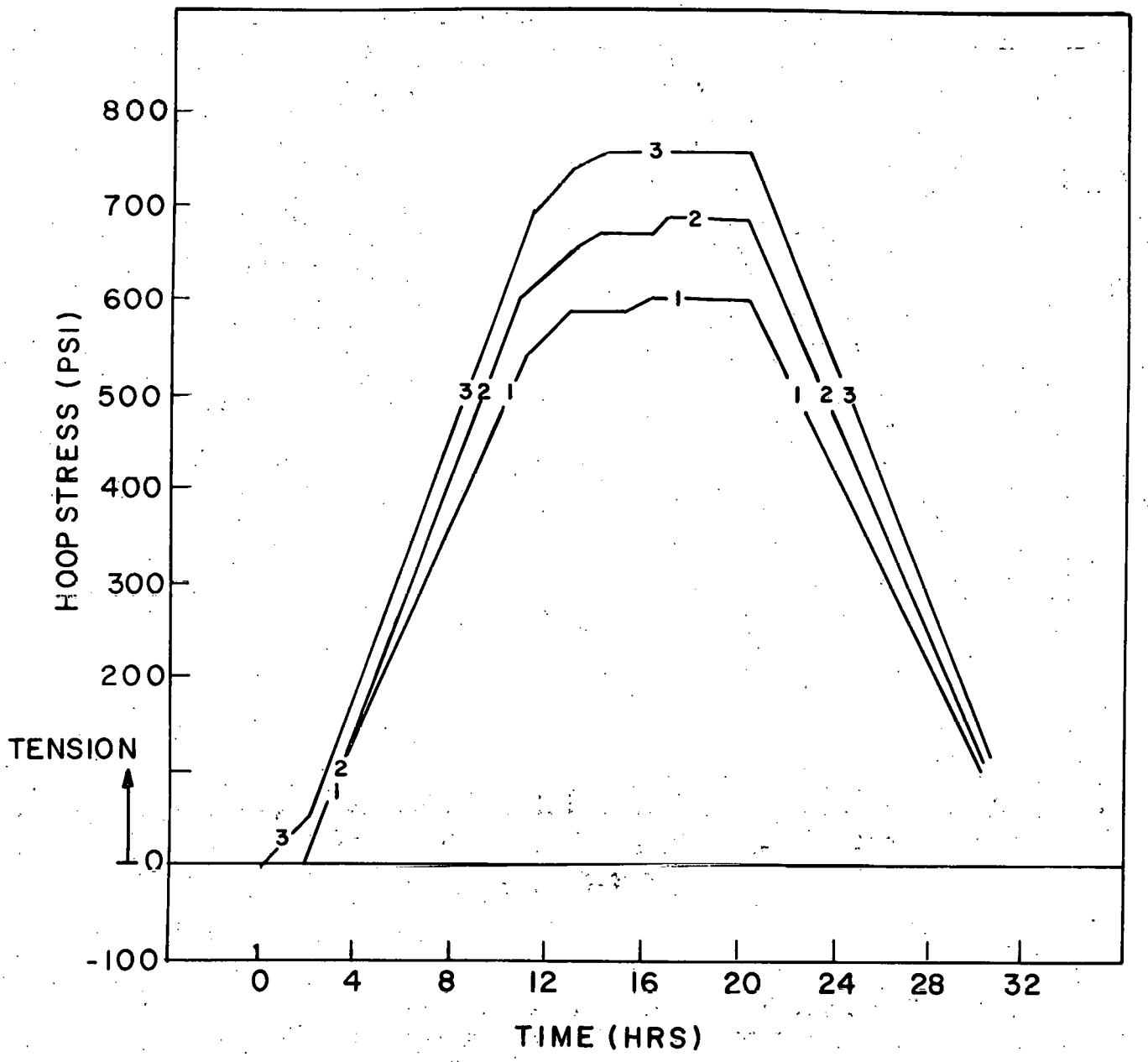

FIGURE 142 (CONT'D).

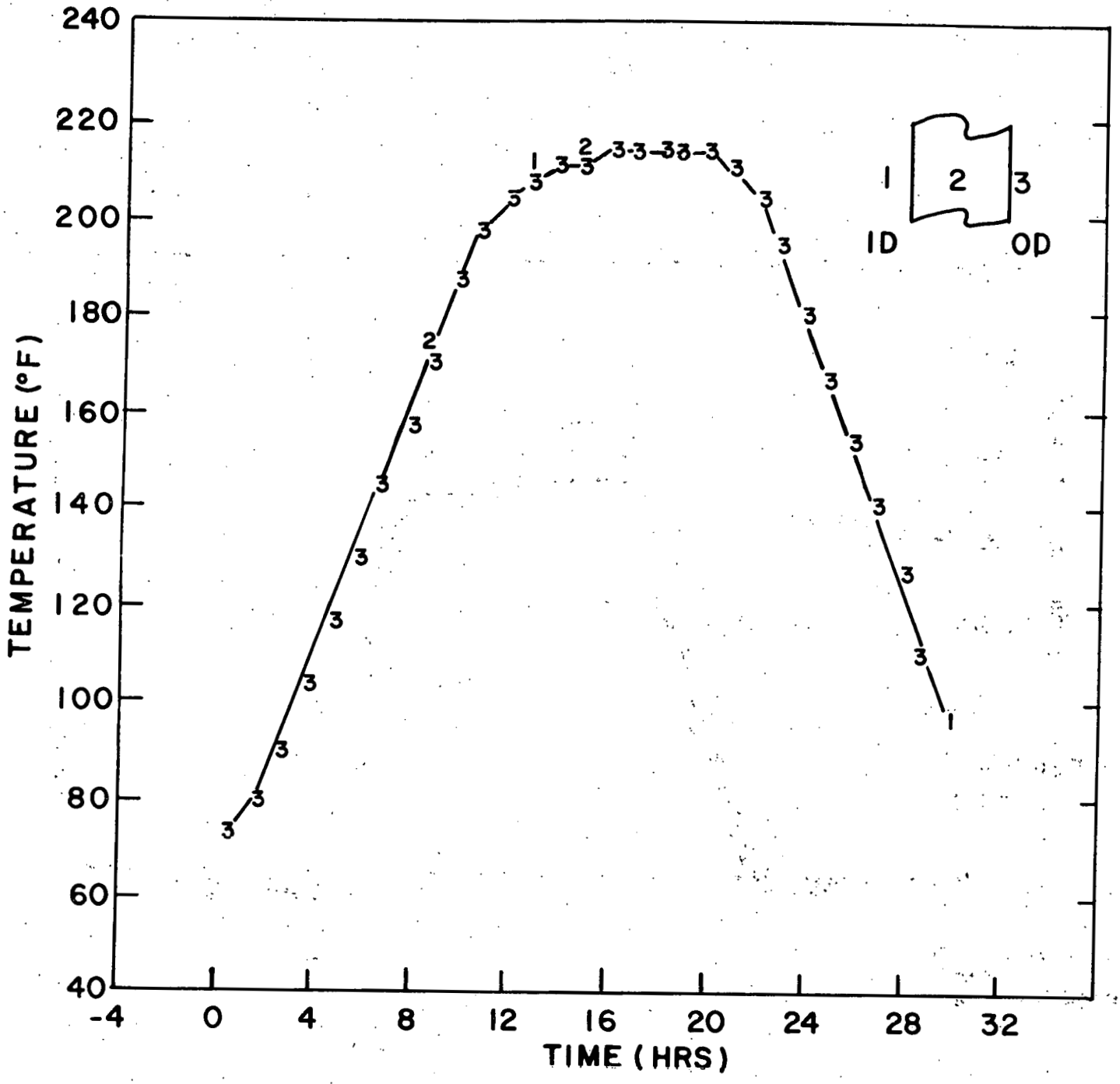

FIGURE 143. Temperature and Hoop Stress Predictions of the 9/8 Inch Carbon Steel Shell of Lining #9 During 200°F/hr. Heat-up to 2000°F.

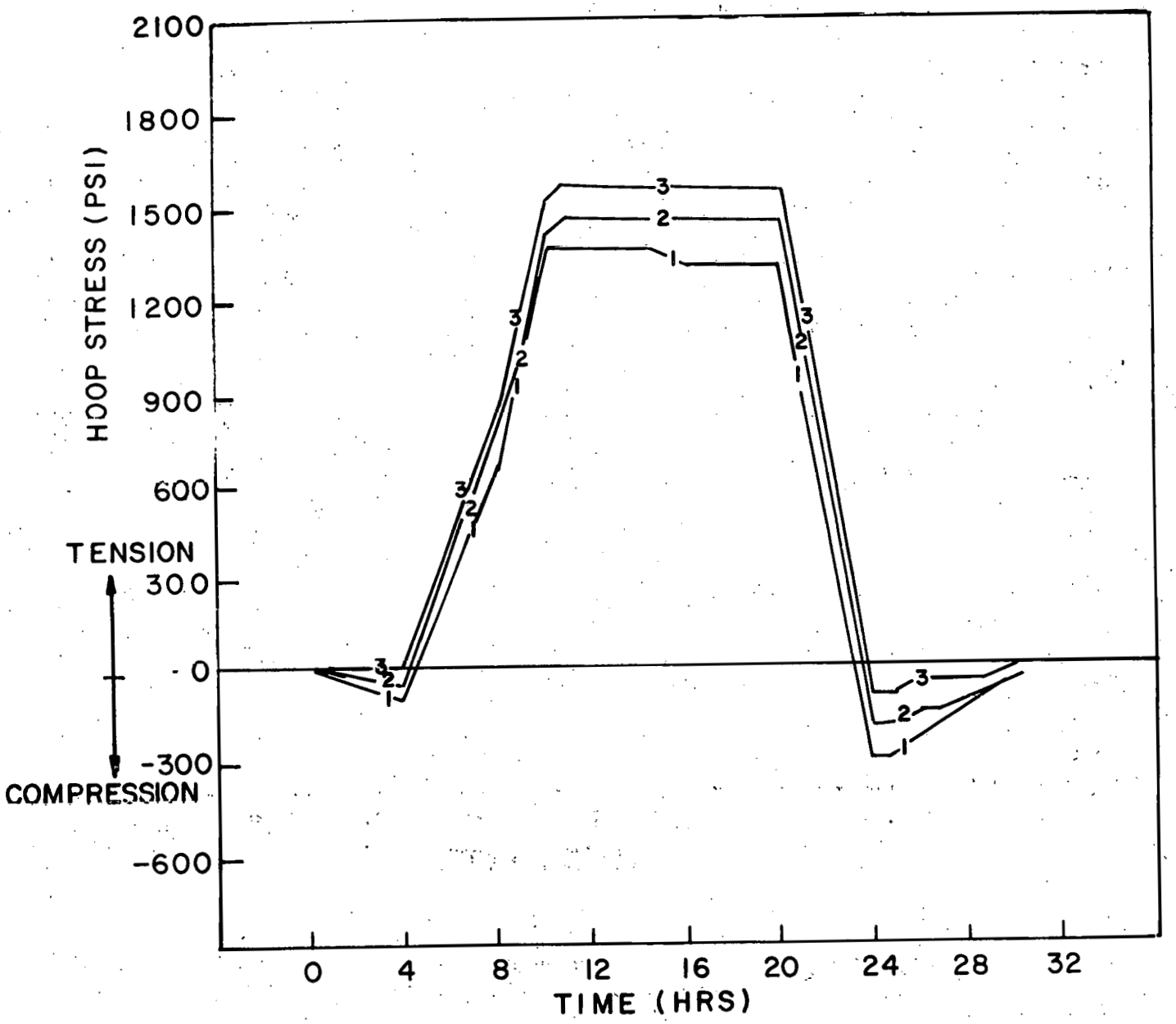

FIGURE 143 (CONT'D).

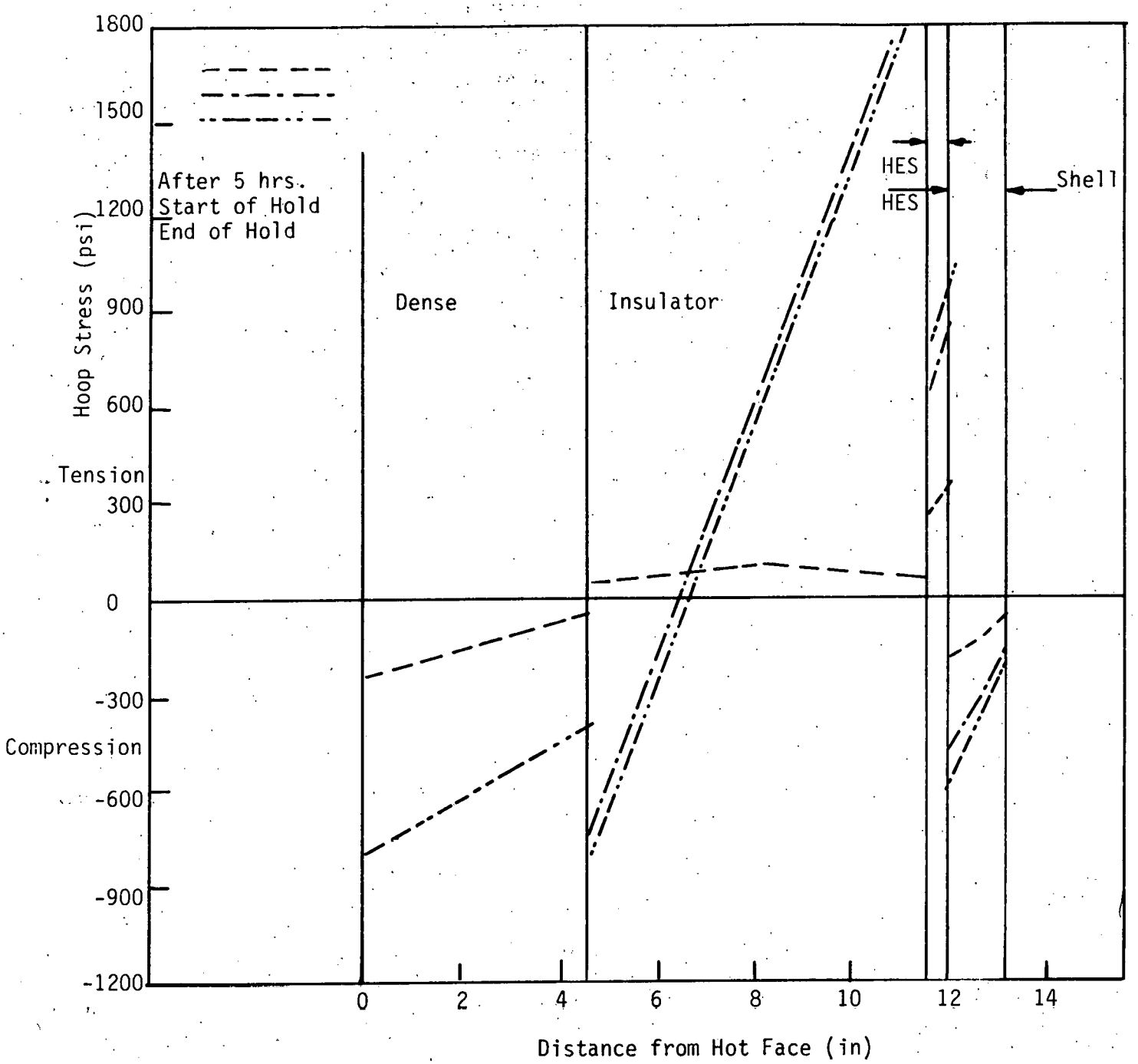

FIGURE 144. Hoop Stress Distribution Prediction of the Lining #9 Configuration With LITECAST 75-28 as the Insulating Component During 200°F/hr Heat-Up to 2000°F.

From these results Lining #9 was expected to perform well in a heat-up test to 2000°F at a rate up to 200°F/hr.

3.4.4. End Effects

In an attempt to explain the large differences between the predicted and measured axial lining strains in the early analyses and lining tests, a study was made of end effects using an elastic finite element program, FESAP. End effects are known to be present in the test vessel but were eliminated as much as possible by using a five (5) foot test section and taking all strain measurements at the center of the test section. Figure 145 is a plot of the minimum principal stress contours in the vessel when subjected to thermal loading due to an experimentally determined radial temperature gradient (1000°F hot face temperature). As shown in Figure 145 the end effects are concentrated in the upper quarter of the vessel (only the upper half was analyzed due to symmetry). Figure 145 illustrates the axial variation of hoop stress along the hot face A-B and along the outside of the shell C-D. As shown in Figure 146 the present generalized plane strain (G.P.S.) model predicts lining stresses very similar to the more elaborate axisymmetric model. However, the shell stresses show considerable differences. To verify the consistency of the results a subsequent analysis was made of a vessel twice as long as the current one. As the vessel becomes longer it must approach generalized plane strain at the center. The stresses along C-D for L=60 inch do in fact, approach the G.P.S. results at A/L=0. It is noted that the peak stresses in the vessel occur near the ends and are similar for the two vessels. More importantly, these results indicate that while a simplified one-dimensional analysis is adequate for lining design, a more sophisticated analysis may be required to insure vessel integrity when interactions between the lining and shell are present.

3.4.5. Gap Effects

The initial predictions of nonlinear effects by the model indicated that cracking could take place at relatively low temperatures due to shrinkage and creep strains. In this case the cracking occurs due to tensile stresses which develop because the lining is constrained from moving freely. As a consequence, Linings #3 and #4 utilized compressible layers between the two linings and between the lining and the shell. These layers served as parting agents to allow the linings to move relative to each other and also served to prevent continuous cracks across the interface. They also were visualized as gaps.

An analytical model was developed to predict the significant effects of gaps. The principal result of the gap analysis was that gaps should be minimized for this particular application since they are detrimental to the lining. Figure 147 illustrates the effect of gaps on the maximum tensile hoop stress in a dual component lining subjected to thermal loading. It also indicates that increasing the gap thickness between the lining components or between the lining and the shell results in higher tensile stresses in both components. A gap between components is less harmful than one at the shell provided that the stress state in the dense component remains compressive. The effect of gaps on shell stresses is just the opposite; increasing the gap reduces any interaction between the lining and shell. Hence, there is an inherent tradeoff, with regard to the presence of gaps, between the stress state in the components of the lining and that in the shell. The effect of pressure, also shown in Figure 147, is relatively minor.

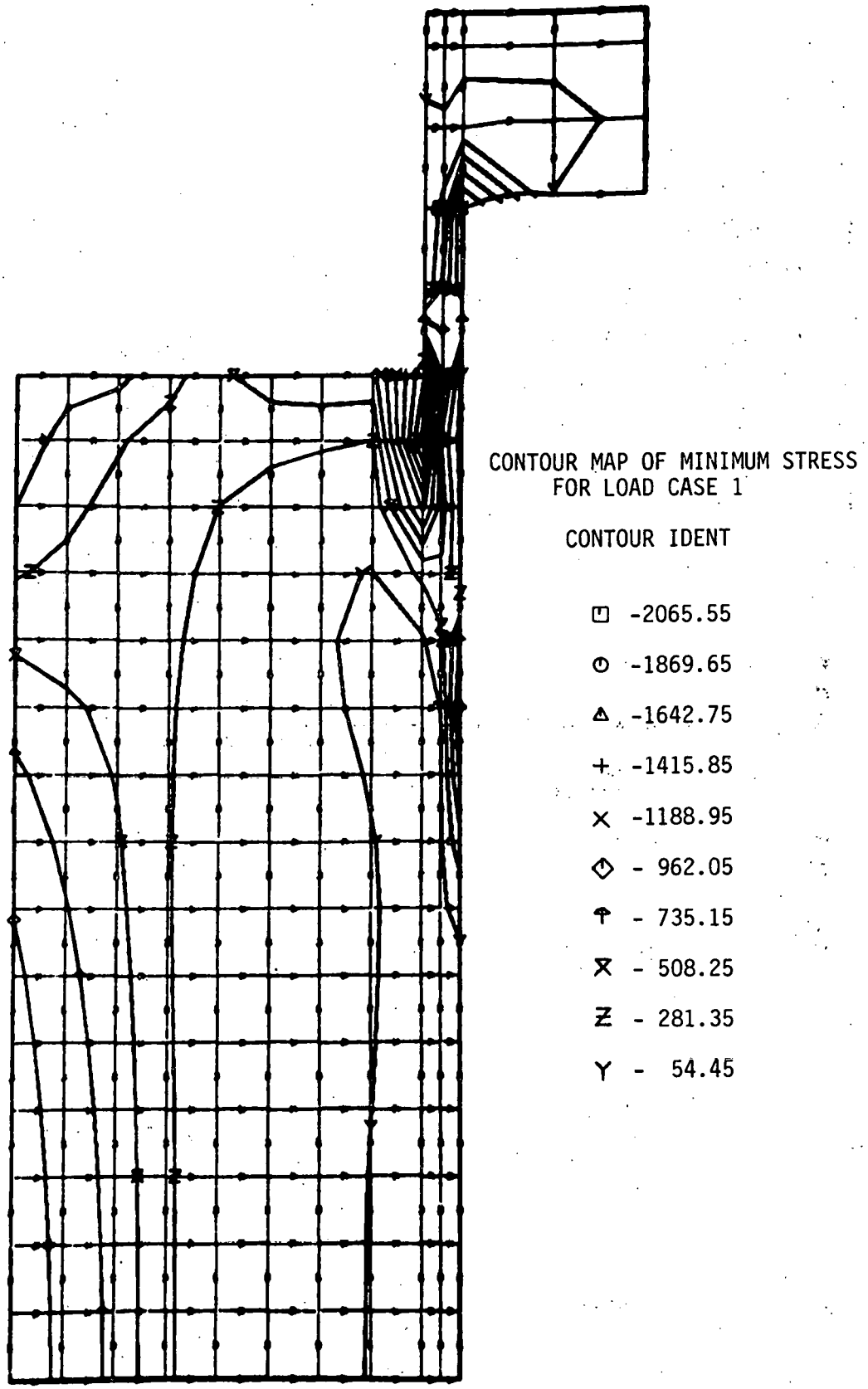

FIGURE 145. Minimum Principal Stress Contours for a Dual Component Refractory Subjected to an Experimentally Determined Radius Temperature Gradient (1000F Hot Face Temperature).

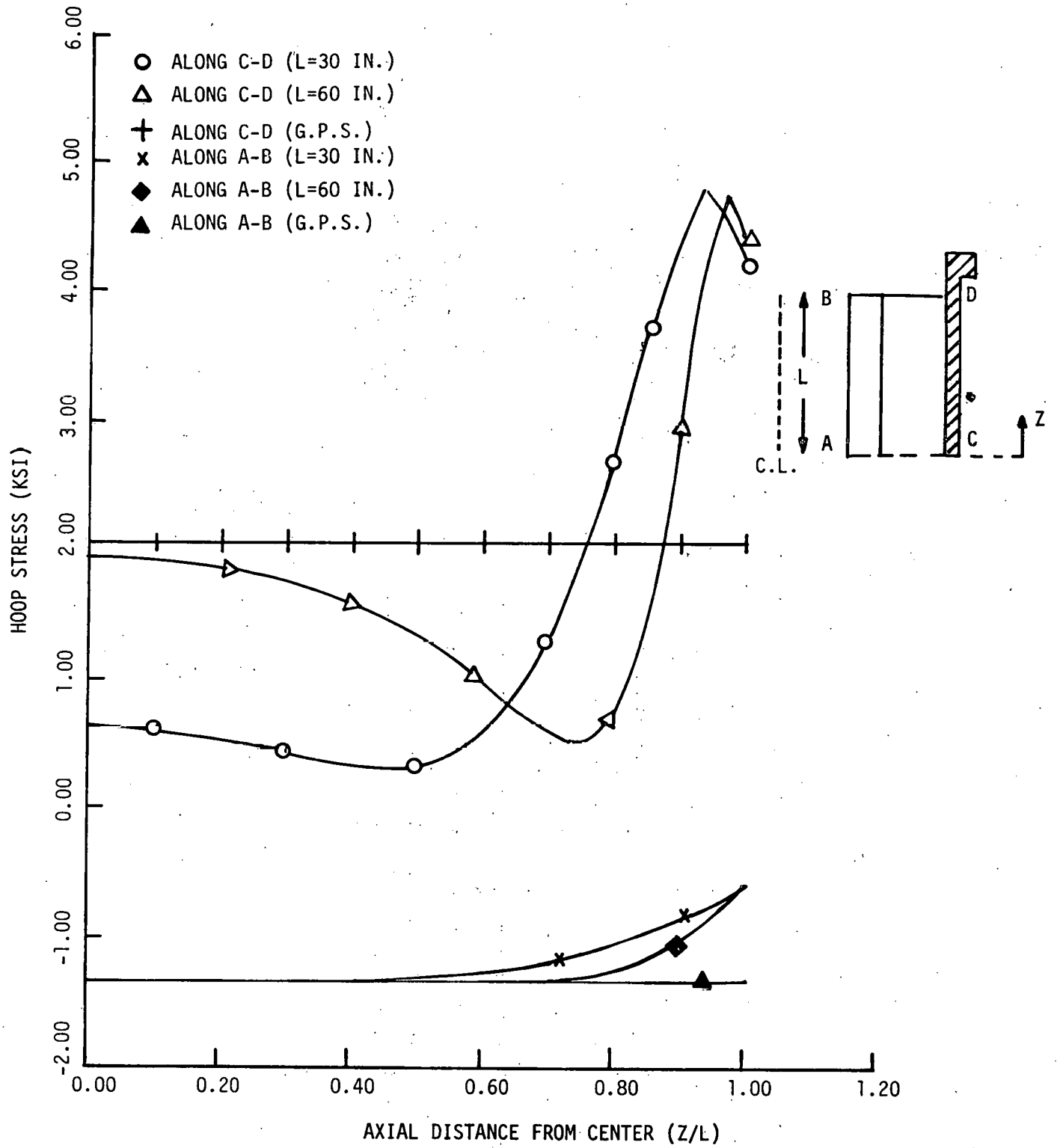

FIGURE 146. Hoop Stress Distributions vs. Axial Distance From Center Along the Hot Face and Along Outside of Shell.

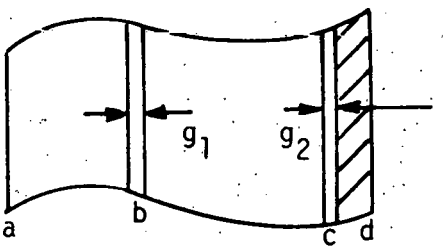

Ta = 1200F
Tb = 900F
Tc = Td = 250F

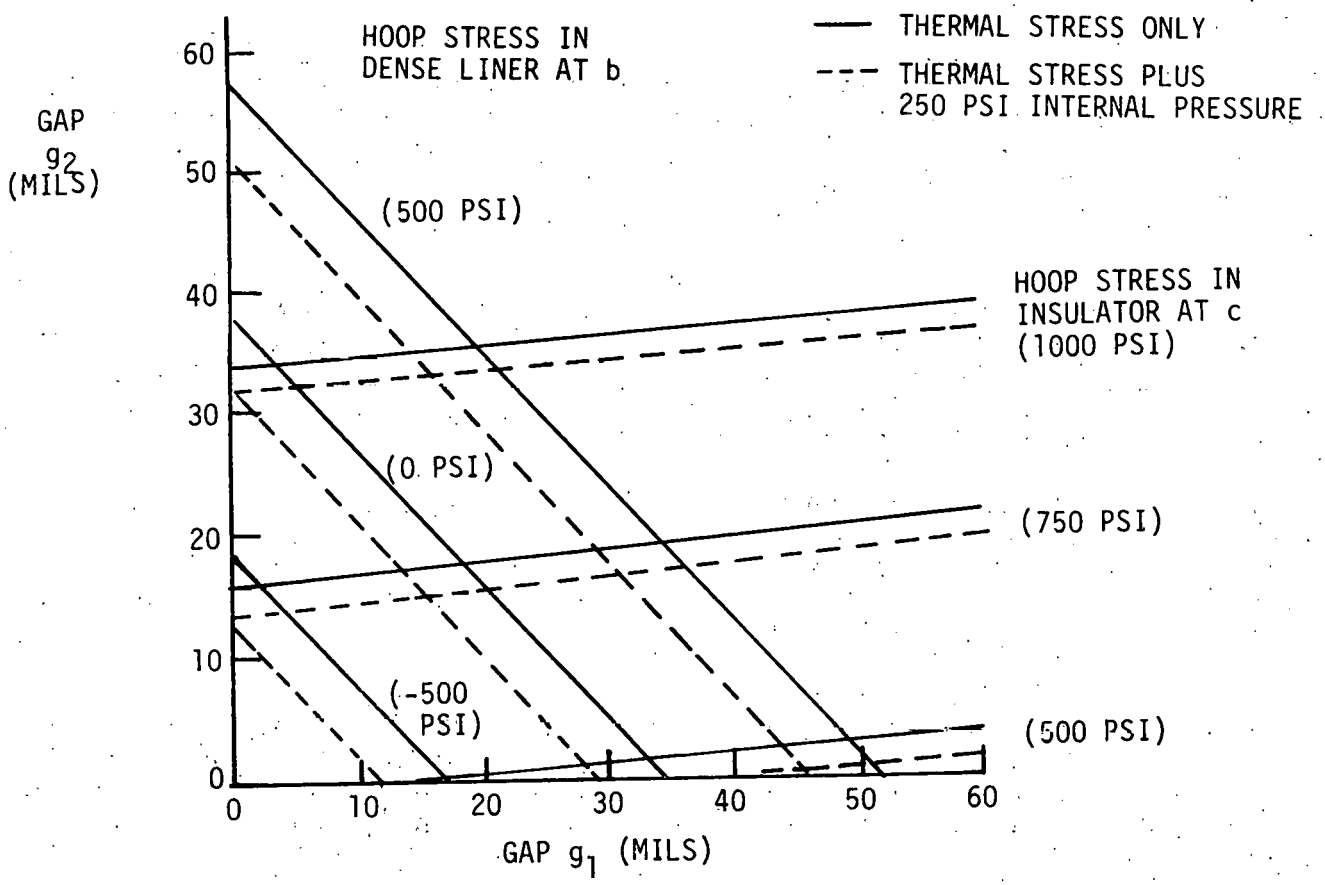

FIGURE 147. Estimate of Gap Effects on the Maximum Hoop Stresses in a Dual Component Refractory Under Combined Thermal and Pressure Loads.

3.5. Lining Tests

3.5.1. General Comments

Once the test equipment was checked out and approved for use, it operated very well and required only minor repairs or modifications. The heaters were the main exception to this since they required constant maintenance, repair, and some modifications. These modifications are described in Section 2.6.1 of this report.

It usually took three to four months to perform a complete lining test plan and required a group of four to six people working three quarter to full time during this period. The instrumentation, installation, post testing and tear out activities were the most time consuming while the test runs, data reduction and analysis of the results were considerably less time consuming by comparison.

The highest vessel temperature recorded during the heat-up tests was about 370°F (measured at the bottom of the vessel). This occurred during the 35 hour soak of the 1850°F, 145 psig steam run on Lining #6. Figure 148 shows schematically the temperatures measured at various locations on the test facility during the test.

During the lining tests run in air, a large volume of steam was released from the lining at a hot face temperature of about 1000°F. This usually caused the steam trap in the bottom of the vessel to begin operating. This trap was constantly in operation during the pressurized steam test. This was partially due to the condensation of steam which was injected directly into the bottom head to keep it hot during the pressurized steam tests.

The steam caused oxidation of the inside of the top and bottom heads and the unlined portions of the vessel shell but the effect was minor. It did not appear to have any major effect on the performance of the heaters whereas temperature did. While the heaters needed to be repaired after the 1700-2000°F runs, they did not after the 1200°F runs.

The steam was found to condense in the top insulation during a test and saturated it. This did not reduce its insulating ability significantly or cause any chimney effects; however, because of the thermal energy required to vaporize it, a cooling effect occurred. This caused the top end of the hot zone to be about 20°F cooler than the lower zones of the lining. This effect was not seen during the high temperature (>1700°F) cycles.

Drill coring was the most efficient method for determining the crack condition of the lining. A series of ten to twenty five drill cores usually permitted the crack depths and gap size to be determined. Core drilling was also used to extract regions around anchors since samples with good integrity could be easily collected. The core drilling equipment was used twice in the field for DOE; once at the CO_2 Acceptor plant in Rapid City, South Dakota and once at the HYGAS plant in Chicago.

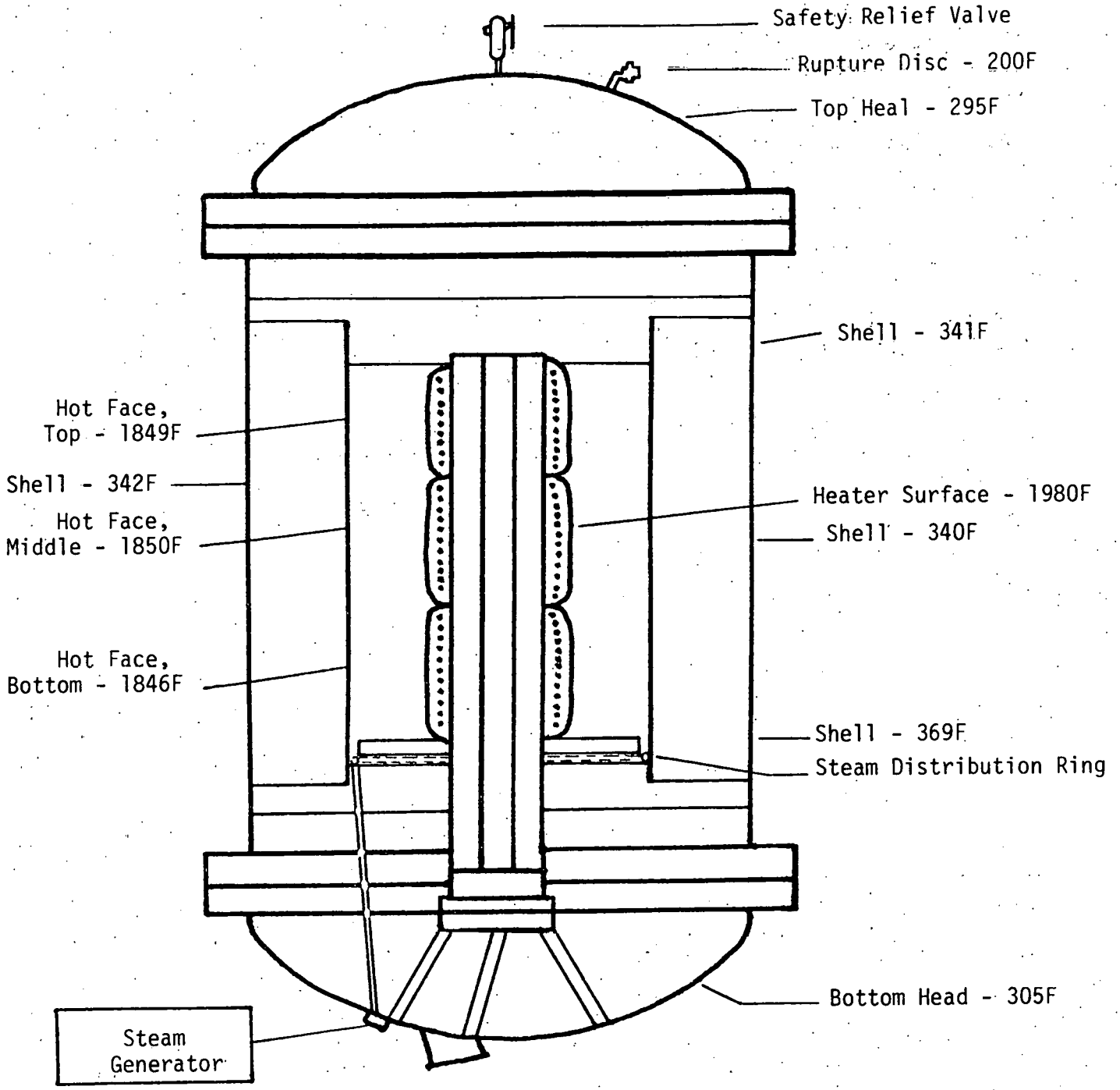

FIGURE 148. Schematic of Test Facility (Indicated Temperatures Measured During 35 Hr. Hold at 1850°F and 145 psig Steam - Lining #6).

The tear out of the linings was generally very difficult. The dense component generally broke up more easily than the insulating component material but the presence of anchors complicated the job. Once bonding barriers and coated anchors at wider anchor spacings were used, the tear out job became easier. It generally took two men one week to completely tear out and clean up a vessel and get it ready for another lining test.

3.5.2. Special Tests on Vessel

Pressure Effect

Prior to the pressurized lining tests, the test facility was checked out to determine how well it maintained pressure and what the radial growth of the shell would be at pressures up to 200 psig. Both compressed asbestos and FLEXITALLIC 1/8 inch thick gaskets worked very well at sealing the flange connections. The vessel was tight enough to maintain 200 psig pressure over a 24 hour period with a loss in pressure of less than 10 psig. The vessel responded quickly to pressure and was found to grow radially an amount equivalent to theoretical predictions.

During later lining tests when good confidence existed in the shell strain gage technique, it was determined that internal vessel pressurization of 150 psig added 4000 psi stress to the shell stresses generated during the heating of the refractory lining.

Thermal Effect

Prior to the installation of Lining #6, a special 400°F heat-up test was run on the empty vessel shell to identify which type shell strain gage was the most reliable and determine the level of thermally induced stresses which occurred independent of lining effects.

The first activity was done to help explain the inconsistent shell stress results obtained with the three types of strain gages used in the first five lining tests. These differences are summarized in Table 29. They indicated that the stresses were predominantly tensile at $\theta = 208°$ and compressive at $\theta = 17°$ for Vessel A on Linings #1, 3 and 5 while they were the same at these same locations for Vessel B on Linings #2 and 4. The results implied that differences in either shell construction or strain gage reliability could be the cause.

To check out these points, it was decided to characterize both shells more fully using the three types of gages of interest in a redundant manner. In addition, this was also considered to be an appropriate time to instrument the vessels to check out end effects. The geometric locations of the original gages as well as the additional gages used on shell A for Lining #6 are indicated in Table 30.

The results obtained during this test are shown in Figure 149 through 153. Figure 149 shows the heating schedule used as sensed by the vessel shell at the midpoint of the lining while Figures 150-153 show comparisons between the LWK, CEA and WK strain gage results at various locations around the midpoint of the vessel and other locations as well.

TABLE 29. Summary of Vessel Shell Stresses Observed from Linings #1 through 5.

Lining No.	Shell "A" or "B"	Gages Used & Stresses Observed at: θ = 17°, Z = 0"	θ = 208°, Z = 0"
1	A	LWK (Compressive)	
2	B	LWK & CEA (Tensile)	CEA (Tensile)
3	A	LWK (Compressive)	WK (Tensile)
4	B	CEA (Compressive)	CEA (Compressive)
5	A	LWK (Compressive)	WK (Tensile)

TABLE 30 - Location of Biaxial Strain Gages on Vessel Shell for Lining #6. Gages were Aligned to Obtain Stresses in the Hoop and Axial Directions.

Shell Strain Gage Location	Circumferential Location 0 - Degrees	Axial Location Z - Inches	Strain Gage Type	Reliable Temperature Limit - °F
1	17	0	CEA	300
2	17	0	LWK*	450
3	17	+27	WK	450
4	17	+15	WK	450
5	17	-15	WK	450
6	17	-27	WK	450
7	118	0	WK	450
8	208	0	CEA	300
9	208	0	WK*	450
10	208	0	WK	450

* Originally installed gages on shell A.

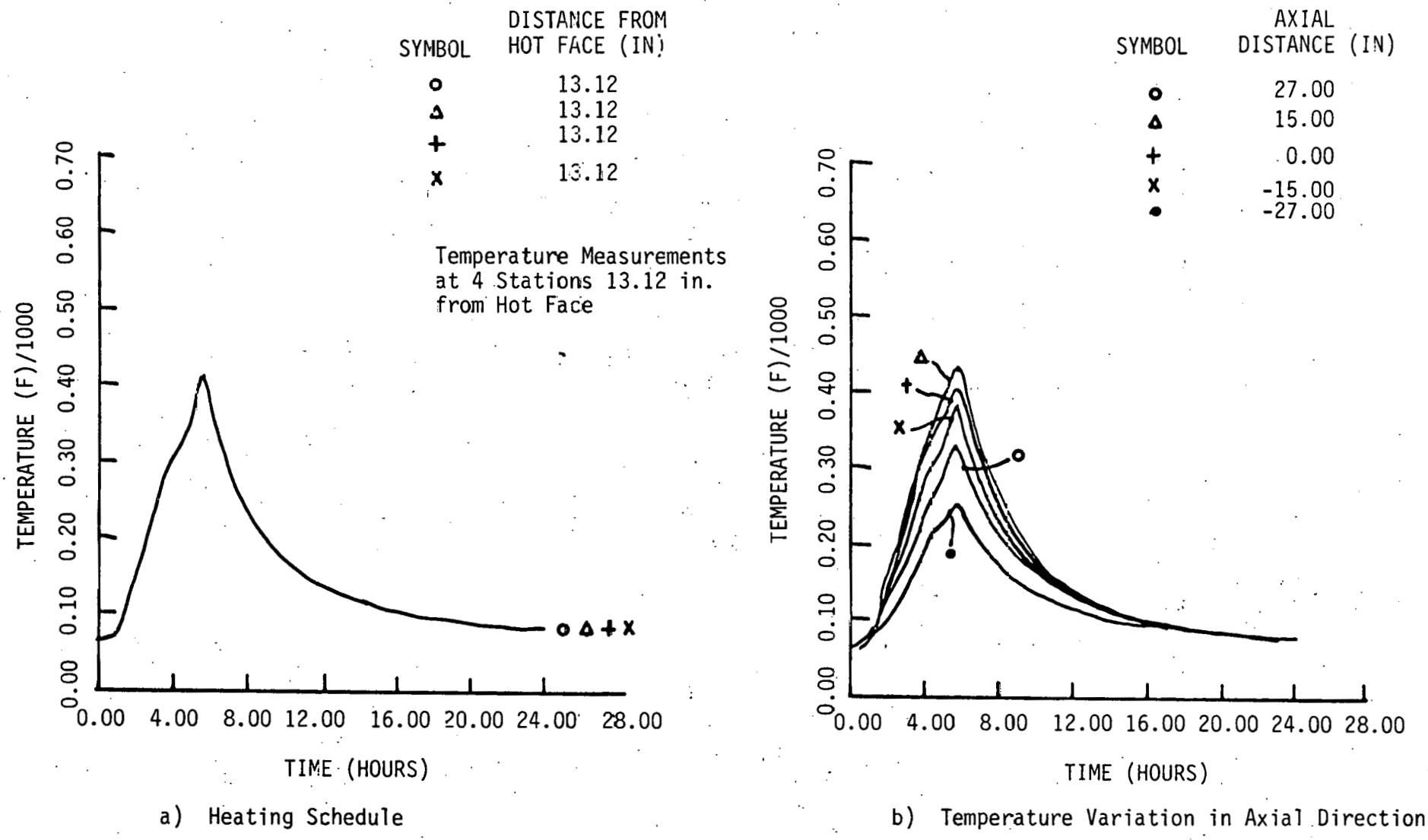

FIGURE 149. Shell Heating Schedule and Temperature Variation In Axial Direction.

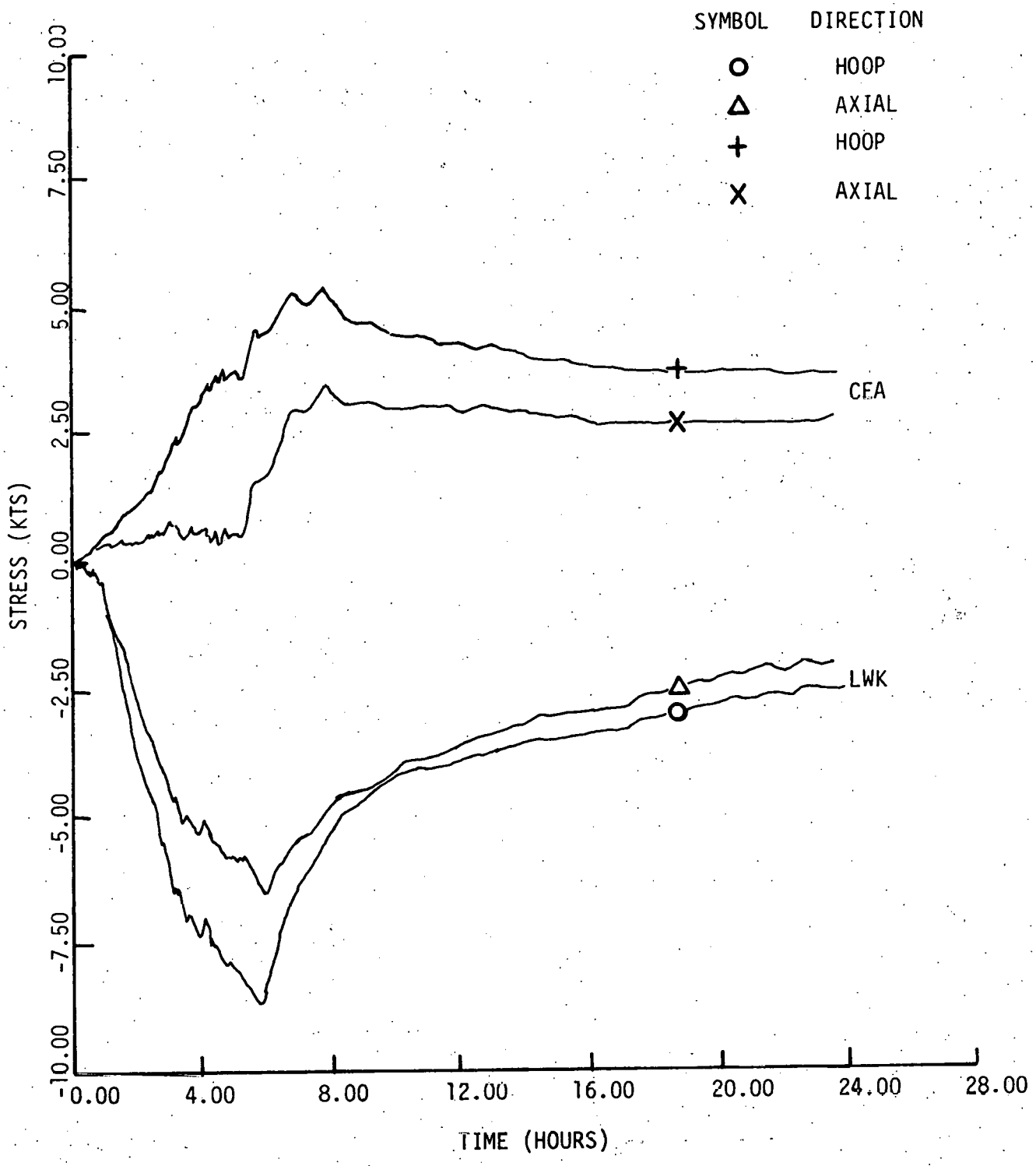

FIGURE 150. Shell Stresses as Determined With CEA and LWK Type Strain Gages During Heat-up Test of Empty Vessel To 400°F (θ = 17°, Z = 0").

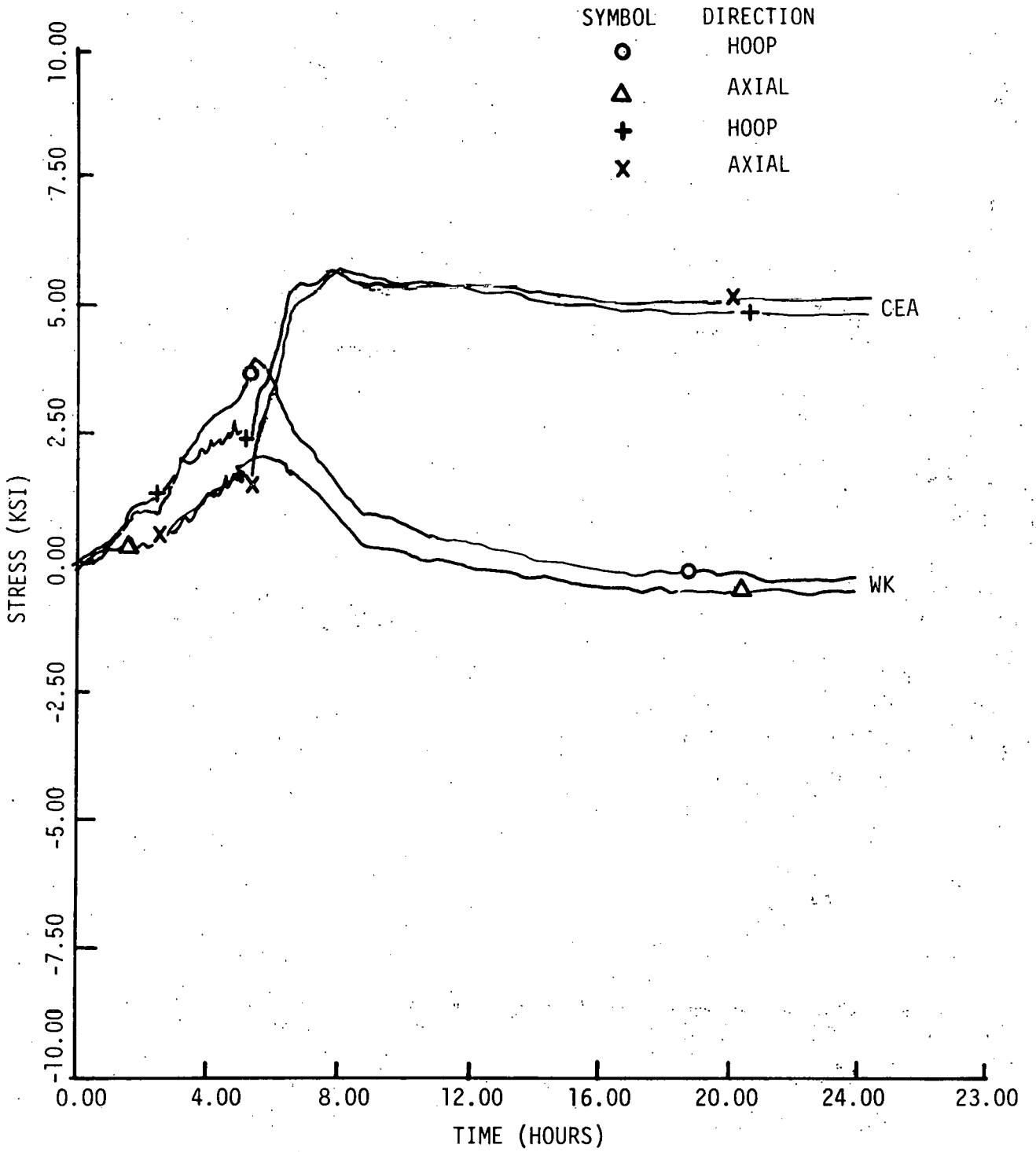

FIGURE 151. Shell Stresses As Determined With WK and CEA Type Strain Gages During Heat-up Test of Empty Vessel to 400°F (θ = 208°, Z = 0").

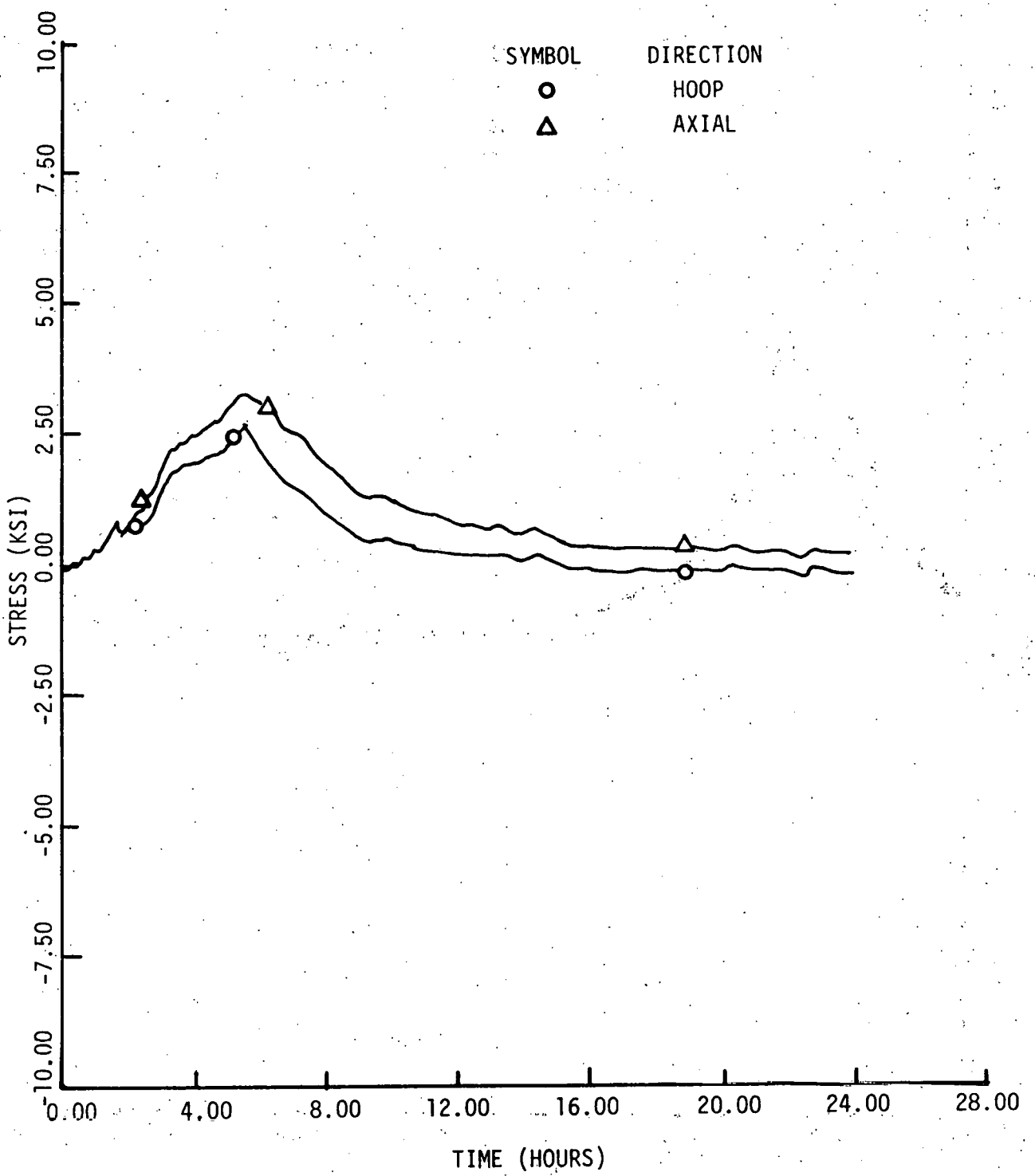

FIGURE 152. Shell Stresses As Determined With WK Type Strain Gage During Heat-up Test of Empty Vessel to 400°F (Θ = 298°, Z = 0").

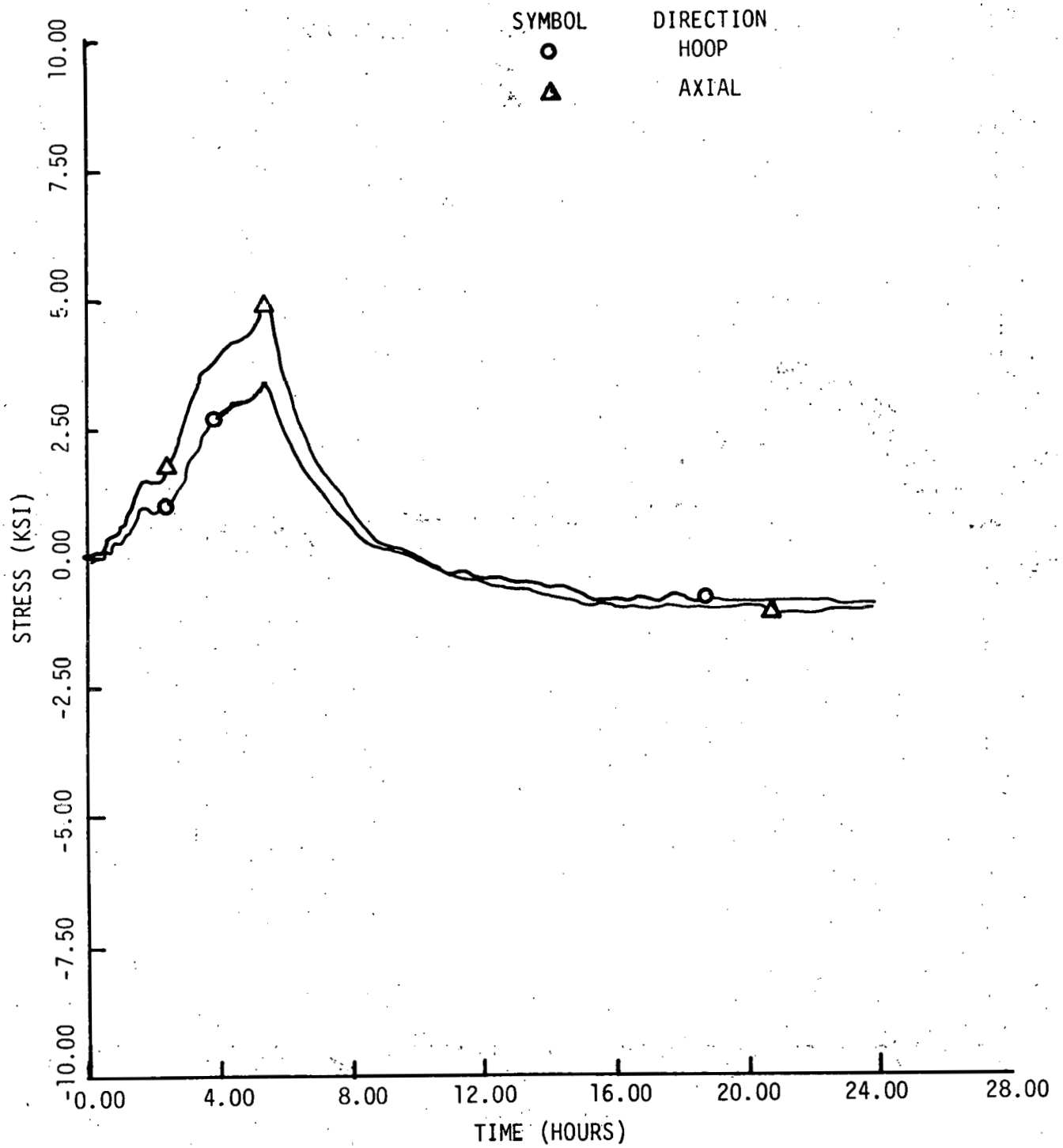

FIGURE 153. Shell Stresses As Determined With WK Type Strain Gages During Heat-up Test of Empty Vessel to 400°F (Θ = 17°, Z = -15").

From a review of these results, it is evident that the WK series gages performed consistently and yielded stresses that were of the same order of magnitude and direction. They furthermore exhibited good zero-return strain states at the completion of the test. This is expected since the apparent strain curve derived for the WK gage when bonded to a separate sample of the shell material retraces itself on cooldown from 450°F with little zero-shift in strain upon return to room temperature. In comparison, the CEA type gage (Figure 151) follows the WK gage results up to a certain point then diverges from the WK results and does not return to a zero strain state. This point corresponds to the upper operating temperature of the CEA gage. An upper operating temperature of 300°F was determined from apparent strain tests run on this gage. While cooling from temperatures above 300°F, the apparent strain curve was found to diverge from the heat-up data, and a large zero-shift in strain occurred upon returning to room temperature. However, when heated to temperatures below 300°F, the cooldown apparent strain curve retraced the heat-up curve, with little zero-shift in strain at room temperature.

With the knowledge that the CEA gages perform reliably at temperatures below 300°F, this gage can be used to evaluate the reliability of the LWK type gage from a comparison of the plots in Figure 150. This comparison clearly demonstrates the unreliable nature of the LWK gage since the resulting stresses are of opposite direction from the CEA gage during the entire duration of the test. Furthermore, these stresses are inconsistent with the results obtained from the WK gages elsewhere on the shell. Although the published temperature limit for reliable operation of the LWK gage was not exceeded, and the gage was found to exhibit good apparent strain characteristics, this gage is believed to be unreliable because of inherent design deficiencies. The primary one is the method of gage attachment to the shell. This is achieved by spot welding a substrate shim to which the gage grid is adhesively bonded. It is suspected that the mechanical strain does not adequately transfer from the shell to the shim, thus causing the gage grid to sense an erroneous strain. An improved method of gage attachment might include a revised spot welding pattern to prevent the shim from warping under load and thereby eliminating erroneous strains to be sensed by the grid. The LWK gage was initially selected to measure shell strains for the lining tests because of its good apparent strain characteristics and the ease with which it can be attached. Although the WK required considerably more time for attachment to the shell (adhesive bonding), it was decided to use this gage for all future lining tests since it was found to be the most reliable.

Once the relationships between the various strain gages were known, the level of thermally induced stresses in the lining tests at the top temperature of the test could be determined. The maximum level was about 4000 psi for a shell temperature of 340°F. This level decreased to about 3000 psi for a shell temperature of 250°F and to about 2300 psi for a shell temperature of 200°F.

Point Loading

The strain results obtained during the point loading experiments on Vessel B to simulate anchor/shell interactions are summarized in Table 31. They indicate that the hoop strains go through maxima and minima depending upon loading distance from the strain gages. This is in general agreement with the trends predicted by theory of thin walled pressure vessels. The results also indicate that point loading of the shell by anchor/refractory interactions are possible and could be having a localized effect on the vessel shell strains. The magnitude of these strains, however, were relatively small and were believed to be of minor overall significance.

TABLE 31 - Shell Strains Determined During Internal Point Loading of Empty Vessel B.

Internal Load (lbs)	Load Angle*	Shell Strain Gages (G.F.S. = 2.00) 17° Hoop	17° Axial	208° Hoop	208° Axial
0	0				
500	0	+6	+6	+3	+6
1000	0	+13	+14	+10	+13
1500	0	+19	+21	+15	+19
2000	0	+26	+29	+20	+25
3000	0	+38	+44	+31	+37
4000	0	+48	+60	+41	+47
5000	0	+59	+71	+49	+56
0	0	-1	0	0	+2
0	1	-1	0	0	+1
500	1	-1	0	+4	+7
1000	1	-1	+2	+8	+13
2000	1	-2	+3	+20	+28
3000	1	-1	+6	+31	+41
4000	1	-2	+8	+41	+55
5000	1	-1	+10	+47	+62
0	1	-1	0	0	0
0	2	-1	0	0	+1
1000	2	-3	-1	0	+3
2000	2	-6	-2	-1	+4
3000	2	-8	-3	-2	+6
4000	2	-9	-5	-2	+7
5000	2	-12	-6	-4	+9
0	2	-1	0	0	+1
0	3	-1	0	0	+1
1000	3	-2	-2	-3	0
2000	3	-6	-5	-6	-1
3000	3	-8	-7	-9	-4
4000	3	-10	-9	-12	-5
5000	3	-11	-11	-15	-6
0	3	0	0	0	+1
0	8	-1	0	0	+1
1000	8	0	0	0	+1
2000	8	0	0	0	+1
3000	8	0	-1	+1	+1
4000	8	+1	-1	+2	0
5000	8	+1	-1	+2	+1
0	8	-1	0	0	+1

* Indicated on Figure 105

3.5.3. Test Conditions

The conditions under which the linings were tested are shown in Table 32. The original test plan included a greater number of linings but it was necessary to deviate from this due to the amount of information generated, the value of running a second or third cycle on each lining, and the time required to analyze and correlate the results of each lining. The plan evolved as information was acquired from the whole program and as experience was gained from the lining tests. Much of the direction of the tests was based on the analytical and experimental findings of Linings #1 and 2 and later on the findings of other DOE contractors who reported good performance of the 50% Al_2O_3 refractory concrete in coal gasifier atmospheres.

The original plan for each lining was to run one heat-up test at one of two heating schedules; or a faster schedule if the linings did not crack at the slower rates. The original heating schedules included one at 100°F/hr with holds at 200°F, 400°F, 1000°F and 2000°F and a second at 50°F/hr to 1000°F and 100°F/hr to 2000°F with no holds except at 2000°F. This plan was changed to include two or more cycles on each lining with the first cycle run to 1200°F or less. This was done because cracking was expected to occur before this temperature was reached and because the embedded strain gages in the dense component were not expected to give reliable strain data on the second and subsequent cycles if used above 1200°F on the first cycle.

The first heating schedule was followed for Lining Nos. 1-3 and the second heating schedule was followed for Lining Nos. 4-7. A third schedule, faster than the first two, was followed for Lining No. 8; and a fourth schedule, slower than the other, was followed for Lining No. 9. A slow cool-down rate (50°F/hr) was followed for Lining No. 1-7 and 9; and a faster (>150°F/hr) cool-down rate was followed for Lining No. 8.

All linings were of the 12 inch dual component configuration with 7-1/2 inches of insulating and 4-1/2 inches dense material. The design configuration included V-type anchors spaced 12 inches apart for the first two linings. The major comparison was uncoated versus coated anchors. The third lining was anchorless, in order to better isolate the material factors contributing to cracking, and Linings #4 through 9 used standard Y-type and independent anchors both spaced at 36 inches apart. The standard design configuration originally started out with intimate bonding between refractory components and the refractory and the shell. However, later linings included ceramic fiber paper, plastic sheet and silicone grease as bonding barriers at these locations to allow each component to shrink independently of one another. The emphasis was also shifted from a 90+% Al_2O_3 dense material to a 50% Al_2O_3 dense refractory concrete material containing metal fibers

3.5.4. Instrumentation

The linings were initially instrumented with embedded strain gages oriented in all three principal stress directions and located at various depths throughout the lining on opposite sides. This was changed to just one side and to the midpoint of each component for Linings #4-6 and 9. Lining #7 had no embedment strain gages.

As noted previously this reduced lining instrumentation was accompanied by an increased anchor and shell instrumentation. The monitoring of internal pore pressure was begun in Lining #4 and accurately measured in Linings #7 and 9.

TABLE 32. Summary of Test Conditions - Lining Nos. 1-9*

LINING NO.	DESIGN	ANCHORS	ATMOSPHERE	HEATING SCHEDULE
1	Standard	Uncoated V 12 Inches	Air	#1 1200, 2000°F
2	Standard	Coated V 12 Inches	Air	#1 1200°F
3	Modified (Barriers)	None	Air, Steam	#1 400, 1200, 2000°F
4	Modified	Semi-Coated Y and Independent 36 Inches	Air, Steam	#2 1200, 1850°F***
5	Modified (Barriers)	Coated Y and Independent 36 Inches	Air, Steam	#2 1200, 1850°F***
6	Modified (Barriers)	Coated Y	Steam	#2 1200,*** 1850°F***
7	Modified (Barriers & Fibers)	Coated Y 36 Inches	Air	#2 1700, 1700,*** 1850°F
8**	Modified (Barriers & Fibers)	Coated Y 36 Inches	Air	#3 1700, 1700°F
9	Mocified (Barriers, Fibers, 3rd Layer)	Coated Y 36 Inches	Air	#4 1850°F

* Nos. 1-4: 90+% Al_2O_3 generic/LITECAST 75-28
Nos. 5-8: 50% Al_2O_3 (KAOCRETE XD 50)/LITECAST 75-28
No. 9: 50% Al_2O_3 (KAOCRETE XD 50)/KAOLITE 2300 LI and HES mortar

** Lining No. 7 left in place and reheated 2 additional cycles
Heating rates: >250°F/Hr. Cooling rates: >150°F/Hr.

*** Vessel pressurized to 150 psig.

3.5.5. Installation

The mixing, casting and initial curing conditions used in each of the eight linings installed are summarized in Tables 33 and 34. Table 33 lists the results for the insulating component materials and Table 34 lists the results for the dense component materials. The LITECAST 75-28 material was generally the most difficult material to place and had the most variability in mixing and casting performance. The ERDA 90 material, on the other hand, was the easiest to place.

The mixers performed very well and permitted lower water levels than had been anticipated in the batches of dense component materials. All the materials flowed well under vibration and filled the vessel cavity satisfactorily. The use of metal fibers in the KAOCRETE XD 50(Mix 36C) material made it somewhat more difficult to pour; however, it flowed well with vibration.

3.5.6. Heat-Up Test Results

The section which follows summarizes the findings of the nine lining tests described in Table 32. These findings are grouped into four or five areas as they relate to the overall objectives of the program. Only the highlights of each lining are discussed. For more details on each lining, the following quarterly and/or annual reports on this contract should be reviewed:

Lining	Report
1	First Annual, Nov. 1977 Fifth Quarterly, Dec. 1977
2	Fifth Quarterly, Dec. 1977 Sixth Quarterly, Jan. 1978
3	Sixth Quarterly, Jan. 1978 Seventh Quarterly, April 1978
4	Seventh Quarterly, April 1978 Second Annual, July 1978
5	Second Annual, July 1978 Ninth Quarterly, Nov. 1978
6	Tenth Quarterly, Jan. 1979
7	Eleventh Quarterly, May 1979 Third Annual, Aug. 1979
8	Included in Appendix E
9	Included in Appendix E

Tables 35 and 36 summarize the crack width and shrinkage results and post test results, respectively, of the nine linings tested. Additional data are included in Appendix E on Linings #7-9.

TABLE 33. Batching Parameters - Insulating Component, Lining Nos. 1-7 and 9.

Parameter	Lining #1 LITECAST 75-28	Lining #2 LITECAST 75-28	Lining #3 LITECAST 75-28	Lining #4 LITECAST 75-28	Lining #5 LITECAST 75-28	Lining #6 LITECAST 75-28	Lining #7 LITECAST 75-28	Lining #9 KAOLITE 2300 LI
Batch Size	600 lbs.	600 lbs.	600 lbs.	450 lbs.	450 lbs.	450 lbs.	450 lbs.	240 lbs.
# Batches	7-1/4	7-1/3	8-1/3	8	8	9	9	10
Material Temp.	76°F	78°F	72°F	62°F	75°F	73.4°F	75°F	76°F
Room Temp.	75°F	78-1/2°F	72°F	64°F	75°F	73.4°F	75°F	70°F
Water Temp.	80°F	77°F	73.5-77°F	74.5°F	75°F	76°F	75°F	76°F
Water Content*	21%	21%	24%	21%	21%	21%	21%	59%
Mix Time Dry	30 sec.	30 sec.	30 sec.	30 sec.	30 sec.	30 sec.	30 sec.	30 sec.
Mix Time Wet	90 sec.	90 sec.	90 sec.	90 sec.	90 sec.	90 sec.	90 sec.	5 min.
Ball-in-Hand	Good	Good	Good/Dry Excel./Wet	Good	Poor	Fair-Good	Good-Excellent	Good-Excellent
Pourability	Fair	Fair	Good	Good	Fair	Good	Very Good	Excellent**
Placement Time	90 min.	58 min.	66 min.	78 min.	57 min.	70 min.	65 min.	120 min.
Cure Temp. Initial-Peak	85 - 129°F	83 - 136°F	77 - 130°F	71 - 119°F	N.D.	78-124°F	74-119°F	78-117°F
Pour Temp.	N.D.	N.D.	N.D.	69 - 71°F	77°F	77°F	77°F	78°F

- - - - - - - -

Legend: N.D. - Not determined
* Basis of dry batch.
** Only metal form vibration was used during casting to prevent damage to HES Mortar.

TABLE 34. Batching Parameters - Dense Component, Lining Nos. 1-7 and 9.

Parameter	Lining #1 90+% Al_2O_3 Generic	Lining #2 90+% Al_2O_3 Generic	Lining #3 90+% Al_2O_3 Generic	Lining #4 90+% Al_2O_3 Generic	Lining #5 50% Al_2O_3 B&W 36-C	Lining #6 50% Al_2O_3 B&W 36-C	Lining #7 50% Al_2O_3 4 w/o Fibers B&W 36-C	Lining #9 50% Al_2O_3 4 w/o Fibers B&W 36-C
Batch Size	800 lbs.	800 lbs.	700 lbs. (ERDA 90/Kaotab)	800 lbs.	600 lbs.	600 lbs.	600+ 24 lbs. fiber	600+ 24 lbs. fiber
# Batches	5-1/2	6	6	6	6	6	5-1/2	6
Material Temp.	76°F	71.5°F	67°F	60°F	79°F	71°F	69°F	79°F
Room Temp.	77°F	76.5°F	68°F	63°F	80°F	75°F	74°F	80°F
Water Temp.	69°F	70°F	77°F	78-83°F	75°F	76°F	74-75°F	77°F
Water Content*	7-3/4 -8%	7-3/4%	7-3/4% - 8-3/4%	7-3/4-8%	7-1/2%	7-1/2%	7-1/2%	7-1/2%
Mix Time Dry	30 sec.	30 sec.	60 sec.	30 sec.-8 min.	30 sec.	30 sec.	30 sec.	30 sec.
Mix Time Wet	90 sec.	90-120 sec.	90 sec.	90-150 sec.	5 min.	5 min.	5 min.	5 min.
Ball-in-Hand	Poor to Excellent	Good to Excellent	Good/Dry Excellent/Wet	Fair to Good	Good	Poor-Fair	Poor/dry-Good/wet	Fair
Pourability	Very Good	Good	Good	Stiff to Fair	Good	Fair	Poor-Fair	Good
Placement Time	44 min.	42 min.	47 min.	60 min.	75 min.	65 min.	75 min.	75 min.
Cure Temp. Initial-Peak	78-114°F	84-109°F	74-98°F	71-90°F	N.D.	80-96°F	74-88°F	81-98°F
Pour Temp.	N.D.	N.D.	N.D.	71°F	81°F	79.5°F	80°F	85°F

Legend: N.D. - Not determined.
* Basis of Dry Batch

TABLE 35. Lining Shrinkage and Crack/Gap Widths After Heat-Up Tests - Lining Nos. 1-9

Lining No.	Temp. (°F)	Shrinkage* (%)	Crack Width** (in.)	Gap Width*** (in.)
1	2000	NA	NA	NA
2	1200	.20	.025	NA
3	400	.06	.005	NM
3	1200	.10	.014	NA
3	2000	.16	.019	.125
4	1200	.09	.013	NA
4	1850	.19	.024	.090
5	1200	.04	.006	NM
5	1850	.23	.032	~.05
6	1200	.05	.008	NM
6	1850	.29	.032	.050
7	1700	.10	.012	.050
7	1700	.095	.009	.050
7	1850	.13	.012	>.050
8****	1700,1700	.13	.014	.055
9	1850	.019	.005	.056

Legend: NA - Not Determined

NM - Not Measurable

* - Linear shrinkage calculations assume summation of crack widths accounts for shrinkage in vertical and horizontal directions from as-cast condition.

** - Average of cracks in vertical and horizontal directions.

*** - Gap width is measured between dense and insulating components.

**** - Lining No. 7 left in place and reheated 2 additional cycles.

TABLE 36. Post Test Physical Properties - Lining Nos. 1-9

						TENSILE STRENGTHS*, PSI									
DENSE COMPONENT	LINING #1	LINING #2	LINING #3 2000°F	LINING #4 1850°F	LINING #5 1200°F	LINING #5 1850°F	LINING #6 As-Cast	LINING #6 1200°F	LINING #6 1850°F	LINING #7 1700°F	LINING #7 1700°F	LINING #7 1850°F	LINING #8 1700°F	LINING #9 As-Cast	LINING #9 1850°F
Hot Face	1870	985	1880	1570	250	715	521	638	879	725	700	845	510	475	435
Interface	--	--	1110	1185	305	--	552	575	781	430	710	765	740	450	420
INSULATING COMPONENT															
Interface	220	200	340	230	270	--	362	401	558	140	200	320	315	90	40
Cold Face	--	--	--	255	250	--	387	370	333	180	220	210	210	90	70
						DENSITY** OF MATERIALS, #/FT^3									
DENSE COMPONENT															
Hot Face	177	175	176	176	139	137	140.7	138.8	139	144	143	144	142	144.5	142.2
Interface	--	--	174	175	139	--	141.3	139	139.4	142	142	140	144	143.4	140
INSULATING COMPONENT															
Interface	81	74.7	82.9	76	85.8	--	86.1	90.5	84.7	83	84	88	82.3	64	59
Hot Face	--	--	--	78	85.8	--	85.2	87.8	88.6	82.5	84	88	84.2	68	62

*Determined by diametral compression test

**Determined by volumetric technique

Standard Lining Design

Cracking occurred in both Lining Nos. 1 and 2 (Standard Design) even though the "V" anchors in No. 2 were wrapped with masking tape (20-30 mil thick). The linings were heated to 1200°F in accordance with the modified Case #1 schedule; and Lining No. 1 was subjected to a second cycle to 2000°F which resulted in propagation of the cracks. The appearances of the two linings are shown in Figures 155-156.

As shown in the figures, the cracking generally followed the principal stress directions of the liner and the anchor spacings. It is further noted that the cracks appear to have propagated across the interface between the two components and became more severe at the higher test temperature. Although the severity of the cracking, considering the small amount of shrinkage (<0.20%), was not anticipated, the cracks do match those as observed in the CO_2 Acceptor and HYGAS gasifiers. Thus, the results indicate that the conditions in the test facility were simulating those of pilot plant and field tests.

When Linings #1 and 2 were post tested, it was found as shown in Figure 157 that the hot face cracks propagated completely through the lining to the shell and followed the anchor orientation and spacing. It was also found that the two components were well bonded to one another and to the shell as shown by the well bonded drill core removed from Lining #2 (see Figure 158). Futhermore, it was found from the lining strain data on these linings, the anchor stresses determined for a strain gaged "V" anchor used in Lining #2 and the shell stress results of Lining #2 which are shown in Figures 159, 160 and 161, respectively, that lining strains and anchor and shell stresses were generated almost instantaneously upon heating of the dense component.

These findings indicated that, initially, the lining acts elastically, interacts severely with the anchors and shell, and is constrained by the shell and anchors from shrinking and contracting on cooldown. This combination of effects appears to have played a significant role in causing the linings to crack. Since the cracking became more severe after the 2000°F heat-up of Lining #1, it also appeared that creep was a significant factor in affecting cracking. Propagation of the cracks was enhanced by the bonding of the two components to each other and to the shell.

These results agreed favorably with the predictions of the REFSAM finite element computer program (Figures 131, 138 and 139) and indicated that the material and design modifications as proposed from the results of the analytical work should be seriously considered.

Modified Lining Designs

Since the anchor/refractory interactions appeared to be so intense, a decision was made to omit all but five of the anchors in Lining #3 and place bonding barriers between the interface and shell so that the components could shrink and contract freely. The five anchors that were used were wrapped with masking tape. Four were used to support strain gages (suspended) and the fifth was strain gaged. A schematic of the lining is shown in Figure 162.

FIGURE 154. As Tested Appearance of Lining #1 After Two Thermal Cycles to 1200° and 2000°F

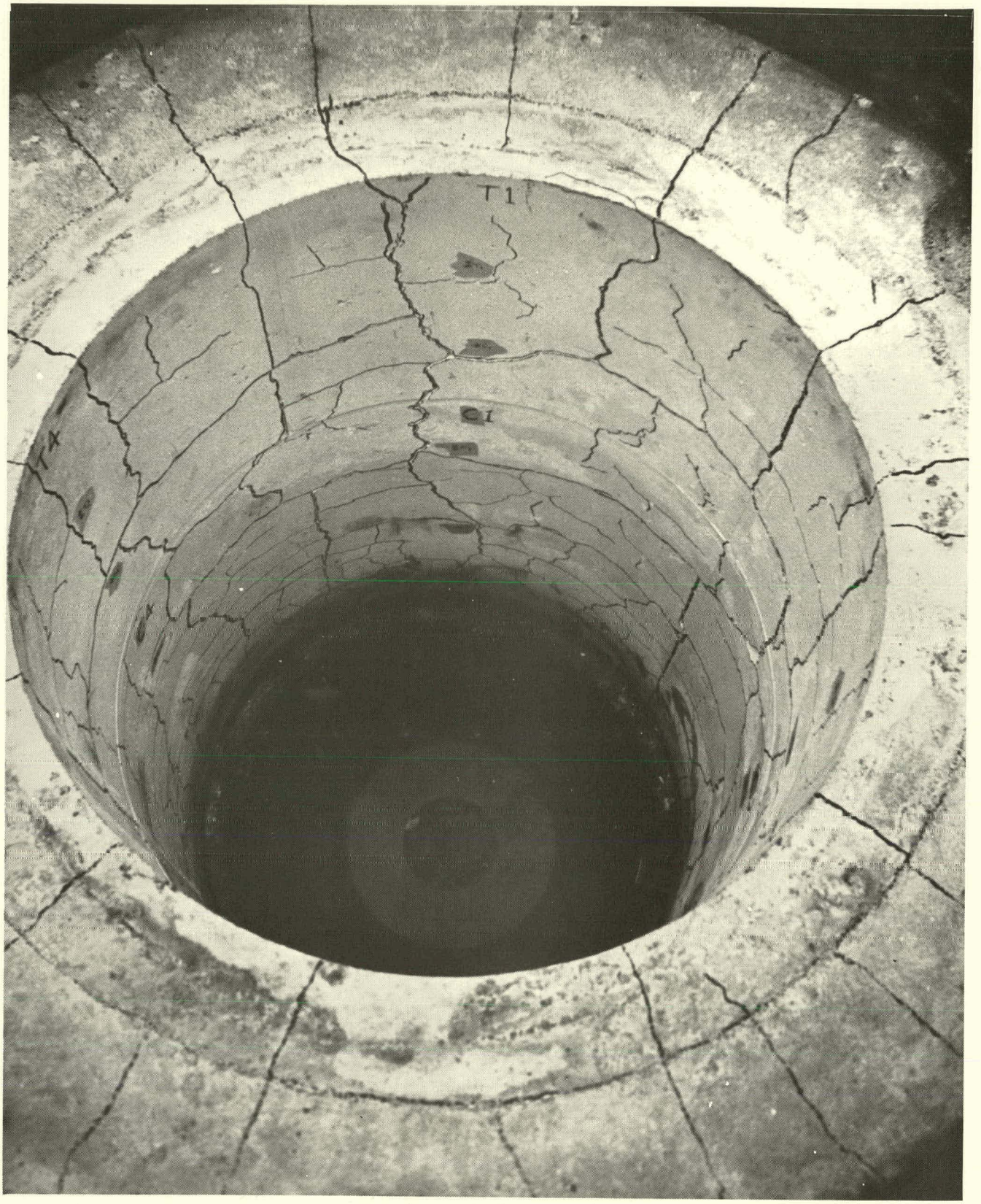

FIGURE 155. Appearance of Lining #1 After Cracks Are Inked Following Two Thermal Cycles to 1200 and 2000°F.

FIGURE 156. Appearance of Lining #2 After Cracks Were Inked Following One Thermal Cycle to 1200°F.

FIGURE 157. Top View of Lining #1 During Tear-Out and Examination. Dense component cut with diamond saw and insulator dressed with a chisel. Cracks are marked with ink. Four foot test zone lies within the arrows.

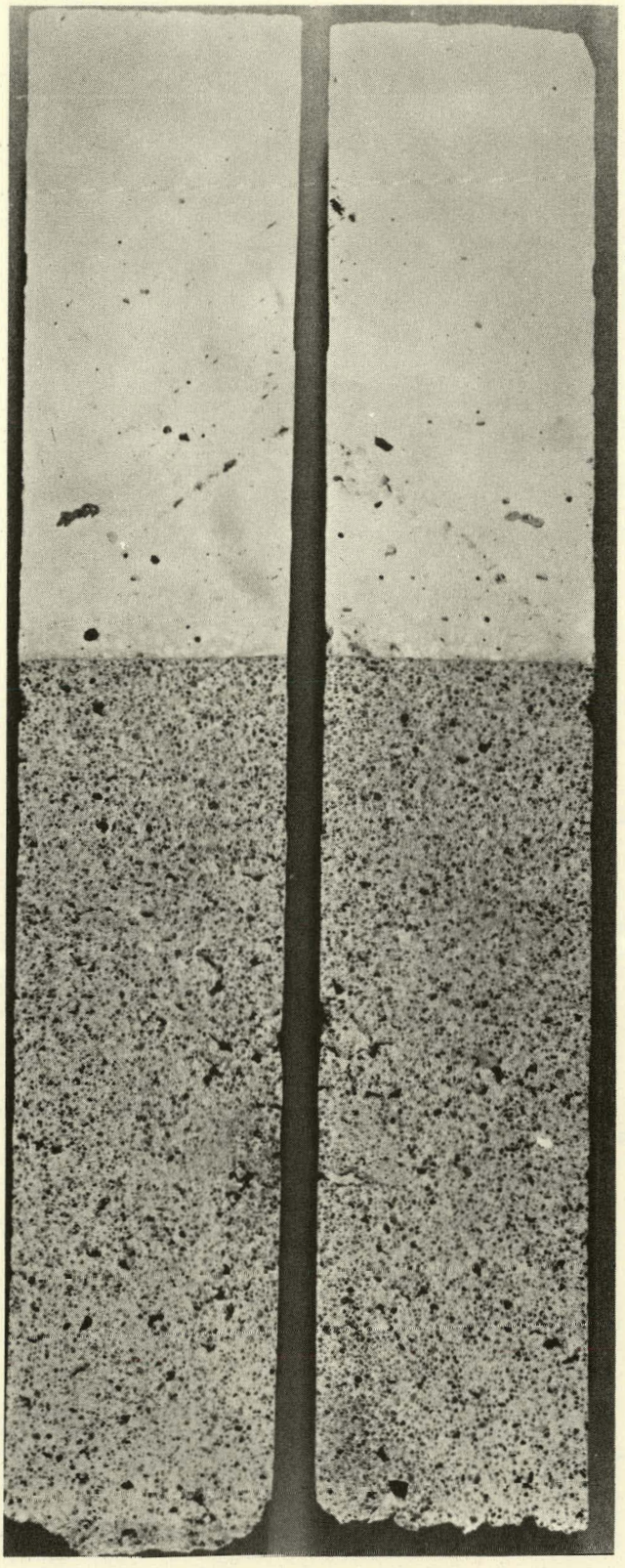

FIGURE 158. Horizontal Cut Through Drill Core Taken From Lining #2 After Test to 1200°F.

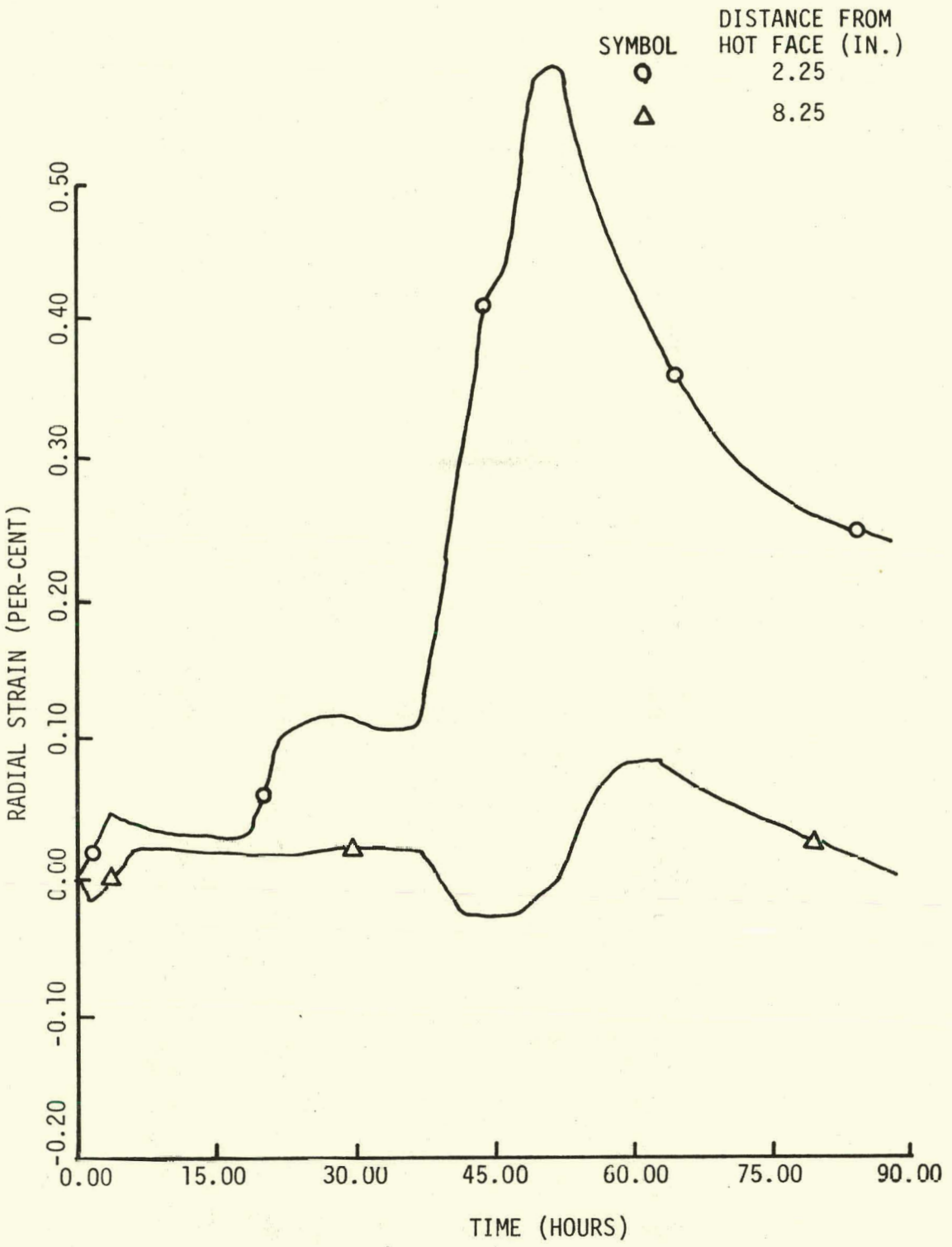

FIGURE 159. Radial Strain History of Lining #2 During Heat-up to (θ = 17°, Z = -6").

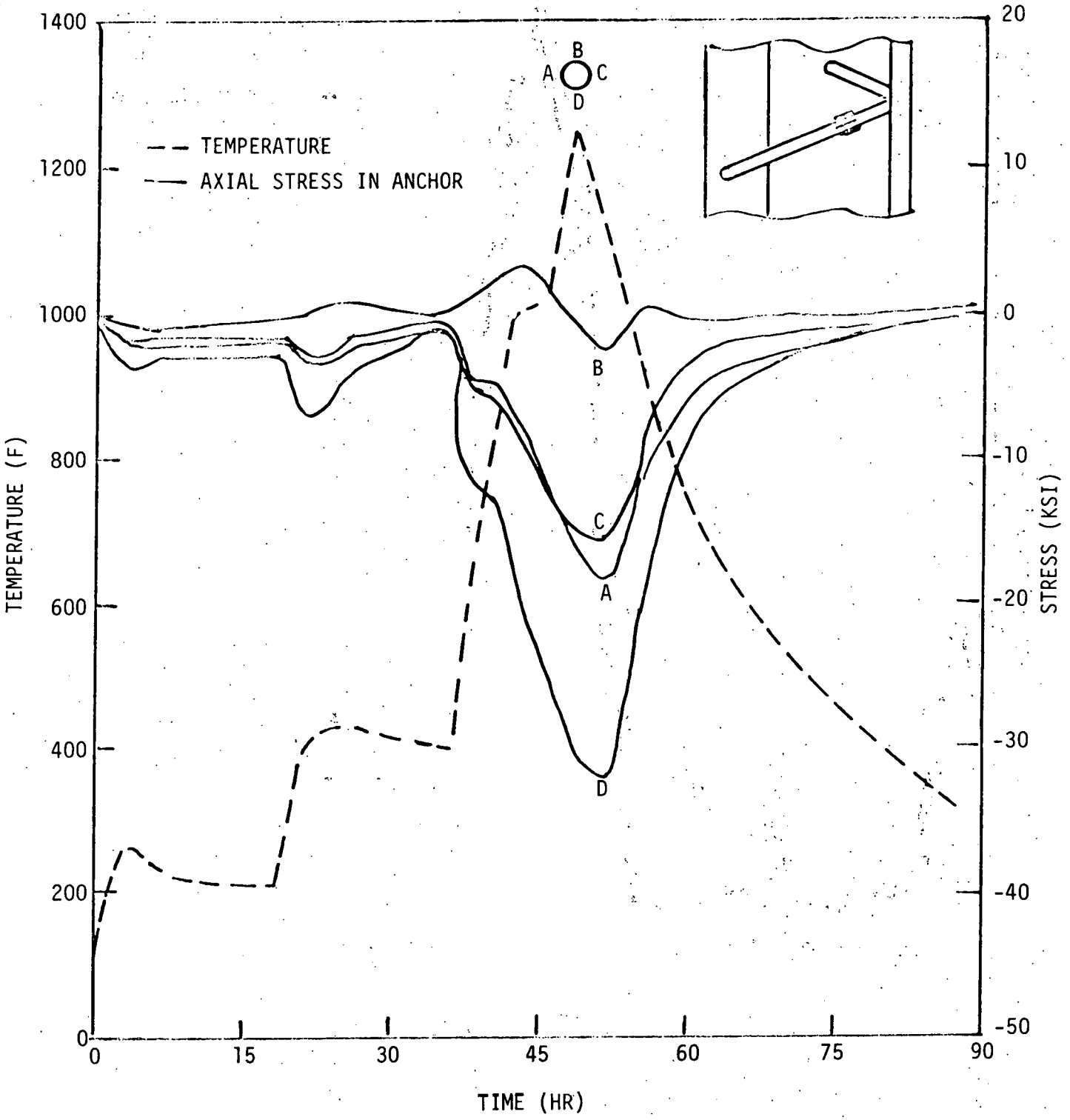

FIGURE 160. "V" Anchor Stresses From Lining #2
1200°F Heat-Up

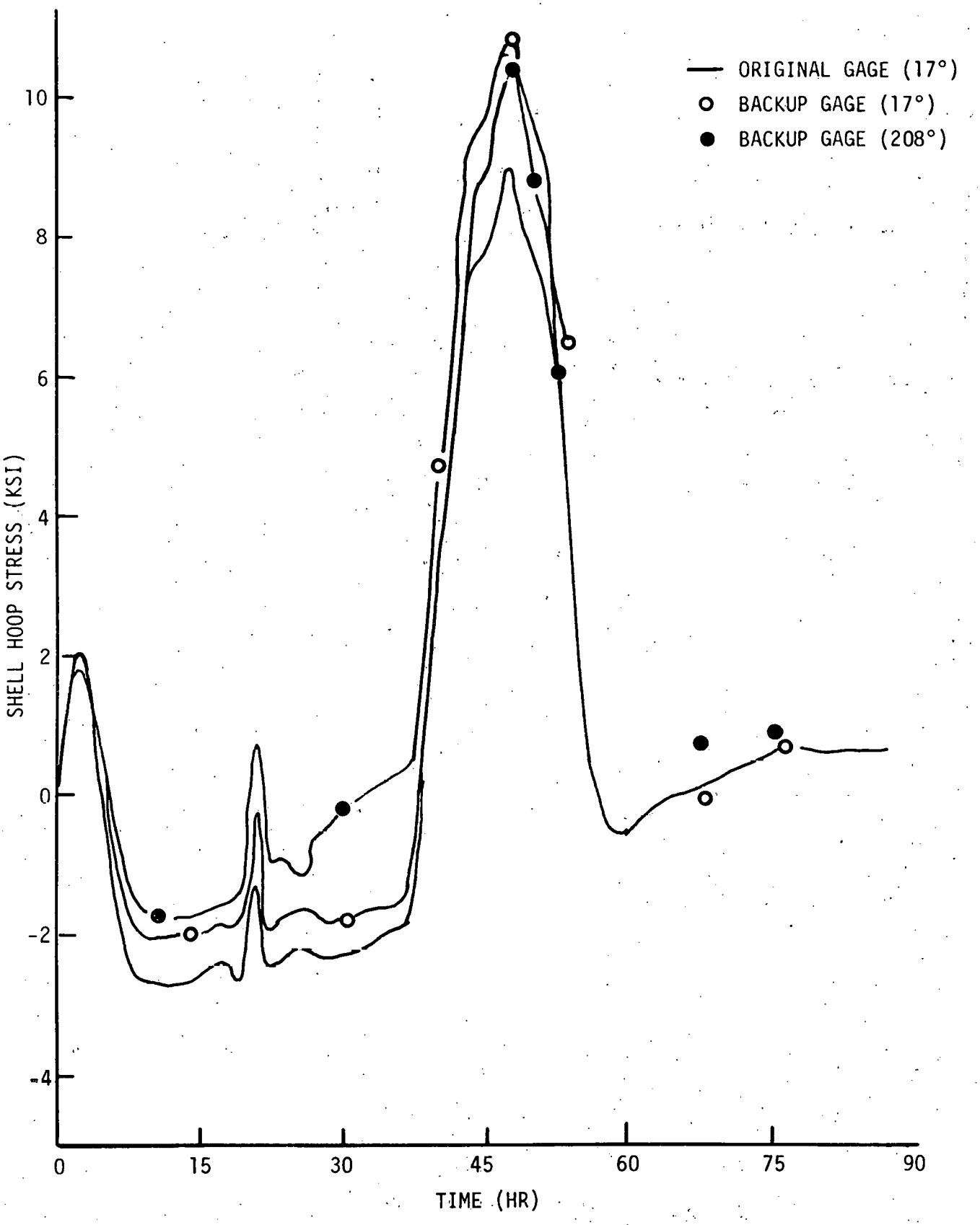

FIGURE 161. Shell Stresses At Different Circumferential Locations During Lining #2 1200°F Heat-up

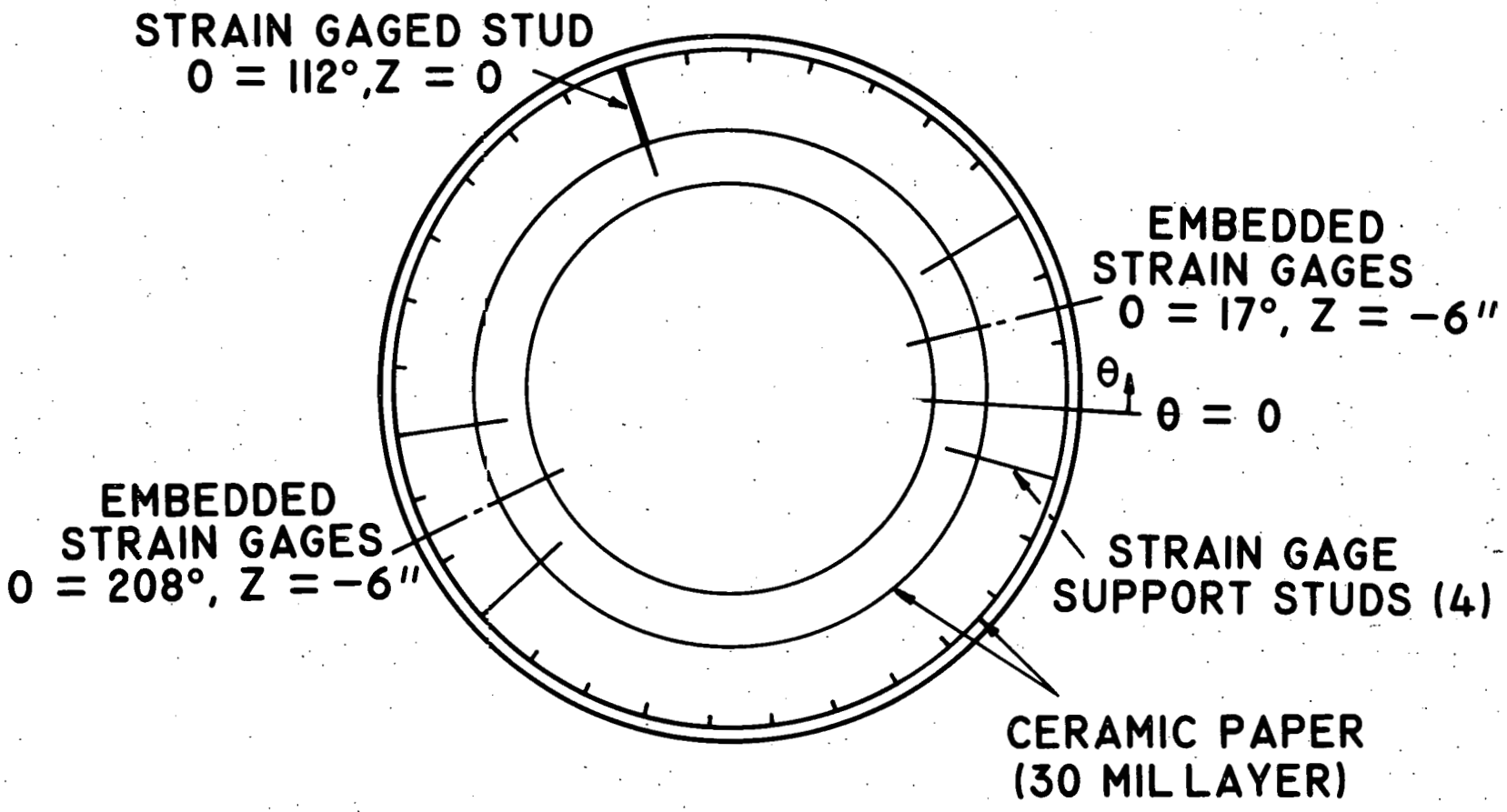

FIGURE 162. Schematic of Lining #3

Lining #3 was heated on three cycles. In addition to being instrumented, it was monitored with a video camera during two of the cycles. The findings of these tests indicated that the 90+% Al_2O_3 (ERDA 90) dense and LITECAST 75-28 materials were still quite susceptible to cracking even when the constraining effect of the anchors were removed and the overall shrinkage of the lining was less than that measured for Linings #1 and 2. However, it was demonstrated that cracks which formed in the dense component could be prevented from propagating into the insulating component by the use of the ceramic fiber paper bonding barrier and that a gap would form between the two components which got progressively larger as the test temperature was increased. Figure 163 shows the appearance of Lining #3 after the 2000°F cycle and Figure 164 shows the interface region of the lining and the presence of a 125 mil gap after the test. As can be seen from these figures, Lining #3 went through a combination of explosive spalling and thermo-mechanical cracking. The cracks in the hot face are more random than those that occurred in Linings #1 and 2 and it appears that the lining material is prone to cracking because of shrinkage and creep.

Even though a substantial amount of tape and ceramic fiber paper coating were applied to the strain gaged anchor, as shown in Figure 165, this anchor was heavily loaded (axially) during the heat-up tests and was expected to have been yielded. Actually, the stresses during the 400°F heat-up were found to be great enough to yield the anchor. This point was checked during the tear out of the lining and as shown in Figures 166 and 167, the anchor was found to be yielded and the insulating component material around it was badly cracked. These findings indicated that greater care was required to assure that an adequate gap would form around the extension nut on the anchor to prevent the dense component from interacting with it. The loading results on the anchor also indicate that hold times in the heat-up schedule at 250°F, 450°F and 1000°F are detrimental to the lining because of cyclic loading each time the hold is started and stopped. This point was checked during subsequent lining tests.

Other features of the lining investigated during the tear-out were: bonding of the insulating component to the shell and the condition of the component. Figure 168 shows the appearance of the insulating component and indicates how heavily, but randomly, cracked it is. This component was well bonded to the shell even though a bonding barrier of ceramic fiber paper was used. During installation, the paper was infiltrated by the cement phase in the insulating component which resulted in a subsequent strong bond that contributed to crack formation in the component.

One additional lining with the standard lining design type materials was tried to determine if the use of a better bonding barrier material (silicone coated ceramic fiber paper at the shell), lower top operating temperature, and a 150 psig pressurized steam atmosphere would help improve the performance of the 90+% Al_2O_3 material. This lining was designated Lining #4.

Experiments were also tried with expansion allowances around the outside of the metal forms for the dense component, use of the Case #2 heat-up schedule, and inclusion of coated, semi-coated and uncoated "Y" anchors at a two to three foot spacing. PRESSTITE* material was used to coat either the entire anchor or the extension portion.

PRESSTITE is a registered trade name of the Virginia Chemical Co., Inc.

FIGURE 163. Top View of Lining #3 After Heat-up Test to 2000°F

FIGURE 164. View of Dual Component Lining With Section of Dense Component Removed to Show Insulator and Gap at Interface.

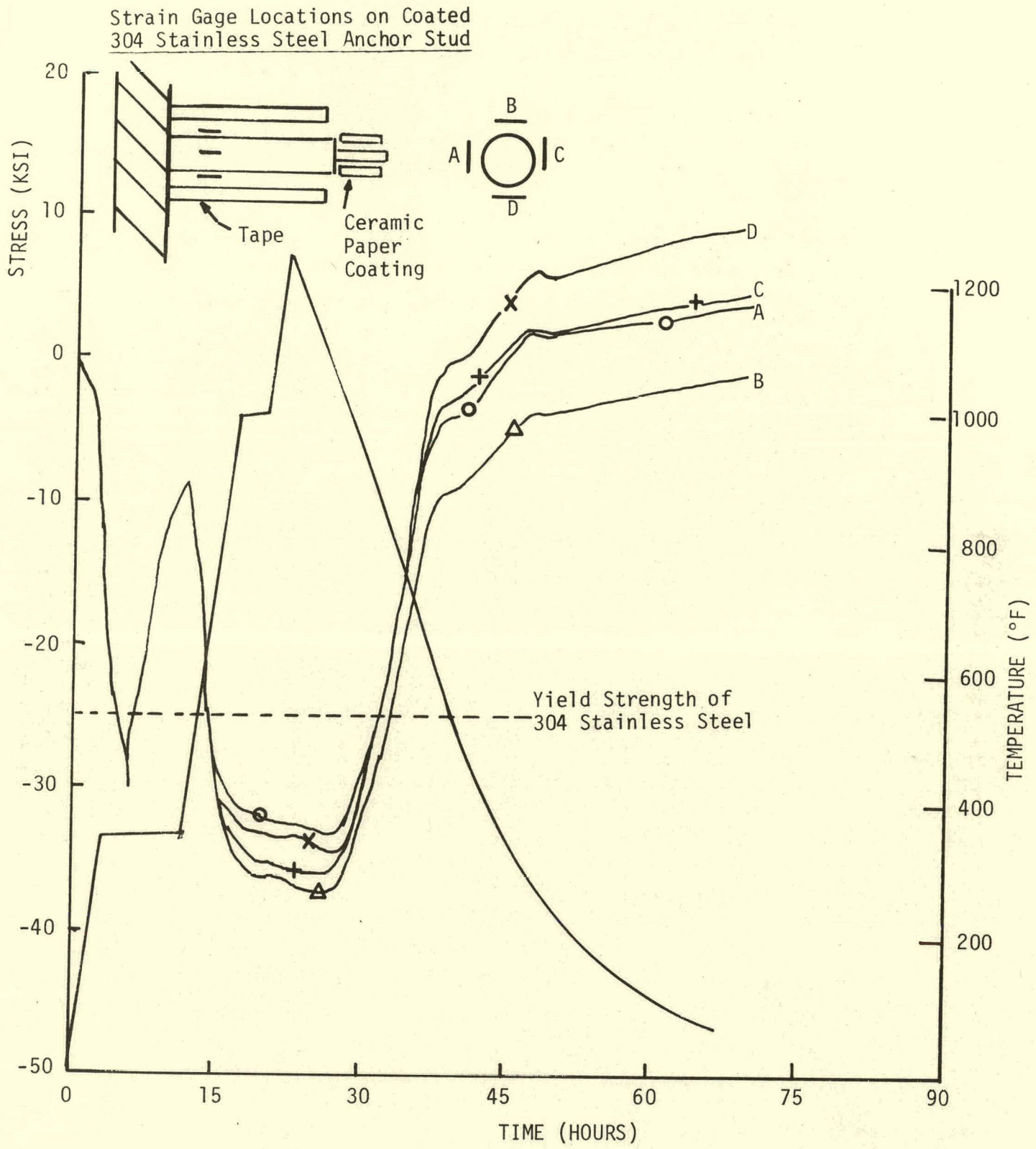

FIGURE 165. Stresses Induced in Radial Anchor During Heat-up of Lining #3 to 1200°F.

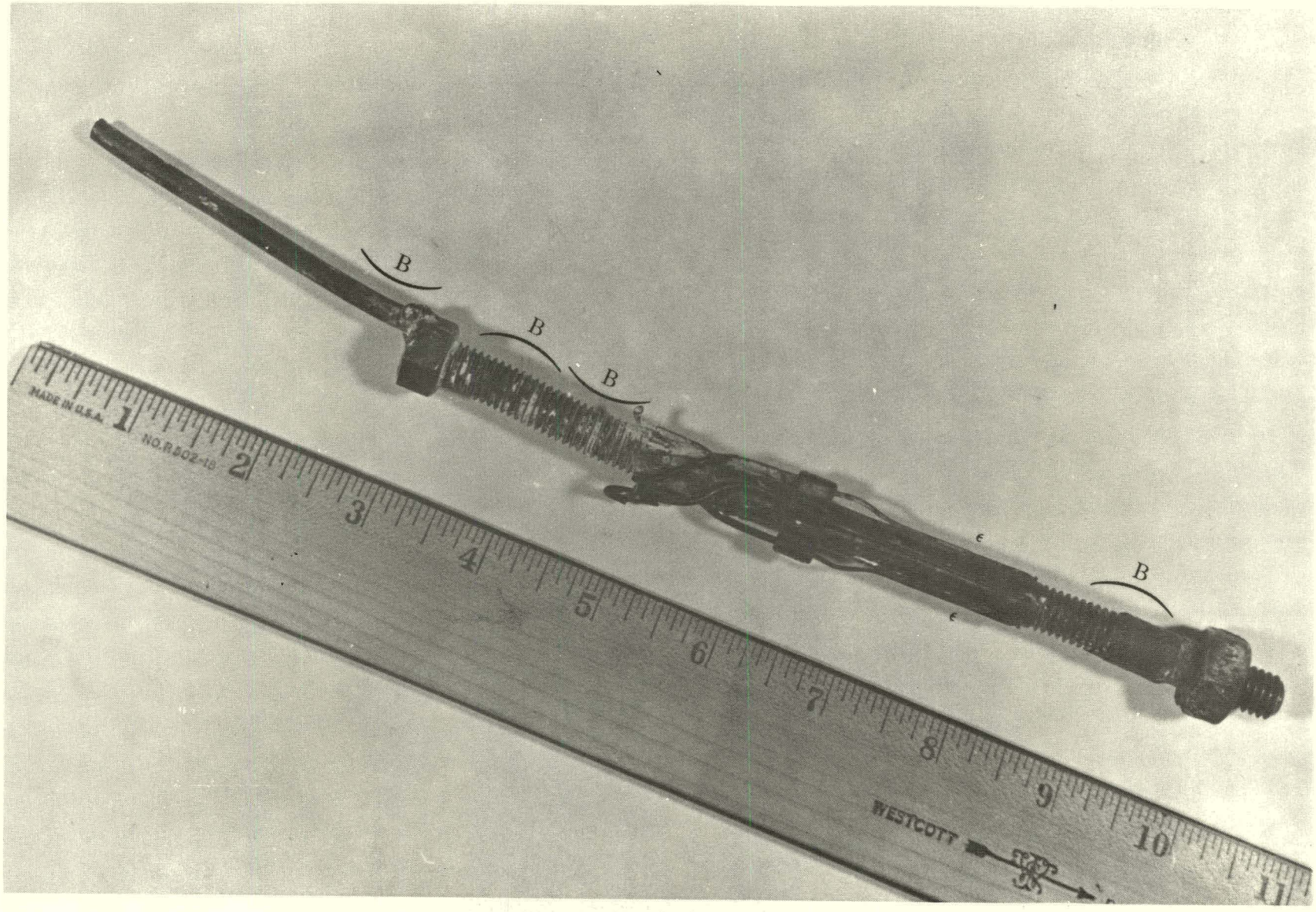

FIGURE 166. Strain Gaged Anchor Removal From Lining #3. Strain Gages are Located 3 In. From End of Anchor. Deformation Was Found in Anchor After Heat-up Test to 2000°F and Can Be Seen Adjacent to Line Markers(B).

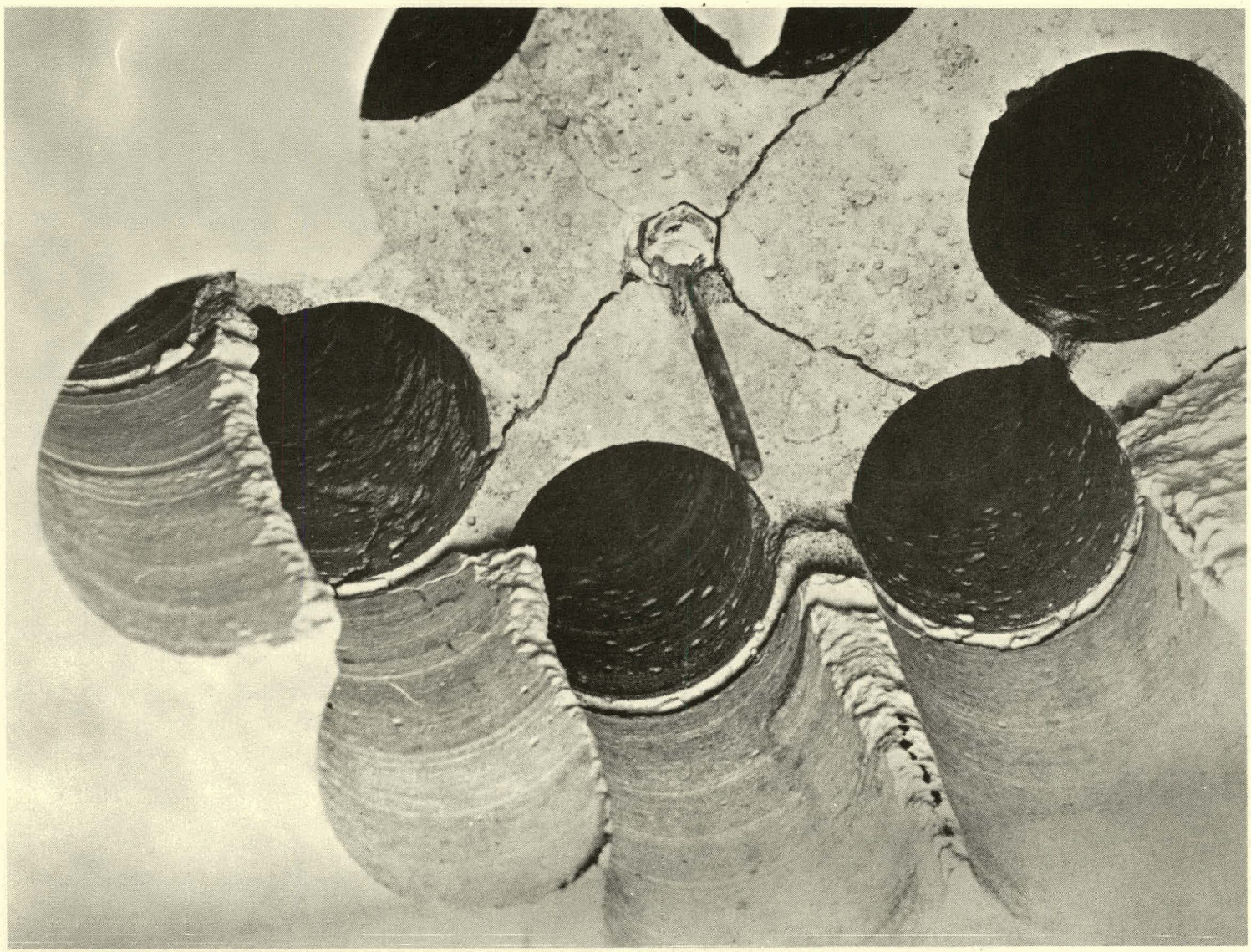

FIGURE 167. Cracking Observed in Insulating Component of Lining #3 Around Nut of Strain Gaged Anchor (Dark Regions Indicate Drill Core Sampling)

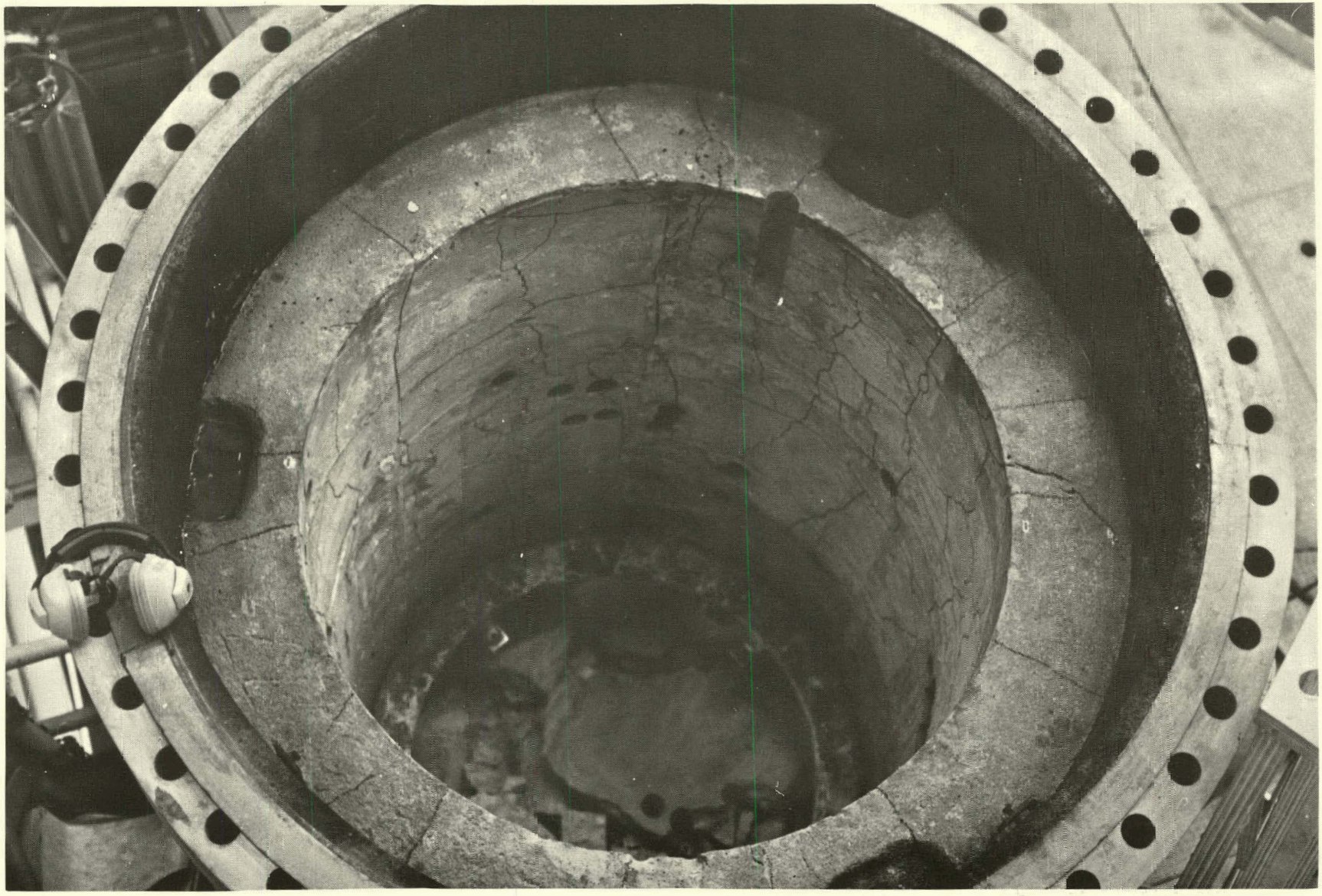

FIGURE 168. Top View of Lining #3 During Tear-out (Dense Component Removal).

Figure 169 shows the appearance of Lining #4 after the 1850°F heat-up test. It has a crack pattern similar to Lining #3 after the 2000°F heat-up cycle; however, it is not as severely cracked and the gap formed between the two components is smaller. The cracks do propagate through the entire lining in both components.

These was no noticeable effect of the pressurized steam on the dense refractory or on the insulating material. However, the shell stresses did increase as predicted by theory relative to internally pressurized vessels. The completely coated strain gaged anchor had a markedly reduced stress compared to the uncoated and partially coated anchor and indicated that the interaction had been essentially eliminated. This is shown in Figure 170 for the three type anchors during the 1200°F heat-up. The results indicate that the bonding of the insulating component material to the shaft of the semi coated anchor is apparently adequate to restrain it from elongating; and can cause it to go into compression.

As can be seen in Figure 171 the coating was completely burned away in the dense component and left an adequate expansion allowance around the extension. The coating did not completely burn away in the insulating component; however, it did create an adequate allowance for expansion.

The results from testing this lining suggested that the use of a slower heating rate (50°F/hr vs 100°F/hr), the elimination of holds during heat-up testing to a lower temperature, and the complete coating of the "Y" type anchor spaced two to three feet apart improved the performance of the lining. Even though the silicone coated ceramic fiber paper did prevent the bonding of the insulating component to the shell, it did not reduce the cracking which occurred in the insulating component. The restraining effect of the independent anchors may have been responsible for the observed crack pattern.

Based on these findings and the interest on the part of DOE in working with a 50% Al_2O_3 dense refractory concrete and experimenting with a material which had better shrinkage characteristics than the 90+% Al_2O_3 dense generic material, Lining #5 was designed to use an improved product, KAOCRETE XD 50(Mix 36C), as the dense component material. This lining was practically identical to Lining #4 in design and test plan and was found to perform as well as, if not better than, Lining #4. Figure 172 shows the appearance of Lining #5 after the 1850°F heat-up. This lining did not show any noticeable reaction with the pressurized steam or any greater resistance to cracking than Lining #4. The cracks propagated completely across the thickness of the dense component but stopped at the interface. The insulating component had a completely independent crack pattern.

One interesting result of this lining test was the very high stress measured for a completely coated anchor which had been strain gaged. The anchor stress results indicated that the anchor would be yielded due to an interaction with the lining. This result was confirmed during the post test and tear out activities on Lining #5 when it was discovered that the coating on the end of the "Y" extension had been rubbed away. This exposed the end of the anchor extension to the dense KAOCRETE XD 50(Mix 36C) material and caused a localized deformation as shown in Figure 173. These results indicate the importance of using a stiff coating material and core during the installation of the anchors and lining.

FIGURE 169. Top View of Lining #4 Hot Face After Heat-up Test to 1850°F and 120 psig Steam.

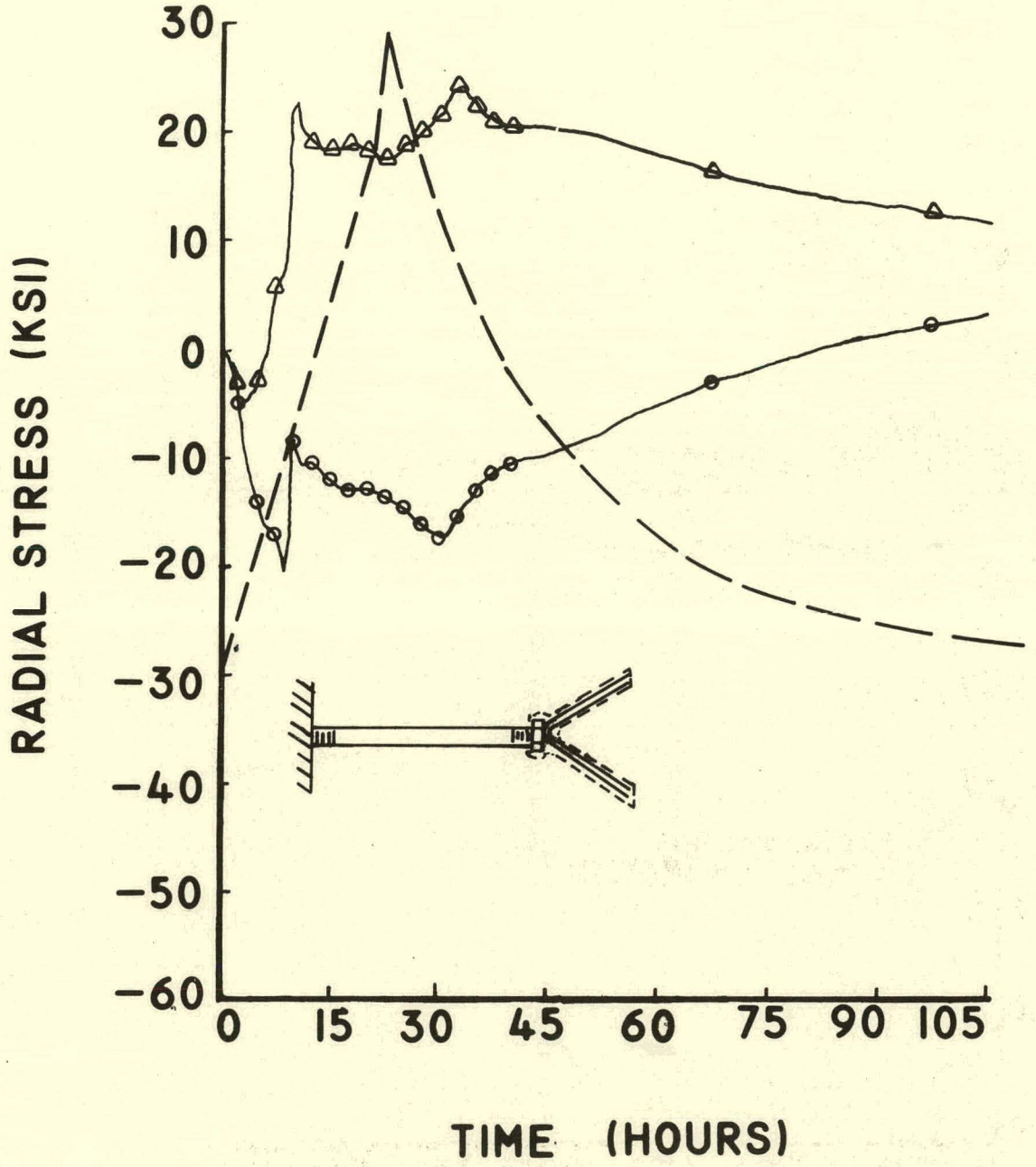

FIGURE 170. Stresses Induced in Anchors During Heat-up of Lining #4 to 1200°F (Z = 0").

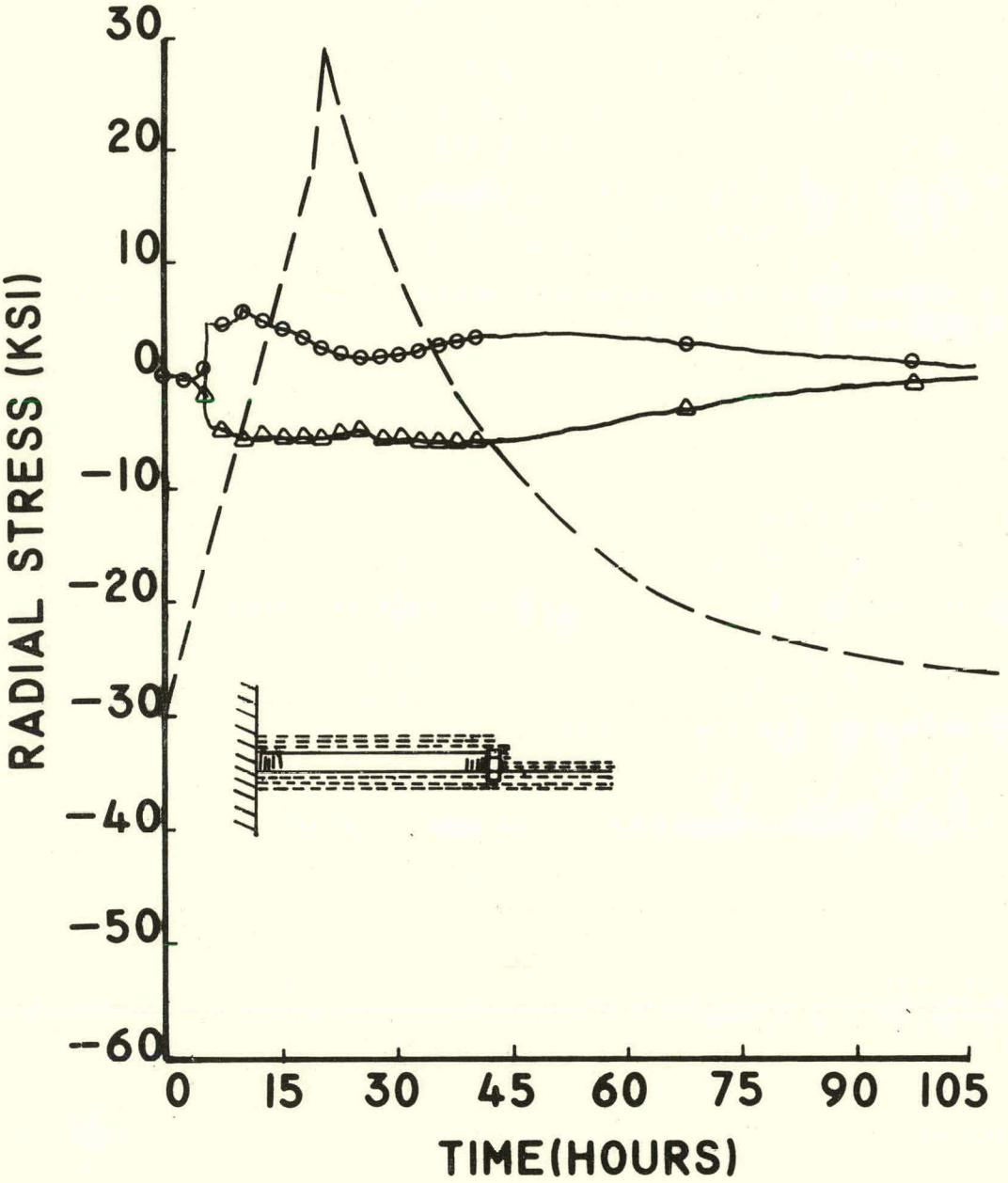

FIGURE 170. (Cont'd).

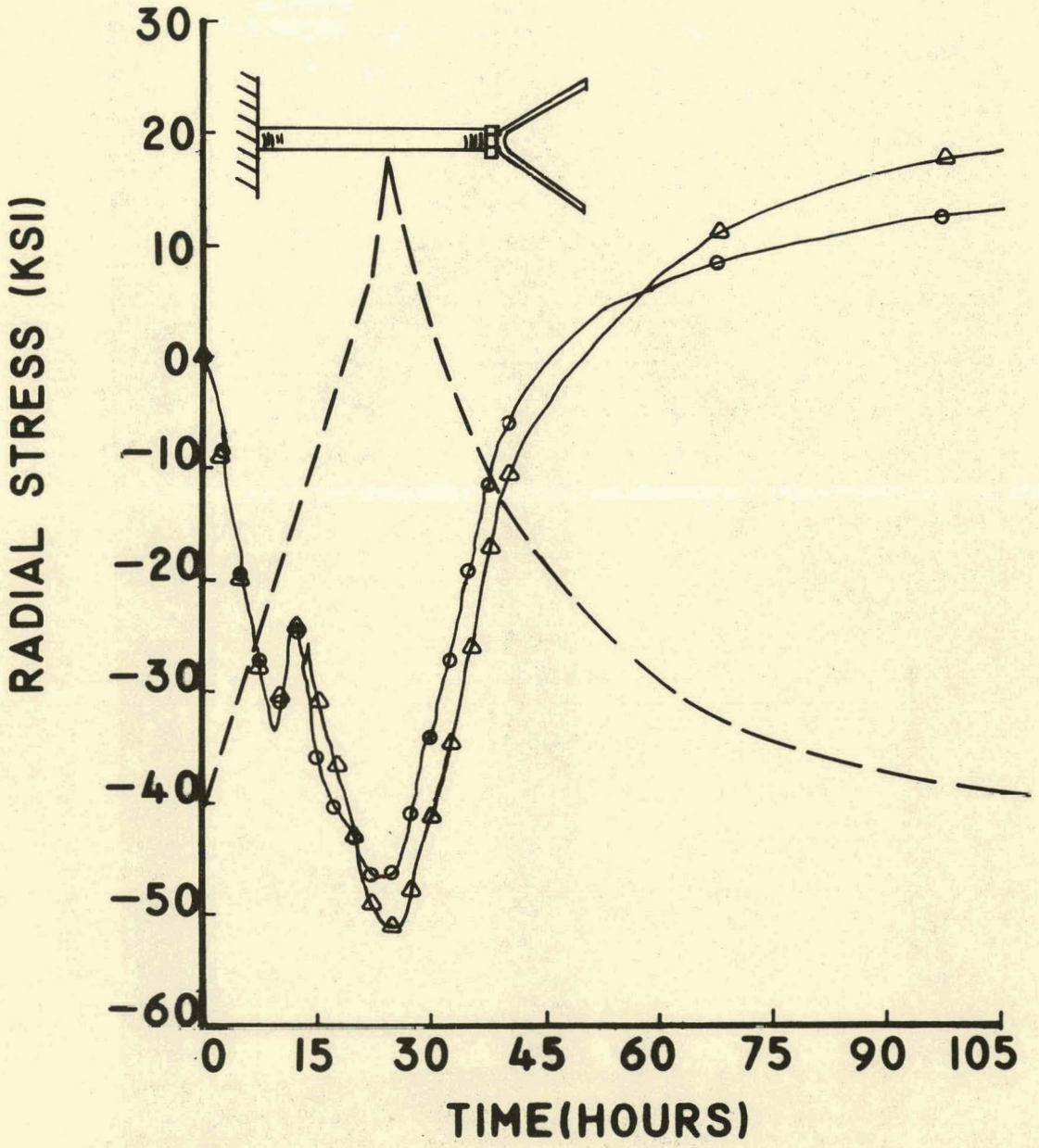

FIGURE 170. (Cont'd.)

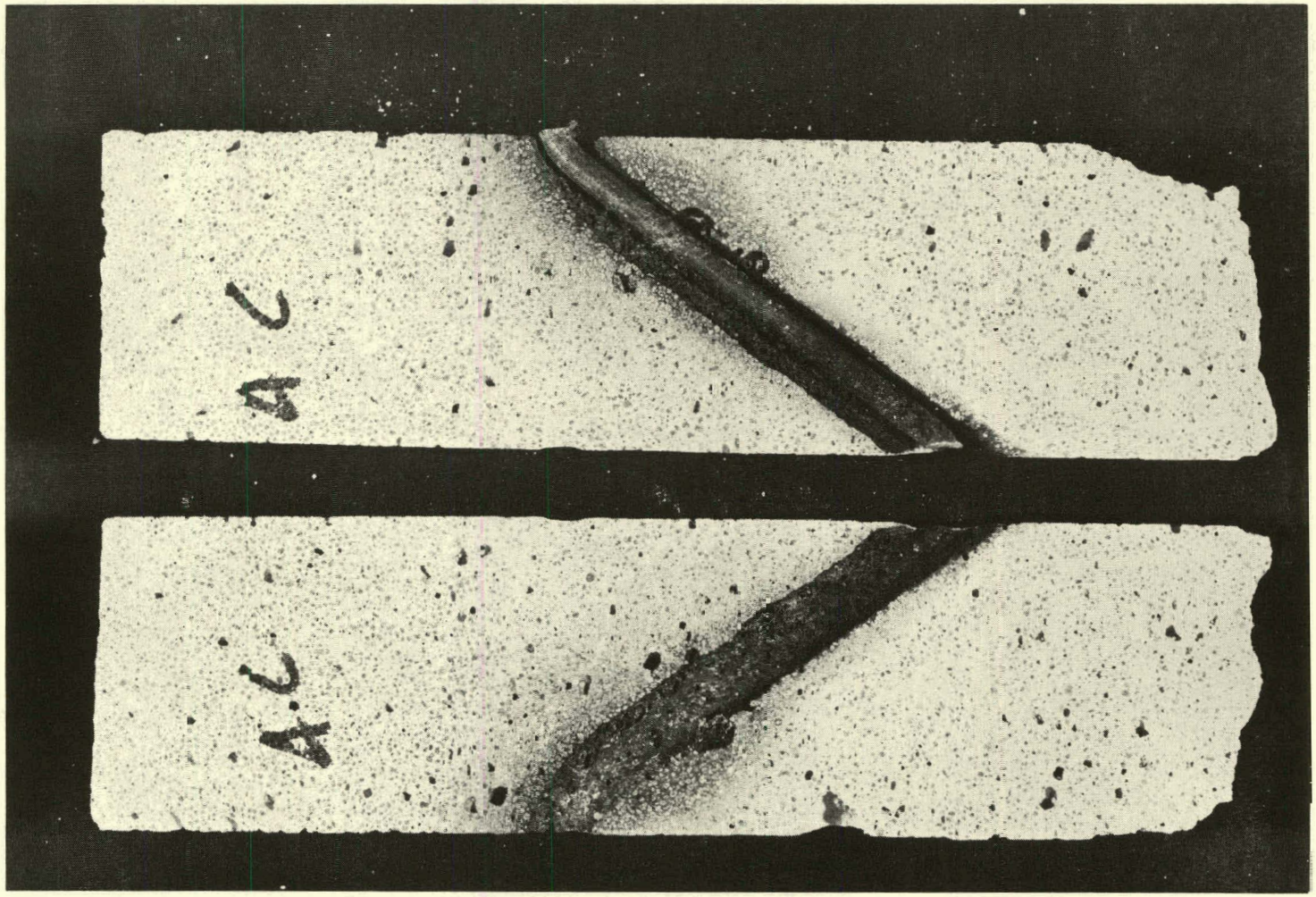

FIGURE 171. Drill Core From Lining #4 After 1850°F Test Showing Gap Around Anchors (Wrapped With 100 Mil Asphalt Tape During Installation).

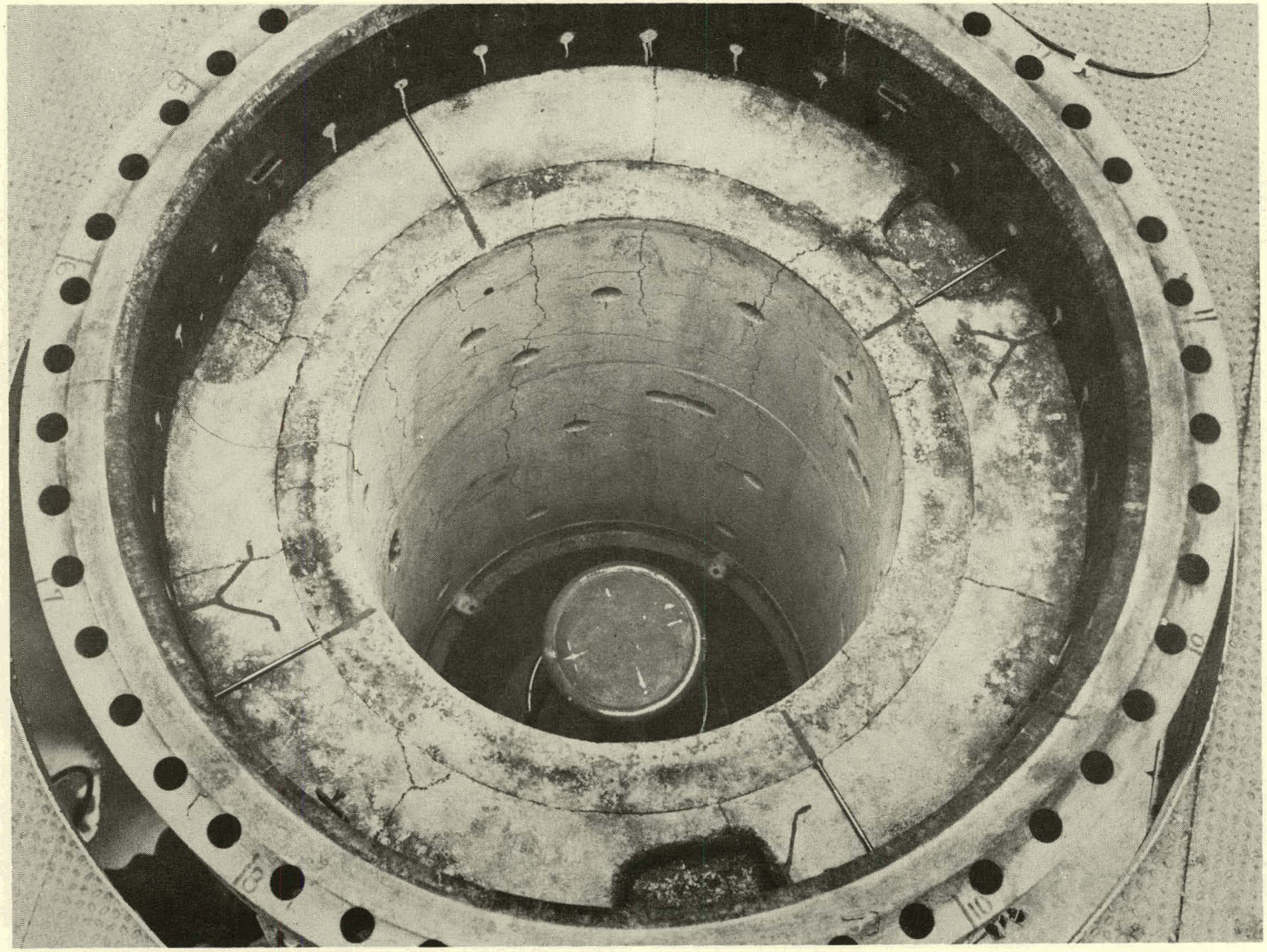

FIGURE 172. Top View of Lining #5 After Heat-up Test to 1850°F and 140 psig Steam (Shaft Locations of Anchors Indicated on Top Surface).

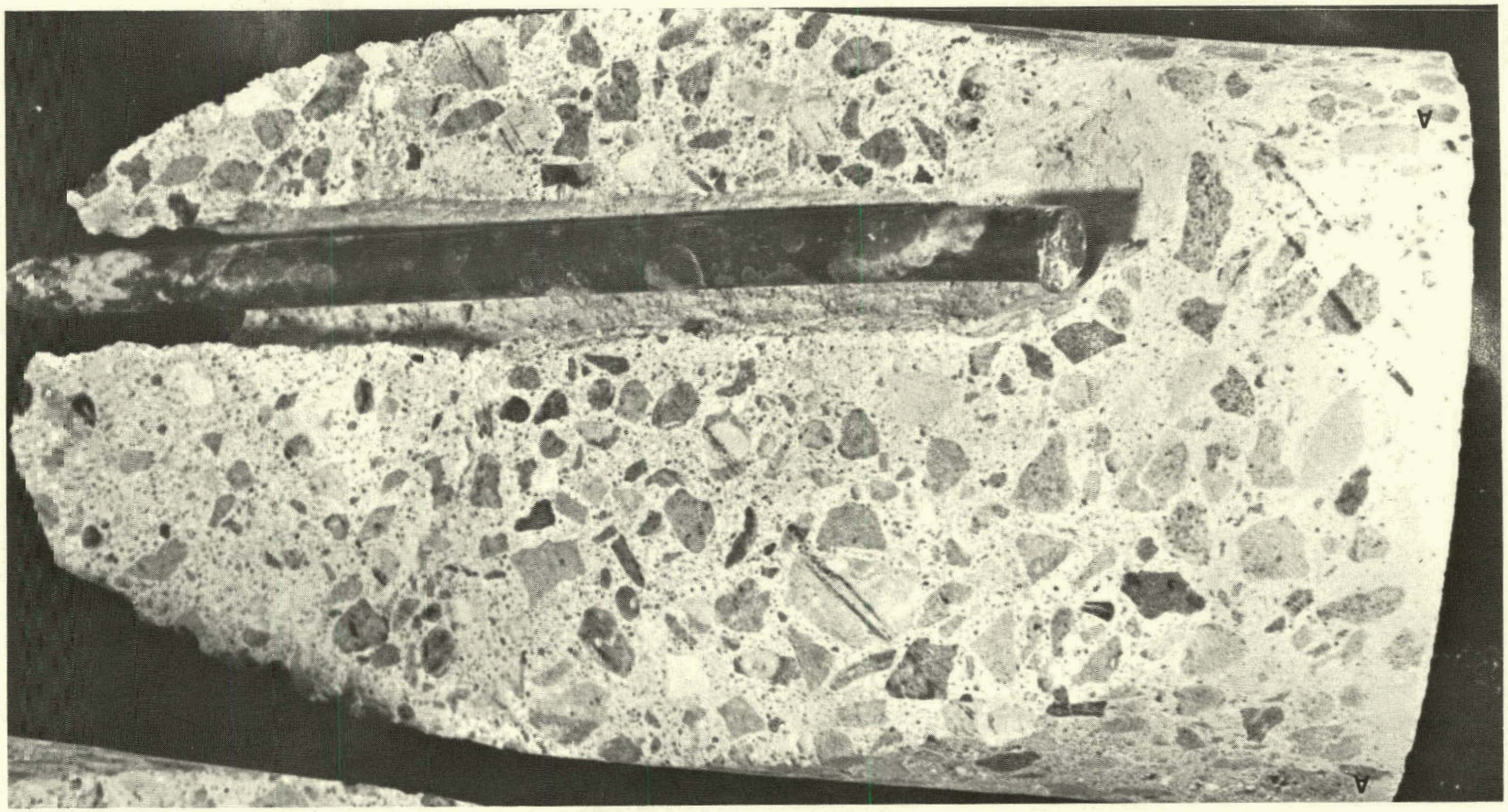

FIGURE 173. Sectioned Drill Cores From Dense Component of Lining #5 After 1850°F Test (Note Gap Around Combustible Coated Anchor).

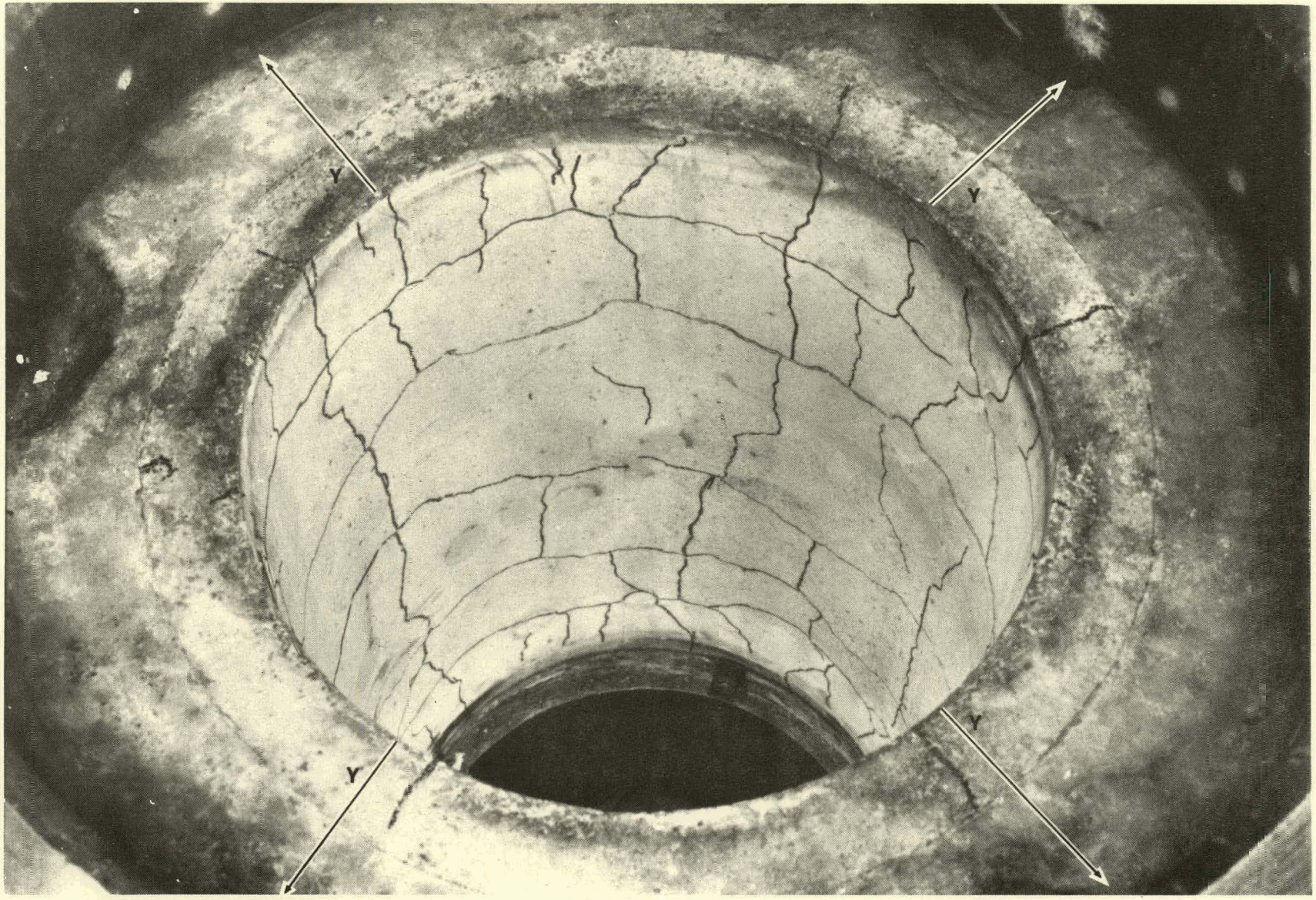

FIGURE 174. Top View of Lining #6 Hot Face After Heat-Up Test To 1850F, 35 Hrs With Steam Pressure of 120-150 psig. Cracks Have Been Highlighted With Blank Ink. Straight Lines (Y) Indicate Location of Top Row of Anchors (Photo No. P-78-638E).

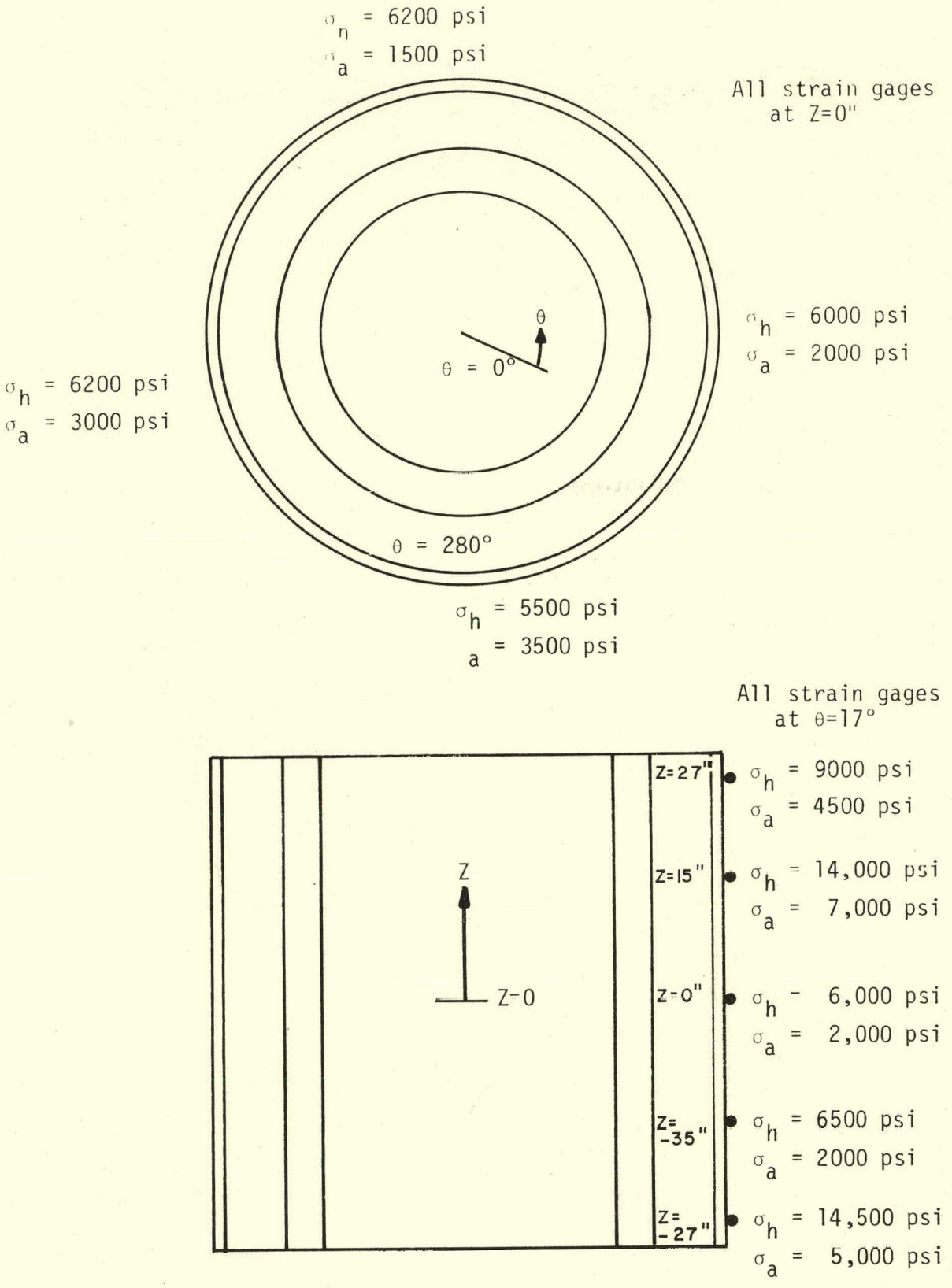

FIGURE 175. Hoop and Axial Shell Stresses at 30 Hrs. Into 1850°F Heat-Up Test of Lining #6.

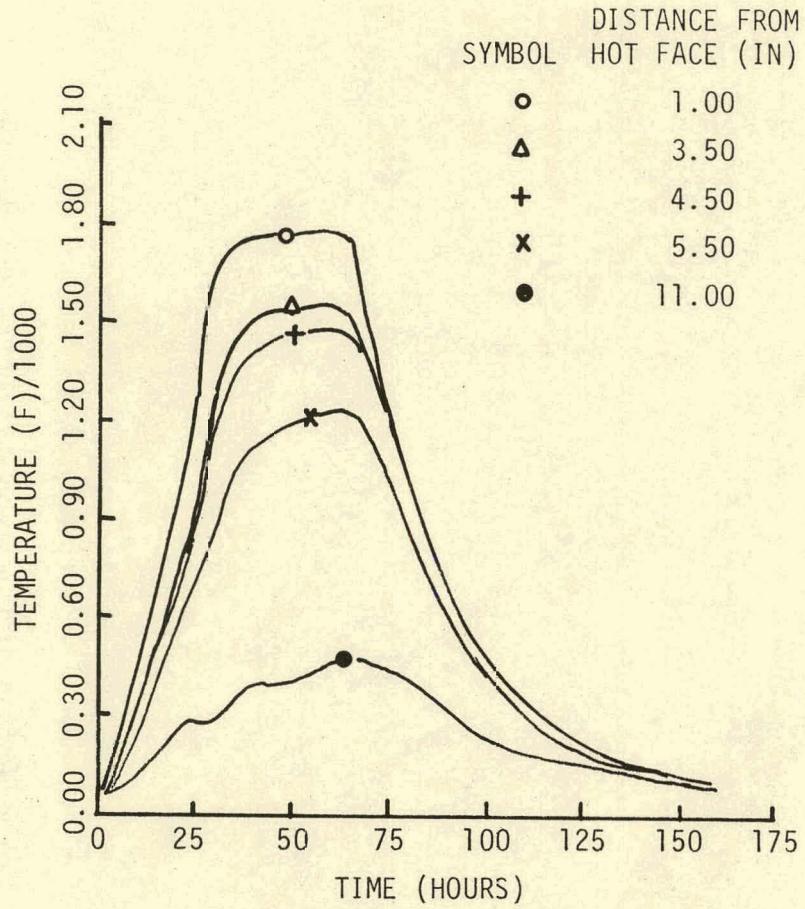

(a) Temperature History

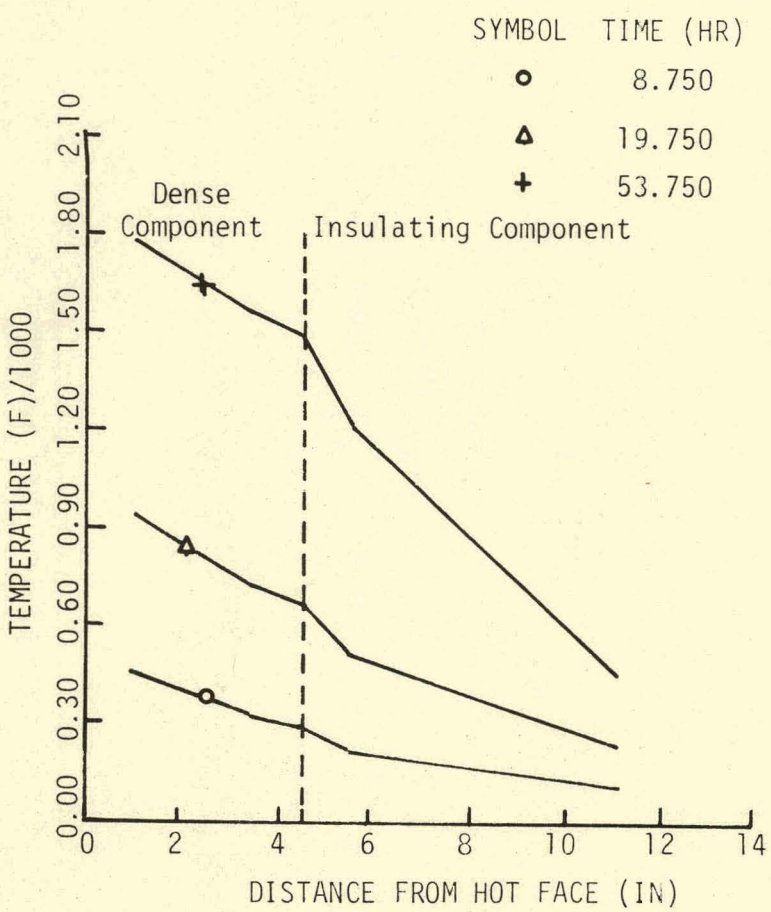

(b) Temperature Profile

FIGURE 176. Temperature History and Profile For Lining #6 During 1850°F Heat-up Test (θ = 266°, Z = -6).

FIGURE 177. Cross Section of Lining #6 After Two Pressurized Steam (120 psig) Heat-Up Tests at 1200 to 1850°F.

Figures 178 and 179 show the appearance of Lining #7 after the first cycle to 1700°F on the Case #2 heat-up schedule, and after three cycles. The lining had very little shrinkage after each cycle (less overall than the previous linings tested) and had a very fine, random crack pattern that did not propagate completely through the lining. It was found that the cracks which had formed during the first cycle to 1700°F had stabilized and not grown during the second and third cycles. Evidence of this is shown in Figure 180 for the dense component. Three drill cores were taken along the same vertical crack, one after each of the three cycles. As can be seen in Figure 180, the crack did not grow from one cycle to the other. This was considered to be a major improvement in performance. The insulating component material acted in the same manner.

The shell stresses indicated quite well the expected differences between the first and subsequent cycles; and similar differences were seen in internal pore pressure between the first and subsequent cycles. These differences in shell stresses are shown in Figure 181-182 for the three heat-up tests and the pore pressure results for the first cycle are presented in Figure 183. The shell stresses induced during the initial heat-up show the immediate interaction between the lining and shell followed by a relaxing of the stress as the lining shrinks. This is followed by a sharp rise and fall in stress which appears to be creep related. This initial lining interaction effect is missing on the second and subsequent cycles and is replaced with a phase of no lining interaction followed by a sharp rise to peak stress. This result suggests that the gap which is known to exist after the first cycle must close first before the lining begins to interact with the shell. The monitoring of shell stresses can therefore be a means of understanding what is happening to the lining during service.

Relatively low, but significant, pore pressures were generated in the lining during the first cycle. These pressures dissipate as the initial heat-up progresses and are higher in the insulating material, because of process water, than the dense material. They are not a factor in the subsequent cycles.

Since Lining #7 was considered to meet the goal of a lining design with reduced cracking, it was reheated at two rapid (>200°F/hr) heat-up and cooldown cycles to determine if its performance changed significantly. The results of the tests indicated that only minor additional surface cracking of the dense component occurred; however, there was further cracking in the insulating component although it was not considered severe. Another drill core was taken from along the same vertical crack and compared to the previous three drill cores. As shown in Figure 184, the crack depth in the fourth core is approximately equal to that of the previous three. These results suggest that the 310 stainless steel fiber addition to the KAOCRETE XD 50 improved its fracture toughness and reduced its tendency to crack even though the fibers degrade its creep resistance.

Based on these results, the findings of the stress analyses, the hollow cylinder work, contacts with R. Pierce of Pennwalt Corrosion Engineering Div., N. Severin of Hotworks Services and the DOE; a decision was made to modify both the insulating material and the design of Lining #7 to futher improve its performance. This lining was designated Lining #9 and was composed of three layers of material instead of the two used in all the previous linings. It was to be heated at a slower heating rate than was used in any of the previous tests (25°F/hr vs 50°F/hr). The lining was designed with an acid resistant mortar which had good refractoriness and would stretch as it was heated and cured. The idea behind using this material was that a third layer was considered a good

FIGURE 178. Top View of Lining #7 Showing Oxidized Metal Fibers (Dark Spots) After 1850°F Heat-Up Test In Air.

FIGURE 179. Top View of Lining #7 After Three Thermal Cycles (1700°F in Air, 1700°F in 100 psig Air, and 1850°F)

FIGURE 180. Drill Cores of Dense Component Adjacent to Same Vertical Crack (Lining #7 - Three Thermal Cycles).

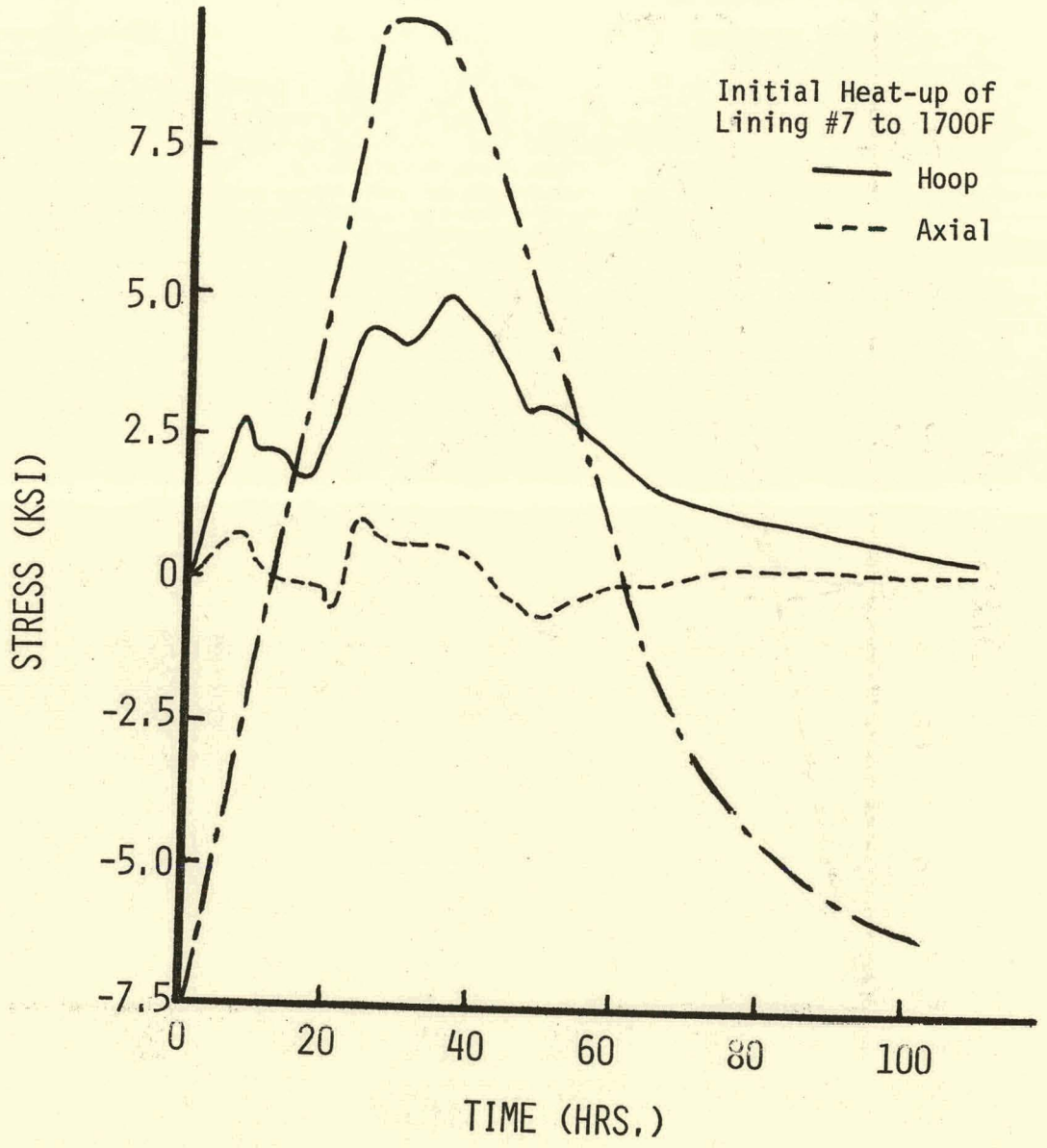

Figure 181. Shell Stresses for Lining #7 During First Heat-up to 1700°F on Case #2 Schedule

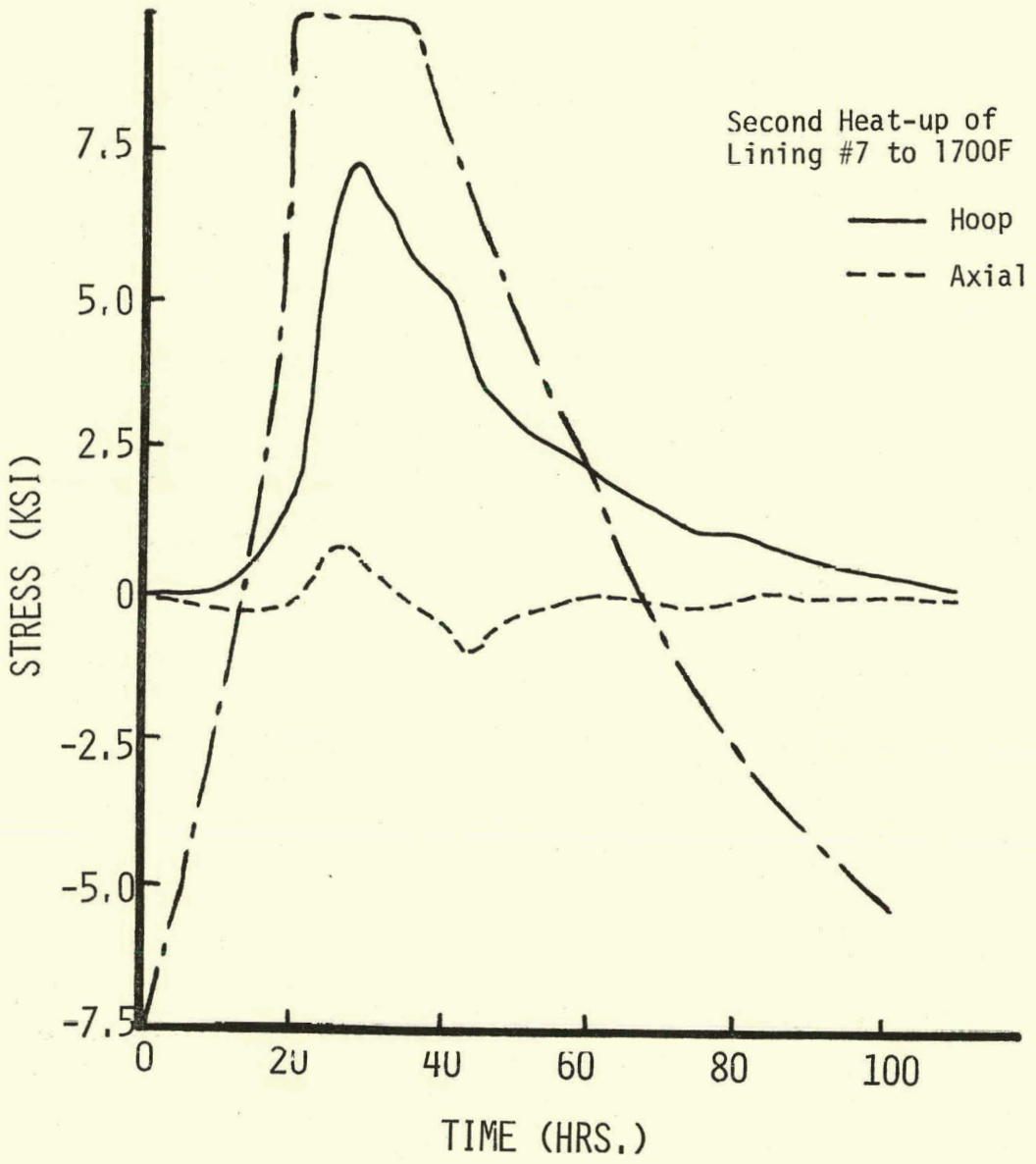

Figure 182. Shell Stresses for Lining #7 During Second Heat-up to 1700°F on Case #2 Schedule

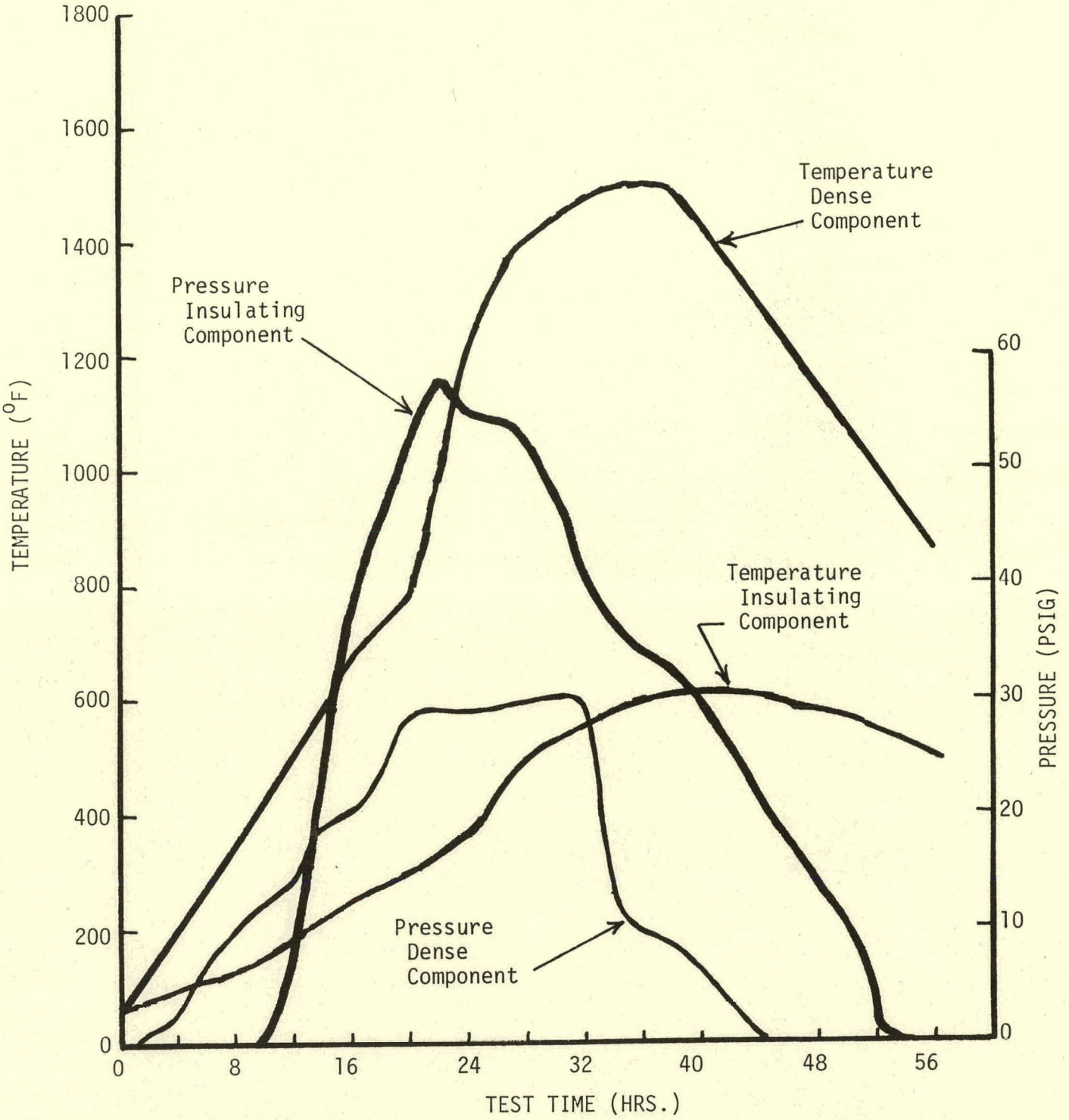

FIGURE 183. Internal Refractory Pressure during Initial Heat-up of Lining #7 to 1700°F.

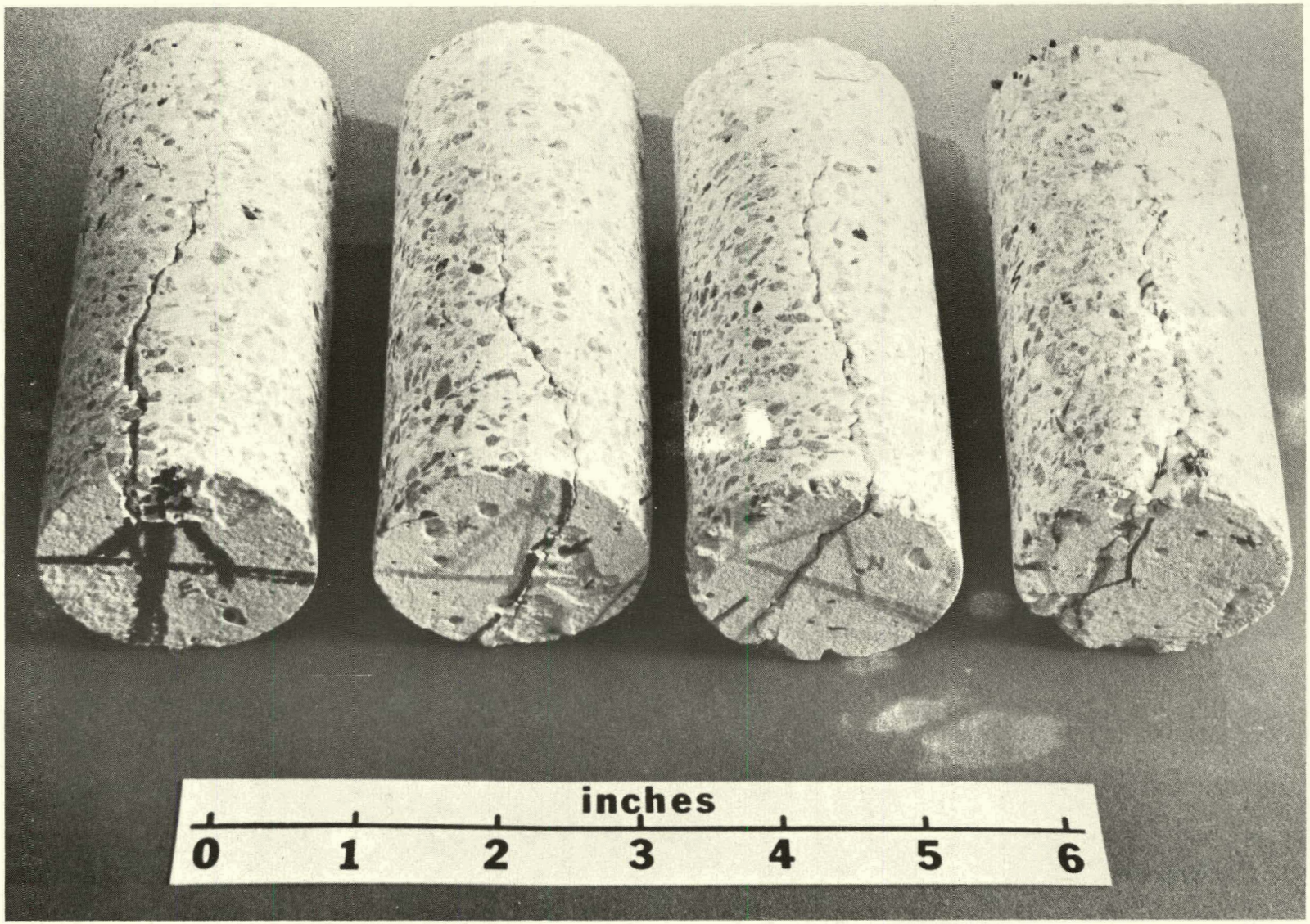

FIGURE 184. Drill Cores of Dense Component Adjacent to Same Vertical Crack (Lining #7 - Five Thermal Cycles).

approach to lower stresses and temperatures. In addition, if it were acid resistant, it could afford added protection to the vessel shell in a corrosive coal gasification type environment. This layer was bonded securely to the shell using the procedure outlined below and then covered with four mil plastic sheet to protect it while the rest of the lining was installed. KAOLITE 2300 LI was used as the insulating component material instead of the LITECAST 75-28 and KAOCRETE XD 50 with 4 w/o 310 stainless steel fibers was the dense component refractory material. Figure 185 is a schematic of this lining design.

The KAOLITE 2300 LI was used to determine how a weaker, less stiff, but better insulating material than LITECAST 75-28 affected the performance of the lining. The use of the slow continuous heat-up rate was based on the previous results and input from N. Severin of Hotworks Services on field practices.

HES Lining And Installation

Prior to installation of the HES* layer, the inside surface of the vessel shell was sandblasted to promote good bonding of the acid resistant material. No bonding barrier was used between the HES layer and the shell. This component was troweled onto the shell surface in two 1/4 inch thick layers for a total thickness of 1/2 inch. During installation the processing parameters for the HES mortar material were carefully monitored in a manner similar to that for the refractory castables. The mortar was a two component system of cement and aggregate to which water was added. It was mixed with a Hobart mixer to achieve a workable material. Important processing conditions are listed in Table 37. Figure 186 is an overhead view of the vessel during the HES installation.

After the HES material was installed, the heating assembly was placed in the vessel and used for curing. The curing schedule was based upon a recommendation by the Pennwalt Corporation. The schedule was 20 hours to reach 200°F and a 35 hr. soak at 200°F.

To determine if the use of 150 psig steam during the entire dry-out and heat-up would benefit the performance of the lining, Lining #6 was run on two cycles to 1200°F and 1850°F. This lining was almost identical to Lining #5 in design except that the independent anchors were not used and a new series of strain gages were applied to the shell to generate more reliable shell stress data around its circumference and along its length. This latter instrumentation was to check for end effects. One other experiment planned involved running the tests for up to 40 hours at temperature and pressure to determine if steady heat transfer conditions would occur and how this would affect cracking.

Figure 174 shows the appearance of Lining #6 after the 1850°F cycle. The crack pattern is similar to that of Lining #5 after a much shorter test but it has a fairly large 30-40 mil horizontal crack in it which suggests the dense component had been constrained from contracting freely during the cooldown of the 1200°F run. The shell stresses showed variations both circumferentially and axially which did not correspond clearly to end effects, but rather to localized temperature effects (See Figure 175). The stress levels were lower, however, than they had been for the standard lining design. The temperature profile through the lining as shown in Figure 176 indicated that steady state conditions were being approached in 35 to 40 hours at 1850°F and that the temperatures were high enough to cause both shrinkage and creep to occur.

*Registered Trademark, Pennwalt Co.

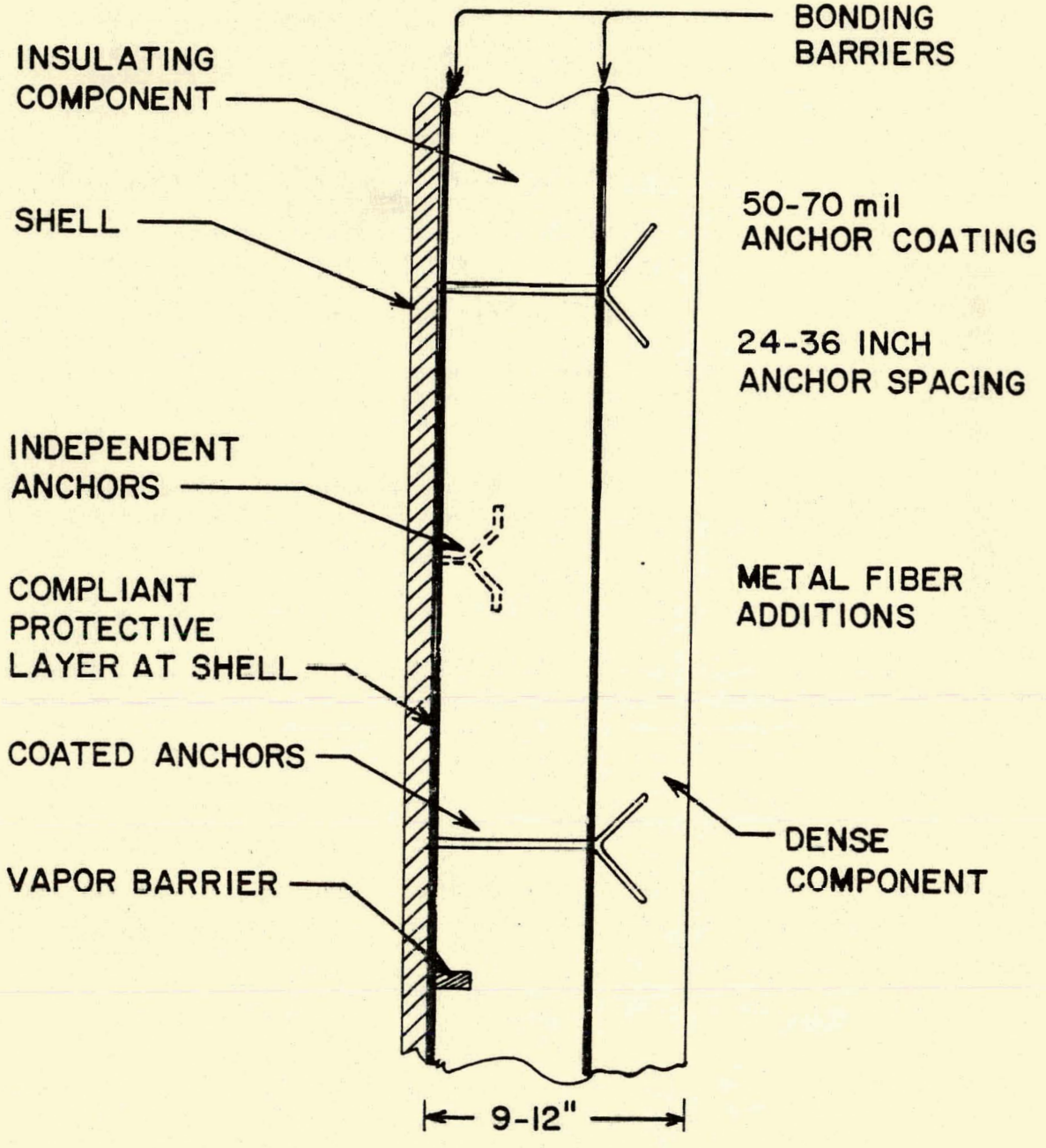

FIGURE 185. Schematic of Improved Lining Design.

TABLE 37. Processing Conditions for HES Component in Lining #9

Steel Temperature - 81-83.5°F
Mixing Water Temperature - 80°F
Material Temperature - 80°F
Mixing Water pH - 6.6
Steel Surface pH - ~ neutral
Air Temperature - 80-85°F
Wet Bulb Temperature - 75°F (70% Saturation)
Steel Dew Point Temperature - 74°F
Installation Time of 1st Layer - 6 hrs.
Installation Time of 2nd Layer - 3 hrs.

FIGURE 186. Installation Technique Used to Place HES Mortar on Inside of Vessel For Lining #9 Test.

The LITECAST 75-28 insulating component, as cast, was found to be denser and considerably stronger than it had been in previous linings, but it was again severely cracked and had a similar pattern to the other linings. This can be seen in Figure 177 for both the dense and insulating components. No strength enhancement was detected in either material after the pressurized steam runs.

Since no major changes occurred in the linings when the 90+% Al_2O_3 dense generic was replaced with a 50% Al_2O_3 dense material in the modified design (except from some additional insulation effect), plans were developed to try other materials and designs while continuing to work with the 50% Al_2O_3 dense refractory concrete. The first change involved the use of stainless steel fibers. This was considered to be applicable to coal combustors, but concern was raised about how well these fibers would stand up to a coal gasification atmosphere. To resolve this question, samples of castables containing stainless steel fibers were sent to the U.S. Bureau of Mines in Tuscaloosa and tested in both clean and sour coal gases at high pressures. The results [25] were very encouraging and showed little or no effect of H_2S and other corrosive gases in a short term (500-1000 hr) test.

Based on these results, Lining #7 was planned. It was to include 4 w/o 310 stainless steel fibers in the 50% Al_2O_3 dense component material (KAOCRETE XD 50) coated "Y" anchors, and running two or more heat-up tests to 1700°F or higher without stopping at 1200°F as was done in all previous lining tests. It also included monitoring the internal pore pressure of the lining during the first heat-up.

The other two components of Lining #9 were cast in a manner similar to the previous linings. They were 7" of Kaolite 2300LI and 4-1/2" of the 50% Al_2O_3 dense castable. The mixing and casting summary is presented in Tables 33 and 34. The Lining #9 installation also included 4 mil thick plastic sheet bonding barriers between the HES layer and the insulating component and at the interface between the insulating and dense refractory concrete material. Only one type of anchor was used in this lining. This was a standard "Y" anchor, used in previous linings, coated with approximately 80 mils of an asphalt tape. This was 20 mils thinner than previous anchor coatings. These anchors were spaced 30-36 inches apart. The V leg extensions of all anchors were oriented vertically to be consistent with earlier linings. Figure 187 shows the plastic bonding barrier and coated anchors prior to installation of the dense component.

Instruments were installed at the vessel shell and within each component to measure the internal pore pressure during the heat-up test. Techniques similar to those used in Linings #6 and #7 were used in Lining #9. Oxidized stainless steel tubes (1/4"OD) were embedded into both the dense and insulating components to measure pressure at the midpoint of each. During casting, the tubes were filled with removable wire to prevent the castable from entering the tube. These tubes were monitored with pressure transducers which were connected to the computerized data acquisition system; a millivolt recorder provided a continuous record of fluctuations. Pressure gages were also attached to penetrations through the vessel shell to monitor pressure on both sides of the HES.

Figure 188 is the appearance of Lining #9 after a 25°F/hr continuous heat-up to 1850°F. The dense component had some very fine, hairline type cracks in it but they did not propagate very far into the material as indicated by

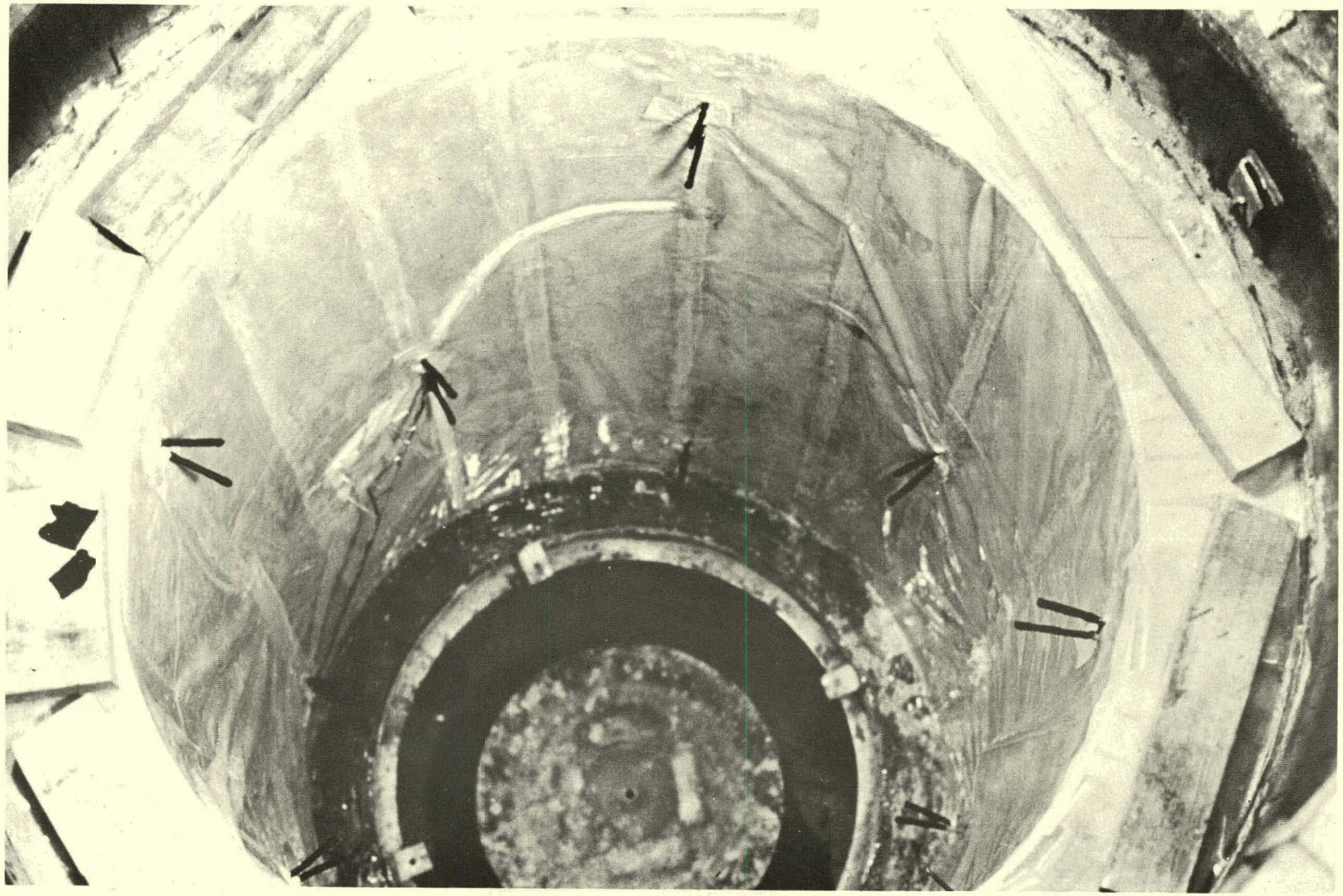

FIGURE 187. Appearance of Lining #9 After Installation of KAOLITE 2300 LI, Plastic Bonding Barrier, and Coated Anchor Extensions.

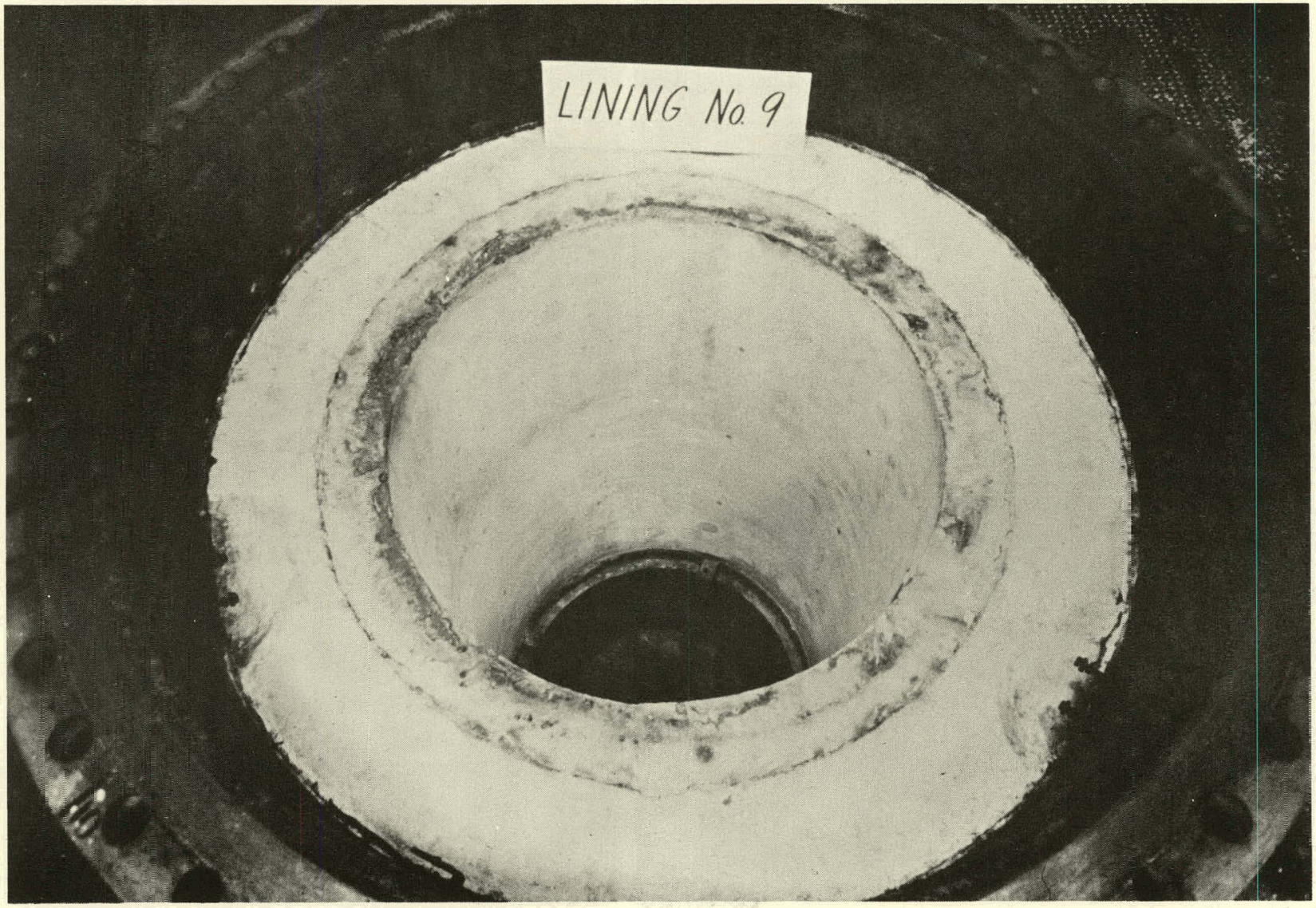

FIGURE 188. Appearance of Lining #9 After Heat-Up Test to 1850°F.

the appearance of the drill core in Figure 189. The insulating component was cracked badly and many of the cracks propagated to the shell. As shown in Table 35, Lining #9 shrank very little compared to the other linings; however, a gap formed between the components. Figures 190-193 show the thermal and stress history of Lining #9. The lining had the lowest shell stresses, shell temperature, pore pressure and lining strains of any of the linings previously tested at high temperatures. The lining temperature and shell stress results agree favorably with the thermal and stress analyses done on Lining #9 with REFSAM and indicate that the proper choice of materials and design parameters had been used to give an optimized design. It also appears that the use of a slow continuous heat-up schedule to top temperature without stopping at 1200°F has a beneficial effect on lining performance.

FIGURE 189. Drill Cores of Lining #7 and #9
After 1850°F Heat-Up Tests.

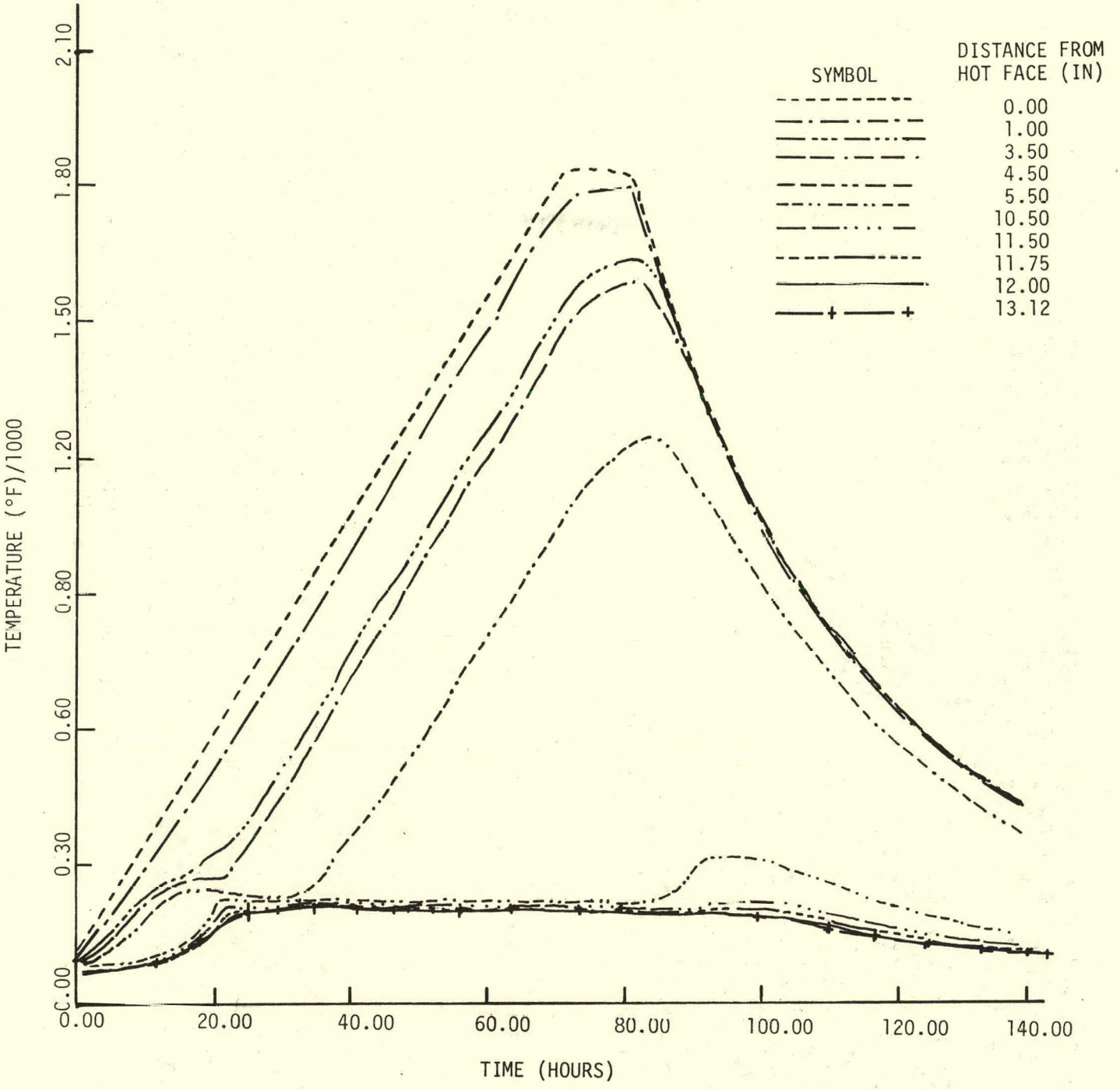

FIGURE 190. Temperature History of Lining #9 During Heat-Up Test to 1850°F.

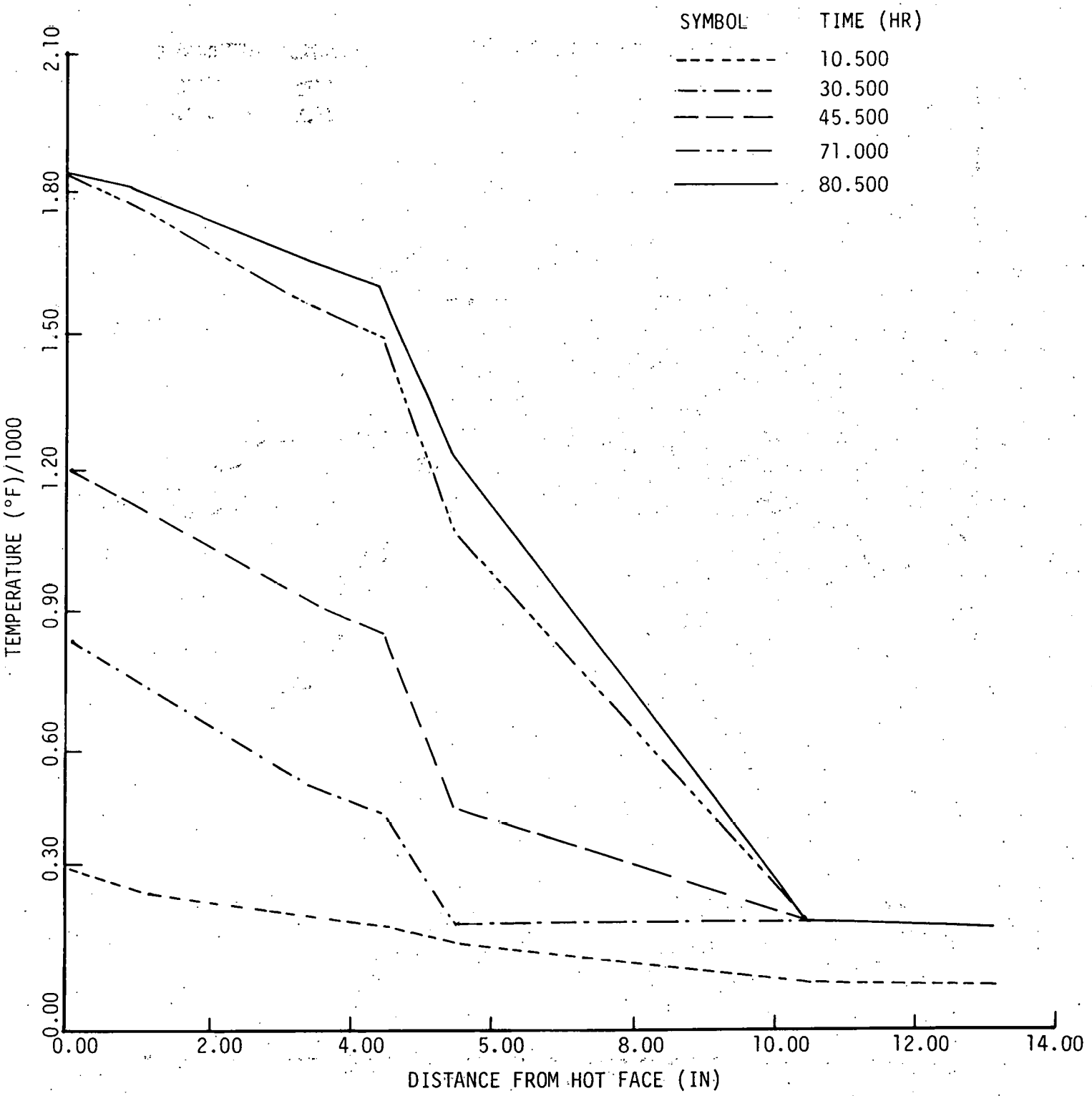

FIGURE 191. Temperature Profile of Lining #9 During Heat-Up Test to 1850°F.

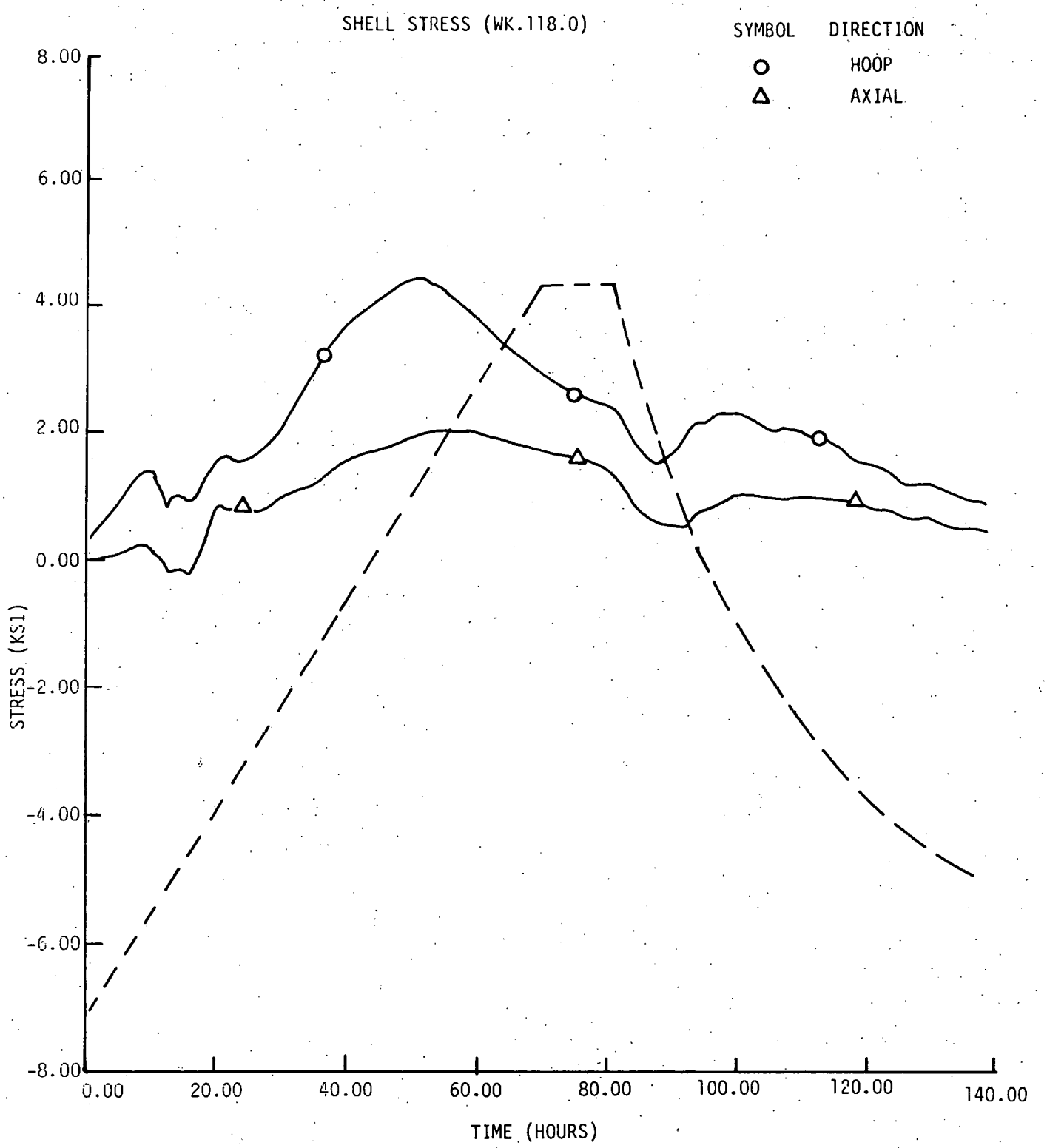

FIGURE 192. Hoop and Axial Shell Stresses During Heat-Up Test of Lining #9 to 1850°F.

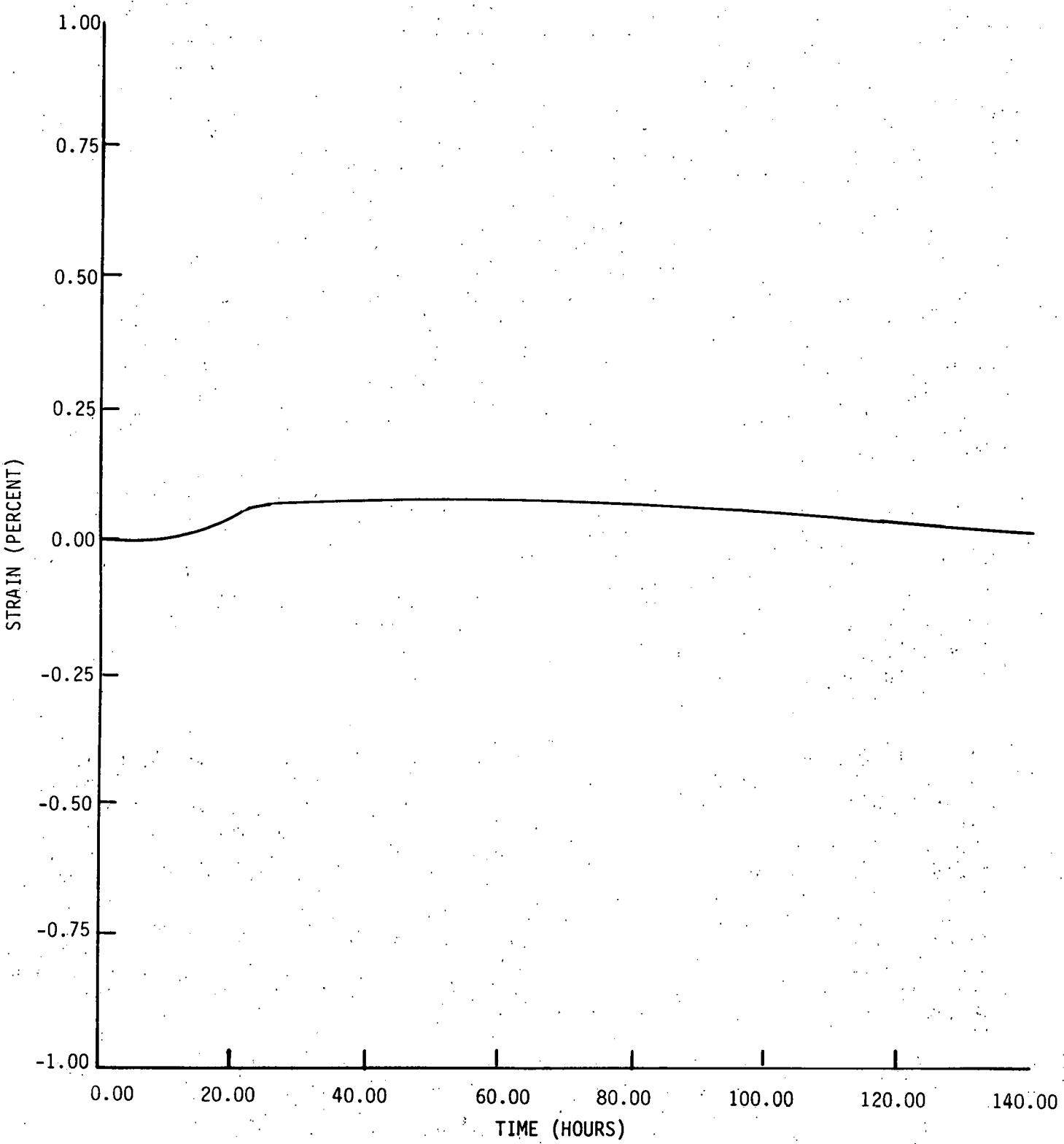

FIGURE 193. Hoop Strain in HES Mortar Layer During Heat-Up Test of Lining #9 to 1850°F.

3.5.7. Acoustic Emission

During the course of this investigation, fifteen full-scale lining tests were monitored for acoustic emission activity. Those tests were designated 1, 1-A, 2, 3-A, 3-B, 3-C, 4-A, 4-B, 5-A, 6-B, 6-C, 7-A, 7-B, 7-C, and 9. Table 38 contains a summary of the AE results obtained from those tests. In some instances, both AE systems (Dunegan-single channel, and AETC-multichannel) were used to record the activity. In those cases the total ringdown counts and total event counts listed in the table were obtained from the single channel AE system's data. Table 38 also lists the maximum hot face temperature reached during the tests, since this parameter influenced the relative amount of AE generated in a given test.

An interesting observation from the data listed in Table 38 is that the accumulated ringdown counts were always greater in the second and third thermal cycles of any one lining configuration. For example, test 7-A was the first thermal cycle of the "lining 7" configuration and produced 202,000 ringdown counts. Tests 7-B and 7-C were subsequent firings of the same lining (no new refractory installed) and produced 466,000 and 533,000 counts, respectively. The same was true of lining configurations 3, 4, and 6, each of which had multiple firings monitored for AE. An exception to this observation occurred in the results for test 3-A, which had 2,550,000 counts recorded due to an equipment malfunction. (This was an obvious electronic failure; i.e., counts were recorded even without sensors connected.)

The above observations imply that a greater amount of lining degradation was induced during additional thermal cycling of the linings. The observations also support the assumption that the acoustic emission detected during these tests was the result of liner degradation by cracking and not by less severe effects such as steam release. Most of the free water held in the uncured refractory linings was forced out during the first thermal cycle. Subsequent firings, however, generated greater amounts of AE, suggesting that steam release was not a significant influence in the AE results.

Figures 194 - 208 are the plots of Relative Energy per Event for each of the large scale lining tests monitored for acoustic emission. Each figure also has the hot face temperature profile overlayed on the AE data for reference. These figures are intended to show when significant degradation was occurring in each test. It is difficult to form correlations from test to test because each lining had a different configuration (material composition, heating rates, anchor types, anchor positions, internal pressure, plastic coatings at component interfaces, ceramic paper coatings at component interfaces, etc.). Even second and third cycles of the same lining design represented new test conditions because the refractory materials had been altered by the previous thermal cycles. In spite of the variable test conditions, several generalized statements can be made concerning the relationship of the Relative Energy per Event data to other measured parameters. Those relationships are as follows:

- There was increased AE activity plus larger Relative Energy per Event occurring during the dynamic portions of the temperature cycles. The largest amplitudes correspond to the largest slopes (rapid changes) in the heating rate.

TABLE 38. Summary of Lining Tests Monitored With Acoustic Emission Instrumentation

Lining Test No.	Maximum Hot Face Temp. (^{o}F)	AE System(s) Used	Total Ringdown Counts	Total Envelope Counts	System Gain (Total)	Remarks
1	1200	Dunegan & AETC	375,000	16,000	≈ 60 dB	
1-A	2000	Dunegan & AETC	750,000	16,000	≈ 60 dB	
2	1280	Dunegan	1,050,000	63,000	≈ 85 dB	
3-A	400	Dunegan	2,550,000 (Equipment Problem)	64,000	≈ 84 dB	• Detected Electrical Noise from Other Instrumentation
3-B	1200	Dunegan	11,500	2,500	≈ 84 dB	• Explosive Spall @ 16.7 hrs.
3-C	2000	AETC	19,000	140	≈ 75 dB	
4-A	1200	Dunegan	83,000	4,200	≈ 81 dB	• Ceramic paper w/silicone between shell and insulator compcnent
4-B	1850	Dunegan	770,000	11,000	≈ 80 dB	
5-A	1200	Dunegan & AETC	45,500	1,310	≈ 80 dB	• Plastic at both component interfaces • Different dense component material
6-B	1200	Dunegan	130,000	3,250	≈ 77 dB	• 50 Al_2O_3 dense component • Pressurized with steam
6-C	1850	Dunegan	341,000	4,940	≈ 77 dB	• Pressurized with steam • Rupture disc failure
7-A	1700	Dunegan	202,000	6,500	≈ 76 dB	• Metal fibers added
7-B	1700	Dunegan	466,000	9,000	≈ 76 dB	• Metal fibers added
7-C	1850	Dunegan	533,000	6,100	≈ 76 dB	• Metal fibers added
9	1200	Dunegan & AETC	900,000	5,300	≈ 76 dB	• HES costing on inside of shell

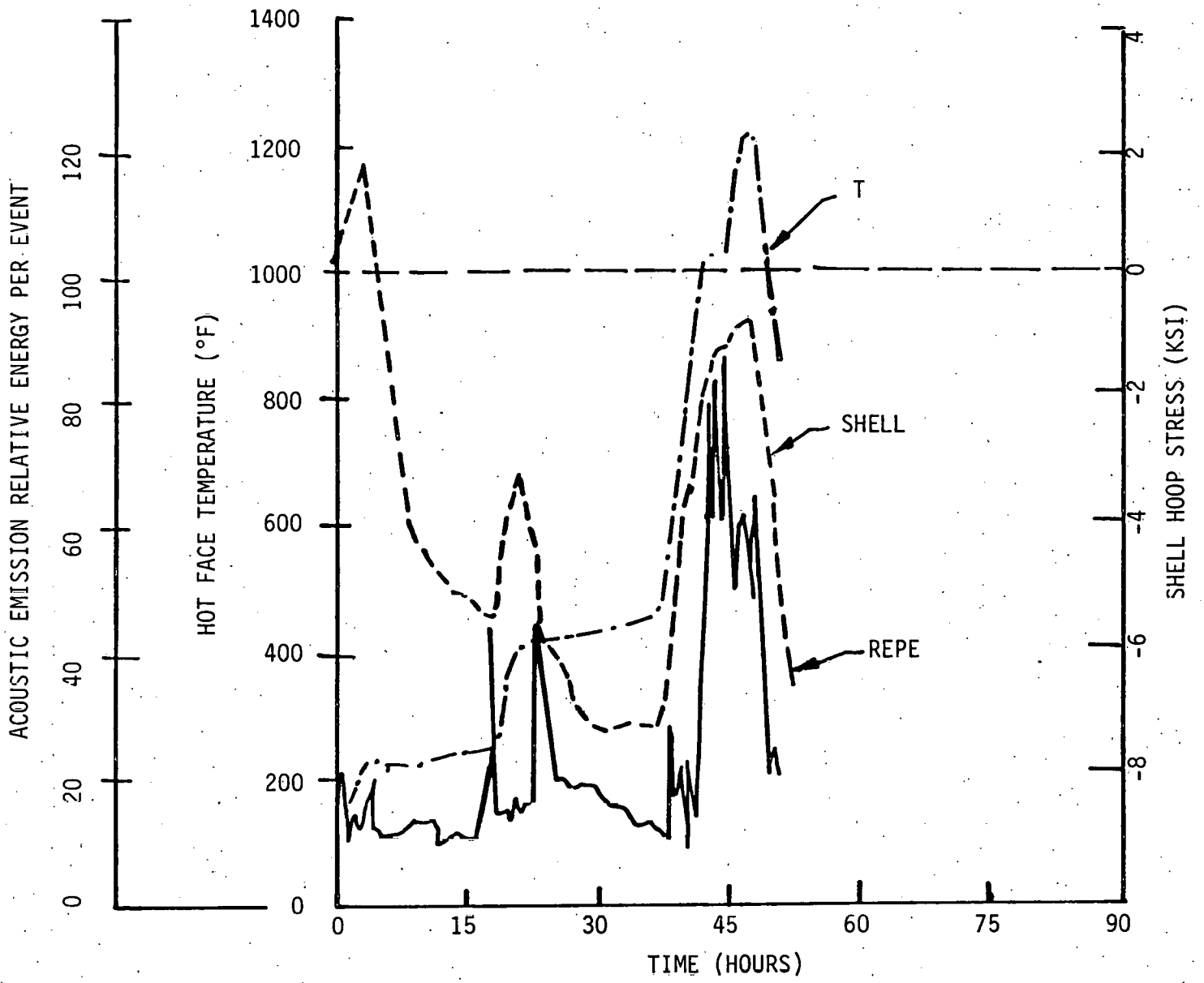

FIGURE 194. Acoustic Emission Data and Hot Face Temperature Recorded During Lining Test #1.

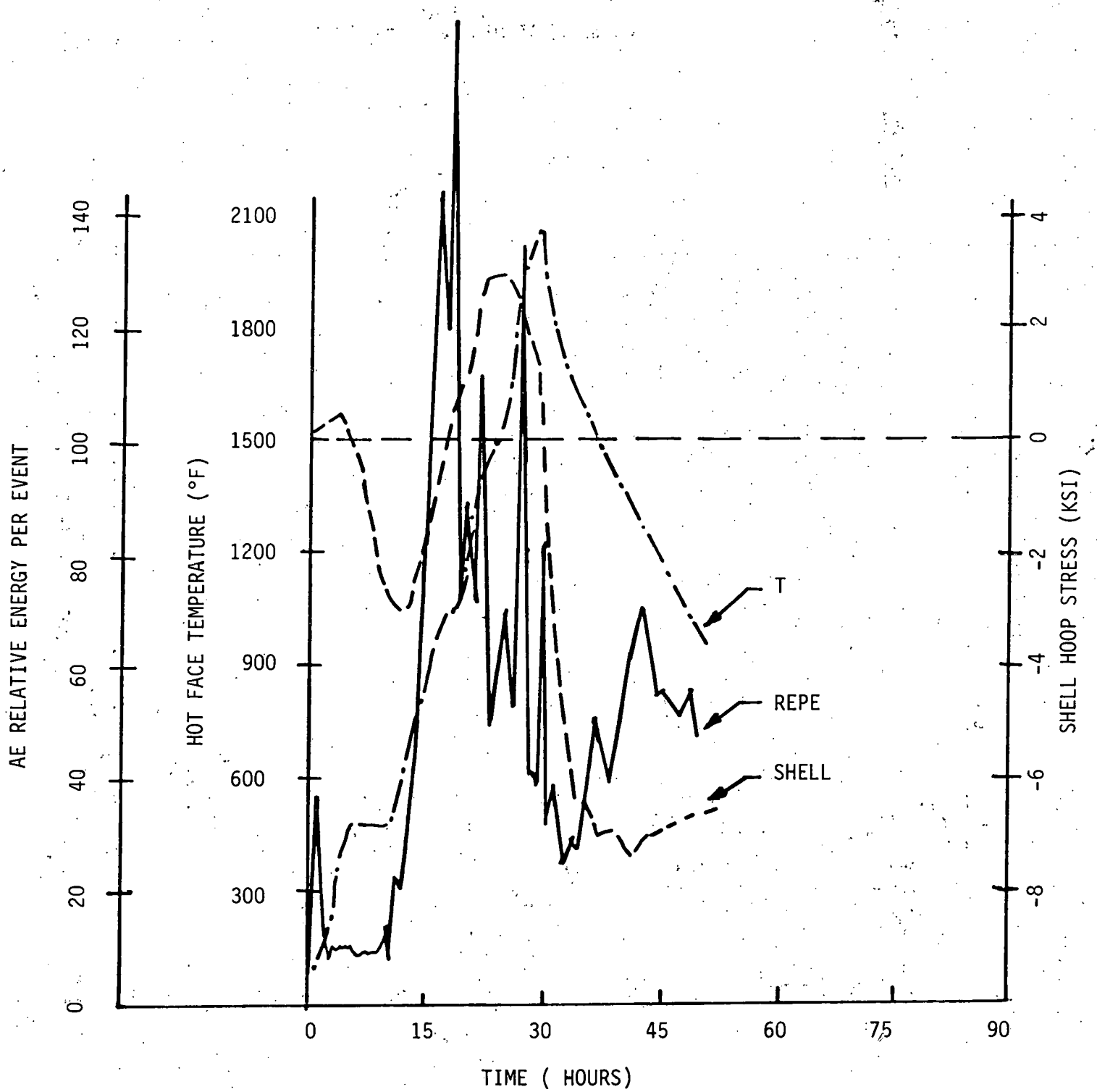

FIGURE 195. Acoustic Emission Data and Hot Face Temperature Recorded During Lining Test #1-A.

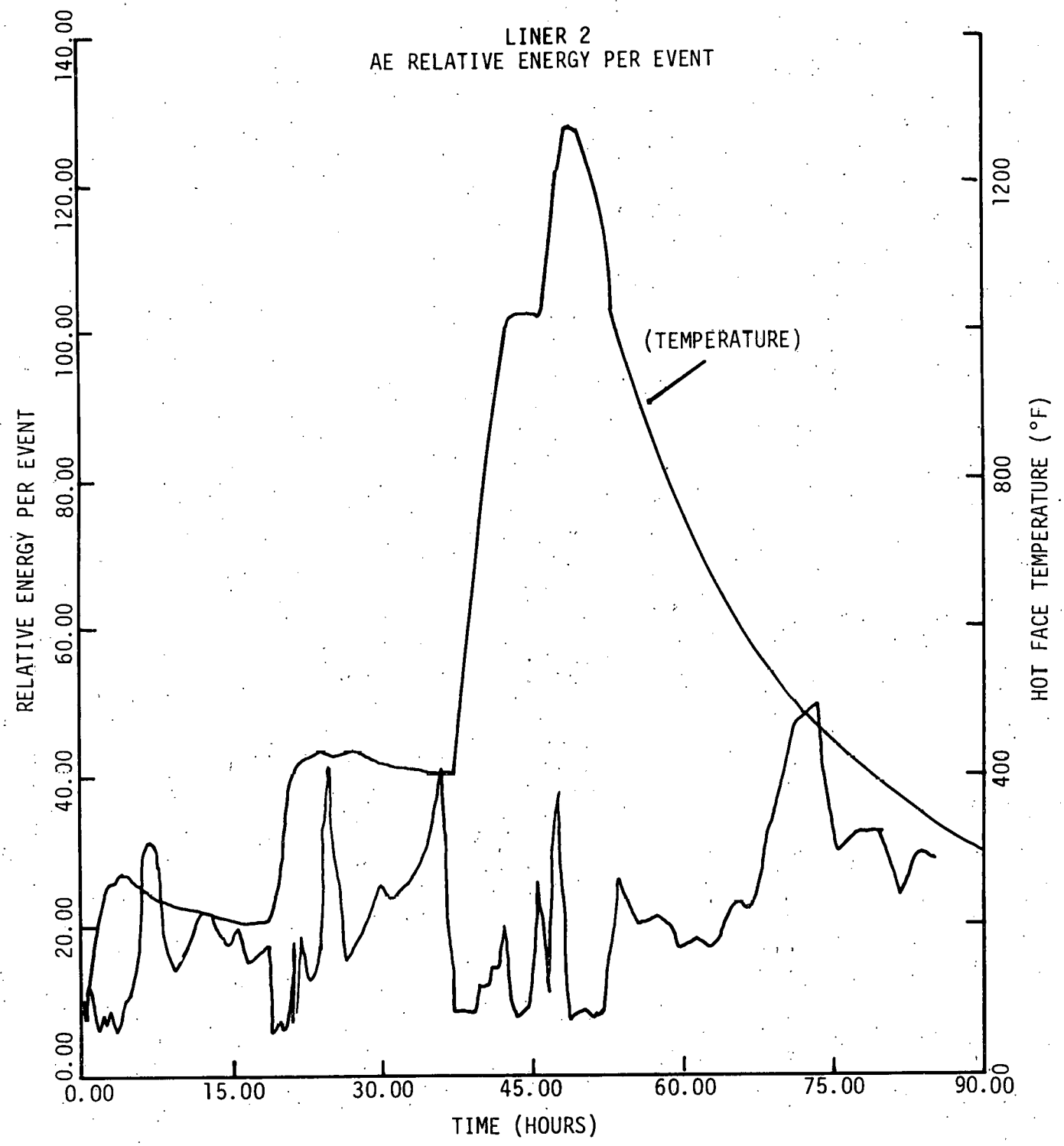

FIGURE 196. Acoustic Emission Data and Hot Face Temperature Recorded During Lining Test #2.

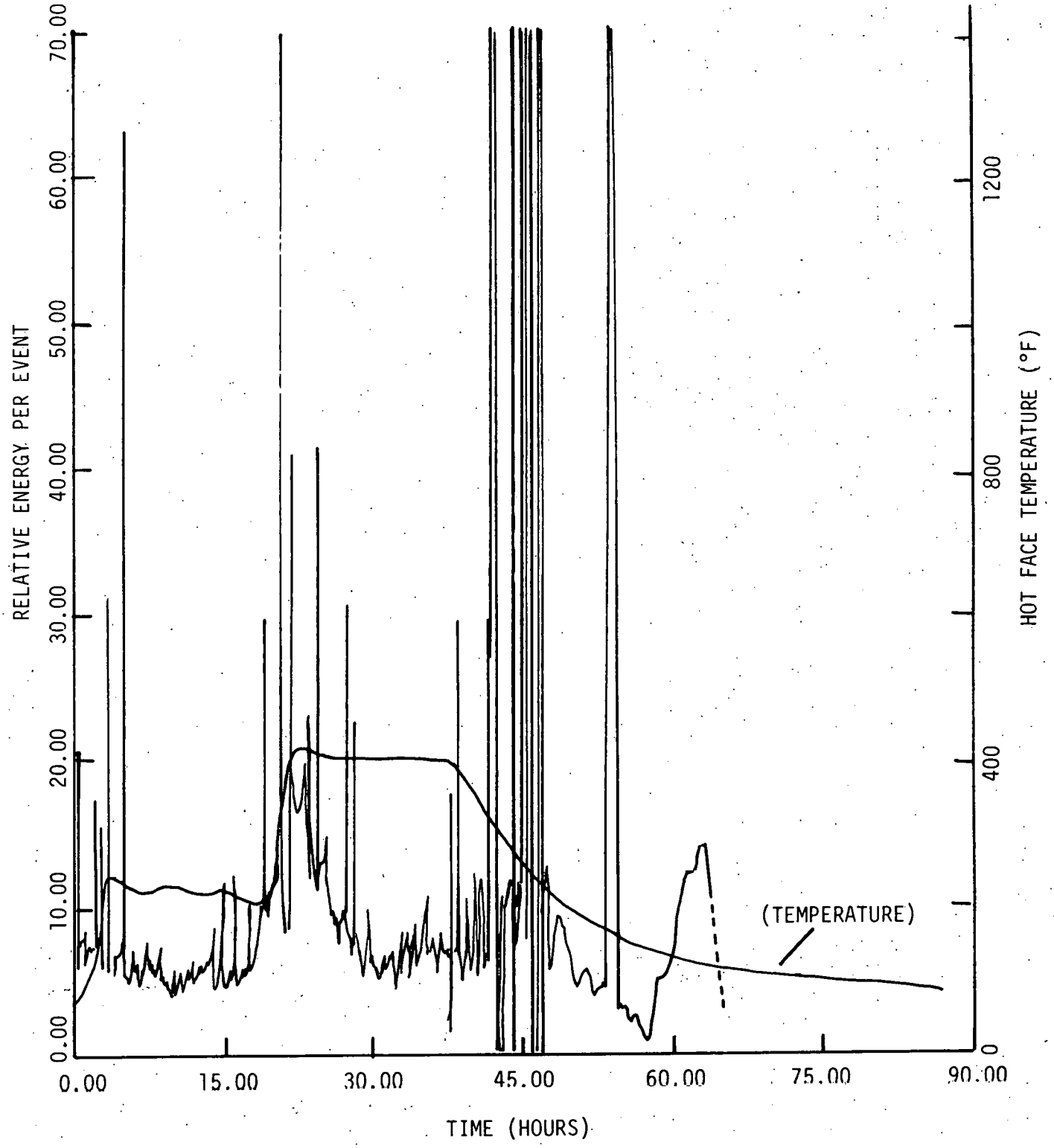

FIGURE 197. Acoustic Emission Data and Hot Face Temperature Recorded During Lining Test #3-A.

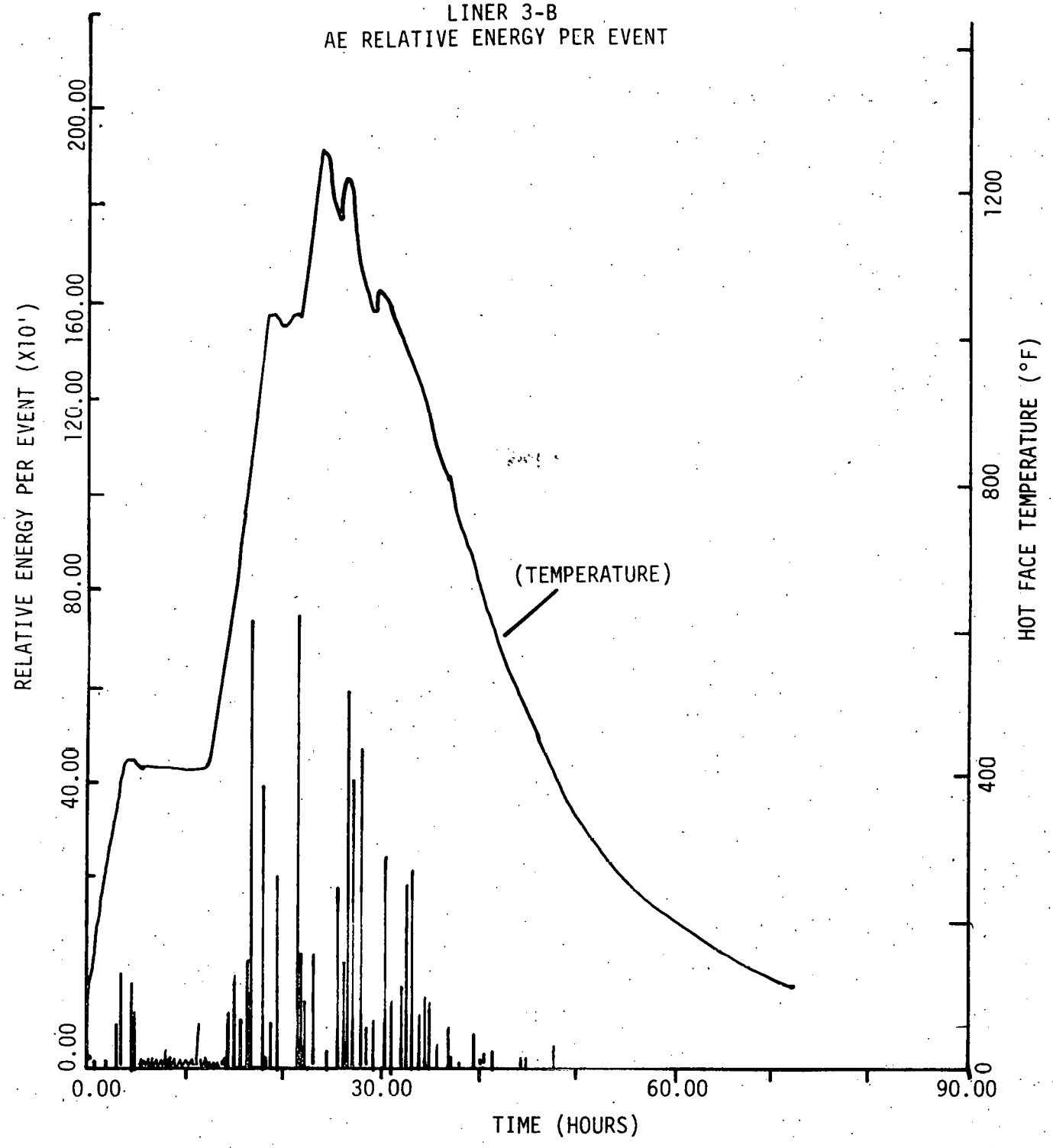

FIGURE 198. Acoustic Emission Data and Hot Face Temperature Recorded During Lining Test #3-B.

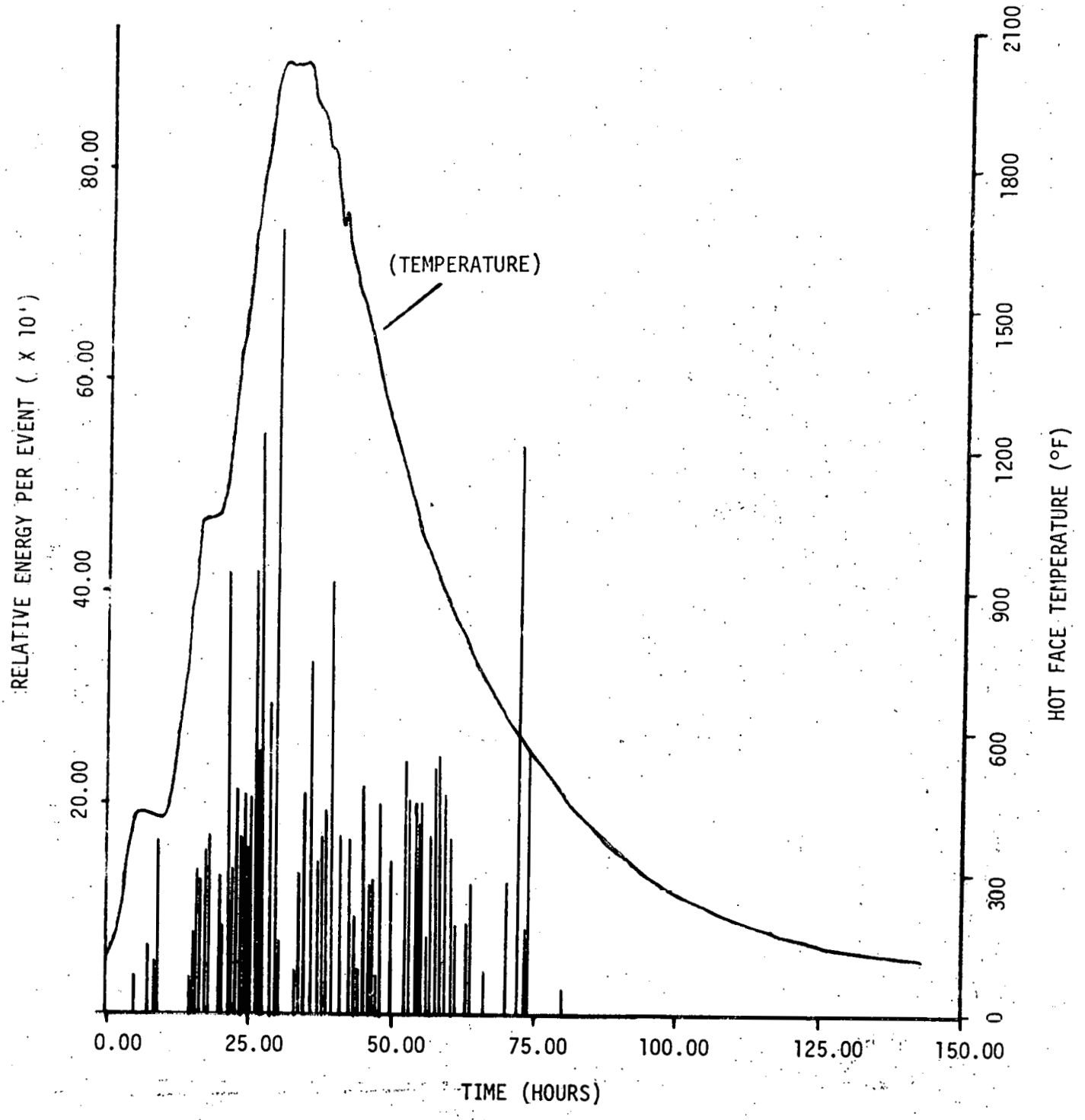

FIGURE 199. Acoustic Emission Data and Hot Face Temperature Recorded During Lining Test #3-C

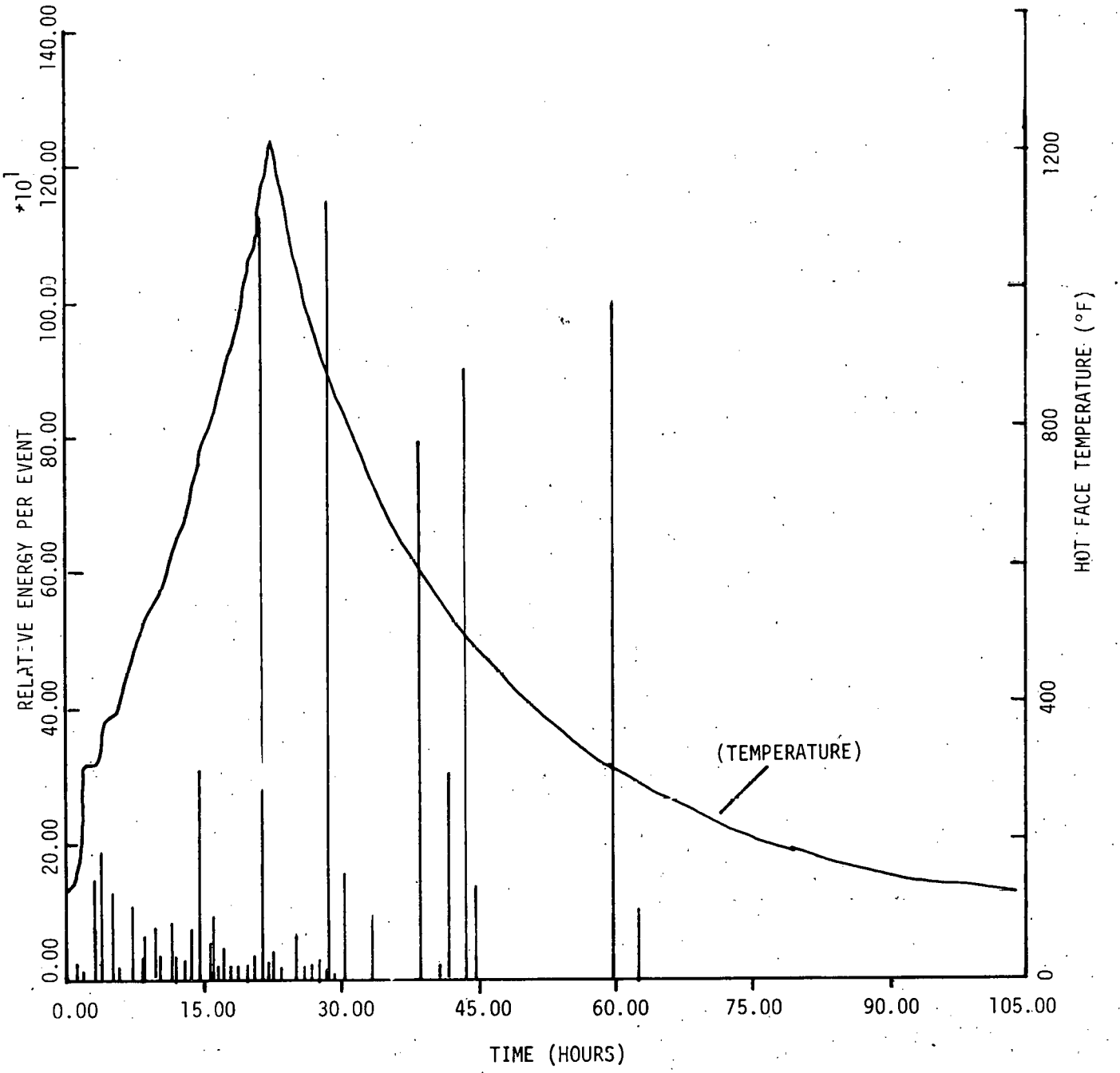

FIGURE 200. Acoustic Emission Data and Hot Face Temperature Recorded During Lining Test #4-A.

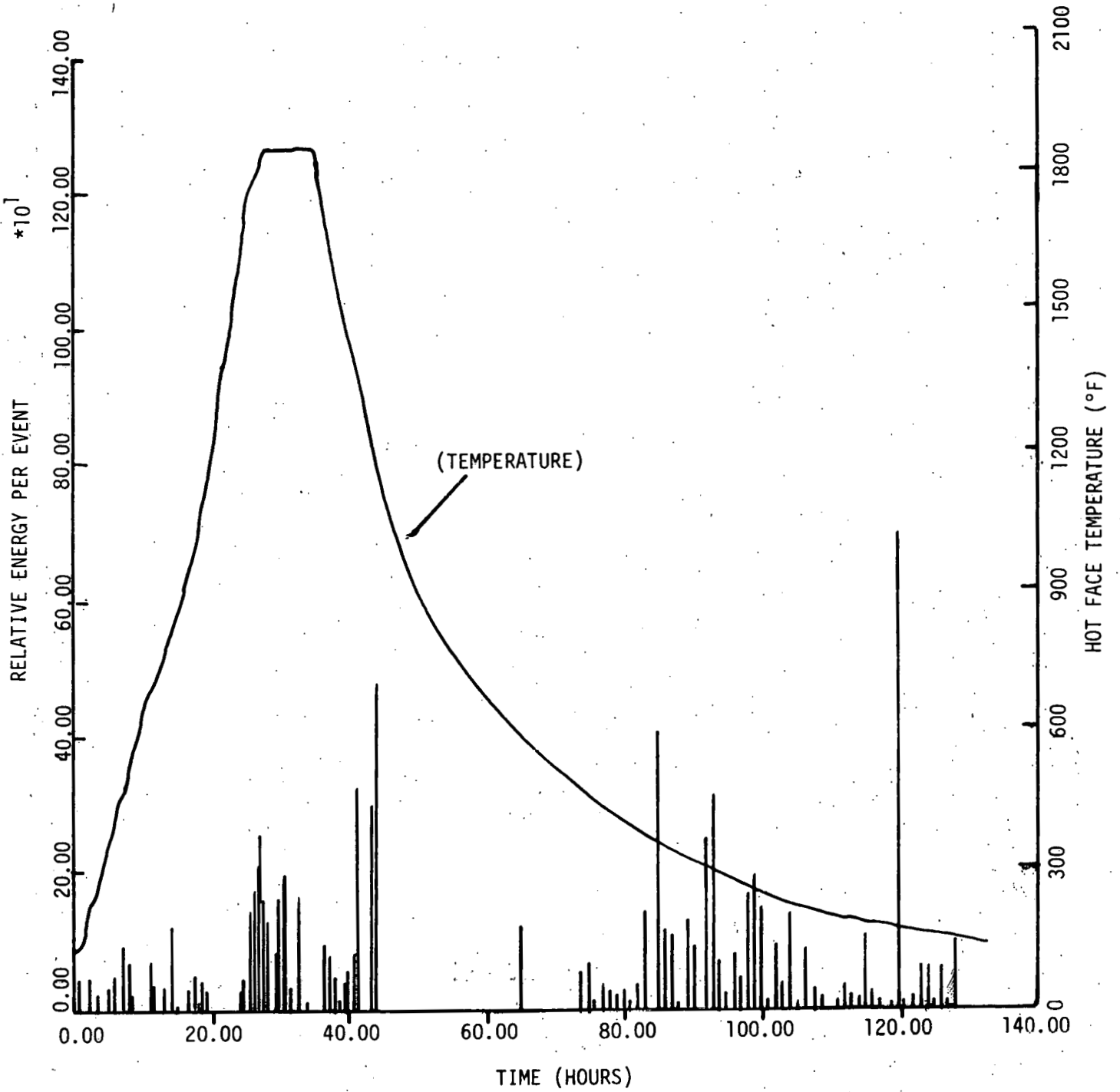

FIGURE 201. Acoustic Emission Data and Hot Face Temperature Recorded During Lining Test #4-B.

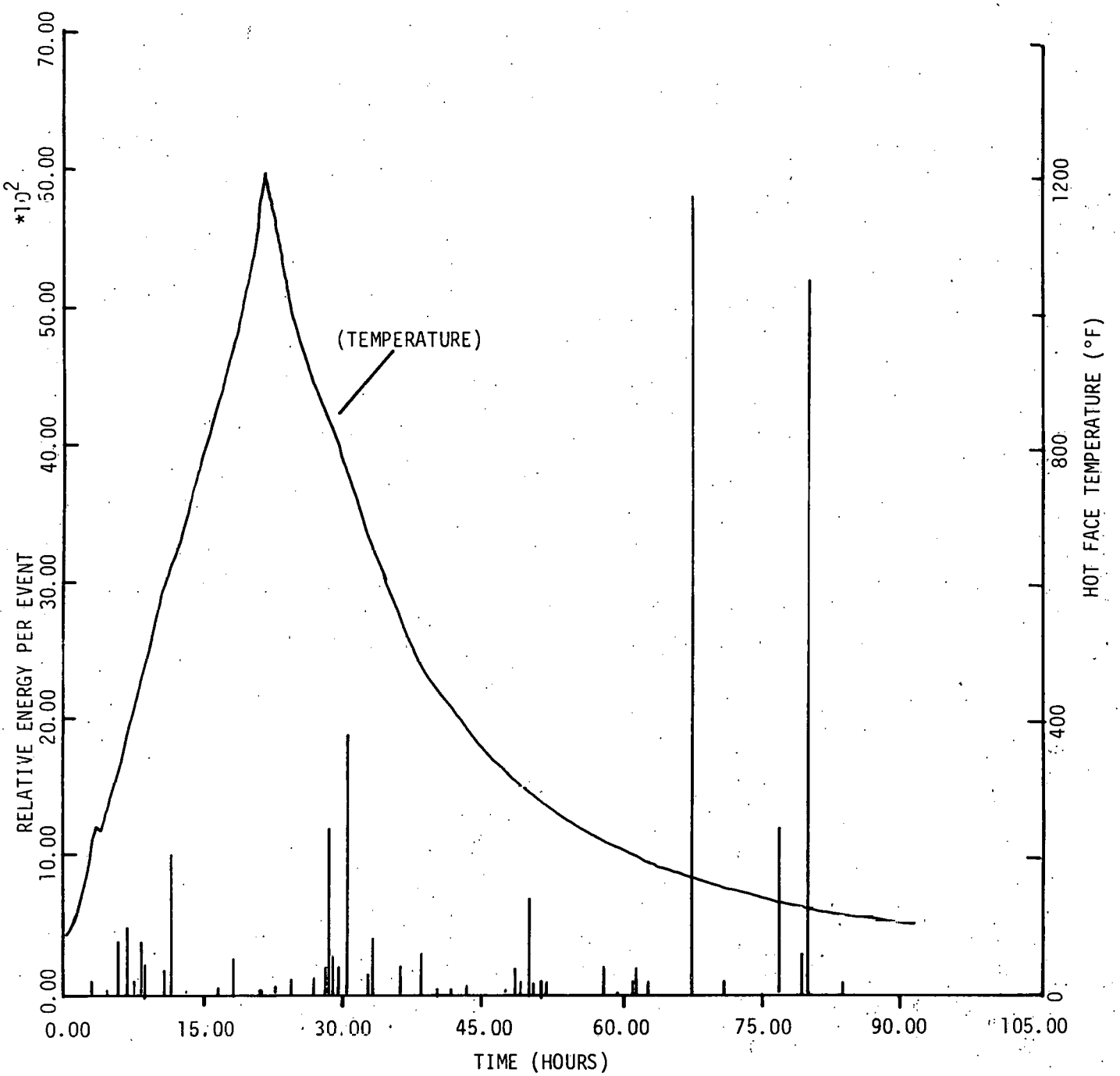

FIGURE 202. Acoustic Emission Data and Hot Face Temperature Recorded During Lining Test #5-A.

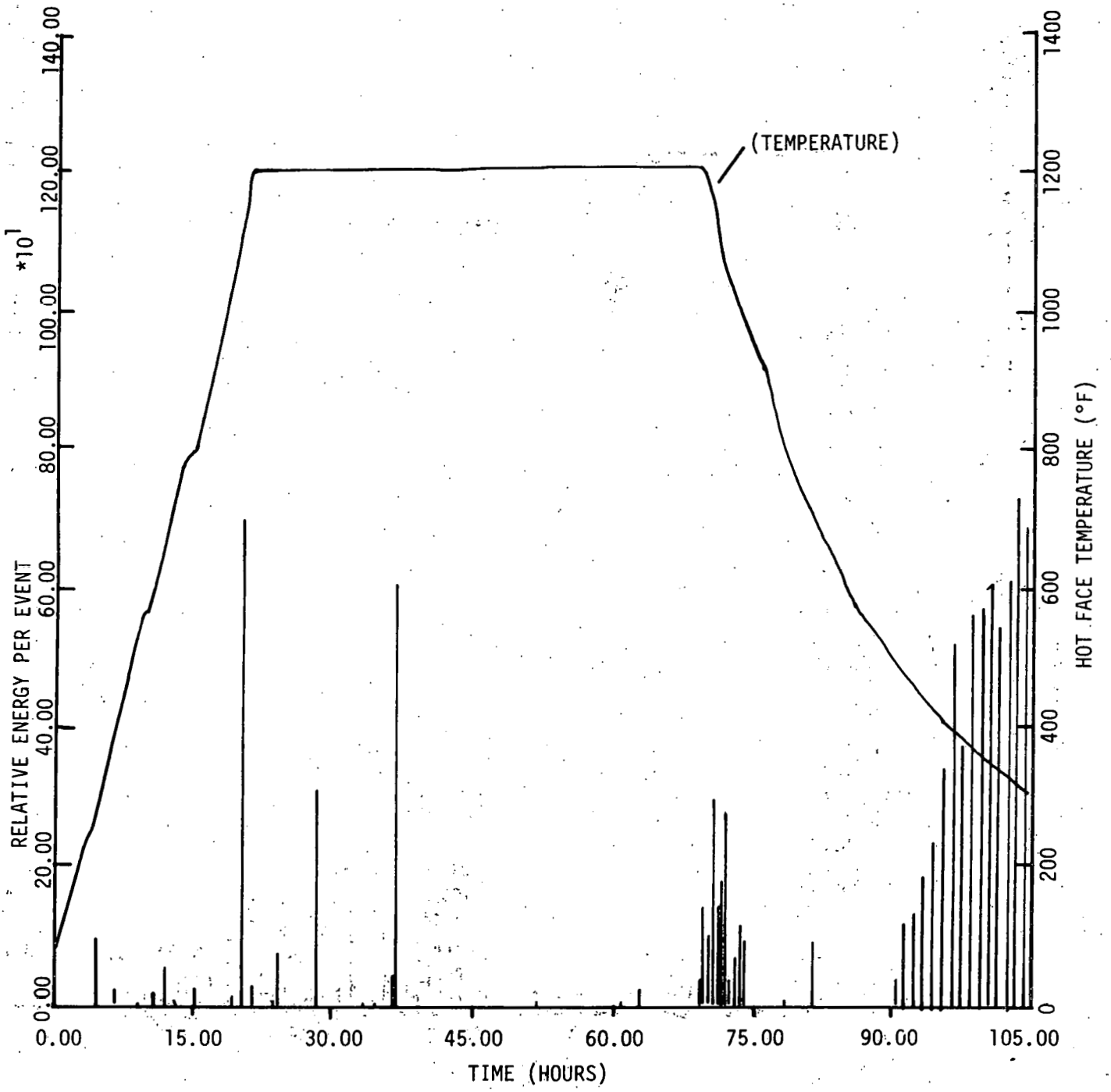

FIGURE 203. Acoustic Emission Data and Hot Face Temperature Recorded During Lining Test #6-B.

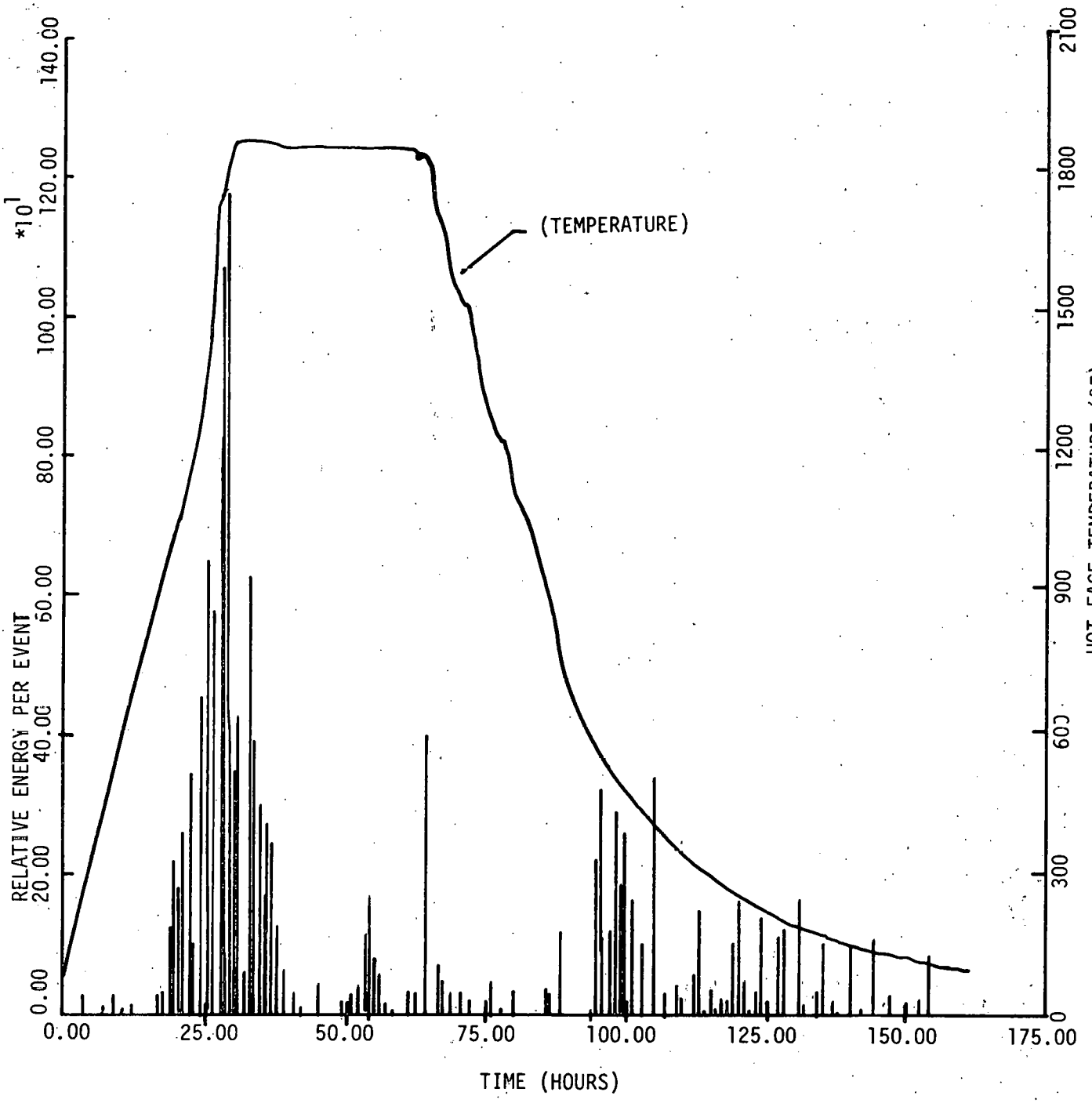

FIGURE 204. Acoustic Emission Data and Hot Face Temperature Recorded During Lining Test #6-C.

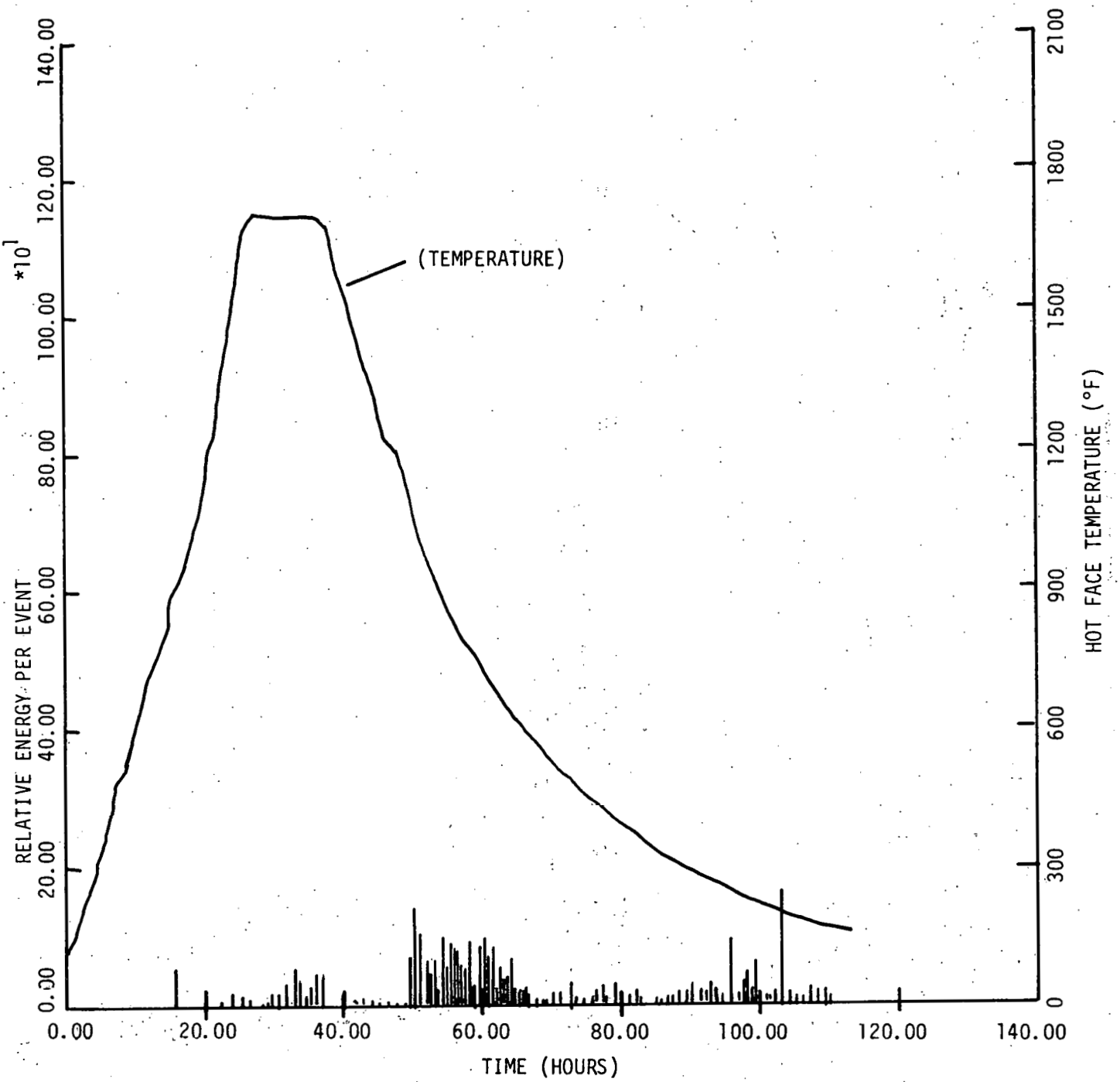

FIGURE 205. Acoustic Emission Data and Hot Face Temperature Recorded During Lining Test #7-A.

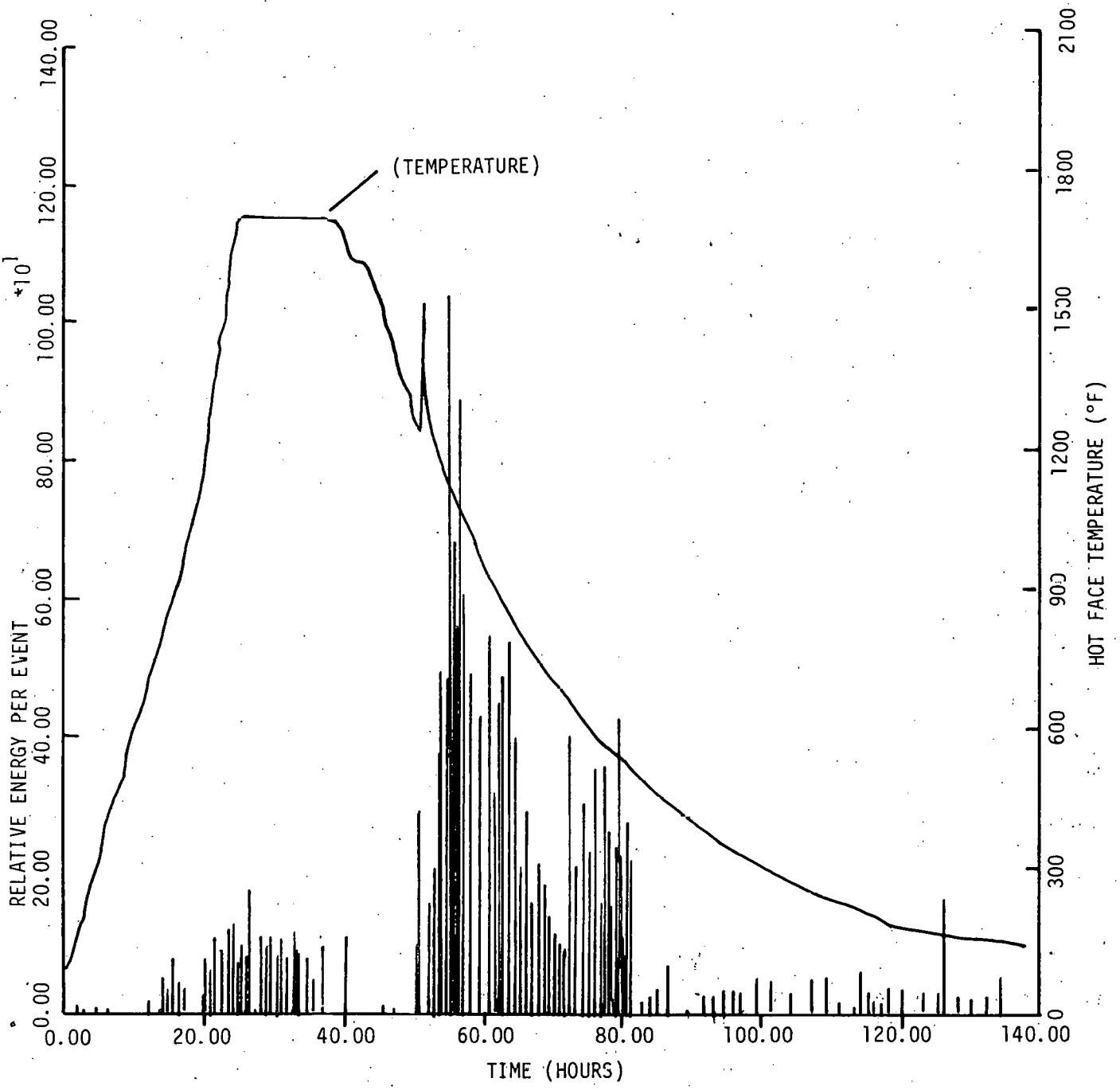

FIGURE 206. Acoustic Emission Data and Hot Face Temperature Recorded During Lining Test #7-B.

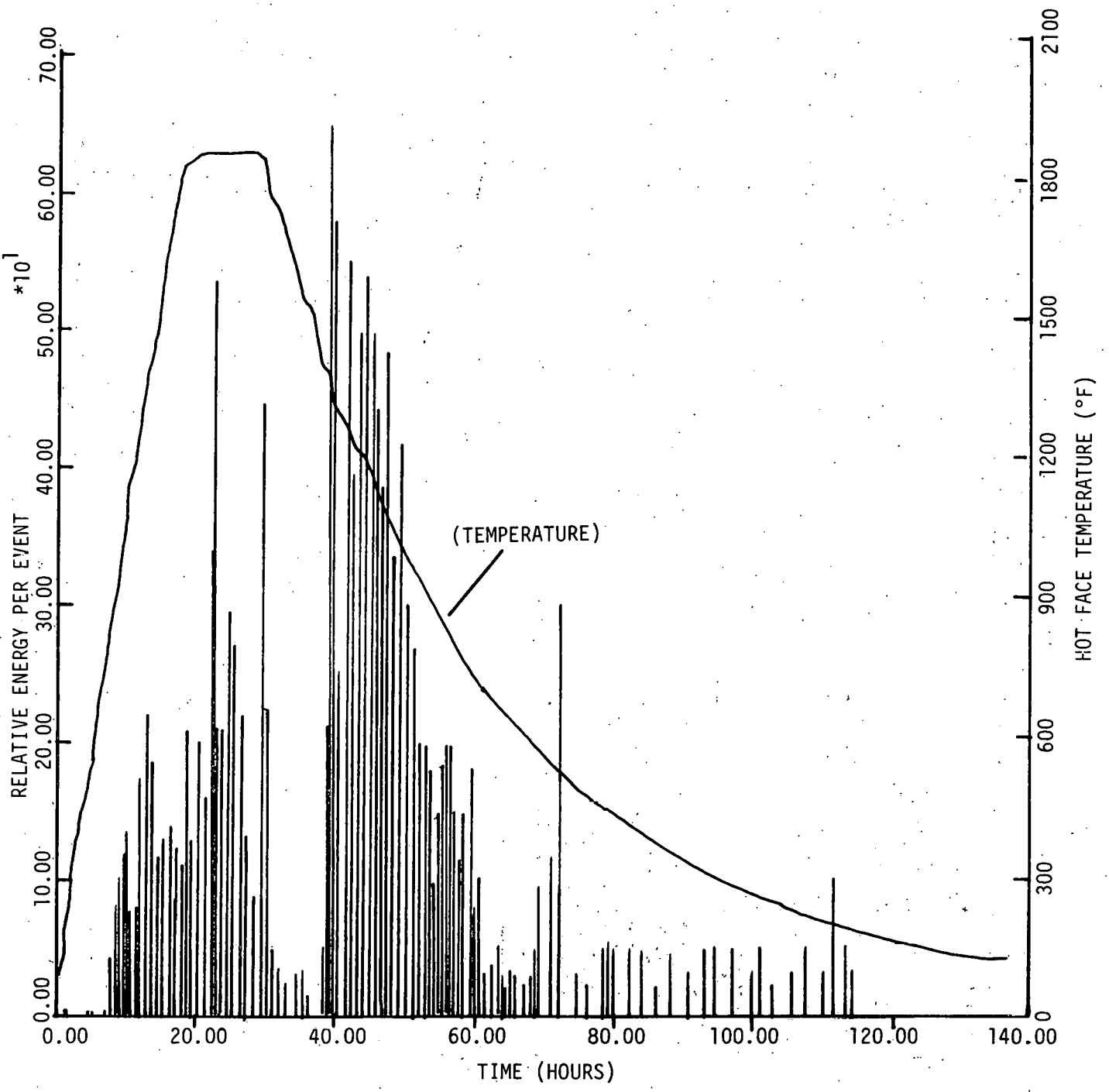

FIGURE 207. Acoustic Emission Data and Hot Face Temperature Recorded During Lining Test #7-C.

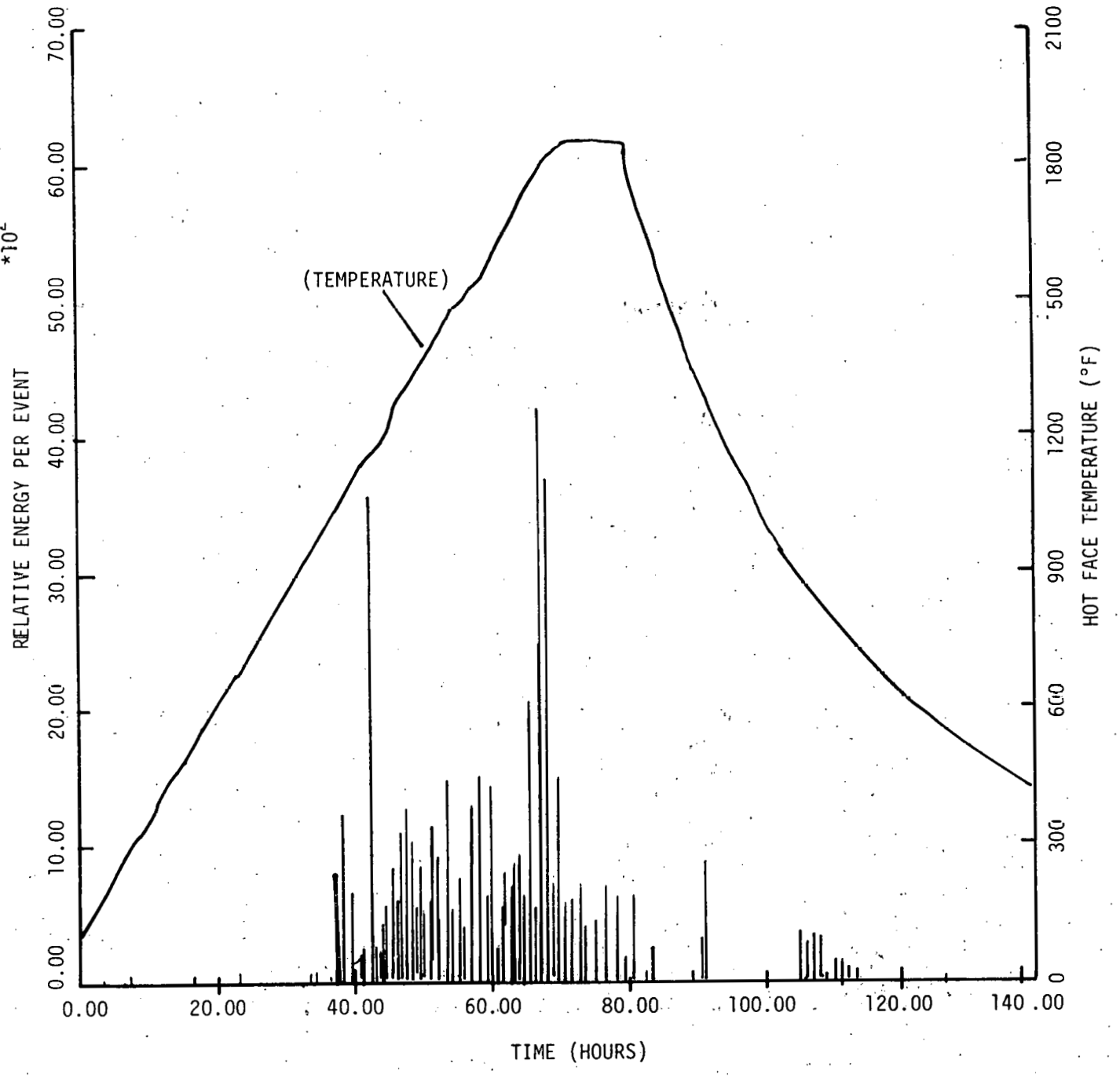

FIGURE 208. Acoustic Emission Data and Hot Face Temperature Recorded During Lining Test #9-A.

- Large Relative Energy per Event spikes generally preceded or coincided with positive or negative changes in the shell stress measurements.

- When strain-gaged anchors went into compression, AE had greater Relative Energy per Event than the average for a given test. Also the "time density" or rate of occurrence of high energy emissions was greater while anchors were in compression.

- In those instances when visual and audible verification of spalling was obtained, spikes were noted at and prior to that time in the Relative Energy per Event plots.

An additional observation of the trends exhibited by the Relative Energy per Event plots in Figures 194-208 is that the AE activity appears to group into three general "time windows". For discussion purposes, these groupings are termed Group I, Group II, and Group III activities. Figure 209 is an idealized drawing showing the typical occurrence of these groups, relative to time and hot face temperature.

Group I activity begins in approximately the same temperature range in each test. That temperature range is between 800°F to 100°F on heat-up, when using heating rates of 50°F/hr. to 100°F/hr. The amplitude and total number of emissions in Group I depend both on the smoothness of the heating rate curve and the linings' history of thermal cycles. Abrupt changes in heating rate generate additional AE and presumably corresponding refractory degradation. The effect was first noted in the heat-up tests of linings 1-5 where various heating rates and temperature soaks (holds) were tried before reaching maximum temperature. The effect was not as evident in test 6-B when overall activity was minimal by comparison to preceding tests. Tests on Lining #7 and #9 used rounded heating rate changes that reduced this effect.

The linings' history of thermal cycles also influences the number and amplitude of Group I emissions. The initial firing of the as-cast linings produced fewer total emissions than following tests on the same lining, but each successive firing showed increased Group I (heat-up) activity over the previous firing.

A quiescent period follows the Group I emissions in which little acoustic activity occurs. This quiescence is very similar to that noted in the brick test data reported in Section 2.5.3. Additional Small-Scale Brick Testing. The quiescent state usually appeared during the holds at maximum temperature after many hours. The quiescent period did not occur during short hold periods presumably because a steady-state stress distribution was not developed. In these cases, Group I activities did not cease before cooldown had started. A brief quiescence will occur as the hot face cools through a temperature distribution at which the stresses are minimal, but the temperature and the time that quiescence occurs is difficult to predict. It will depend strongly upon the heating rate used, the maximum temperature attained, length of time during a hold (if any), and the cooling rate.

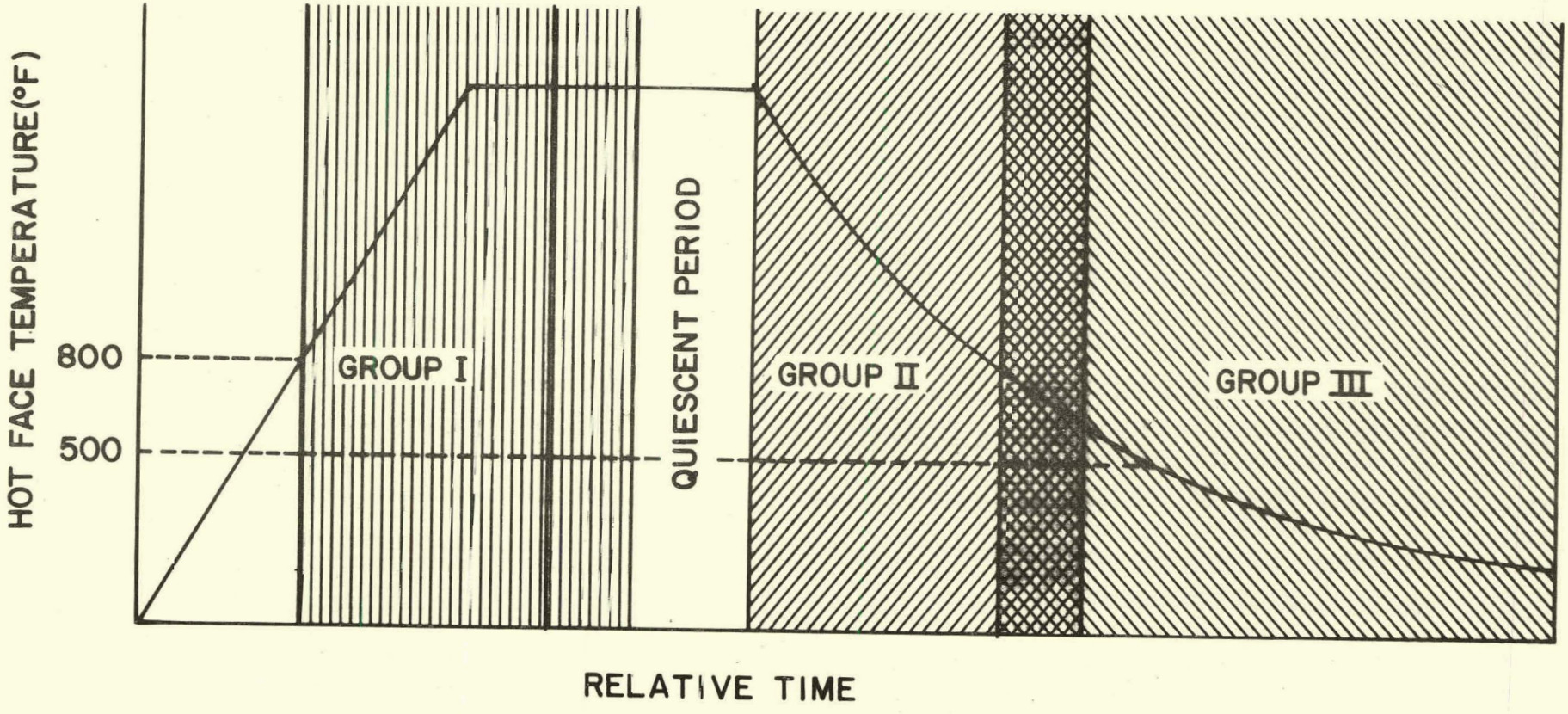

FIGURE 209. Generalized Grouping of Acoustic Emission Responses During Typical Lining Test

Group II activities start immediately with the beginning of cooldown, provided quiescence has been attained during the soak period. Group II emissions are similar to Group I in the sense that they arise from the stresses created by dynamic thermal gradients through the thickness of the lining components. Group II activity continues until approximately 900-500°F, and may overlap Group III emissions.

Group III activity is sometimes difficult to distinguish from Group II emissions. The activity generally overlaps Group II as shown in the figure, starting below 600°F on cooldown. The least overlap or greatest time separation between Group II and Group III occurs during the initial firing of a given lining, with generally less separation with successive thermal cycles. Thermal cycle history effects, however, are not as pronounced upon Group II and Group III activities as they are upon Group I.

It has been postulated that Group III activity results from tensile stresses on the hot face as the surface cools. The tensile stresses develop only during the latter stages of cooldown as the dense component contracts. While the lining is soaked at high temperature, the effects of creep relieve compressive stresses that have built up in the components during heat-up. The quiescent period which occurs during the hold (given sufficient time) supports the statement that stress relief occurs. The stresses, however, are relieved at elevated temperatures, where the materials are in an expanded state. Upon cooling, the components contract again, placing the hot face in a state of tension. It is hypothesized that the tension becomes great enough below 600°F to cause cracking, as indicated by the AE response. This analysis is supported by the math model predictions for the time of cracking during cooldown.

3.6 Seminar

A one and one half day seminar was held at the Lynchburg Research Center of Babcock and Wilcox on September 17 and 18, 1980, to review the results of the work and discuss the recommendations with invited personnel from various industries.

Included in Appendix F is the announcement of the seminar which was sent to approximately sixty companies or people known to be involved and/or interested in refractory lining designs for coal gasifiers. A list of attendees is also included in the appendix. The minimal $60 fee was found to cover the transportation and meal expenses incurred during the seminar.

The seminar was well received and a considerable amount of interchange occurred among the attendees and the speakers. There were many recommendations that the seminar be longer if held again; and several of the attendees suggested that it should be a follow-up after the final report and math model users manual were published. All those in attendance at the seminar were informed that they would receive copies of the final report and manual. They were also informed that they could acquire a copy of the REFSAM and RESGAP programs through Babcock & Wilcox Company.

4. CONCLUSIONS AND RECOMMENDATIONS

4.1 Conclusions

1. From the lining test results obtained, it has been concluded that

- The results confirm the model analyses performed on both the standard and the experimental linings.

- Cracking of the standard lining design occurs by 1200°F and probably at temperatures as low as 400°F.

- 50% Al_2O_3 dense refractory concretes have thermomechanical properties which make them good candidates for the dense, working lining of non-slagging coal gasification process vessels.

- Since the tests on the standard lining design agree with the field results, the improvements achieved with Linings #7 and 9 should be possible in field applications.

- 150 psi pressurized steam has no apparent effect on the thermomechanical properties and performance of either the standard or improved linings.

- Rapid heating rates (>250°F/hr) in the 800-1000°F hot face temperature range should be prevented for 90+% Al_2O_3 dense refractory concretes during the initial heat-up to avoid explosive spalling.

- Improved lining performance which is achieved on the first heat-up cycle is maintained on subsequent cycles.

- The high tensile stresses developed in the shell during the heat-up of the standard type lining indicate that additional safety factors should be added to the code calculations on pressure vessels.

- The use of 4 w/o 310 SS fibers in the KAOCRETE XD 50 dense component used in Linings #7 and 9 makes this component react more uniformly to thermal and mechanical loading, reduces the tendency for cracks to grow and generally makes it tougher.

- Permitting the dense inner component of a dual component lining to shrink and contract freely by reducing the constraining effects of anchors and bonding at the interface have reduced its tendency to crack.

2. Cracking of monolithic refractory concrete linings can be reduced or eliminated by using

- Materials which expand, shrink, and creep less than the standard design type materials.

- A 50% Al_2O_3 dense refractory concrete, such as the KAOCRETE XD 50 material in the dense component.

- Up to 4 w/o 310 SS fibers in the dense component.

- A low iron 50+% Al_2O_3 insulating refractory concrete with a compressive strength of at least 400 psi.

- Five (5) mil or less bonding barriers at the shell and between the two refractory components.

- Spacings between anchors of two to three feet.

- Anchors carefully coated with 60-70 mils of an organic type material to prevent bonding.

- A uniform lining thickness.

- Thin (0.5" or less) corrosion resistant layer at shell.

- The lowest water level which will permit good placement and vibration.

- As poured and curing temperatures of 70°F or slightly higher, and moist surface during curing.

- Slow (25-50°F/hr) continuous heating rates with no temperature holds until the maximum temperature is reached.

- Gradual rather than abrupt changes in heat-up or cool-down.

- 100°F/hr or slower cool-down rates.

- Pressurization and depressurization rates of 50 psi/hr or less.

- Casting forms which will produce rough surfaces on the hot face of the lining.

3. Good agreement has been achieved between the predicted (mathematical model) performance and the experimental lining test results. This indicates that the REFSAM and RESGAP computer programs are very useful design tools for optimizing the performance of single and multi-component monolithic refractory lined vessels used to 2000°F.

4. From the elastic and inelastic stress analyses run on the single and multi-component monolithic refractory vessels, it has been concluded that

- Refractory lining/vessel shell interactions during the initial dry-out and heat-up of a twelve inch thick lining can induce tensile stresses which exceed the yield strength in thin (0.5" or less) carbon steel shells.

- The use of one inch or greater shell thicknesses will reduce the effect of this interaction and lower the stresses induced in the shell to acceptable levels.

- For a given shell thickness, the use of thinner linings (<12 in.) or twelve inch thick linings with lower average thermal expansion coefficients and stiffnesses than the standard type lining design reduce the effect of the lining/vessel shell interactions.

- Steady state stresses at maximum temperature are much higher than those produced during a 100°/hr heatup in a standard lining design.

- Shrinkage and creep are the principal factors which affect cracking of the standard lining design during the initial heat-up, assuming cracking/explosive spalling caused by steam entrapment can be prevented.

- Shrinkage and creep strains cause tensile stresses, which exceed the strength of the refractory, to develop at the hot face on cooldown. Good bonding of the refractory to the shell and/or bonding between the dense and the insulating components increases this stress and should be prevented.

- Materials with lower shrinkage (<0.1%) and better creep resistance than the 90+% Al_2O_3 dense refractory concrete will reduce cracking of the hot face of the lining.

- The presence of gaps or expansion allowances between the components of a lining and between the lining and the vessel will reduce the interactions between these components and the shell and also reduce the tensile cracking of the hot face on cooldown due to the creep effect. If, however, these gaps are greater than 10 mils, tension stresses can form on the cold face side of the components during heat-up which will crack the lining.

- From the predictions obtained with the REFSAM model, lining designs which keep the hot face in a mild state of compression (1000 psi or less) and the shell in a low level of tensile stress (3000 psi or less) during the initial heat-up will result in the least cracking.

5. The evidence provided by the acoustic emission tests is largely qualitative; however, it does suggest that AE monitoring provides a means to reliably assess cracking tendencies during thermal cycling of monolithic refractory linings. The AE method is easily applied, does not interfere with the installation of the refractory linings, and provides real-time analysis capabilities.

A real-time AE monitoring system could be constructed based upon the Relative Energy per Event criteria. The system could be used to monitor the thermal cycling of field installed linings. For a fixed lining configuration and heating schedule, baseline acoustic emission response could be established. Significant deviations from that baseline response would be indicative of lining degradation, allowing corrective action to be taken.

6. A creep model has been developed which uses data from a short term "stepwise" creep test and the unit creep technique employed in the concrete industry. This permits stress analyses, including the effect of creep, to be done on monolithic refractory concrete linings during the initial dry-out and heat-up. This model is thoroughly discussed in the REFSAM and RESGAP user manual written under separate cover on this contract.

7. The mechanical property test results indicate that:

- Up to 1700°F, the 90% Al_2O_3 phosphate bonded monolithic refractories are the strongest; however, above that temperature the 90+% Al_2O_3 dense refractory concrete and the KAOCRETE XD 50 are stronger, especially in compressive creep.

- Lowering the cement content of the 50% Al_2O_3 dense refractory concrete and optimizing the grain sizing have reduced the shrinkage and improved the creep resistance without detrimentally affecting strength.

- The modulus of elasticity of refractory concretes and phosphate bonded monolithic refractories are comparable to fully set conventional concretes at room temperature. Typical values are in the 0.75 to 1.5×10^6 psi range depending upon the density of the material. These values are reduced to one-half or less with heating to 500°F.

- Within the creep test conditions used, the creep resistance of the refractory concretes and phosphate bonded monolithic refractories is more temperature dependent than stress dependent. This indicates that the refractoriness of the bond is a controlling factor in creep resistance.

- The temperatures at which creep becomes significant for the various materials tested are:

90+% Al_2O_3 dense refractory concrete	-	1800°F
50% Al_2O_3 dense refractory concrete	-	1700°F
KAOCRETE XD 50	-	1800°F
90% Al_2O_3 Phosphate Bonded	-	1700°F
LITECAST 75-28	-	1250°F

- The addition of 2 to 4 w/o 310 or 446 stainless steel fibers improves the toughness of the dense and insulating refractory concretes tested but reduces the creep resistance at 2000°F and at stresses above 1000 psi. This high temperature effect is more pronounced for the concretes with 446 SS fiber. This difference is thought to be due to the lower hot strength of the 446 SS fibers.

- The combination of the lower coefficient of thermal expansion, shrinkage, thermal conductivity, modulus of elasticity and strength, and equivalent creep properties of the KAOCRETE XD 50 compared to the 90+% Al_2O_3 dense refractory concrete (ERDA 90) made it well suited for reducing the stresses induced in a lining during heat-up and cool-down and insulating the vessel.

- The properties of refractory concretes are markedly affected by the water level used. Every attempt should be made to use the lowest possible water levels.

4.2 Recommendations

1. The material, design, installation and operating guidelines outlined in the conclusions section of this report are recommended to produce non-slagging coal gasifier monolithic refractory concrete linings with little or no cracking and generally improved performance.

2. Lining #9 can be used as a model for the above recommendation. The use of an impervious chemical barrier at the inner surface of the shell to give added chemical and thermal protection to the shell and to act as a compliant layer which reduces stresses is also recommended.

3. Field testing of these guidelines should be arranged as soon as possible and evidence sought for the long range benefits of the short range improvements obtained.

4. A thorough parameter study on various types of lining designs, should be undertaken with the REFSAM and RESGAP computer programs developed. The results of other DOE contractor's studies could be factored into this effort.

5. A study should be undertaken to combine the two stress analysis computer programs (REFSAM and RESGAP) into one all inclusive program and to determine how to expand it for analysis of brick linings.

6. Strain gaging of the vessel shell and other components of a gasifier with the WK type weldable electric resistance strain gage is recommended as an accurate method to monitor the performance of a refractory lining during service and the shell during operation.

7. Further examination and evaluation of the embedment strain gage, acoustic emission monitoring and pore pressure techniques developed and/or expanded on this program should be done. The development of devices which would generate results in real time would be the expected output of the work and would aid those responsible for the safe and successful dryout and heat-up of a new lining and would complement the shell stress monitoring technique recommended.

8. Since large gasifier linings are gunned rather than cast, refractory companies should be encouraged to make gunning refractory concretes with properties as close as possible to those of the KAOCRETE XD 50 type material.

9. A separate project should be undertaken to bring together the results of all the DOE-approved programs on monolithic refractory concretes and phosphate bonded refractories. This could indicate the need for further work in this area relative to the advancements being made in gasification.

5. REFERENCES

1 Best, R. H., Malik, S. N. and Schroedl, M. A., "User's Manual for Refractory Failure and Stress Analysis Model, REFSAM", DOE Contract EX-76-C-01-2218 (Old No.), DE-AC05-76OR10434 (New No.), February, 1981.

2 Bathe, K. J., "Static and Dynamic Geometric and Material Nonlinear Analysis Using ADINA", MIT Report 82448-2, May, 1976.

3 Bathe, K. J. and Wilson, E. L., Numerical Methods in Finite Element Analysis, Prentice-Hall Inc., Englewood Cliffs, New Jersey, 1976.

4 England, G. L. and Sharp, T. J., "Migration of Moisture and Pore Pressures in Heated Concrete", First Int. Conf. on Struct. Mech. of Refractory Technology.

5 Bazant, Z. P. and Thongulhu, W., "Pore Pressure in Heated Concrete Walls: Theoretical Prediction", Magazine of Concrete Res. 31, 107, June 1979.

6 J. H. Ainsworth and R. H. Herron, "High Temperature Fracture Energy of Refractories", Cer. Bull. 55, 7, 655, 1976.

7 P. J. Pike, O. Buyukozturk and J. J. Connors, "Thermo-Mechanical Analysis of Refractory Concrete Lined Coal Gasification Vessels", MIT Research Report No. R80-2, Jan. 1980.

8 Wygant, J. F. and Crowley, M. S., "Designing Monolithic Refractory Vessel Linings", Am. Cer. Soc. Bull. 43, 3, 173, 1964.

9 Carneglie, S. C., et al., "Low-Temperature Deformation Test for Tar-Bonded Basic Refractories", Am. Cer. Soc. Bull. 53, 7, 539, 1974.

10 Chuang, J. W., et al., "An Approach to Estimating Long-Term Multiaxial Creep Behavior from Short Term Uniaxial Creep Results", Research Report 2864-3, Univ. of Texas, Austin, Tex., June 1970.

11 Kistler, C., "Pressure Build-up in Refractory Panels", Feb. 1977, Personal Communication, (Battelle Columbus Laboratory).

12 Marion, R. H., and Johnstone, J. K., "A Parametric Study of the Diametral Compression Test for Ceramics", American Ceramic Society Bull., 56, 11, 998, 1977.

13 Huggett, L. G., "Lining of Secondary Reformers", Proc. Mat. Tech. Symposium, Pergamon Press, 305, (1966).

14 Crowley, M. S., "Hydrogen-Silica Reactions in Refractories: II", Am. Ceram. Soc. Bull., 49, 5, 527, 1970.

15 Fuller, E. R. and Robbins, C. R., "Effect of Elevated Pressure Steam on the Strength of Refractory Concretes", Refr. Div. of Am. Ceram. Soc. Meeting, Bedford, PA. (1975).

16 Raymon, N. S. and Sadler, L. Y., "Refractory Lining Materials for Coal Gasification", U.S. Bureau of Mines Circ. 8721 (1976).

17 Gac, F. D. and Day, D. E., "Exposure of Refractory Castables to Steam - N_2 and Steam - Co Atmospheres", Refr. Div. of Am. Ceram. Soc. Meeting, Bedford, PA. (1975).

18 Crowley, M. S. and Johnson, R. C., "Guidelines for Installing and Drying Refractory Concrete Linings in Petroleum and Petro-Chemical Units", Amer. Ceram. Soc. Bull., 51, 3, 226, 1972.

19 Haydl, H. M., and Sherbourne, A. N., "Thermal Stress in Refractory Lined Steel Cylinders", Proc. Instn. Civ. Engrs., Part 2, 63, 195-202, (Mar. 1977).

20 Pierce, R. R., "Engineering Brick Lined Process Vessels", Mat. Protection and Performance, NACE, (Dec. 1972).

21 McCullough, J. M. and Rigby, G. R., "Mechanical Properties of Refractory Castables", J. Brit. Cer. Soc., 71, 233, 1972.

22 McGee, T. D., Smyth, J. R., and Bray, D. J., "Creep of 90+% Al_2O_3 Refractory Concrete", Am. Cer. Soc. Bull., 59, 7, p. 706, 1980.

23 C. E. Zimmer and E. M. Anderson, "Effects of Various Parameters on Monolithic Refractory Linings for Coal Gasifiers", Industrial Heating, November 1978, p. 30.

24 C. E. Zimmer and E. M. Anderson, "Processing Variables Affecting the Thermomechanical Degradation of Monolithic Refractory Concretes", Processing of Crystalline Ceramics, 1978, pp. 505-514.

25 Heystek, H., Raymon, N. S. and Ivey, K. H., "Testing and Development of Refractory Linings for Coal Gasification Process Equipment", Third Quarterly Report 1979, USBM.

APPENDIX B

Additional Material Properties on Monolithic Refractories Tested

Appendix B. Additional Material Properties

The tables and figures in this appendix summarize the property data collected on the materials specified to be tested in the program but not used in the lining tests or stress analyses. They also include the properties of the original 50 and 90+% Al_2O_3 dense generics formulations before they were changed to contain casting grade CA-25 cement instead of regular grade and changed to make them mix and cast more easily in large mixers. Furthermore, they present the stress-strain and creep strain data generated on the key refractories and an example of how the creep strain is reduced to Unit Strain-data for use in a Unit Creep Plot. The special test data relative to the monolithic refractories discussed in Section 3.2. of this report are included.

Tables B-1 through B-3 list the bulk density, apparent porosity, mean pore size and loss on ignition (LOI) data generated on the above mentioned materials. Tables B-4 through B-9 list the linear shrinkage, coefficient of thermal expansion, modulus of rupture, crushing strength, modulus of elasticity, splitting tensiles and some other miscellaneous properties of the materials, some of which were from the lining pours. Figures B-1 through B-5 show the thermal expansion characteristics of the phosphate bonded refractories and some of the dense and insulating monolithic refractories mixed with different amounts of water and stored in different environments. These figures also show the hot compressive strength curves of the phosphate bonded refractories and the stress relaxation curves generated on the standard 50% Al_2O_3 dense generic, the modified 90+% Al_2O_3 dense generic and LITECAST 75-28 at different temperatures and loads.

Table B-10 and Figures B-6 through B-8 are the typical output data of the computer program developed for the HP 9830 computer to reduce and plot modulus of rupture, compressive strength and modulus of elasticity properties versus temperature. The table is output on the compressive strength and stress-strain results of one specimen of the standard 90+% Al_2O_3 dense generic refractory concrete. The figures are uncorrected stress-strain plots of the 50% Al_2O_3 generic, the standard 90+% Al_2O_3 dense generic and the LITECAST 75-28 developed from the compressive strength tests.

Tables B-11 through B-24 summarize the creep and hot load results obtained on the key monolithic refractories (different water levels, densities, fiber additions, and pretreatments), and the phosphate bonded monolithic refractories (different stress levels and temperatures). Figures B-9 and B-11 are the stepwise creep or Unit Creep plots of the phosphate bonded refractories and the modified 90+% Al_2O_3 dense generic refractory concrete at different water levels.

From a review of the physical property data presented, the effect of water level variations on the bulk density, porosity, shrinkage, strength and creep properties of the various refractories tested is evidenct. Levels above the optimum level generally decreased bulk density, thermal expansion, strength and creep resistance; and increased porosity and shrinkage. These findings emphasized the importance of using as low water levels as possible to get good lining performance.

From a review of these data, it is evident that the physical and strength properties of the dense 50% Al_2O_3 generic castable appeared to be detrimentally affected by formulation change even though it mixed and cast better than the standard formulation. The reduced fines may have contributed to the reduction in density and strength obtained. Two other factors may have contributed to the reduced properties. One was the use of the regular grade of CA-25 cement and a boric acid addition. The other was that the test bars were made from a 600 lb. batch of the modified formulation after the majority of it was used to cast test panel #9 and an arc segment. The modifications of the modified 90+% Al_2O_3 generic had very little effect on physical and strength properties.

The results give further evidence that the original and modified generic castables have comparable properties to commercial 50 and 90+% Al_2O_3 castables. They also indicate that the use of the casting grade CA-25 cement in the generic formulations improves their physical and mechanical properties and hot load and creep characteristics. Since the use of this cement also improved the casting characteristics of these generic castables, the decision was made to continue working with the modified casting mixes.

Unlike the dense monolithic refractory concretes, the phosphate bonded monolithic refractories had strengths that were strongly temperature dependent. The strengths were generally equal to or greater than the dense concrete in the as-cured state, but increased with temperature to 1500°F before dropping off rapidly above 1750°F. This sharp strength loss correlates with the significant loss in creep resistance of these materials above 1800°F.

Both the 45 and the 90% Al_2O_3 phosphate bonded refractories have smooth thermal expansion curves compared to the as-cured refractory concretes. They do not appear to be affected by storage conditions on time as the refractory concretes are. These features of the phosphate bonded materials make them attractive materials for linings operating to 1800°F to 2000°F.

The fracture energy results which were obtained on notched bend specimens and were presented in Section 3.2. of the report were found to be in same order of magnitude for refractories as other investigators have reported. The results indicated that the standard 50% Al_2O_3 generic castable had better resistance to cracking than either the standard or modified 90+% Al_2O_3 generic castables. The insulating castable had the least cracking resistance. There is, however, some concern about the reliability of these fracture energy results for two reasons. One was that the results follow the same trends as the hot bending strength curves. The other was that the deflections measured with the LVDT set-up were very small and the standard deviation was high.

The hot load and creep data give added support to the results discussed in Section 3.2. of this report and clearly show the detrimental effects of higher water levels and lower densities on creep. The 90+% Al_2O_3 dense generic, for example, deforms 0.5 to 1.0% more at the same test conditions when the water level is increased from 8.5 to 9.0%. The insulating refractory showed more dramatic increases in deformation (1.2 to 2.3% or higher) when the water level was raised from 21 to 24%.

The creep data also indicates how poor the creep resistance of the KAOLITE 2300 LI is compared to the LITECAST 75-28 and that the KAOCRETE XD 50 (Mix 36C) with 4 w/o 310 SS fibers is better in creep resistance than the same material with 2 or 4 w/o 446 SS fibers. This difference appears to correlate with the higher fiber tensile strength at 1600°F (2200 psi vs 7650 psi) of the 310 SS than the 446 SS.

The creep results also indicate that modifying the 50% Al_2O_3 dense generic refractory concrete with regular CA-25 cement and a boric acid addition had a detrimental effect. This was especially noticed when the short term creep results at 1800°F were compared. The modified generic material deformed more than the standard when tested at 1500 psi stress and failed after 1.25 hours at 2500 psi stress. The commercial-LOABRADE 50% Al_2O_3 dense refractory concrete deformed more than the modified generic material at 1800°F and 1500 psi and would probably fail at the higher stress level.

Finally, the hot load and creep data indicate that the 45% and 90% Al_2O_3 phosphate bonded monolithic refractories have better creep resistances at and below 1800°F than the 50 and 90+% Al_2O_3 dense refractory concretes but worse creep resistance above 1800°F.

Since stress relaxation and creep are related and the stress relaxation test procedure is relatively fast and commonly done on an Instron type test machine, some experiments were performed on the dense and insulating castables during the hot compressive test work. The main experiments performed involved determining the level of relaxation at different temperatures, stress levels and times. Since the experiments were combined with the compressive strength testing, it was planned to stop the experiments when the relaxation leveled off. The stress relaxation results were obtained during the hot compressive strength tests by stopping the Instron crosshead at loads that would not crush the sample. The decay of this load with time was observed as the sample deformed to relieve the stress. The results follow the same temperature and stress dependent relationships as the creep results on the same materials.

The initial findings (see Figure B-5) indicated that no relaxation occurred below 1000°F for the insulating castable or below 1500°F for the dense castables tested. These results agreed favorably with the creep results on the same materials. The relaxation above these temperatures occurred very quickly and leveled off in four to five minutes. Further analysis of the results indicated that they could be used in the math model to predict creep effects but longer relaxation times are needed to fully verify this point.

Table B-1. Physical Properties of the Standard and Modified 90+% Al_2O_3 Dense Generic Refractory Concretes at Different Water Levels and with Different Cements

Properties	Standard 90+% Al_2O_3 Generic Castable				Standard 90+% Al_2O_3 Generic With CA - 25 Casting Grade				Modified 90+% Al_2O_3 Generic With CA - 25 Casting Grade
	With CA - 25		With Secar 250						
Water Added, %	9.3	10.2	10.0	10.5	8.8	9.3	9.8	10.3	8.5
Bulk Density, pcf (brick)									
RT Cured	174(175)	173(173)	171(172)	172(170)	176(174)	175(174)	174(172)	172	177
24 hrs. @ 250°F	169(169)	166(166)	169(170)	169(168)	174(172)	173(171)	171(169)	169	175
2 hrs. @ 450°F	-	-	-	-	-	-	-	-	-
2 hrs. @ 1000°F	-	-	-	-	165	167	-	-	-
2 hrs. @ 1500°F	-	-	-	-	166	166	-	-	-
Weight Loss, % (green to fired)									
After 24 hrs. @ 250°F	2.9	4.0	1.7	2.2	1.8	2.0	1.9	2.0	-
After 2 hrs. @ 1000°F	6.9	6.9	9.2	9.5	4.7	5.4	-	-	-
After 2 hrs. @ 1500°F	6.9	7.3	9.2	10.0	6.0	6.5	-	-	-
After 0 hrs. @ 1875°F	7.4	7.4	10.2	10.2	-	-	-	-	-
Apparent Porosity, %									
RT Cured	15.4	-	8.2(2)	-	-	-	-	-	-
24 hrs. @ 250°F	22.4	-	14.8	-	-	-	-	-	-
2 hrs. @ 1000°F	14.0	-	11.9	-	-	-	-	-	-
2 hrs. @ 2000°F(30 hrs.)	17.0	-	15.0(18.0)	-	-	-	-	-	-
Mean Pore Size, µm									
RT Cured	.19	-	.25(2)	-	-	-	-	-	-
24 hrs. @ 250°F	.20	-	.20	-	-	-	-	-	-
2 hrs. @ 1000°F	.24	-	.16	-	-	-	-	-	-
2 hrs. @ 2000°F(30 hrs.)	.42(.46)	-	.65(.88)	-	-	-	-	-	-

Note: RT = Room Temperature

TABLE B-2. Physical Properties of the Standard and Modified 50% Al_2O_3 Dense Generic Refractory Concretes at Different Water Levels and With Different Cements and Commercial Refractory Concretes for Comparison

Properties	Standard 50% Al_2O_3 Generic With CA - 25		Standard 50% Al_2O_3 Generic With Refcon	Modified 50% Al_2O_3 Generic With CA - 25 Casting Grade		Commercial Casting Grade KAOTAB 95		Commercial LAO3RADE		
Water Added, %	10.2	10.8	10.2	10	11	8.0	10	10	11	12
Bulk Density, pcf (brick)										
RT Cured	139(140)	140(142)	141(140)	143(142)	141(141)	177(178)	176(175)	143(143)	138(139)	139(139)
24 hrs. @ 250°F	134(134)	133(133)	138(137)	140(139)	137(136)	172(173)	169(167)	138(137)	136(135)	135(133)
2 hrs. @ 450°F	-	-	-	-	-	-	-	-	-	-
2 hrs. @ 1000°F	-	-	-	133	132	-	-	-	131	129
2 hrs. @ 1500°F	-	-	-	133	132	-	-	-	128	128
Weight Loss, % (Green to fired)										
After 24 hrs. @ 250°F	-	3.5	2.6	2.7	3.7	3.2	-	2.4	2.5	2.9
After 2 hrs. @ 1000°F	-	6.8	7.6	5.5	5.5	6.8	-	-	5.9	6.8
After 2 hrs. @ 1500°F	-	7.2	7.8	6.6	6.5	7.2	-	-	6.2	6.8
After 0 hrs. @ 1875°F	-	7.3	8.6	5.8	-	7.7	-	-	7.3	-
Apparent Porosity, %										
RT Cured	-	14.5(3)	-	-	-	9.0(3)	-	-	-	-
24 hrs. @ 250°F	-	21.4	-	-	-	20.3	-	-	-	-
2 hrs. @ 1000°F	-	17.3	14.7	-	-	13.7	-	-	-	-
2 hrs. @ 2000°F(30 hrs.)	-	16.4(17.8)	15.9(16)	-	-	16.0(16.3)	-	-	-	-
Mean Pore Size, µm										
RT Cured	-	.20(3)	-	-	-	.19(3)	-	-	-	-
24 hrs. @ 250°F	-	.23	-	-	-	.19	-	-	-	-
2 hrs. @ 1000°F	-	.28	.89	-	-	.21	-	-	-	-
2 hrs. @ 2000°F(30 hrs.)	-	.53(.57)	1.3(1.6)	-	-	.42(.47)	-	-	-	-

Note: RT = Room Temperature

Table B-3. Physical Properties of the LITECAST 75-28 and Phosphate Bonded Monolithic Refractories at Different Water Levels or at Different Al_2O_3 Contents

Properties	Commercial LITECAST 75 - 28					Phosphate Bonded Monolithic Refractories		
						45% Al_2O_3 Generic	90% Al_2O_3 Generic	90 RAM Commercial
Water Added, %	21	23	24	26	29	6	5	-
Bulk Density, pcf (brick)								
RT Cured	90	88(91)	85(89)	87(87)	93(83)	-	-	-
24 hrs. @ 250°F	85	80(81)	79(79)	79(79)	78(77)	150	195	182
2 hrs. @ 450°F	-	-	-	-	-	-	-	-
2 hrs. @ 1000°F	82	-	77	77	-	142.5	185	172
2 hrs. @ 1500°F	82	-	77	76	-	-	-	-
Weight Loss, % (Green to fired)								
After 24 hrs. @ 250°F	6.5	7.1	9.2	9.8	11+	-	-	-
After 2 hrs. @ 1000°F	7.0	-	7.6	7.8	-	-	-	-
After 2 hrs. @ 1500°F	7.0	-	7.6	8.2	-	-	-	-
After 0 hrs. @ 1875°F	8.1	-	8.8	-	-	-	-	-
Apparent Porosity, %								
RT Cured	34.8	-	-	-	-	-	-	-
24 hrs. @ 250°F	30.0	-	-	-	-	-	-	-
2 hrs. @ 1000°F	29.1	-	-	-	-	-	-	-
2 hrs. @ 1500°F	31.5	-	-	-	-	-	-	-
Mean Pore Size, μm								
RT Cured	0.6	-	-	-	-	-	-	-
24 hrs. @ 250°F	0.2	-	-	-	-	-	-	-
2 hrs. @ 1000°F	0.3	-	-	-	-	-	-	-
2 hrs. @ 1500°F	1.2	-	-	-	-	-	-	-

Note: RT = Room Temperature

TABLE B-4. Physical and Mechanical Properties of the 90+% Al_2O_3 Dense Generic Refractory Concretes at Different Water Levels and With Different Cements

Properties	Standard 90+% Al_2O_3 Generic With CA - 25		Standard 90+% Al_2O_3 Generic With Secar 250		Standard 90+% Al_2O_3 Generic With CA-25 Casting Grade				Modified 90+% Al_2O_3 Generic With CA-25 Casting Grade
Water Added, %	9.3	10.2	10.0	10.5	8.8	9.3	9.8	10.3	8.5
Shrinkage, % Linear (% Volume)									
Green to 250°F for 24 hrs.	.1(.4)	0(.2)	0(.4)	0(.3)	.1(1.0)	.08(.9)	.1(.5)	0(.6)	.05
Green to 450°F for 24 hrs.	-	-	-	-	-	-	-	-	-
Green to 1000°F for 2 hrs.	-	-	-	-	-	-	-	-	-
Green to 1500°F for 2 hrs.	-	-	-	-	.2(1.2)	.2(1.2)	-	-	-
Green to 1875°F (no hold)	.1?	-	.25	-	.1(.5)	.3(.9)	-	-	-
Coefficient of Thermal Expansion (10^{-6}in/in.F)									
RT - 1875° (2nd cycle)	3.15	-	3.22	-	-	3.94(4.88)	-	-	3.50
700 - 1875°F	4.90	-	4.62	-	-	5.9	-	-	5.36
RT Modulus of Rupture, psi									
As Cured	1235	1205	2895	2325	1940	1775	-	-	-
After 24 hrs. @250°F	1390	1260	1860	1575	-	1680	-	-	1790 ± 330
Hot Modulus of Rupture, psi									
500°F	-	-	-	950 ± 150	-	870	-	-	980 ± 150
1000°F	1130	920	930	840 ± 320	-	1090	-	-	890 ± 170
1250°F	-	-	-	-	-	-	-	-	-
1500°F	-	-	-	685 ± 90	-	815	-	-	865 ± 155
1750°F	-	-	-	690 ± 225	-	640	-	-	610 ± 210
2000°F	820	960	905	615 ± 205	-	1210	-	-	760 ± 320
Hot Crushing Strength, psi									
RT (dried @250°F for 24 hrs.)	4730	-	7285	11120 ± 1030	-	9815	-	-	9100 ± 1750
500°F	-	-	-	6830 ± 605	-	8750	-	-	9220 ± 530
1000°F	-	-	-	7200 ± 570	-	8650	-	-	9690 ± 1040
1250°F	-	-	-	-	-	-	-	-	-
1500°F	-	-	-	8330 ± 580	-	9740	-	-	9130 ± 1480
1750°F	-	-	-	5915 ± 115	-	9680	-	-	7300 ± 1160
2000°F			-	5030 ± 425	-	10440	-	-	8455 ± 420
Hot Modulus of Elasticity, 10^3psi									
RT	-	-	-	1.7 ± .8	-	1.19	-	-	1.5
500°F	-	-	-	.7 ± .3	-	.77	-	-	.78
1000°F	-	-	-	.5 ± .2	-	.62	-	-	.75
1250°F	-	-	-	-	-	-	-	-	-
1500°F	-	-	-	.4 ± .1	-	.58	-	-	.71
1750°F	-	-	-	.3 ± .1	-	.60	-	-	.36
2000°F	-	-	-	.2 ± .1	-	.56	-	-	.44
Thermal Conductivity, Btu/in/hr.ft^{2}F	-	-	-		-	13.1	-	-	13.1

TABLE B-5. Physical and Mechanical Properties of the 50% Al_2O_3 Dense Generic Refractory Concrete at Different Water Levels and With Different Cements and the Commercial Refractory Concretes for Comparison

Properties	Standard 50% Al_2O_3 Generic With CA - 25		Standard 50% Al_2O_3 Generic With Refcon	Modified 50% Al_2O_3 Generic With CA-25 Casting Grade			Commercial KAOTAB 95	
Water Added, %	10.2	10.8	10.2	10	11	11 (Large Batch)	8.0	10
Shrinkage, % Linear (% Volume)								
Green to 250°F for 24 hrs.	0(.4)	0(.4)	0(.6)	0(.9)	.1(.6)	.08	.1(.4)	0(.1)
Green to 450°F for 24 hrs.				-	-	-	.14	-
Green to 1000°F for 2 hrs.				.2(1.2)	.2(1.2)	.1	-	-
Green to 1500°F for 2 hrs.				.1(.6)	.1(.5)	.1	-	-
Green to 1875°F (no hold)	.22	.2	.19	.2	.2	.1	.1	-
Coefficient of Thermal Expansion (10^{-6}in/in°F)								
RT - 1875° (2nd cycle)	-	1.79	1.85	2.1	2.06	2.71	3.84	-
700 - 1875°F	-	2.54	2.44	2.9	2.90	3.15	5.30	-
RT Modulus of Rupture, psi								
As Cured	1340	1315	-	1460	1425	-	1695	1200
After 24 hrs. @250°F	1100	1225	1650	-	1125 ± 140	980	1620	1220
Hot Modulus of Rupture, psi								
500°F	-	-	-	-	860 ± 85	-	-	-
1000°F	830	980	1130	-	890 ± 50	950	1320	855
1250°F	-	-	-		-	-	-	-
1599°F	-	-	-	-	1030 ± 150	1080	-	-
1750°F	-	-	-	-	660 ± 85	-	-	-
2000°F	765	940	1010	-	435 ± 90	850	1320	800
Hot Crushing Strength, psi								
RT (dried @250°F for 24 hrs.)	-	3760	5200	-	8020 ± 880	4000	5940	-
500°F	-	-	-	-	6705 ± 850	4195	-	-
1000°F	-	-	-	-	8570 ± 910	3770	-	-
1250°F	-	-	-	-	-	-	-	-
1500°F	-	-	-	-	10130 ± 470	5680	-	-
1750°F	-	-	-	-	8090 ± 390	4550	-	-
2000°F	-	-	-	-	6300 ± 1020	3865	-	-
Hot Modulus of Elasticity, 10^6psi								
RT	-	-	-	-	.9 ± .5	.2	-	-
500°F	-	-	-	-	.6 ± .3	.2	-	-
1000°F	-	-	-	-	1 ± .4	.2	-	-
1250°F	-	-	-	-	-	-	-	-
1500°F	-	-	-	-	.6 ± .2	.2	-	-
1750°F	-	-	-	-	.6 ± .3	.1	-	-
2000°F	-	-	-	-	.2 ± .1	.1	-	-

TABLE B-6. Physical and Mechanical Properties of the Insulating Refractory Concretes anc Phosphate Bonded Monolithic Refractories at Different Water Levels and With Different Al_2O_3 Contents

Properties	Commercial LITECAST 75 - 28					Commercial KACLITE 2300 LI	Phosphate Bonded Monolithic Refractories 45% Al_2O_3 Generic	90% Al_2O_3 Generic	90 RAM Commercial
Water Added, %	21	23	24	26	29	59	6	5	-
Shrinkage, % Linear (% Volume)									
Green to 250°F for 24 hrs.	.1(.6)	.1(.8)	.4(1.1)	.1(.8)	.1(1.0)	.09	-	-	-
Green to 450°F for 24 hrs.	-	-	-	-	-	-	.2	.2	.3
Green to 1000°F for 2 hrs.	.3(1.5)	-	.2(1.1)	.3(1.1)	-	.4	-	-	-
Green to 1500°F for 2 hrs.	.3(1.2)	-	.3(1.3)	.4(1.4)	-	.6	-	-	-
Green to 1875°F (no hold)	.3	-	4	-	-	-	.2	.1	-
Coefficient of Thermal Expansion (10^{-6} in/in.°F)									
RT - 1875° (2nd cycle)	2.61(4.1)	-	.42	-	-	-.12(3.3)	3.24	4.84	-
700 - 1857°F	4.04	-	2.8	-	-	1.19	3.83	5.45	-
RT Modulus of Rupture, psi									
As Cured	655	-	545	510	-	-	1315 ± 80	2135 ± 50	1790 ± 255
After 24 hrs. @250°F	570 ± 65	-	415	-	-	230	-	-	-
Hot Modulus of Rupture, psi									
500°F	320 ± 30	-	365	-	-	170	1470 ± 210	2155 ± 320	1800 ± 165
1000°F	225 ± 55	-	200	-	-	150	2445 ± 270	3210 ± 890	3290 ± 360
1250°F	220 ± 25	-	150	-	-	140	2360 ± 260	3810 ± 320	3205 ± 160
1500°F	185 ± 115	-	100	-	-	-	-	-	-
1750°F	-	-	-	-	-	150	2800 ± 105	3830 ± 50	1320 ± 460
2000°F	-	-	-	-	-		1770 ± 60	1260 ± 160	165 ± 90
Hot Crushing Strength, psi									
RT (dried @250°F for 24 hrs.)	3945 ± 350	-	-	-	-	430	2480 ± 345	2680 ± 385	3490 ± 1050
500°F	3490 ± 180	-	-	-	-	505	3480 ± 715	4830 ± 545	3740 ± 1825
1000°F	3940 ± 340	-	-	-	-	540	5205 ± 480	6670 ± 800	6770 ± 2330
1250°F	4245 ± 740	-	-	-	-	560	6080 ± 1100	8000 ± 630	6840 ± 2030
1500°F	5330 ± 450	-	-	-	-	-	-	-	-
1750°F	-	-	-	-	-	820	8080 ± 455	6370 ± 710	4160 ± 980
2000°F	-	-	-	-	-	-	3640 ± 640	1530 ± 540	1260 ± 405
Hot Modulus of Elasticity, 10^3psi									
RT	.6 ± .3	-	-	-	-	.02	.3 ± .2	.2 ± .1	.1 ± 0
500°F	.3 ± .1	-	-	-	-	-	.2 ± .1	.3 ± .2	.3 ± .3
1000°F	.4 ± .2	-	-	-	-	.02	.5 ± .3	.4 ± .2	.6 ± .3
1250°F	.4 ± .2	-	-	-	-	-	-	-	-
1500°F	.2 ± .1	-	-	-	-	.03	.4 ± .2	.4 ± .2	.4 ± .2
1750°F	-	-	-	-	-	-	.4 ± .2	.3 ± .2	.1 ± .1
2000°F	-	-	-	-	-	-	.2 ± .1	.1 ± 0	.1 ± .1
Thermal Conductivity, Btu/in/hr.ft²F	2.8	-	2.6	-	-	1.6	7.2	15.5	15.5

TABLE B-7. Physical and Mechanical Properties of Various Refractory Concretes from Different Linings or With Different Pretreatments

Properties	Improved 90+% Al_2O_3 Generic With CA - 25 Casting Grade				KAOCRETE XD 50 (Mix 36C)						Commercial LITECAST 75 - 28		
	Lining #3+	#4	1200F Steam* #4	1850F Steam #4	Lining #5	1200F Steam #5	1850F Steam #5	Lining #6	1200F Steam #6	1850F Steam #6	Lining #6	1200F Steam #6	1850F Steam #6
Shrinkage % Linear													
Green to 250°F for 24 hrs.	.03	.05	-	-	.04	-	-	.04	-	-	.1	0	0
Green to 1000°F for 2 hrs.	-	-	-	-	-	-	-	-	-	-	-	0	0
Green to 1500°F for 2 hrs.	.2	-	.1	0	-	0	0	-	0	0	-	0	0
Green to 2000°F for 2 hrs.	.2	-	.1	.05	-	-	-	-	-	-	-	-	-
Coefficient of Thermal Expansion (10^{-6}in/in./°F)													
RT - 1875°F (Second cycle)	3.86(4.8)	-	4.87	4.73	-	3.16	3.67	2.39	2.94	3.50	2.02	5.06	4.37
700° - 1875°F	5.42	-	-	-	-	3.06	3.46	2.62	2.79	3.47	3.88	-	
Modulus of Rupture, psi (dried @250°F for 24 hrs)	2550	-	1325	1500	-	1360	1120	-	-	-	1080	790	660
Crushing Strength, psi (dried @250°F for 24 hrs)	12140	9170	10160	7185	-	6780	8430	-	-	-	-	2150	2335
Splitting Tensile Strength, psi (dried @250°F for 24 hrs)	1880	-	-	1560	715	380	580	535	638	879	375	370	333

* 150 psig steam
\+ Samples were prepared while the linings were being cast.

TABLE B-8. Physical and Mechanical Properties of KAOCRETE XD 50(Mix 36C) with Different Levels and Types of Stainless Steel Fibers

Properties	KAOCRETE XC50 (Mix 36C) 2% 446SS	4% 446SS	4% 310SS (Lining #7)
Bulk Density, pcf (220°F Dried)	142	143	
Linear Shrinkage, % (-1875°F)	.04	.04	.05
Coefficient of Thermal Expansion x (10^{-6} in/in/°F)			
RT - 1875°F (second cycle)	3.32	3.81	5.0(4.51)
680 - 1875°F	3.65	4.02	5.73
Hot Modulus of Rupture, psi			
RT	1150 ± 225	1460 ± 135	1990±430
500°F	585 ± 120	675 ± 85	1080±430
1000°F	650 ± 140	565 ± 140	1070±190
1500°F	570 ± 170	650 ± 60	990±175
1800°F	510 ± 80	460 ± 30	730± 90
2000°F	470 ± 75	390 ± 55	575±160
Hot Crushing Strength, psi			
RT	2560 ± 635	3350 ± 600	3220±410
500°F	3965 ± 1055	4300 ± 460	3480±850
1000°F	3820 ± 1290	4660 ± 560	3520±650
1500°F	6960 ± 1250	6090 ± 670	4725±370
1800°F	6180 ± 950	4080 ± 2115	4380±435
2000°F	5630 ± 1220	4460 ± 610	3680±270
Hot Modulus of Elasticity x 10^6 psi			
RT	-	-	.13
500°F	-	-	.14
1000°F	-	-	.15
1500°F	-	-	.14
1750°F	-	-	.12
2000°F	-	-	.10

TABLE B-9. Shrinkage Results on ERDA 90 and LITECAST 75-28 After Different Storage Conditions

Storage Conditions	ERDA 90 (7.8% Water)						LITECAST 75-28 (21% Water)					
	200 F/hr to 1200 F @ 2 hrs			Case #1 to 2000 F @ 5 hrs			200 F/hr to 900 F @ 2 hrs			Case #1 to 1500 F @ 5 hrs		
	ΔL/L,%	ΔV/V,%	Wt. Loss %	ΔL/L,%	ΔV/V,%	Wt. Loss %	ΔL/L,%	ΔV/V,%	Wt. Loss %	ΔL/L,%	ΔV/V,%	Wt. Loss %
In Air (Ambient)												
5 Days	0.2	0.3	3.4	0.2	0.5	3.8	0.3	0.8	16.1	--	--	--
18 Days	0.1	0.3	2.7	--	--	--	0.2	0.5	5.2	0.3	0.3	5.8
100% Humidity												
5 Days	0.2	0.4	4.0	--	--	--	0.4	0.9	16.1	--	--	--
18 Days	0.2	0.5	5.5	--	--	--	0.3	0.3	8.5	--	--	--

NOTE: Sample test bars were cured overnight at ambient conditions in molds, then removed from molds and either stored in air or placed in 100% humidity environment (a Desiccator containing water) at 72 F (30 C) for the prescribed period before the shrinkage tests were run. Separate samples were used for each test.

TABLE B-10. Uniaxial Compression Test Data for Lining #5

SAMPLE # 1

SAMPLE TITLE	DIMENSIONS(IN)	TEMP(F)	SOAK(MIN)	P-MAX(LB)
	1.02 X 1.06 X 0.52	500	30	5201

CRUSHING STRENGTH = 9436 PSI

P(LB)	Y(MILS)	STRESS(PSI)	STRAIN(MILS/IN)
0	0.00	0	0.00
39	1.35	71	0.11
82	2.60	149	0.76
126	3.90	229	1.71
180	5.40	327	2.99
255	7.10	463	4.52
335	9.00	608	6.21
445	10.75	807	7.73
580	12.20	1052	8.94
750	13.20	1361	9.71
930	14.25	1687	10.55
1300	15.80	2358	11.75
1550	16.50	2812	12.27
1800	17.25	3266	12.83
2050	18.00	3719	13.39
2300	18.80	4173	14.00
2550	19.25	4626	14.27
2800	20.00	5080	14.83
3100	21.00	5624	15.60
3400	21.75	6168	16.13
3650	22.75	6622	16.94
3900	23.75	7075	17.74
4200	24.80	7620	18.56
4500	26.00	8164	19.53
4750	27.30	8618	20.63
5000	28.50	9071	21.63
5200	30.00	9434	22.97
5201	31.50	9436	24.44

TABLE B-11. Percent (%) Deformation During Creep Tests on LITECAST 75-28 with Varying Water Levels Subjected to 700 psi or Less Strain

	700 psi					500 psi	
	21% H_2O	24% H_2O	24% H_2O	24% H_2O	26% H_2O	26% H_2O	26% H_2O
Starting Density (pcf)	85.5	79.1	75.9	79.5	77.8	78.0	79.0
Time (hrs)/Temperature (°F)							
1 hr. / 75°F	-	.14	-	-	-	-	-
3 hrs. / 500°F	.31	.29	-	-	-	-	-
3 hrs. / 1000°F	.22	.15	.39 (10 hrs.)	-	.57 (10 hrs.)	.45 (30 hrs.)	.86 (30 hrs.)
3 hrs. / 1500°F	1.51 (10 hrs.)	2.26 (10 hrs.)	-	8.66 (10 hrs.)	-	-	-
3 hrs. / 1800°F	-	-	-	-	-	-	-
10 hrs. / 2000°F	-	-	-	-	-	-	-
Post Test Density (pcf)	82.2	76.2	73.6	76.4	74.6	75.2	76.9

pcf = lb/ft^3

TABLE B-12. Percent (%) Deformation During Creep Tests on Various Monolithic Refractories Subjected to 1000 PSI Stress

	KAOCRETE XD 50 (Mix 36C)					LITECAST 75-28			Phosphate Bonded Monolithic Refractories			
		Lining #5	Lining #6	w/2% 310SS	w/4% 446SS	w/21% H_2O	w/21% H_2O	w/24% H_2O	90P	90P	90RAM	45P
Starting Density pcf	-	138.9	143.6	-	145.9	84.9	84.7	80.4	187	186.1	181	145.0
Time(hrs)/ Temperature(°F)												
1 hr. / 75°F	.07	.05	.06	.06	.08	-	.22	.15	.02	.04	.02	.03
3 hrs. / 500°F	.15	-	.17	.16	.23	.44	.39	.32	.01	.01	.01	-
3 hrs. / 1000°F	.08	.13	.09	.11	.27	.24	.29	.35	.01	.01	0	.06
3 hrs. / 1500°F	.13	.20	.21	.24	.64	2.08 (10 hrs)	2.93 (10 hrs)	4.97 (3 hrs)	.04	.01	.04	.04
3 hrs. / 1800°F	.16	.30	.18	.24	.27	-	-	-	.76	.53 (10 hrs)	.76	.22 (10 hrs)
10 hrs. / 2000°F	.53	1.44	.76	1.38	1.58	-	-	-	1.26 (failed 12 min)		1.68 (failed 12min)	-
Post Test Density (pcf)	-	137.6	140.6	-	143.6	81.6	81.7	76.4	-	184.9	-	143.3

pcf = lb/ft^3

TABLE B-13. Percent(%) Deformation During Creep Tests on Various Monolithic Refractories Subjected to 1500 and 2000 PSI Stresses

1500 psi

	90+% Al_2O_3 Generic with Secar 250	KAOCRETE XD 50 (Mix 36C) 1st Cycle	KAOCRETE XD 50 w/310SS (Retest)	50% Al_2O_3 Generic with CA-25 Standard	50% Al_2O_3 Generic with CA-25 Standard	50% Al_2O_3 Generic with CA-25 Modified	Commercial LOABRADE	LITECAST 75-28 21% H_2O	LITECAST 75-28 21% H_2O
Starting Density (pcf)	172.4	145.4	143.4	132.8	136.0	137.8	134.6	84.6	85.4
Time(hrs)/Temperature(°F)									
1 hr. / 75°F	-	.14	.02	-	-	.14	-	-	.03
3 hrs. / 500°F	-	.27	.02	-	-	.19	-	.21	.22
3 hrs. / 1000°F	.35(30 hr)	.20	.14	.47*(34 hr)	.25	.25	.20	.26	.40
3 hrs. / 1500°F	-	.37	.27	-	.31	.39	.36	3.10(10 hr)	3.81(10 hr)
3 hrs. / 1800°F	-	.38	.27	-	.65(10 hr)	.55	1.05(10 hr)	-	-
10 hrs. / 2000°F	-	2.08	1.32	-	-	.73	-	-	-
Post Test Density (pcf)	166.9	143.4	-	129.0	132.6	133.5	128.6	81.2	81.3

* Average of two samples which had 0H6 & 0.48% Deformation

2000 psi

	Modified 90+% Al_2O_3 Generic With CA-25 Casting Grade			KAOCRETE XD 50 (Mix 36C) Lining #6	1200°F Steam* Lining #5	w/2% 310SS	w/4% 310SS	Lining #7 w/4%310SS	w/4% 446SS	Phosphate Bonded Monolithic Refractory 45P
Starting Density (pcf)	169.8	171.8	175.4	146.3	-	137.7	143.0	141.3	141.6	145.0
Time(hrs),Temperature(°F)										
1 hr. / 75°F	-	.08	.01	.09	.23	.11	.10	.29	.06	.01
3 hrs. / 500°F	-	.13	.13	.12	.25	.38	.29	.52	.12	-
3 hrs. / 1000°F	.25	.12	.02	.28	.24	.22	.28	.28	.18	.24
3 hrs. / 1500°F	.44	.29	.16	.56	.46	.50	.54	.50	.36	.13
3 hrs. / 1800°F	-	.51	.29	.88	.44	.60	.71	.49	.36	.49 (10 hrs)
10 hrs. / 2000°F	2.4	2.52	1.65	3.77	2.18	failed	failed	failed	1.44	-
Post Test Density (pcf)	161.7	163.6	168.7	142.0	-	-	-	-	138.5	143.3

TABLE B-14. Percent (%) Deformation During Creep Tests on Various Refractories Subjected to 2500 and 3300 PSI Stresses

	2500 PSI		
		50% Al_2O_3 Generic	
	KAOCRETE XD50 (Mix 36C) Lining #6	Standard	Modified
Starting Density (pcf)	142.1	139.8	137.2
Time(hrs)/Temperature(°F)			
1 hr/75°F	.05	---	.09
3 hrs/500°F	.08	.29	.27
3 hrs/1000°F	.11	.16	.22
3 hrs/1500°F	.37	.41	.94
3 hrs/1800°F	.46	.87 (10 hrs)	1.85 (failed 1.25 hrs)
Post Test Density (pcf)	138.7	134.9	---

	3300 PSI		
	90+% Al_2O_3 Generic With CA-25 Casting Grade		
	9.3% H_2O	8.5% H_2O	9.0% H_2O
Starting Density (pcf)	169.8	174.4	174.8
Time(hrs)/Temperature(°F)			
1 hr/75°F	---	.03	.16(3 hrs)
3 hrs/500°F	.57	.52	.54
3 hrs/1000°F	.22	.16	.24
3 hrs/1500°F	.35	.36	.49
3 hrs/1800°F	---	.58	1.32
10 hrs/2000°F	2.22	3.62	3.65(7 hrs)
Post Test Density (pcf)	163.7	166.8	162.1

TABLE B-15. 11 Hour Hot Load Deformation of 90+% Al_2O_3 Generic With CA-25 and Phosphate Bonded Refractories

90+% Al_2O_3 Generic

Material	Density (pcf) Before	Density (pcf) After	% Deformation @ 1800°F 100 psi	% Deformation @ 1800°F 200 psi	% Deformation @ 2000°F 100 psi	% Deformation @ 2000°F 200 psi
Standard	168.9	161.0	.18	-	-	-
"	172.5	165.5	-	.23	-	-
"	177.1	170.4	-	-	.08	-
"	172.8	166.2	-	-	-	.31
Lining #4	169.9	152.8	-	-	.044	-
"	172.3	163.8	-	-	-	.09
"	175.2	165.5	-	-	.044	-
"	-	-	-	-	-	.17
Modified/ Casting Grade	170.9	162.3	-	-	.033	-
"	172.7	164.3	-	-	.028	-
Modified/ Casting Grade	171.2	162.6	-	-	+.083	-
"	175.4	168.7	-	-	.011	-
"	173.6	164.9	-	-	.033	-
"	177.0	164.9	-	-	.022	-

Note: + = Expansion

Phosphate Bonded Refractories

Material	Density (pcf) Before	Density (pcf) After	% Deformation @ 1500°F 100 psi	% Deformation @ 1500°F 200 psi	% Deformation @ 2000°F 100 psi	% Deformation @ 2000°F 200 psi
90P	183.6	184.3	-	-	-	.81
"	181.9	180.2	-	-	-	.133
"	179.0	177.7	-	-	.43	-
90 RAM	165.1	162.9	-	-	1.18	-
"	164.9	163.3	.045	-	-	-
"	170.3	168.7	.08	-	-	-
45P	138.0	138.0	-	-	-	.83
"	139.0	138.8	-	-	.63	-
"	140.9	140.0	-	-	.33	-
"	137.2	135.5	-	.07 } 1800F	-	-

TABLE B-16. 11 Hour Hot Load Deformation of 50% Al_2O_3 Monolithic Refractories

Material	Density (pcf)		% Deformation @ 1500°F		% Deformation @ 1800°F		% Deformation @ 2000°F	
	Before	After	100 psi	200 psi	100 psi	200 psi	100 psi	200 psi
50% Al_2O_3 Generic	133.9	127.6	-	-	-	.31	-	-
	135.3	129.0	-	-	.18	-	-	-
KAOCRETE XD 50 Lining #5	135.7	132.3	-	-	-	-	.28	-
"	135.2	132.3	-	-	-	-	-	.43
Lining #6	140.8	138.3	-	-	-	-	.37	-
"	139.8	137.5	-	-	-	-	-	.47
Lining #7*	146.7	144.5	-	-	-	-	-	.62
"	144.2	141.8	-	-	-	-	-	.71
KAOCRETE XD 50	139.1	134.0	-	-	-	-	.41	-
"	138.7	133.0	-	-	-	-	.22	-
"	134.9	129.1	.11	-	-	-	-	-
"	139.6	133.4	-	-	.22	-	-	-
LOABRADE	137.3	130.3	-	-	-	-	.53	-
"	136.2	130.8	-	-	-	-	-	.82
"	134.9	129.9	.15	-	-	-	-	-
"	136.7	131.4	-	.23	-	-	-	-
"	134.3	130.3	.08 } 1000F	-	-	-	-	-
"	133.5	129.6	.11 }	-	-	-	-	-
"	132.2	128.2	-	-	-	-	1.3	-
KAOCRETE XD 50 w/10% Kymte	140.1	135.7	-	-	-	-	-	.12
"	146.7	139.9	-	-	-	-	-	.61
KAOCRETE XD 50 w/2% 446SS	136.7	133.4	-	-	-	-	-	.54
"	145.1	141.8	-	-	-	-	-	.54
"	133.6	130.6	-	-	-	-	-	.63
"	137.7	134.1	-	-	-	-	-	.46

* This material has 4 w/o 310SS Fibers added to it.

TABLE B-17. 11 Hour Hot Load Deformation of Insulating Monolithic Refractories

Material	Density (lb/ft^3)		% Deformation @ 1500°F	% Deformation @ 1800°F		% Deformation @ 2000°F	
Litecast 75-28	Before	After	100 psi	100 psi	200 psi	100 psi	200 psi
w/21% H_2O	83.8	81.3	-	-	3.32	-	-
"	85.3	82.7	-	1.46	-	-	-
"	85.4	81.7	.25	-	-	-	-
"	87.9	83.9	.29	-	-	-	-
w/24% H_2O	79.1	77.2	-	-	5.76	-	-
"	77.4	73.5	.41	-	-	-	-
"	79.1	75.2	-	1.93	-	-	-
"	76.5	73.5	1.11	-	-	-	-
"	80.5	77.4	1.04	-	-	-	-
"	80.0	75.4	.24 } 1000F	-	-	-	-
"	80.4	76.7	.25 } 1000F	-	-	-	-
w/26% H_2O	78.5	74.6	.42	-	-	-	-
"	86.3	82.9	-	1.4	-	-	-
"	81.2	78.4	.26 } 30 hr	-	-	-	-
"	77.3	74.9	.31 } 30 hr	-	-	-	-
Lining #4	-	-	-	-	-	-	Failed
"	79.8	75.8	-	-	4.03	-	-
"	76.7	73.2	-	-	4.1	-	-
Lining #5	-	-	-	-	-	-	Failed
"	83.6	80.5	-	-	3.31	-	-
"	83.2	78.6	-	-	2.27	-	-
Lining #6	-	-	-	-	-	3.14	-
"	-	-	-	-	-	3.32	-
"	91.8	87.8	-	-	-	4.24	-
"	-	-	-	-	-	-	Failed
"	89.2	85.1	-	-	-	3.62	-
Lining #7	-	-	-	-	-	-	Failed
"	84.9	81.1	-	-	-	6.48	-
"	84.1	80.1	-	-	-	4.42	-
"	81.6	-	-	-	-	-	Failed
w/4% 31055	-	-	-	-	-	-	Failed
"	92.5	89.4	-	-	-	3.67	-
Kaolite 2300LI	62.2	59.4	-	-	-	7.73	-
"	-	-	-	-	-	7.86	-
"	-	-	-	-	-	-	Failed

TABLE B-18. Creep and Deformation Results on the Modified 90+% Al_2O_3 Dense Generic Refractory Concrete at Different Stress Levels and Temperatures

Temperature		RT	500°F	1000°F	1500°F	1800°F	2000°F	Total Def. %
Stress					1500 PSI			
Time	Log T	(Bulk Density, pcf)			(170.0)			
0	0	0	-	0.0099	.0212	0.0383	0.0904	-
3 Minutes	-1.301	0	-	.0105	.0243	.0486	.0937	-
6 Minutes	-1.000	.0001	-	.0143	.0294	.0510	.0967	-
12 Minutes	-0.699	.0002	-	.0164	.0318	.0548	.1012	-
15 Minutes	-0.602	.0003	-	.0189	.0340	.0565	.1031	-
30 Minutes	-0.301	.0004	-	.0203	.0360	.0650	.1128	-
45 Minutes	-0.125	.0006	-	.0213	.0373	.0696	.1178	-
1 Hour	0.000	.0008	-	.0227	.0382	.0738	.1214	-
2 Hours	0.301	.0010	-	.0230	.0405	.0825	.1372	-
3 Hours	0.477	.0011	-	.0256	.0423	.0934	.1447	-
4 Hours	0.602	-	-	-	-	-	.1522	-
5 Hours	0.699	-	-	-	-	-	.1597	-
10 Hours	1.000	-	-	-	-	-	.1970	-
% Deformation		0.02	-	0.26	0.34	0.90	1.7 (3.22)	3.22

(Post Test Deformation Measured RT on Stepwise Tested Specimen)
* Sample Was Slightly "S" Shaped After Test)

Temperature		RT	500°F	1000°F	1500°F	1800°F	2000°F	Total Def. %
Stress					2000 PSI			
Time	Log T				(171.8)			
0	0	0	0.0084	0.0199	0.0200	0.0393	0.0515	-
3 Minutes	-1.301	0.0046	.0146	.0230	.0257	.0430	.0575	-
6 Minutes	-1.000	.0046	.0150	.0232	.0272	.0438	.0610	-
12 Minutes	-0.699	.0046	.0153	.0235	.0273	.0450	.0625	-
15 Minutes	-0.602	.0047	.0159	.0235	.0278	.0454	.0655	-
30 Minutes	-0.301	-	.0168	.0238	.0285	.0475	.0735	-
45 Minutes	-0.125	-	.0180	.0239	.0294	.0492	.0800	-
1 Hour	0.000	-	.0190	.0240	.0300	.0512	.0845	-
2 Hours	0.301	-	.0220	.0248	.0320	.0555	.1010	-
3 Hours	0.477	-	.0228	.0248	.0327	.0587	.1125	-
4 Hours	0.602	-	-	-	-	-	.1215	-
5 Hours	0.699	-	-	-	-	-	.1295	-
10 Hours	1.000	-	-	-	-	-	.1600	-
% Deformation		0.08	0.23	0.08	0.20	0.32	1.8 (2.36)	2.71

Temperature		RT	500°F	1000°F	1500°F	1800°F	2000°F	Total Def. %
Stress					3300 PSI			
Time	Log T				(174.4)			
0	0	0	0.0097	0.0339	0.0337	0.0686	0.0903	-
3 Minutes	-1.301	0.0090	-	.0401	.0450	.0070	.1035	-
6 Minutes	-1.000	-	-	-	-	-	-	-
12 Minutes	-0.699	-	.0234	-	-	-	-	-
15 Minutes	-0.602	.0096	-	.0413	.0413	.0822	.1209	-
30 Minutes	-0.301	-	.0268	.0418	.0418	.0857	.1330	-
45 Minutes	-0.125	-	.0296	-	-	-	-	-
1 Hour	0.000	-	.0323	.0420	.0420	.0914	.1602	-
2 Hours	0.301	-	.0393	.0428	.0428	.0986	.1973	-
3 Hours	0.477	-	.0417	.0434	.0434	.1037	.2187	-
4 Hours	0.602	-	-	-	-	-	.2381	-
5 Hours	0.699	-	-	-	-	-	.2543	-
10 Hours	1.000	-	-	-	-	-	.3108	-
% Deformation		0.16	0.52	0.16	0.52	0.58	3.6 (5.00)	5.38

TABLE B-19. Creep and Deformation Results on the Modified 90+% Al_2O_3 Dense Generic (ERDA 90-Lining #4) Refractory Concrete at Different Stress Levels and Temperatures.

Temperature		RT	1000°F	1500°F	1800°F	2000°F	Total Def. %
Stress				1500 psi			
Time	Log T	(Bulk Density, pcf)		(174.4)			
0	0	-	0.0054	0.0067	0.0128	0.0222	
3 Minutes	-1.301	0.0016	0.0093	0.0116	0.0205	.0367	
6 Minutes	-1.000	0.0017	0.0094	0.0119	0.0226	.0377	
12 Minutes	-0.699	0.0018	0.0096	0.0120	0.0255	.0394	
15 Minutes	-0.602	0.0019	0.0096	0.0121	0.0266	.0401	
30 Minutes	-0.301	0.0019	0.0098	0.0127	0.0306	.0435	
45 Minutes	-0.125	0.0020	0.0099	0.0134	0.0330	.0463	
1 Hour	0.000	0.0021	0.0101	0.0139	.0360	.0486	
2 Hours	0.301	-	0.0104	0.0145	.0402	.0560	
3 Hours	0.477	-	0.0106	0.0152	.0431	.0627	
4 Hours	0.602	-	-	-	-	.0688	
5 Hours	0.699	-	-	-	-	.0743	
10 Hours	1.000	-	-	-	-	.0997	
% Deformation		0.03	0.08	0.14	0.49	1.08 (1.45)	1.82

(Post Test Deformation measured at RT on Stepwise Tested Specimen)

Temperature		RT	1000°F	1500°F	1800°F	2000°F	Total Def. %
Stress				2500 psi			
Time	Log T			(176.2 pcf)			
0	0	0	0.0110	0.0182	0.0315	0.0703	
3 Minutes	-1.301	0.0074	.0227	.0281	.0441	.0761	
6 Minutes	-1.000	.0076	.0232	.0288	.0487	.0777	
12 Minutes	-0.699	.0080	.0239	.0296	.0529	.0802	
15 Minutes	-0.602	.0080	.0240	.0300	.0548	.0809	
30 Minutes	-0.301	.0084	.0246	.0311	.0618	.0850	
45 Minutes	-0.125	.0086	.0249	.0322	.0663	.0887	
1 Hour	0.000	.0087	.0252	.0333	.0699	.0923	
2 Hours	0.301	-	.0259	.0361	.0783	.1046	
3 Hours	0.477	-	.0262	.0375	.0831	.1136	
4 Hours	0.602	-	-	-	-	.1234	
5 Hours	0.699	-	-	-	-	.1310	
10 Hours	1.000	-	-	-	-	.1643	
% Deformation		0.1	0.25	0.32	0.[illegible]	1.54 (2.33)	3.00

Temperature		RT	1000°F	1500°F	1800°F	2000°F	Total Def. %
Stress				3300 psi			
Time	Log T			(179.5 pcf)			
0	0	0	0.0079	0.0110	0.0275	0.0772	
3 Minutes	-1.301	0.0040	.0194	0.0240	.0381	0.0876	
6 Minutes	-1.000	.0042	.0198	0.0250	.0406	.0904	
12 Minutes	-0.699	.0044	.0200	.0262	.0445	.0946	
15 Minutes	-0.602	.0045	.0200	.0267	.0460	.0963	
30 Minutes	-0.301	.0046	.0201	.0290	.0524	.1039	
45 Minutes	-0.125	.0047	.0202	.0304	.0579	.1108	
1 Hour	0.000	.0048	.0204	.0315	.0631	.1174	
2 Hours	0.301	-	.0210	.0346	.0830	.1428	
3 Hours	0.477	-	.0215	.0362	.0927	.1616	
4 Hours	0.602	-	-	-	-	.1781	
5 Hours	0.699	-	-	-	-	.1938	
10 Hours	1.000	-	-	-	-	.250[illegible]	
% Deformation		0.08	0.22	0.40	0.87	2.77 (3.75)	4.34

TABLE B-20. Creep (Inches) and Deformation (%) Results on 50% Al_2O_3 Dense Generic Refractory Concrete at Different Stress Levels and Temperature (6 Inch Long Specimens)

Temperature		RT	250°F	500°F	1000°F	1500°F	1800°F	Total Def. %
Stress				2500 psi				
Time	Log T			(140.0)				
0	0	-	0	0.008	0.0250	0.0310	0.0510	
3 Minutes	-1.301	-	0.0050	.0165	.0300	.0410	.0620	
6 Minutes	-1.000	-	.0075	.0180	.0305	.0430	.0650	
12 Minutes	-0.699	-	-	.0190	.0310	.0455	.0710	
15 Minutes	-0.602	-	.0080	.0195	.0315	.0460	.0730	
30 Minutes	-0.301	-	.0085	.0205	.0315	.0480	.0775	
45 Minutes	-0.125	-	.0085	.0210	.0315	.0495	.0815	
1 Hour	0.000	-	.0090	.0215	.0315	.0510	.0845	
2 Hours	0.301	-	.0095	.0250	.0320	.0540	.0880	
3 Hours	0.477	-	.0100	.0260	.0320	.0560	.0900	
4 Hours	0.602	-	-	-	-	-	.0920	
5 Hours	0.699	-	-	-	-	-	.0940	
10 Hours	1.000	-	-	-	-	-	.1040	
% Deformation		-	0.08	0.30	0.11	0.41	0.87 (1.70)	1.76

Temperature		RT	1000°F	1500°F	1800°F	Total Def. %
Stress				1500 psi		
Time	Log T		(Bulk Density, pcf)	(136.0)		
0	0	-	0	0.0090	0.0247	-
3 Minutes	-1.301	-	0.0080	.0180	.0315	-
6 Minutes	-1.000	-	.0090	.0200	.0350	-
12 Minutes	-0.699	-	.0110	.0210	.0370	-
15 Minutes	-0.602	-	.0115	.0220	.0380	-
30 Minutes	-0.301	-	.0119	.0230	.0410	-
45 Minutes	-0.125	-	.0120	.0240	.0430	-
1 Hour	0.000	-	.0120	.0245	.0450	-
2 Hours	0.301	-	.0125	.0265	.0500	-
3 Hours	0.477	-	.0125	.0280	.0530	-
4 Hours	0.602	-	-	-	.0550	-
5 Hours	0.699	-	-	-	.0570	-
10 Hours	1.000	-	-	-	.0642	-
% Deformation		-	0.07	0.31	0.65 (1.0)*	51.03

(Post Test Deformation Measured at RT on Stepwise Tested Specimen)

* Sample was slightly "S" shaped after test.

TABLE B-21. Creep and Deformation Results on KAOCRETE XD 50 (Mix 36C) Refractory Concrete at Different Stress Levels and Temperatures.

Temperature		RT	500°F	1000°F	1500°F	1800°F	2000°F	Total Def. %
Stress					1000 PSI			
Time	Log T	(Bulk Density, pcf)			(143.6)			
0	0	0	0.0058	0.0177	0.0264	0.0384	0.0466	-
3 Minutes	-1.301	0.0031	.0115	.0218	.0328	.0430	.0531	-
6 Minutes	-1.000	.0032	.0123	.0219	.0335	.0435	.0546	-
12 Minutes	-0.699	.0034	.0128	.0222	.0343	.0443	.0566	-
15 Minutes	-0.602	.0035	.0130	.0223	.0345	.0446	.0574	-
30 Minutes	-0.301	.0037	.0134	.0225	.0356	.0457	.0606	-
45 Minutes	-0.125	.0038	.0137	.0227	.0364	.0464	.0631	-
1 Hour	0.000	.0039	.0140	.0228	.0368	.0469	.0652	-
2 Hours	0.301	-	.0152	.0231	.0385	.0485	.0709	-
3 Hours	0.477	-	.0163	.0232	.0396	.0496	.0751	-
4 Hours	0.602	-	-	-	-	-	.0781	-
5 Hours	0.699	-	-	-	-	-	.0811	-
10 Hours	1.000	-	-	-	-	-	.0936	-
% Deformation		0.06	0.17	0.09	0.21	0.18	0.76 (1.06)	1.47

(Post Test Deformation Measured at RT on Stepwise Tested Specimen)

Temperature		RT	500°F	1000°F	1500°F	1800°F	2000°F	Total Def. %
Stress					2000 PSI			
Time	Log T				(141.0)			
0	0	0	0.0042	0.018	0.0257	0.0432	0.0620	-
3 Minutes	-1.301	0.0046	.0115	.0253	.0355	.0535	.0738	-
6 Minutes	-1.000	.0048	.0120	.0254	.0367	.0551	.0770	-
12 Minutes	-0.699	.0049	.0130	.0257	.0381	.0573	.0816	-
15 Minutes	-0.602	.0049	.0134	.0258	.0385	.0582	.0835	-
30 Minutes	-0.301	.0051	.0140	.0261	.0404	.0615	.0901	-
45 Minutes	-0.125	.0052	.0150	.0264	.0416	.0635	.0972	-
1 Hour	0.000	.0053	.0157	.0266	.0425	.0651	.1016	-
2 Hours	0.301	-	.0169	.0269	.0447	.0702	.1174	-
3 Hours	0.477	-	.0178	.0270	.0465	.0736	.1302	-
4 Hours	0.602	-	-	-	-	-	.1399	-
5 Hours	0.699	-	-	-	-	-	.1437	-
10 Hours	1.000	-	-	-	-	-	.1826	-
% Deformation		0.08	0.22	0.14	0.34	0.49	1.95 (2.73)	3.22

Temperature		RT	500°F	1000°F	1500°F	1800°F	2000°F	Total Def. %
Stress					2500 PSI			
Time	Log T				(142.3)			
0	0	0	0.0076	0.0173	0.0282	0.0507	0.0688	-
3 Minutes	-1.301	0.0026	.0105	.0209	.0352	.0572	.0812	-
6 Minutes	-1.000	.0027	.0105	.0212	.0367	.0589	.0860	-
12 Minutes	-0.699	.0027	.0107	.0214	.0386	.0610	.0934	-
15 Minutes	-0.602	.0028	.0108	.0215	.0392	.0618	.0966	-
30 Minutes	-0.301	.0028	.0111	.0224	.0414	.0646	.1099	-
45 Minutes	-0.125	.0029	.0113	.0227	.0434	.0687	.1197	-
1 Hour	0.000	.0030	.0116	.0230	.0446	.0706	.1270	-
2 Hours	0.301	-	.0125	.0237	.0487	.0756	.1518	-
3 Hours	0.477	-	.0125	.0239	.0511	.0789	.1681	-
4 Hours	0.602	-	-	-	-	-	.1821	-
5 Hours	0.699	-	-	-	-	-	.1914	-
10 Hours	1.000	-	-	-	-	-	.2345	-
% Deformation		0.04	0.08	0.10	0.37	0.46	2.69 (3.45)	3.74

TABLE B-22. Creep and Deformation Results on KAOCRETE XD 50 (Mix 36C) 4 w/o 310 SS Fibers Refractory Concrete at Different Stress Levels and Temperatures.

Temperature		RT	500°F	1000°F	1500°F	1800°F	2000°F	Total Def. %
Stress					1000 psi			
Time	Log T	(Bulk Density pcf)			(145.9)			
0	0	0	0.0001	0.006	0.0145	0.0335	0.0458	-
3 Minutes	-1.301	0.0038	.0068	.0150	.0264	.0400	.0571	-
6 Minutes	-1.000	.0040	.0070	.0153	.0272	.0408	.0606	-
12 Minutes	-0.699	.0040	.0073	.0156	.0281	.0418	.0655	-
15 Minutes	-0.602	.0047	.0076	.0157	.0284	.0422	.0676	-
30 Minutes	-0.301	.0048	.0087	.0160	.0301	.0438	.0728	-
45 Minutes	-0.125	.0049	.0093	.0162	.0313	.0449	.0788	-
1 Hour	0.000	.0050	.0099	.0164	.0326	.0457	.0838	-
2 Hours	0.301	-	.0121	.0168	.0344	.0481	.0985	-
3 Hours	0.477	-	.0142	.0171	.0359	.0499	.1087	-
4 Hours	0.602	-	-	-	-	-	.1168	-
5 Hours	0.699	-	-	-	-	-	.1236	-
10 Hours	1.000	-	-	-	-	-	.1484	-
% Deformation		0.03	0.23	0.18	0.35	0.27	1.68 (1.78)	2.79

(Post Test Deformation Measured at RT on Stepwise Tested Specimen)

Temperature		RT	500°F	1000°F	1500°F	1800°F	2000°F	Total Def. %
Stress					1500 psi			
Time	Log T				(145.4)			
0	0	0	0.0043	0.0178	0.0296	0.0477	0.0632	-
3 Minutes	-1.301	0.0062	.0144	.0280	.0419	.0563	.0747	-
6 Minutes	-1.000	.0063	.0150	.0282	.0432	.0573	.0776	-
12 Minutes	-0.699	.0064	.0166	.0284	.0439	.0588	.0822	-
15 Minutes	-0.602	.0068	.0174	.0285	.0445	.0594	.0840	-
30 Minutes	-0.301	.0072	.0174	.0290	.0464	.0616	.0927	-
45 Minutes	-0.125	.0080	.0179	.0292	.0472	.0631	.0981	-
1 Hour	0.000	.0082	.0195	.0294	.0488	.0646	.1031	-
2 Hours	0.301	-	.0198	.0297	.0504	.0680	.1212	-
3 Hours	0.477	-	.0209	.0299	.0523	.0707	.1344	-
4 Hours	0.602	-	-	-	-	-	.1453	-
5 Hours	0.699	-	-	-	-	-	.1545	-
10 Hours	1.000	-	-	-	-	-	.1894	-
% Deformation		2.79	0.27	0.20	0.37	0.38	2.08 (2.29)	3.44

Temperature		RT	500°F	1000°F	1500°F	1800°F	2000°F	Total Def. %
Stress					2000 psi			
Time	Log T				(141.3)			
0	0	0	0.0038	0.0266	0.0380	0.0614	0.0791	-
3 Minutes	-1.301	0.0162	.0242	.0412	.0555	.0724	.0986	-
6 Minutes	-1.000	.0165	.0267	.0414	.0570	.0738	.1035	-
12 Minutes	-0.699	.0167	.0278	.0416	.0591	.0757	.1118	-
15 Minutes	-0.602	.0168	.0278	.0417	.0602	.0765	.1150	-
30 Minutes	-0.301	.0172	.0283	.0421	.0623	.0793	.1309	-
45 Minutes	-0.125	.0173	.0299	.0424	.0636	.0814	.1431	-
1 Hour	0.000	.0174	.0302	.0427	.0649	.0829	.1538	-
2 Hours	0.301	-	.0335	.0431	.0670	.0874	.1916	-
3 Hours	0.477	-	.0354	.0436	.0685	.0911	.2170	-
4 Hours	0.602	-	-	-	-	-	.2427	-
5 Hours	0.699	-	-	-	-	-	-	-
10 Hours	1.000	-	-	-	-	-	Failed @ 3.64% after 5.5 hrs.	-
% Deformation		0.29	0.52	0.28	0.50	0.49		5.72 = Failure

TABLE B-23. Creep and Deformation Results on LITECAST 75-28 Refractory Concrete at Different Stress Levels and Temperatures.

Temperature / Stress / Time	Log T	RT	250°F	500°F	1000°F	1250°F	1500°F	Total Def. %
				700 psi				
		(Bulk Density, pcf)			(85.0)			
0	0		0	.0045	.0165	-	.0265	
3 Minutes	-1.301	-	.0047	.0115	.0250	-	.0450	
6 Minutes	-1.000	-	-	-	-	-	-	
12 Minutes	-0.699	-	-	-	-	-	-	
15 Minutes	-0.602	-	.0048	.0135	.0265	-	.0560	
30 Minutes	-0.301	-	.0048	.0160	.0270	-	.0625	
45 Minutes	-0.125	-	-	-	-	-	-	
1 Hour	0.000	-	.0049	.0200	.0275	-	.0730	
2 Hours	0.301	-	-	.0220	.0280	-	.0850	
3 Hours	0.477	-	-	.0230	.0290	-	.0920	
4 Hours	0.602	-	-	-	-	-	.0988	
5 Hours	0.699	-	-	-	-	-	.1030	
10 Hours	1.000	-	-	-	-	-	.1175	
% Deformation			0.08	0.30	0.2.	-	1.50 (1.73)	2.08

(Post Test Deformation Measured at RT on Stepwise Tested Specimen)

Temperature / Stress / Time	Log T	RT	250°F	500°F	1000°F	1250°F	1500°F	Total Def. %
				1000 psi				
					(84.8)			
0	0	0	0.0066	0.0182	0.0350	0.0436	0.0627	
3 Minutes	-1.301	0.0125	.0205	.0352	.0463	0.0545	.0912	
6 Minutes	-1.000	-	.0205	.0356	.0471	.0552	.0979	
12 Minutes	-0.699	-	-	-	-	-	-	
15 Minutes	-0.602	.0125	.0211	.0364	.0479	.0565	0.1102	
30 Minutes	-0.301	.0130	.0213	.0373	.0492	.0582	.1302	
45 Minutes	-0.125	-	-	-	-	-		
1 Hour	0.000	.0131	.0213	.0387	.0503	.0606	.1494	
2 Hours	0.301	-	.0222	.0408	.0523	.0636	.1784	
3 Hours	0.477	-	.0233	.0422	.0529	.0660	.1953	
4 Hours	0.602	-	-	-	-	-	.2057	
5 Hours	0.699	-	-	-	-	-	.2156	
10 Hours	1.000	-	-	-	-	-	.2429	
% Deformation		0.21	0.27	0.39	0..	0.36	2.93 (3.79)	4.45

Temperature / Stress / Time	Log T	RT	250°F	500°F	1000°F	1250°F	1500°F	Total Def. %
				1500 psi				
					(85.0)			
0	0	0	0.0065	0.0191	0.0346	0.0428	0.0638	
3 Minutes	-1.301	.0016	.0179	0.0334	.0477	.0567	.1104	
6 Minutes	-1.000	.0105	.0184	.0341	.0482	.0580	.1230	
12 Minutes	-0.699	-	-	-	-	-	-	
15 Minutes	-0.602	.0112	.0193	.0362	.0497	.0601	.1447	
30 Minutes	-0.301	.0118	.0203	.0385	.0504	.0628	-	
45 Minutes	-0.125	-	-	-	-	-	-	
1 Hour	0.000	-	.0204	.0410	.0517	.0660	.1916	
2 Hours	0.301	-	.0234	.0442	.0535	.0703	.2340	
3 Hours	0.477	-	.0237	.0463	.0547	.0732	.2726	
4 Hours	0.602	-	-	-	-	-	.3060	
5 Hours	0.699	-	-	-	-	-	.3346	
10 Hours	1.000	-	-	-	-	-	.4104	
% Deformation		0.19	0.28	0.44	0..	0.50	5.66 (6.40)	7.40

TABLE B-24. Example of Reduced Creep Data to Unit Strain (in/in/psi) on 50% Al_2O_3 Dense Generic Refractory Concrete

DATA SET 27 GAGE LENGTH= 6.0560

TEMPERATURE(F)= 1800.0 STRESS(PSI)= 1500.0

TIME(HR)	LOG TIME	ELONG.(IN)	STRAIN(IN/IN) *10**6	UNIT STRAIN *10**6
.1000	-1.0000	.0105	1734.	1.1559
.2000	-.6990	.0127	2097.	1.3981
.2500	-.6021	.0133	2196.	1.4641
.5000	-.3010	.0162	2675.	1.7834
.7500	-.1249	.0185	3055.	2.0365
1.0000	0.0000	.0205	3385.	2.2567
2.0000	.3010	.0255	4211.	2.8071
3.0000	.4771	.0285	4706.	3.1374
4.0000	.6021	.0305	5036.	3.3576
6.0000	.7782	.0345	5697.	3.7979
8.0000	.9031	.0370	6110.	4.0731
10.0000	1.0000	.0395	6522.	4.3483
15.0000	1.1761	-0.0000	0.	0.0000
20.0000	1.3010	-0.0000	0.	0.0000
25.0000	1.3979	-0.0000	0.	0.0000
30.0000	1.4771	-0.0000	0.	0.0000

DATA SET 25 GAGE LENGTH= 6.0560

TEMPERATURE(F)= 1000.0 STRESS(PSI)= 1500.0

TIME(HR)	LOG TIME	ELONG.(IN)	STRAIN(IN/IN) *10**6	UNIT STRAIN *10**6
.1000	-1.0000	.0095	1569.	1.0458
.2000	-.6990	.0105	1734.	1.1559
.2500	-.6021	.0112	1849.	1.2329
.5000	-.3010	.0120	1982.	1.3210
.7500	-.1249	.0120	1982.	1.3210
1.0000	0.0000	.0120	1982.	1.3210
2.0000	.3010	.0122	2015.	1.3430
3.0000	.4771	.0122	2015.	1.3430
4.0000	.6021	-0.0000	0.	0.0000
6.0000	.7782	-0.0000	0.	0.0000
8.0000	.9031	-0.0000	0.	0.0000
10.0000	1.0000	-0.0000	0.	0.0000
15.0000	1.1761	-0.0000	0.	0.0000
20.0000	1.3010	-0.0000	0.	0.0000
25.0000	1.3979	-0.0000	0.	0.0000
30.0000	1.4771	-0.0000	0.	0.0000

DATA SET 26 GAGE LENGTH= 6.0560

TEMPERATURE(F)= 1500.0 STRESS(PSI)= 1500.0

TIME(HR)	LOG TIME	ELONG.(IN)	STRAIN(IN/IN) *10**6	UNIT STRAIN *10**6
.1000	-1.0000	.0105	1734.	1.1559
.2000	-.6990	.0125	2064.	1.3760
.2500	-.6021	.0130	2147.	1.4311
.5000	-.3010	.0140	2312.	1.5412
.7500	-.1249	.0150	2477.	1.6513
1.0000	0.0000	.0161	2659.	1.7723
2.0000	.3010	.0175	2890.	1.9265
3.0000	.4771	.0190	3137.	2.0916
4.0000	.6021	-0.0000	0.	0.0000
6.0000	.7782	-0.0000	0.	0.0000
8.0000	.9031	-0.0000	0.	0.0000
10.0000	1.0000	-0.0000	0.	0.0000
15.0000	1.1761	-0.0000	0.	0.0000
20.0000	1.3010	-0.0000	0.	0.0000
25.0000	1.3979	-0.0000	0.	0.0000
30.0000	1.4771	-0.0000	0.	0.0000

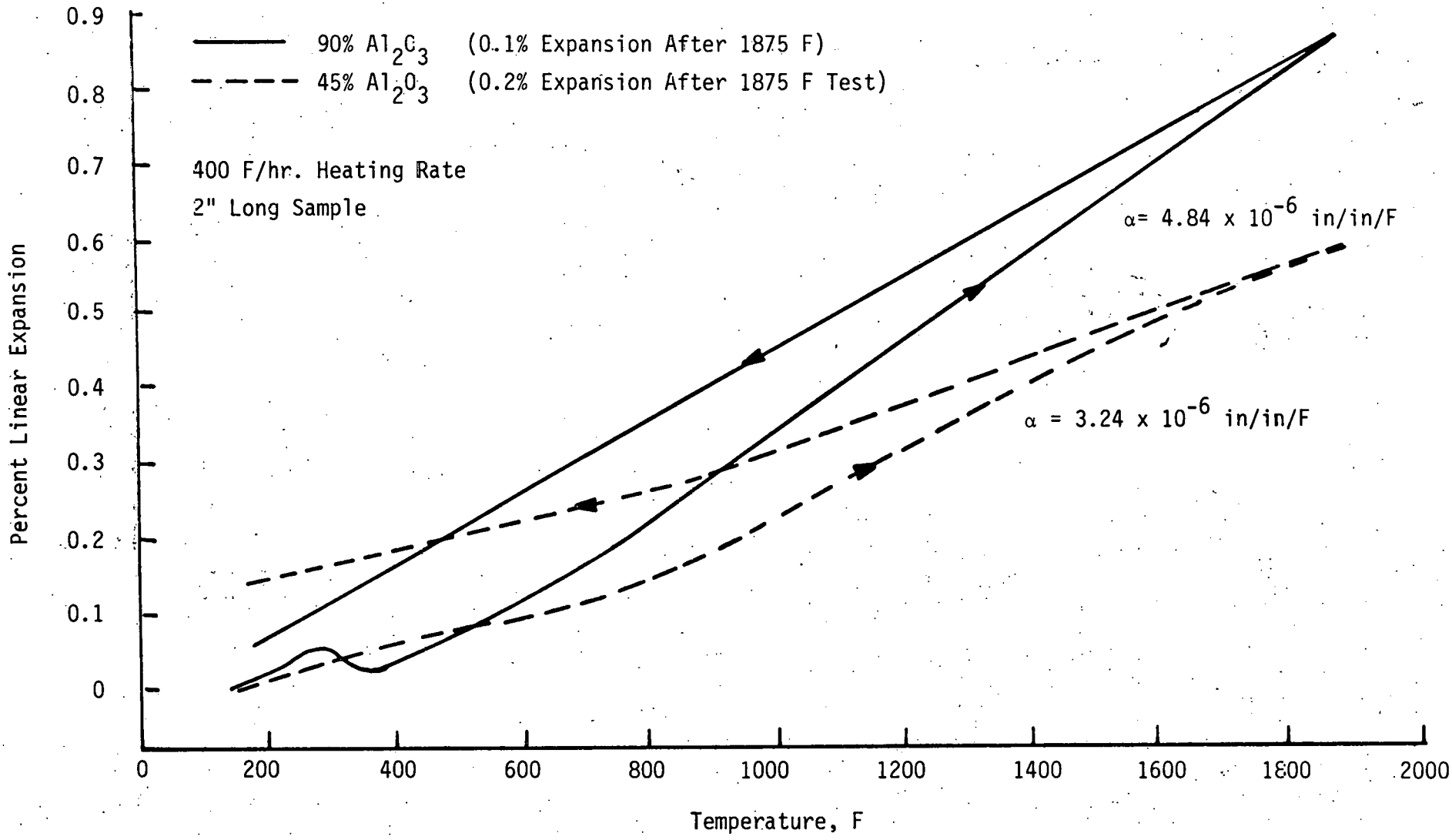

FIGURE B-1. Thermal Expansion of 45 and 90% Al_2O_3 Generic Phosphate Bonded Ramming Mixes (Stored At Room Temperature).

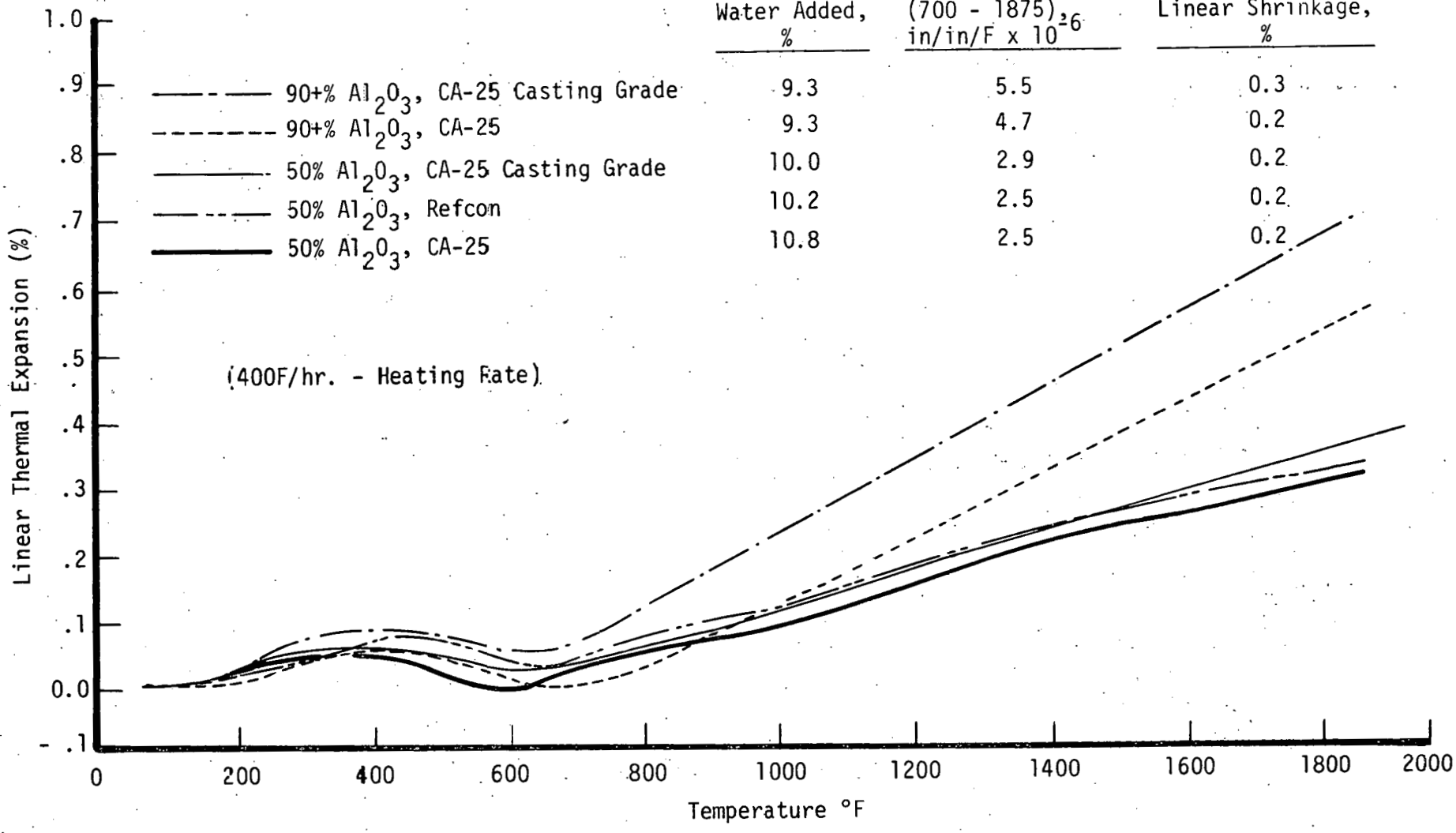

FIGURE B-2. Thermal Expansion of 50 and 90+ Al_2O_3 Generic Castables On Initial Heat-Up (Stored at Room Temperature).

EFFECT OF STORAGE CONDITION ON INSULATING COMPONENT

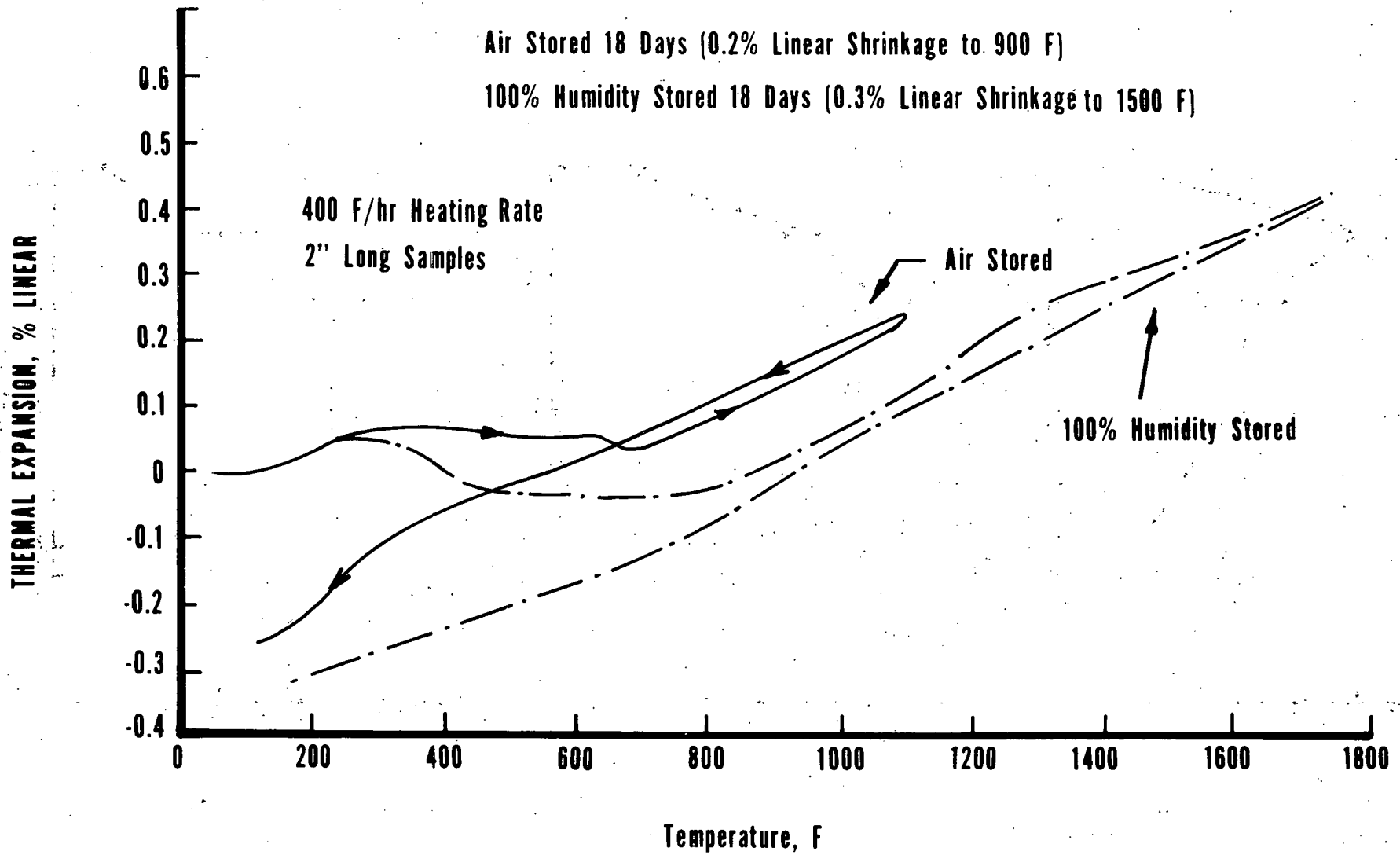

FIGURE B-3. Thermal Expansion of LITECAST 75-28 (21% Water) After Storage in Air or High Humidity Environment.

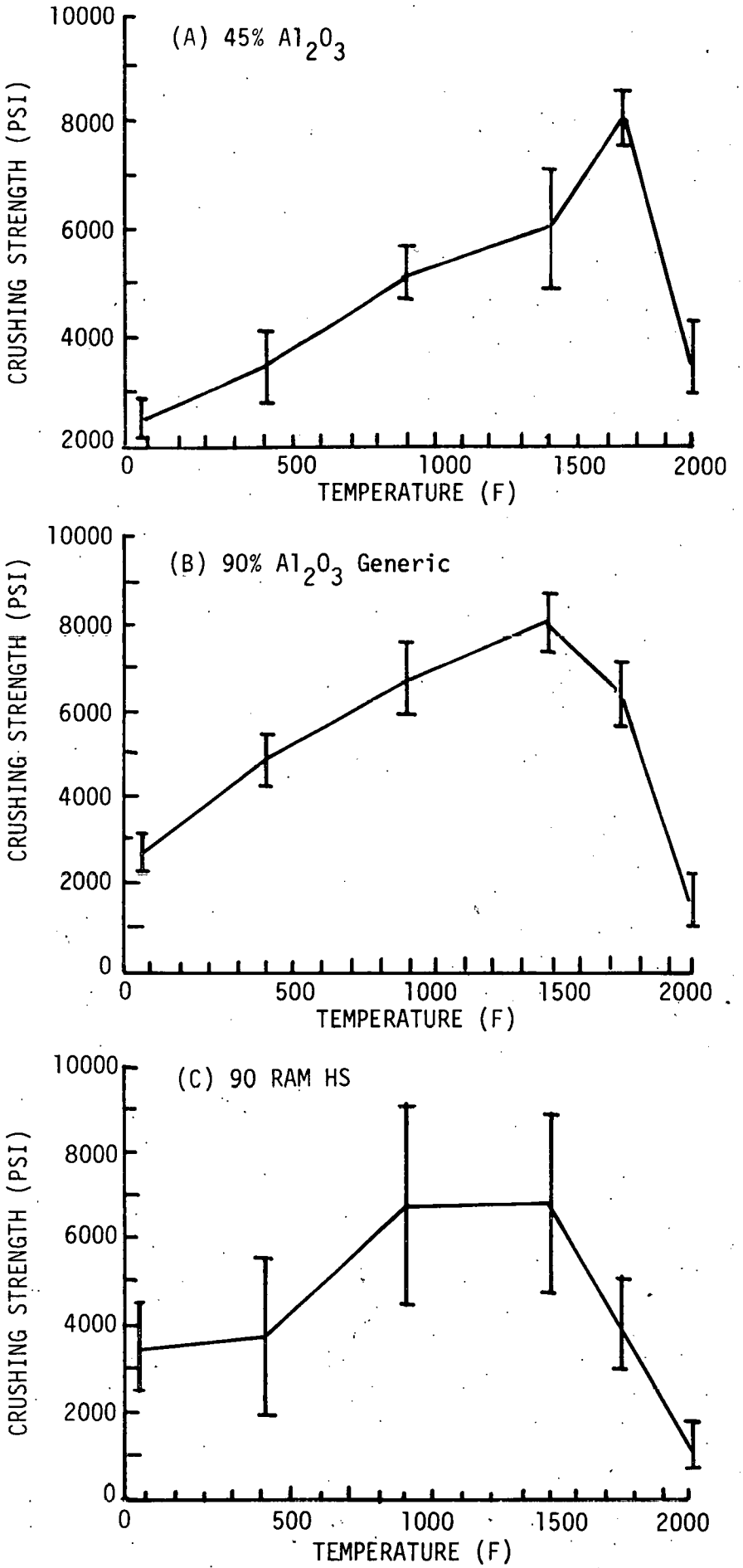

FIGURE B-4. Hot Crushing Strength of the Phosphate Bonded Monolithic Refractories.

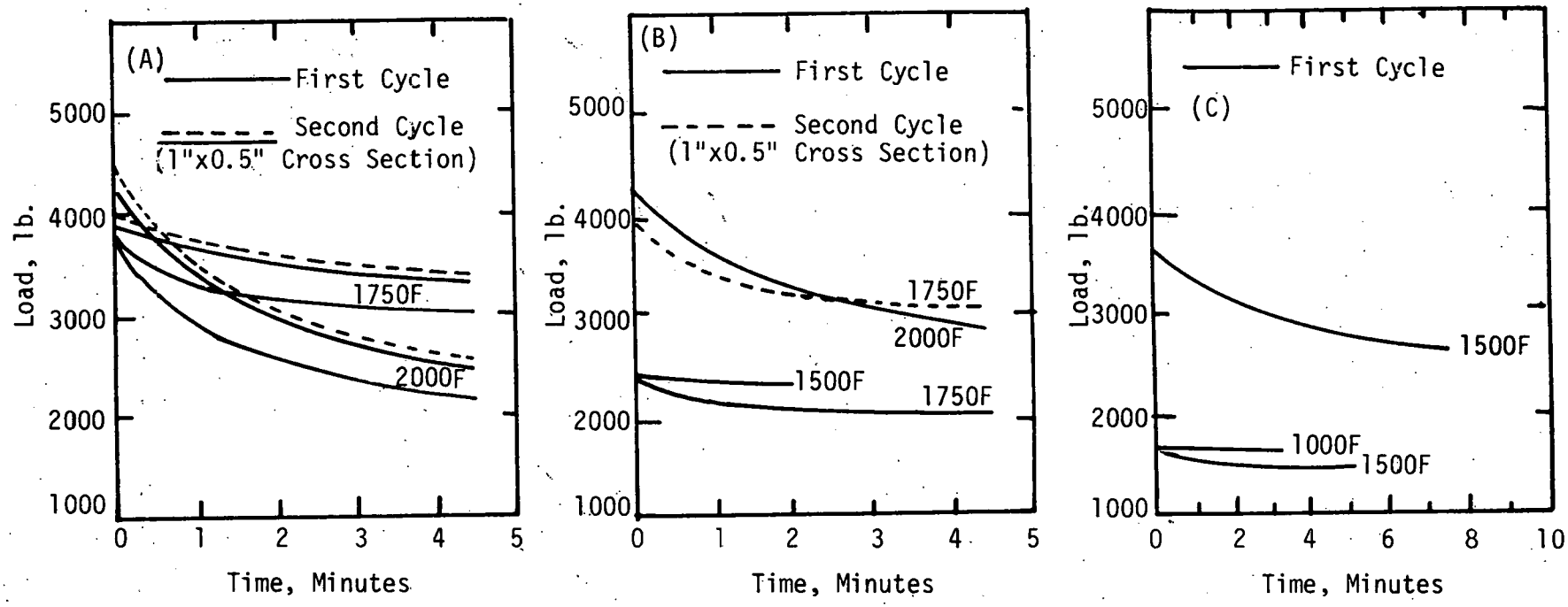

(a) 50% Al_2O_3 Generic (Standard Formulation)

(b) 90+% Al_2O_3 Generic (Modified Formulation)

(c) LITECAST 75-28

FIGURE B-5. Stress Relaxation Curves of Uniaxial Compression Tested Specimens of Castables.

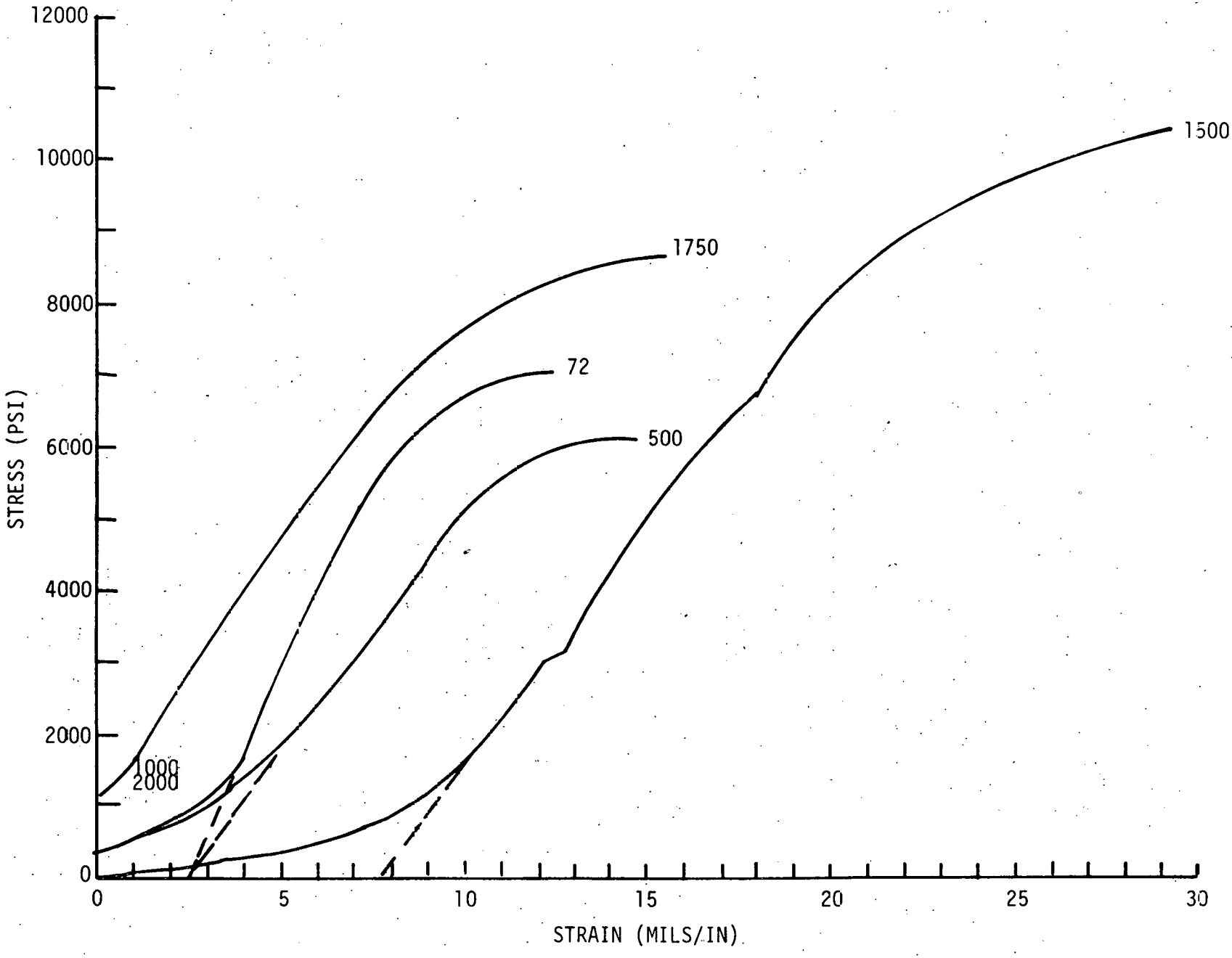

FIGURE B-6. Stress-Strain Curves For 50% Al_2O_3 Dense Refractory Concrete.

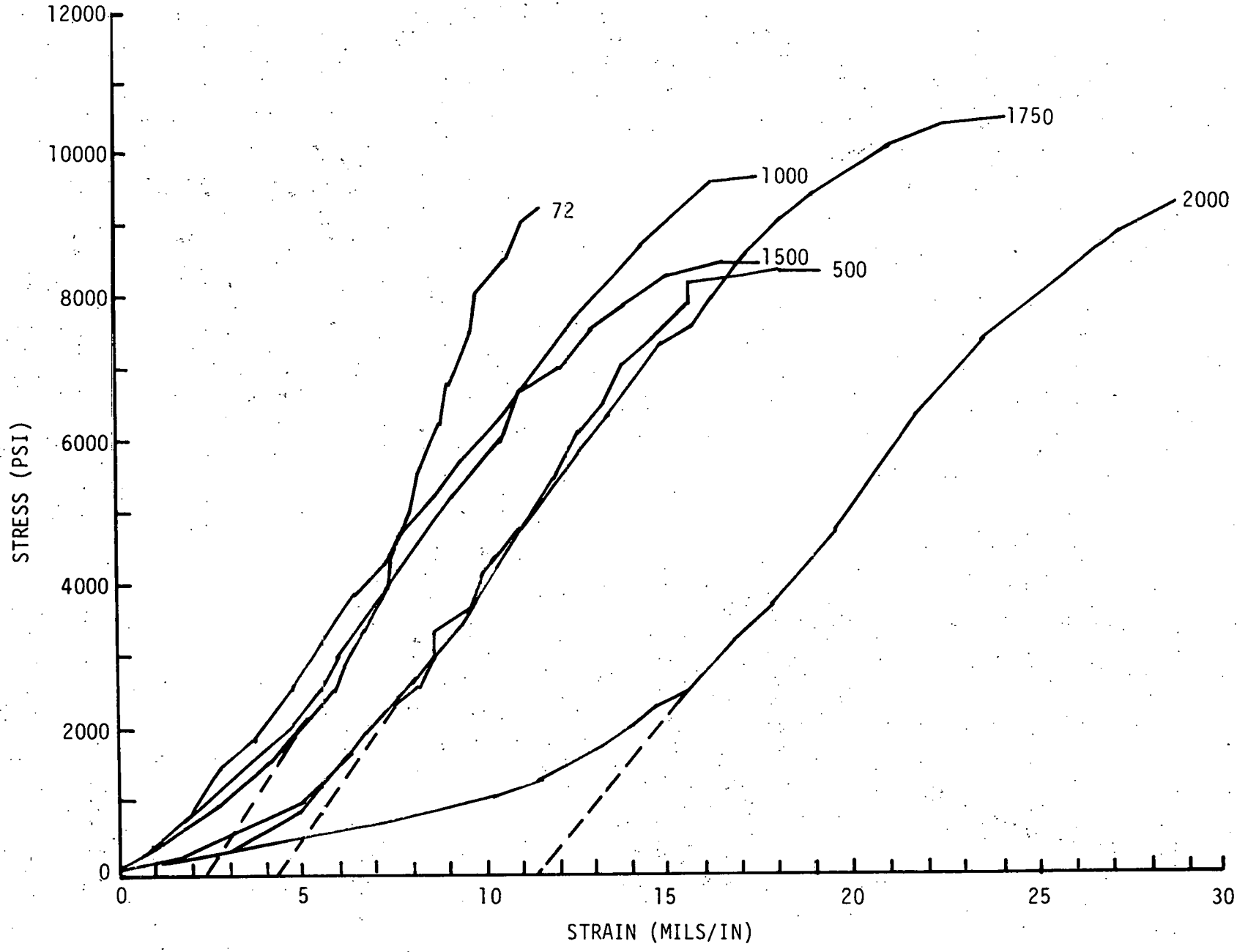

FIGURE B-7. Stress-Strain Curves For Standard 90+% Al_2O_3 Dense Refractory Concrete.

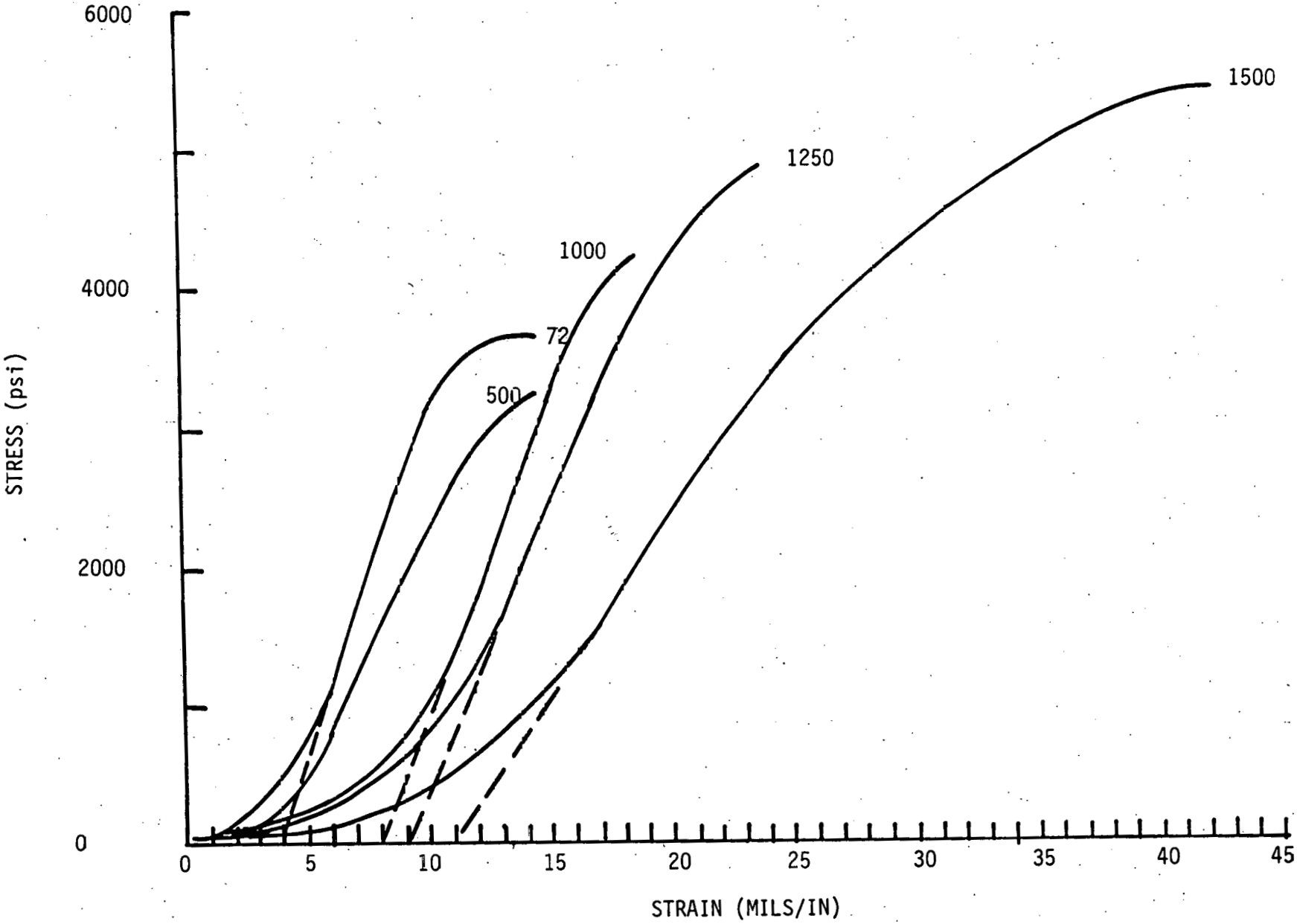

FIGURE B-8. Stress-Strain Curves for LITECAST 75-28 Insulation Castable.

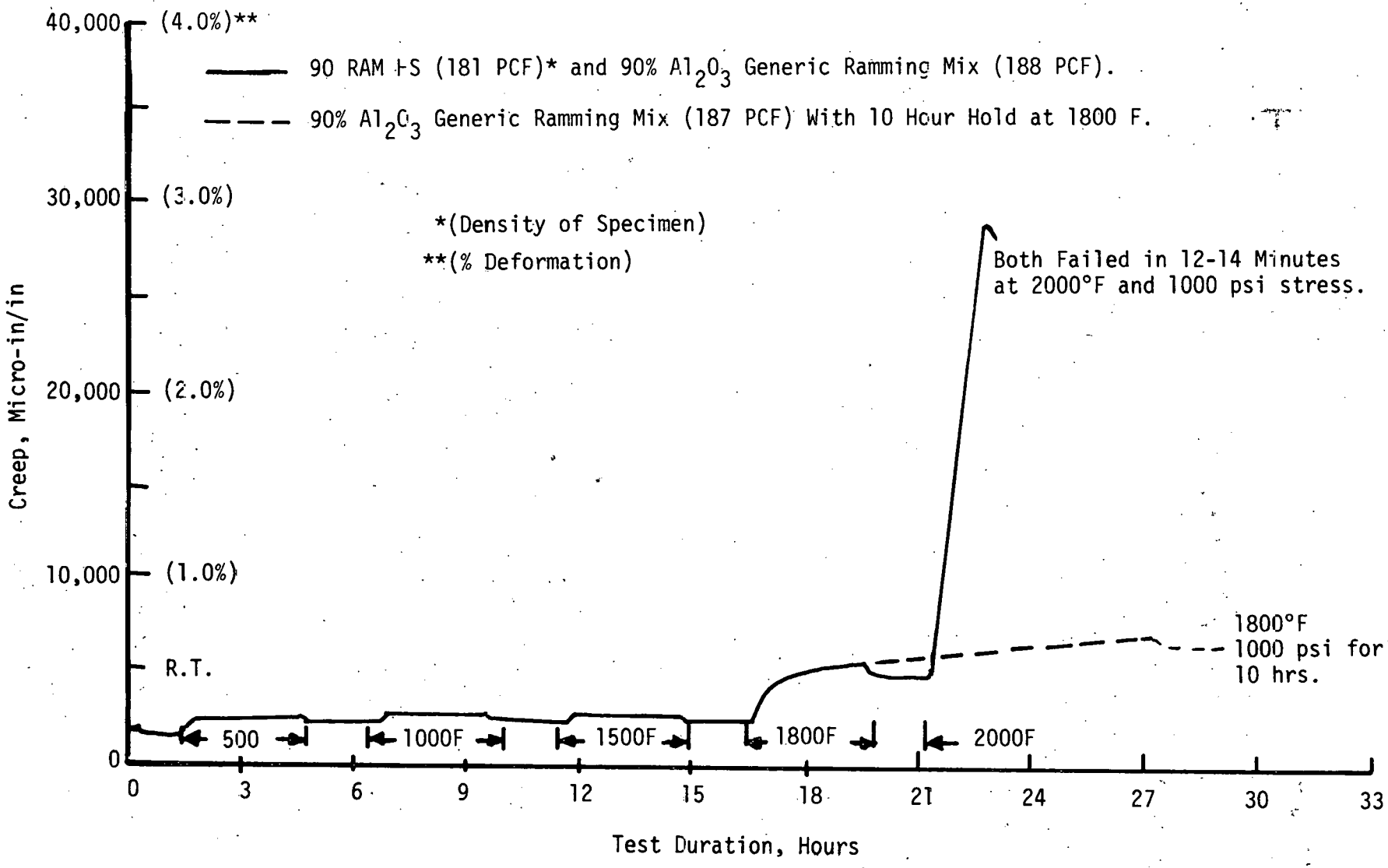

FIGURE B-9. Creep Curves For 90 RAM HS and 90% Al_2O_3 Generic Phosphate Bonded Ramming Mix.

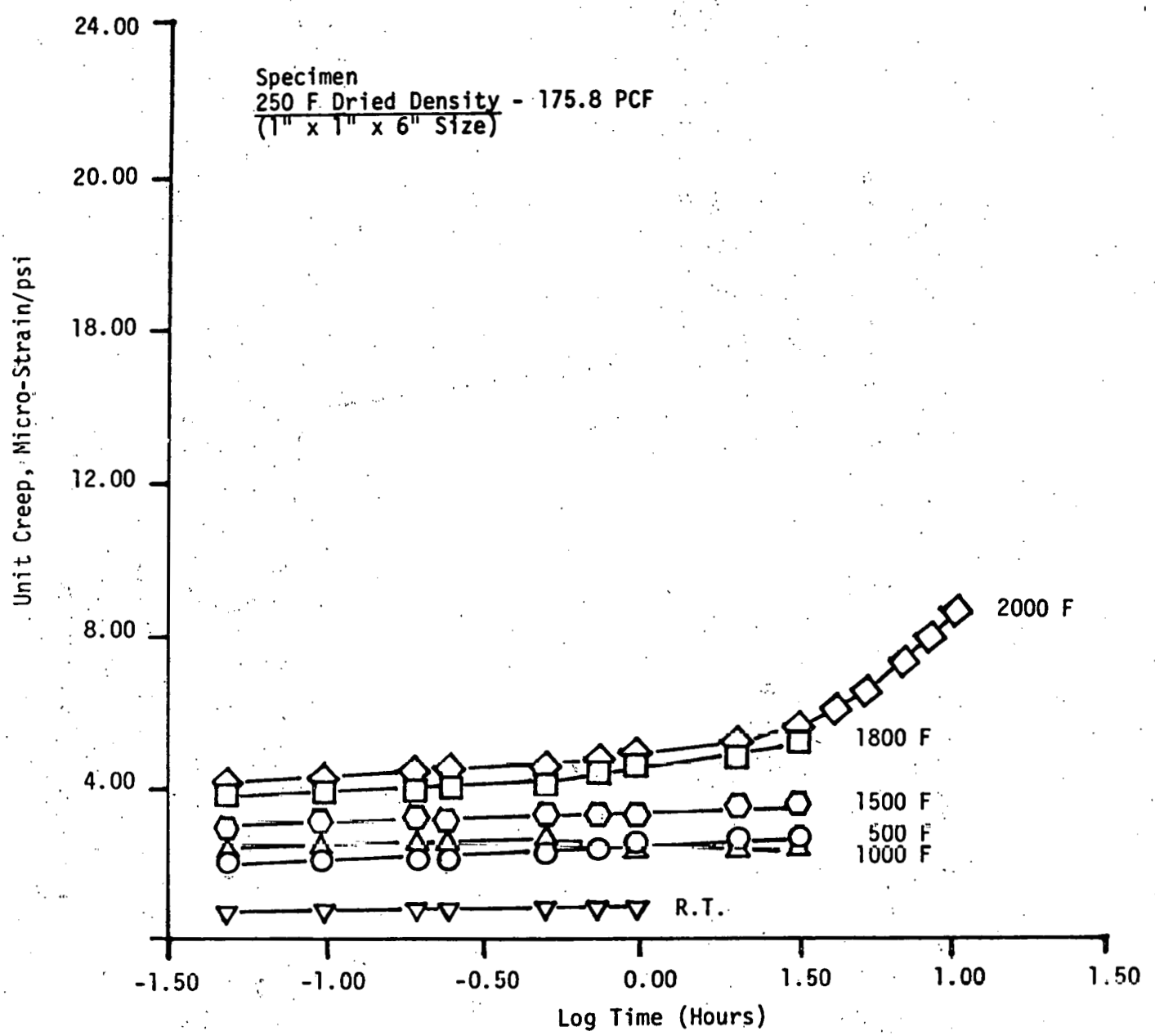

FIGURE B-10. Unit Creep Curves For Modified 90+% Al_2O_3 Dense Generic Concrete (9.0% Mix Water) Tested at 1000 psi.

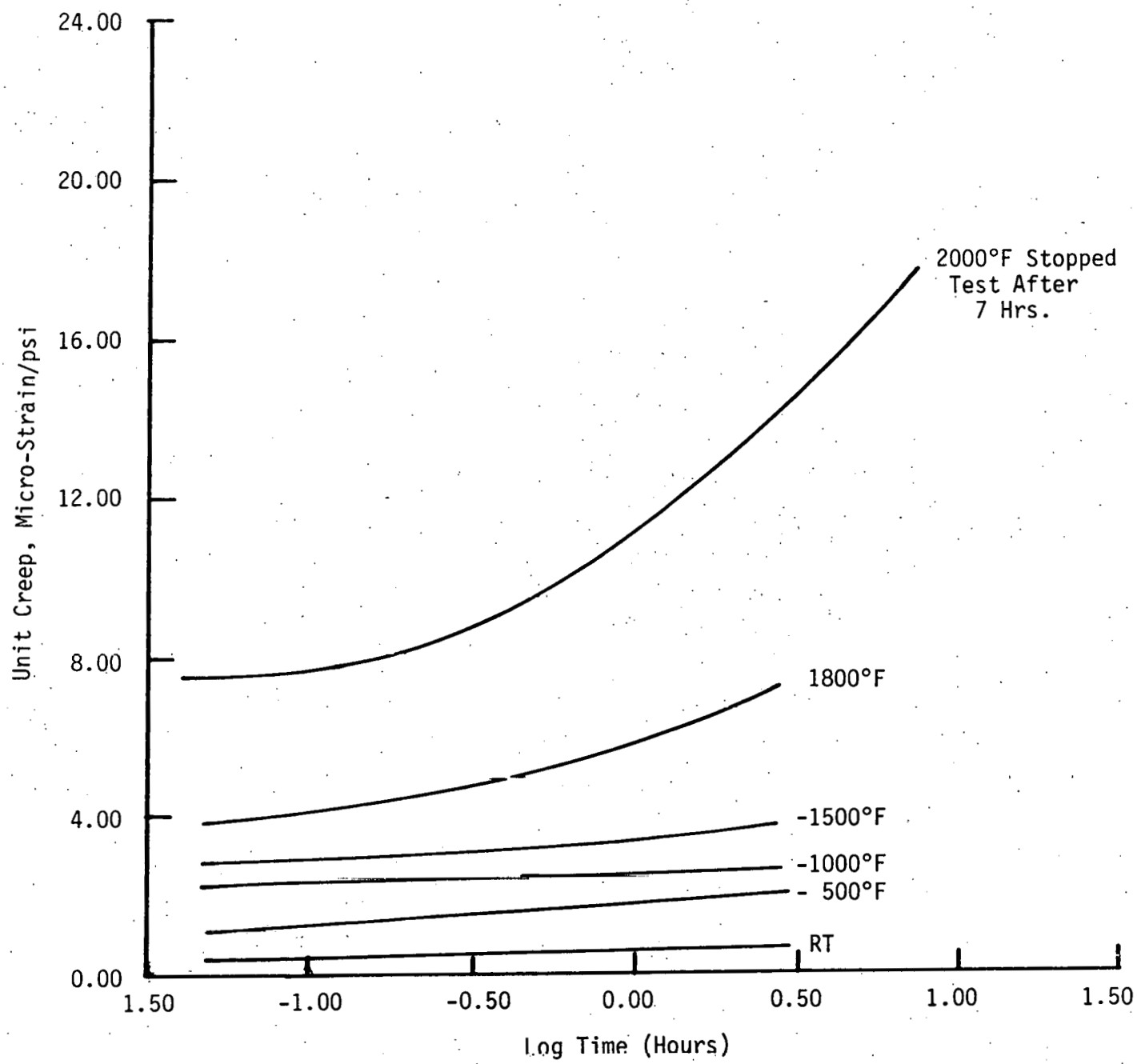

FIGURE B-11 Unit Creep Curves For Modified 90+% Al_2O_3 Dense Generic Concrete (9.0% Mix Water) Tested at 3300 psi.

THIS PAGE

WAS INTENTIONALLY

LEFT BLANK

APPENDIX C

Weight Loss Vs. Time Curves for Pore Pressure Calculations

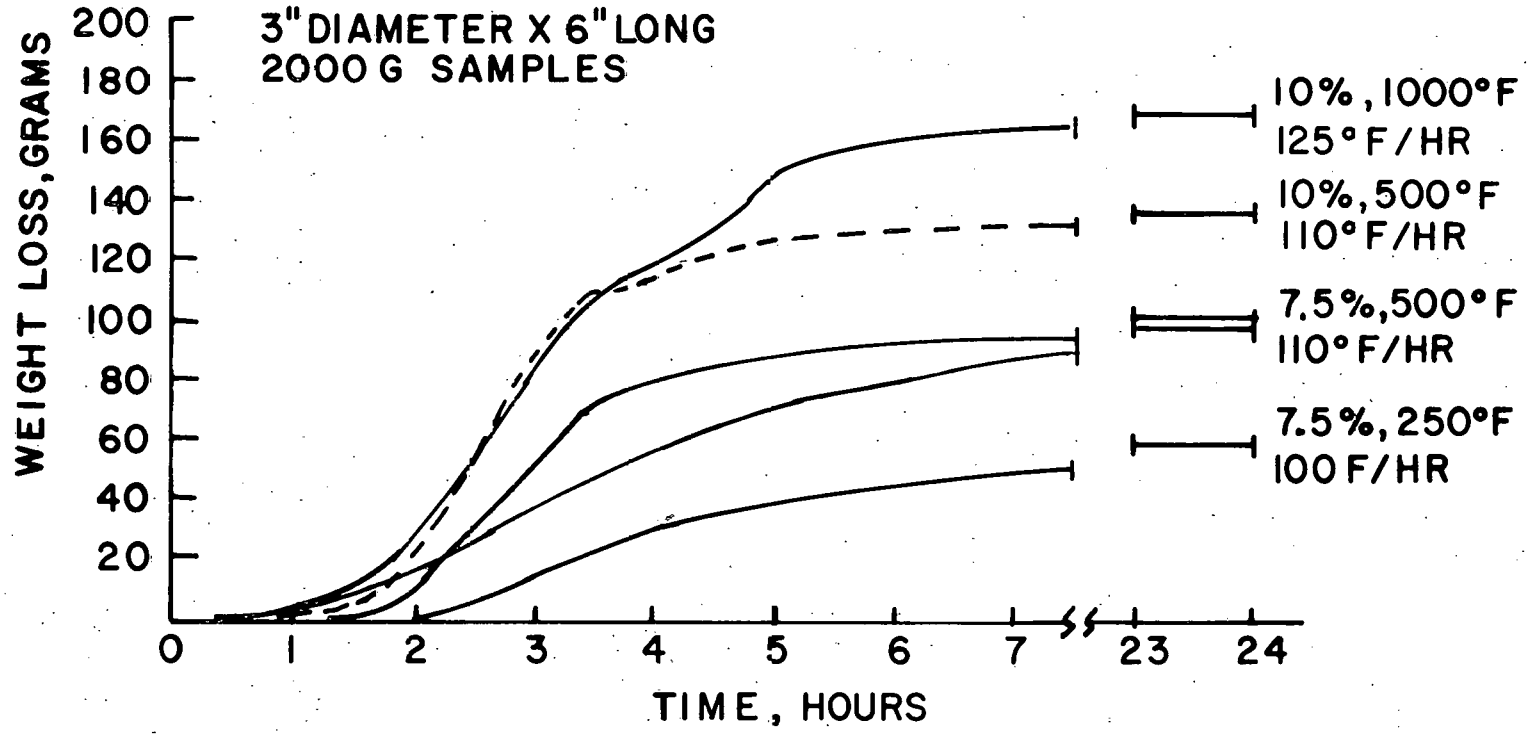

Figure C-1. Weight Loss vs Time Curves of As-Cured Solid Cylinders of ERDA 90 at Different Water Levels and Heat-up Rates

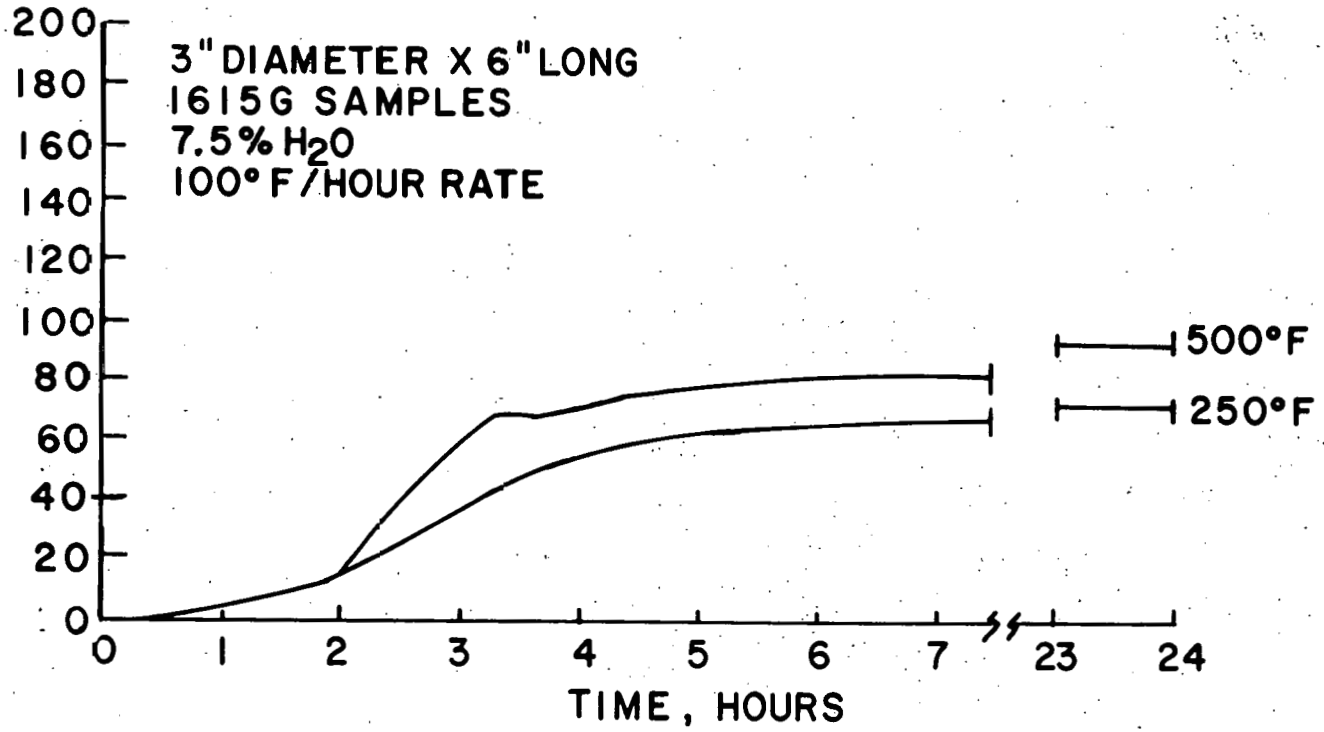

Figure C-2. Weight Loss vs Time Curves of As-Cured Solid Cylinders of KAOCRETE XD 50 (Mix 36C)

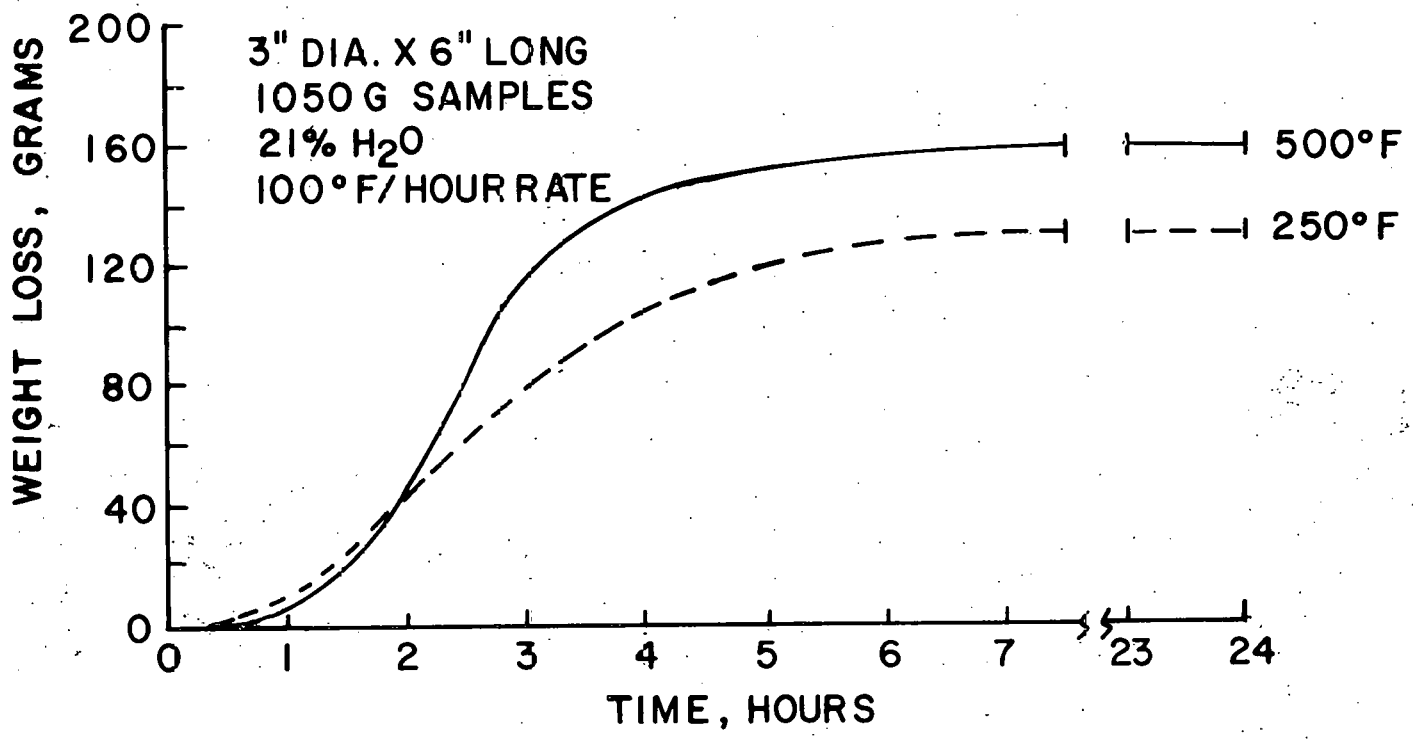

Figure C-3. Weight Loss vs Time Curves of As-Cured Solid Cylinders of LITECAST 75-28

APPENDIX D

Tensile Strength and Shrinkage of Linings

TABLE D-1. Crack Widths and Shrinkage Measurements on the Hot Face of Lining #9 After Heat-up to 1850°F

Vertical Cracks Location*	Sum of Cracks, in.	
15"	.013 (2)	Average = .006
		Sum = .014
30"	.014 (3)	Circumference = 115.9
		Shrinkage = .012%
45"	.012 (2)	

Horizontal Cracks Location**		
0°	.009 (3)	Average = .004
		Sum = .0125
90°	.015 (5)	Height = 48
		Shrinkage = .026%
180°	.013 (3)	
270°	.013 (3)	

Hot Face Diameter Shrinkage	.25%	Consider shrinkage over total 5 ft. height of lining. Shrinkage value is closer to that of circumference value, 0.021%.

Linear shrinkage calculations assume summation of crack widths accounts for shrinkage in vertical and horizontal directions.

*Measured at distance of 15, 30 and 45 inches from top of lining.

**Measured at vertical lines located at 45° apart around circumference of lining.

(#)Number of cracks measured.

TABLE D-2. Crack Widths and Shrinkage Measurements on the Hot Face of Lining #7 and #8(7A) After Testing

Vertical Cracks Location*	#7 1st 1700°F Test Sum of Cracks, in.	#7 2nd 1700°F Test Sum of Cracks, in.	#7 1850°F Test Sum of Cracks, in.	#8(7A) 2 Tests to 1700°F Sum of Cracks, in.
15"	.1045 (12)	.078 (9)	.117 (13)	.122 (11)
30"	.119 (8)	.114 (10)	.161 (9)	.165 (10)
45"	.097 (9)	.086 (11)	.134 (10)	.154 (10)
	Average = .012 Sum = .107 Circumference = 115.9 Shrinkage = .09%	Average = .009 Sum = .093 Circumference = 115.9 Shrinkage = .08%	Average = .013 Sum = .137 Circumference = 115.9 Shrinkage = .12%	Average = .014 Sum = .147 Circumference = 115.9 Shrinkage = .127%
Horizontal Cracks Location**				
0°	.068 (8)	.057 (8)	.078 (9)	.051 (6)
90°	.046 (5)	.047 (7)	.058 (6)	.058 (4)
180°	.056 (8)	.051 (5)	.075 (5)	.084 (6)
270°	.038 (4)	.061 (7)	.074 (7)	.077 (4)
	Average = .008 Sum = .052 Height = 48 Shrinkage = .11%	Average = .008 Sum = .054 Height = 48 Shrinkage = .11%	Average = .011 Sum = .071 Height = 48 Shrinkage = .15%	Average = .014 Sum = .068 Height = 48 Shrinkage = .142%
Hot Face Diameter Shrinkage	.25% ΔS = .25%	.38% ΔS = .13%	.38% ΔS = 0%	.38% ΔS = 0%

Shrinkage values determined from as-cast condition.

Linear shrinkage calculations assume summation of crack widths accounts for shrinkage in vertical and horizontal directions.

*Measured at distance of 15, 30 and 45 inches from top of lining.

**Measured at vertical lines located 45° apart around circumference of lining.

(#)Number of cracks measured.

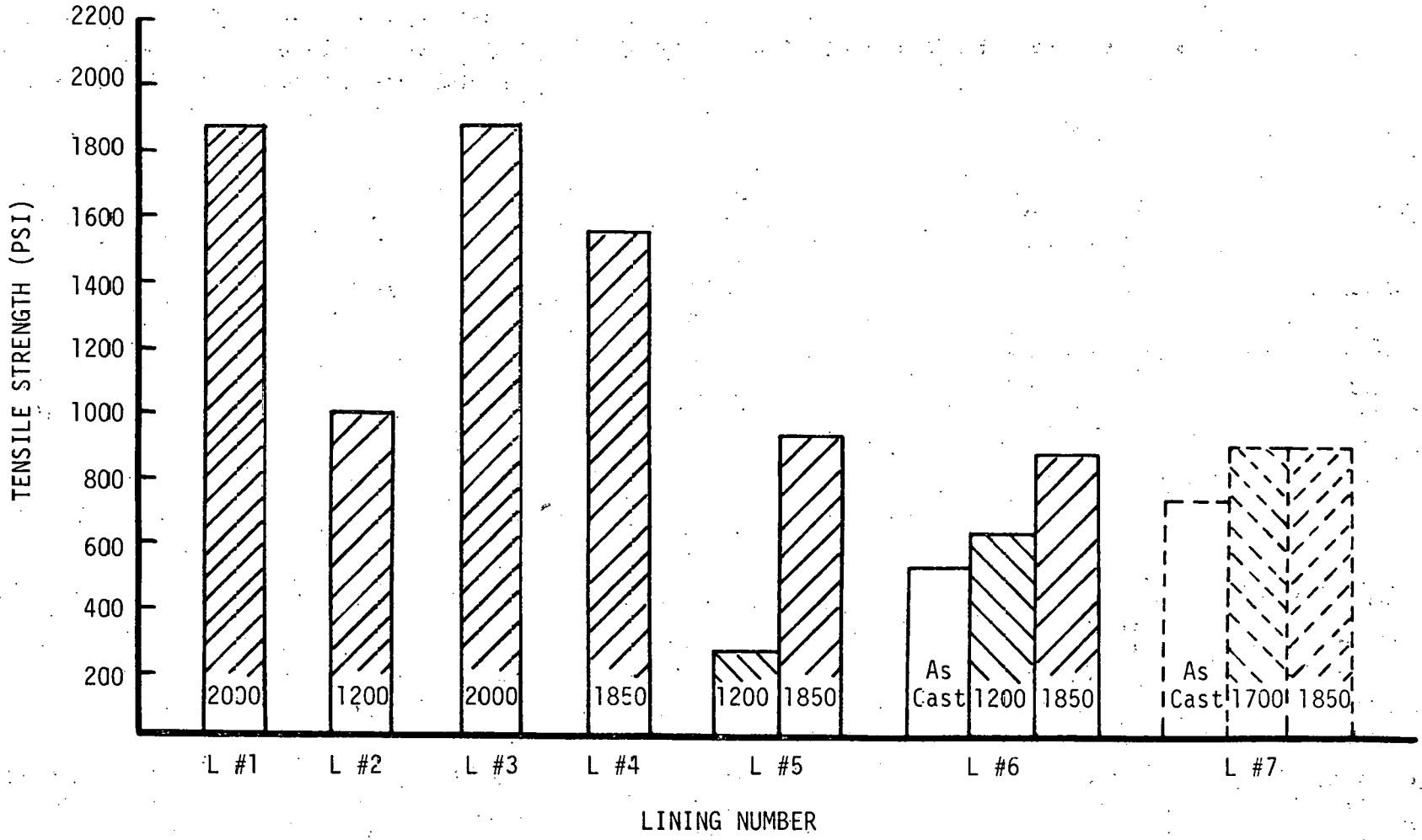

FIGURE D-1. Tensile Strengths of Dense Castables Used in Linings #1-#7 (Diametral Compression Test).

APPENDIX E

Seminar Agenda and List of Attendees

A Seminar
on
Monolithic Refractory Lining Design for Process Vessels
will be held at the Research & Development Division
Babcock & Wilcox
at
Lynchburg, Virginia on September 17-18, 1980

Babcock & Wilcox Company has been under contract to the Department of Energy in a multi-year study to develop improved monolithic refractory lining designs, materials and operating procedures for coal gasifiers. Transfer of the technology to the appropriate industries will be accomplished through a seminar planned at the Babcock & Wilcox Company Lynchburg Research Center in Lynchburg, Virginia. The one-and-one-half day seminar is planned for Wednesday and Thursday, September 17-18, 1980.

An outline of the seminar follows:

Wednesday Morning

- Introduction - W. G. Long

- Overview of DOE/Fossil Energy Refractories Development Programs - Ron Bradley, Manager of Fossil Energy Materials Programs - Oak Ridge National Laboratory

- Overview of Contract - E. M. Anderson
  Ed will discuss the objectives and scope of the program, the approach to study potential improvements in monolithic refractory linings, and the refractory materials and properties of interest.

- Strain Gage Development - R. P. Glasser
  Dick will discuss the techniques used to measure lining and shell strains during the lining tests.

Wednesday Afternoon

Discussion of Acoustic Emission Techniques - R. W. Sheriff
Rob will discuss the acoustic emission techniques employed to correlate cracking in the refractory concrete lining with other data in this program.

- Tour of Test Facilities

- Mathematical Model Development - Ray Best
  Ray will describe the development of the 1-D and 2-D models. Comparison will be made with the MIT modeling program.

- Model Development at MIT

- Creep Testing at Iowa State

Thursday Morning

- Lining Test Results - Anderson, Glasser and Best
  The lining test results will be presented and correlated with the model predictions. The recommended guidelines for improved performance will be presented.

- 11:00 AM Wrap-up - E. M. Anderson

LIST OF SEMINAR ATTENDEES

Alcoa Research Lab - George MacZura

Battelle Columbus Labs - Gene Hulbert

Bechtel - Doc Lou

C-E Refractories - Edward Snajdr

Chicago Bridge & Iron Co. - Elmar Rothrock

Dept. of Energy - Gene Hoffman

Dravo Corp. - Jack Hyde

Foster-Wheeler - Anthony Mondok

Fluidyne Eng. Co. - Ron Smyth

Fluor Engineers & Constructors, Inc. - George Smith

A. P. Green - Craig Campbell

Gulf Oil Research & Development Corp. - Pat Dolan

Harbison-Walker - Hugh Criss

Hotwork, Inc. - Kerry Higgins

IIT Research Institute - Ross Firestone

Iowa State University - Tom McGee

Koppers Co. - Jan Reiser
- Paul Musiol

Lone Star LaFarge - Ken Moody

Davey McKee Co. - Jim Cheraso

MIT - Oral Buyukozturk

Monsanto Co. - Bill Netter

Oak Ridge National Lab - Ron Bradley
Joe Hammond

Ralph M. Parson Co. - Lynn McRae

Pennwalt Corp. - Bob Pierce

Plibrico - Ken Krietz

Pullman Kellogg - Tom Thweatt

Shell Development Corp. - Bill Gottenburg

Stone & Webster - William Hsu

TVA - Bill Goins

Texaco - Don Newlin

UOP - Bud Krause

UTSI - Troy Shaver

VPI - Curtis Martin

Air Products & Chemicals, Inc. - Joe Slusser

P&M Coal Mining Co. - Larry Sluzalis

Montana Tech - Kathy Kitto

Lal Singh - Pro-Con

R&W

Walt Alexanderson
Ed Anderson
Ray Best
Ted Cook
Ted Engelder
Allen Ferguson
Dick Glasser
Ron Komoroski
Bill Long
Gene Lynch
Dan Petrak
Paul Probert
Rob Sheriff
Joe Snyder

DISTRIBUTION: LRC-5258

LRC

C. E. Bell
A. H. Bremser
D. A. Button
T. C. Engelder
R. P. Glasser
A. E. Holt
W. G. Long
E. D. Lynch
H. H. Moeller
R. A. Potter (5)
S. R. Schenck
R. W. Sheriff
J. E. Snyder
Library
4495 File

ARC

P. S. Ayres
R. K. Bhada
R. W. Curtis
J. M. Nielsen
J. M. Rackley
S. Reid
M. A. Schroedl
K. H. Schulze
P. E. Sensmeier
D. B. VanFossen
Library

DOE Fossil Energy

S. J. Dapkunas (3)

CRD

A. C. Rogers
M. A. Rushing
N. F. Smith

TPD

H. Madden

IITRI

R. Firestone

Pennwalt

R. Pierce

Refractories Div.

W. H. Alexanderson
W. C. Bohling
T. H. Cook
C. E. Hopson
J. O'Keefe
H. A. Uzpurvis

FPGD

J. Davis
C. R. Ferguson
P. B. Probert

Battelle Columbus

C. Kistler
J. R. Schorr

Argonne National Laboratory

W. A. Ellingson
C. R. Kennedy
M. Shackelford

National Bureau of Standards

E. R. Fuller
S. J. Schneider (2)
S. M. Wiederhorn

United States Bureau of Mines

H. Heystek

University of Missouri at Rolla

D. E. Day

VPI

J. J. Brown

Pennsylvania State University

R. Bradt

Science Applications, Inc.

Jim Pope

Lone Star LaFarge

J. Fishwick

Alcoa

G. MacZura

Amco Research Center

M. S. Crowley

Iowa State University

T. McGee/J. Smyth

EPRI

W. T. Bakker
J. Stringer

MIT

O. Buyukozturk/
J. Connor

Exxon Research & Eng. Co.

G. Sorell

Oak Ridge Nat. Lab

TIC
R. A. Bradley

Dorr-Oliver

L. Alford/
G. Van Dyke

Phillips Petroleum

C. Venable

DOE Patent Department

Chicago

Stearns-Roger

P. E. Dempsey
M. R. Schultz

Curtis Wright

A. De Feo

Institute of Gas Tech.

J. Arnold

Northwestern University

Z. P. Bazant

Shell Development Co.

L. W. R. Dicks

DISTRIBUTION CONT'D.

Bechtel

Doc Lou

C-E Refractories

Edward Snajdr

Chicago Bridge & Iron Co.

Elmar Rothrock

Dept. of Energy

Gene Hoffman

Dravo Corp.

Jack Hyde

Foster-Wheeler

Anthony Mondok

Fluidyne Eng. Co.

Ron Smyth

Fluor Engineers

George Smith

A.P. Green

Craig Campbell

Gulf Oil

Pat Dolan

Harbison-Walker

Hugh Criss

Montana Tech

Kathy Kitto

Hotwork, Inc.

Kerry Higgins

IIT Research Institute

R. F. Firestone

Iowa State Univ.

Tom McGee

Koppers Co.

Jan Reiser
Paul Musiol

Lone Star LaFarge

Ken Moody

Davey McKee Co.

Jim Cheraso

MIT

Oral Buyukozturk

Monsanto Co.

Bill Netter

Oak Ridge National Lab

Ron Bradley
Joe Hammond

Ralph M. Parson Co.

Lynn McRae

Pittsburgh & Midway Coal Mining Co.

Larry Sluzalis

Pennwalt Corp.

Bob Pierce

Plibrico

Len Krietz

Pullman Kellogg

W. T. Thweatt

Shell Development Corp.

Bill Gottenburg

Stone & Webster

W. Hsu

Tennsesee Valley Autho.

W. D. Goins

Texaco

Don Newlin

UOP

Don Jaeger
Bud Krause

UTSI

Troy Shaver

VPI

Curtis Martin

Air Products & Chemicals

Joe Slusser